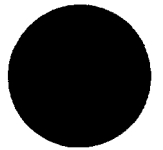
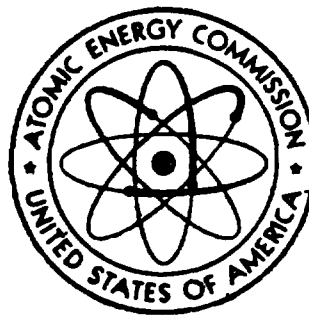


NVO-140  
VOLUME II

5258



# ENEWETAK RADIOLOGICAL SURVEY



OCTOBER 1973

UNITED STATES ATOMIC ENERGY COMMISSION  
NEVADA OPERATIONS OFFICE  
LAS VEGAS, NEVADA

## Appendix II - Survey Results by Island

Introduction . . . . .	iii
Map of Enewetak Atoll . . . . .	iv
Cross-reference list of island names . . . . .	v
Individual photomap scale factors . . . . .	vi
Contour map key for use with the EG&G aerial radiological survey figures . . . . .	vii
Survey results, Volume II	B.
ALICE . . . . .	.B. 1. 1
BELLE . . . . .	.B. 2. 1
CLARA . . . . .	.B. 3. 1
DAISY . . . . .	.B. 4. 1
EDNA . . . . .	.B. 5. 1
IRENE A . . . . .	.B. 6. 1
IRENE B . . . . .	.B. 7. 1
JANET . . . . .	.B. 8. 1
KATE . . . . .	.B. 9. 1
LUCY . . . . .	.B. 10. 1
PERCY . . . . .	.B. 11. 1
MARY . . . . .	.B. 12. 1
NANCY . . . . .	.B. 13. 1
OLIVE . . . . .	.B. 14. 1
PEARL . . . . .	.B. 15. 1
RUBY . . . . .	.B. 16. 1
SALLY . . . . .	.B. 17. 1
TILDA . . . . .	.B. 18. 1
URSULA . . . . .	.B. 19. 1
VERA . . . . .	.B. 20. 1
WILMA . . . . .	.B. 21. 1
YVONNE A . . . . .	.B. 22. 1
Survey results, Volume III	
YVONNE B . . . . .	.B. 23. 1
YVONNE C . . . . .	.B. 24. 1
YVONNE D . . . . .	.B. 25. 1
YVONNE E . . . . .	.B. 26. 1
YVONNE F . . . . .	.B. 27. 1



Survey results (continued)

SAM . . . . .	.B. 28.1
TOM . . . . .	.B. 29.1
URIAH . . . . .	.B. 30.1
VAN . . . . .	.B. 31.1
ALVIN . . . . .	.B. 32.1
BRUCE . . . . .	.B. 33.1
CLYDE . . . . .	.B. 34.1
DAVID . . . . .	.B. 35.1
REX . . . . .	.B. 36.1
ELMER A . . . . .	.B. 37.1
ELMER B . . . . .	.B. 38.1
ELMER C . . . . .	.B. 39.1
ELMER D . . . . .	.B. 40.1
WALT . . . . .	.B. 41.1
FRED A . . . . .	.B. 42.1
FRED B . . . . .	.B. 43.1
FRED C . . . . .	.B. 44.1
FRED D . . . . .	.B. 45.1
FRED E . . . . .	.B. 46.1
FRED F . . . . .	.B. 47.1
GLENN . . . . .	.B. 48.1
HENRY . . . . .	.B. 49.1
IRWIN A . . . . .	.B. 50.1
IRWIN B . . . . .	.B. 51.1
JAMES . . . . .	.B. 52.1
KEITH . . . . .	.B. 53.1
LEROY . . . . .	.B. 54.1
Summary of Experimental Data . . . . .	.C.

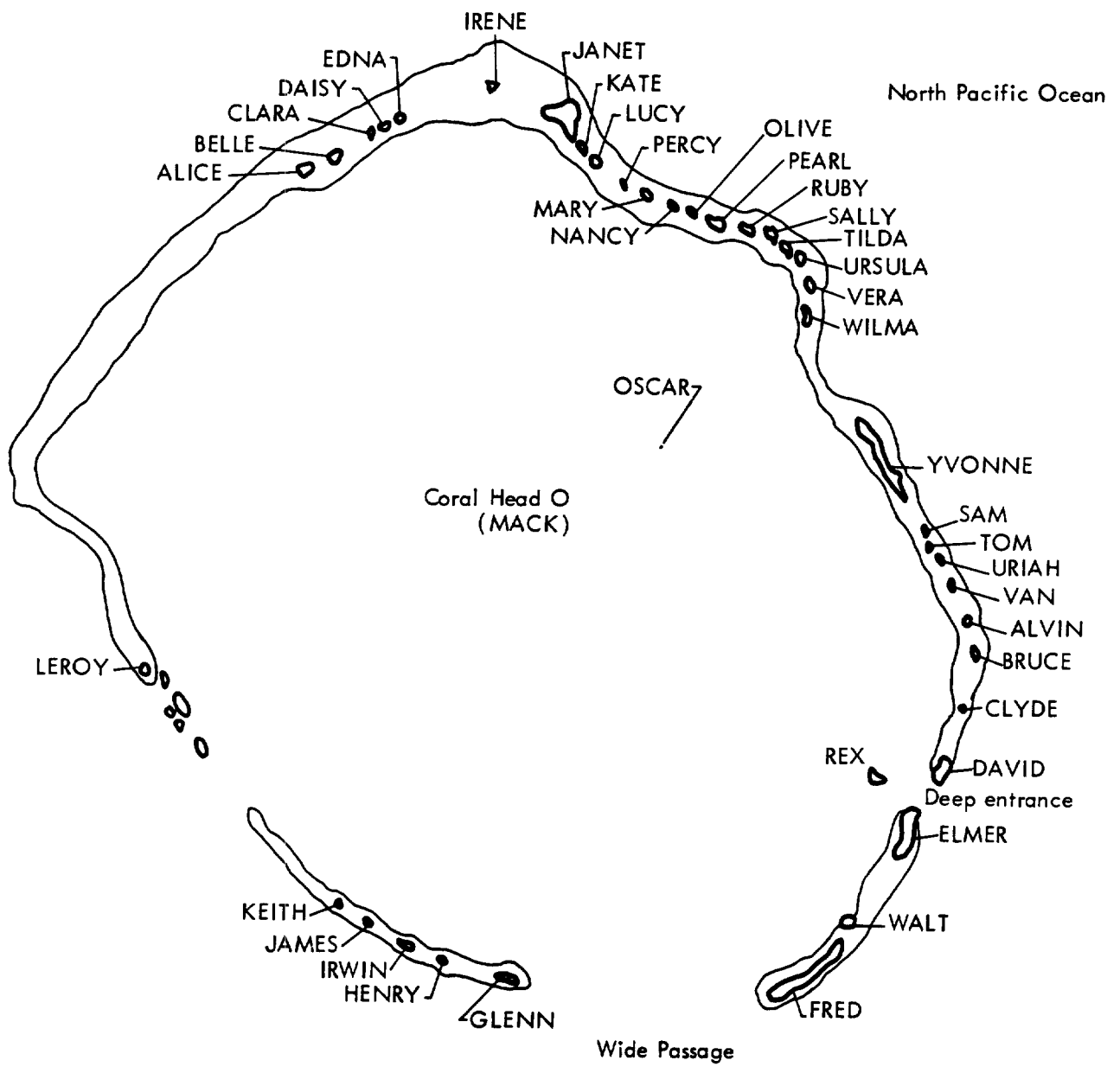
## INTRODUCTION

This appendix is a compilation of radiological survey results for each of the islands in Enewetak Atoll. The information for each island includes a color aerial photograph, a series of photographs overprinted with survey data, and a set of analytical data. It should be noted that several islands (i.e., IRENE, YVONNE, ELMER, FRED, and IRWIN) have been subdivided into sections (e.g., IRENE A and IRENE B) because of their relatively large size. In addition, it should be pointed out that the sets of overprints are not necessarily the same for all islands. Thermoluminescent detectors (TLD's), for example, were not used on all islands. For ease of comparison and clarity, the same data parameter for each island is overprinted on the same color of photograph.

For a discussion of the techniques used in collecting the data presented on the photographic overprints, the reader is referred to the appropriate section in Vol. I of this document.

A typical set of survey results is outlined below for ALICE, together with the page and figure designation scheme used.

	<u>ALICE</u>	<u>Fig.</u> <u>No.</u>
Current condition . . . . .		
a. Color photograph . . . . .		B. 1. 1a
b. 0-3 MeV EG&G isopleth . . . . .		B. 1. 1b
c. 0-300 keV EG&G isopleth . . . . .		B. 1. 1c
d. Ground measurements with Baird Atomic . . . . .		B. 1. 1d
f. Soil-sampling locations . . . . .		B. 1. 1f
g. Vegetation sampling locations . . . . .		B. 1. 1g
h. TLD locations . . . . .		B. 1. 1h
i. <sup>239</sup> Pu soil content isopleths . . . . .		B. 1. 1i
j. <sup>90</sup> Sr soil content isopleths . . . . .		B. 1. 1j
k. <sup>137</sup> Cs EG&G isopleths . . . . .		B. 1. 1k
l. <sup>137</sup> Cs soil data . . . . .		B. 1. 1l
m. <sup>60</sup> Co EG&G isopleths . . . . .		B. 1. 1m
n. <sup>60</sup> Co soil data . . . . .		B. 1. 1n
o. Animal sampling location . . . . .		B. 1. 1o
Analytical data for soils . . . . .		
a. through m. Soil profile data plots . . . . .		B. 1. 2a through B. 1. 2m



Map of Enewetak Atoll

At the end of Volume III, after the section on LEROY, is a section containing microfiche transparencies reproducing all of the analytical data obtained in this survey. Instructions on the use of microfiche film are also included in that section.

Table B.1. Cross-reference list of island names.

Site	Native names from U. S. Hydrographic Office charts		Native names from Dr. Jack A. Tobin
	1946	1968	
ALICE	Bogallua	Bogallua	BOKOLUO
BELLE	Bogombogo	Bogombogo	BOKOMBAKO
CLARA	Ruchi	Eybbiyae	— <sup>a</sup>
DAISY	— <sup>a</sup>	Lidilbut	LOUJ
EDNA	— <sup>a</sup>	— <sup>a</sup>	— <sup>a</sup>
HELEN	Bogairikk	Bogeirik	BOKAIDRIK
IRENE	Bogon	Bogon	BOKEN
JANET	Engebi	Engebi	ENJEBI
KATE	Muzinbaarikku	Mujinkarikku	MIJIKADREK
LUCY	Kirinian	Billee	KIDRINEN
PERCY	— <sup>a</sup>	— <sup>a</sup>	— <sup>a</sup>
MARY	Bokonaarappu	Bokonarppu	BOKENELAB
NANCY	Yeiri	Yeiri	ELLE
OLIVE	Aitsu	Aitsu	AEJ
PEARL	Rujoru	Rujiyoru	LUJOR
RUBY	Eberiru	Eberiru	ELELERON
SALLY	Aomon	Aomon	AOMON
TILDA	Bijiri	Bijiri	BIKILE
URSULA	Rojoa	Rojoa	LOJWA
VERA	Aaraanbiru	Arambiru	ALEMBEL
WILMA	Piiraai	Piirai	BILLAE
YVONNE	Runit	Runit	RUNIT
SAM	— <sup>a</sup>	— <sup>a</sup>	— <sup>a</sup>
TOM	— <sup>a</sup>	— <sup>a</sup>	ANEROWIJ
URIAH	— <sup>a</sup>	— <sup>a</sup>	— <sup>a</sup>
VAN	— <sup>a</sup>	— <sup>a</sup>	— <sup>a</sup>
ALVIN	Chinieero	— <sup>a</sup>	JINEDROL
BRUCE	Aniyaanii	Japtan	ANANIJ
CLYDE	Chinimi	Chinimi	JINIMI
DAVID	Japtan	Muti	JAPTAN
ELMER	Parry	Parry	MEDREN
WALT	— <sup>a</sup>	— <sup>a</sup>	— <sup>a</sup>
FRED	Eniwetok	Eniwetok	ENEWETAK

Table B.1 (Continued)

Site	Native names from U. S. Hydrographic Office Charts		Native names from Dr. Jack A. Tobin
	1946	1968	
GLENN	Igurin	Igurin	IKUREN
HENRY	Mui	Buganegan	MUT
IRWIN	Pokon	Bogan	BOKEN
JAMES	Ribaion	Libiron	RIBEWON
KEITH	Giriinien	Grinem	KIDRENEN
LEROY	Rigili	Rigili	BIKEN
REX	Jieroru	Bogen	JEDROL
OSCAR	— <sup>a</sup>	— <sup>a</sup>	DREKATIMON
MACK	— <sup>a</sup>	— <sup>a</sup>	UNIBOR

<sup>a</sup>No native name.

Table B.2. Enewetak Atoll individual photomap scale factors.

Island	Altitude flown, ft	Scale
ALICE	5000	1 cm = 37 m
BELLE	5000	34
CLARA	3000	23
DAISY	3000	25
EDNA	5000	38
IRENE A, B	5000	51
JANET	10000	87
KATE	3000	24
LUCY	3000	26
PERCY	3000	21
MARY	3000	24
NANCY	5000	33
OLIVE	5000	38
PEARL	5000	44
RUBY	3000	17
SALLY	8000	67
TILDA	5000	36
URSULA	5000	33
VERA	5000	31
WILMA	3000	27
YVONNE A, B, C, D	5000	51
SAM	1000	13

Table B.2 (Continued)

Island	Altitude flown, ft	Scale
TOM	2000	1 cm = 8 m
URIAH	2000	17
VAN	4000	20
ALVIN	2000	15
BRUCE	5000	42
CLYDE	2000	12
DAVID	5000	44
REX	2000	18
ELMER A, B, C, D	5000	47
WALT	2000	15
FRED A, B, C, D, E, F	5000	48
GLENN	9000	77
HENRY	6000	55
IRWIN A, B	3000	29
JAMES	3000	16
KEITH	3000	26
LEROY	3000	20
YVONNE E, F	10000	95

Table B.3. Contour map key for use with the EG&G aerial radiological survey figures in Appendix II.<sup>a</sup>

Sym- bol	<sup>241</sup> Am concentration <sup>b</sup> (assumed 10-cm relaxation depth)		<sup>137</sup> Cs <sup>c</sup>		<sup>60</sup> Co <sup>d</sup>		Gross count exposure rate, <sup>e</sup> μR/hr
	Total μCi/m <sup>2</sup>	averaged over top 10 cm, pCi/g	Concentration ±50% for 1 cm (relaxation depth < 10 cm), μCi/m <sup>2</sup>	Exposure rate, μR/hr	Concentration ±50% for 1 cm (relaxation depth < 10 cm), μCi/m <sup>2</sup>	Exposure rate, μR/hr	
A <sup>-</sup>			0-0.1	0-0.34			
A <sup>-</sup>			0.1-0.2	0.34-0.68	0-0.04	0-0.59	
A	0-21	0-9	0.2-0.4	0.68-1.36	0.04-0.08	0.59-1.14	0-1.0
B	21-30	9-13	0.4-0.6	1.36-2.0	0.08-0.12	1.14-1.7	1.0-1.5
C	30-45	13-19	0.6-0.8	2.0-2.7	0.12-0.16	1.70-2.3	1.5-2.0
D	45-66	19-28	0.8-1.6	2.7-5.4	0.16-0.32	2.3-4.6	2.0-4
E	66-100	28-42	1.6-3.1	5.4-11	0.32-0.64	4.6-0.9	4-8
F	100-145	42-61	3.1-6.2	11-22	0.64-1.3	9.2-18	8-16
G	145-210	61-89	6.2-12	22-44	1.3-2.5	18-36	16-33
H	210-300	89-130	12-25	44-88	2.5-5.0	36-72	33-66
I	300-450	130-190	25-50	88-170	5-10	72-140	66-130
J			50-100	170-340	10-20	140-290	130-260
K			100-200	340-700	20-40	290-580	260-520
L			200-400	700-1400	40-80	580-1200	520-1050

<sup>a</sup>See chapter on the EG&G aerial radiological survey in Vol. 1.<sup>b</sup>Shown in "c" figures in this Appendix.<sup>c</sup>Shown in "k" figures in this Appendix.<sup>d</sup>Shown in "m" figures in this Appendix.<sup>e</sup>Shown in "b" figures in this Appendix.



100 METERS

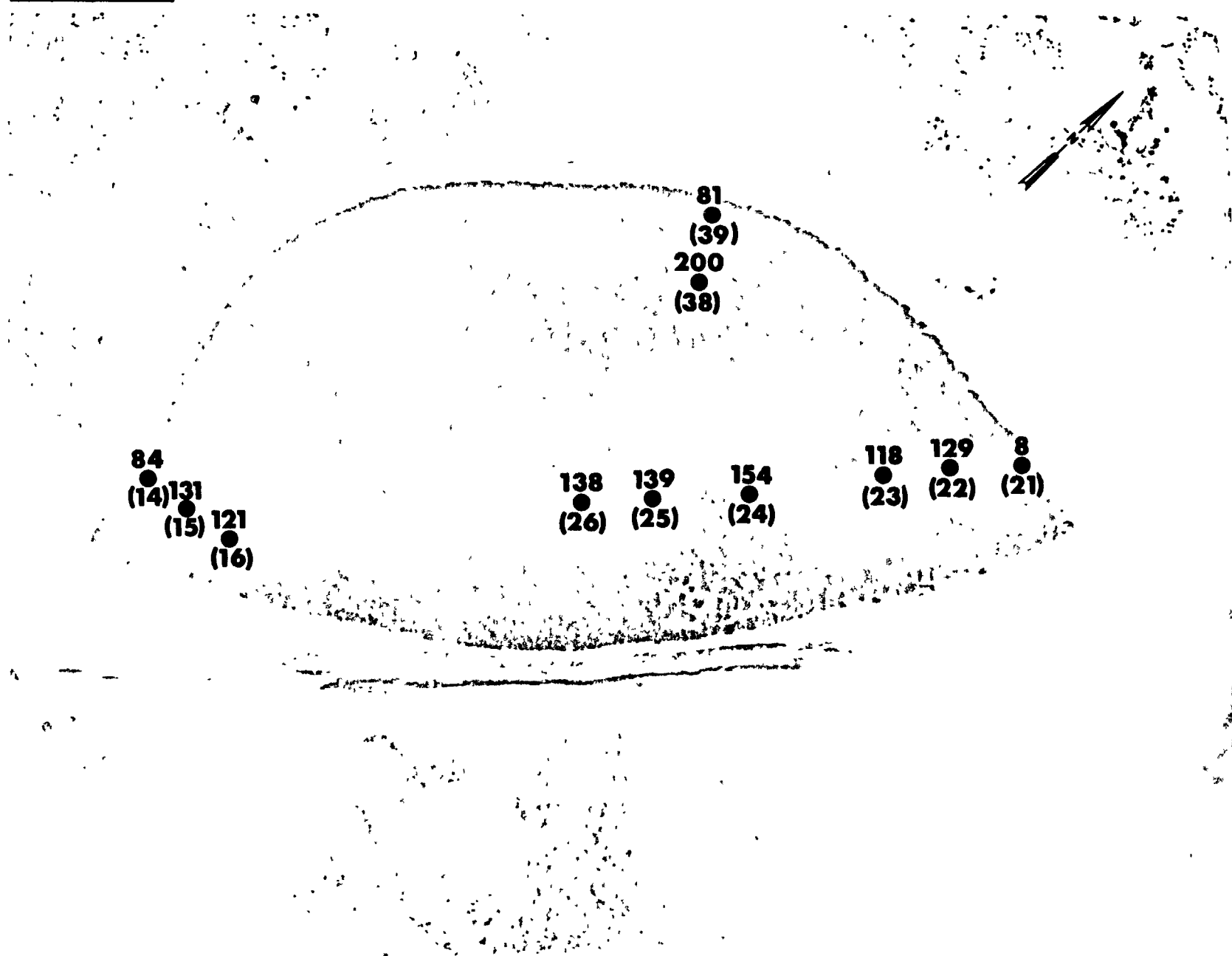
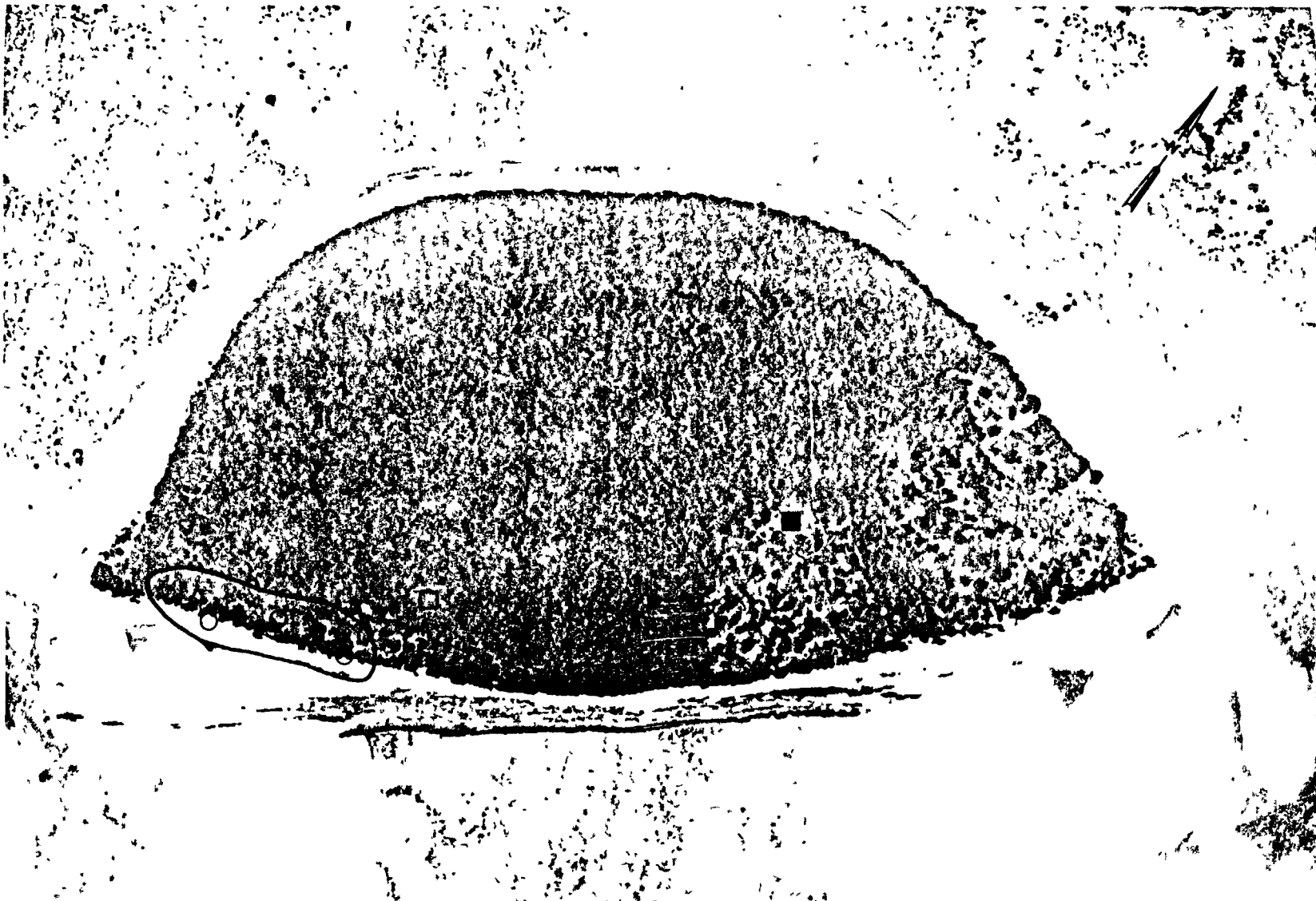


Fig. B.2.1.h. The gamma-ray exposure rates ( $\mu\text{R/hr}$ ) measured 1 m above the ground by the LiF thermoluminescent dosimeters (TLD). The numbers shown in parentheses denote the location identification numbers.



100 METERS



△ △ △ MESSERSCHMIDIA

○ ○ ○ SCAEVOLA

■ PANDANUS

□ GUETTARDA

Fig. B.2.1.g. Vegetation sample locations.

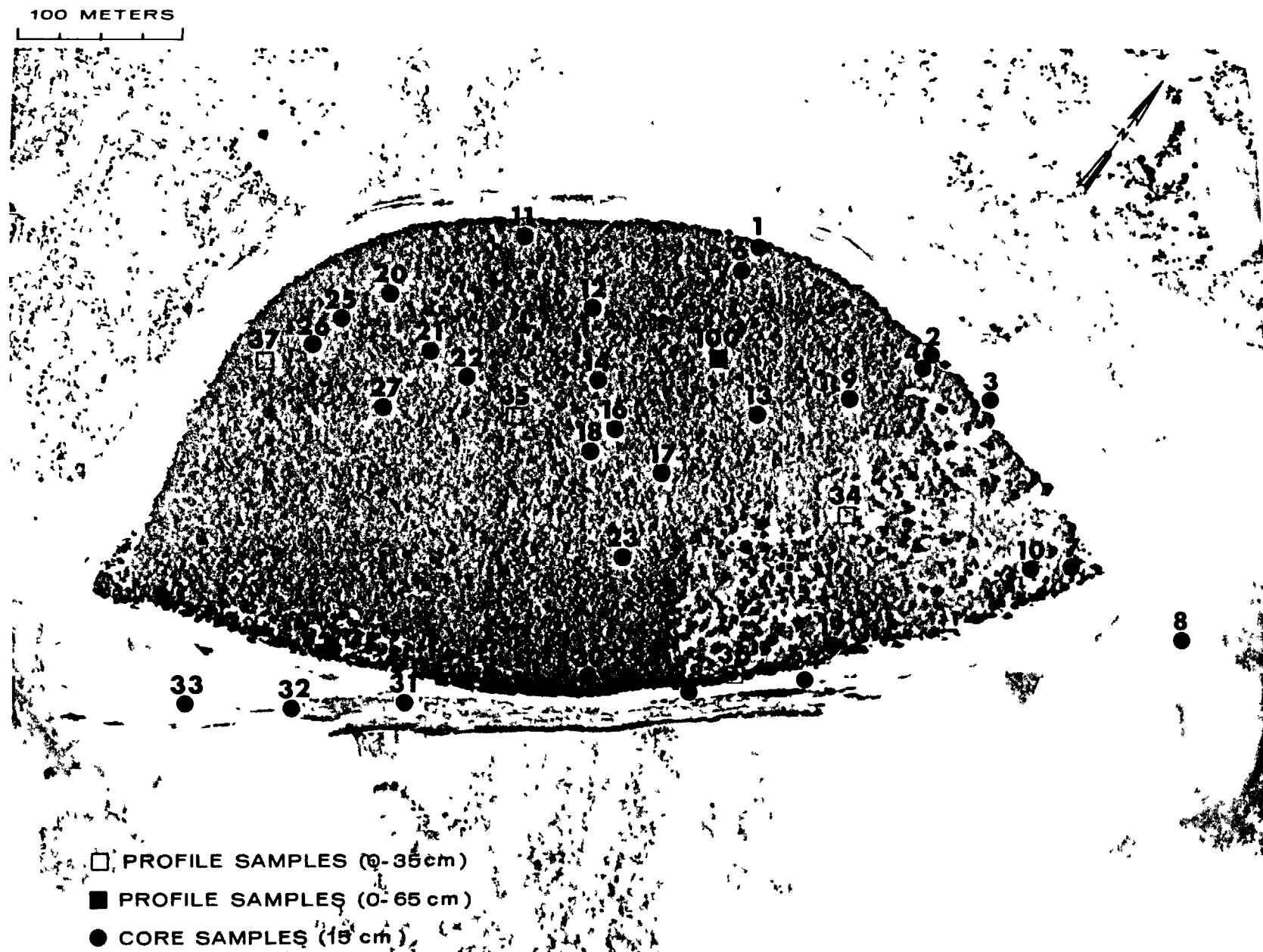


Fig. B.2.1.f. Soil-sample locations.

100 METERS

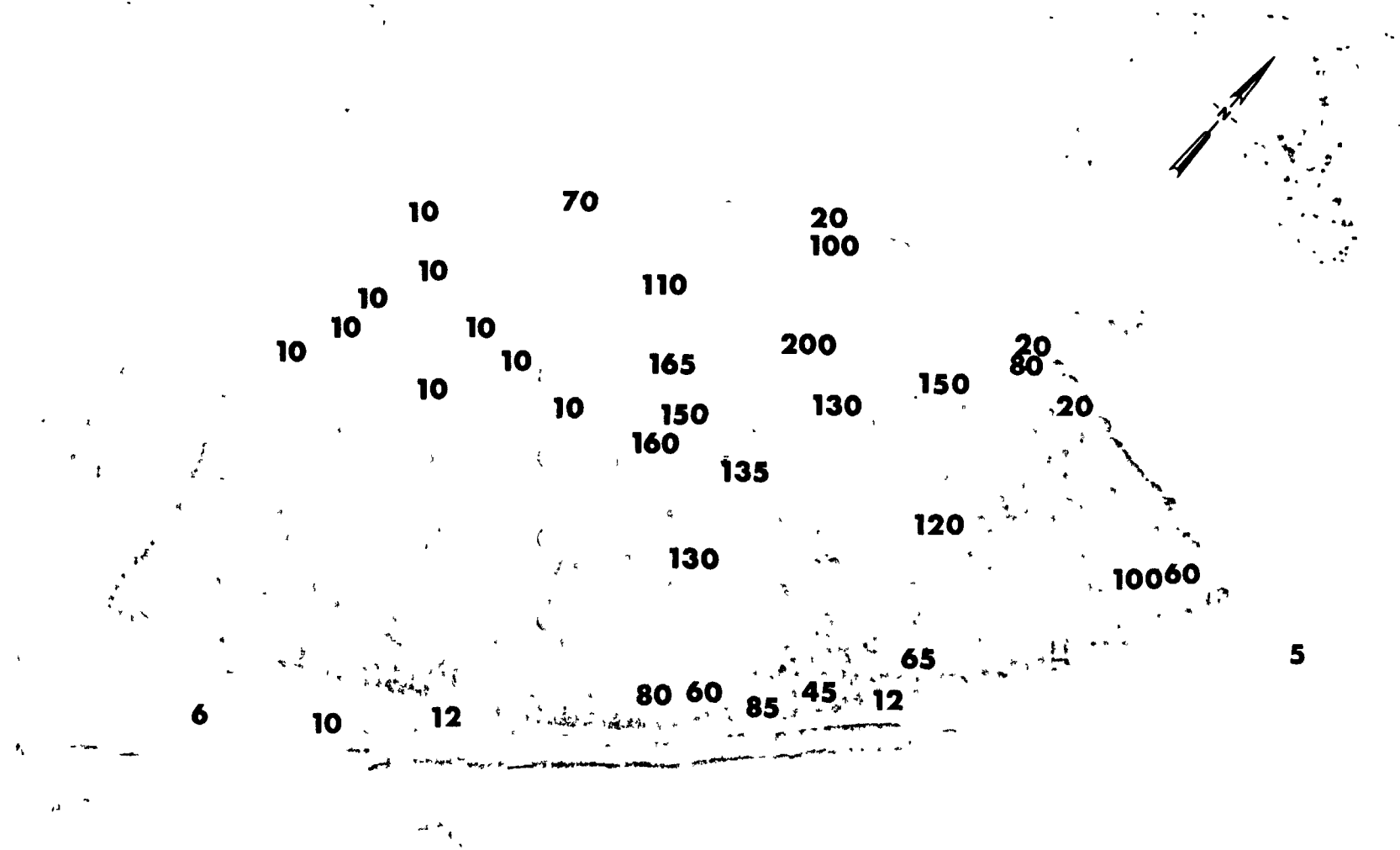
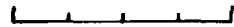


Fig. B.2.1.d. The gamma background exposure rate ( $\mu\text{R/hr}$ ) at 1 m above the ground, measured with a portable NaI scintillation counter.

100 METERS

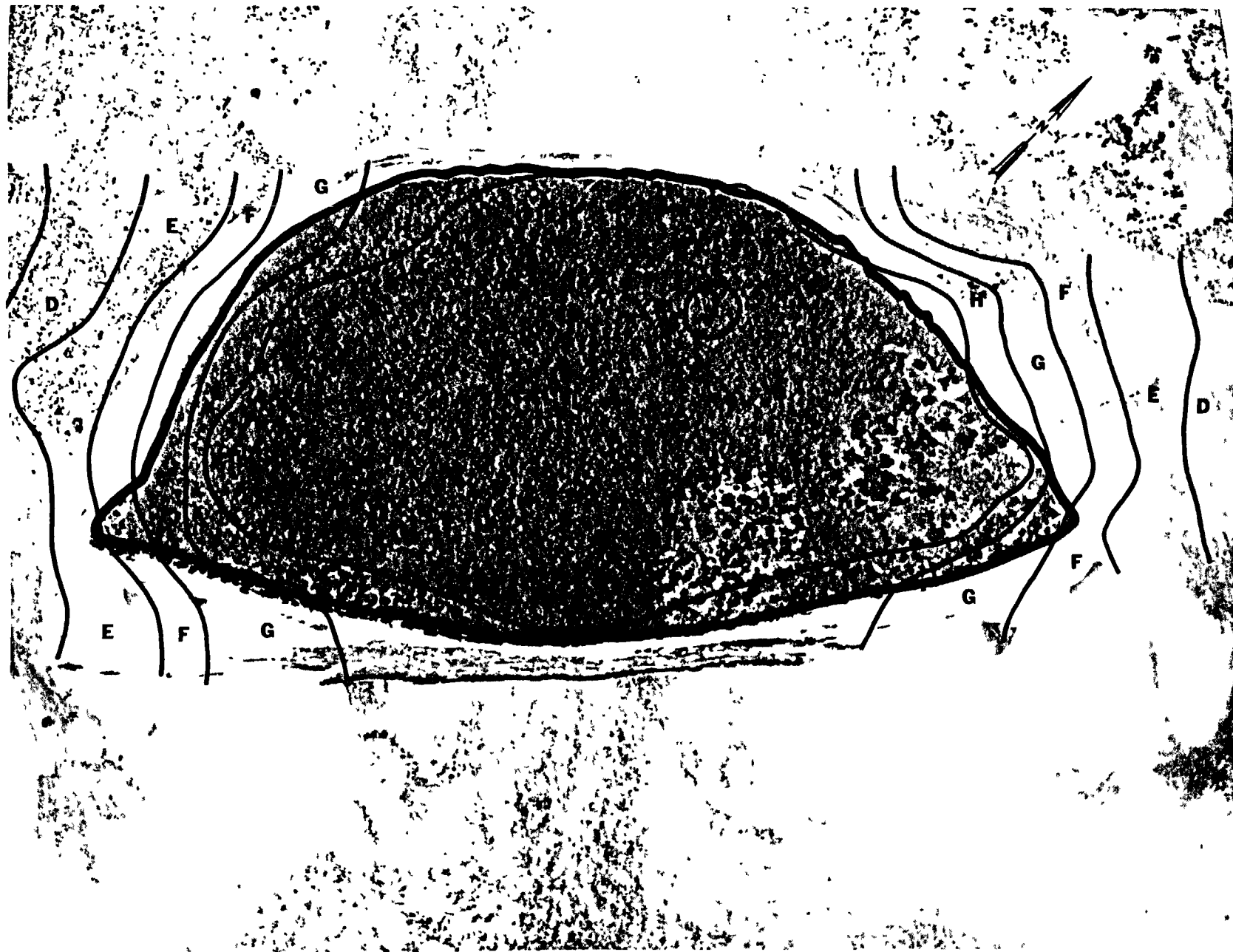


Fig. B.2.1.b. Gross count isoexposure contours. (Refer to alphabetic symbol key in this appendix.)

100 METERS

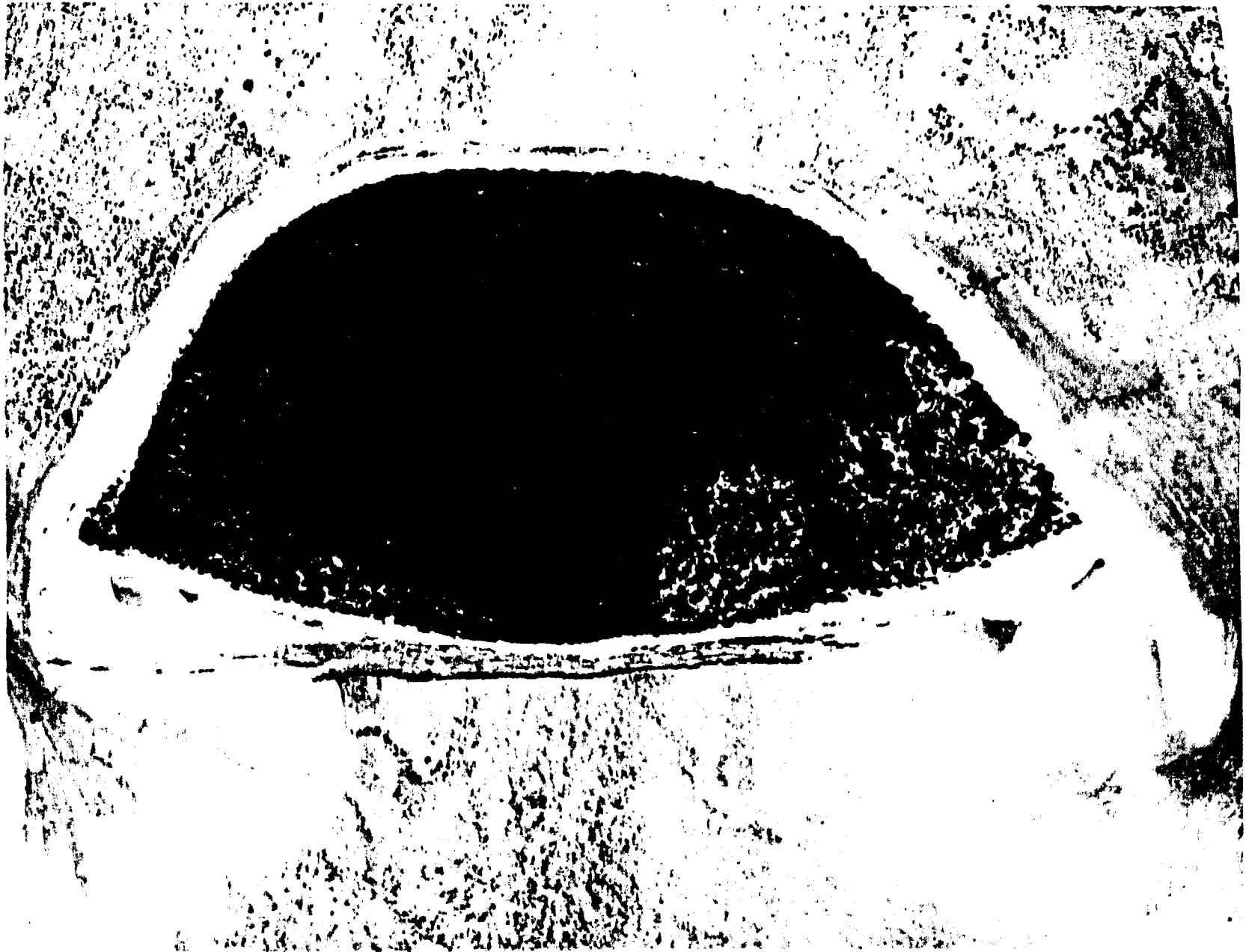


Fig. B.2.1.a.

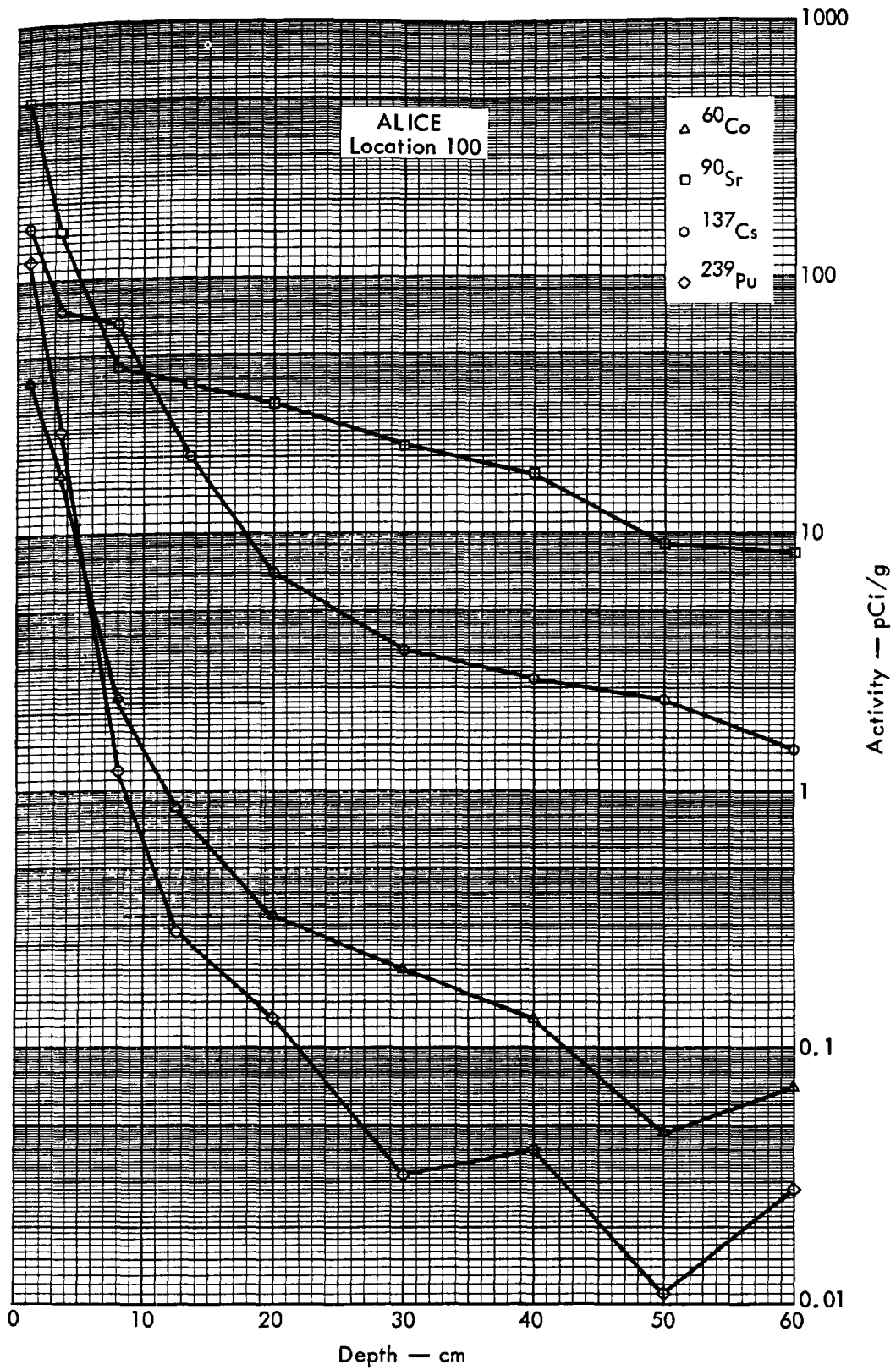


Fig. B.1.2e. Activities of selected radionuclides as a function of soil depth.

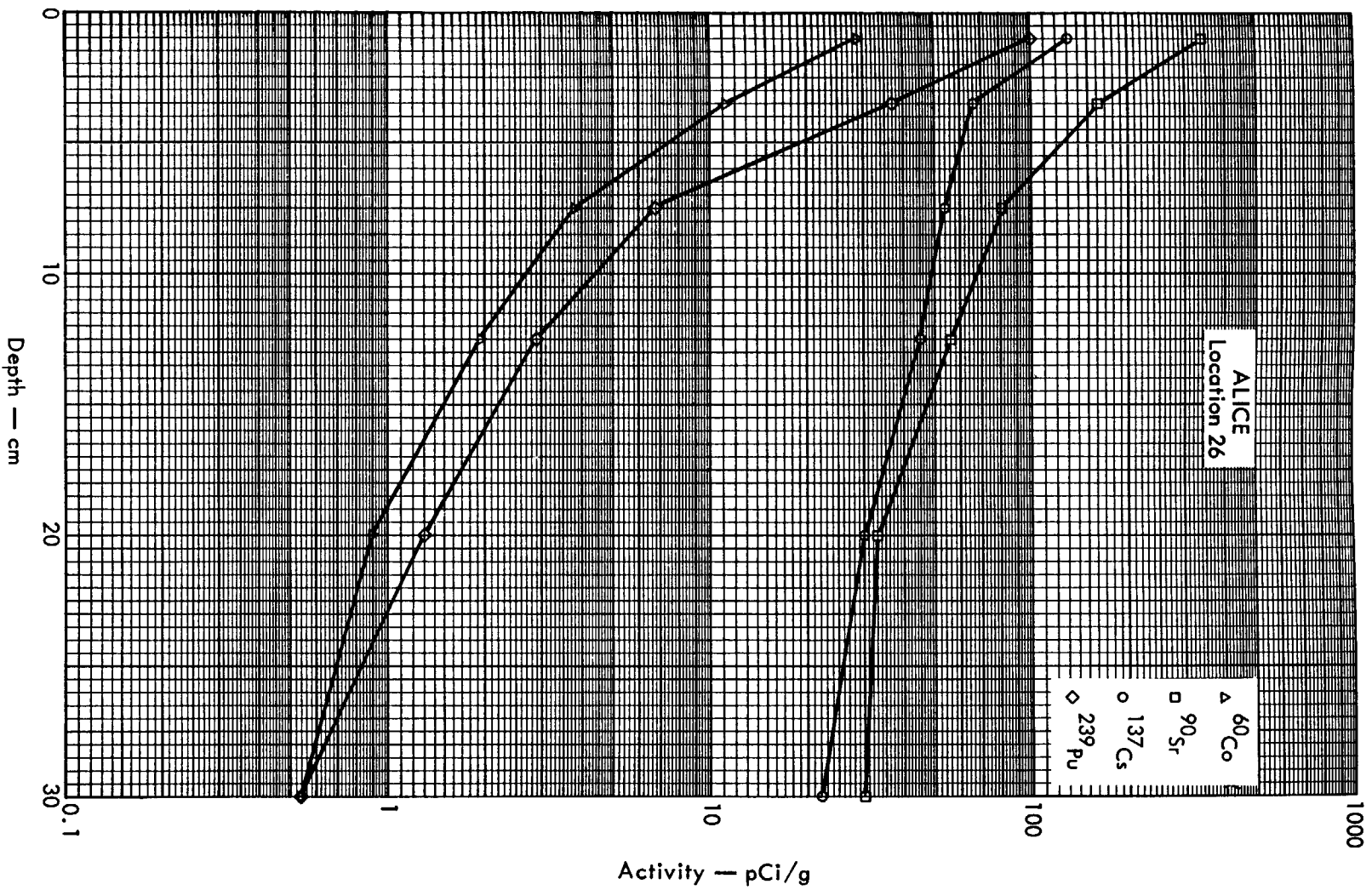


Fig. B. 1. 2d. Activities of selected radionuclides as a function of soil depth.

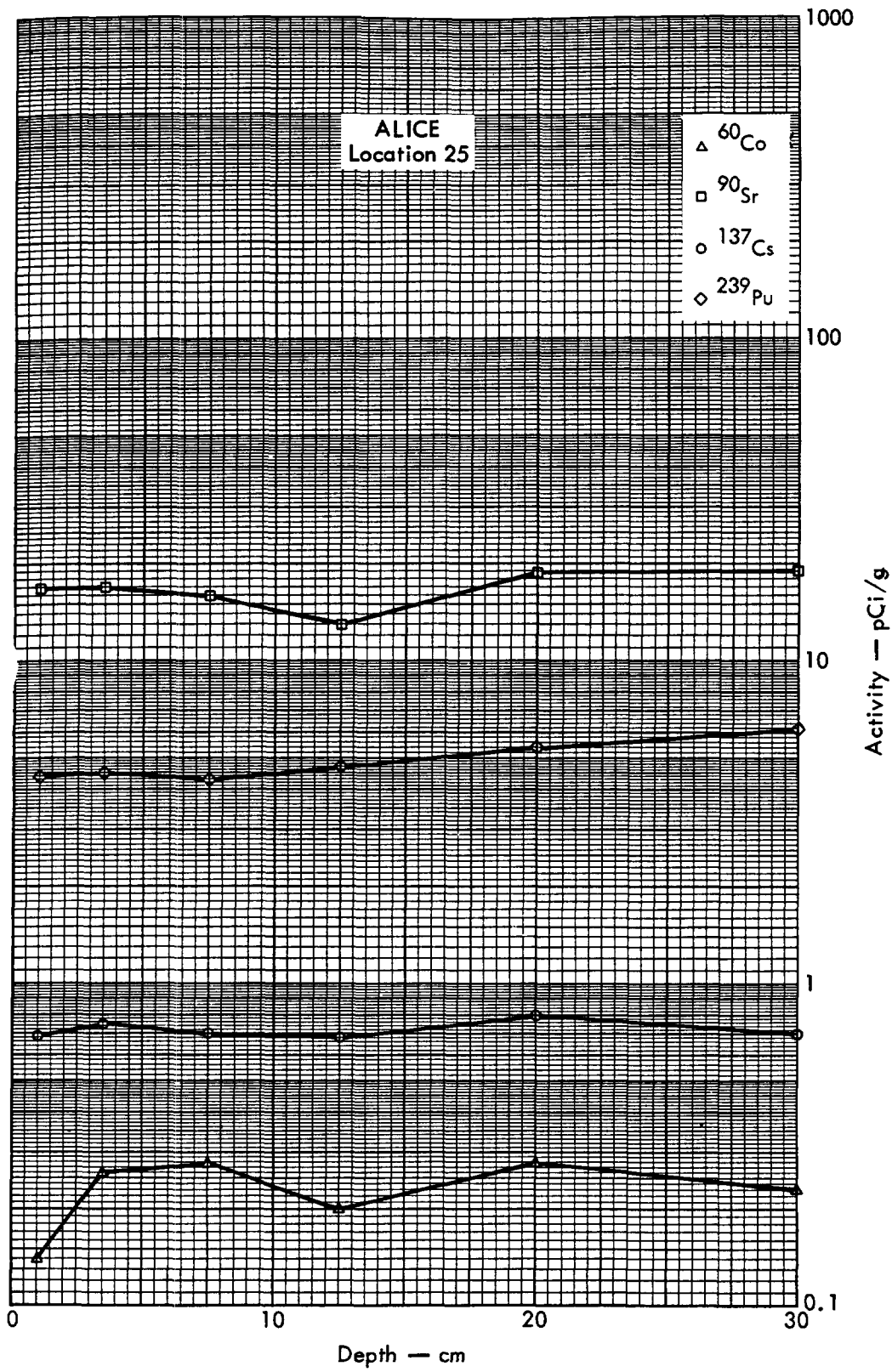


Fig. B. 1. 2c. Activities of selected radionuclides as a function of soil depth.



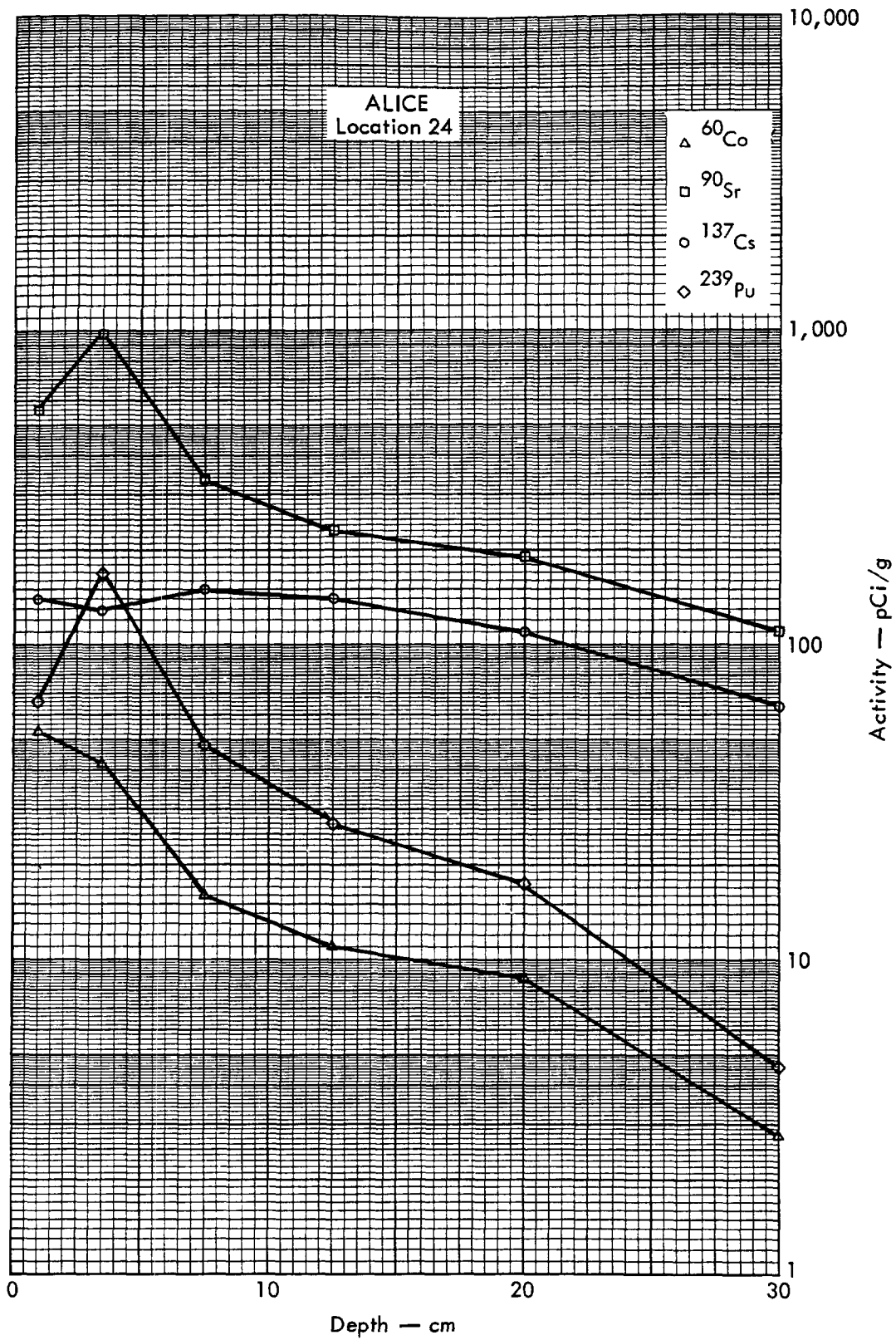


Fig. B. 1. 2b. Activities of selected radionuclides as a function of soil depth.

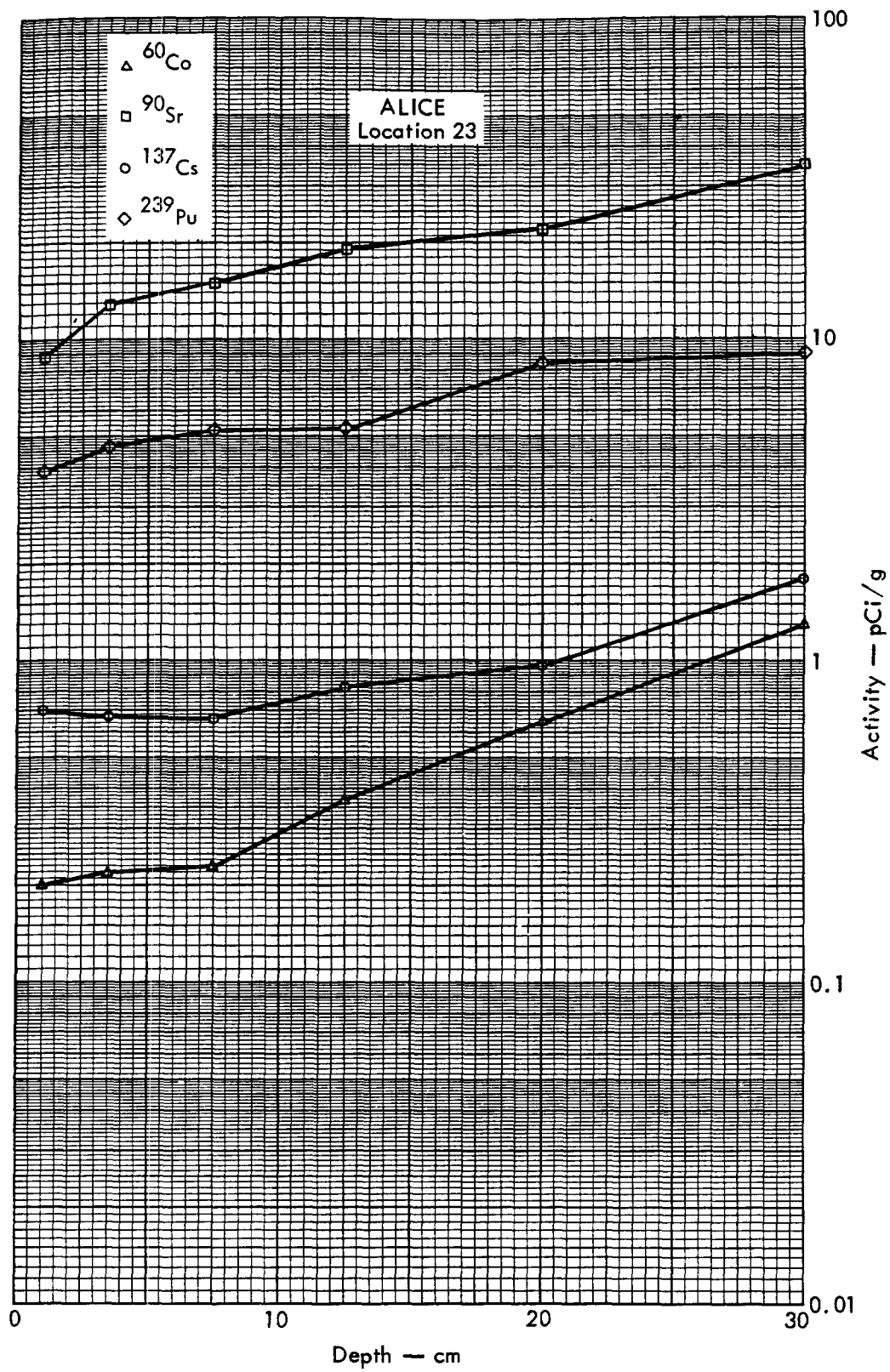
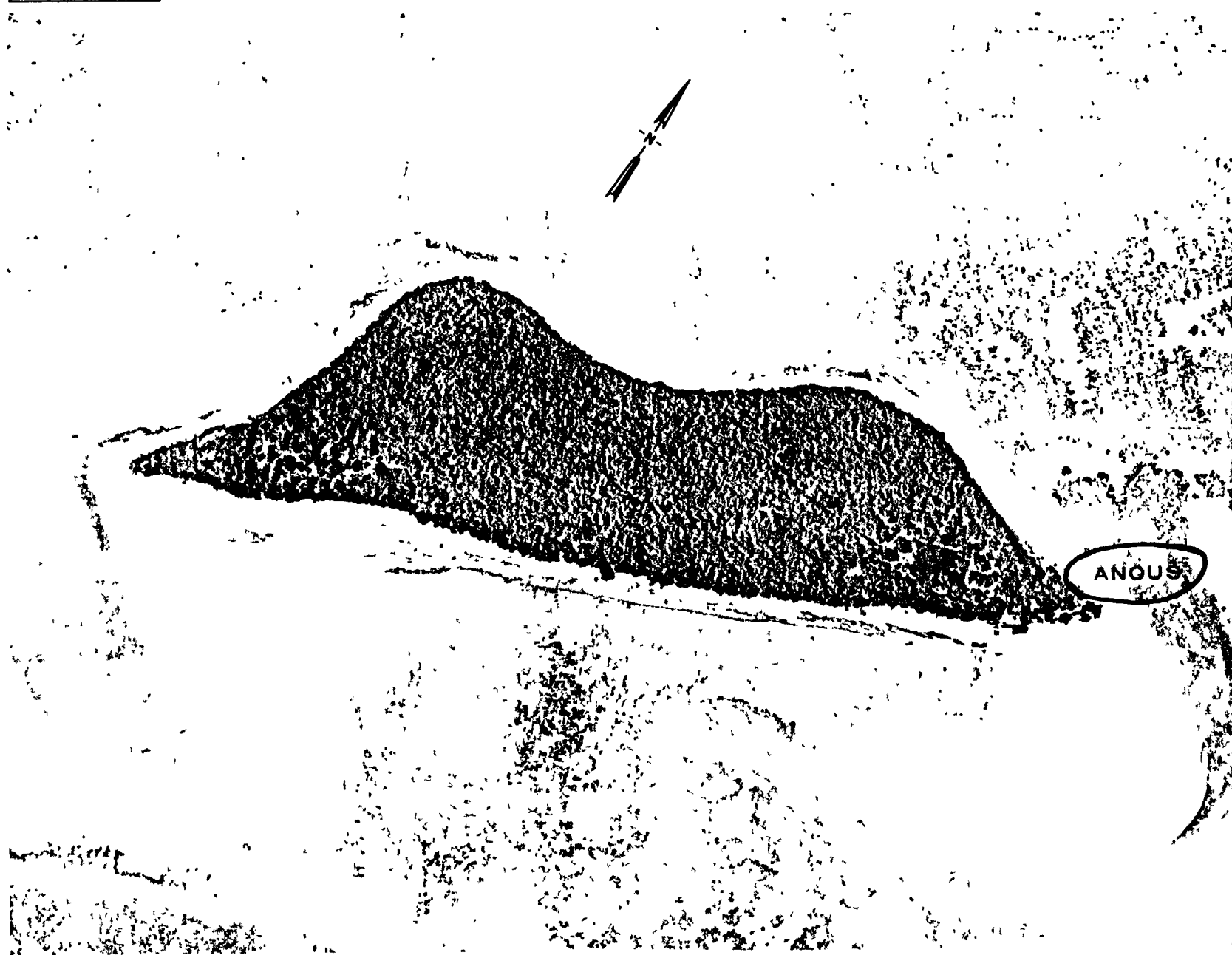


Fig. B. 1. 2a. Activities of selected radionuclides as a function of soil depth.

100 METERS



ANOUS

Fig. B.1.1.o. Terrestrial animal sample locations.

100 METERS

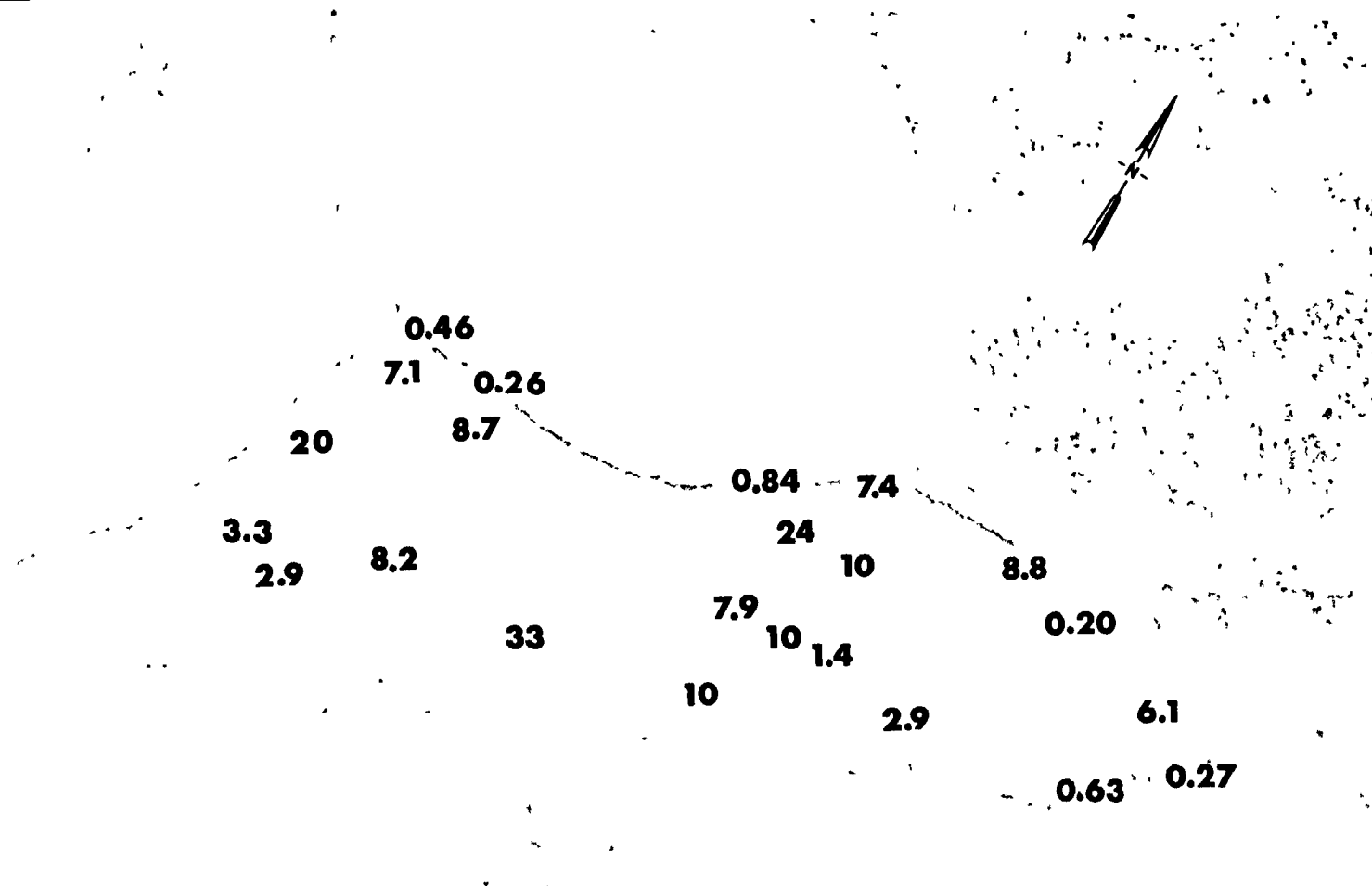


Fig. B.1.1.n. The average <sup>60</sup>Co activities (pCi/g) in soil samples collected to a depth of 15 cm.

100 METERS

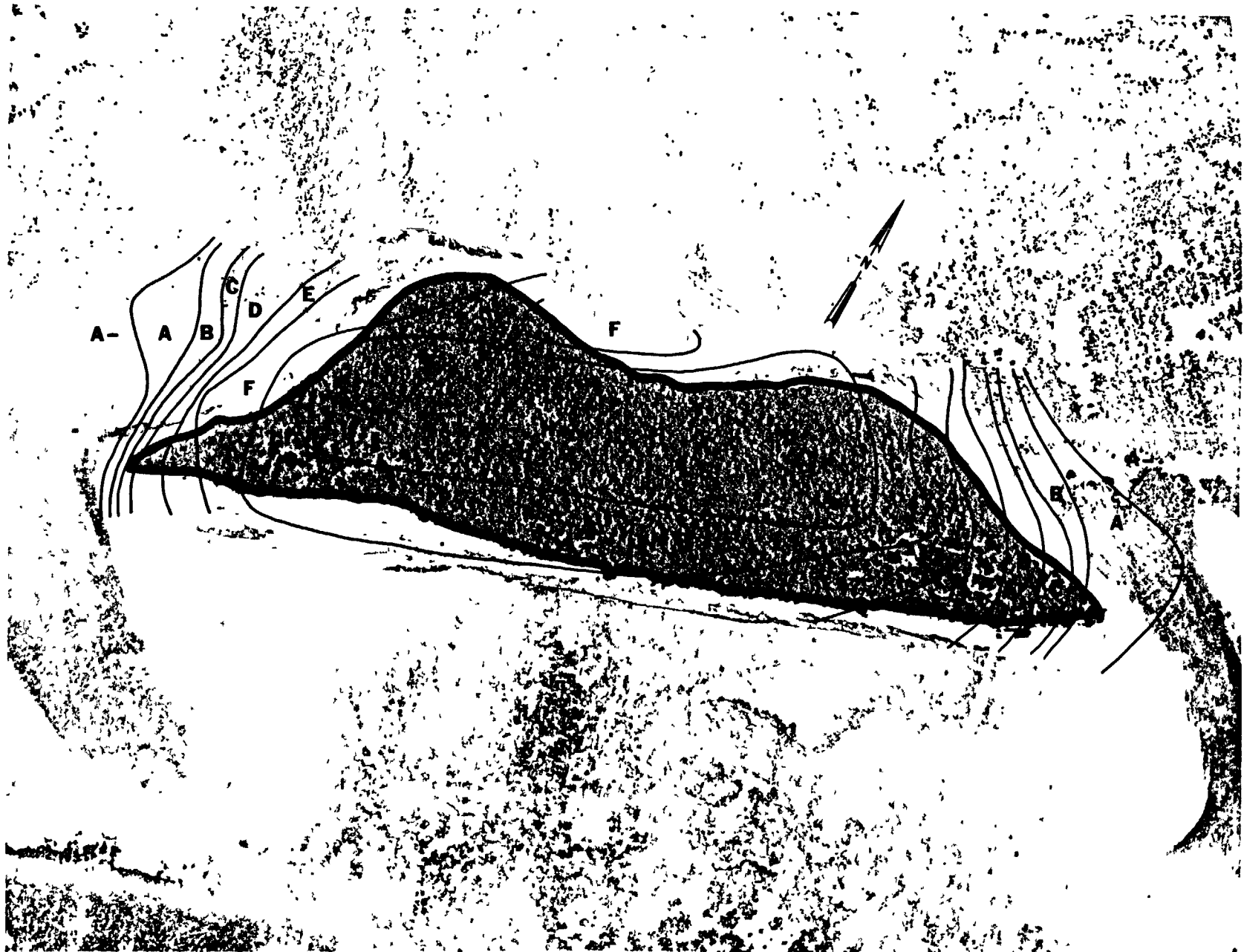
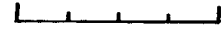


Fig. B.1.1.m.  $^{60}\text{Co}$  isoexposure and isoconcentration contours. (Refer to alphabetic symbol key in this appendix.)

100 METERS

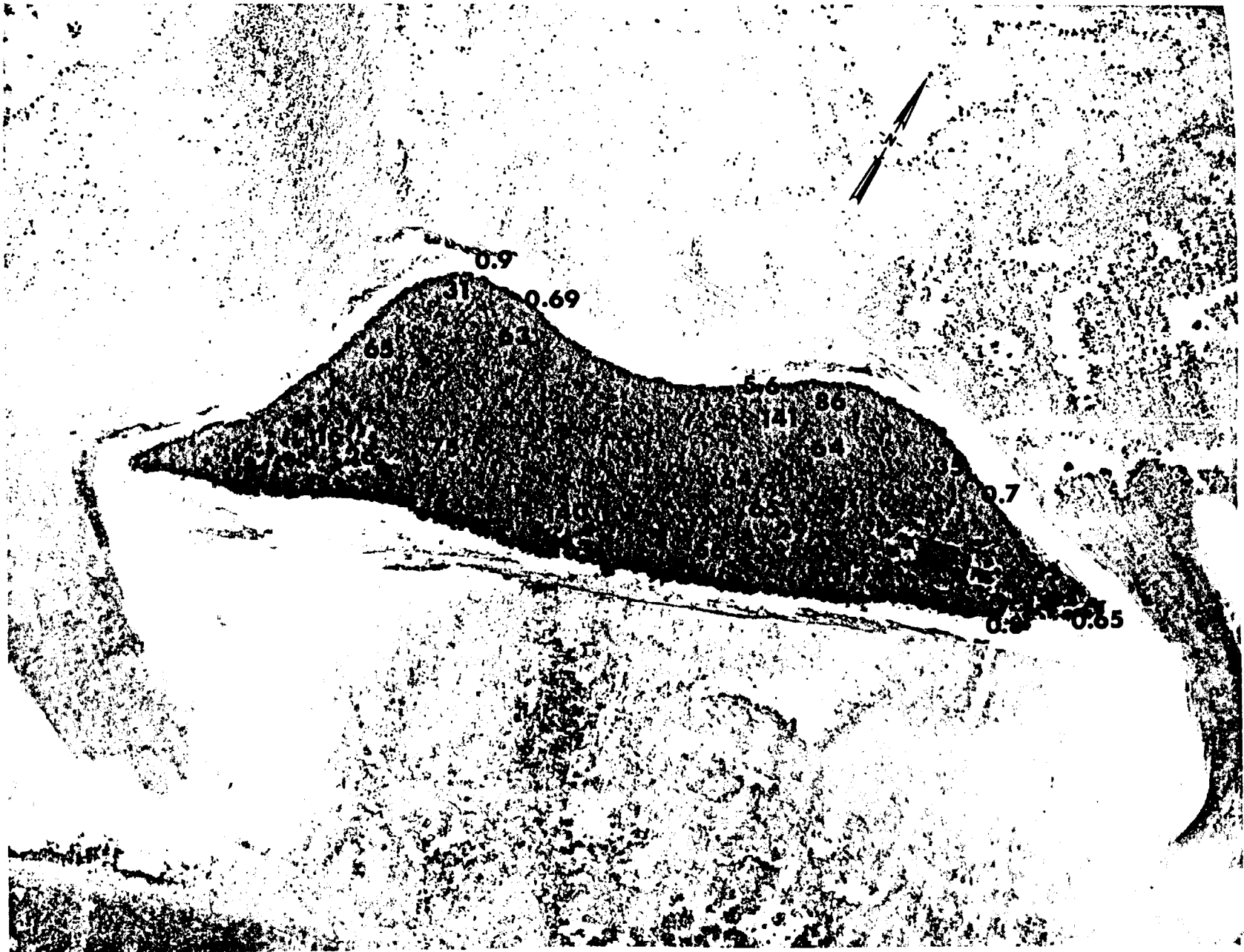


Fig. B.1.1.1. The average  $^{137}\text{Cs}$  activities (pCi/g) in soil samples collected to a depth of 15 cm.

100 METERS

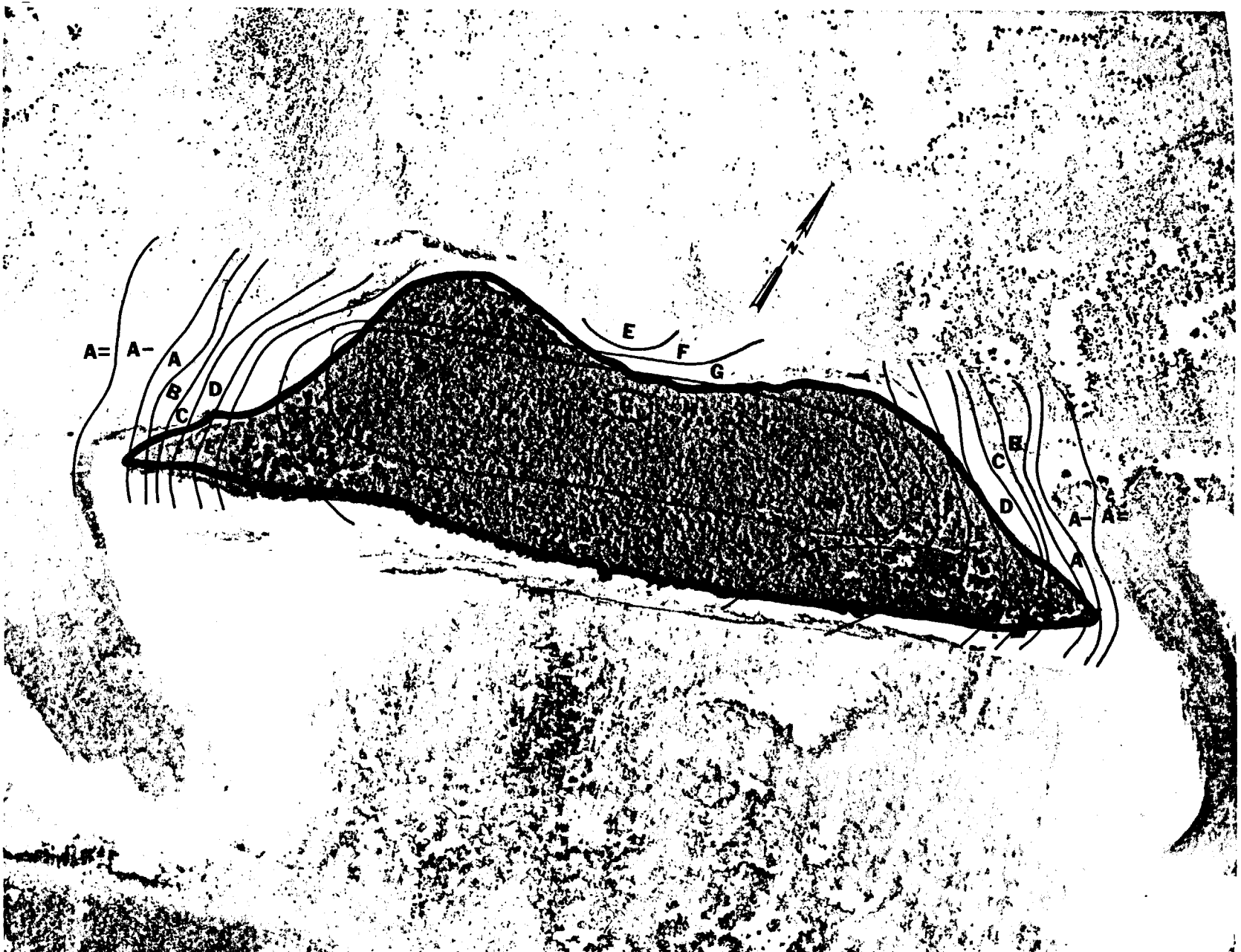
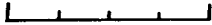


Fig. B.1.1.k.  $^{137}\text{Cs}$  isoexposure and isoconcentration contours. (Refer to alphabetic symbol key in this appendix.)

100 METERS

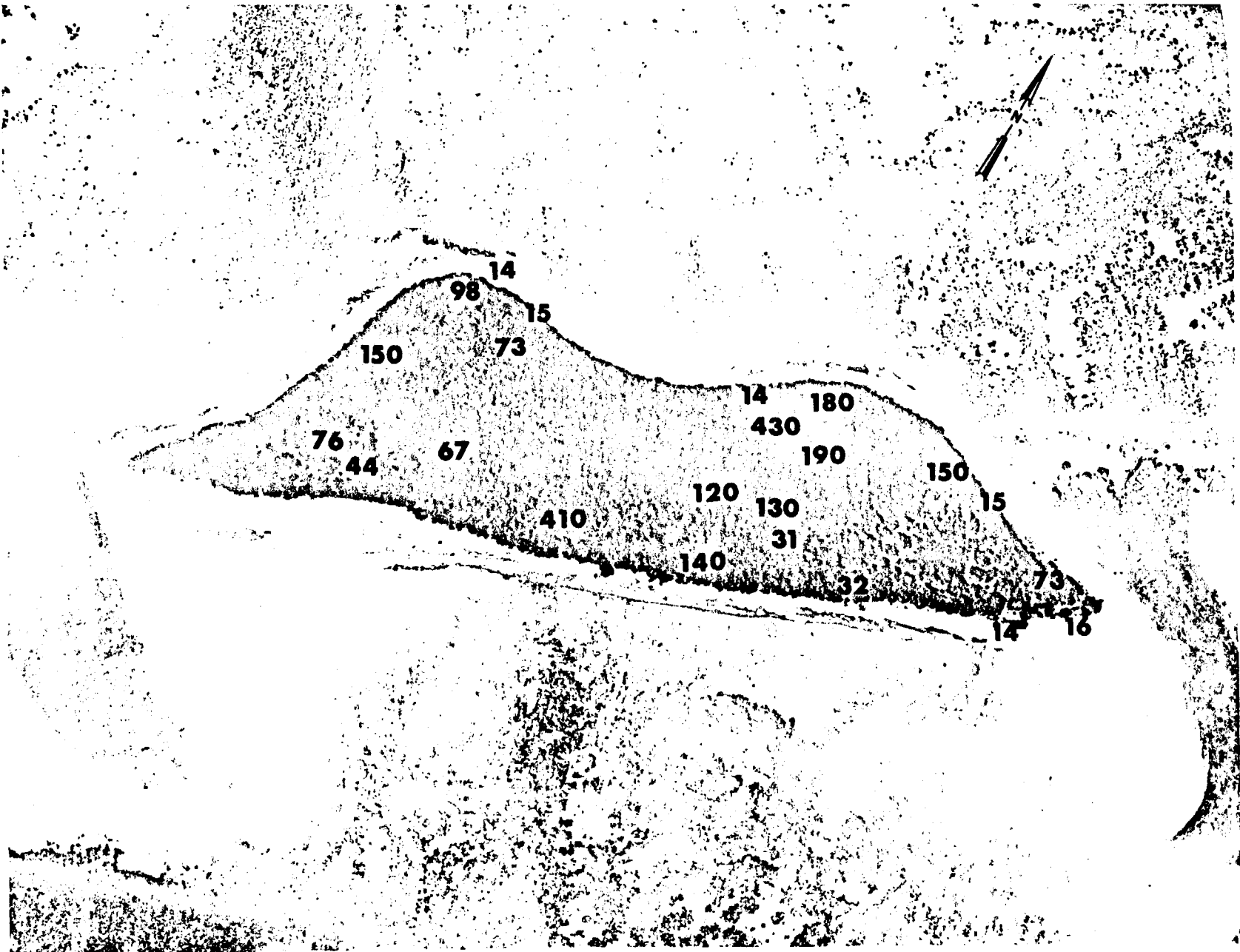


Fig. B.1.1.j. The average  $^{90}\text{Sr}$  activities (pCi/g) in soil samples collected to a depth of 15 cm.



100 METERS

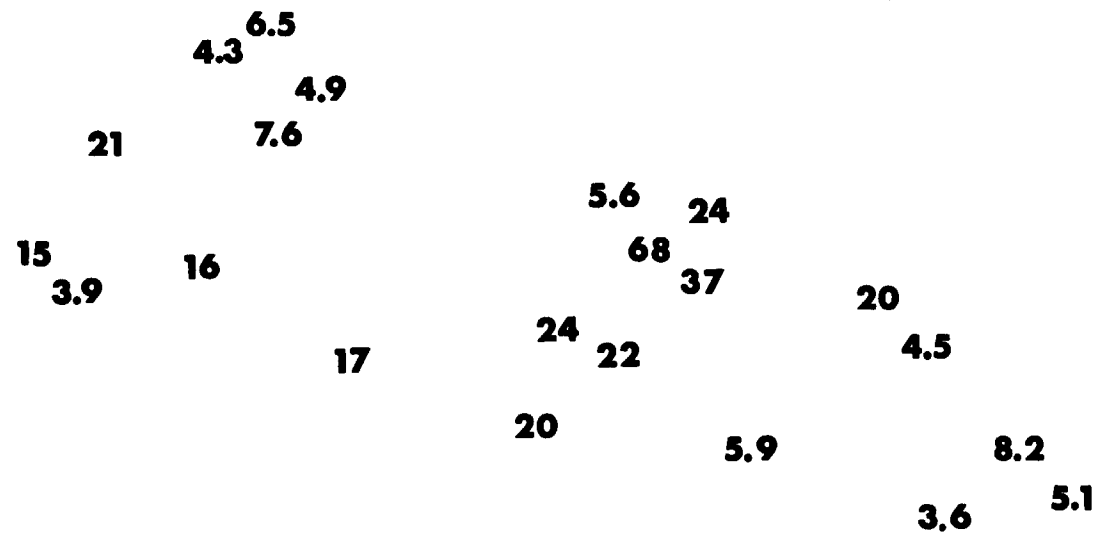


Fig. B.1.1.i. The average  $^{239}\text{Pu}$  activities (pCi/g) in soil samples collected to a depth of 15 cm.

100 METERS

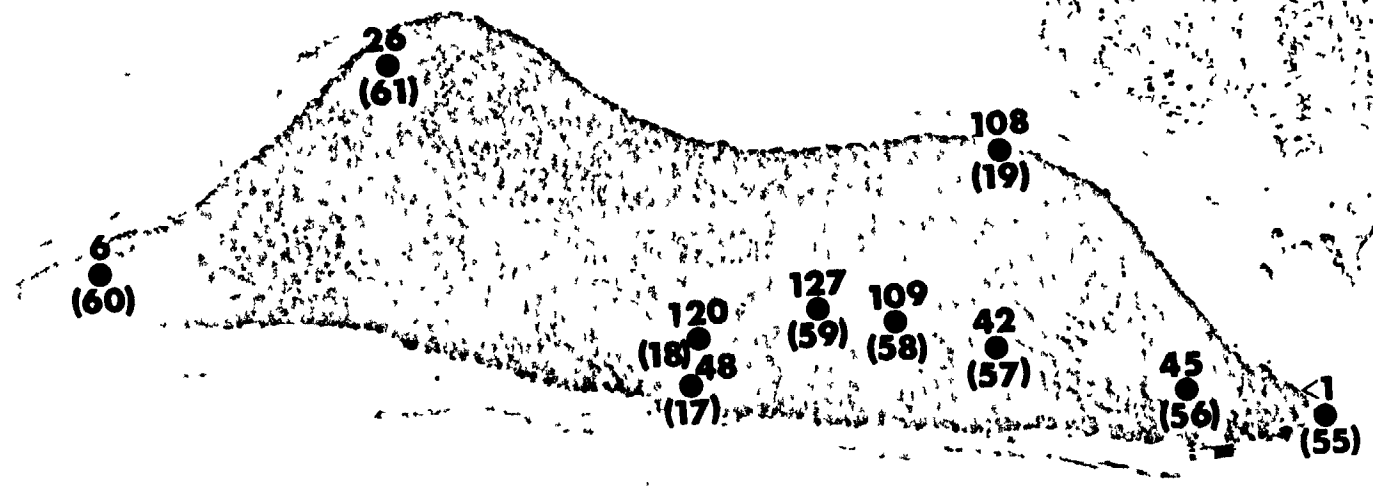
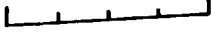


Fig. B.1.1.h. The gamma-ray exposure rates ( $\mu\text{R/hr}$ ) measured 1 m above the ground by [unclear] detectors (TLD). The numbers shown in parentheses denote [unclear]

100 METERS

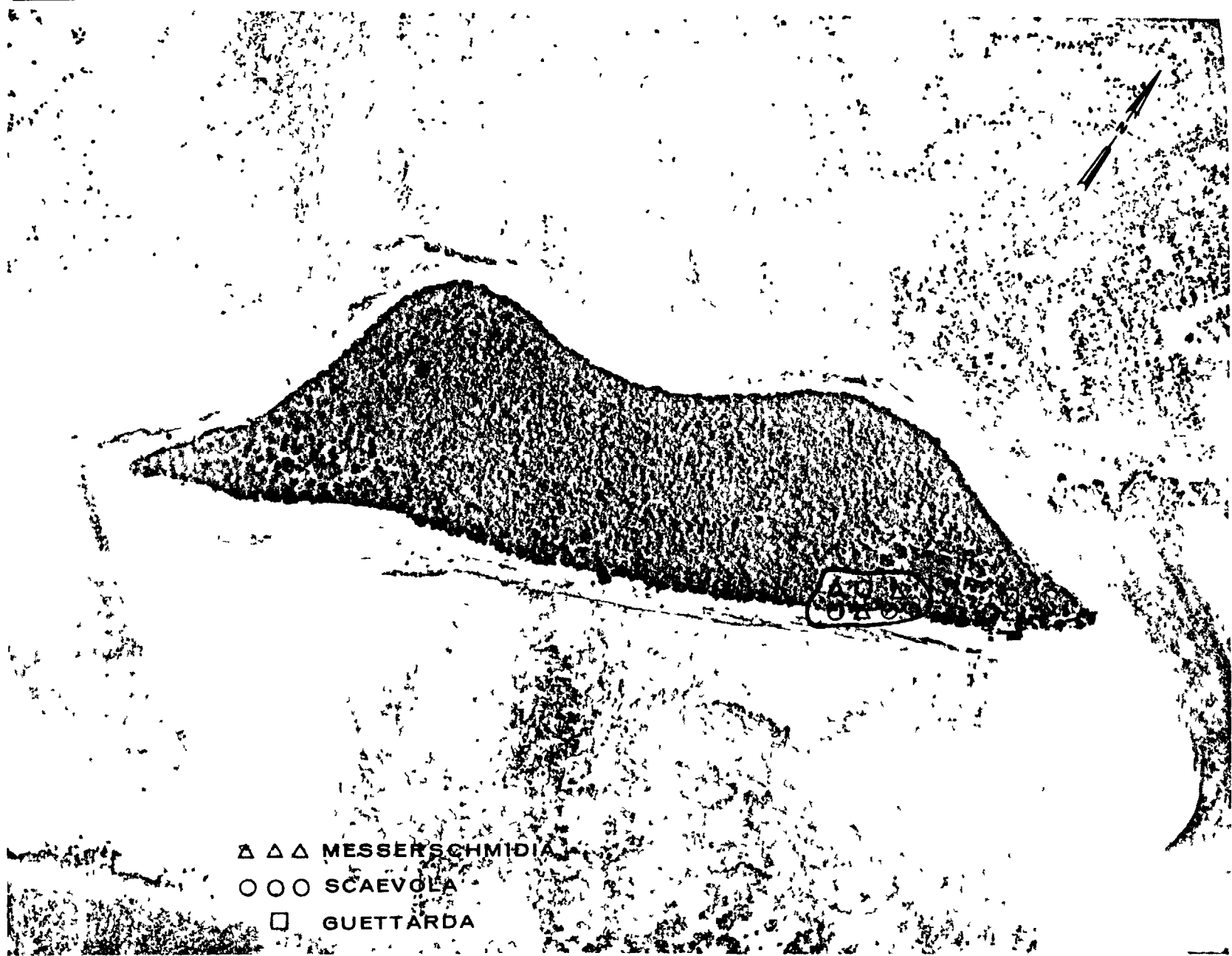
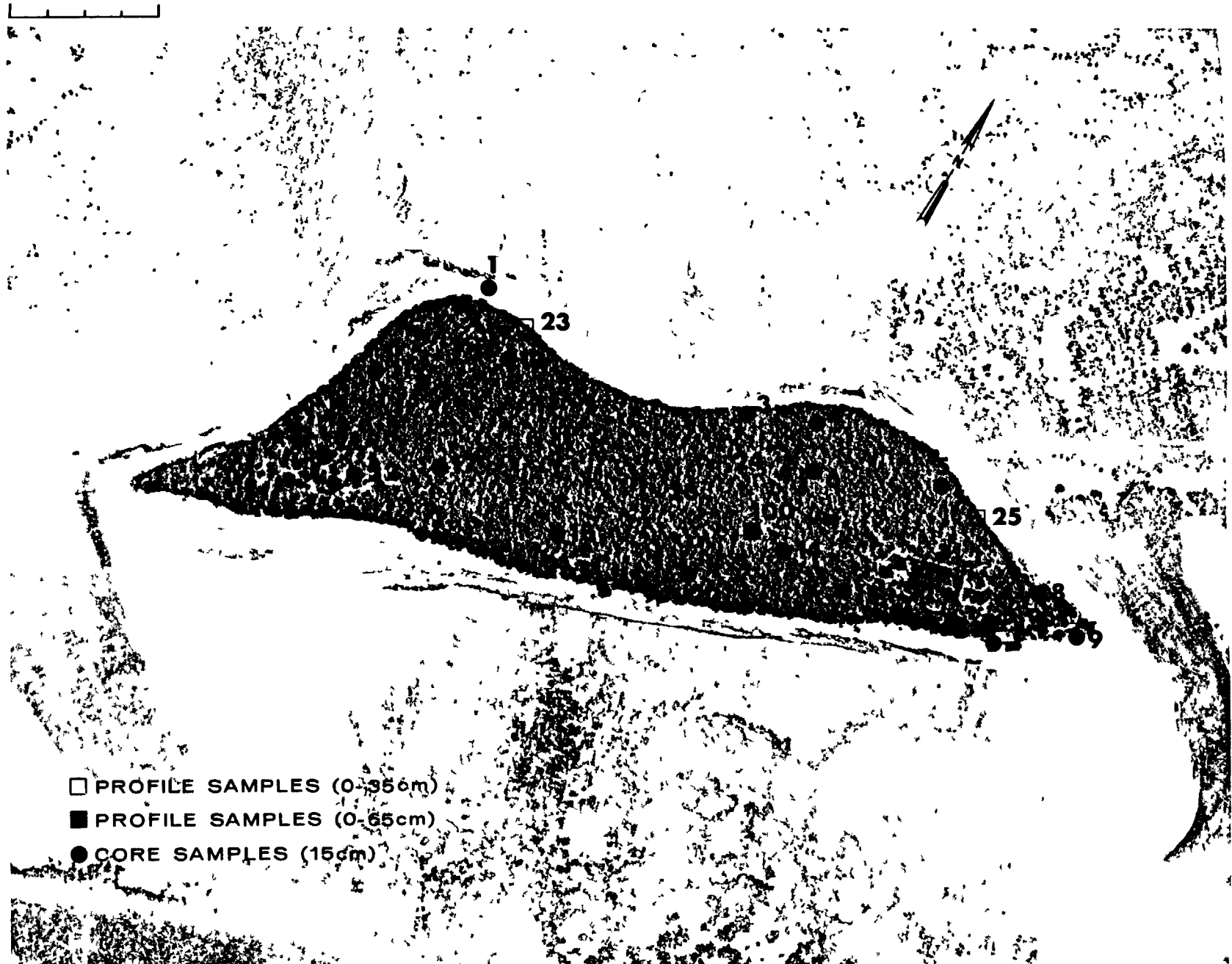


Fig. B.1.1.g. Vegetation sample locations.

100 METERS



□ PROFILE SAMPLES (0-35cm)

■ PROFILE SAMPLES (0-65cm)

● CORE SAMPLES (15cm)

Fig. B.1.1.f. Soil-sample locations.

100 METERS

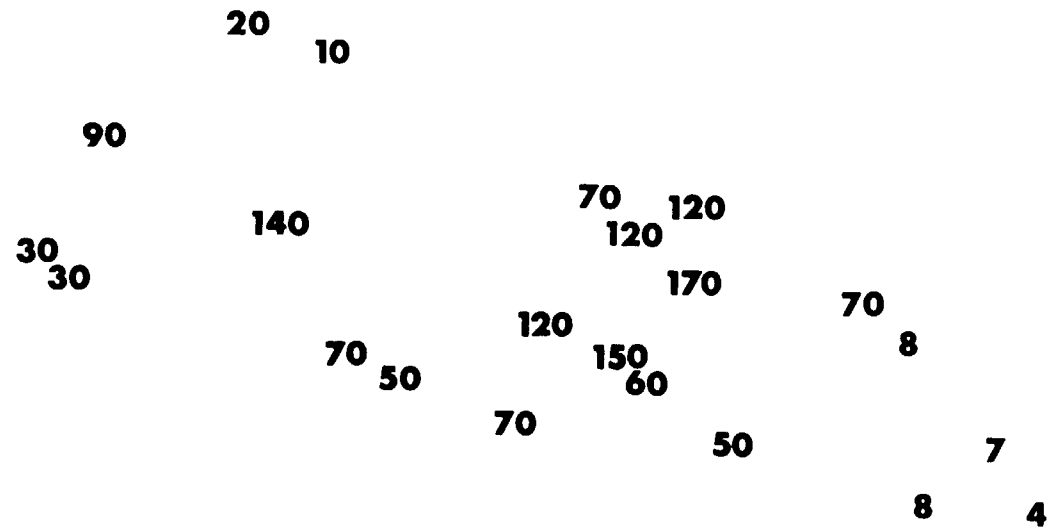


Fig. B.1.1.d. The gamma background exposure rate ( $\mu\text{R/hr}$ ) at 1 m above the ground, measured with a portable NaI scintillation counter.

100 METERS



Fig. B.1.1.b. Gross count isosexposure contours. (Refer to alphabetic symbol key in this appendix.)

100 METERS



Fig. B.1.1.a.

100 METERS

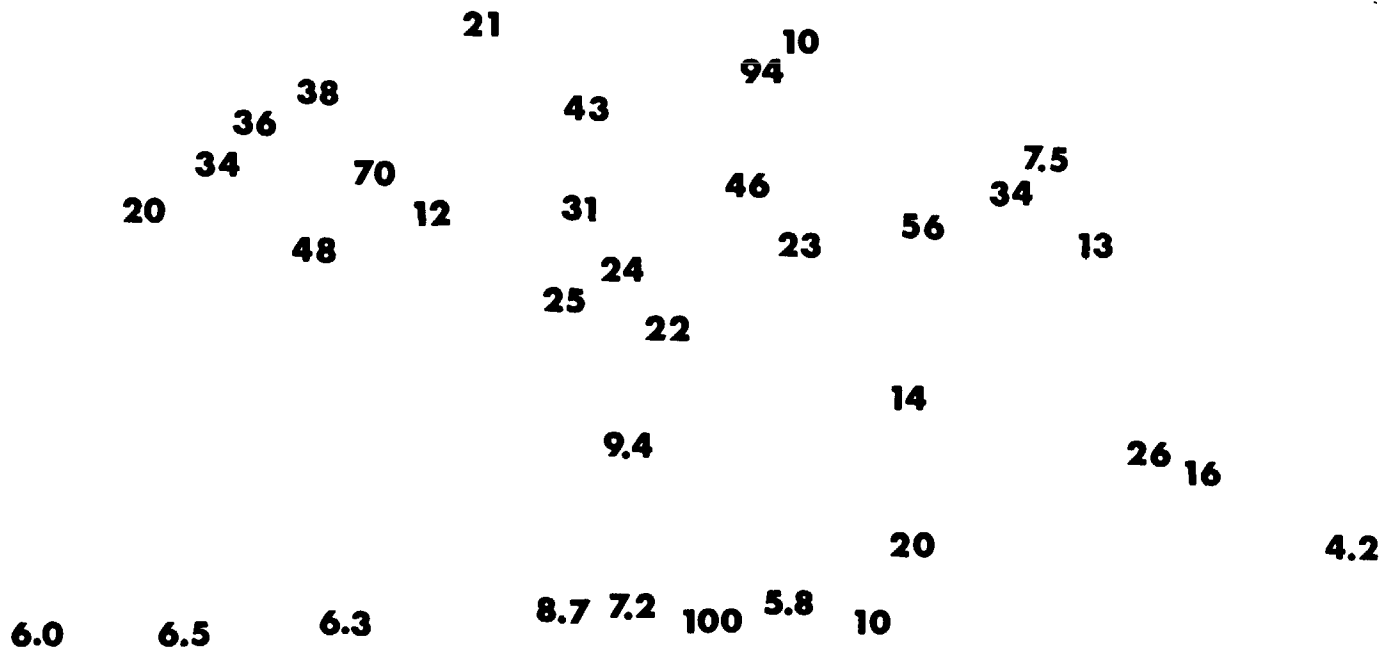


Fig. B.2.1.i. The average <sup>239</sup>Pu activities (pCi/g) in soil samples collected to a depth of 15 cm.



100 METERS

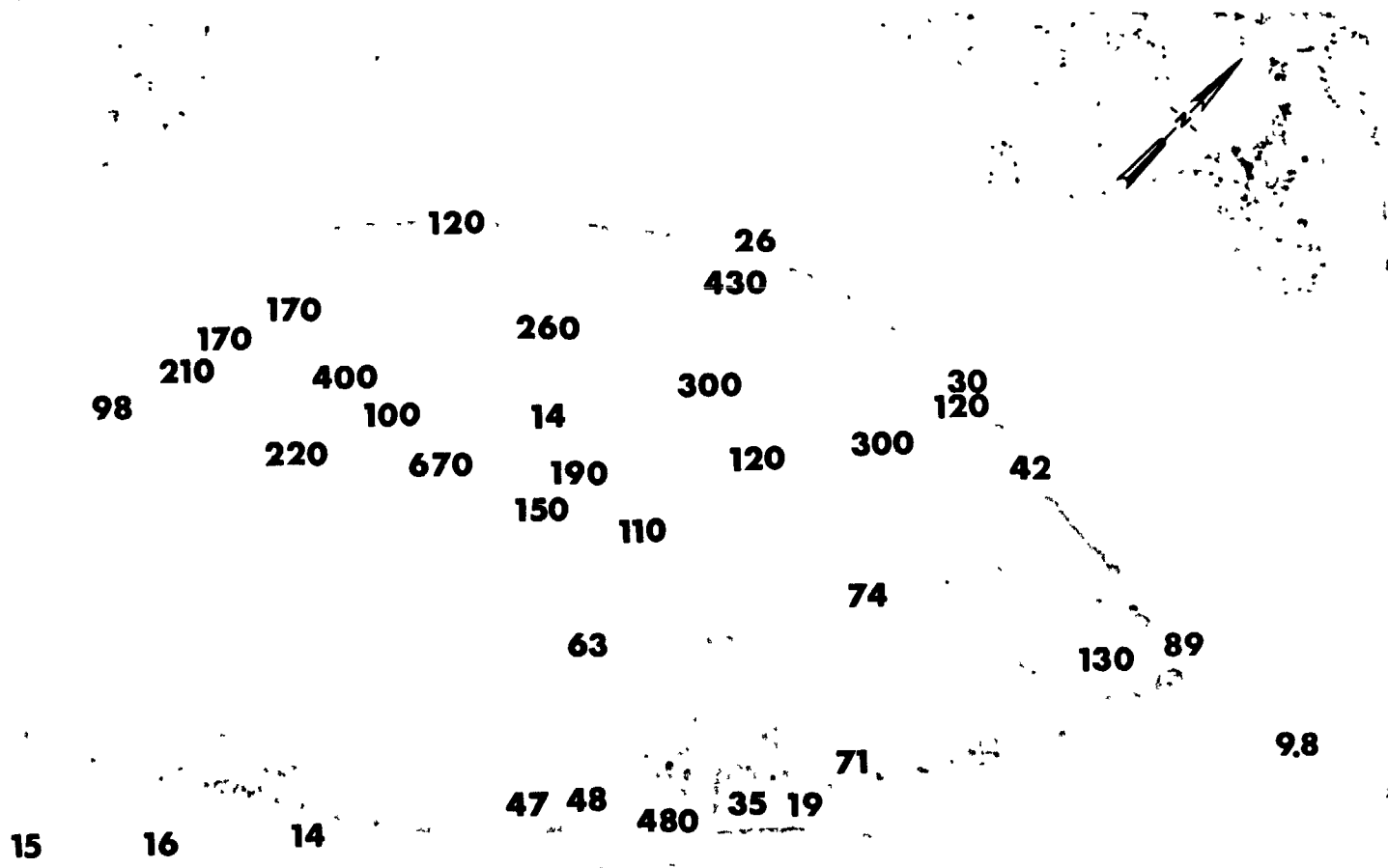


Fig. B.2.1.j. The average  $^{90}\text{Sr}$  activities (pCi/g) in soil samples collected to a depth of 15 cm.

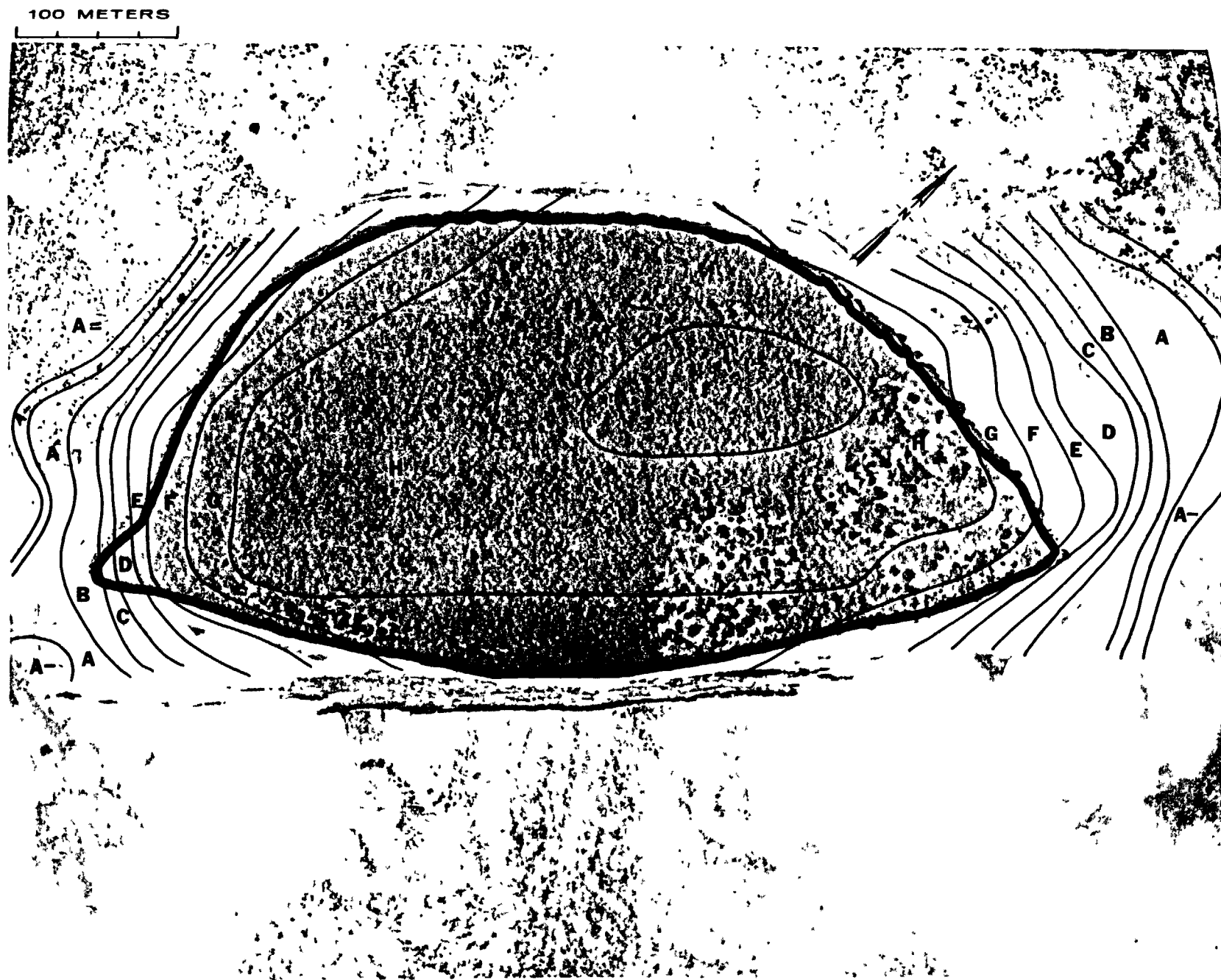


Fig. B.2.1.k.  $^{137}\text{Cs}$  isoexposure and isoconcentration contours. (Refer to alphabetic symbol key in this appendix.)

100 METERS

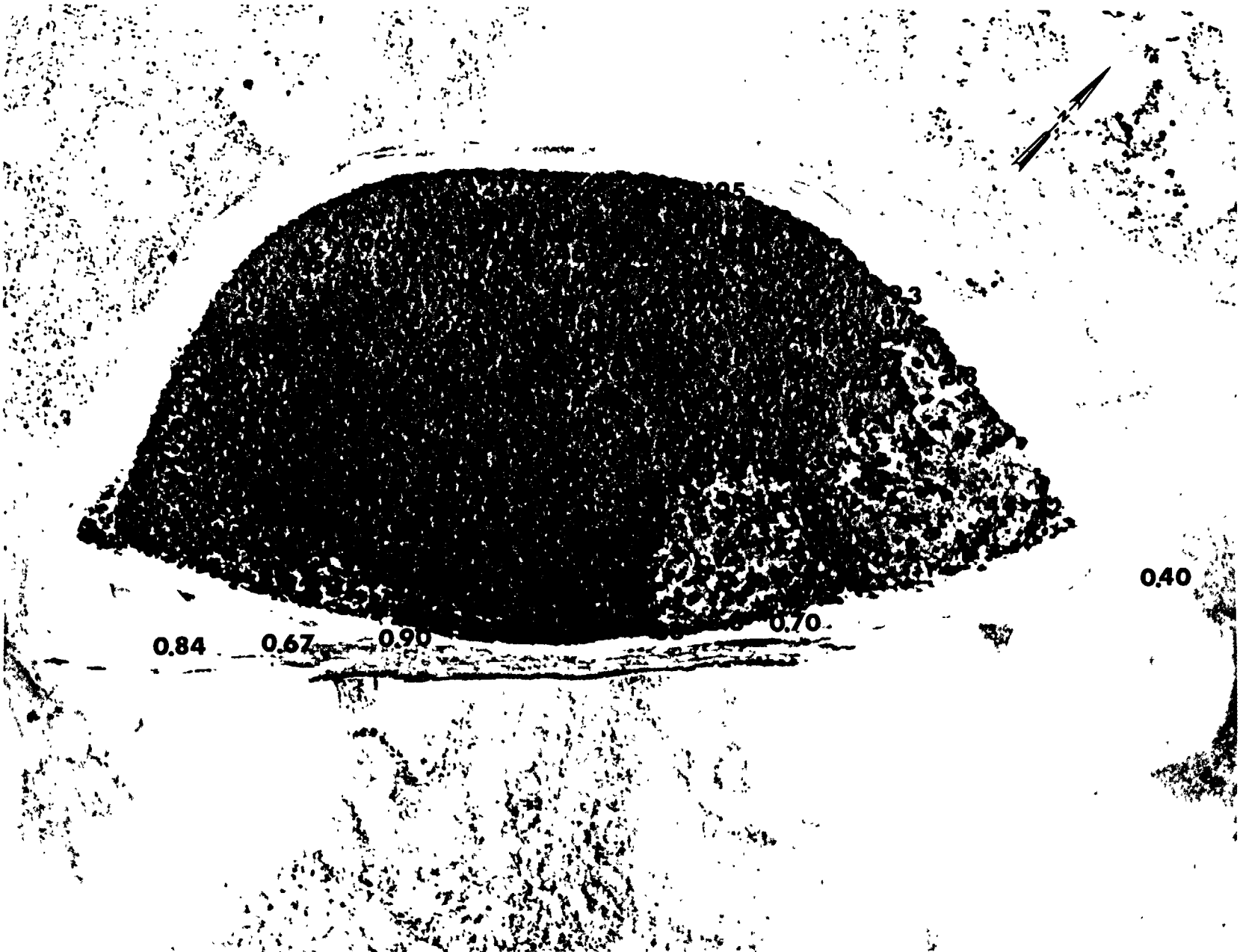


Fig. B.2.1.1. The average  $^{137}\text{Cs}$  activities (pCi/g) in soil samples collected to a depth of 15 cm.

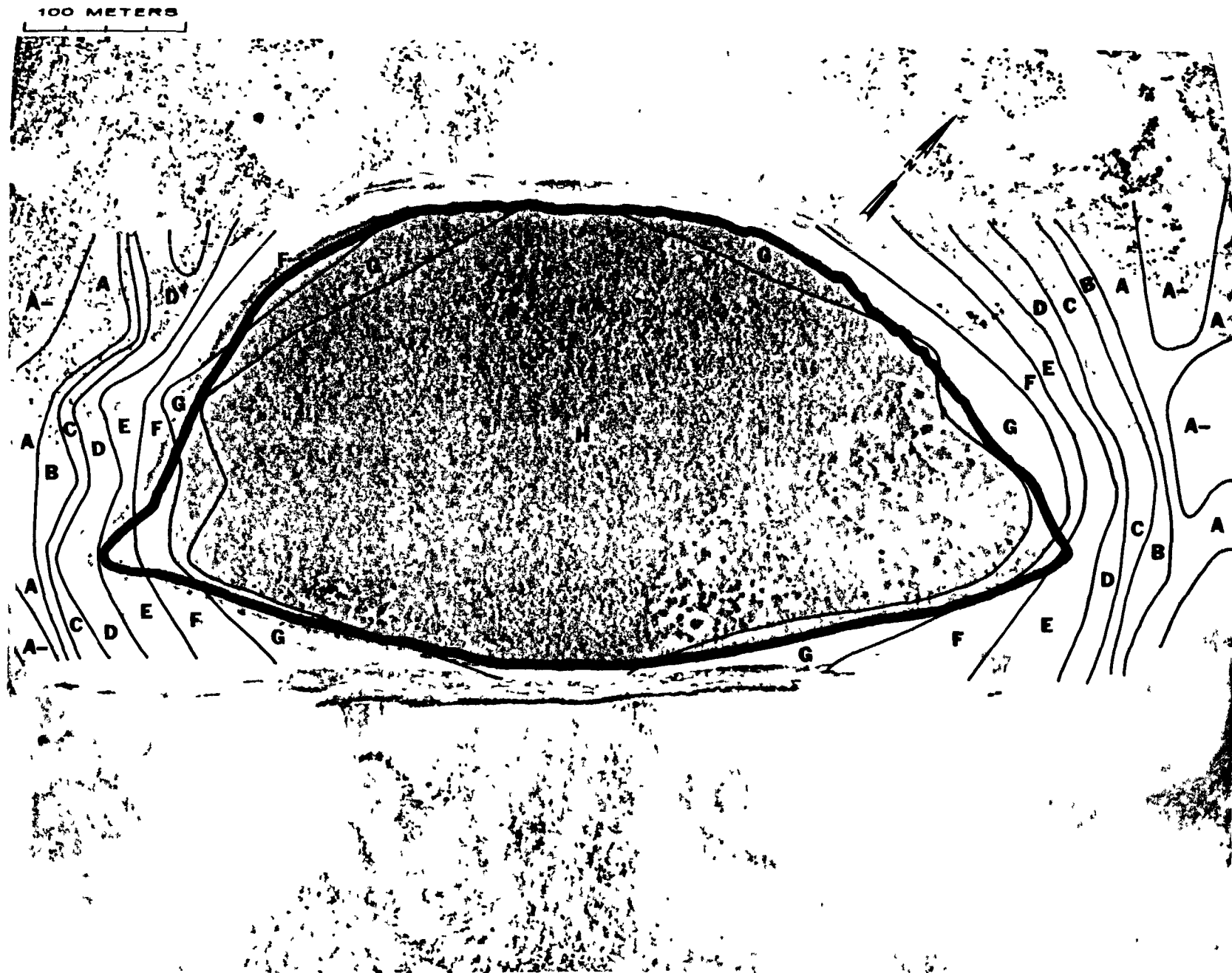


Fig. B.2.1.m.  $^{60}\text{Co}$  isoexposure and isoconcentration contours. (Refer to alphabetic symbol key in this appendix.)

100 METERS

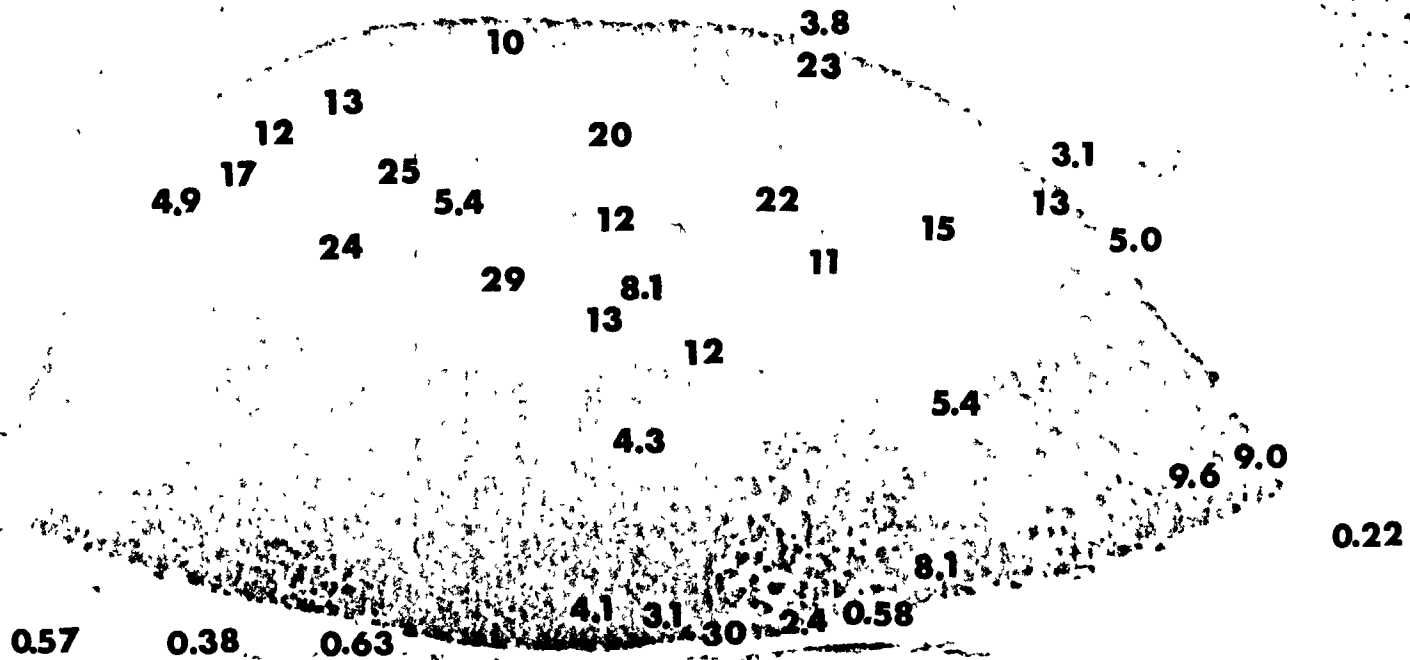


Fig. B.2.1.n. The average  $^{60}\text{Co}$  activities (pCi/g) in soil samples collected to a depth of 15 cm.

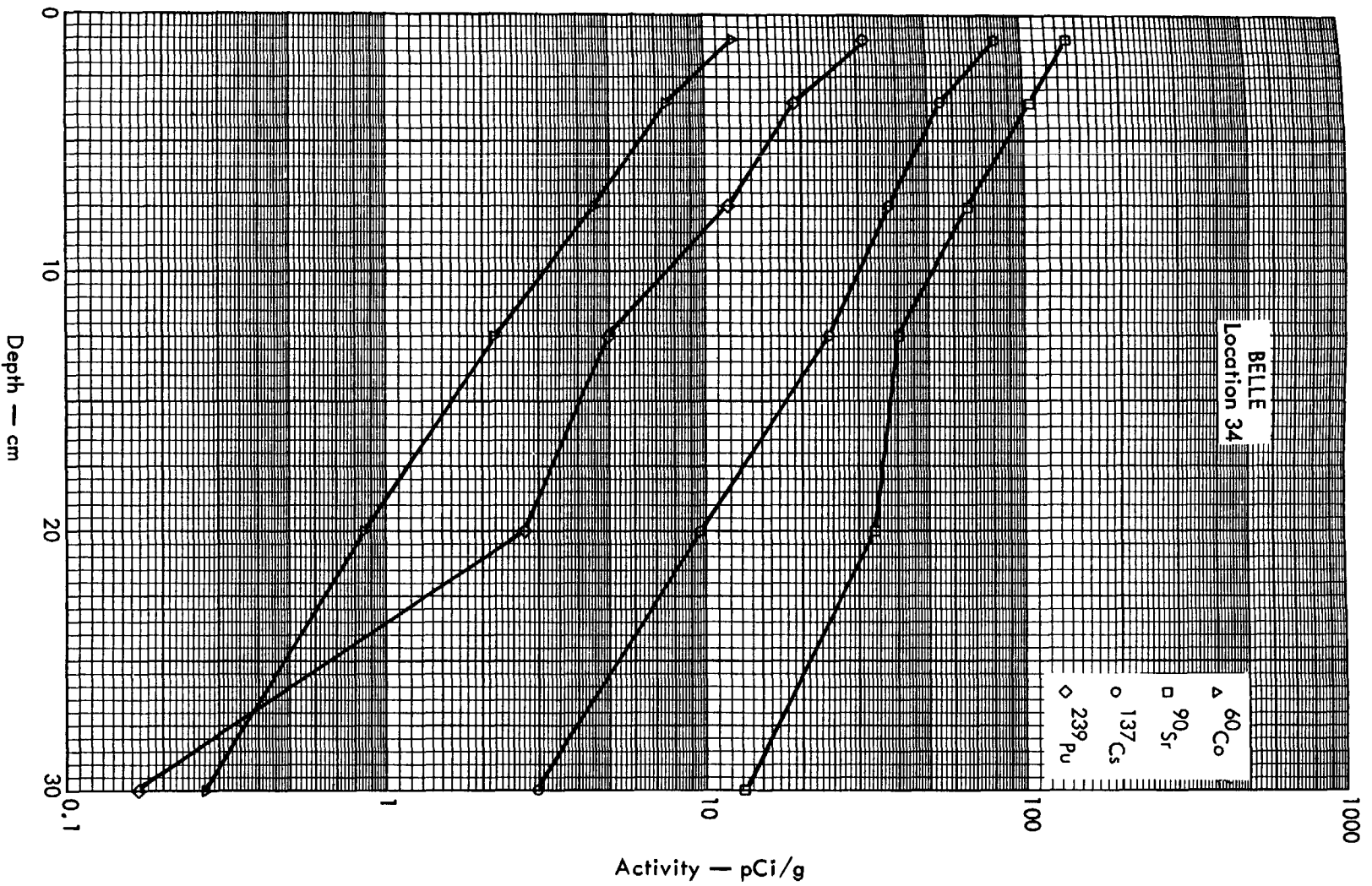


Fig. B. 2. 2a. Activities of selected radionuclides as a function of soil depth.

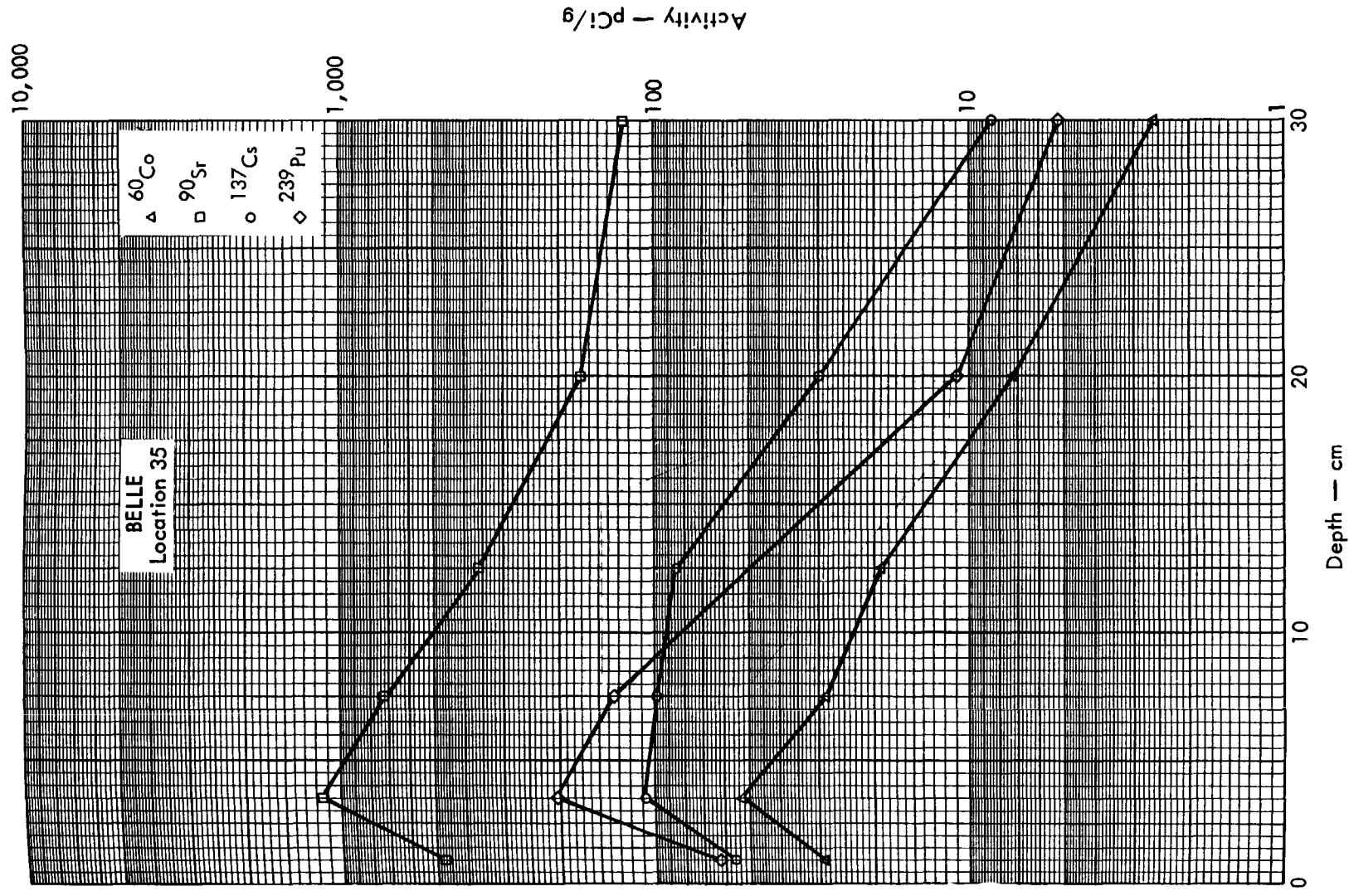


Fig. B.2.2b. Activities of selected radionuclides as a function of soil depth.

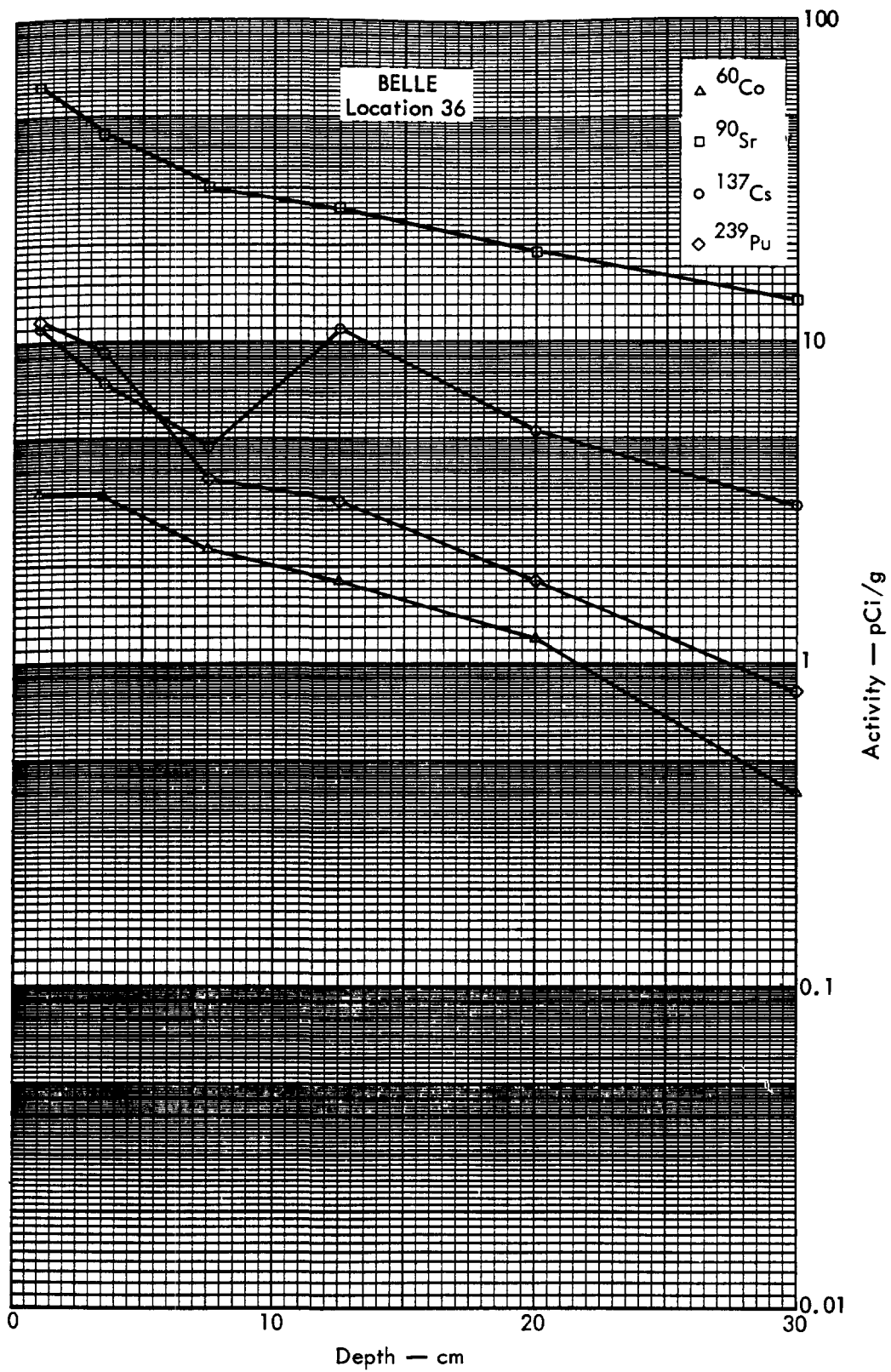


Fig. B.2.2c. Activities of selected radionuclides as a function of soil depth.



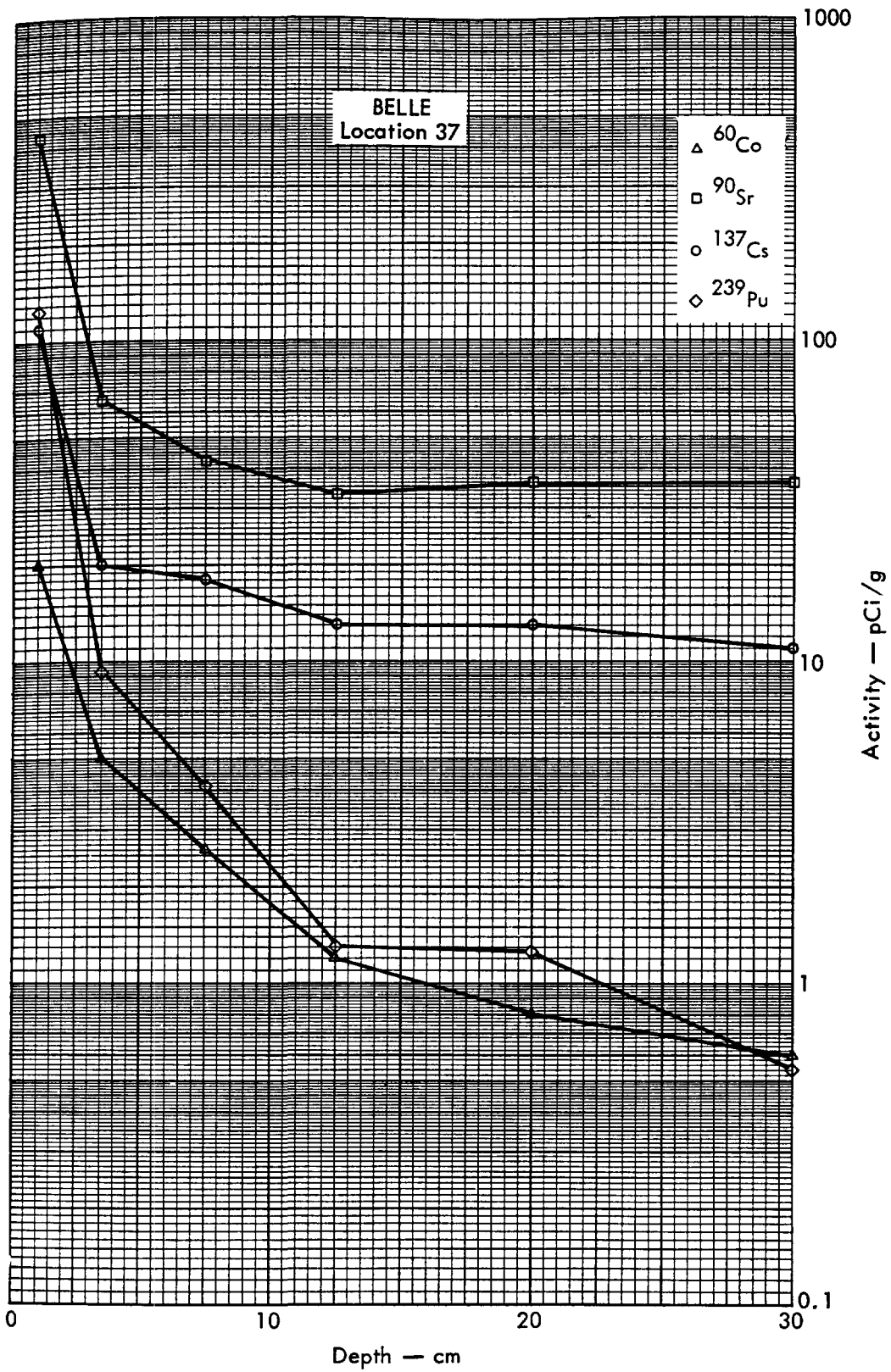


Fig. B. 2. 2d. Activities of selected radionuclides as a function of soil depth.

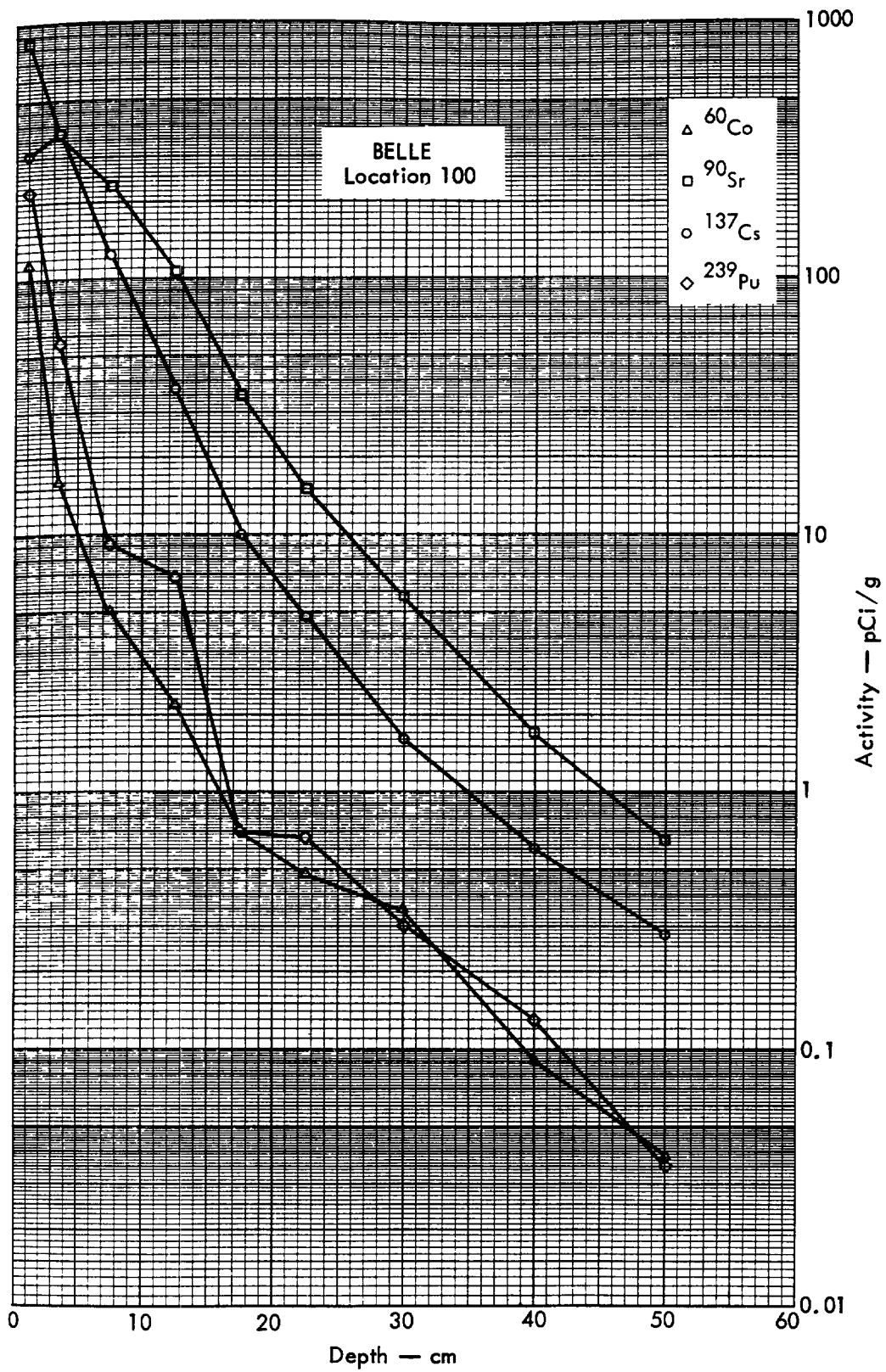


Fig. B.2.2e. Activities of selected radionuclides as a function of soil depth.

100 METERS



Fig. B.3.1.a.

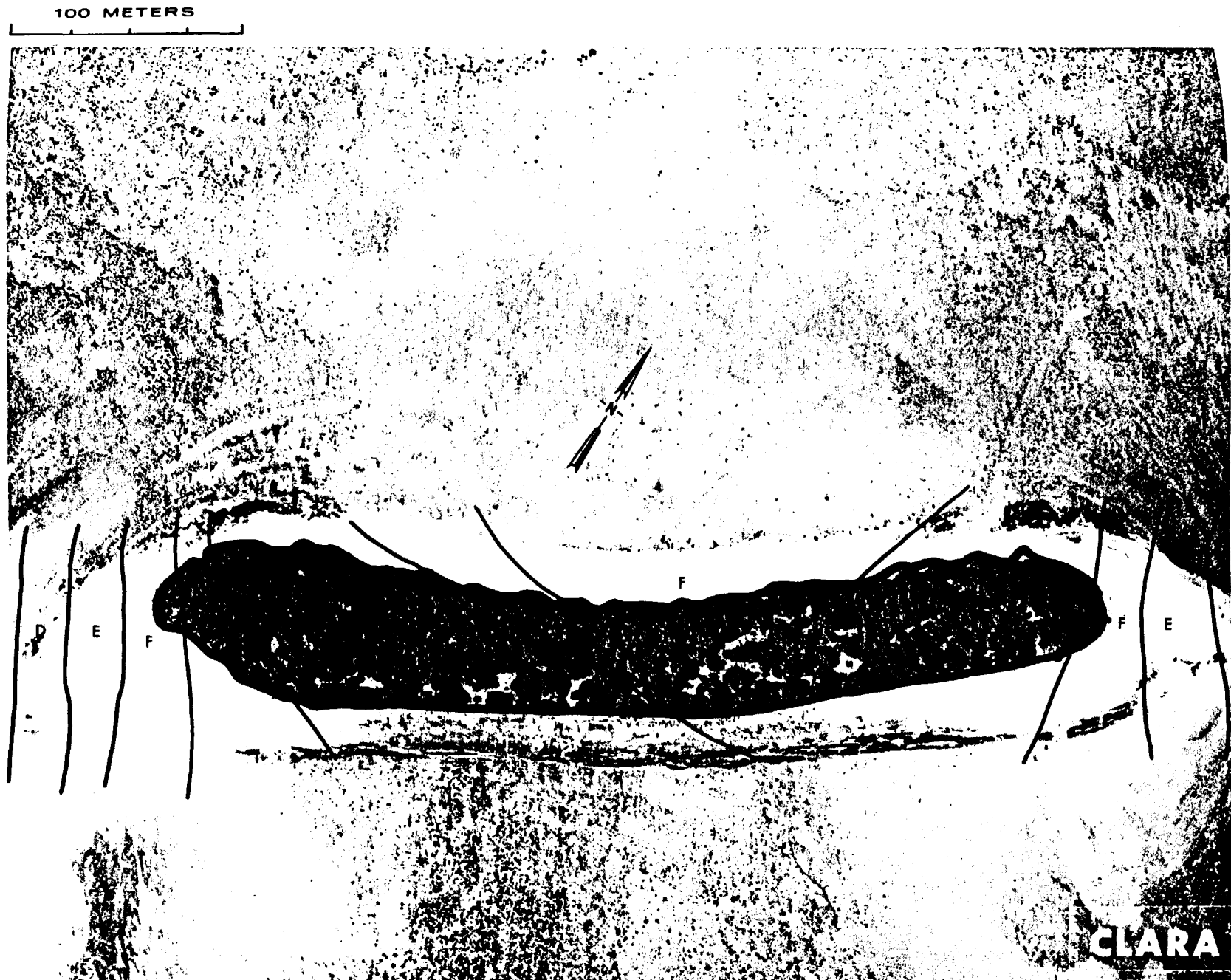


Fig. B.3.1.b. Gross count isosexposure contours. (Refer to alphabetic symbol key in this appendix.)

100 METERS

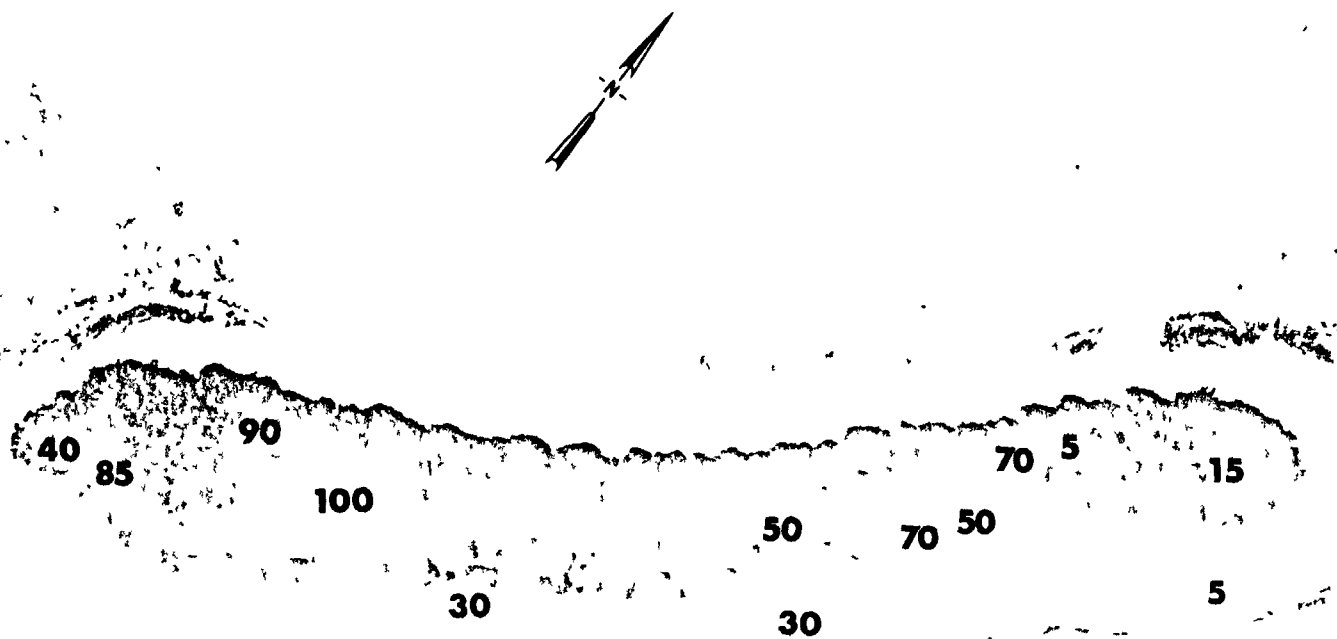


Fig. B.3.1.d. The gamma background exposure rate ( $\mu\text{R/hr}$ ) at 1 m above the ground, measured with a portable NaI scintillation counter.

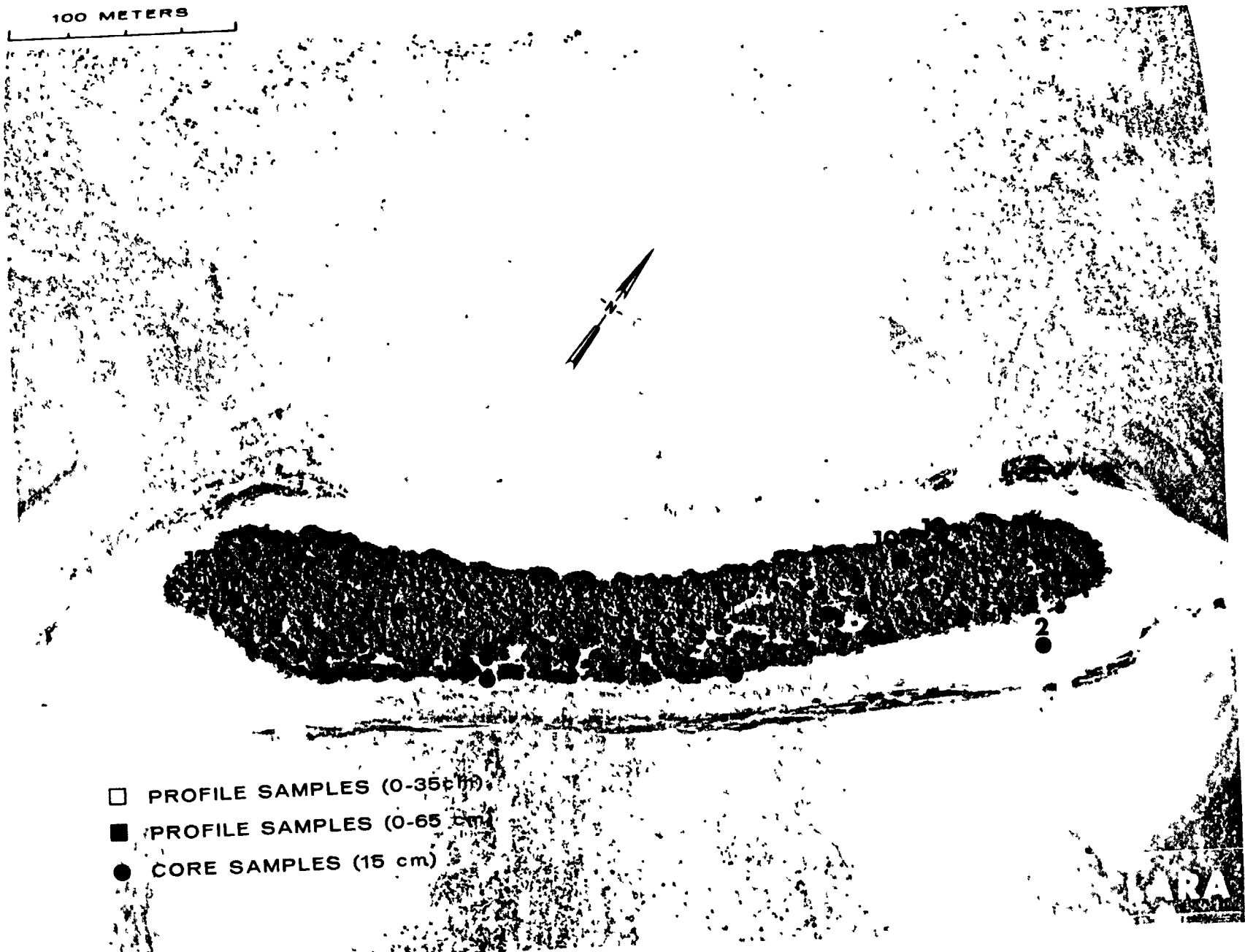


Fig. B.3.1.f. Soil-sample locations.

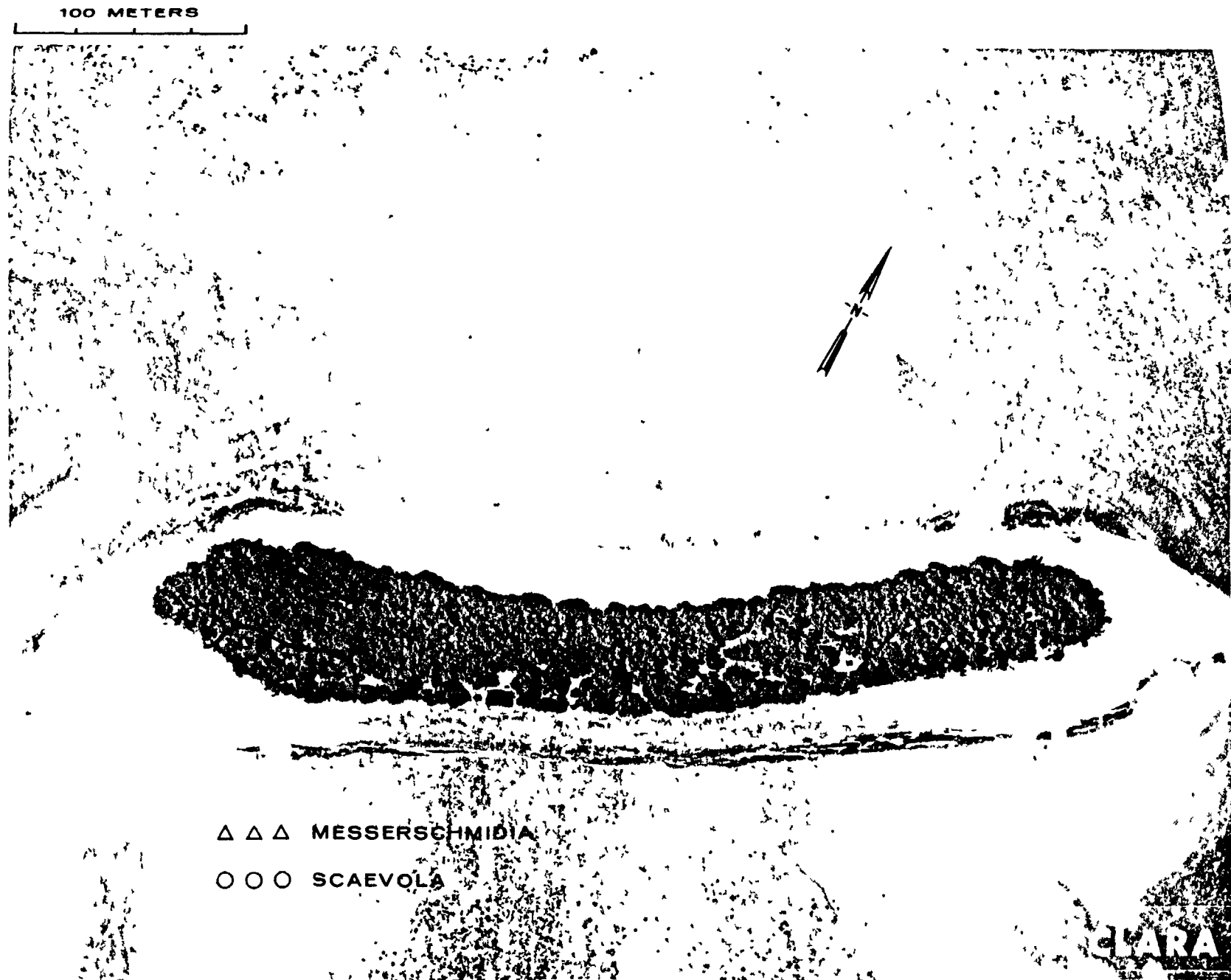


Fig. B.3.1.g. Vegetation sample locations.

100 METERS



Fig. B.3.1.h. The gamma-ray exposure rates ( $\mu\text{R/hr}$ ) measured 1 m above the ground by the LiF thermoluminescent dosimeters (TLD). The numbers shown in parentheses denote the location identification numbers.



100 METERS

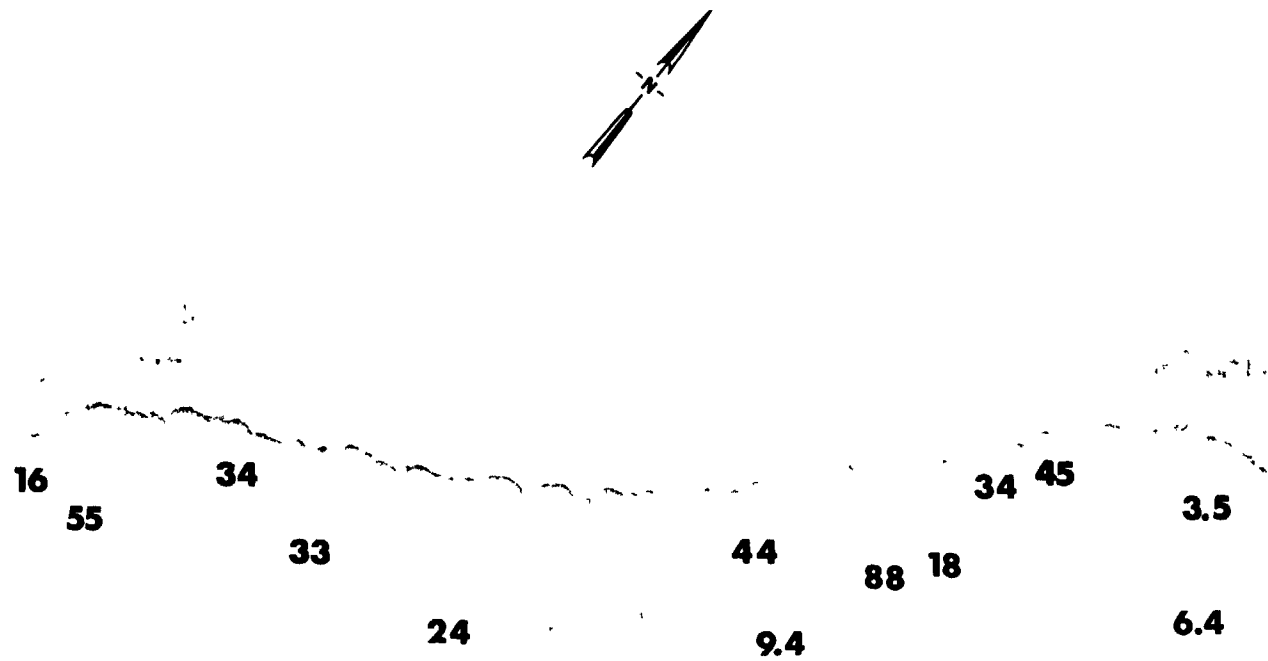


Fig. B.3.1.i. The average <sup>239</sup>Pu activities (pCi/g) in soil samples collected to a depth of 15 cm.



Fig. B.3.1.j. The average  $^{90}\text{Sr}$  activities (pCi/g) in soil samples collected to a depth of 15 cm.

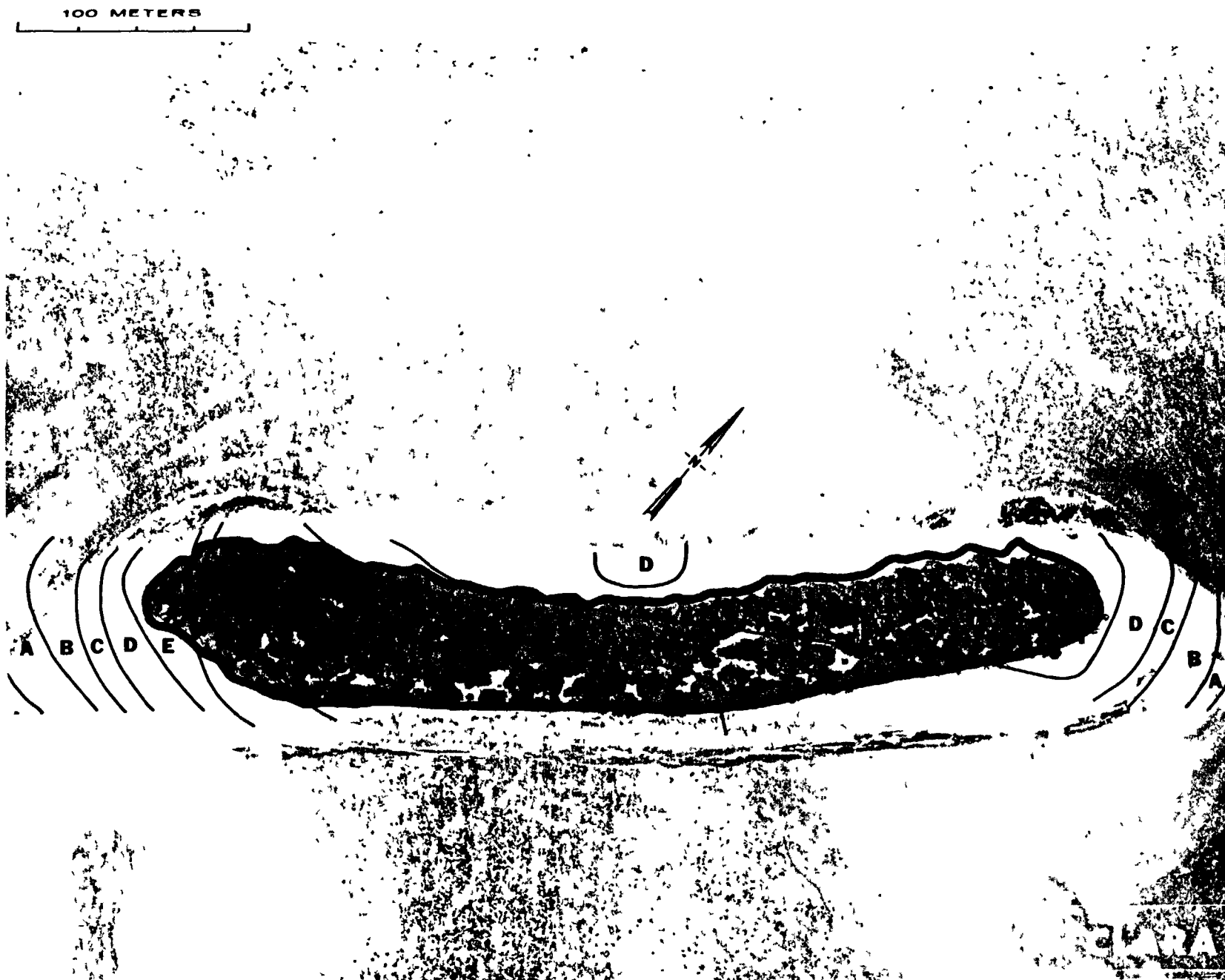


Fig. B.3.1.k. <sup>137</sup>Cs isoexposure and isoconcentration contours. (Refer to alphabetic symbol key in this appendix.)

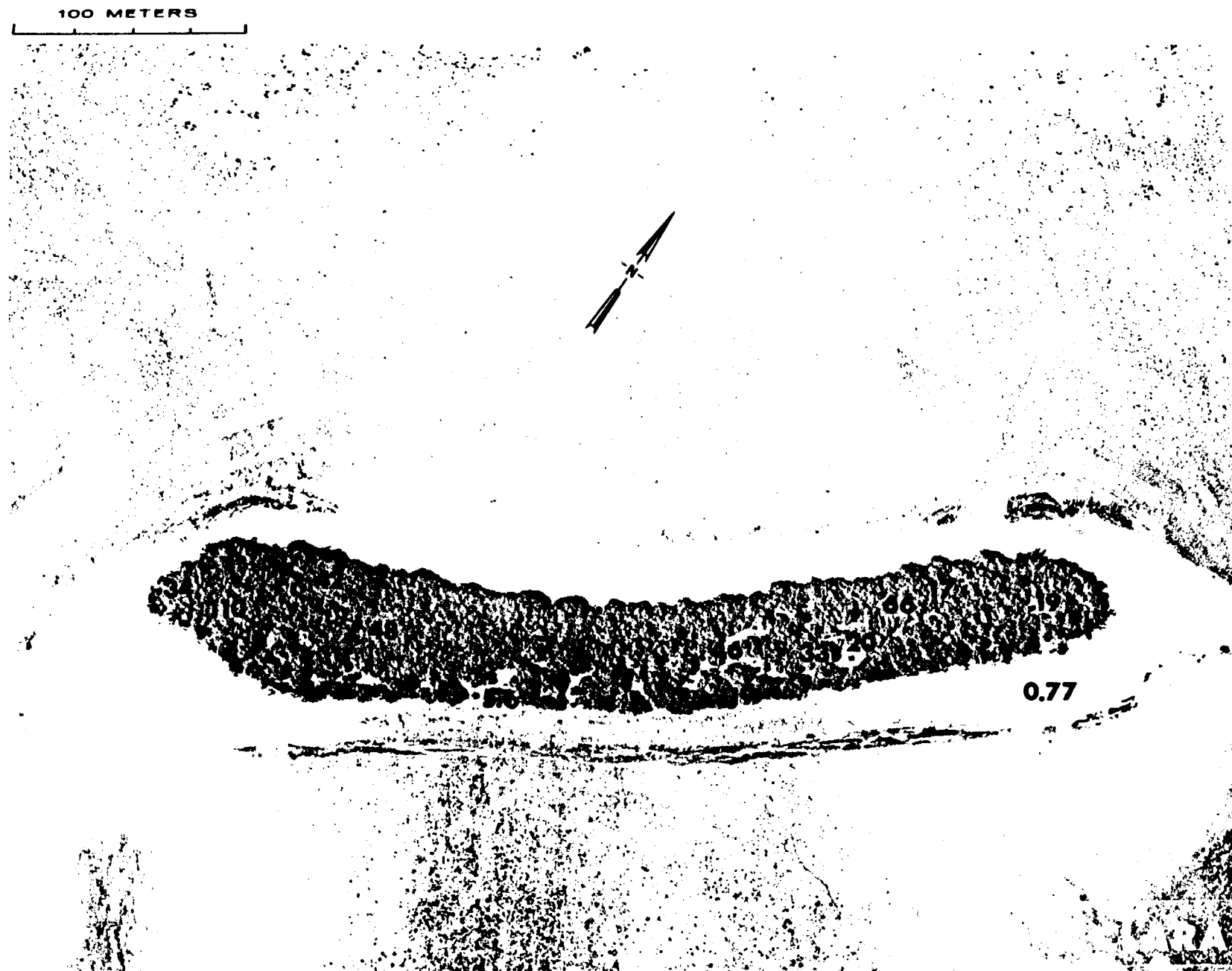


Fig. B.3.1.1. The average  $^{137}\text{Cs}$  activities (pCi/g) in soil samples collected to a depth of 15 cm.

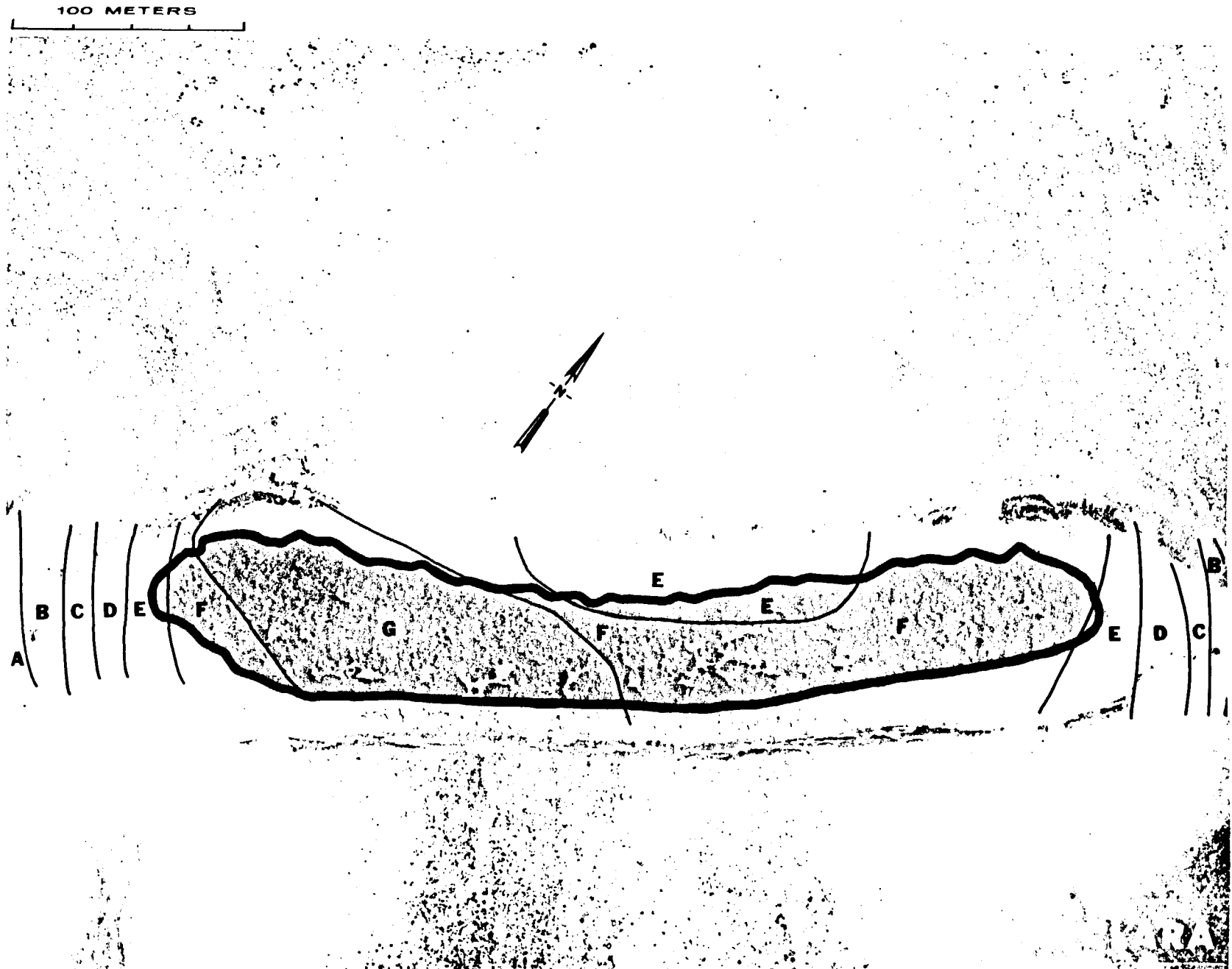


Fig. B.3.1.m. <sup>60</sup>Co isosexposure and isoconcentration contours. (Refer to alphabetic symbol key in this appendix.)

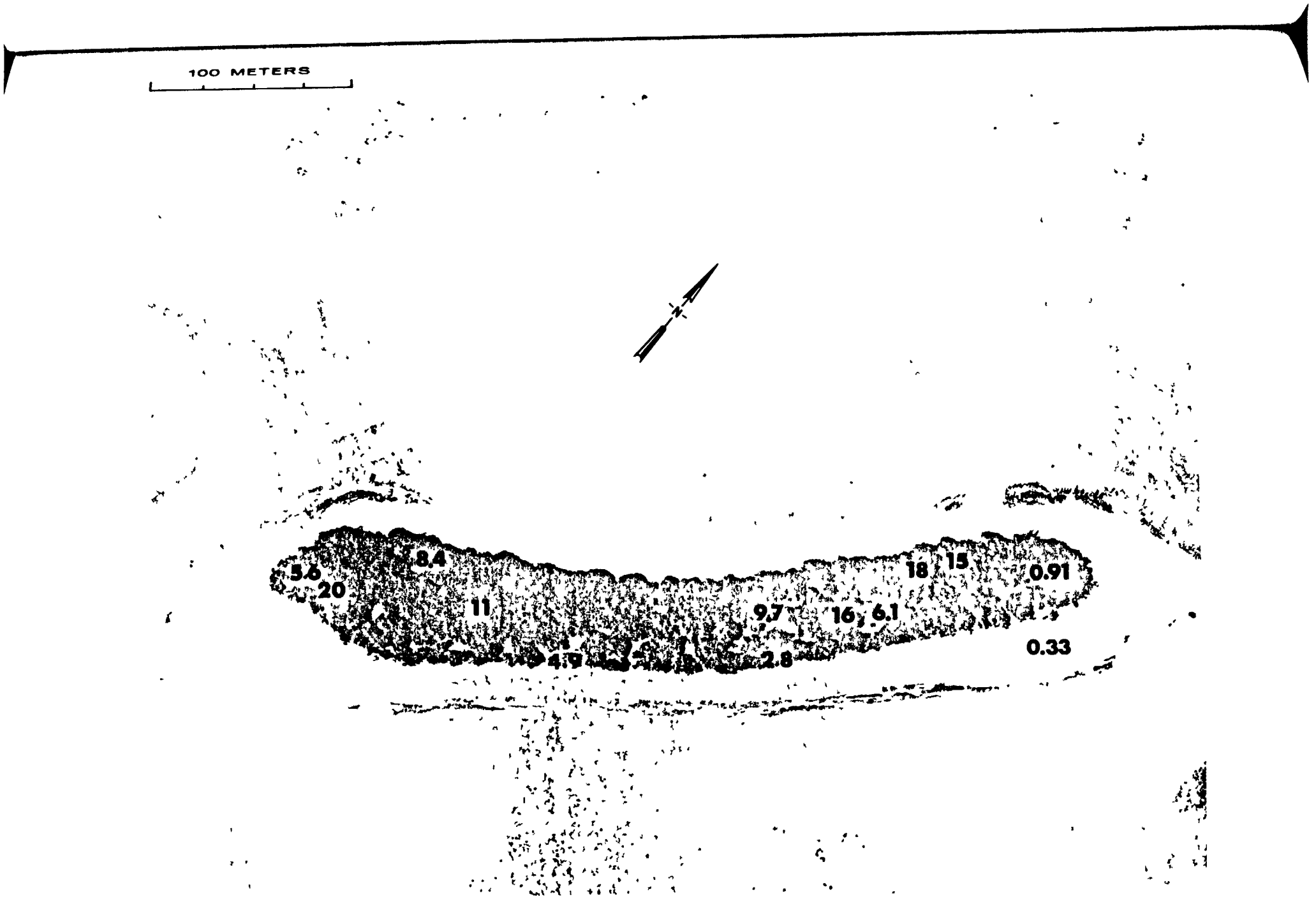


Fig. B.3.1.n. The average  $^{60}\text{Co}$  activities (pCi/g) in soil samples collected to a depth of 15 cm.

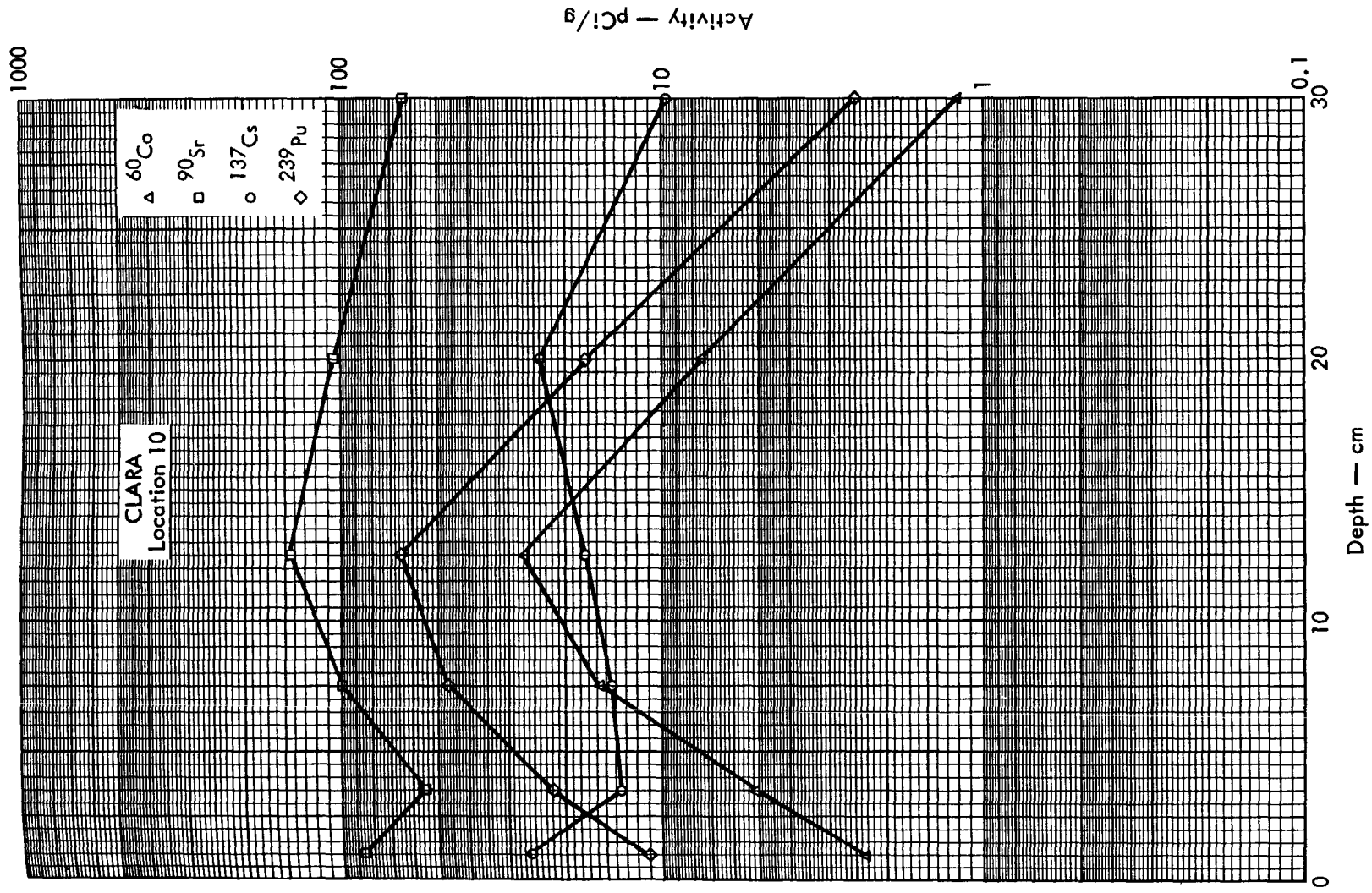


Fig. B. 3. 2a. Activities of selected radionuclides as a function of soil depth.

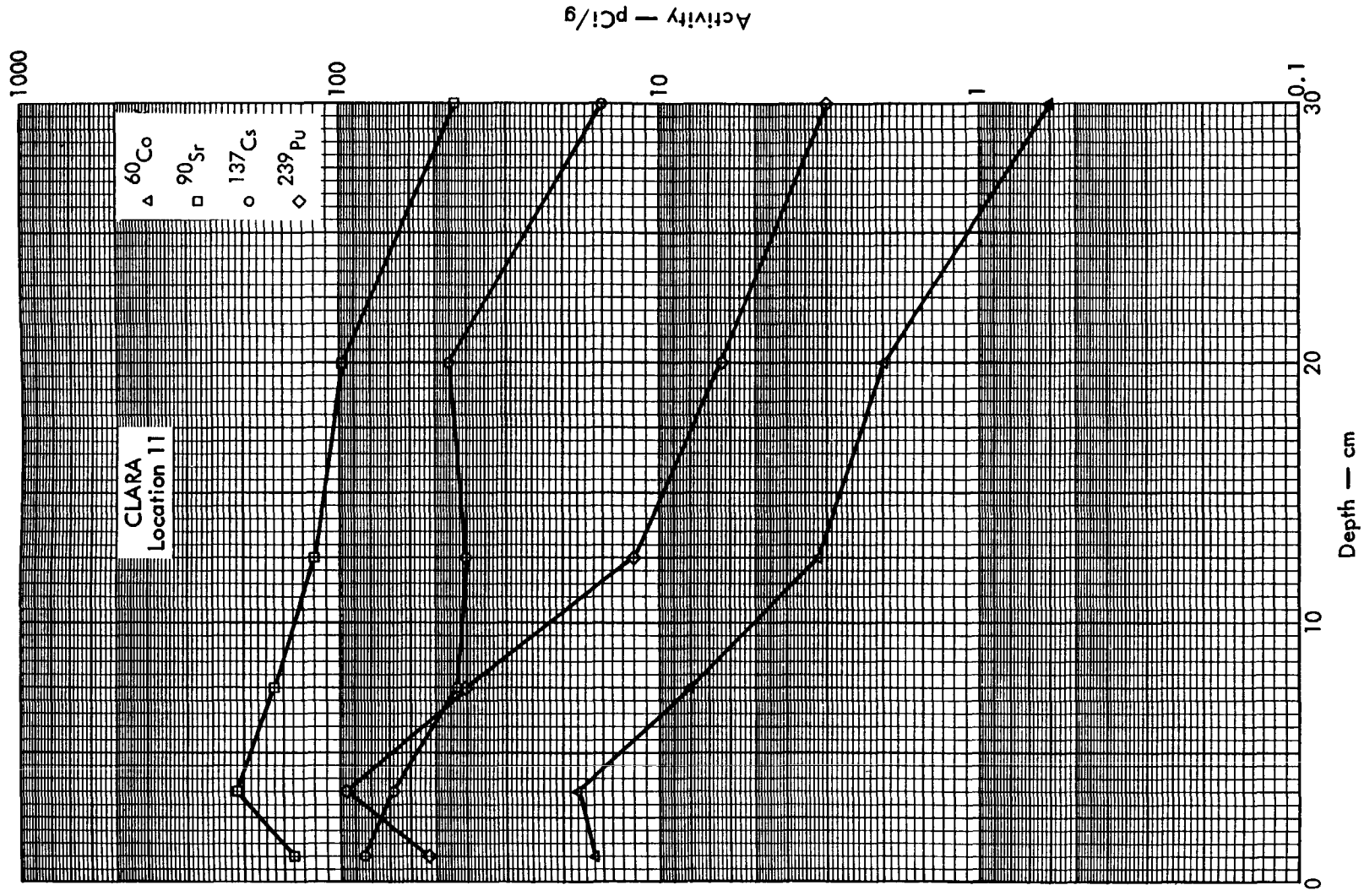


Fig. B. 3. 2b. Activities of selected radionuclides as a function of soil depth.



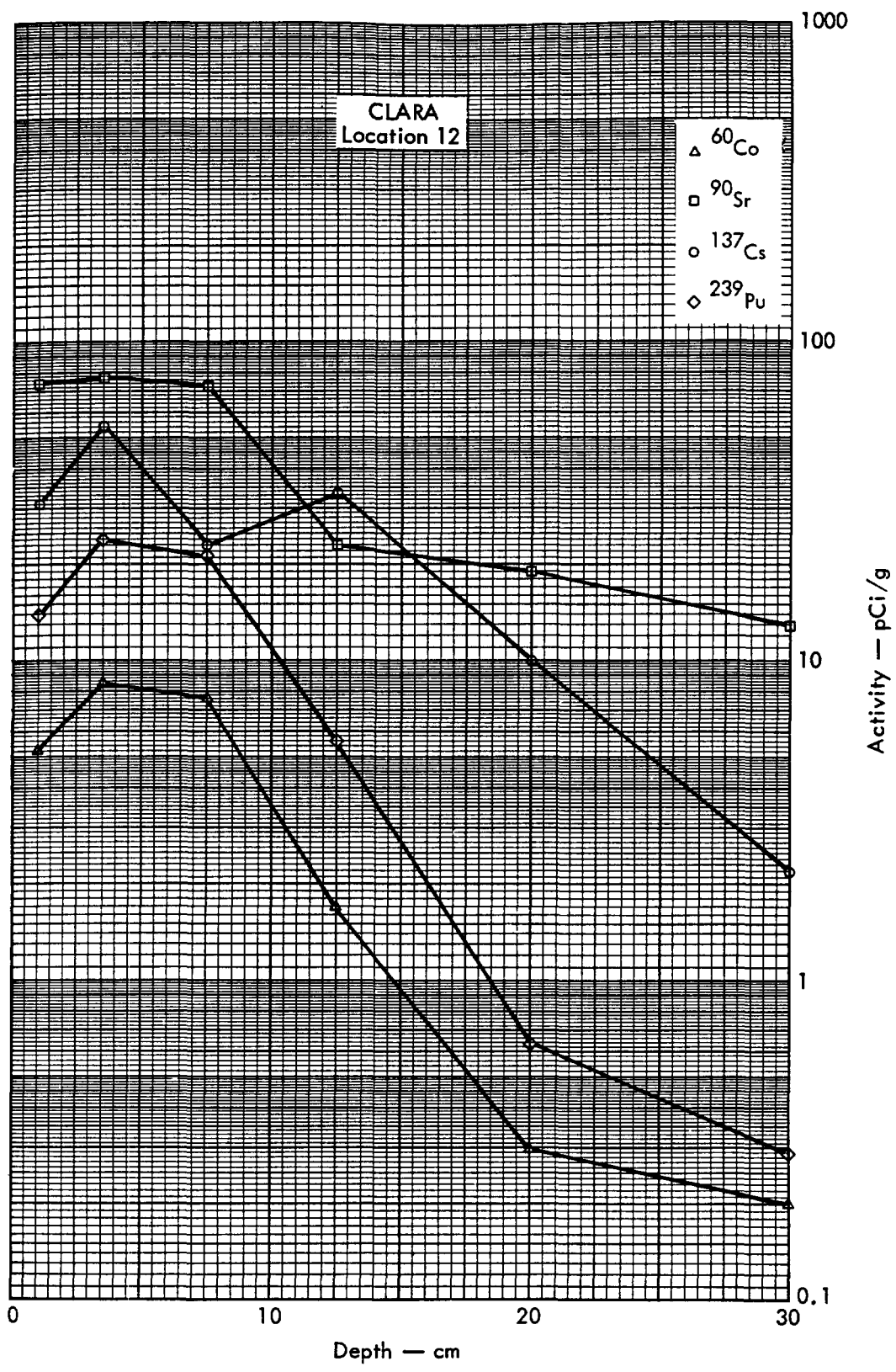


Fig. B.3.2c. Activities of selected radionuclides as a function of soil depth.

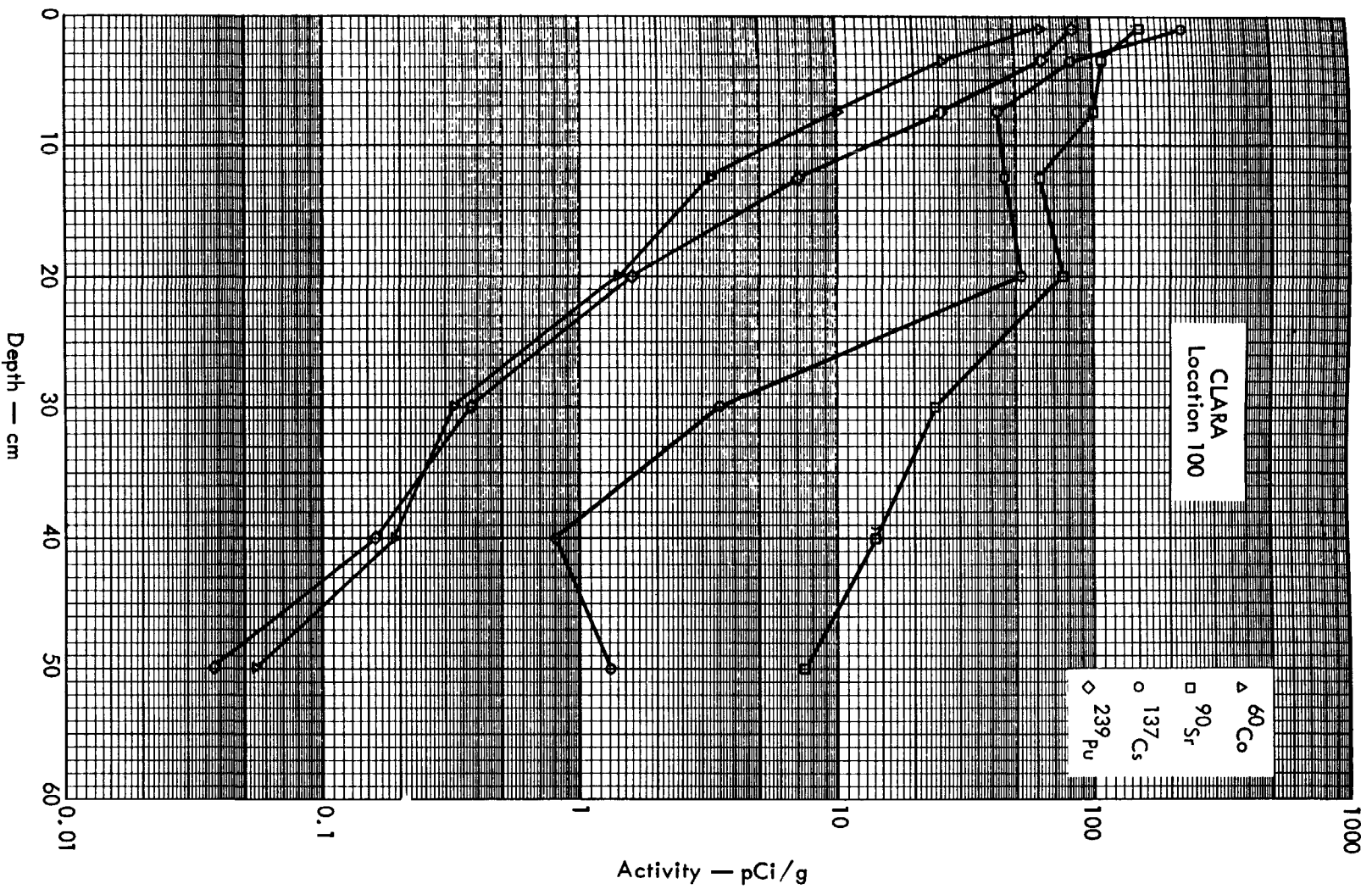


Fig. B. 3. 2d. Activities of selected radionuclides as a function of soil depth.

100 METERS

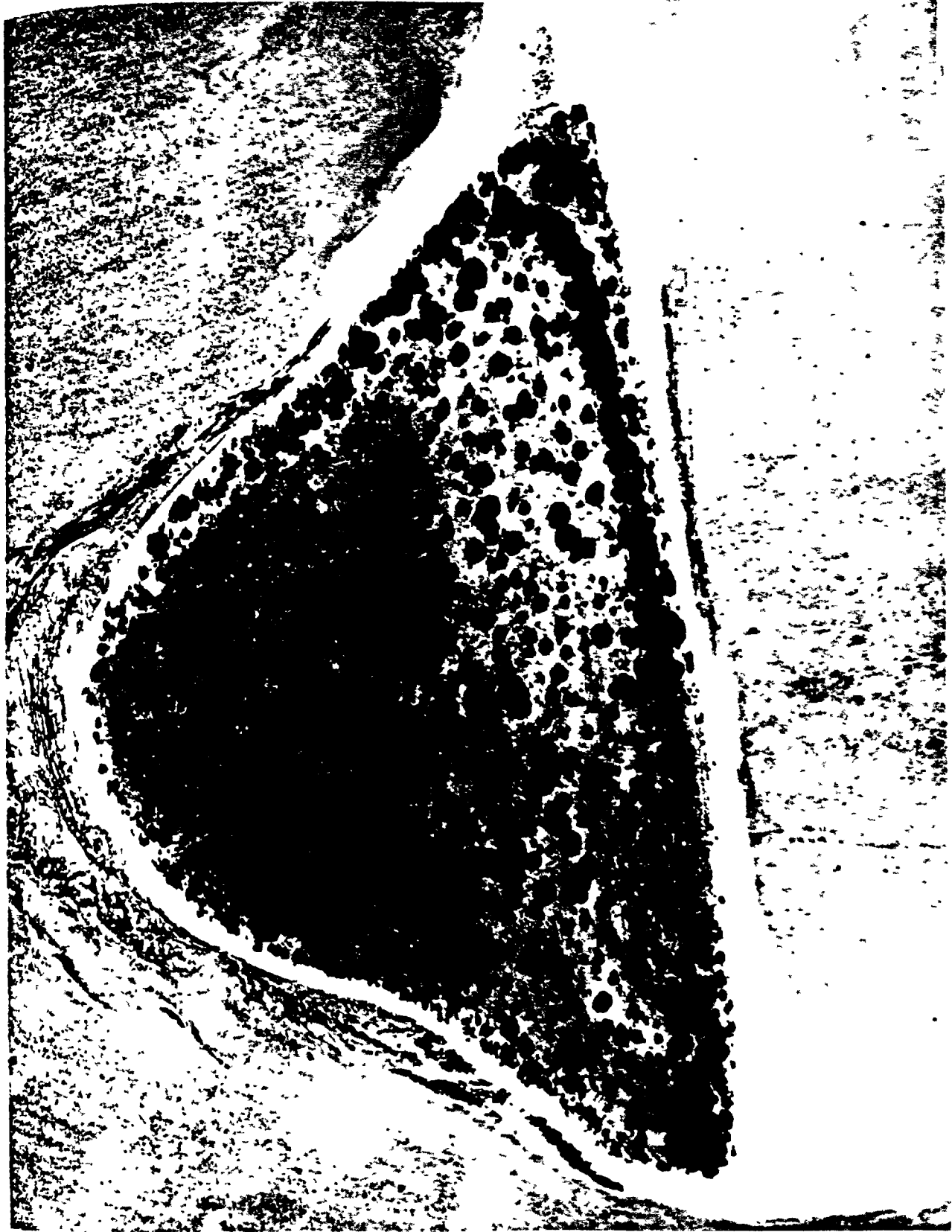


FIG. B.4.1.a.

100 METERS

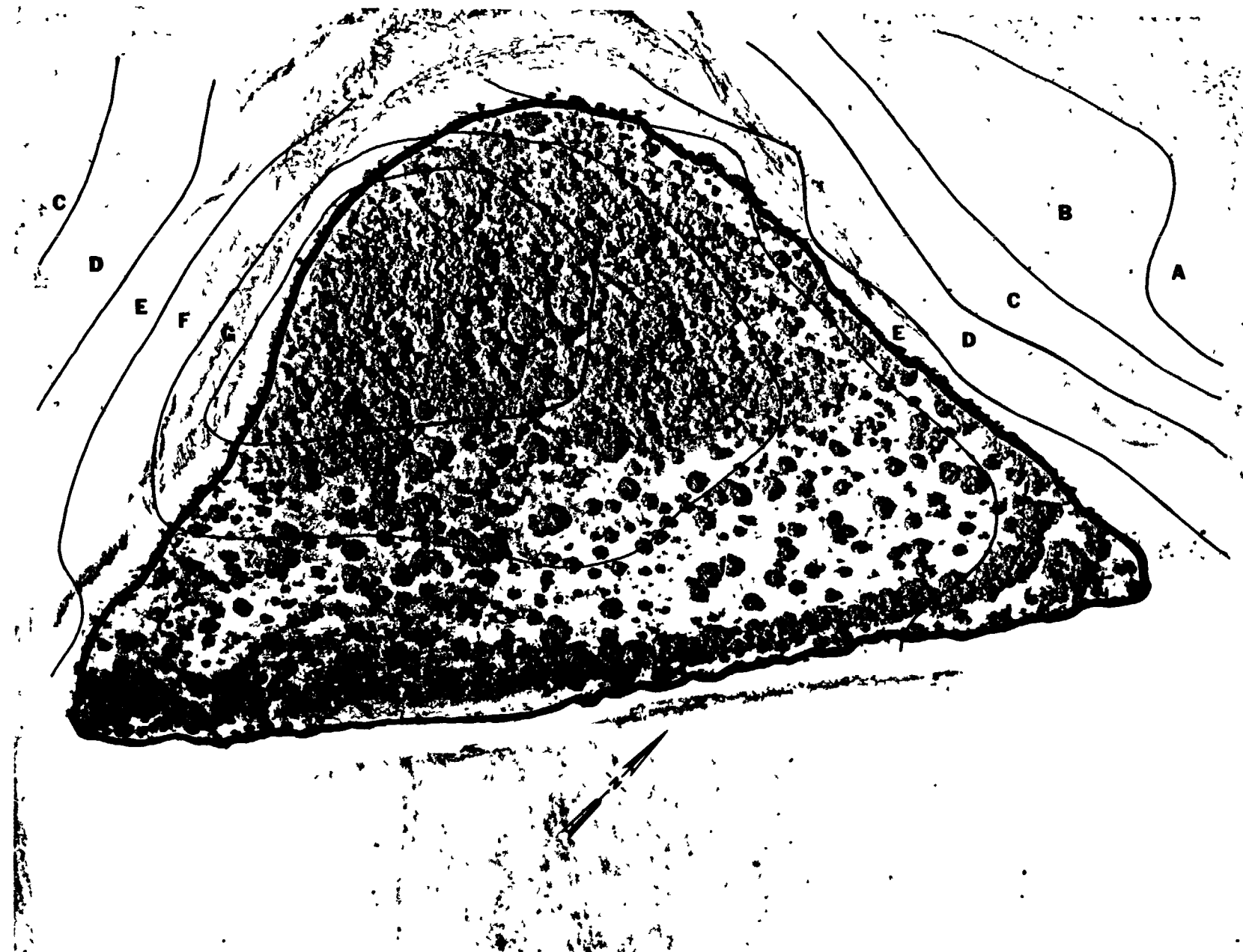


Fig. B.4.1.b. Gross count isosexposure contours. (Refer to alphabetic symbol key in this appendix.)

100 METERS

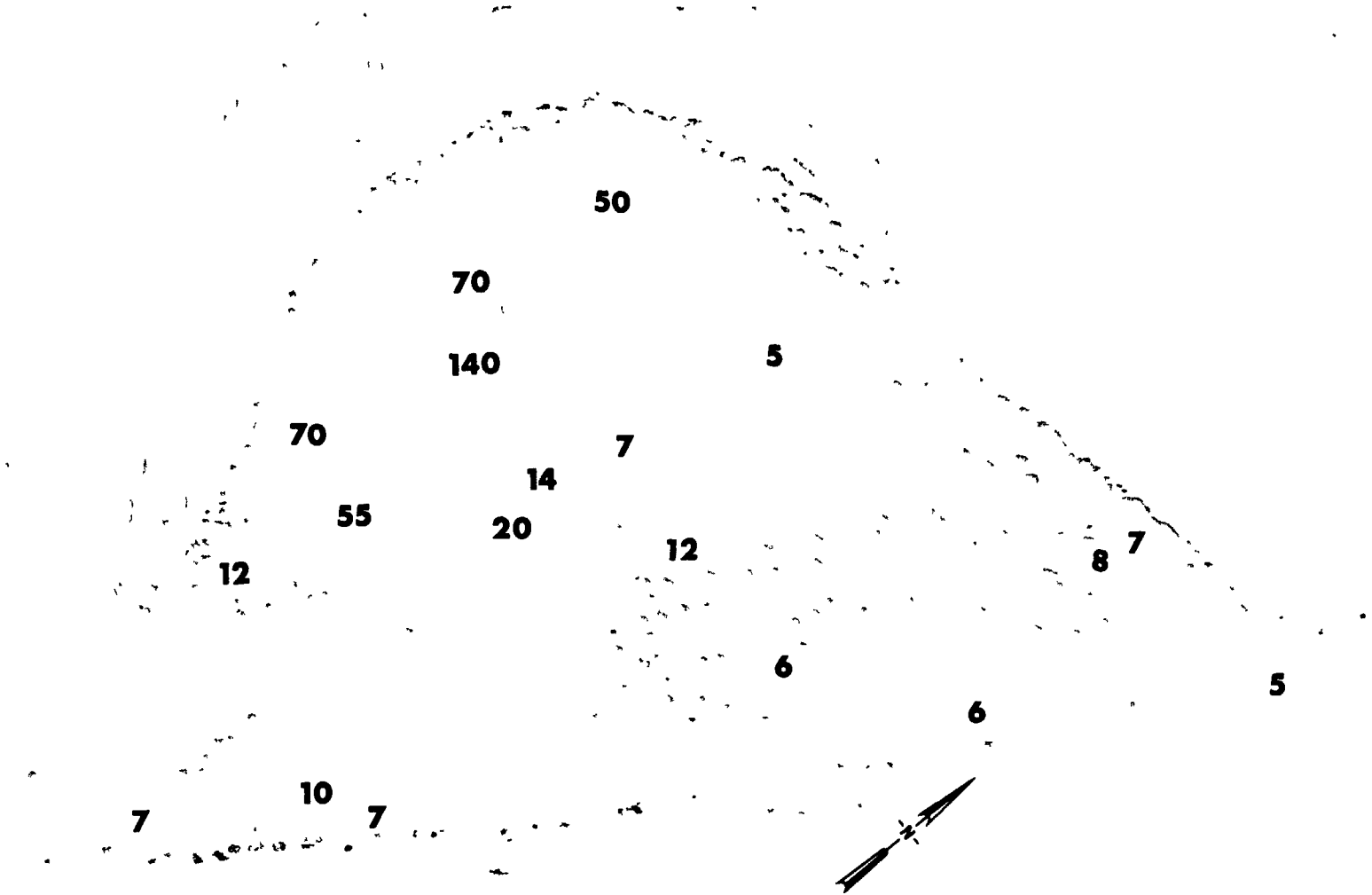
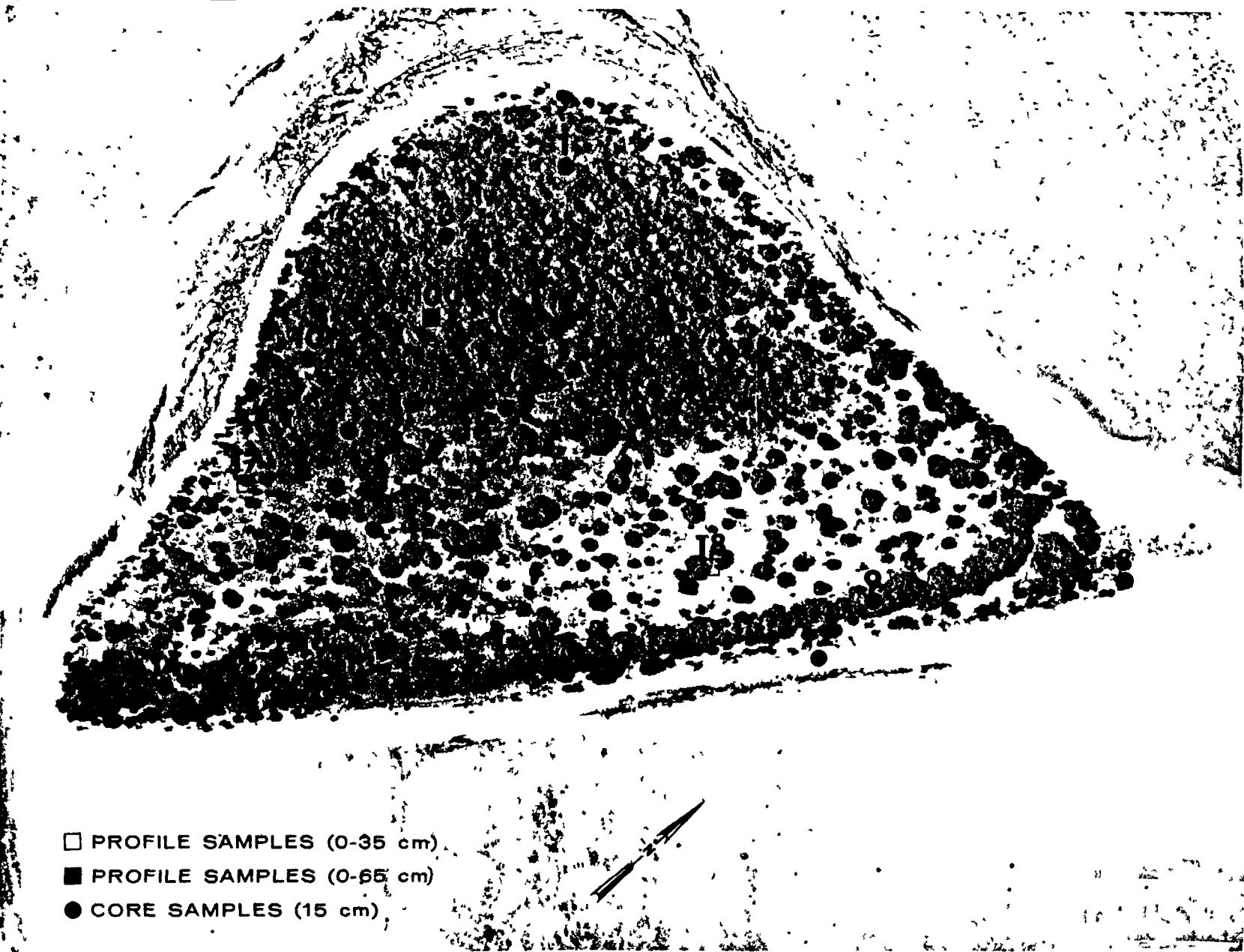


Fig. B.4.1.d. The gamma background exposure rate ( $\mu\text{R/hr}$ ) at 1 m above the ground, measured with a portable NaI scintillation counter.

100 METERS



- PROFILE SAMPLES (0-35 cm)
- PROFILE SAMPLES (0-65 cm)
- CORE SAMPLES (15 cm)

Fig. B.4.1.f. Soil-sample locations.

100 METERS

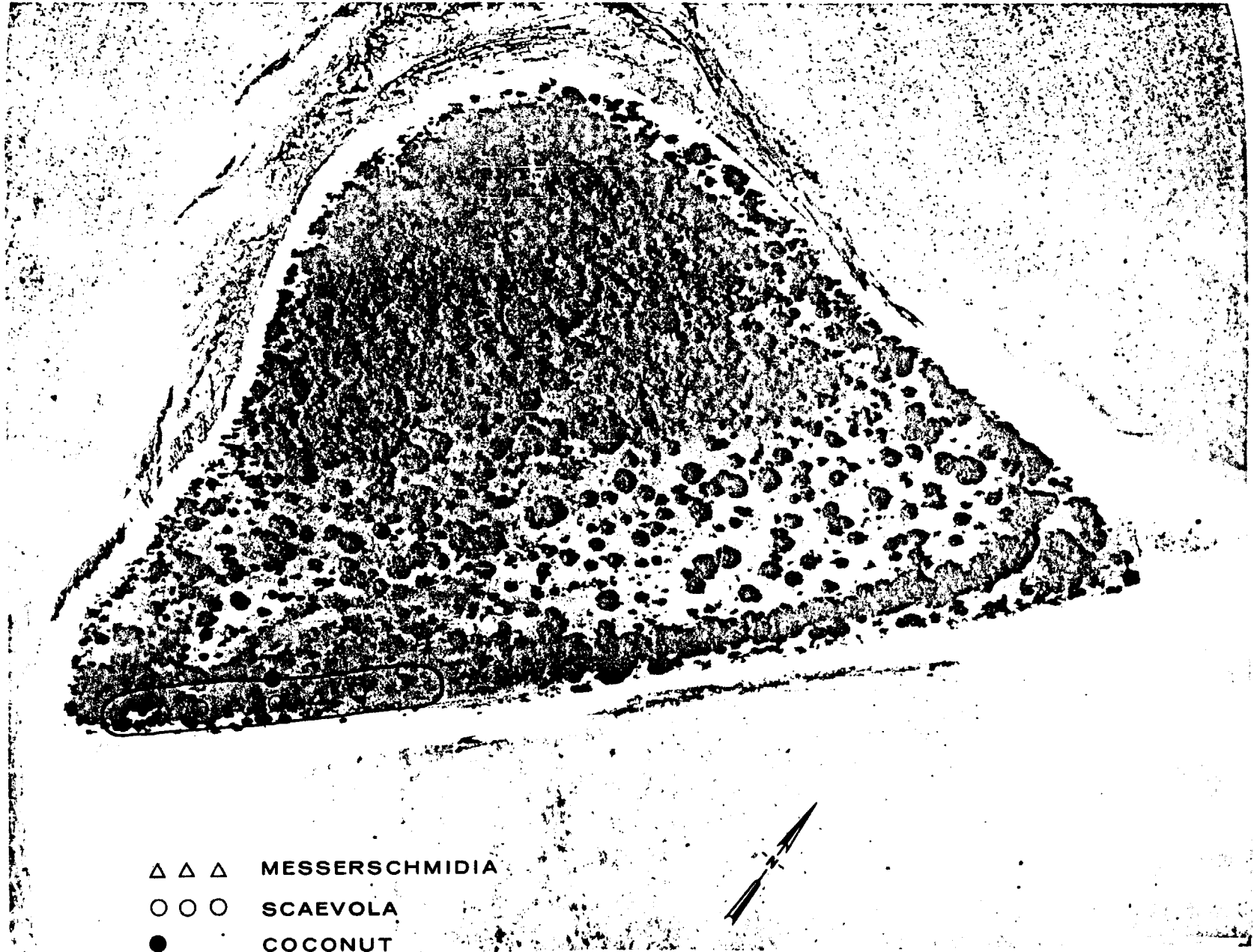


Fig. B.4.1.g. Vegetation sample locations.

100 METERS

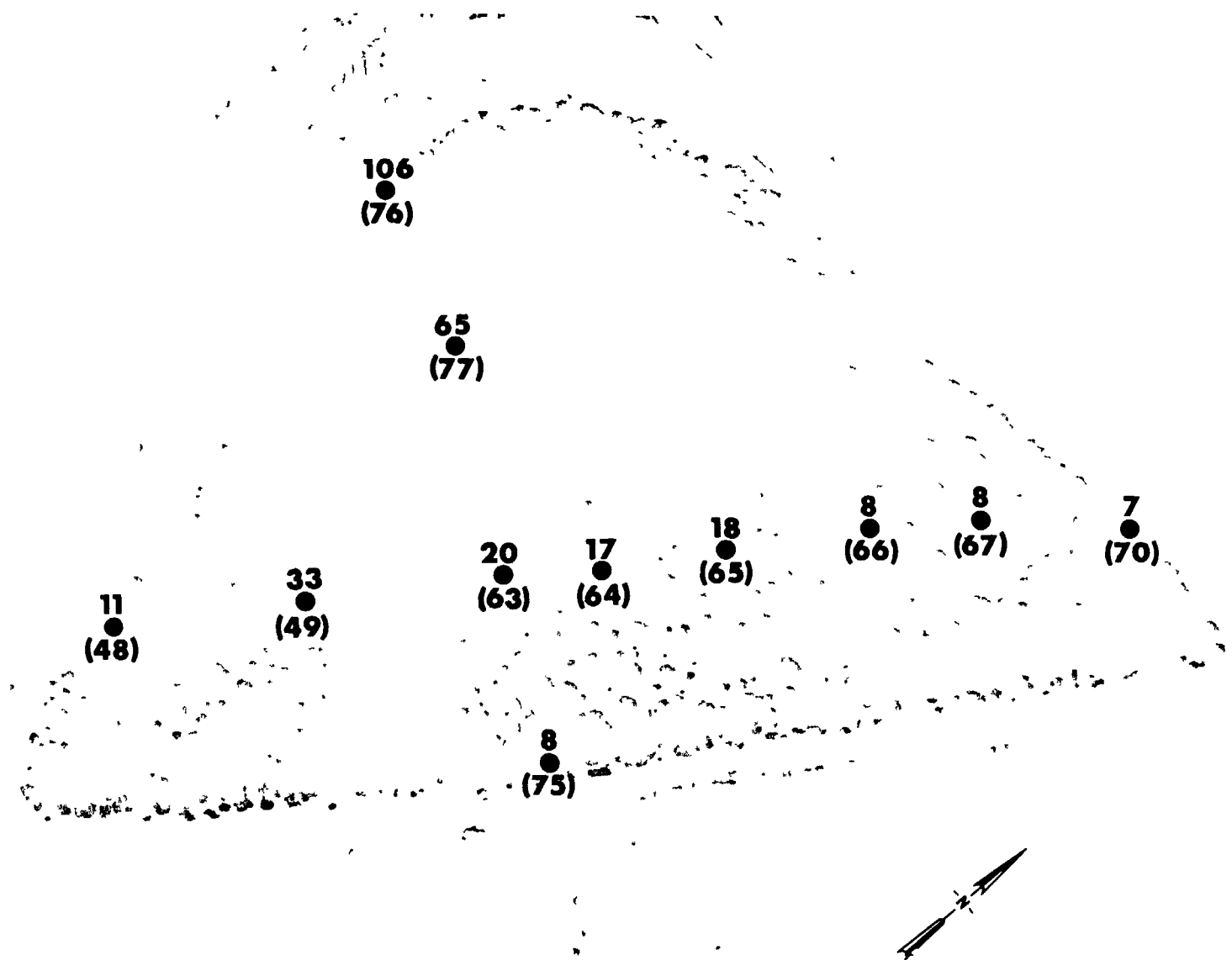


Fig. B.4.1.h. The gamma-ray exposure rates ( $\mu\text{R/hr}$ ) measured 1 m above the ground by the LiF thermoluminescent dosimeters (TLD). The numbers shown in parentheses denote the location identification numbers.



100 METERS

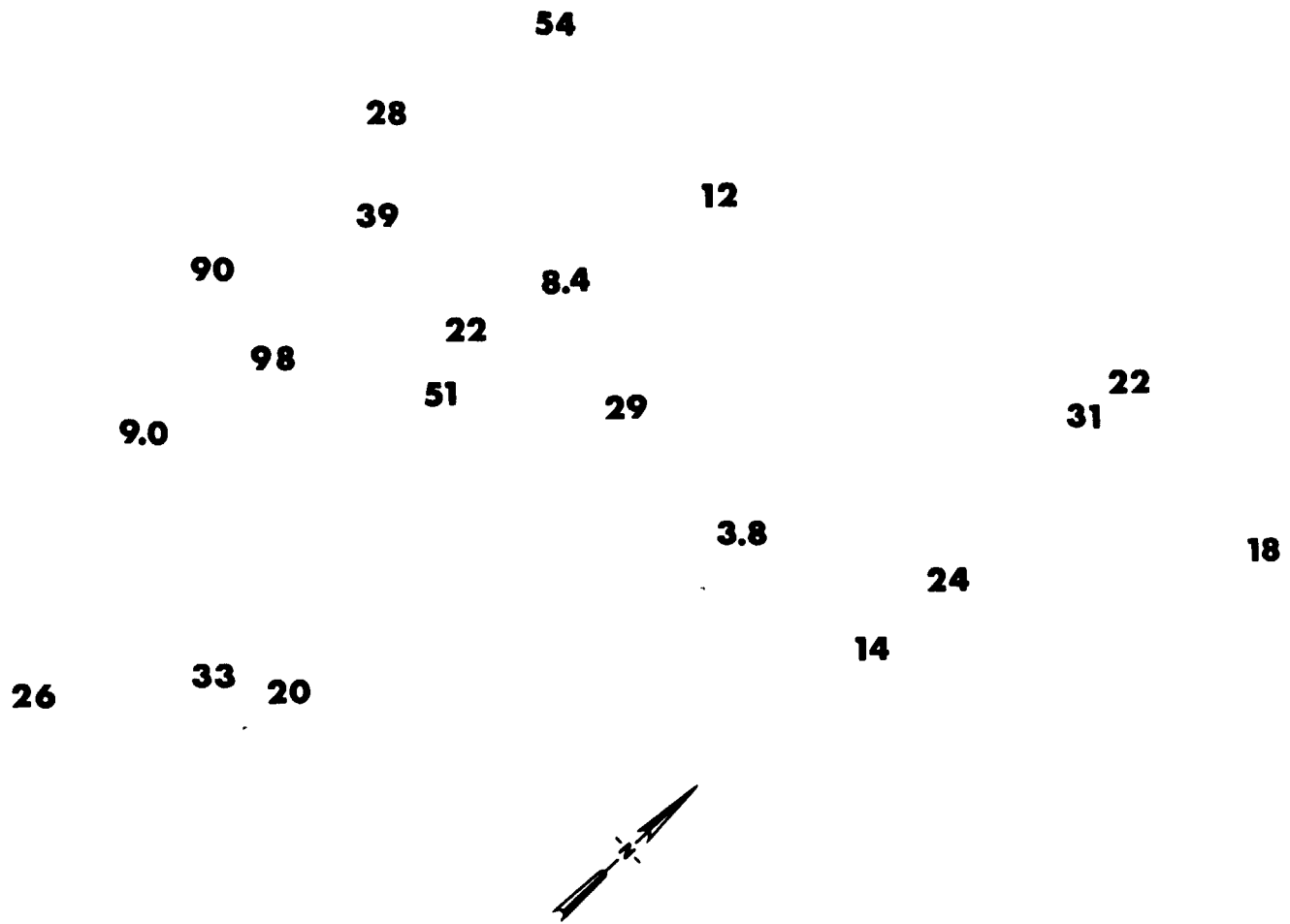


Fig. B.4.1.i. The average  $^{239}\text{Pu}$  activities (pCi/g) in soil samples collected to a depth of 15 cm.

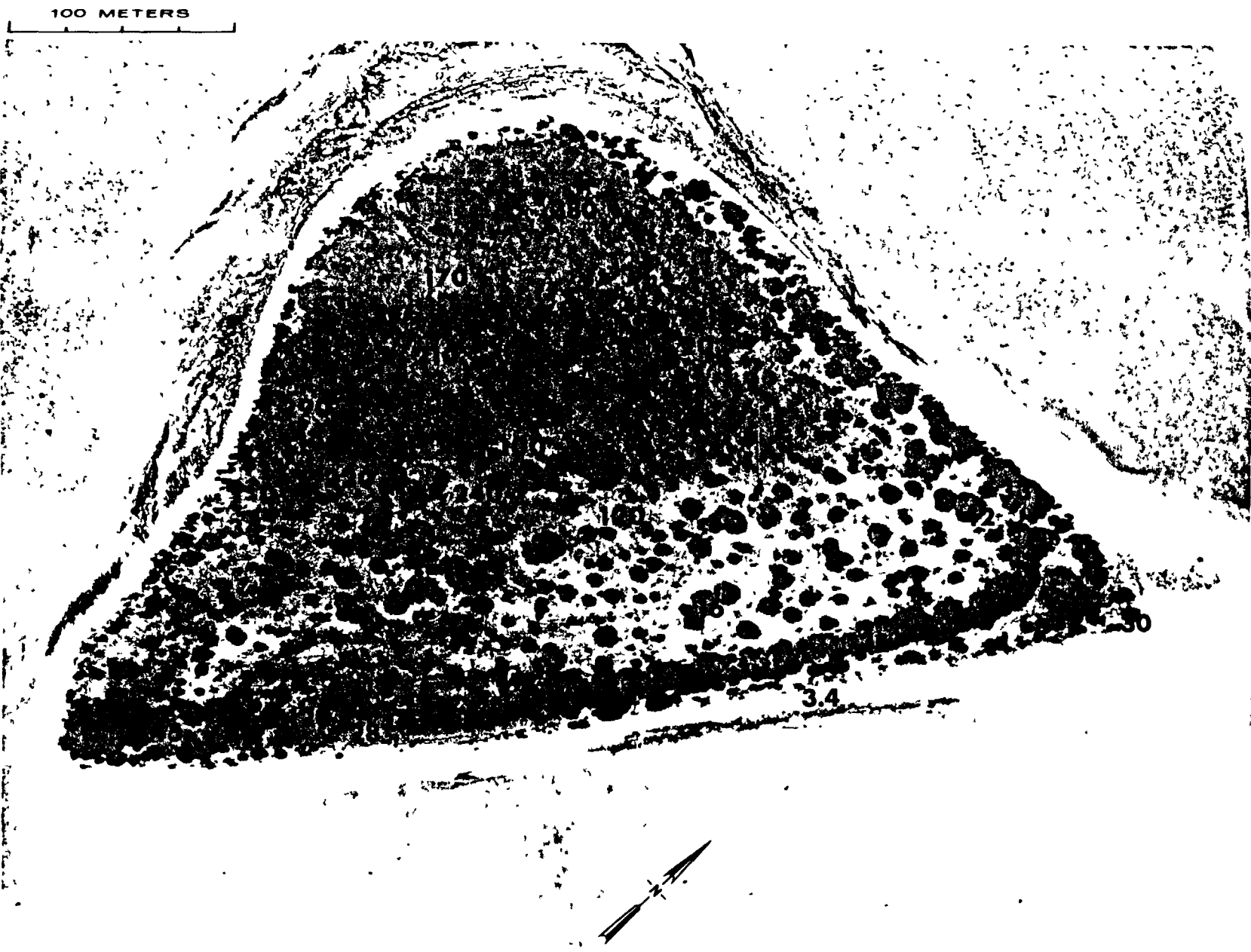


Fig. B.4.1.j. The average  $^{90}\text{Sr}$  activities (pCi/g) in soil samples collected to a depth of 15 cm.

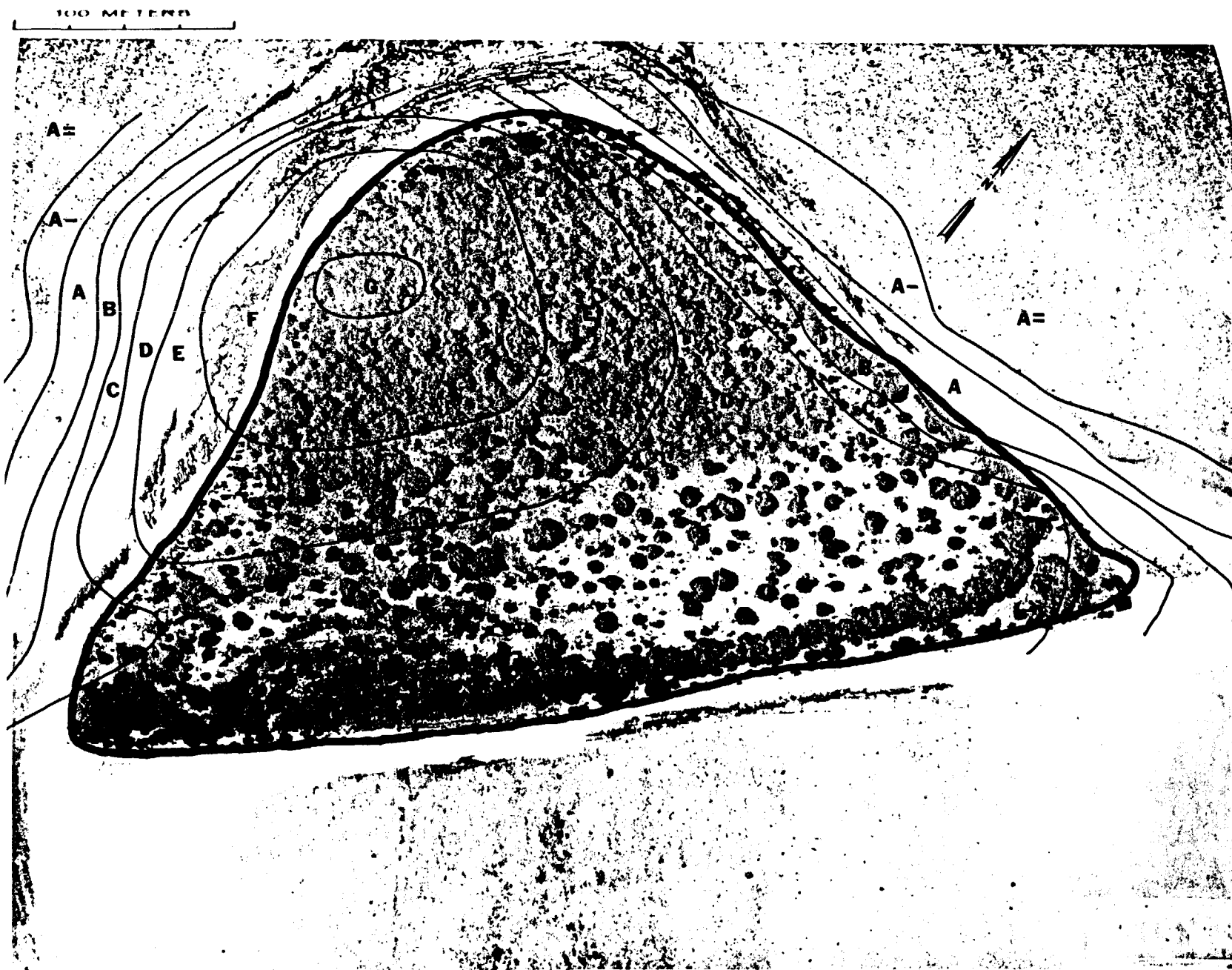


Fig. B.4.1.k.  $^{137}\text{Cs}$  isoexposure and isoconcentration contours. (Refer to alphabetic symbol key in this appendix.)

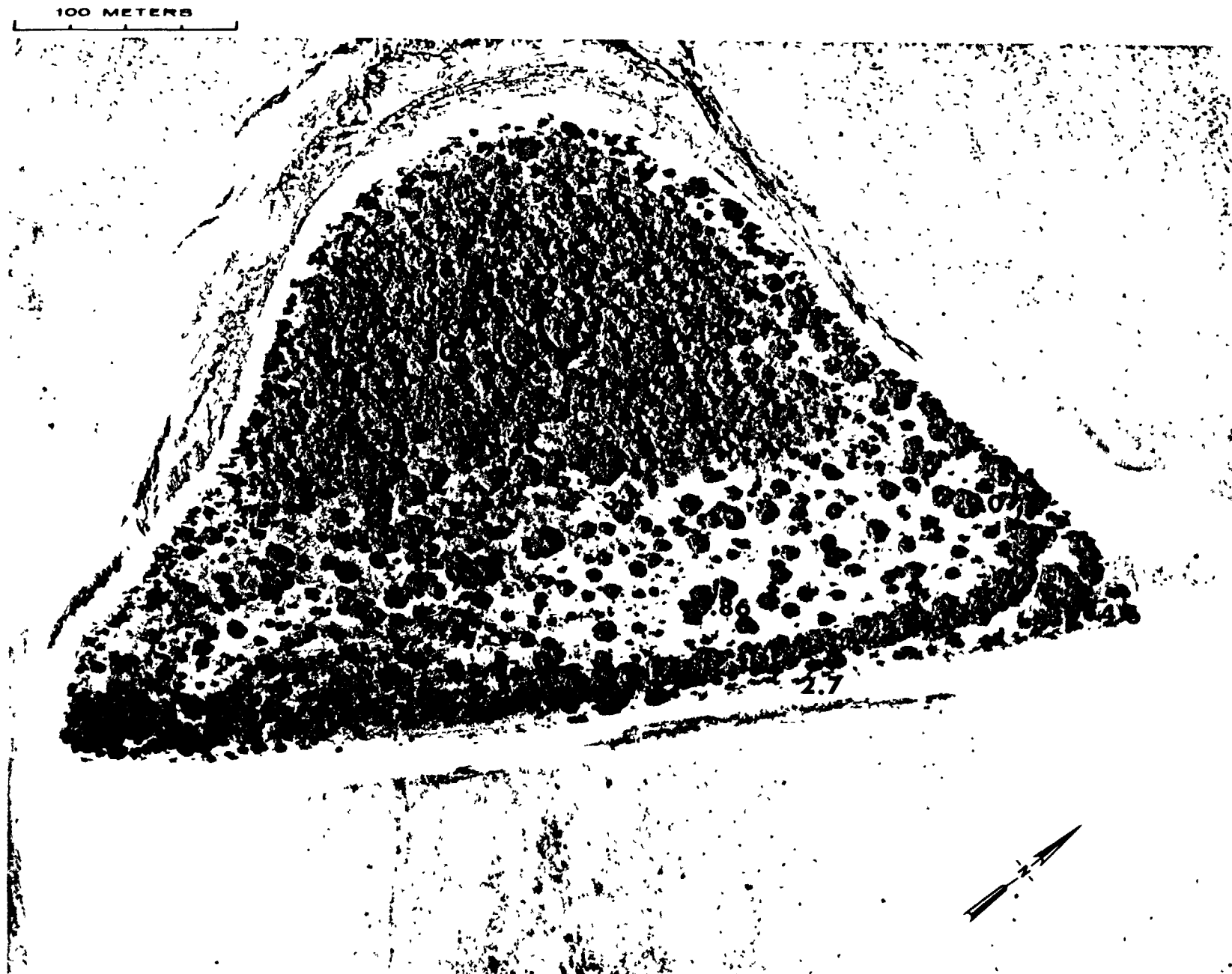


Fig. B.4.1.1. The average  $^{137}\text{Cs}$  activities (pCi/g) in soil samples collected to a depth of 15 cm.

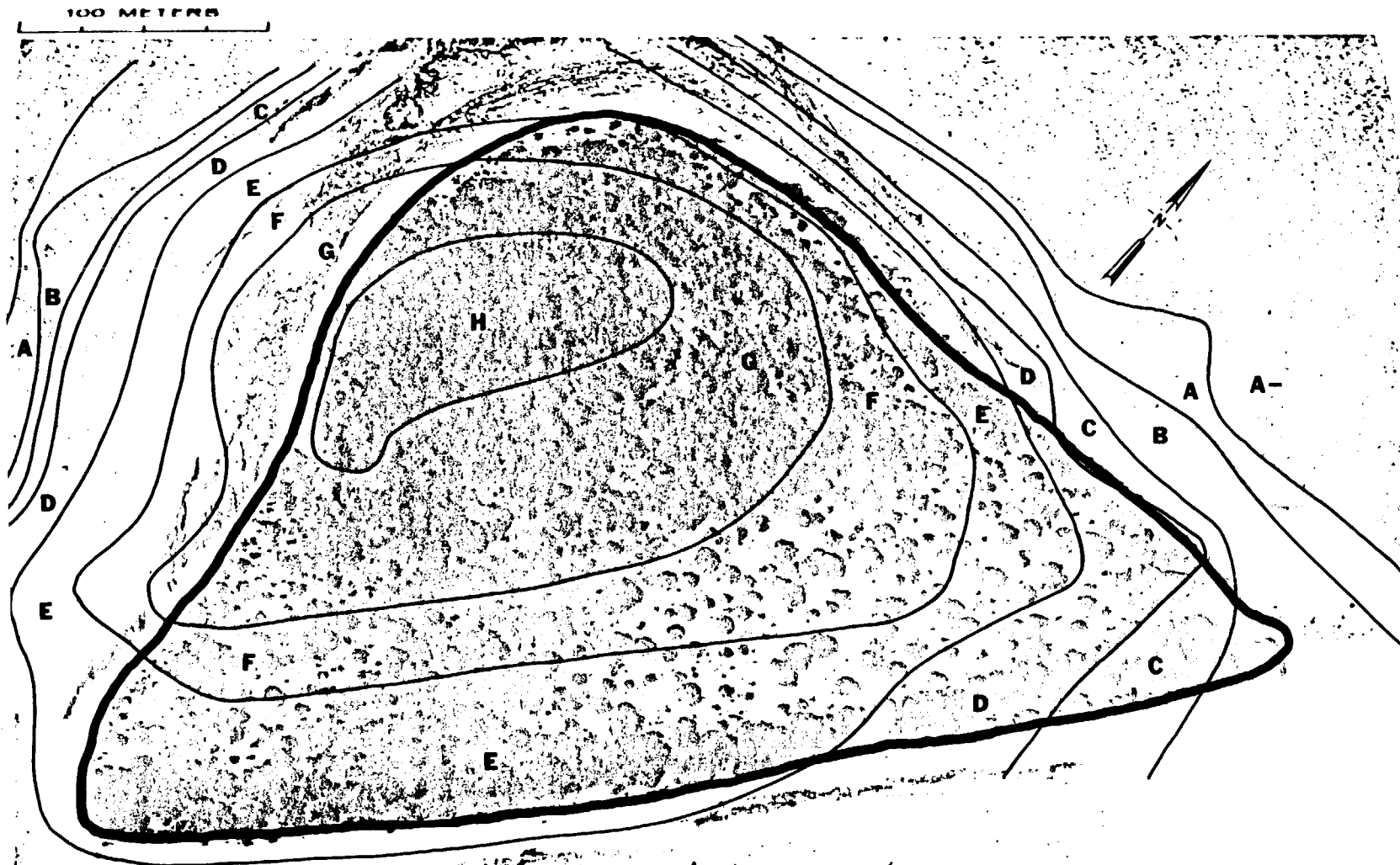


Fig. B.4.1.m.  $^{60}\text{Co}$  isoexposure and isoconcentration contours. (Refer to alphabetic symbol key in this appendix.)

100 METERS

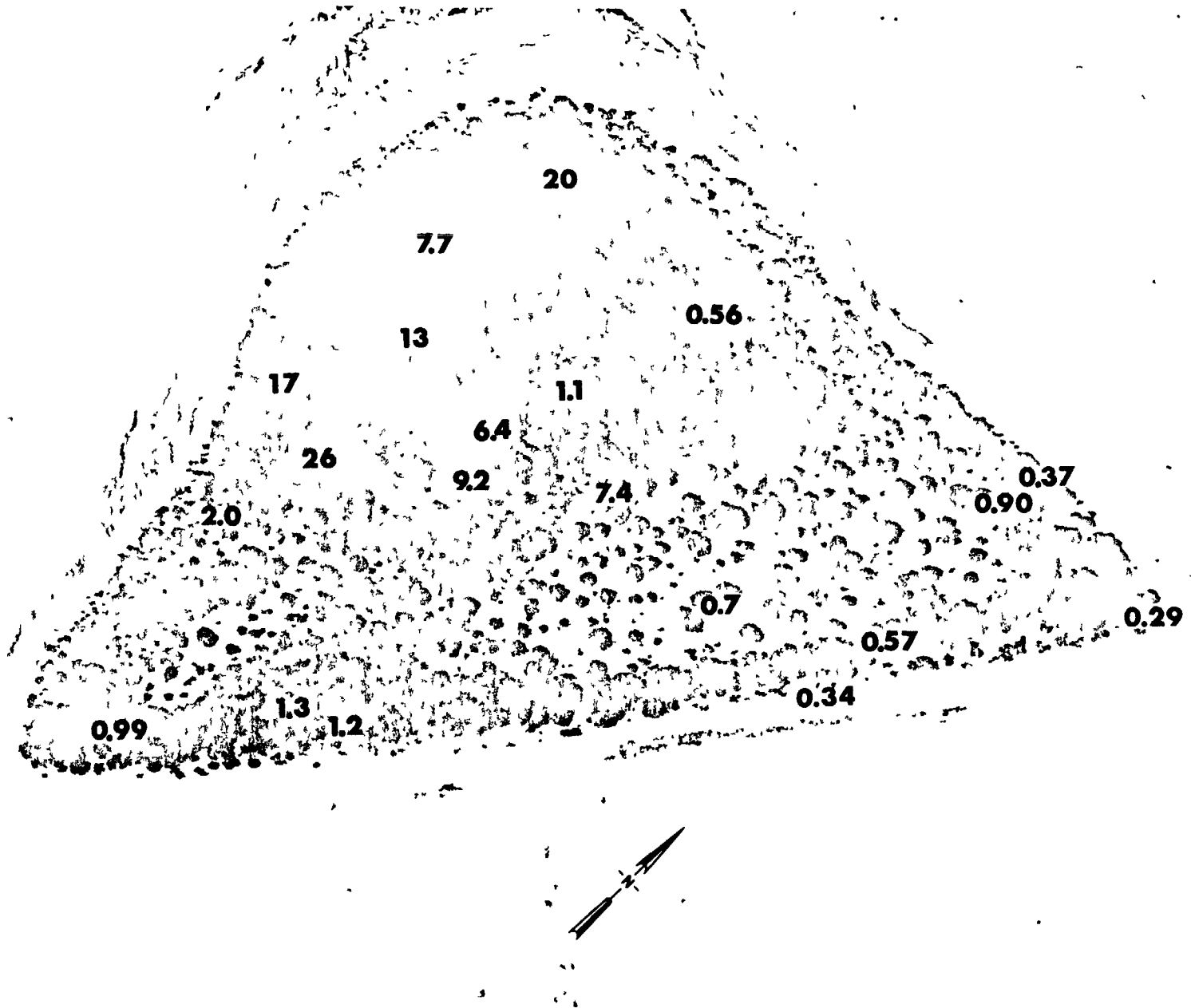


Fig. B.4.1.n. The average <sup>60</sup>Co activities (pCi/g) in soil samples collected to a depth of 15 cm.

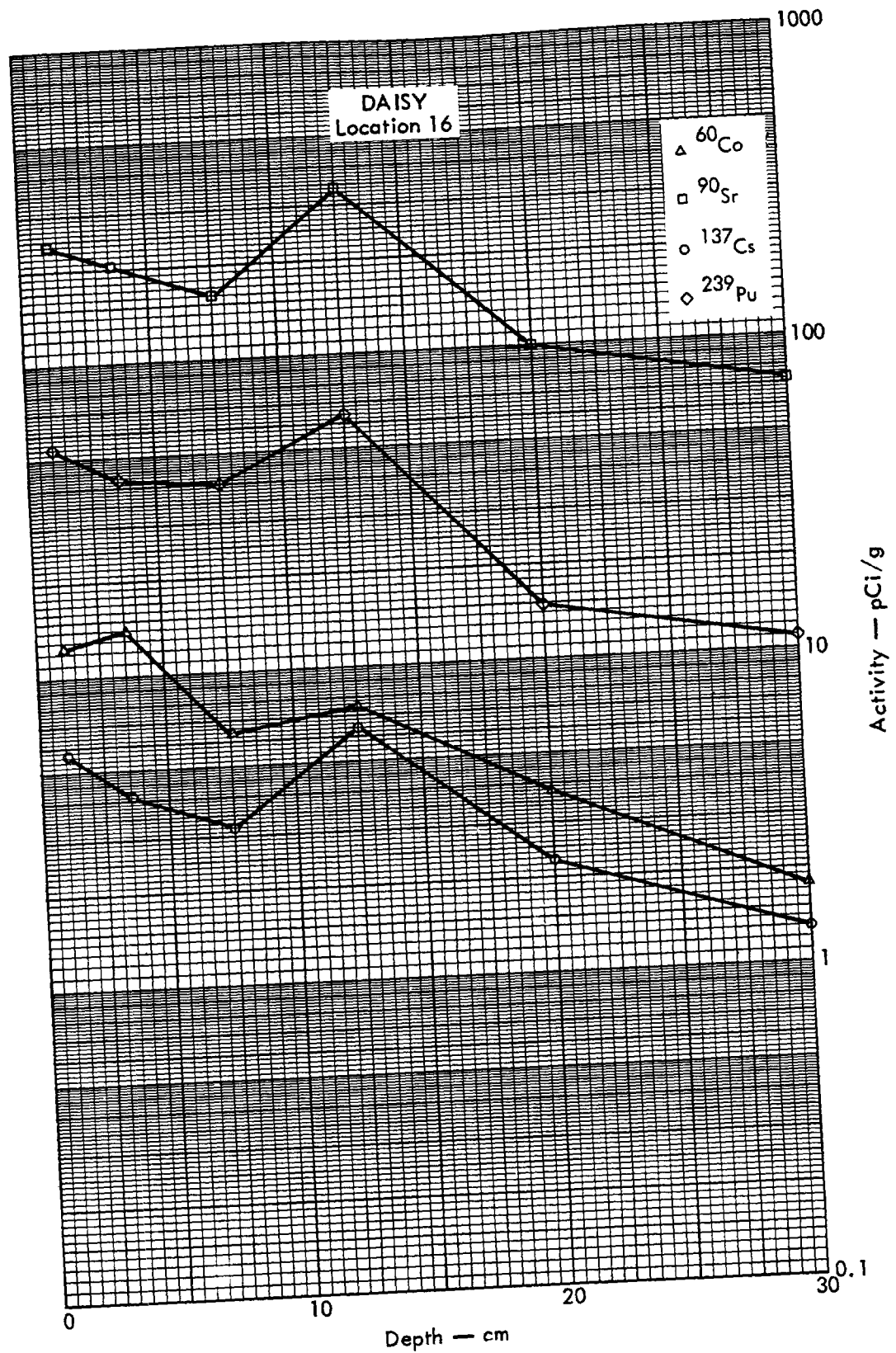


Fig. B.4.2a. Activities of selected radionuclides as a function of soil depth.

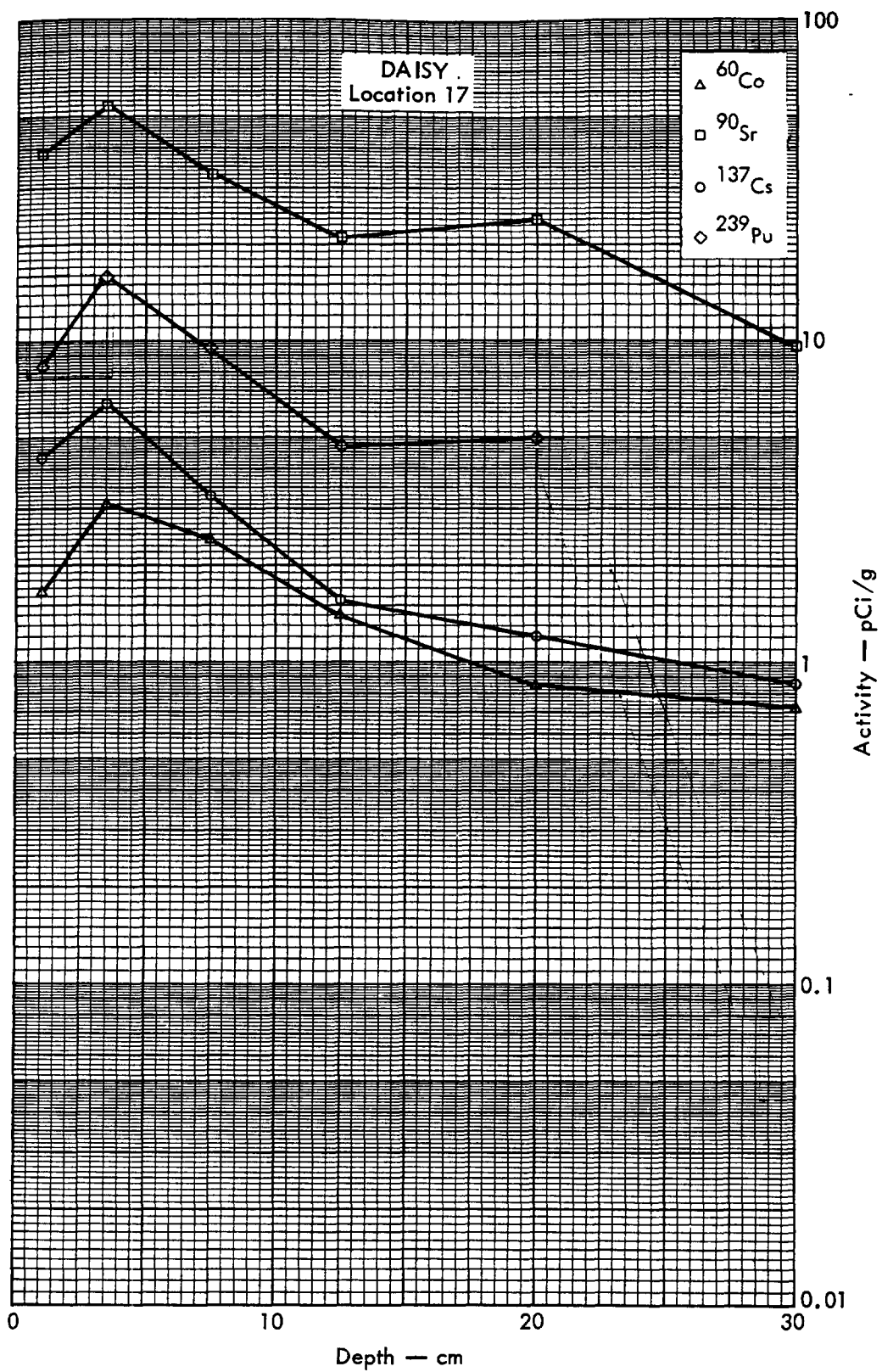


Fig. B. 4. 2b. Activities of selected radionuclides as a function of soil depth.



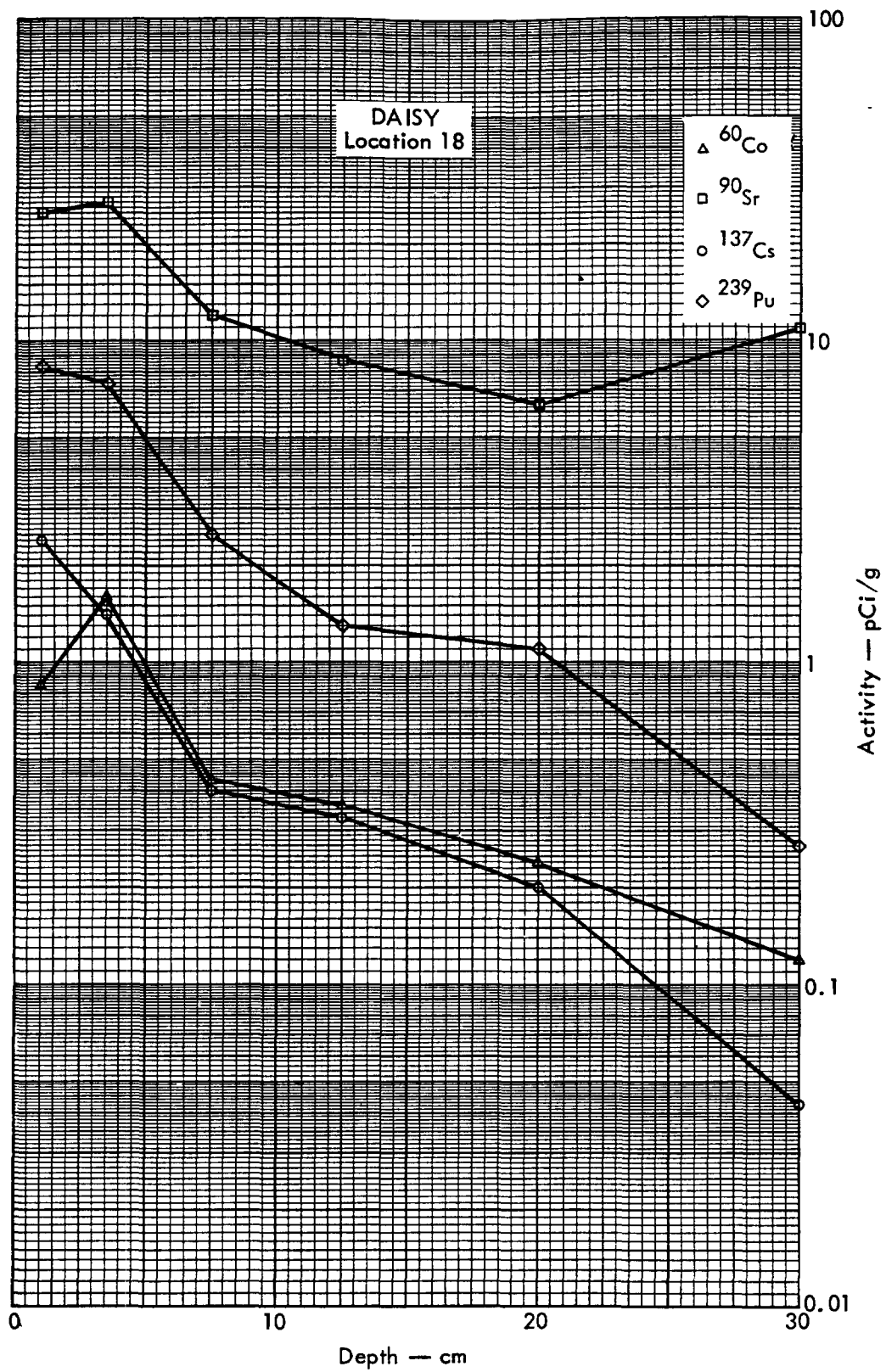


Fig. B. 4. 2c. Activities of selected radionuclides as a function of soil depth.

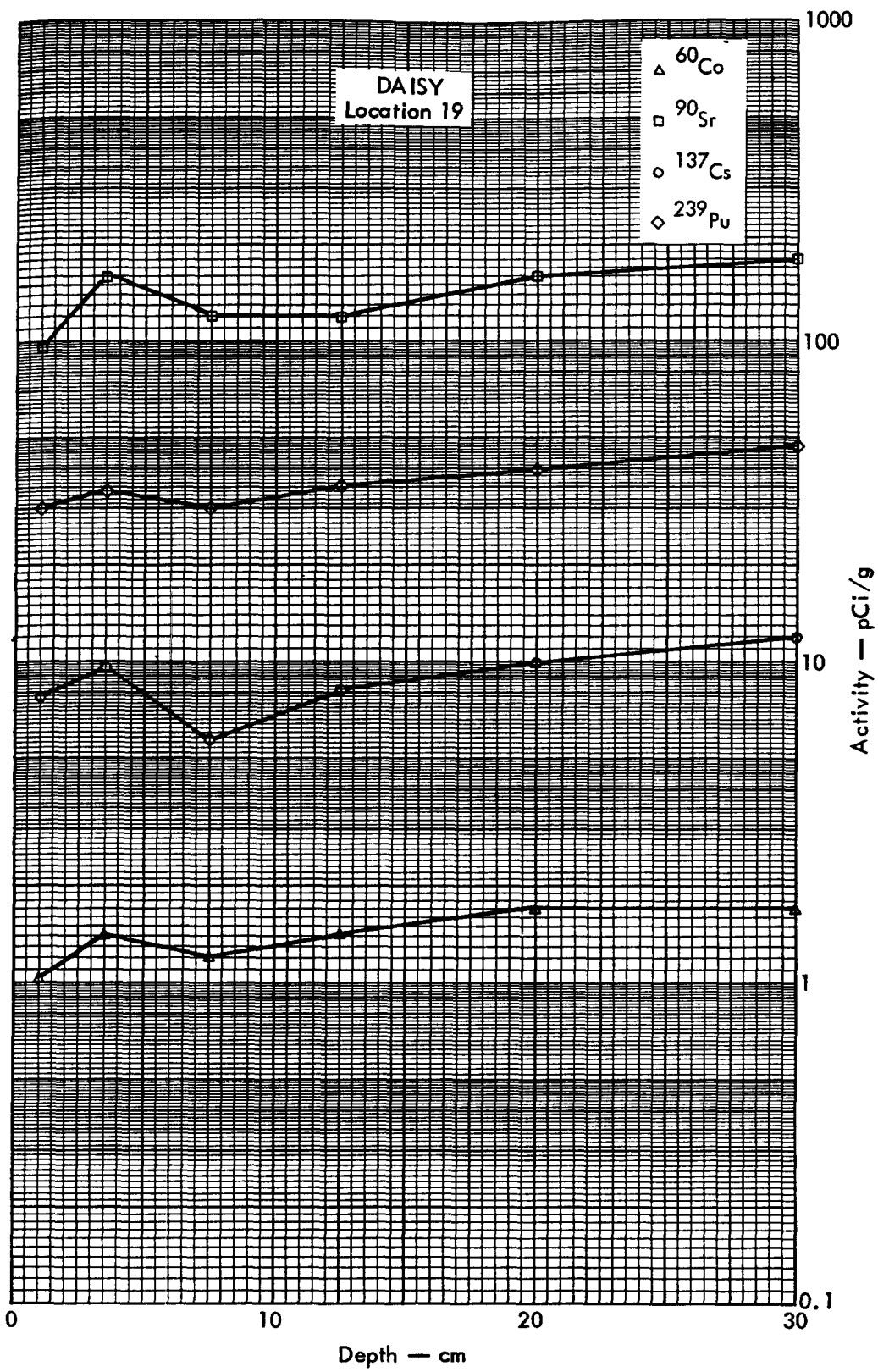


Fig. B. 4. 2d. Activities of selected radionuclides as a function of soil depth.

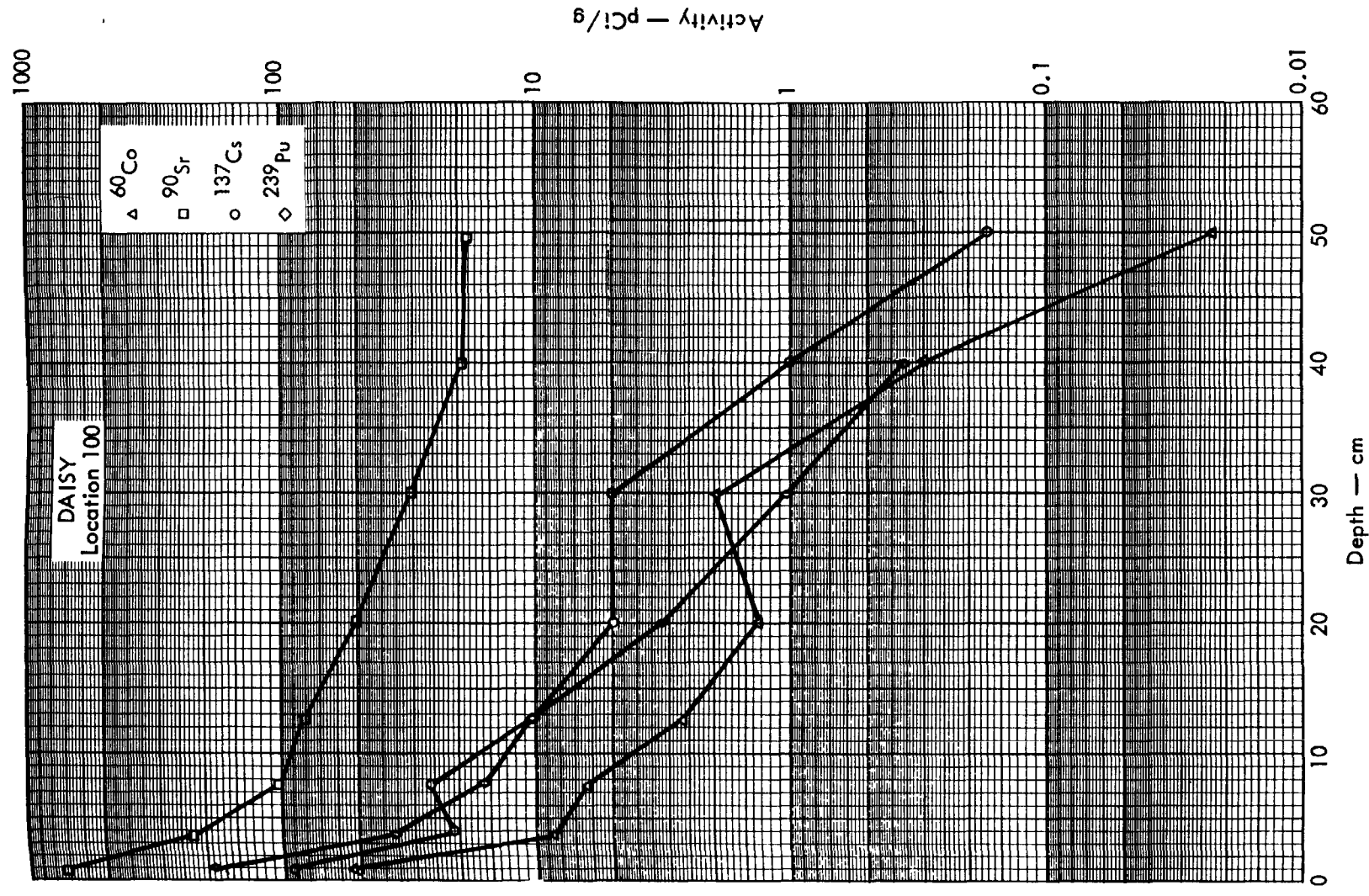


Fig. B.4.2e. Activities of selected radionuclides as a function of soil depth.

100 METERS



EDNA

Fig. B.5.1.a.

100 METERS



Fig. B.5.1.b. Gross count isoexposure contours. (Refer to alphabetic symbol key in this appendix.)

100 METERS



Fig. B.5.1.d. The gamma background exposure rate ( $\mu\text{R/hr}$ ) at 1 m above the ground, measured with a portable NaI scintillation counter.

100 METERS



□ PROFILE SAMPLES (0-35cm)

● CORE SAMPLES (15 cm)

Fig. B.5.1.f. Soil-sample locations.

100 METERS



Fig. B.5.1.g. Vegetation sample locations.



100 METERS

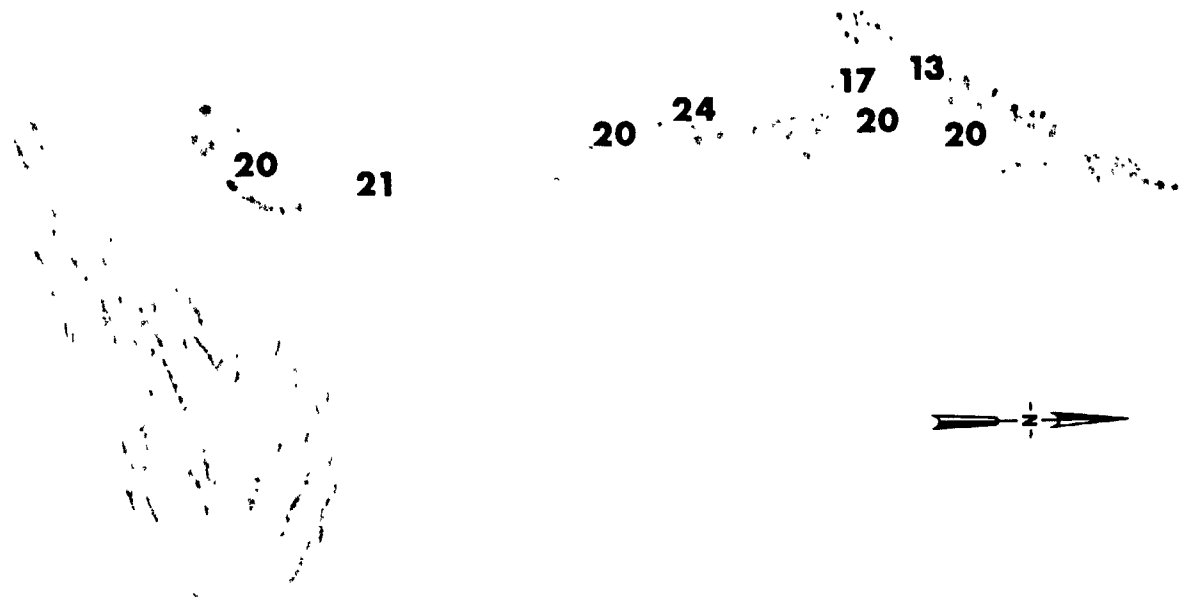


Fig. B.5.1.i. The average  $^{239}\text{Pu}$  activities (pCi/g) in soil samples collected to a depth of 15 cm.

100 METERS



Fig. B.5.1.j. The average <sup>90</sup>Sr activities (pCi/g) in soil samples collected to a depth of 15 cm.

100 METERS

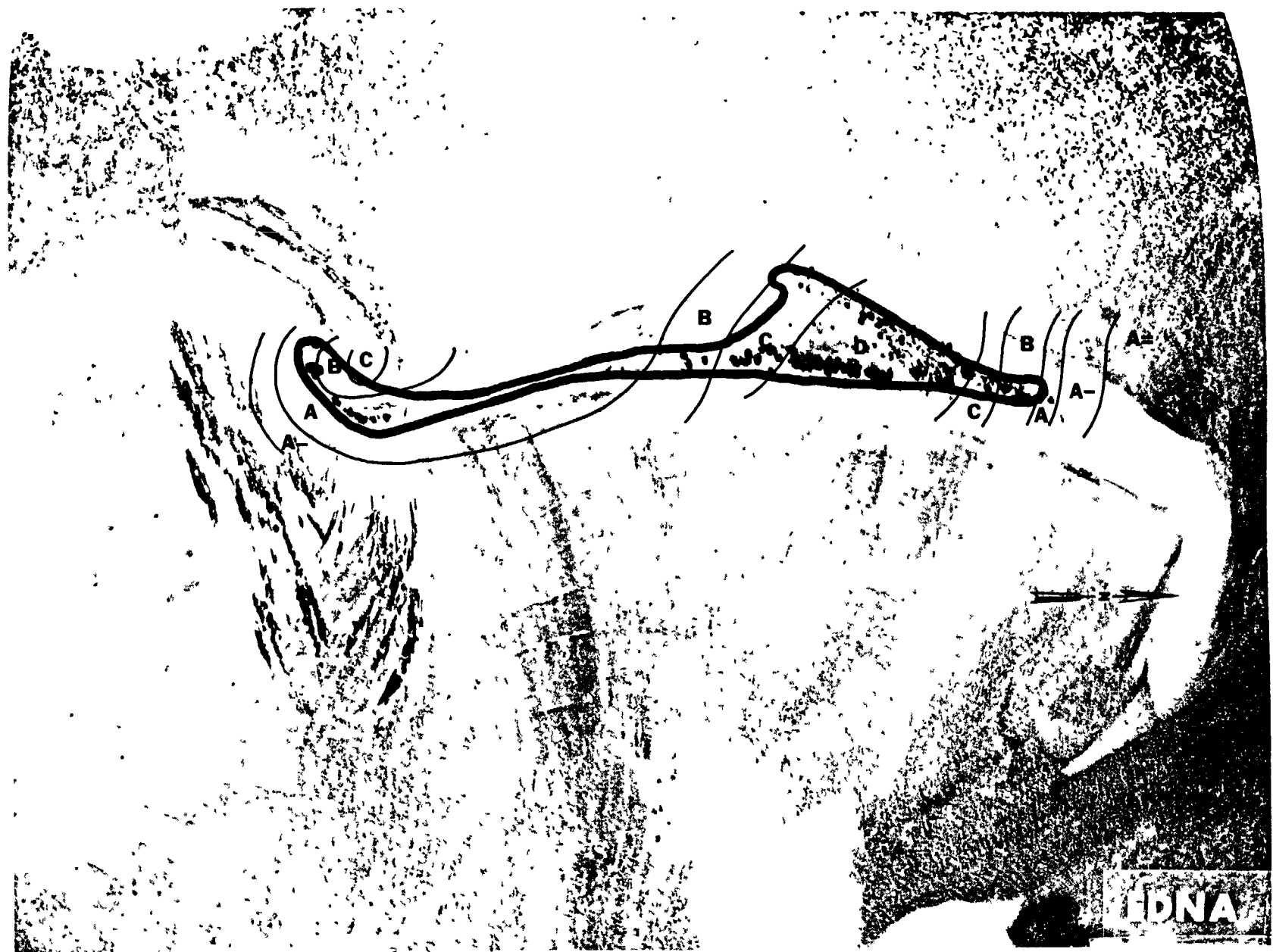


Fig. B.5.1.k.  $^{137}\text{Cs}$  isoexposure and isoconcentration contours. (Refer to alphabetic symbol key in this appendix.)

100 METERS



Fig. B.5.1.1. The average  $^{137}\text{Cs}$  activities (pCi/g) in soil samples collected to a depth of 15 cm.

100 METERS

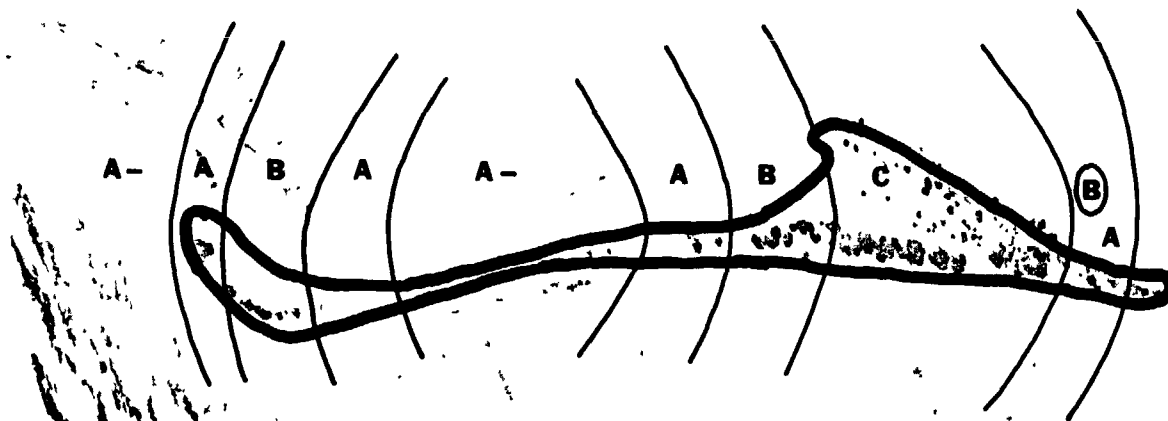


Fig. B.5.1.m. <sup>60</sup>Co isoexposure and isoconcentration contours. (Refer to alphabetic symbol key in this appendix.)

100 METERS

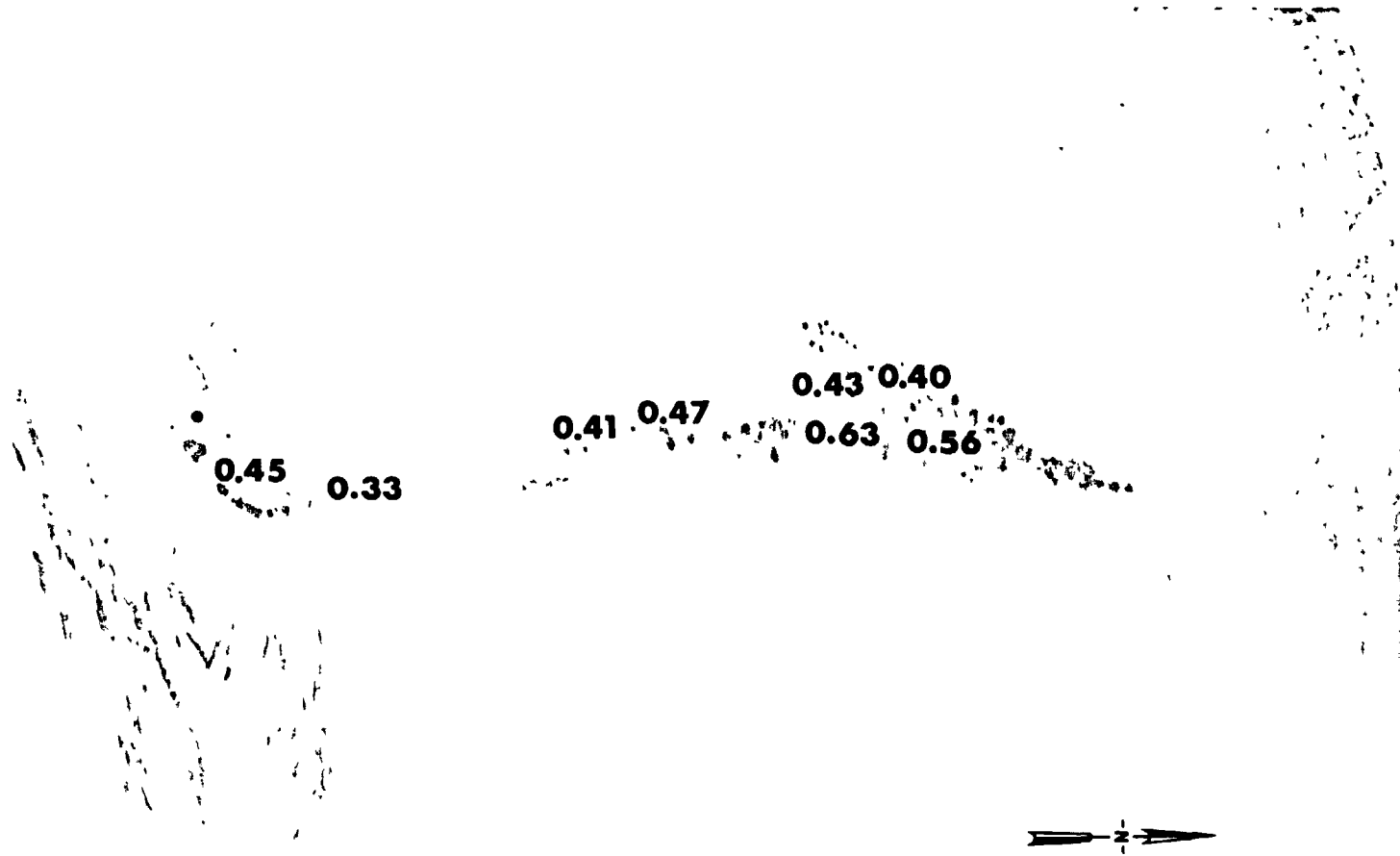


Fig. B.5.1.n. The average  $^{60}\text{Co}$  activities (pCi/g) in soil samples collected to a depth of 15 cm.

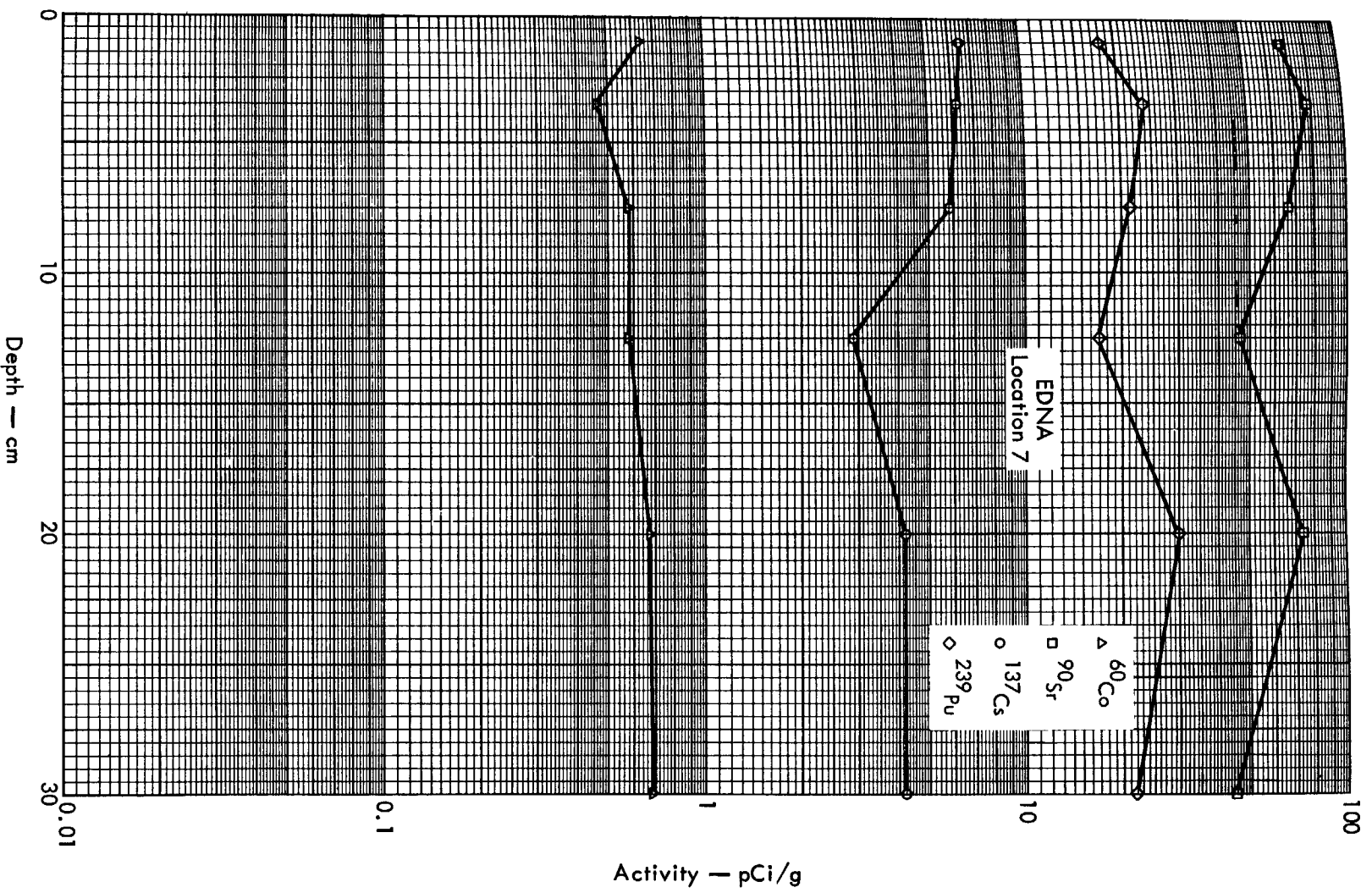


Fig. B. 5. 2a. Activities of selected radionuclides as a function of soil depth.

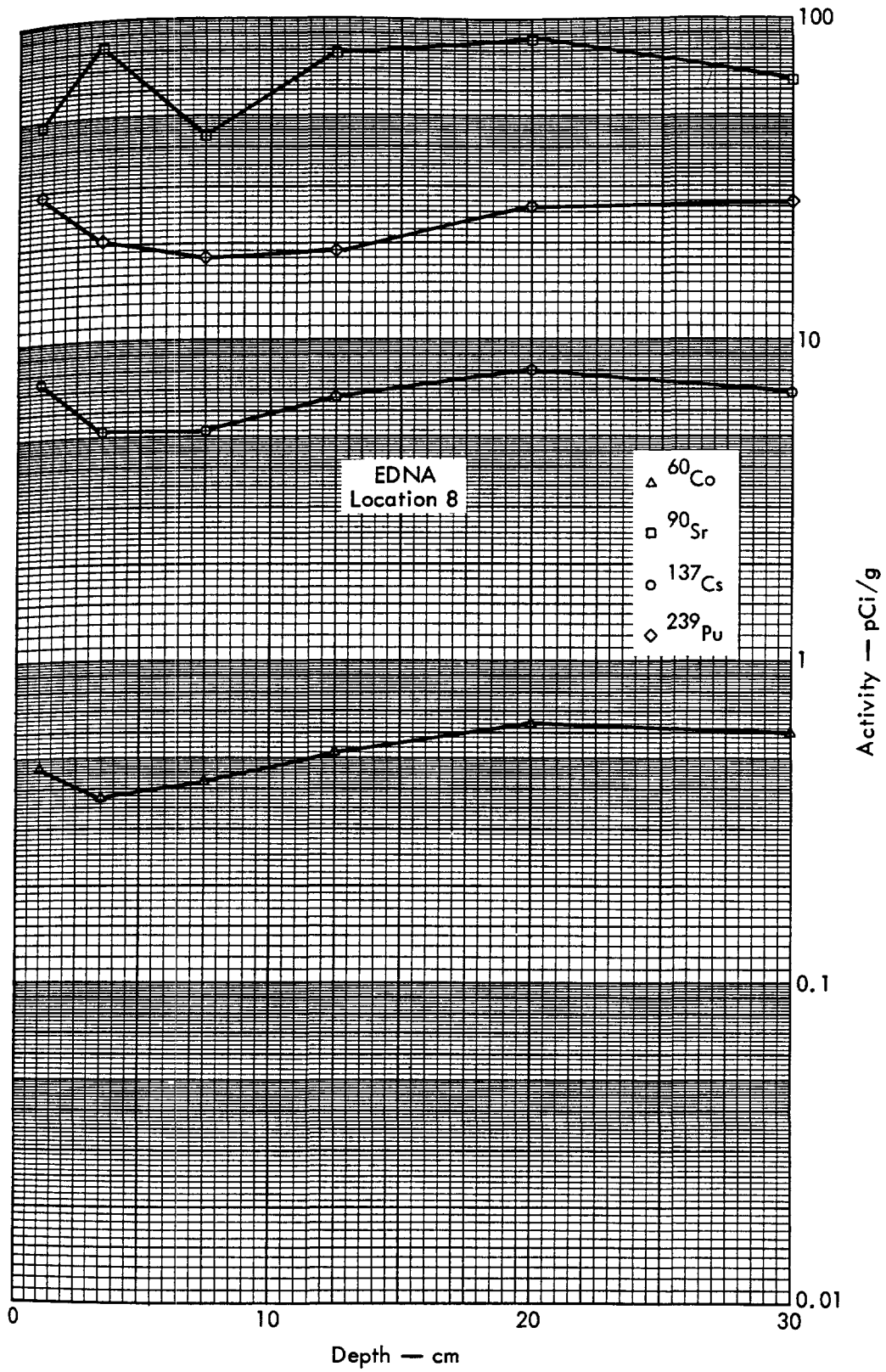


Fig. B.5.2b. Activities of selected radionuclides as a function of soil depth.





Fig. B.6.1.a.

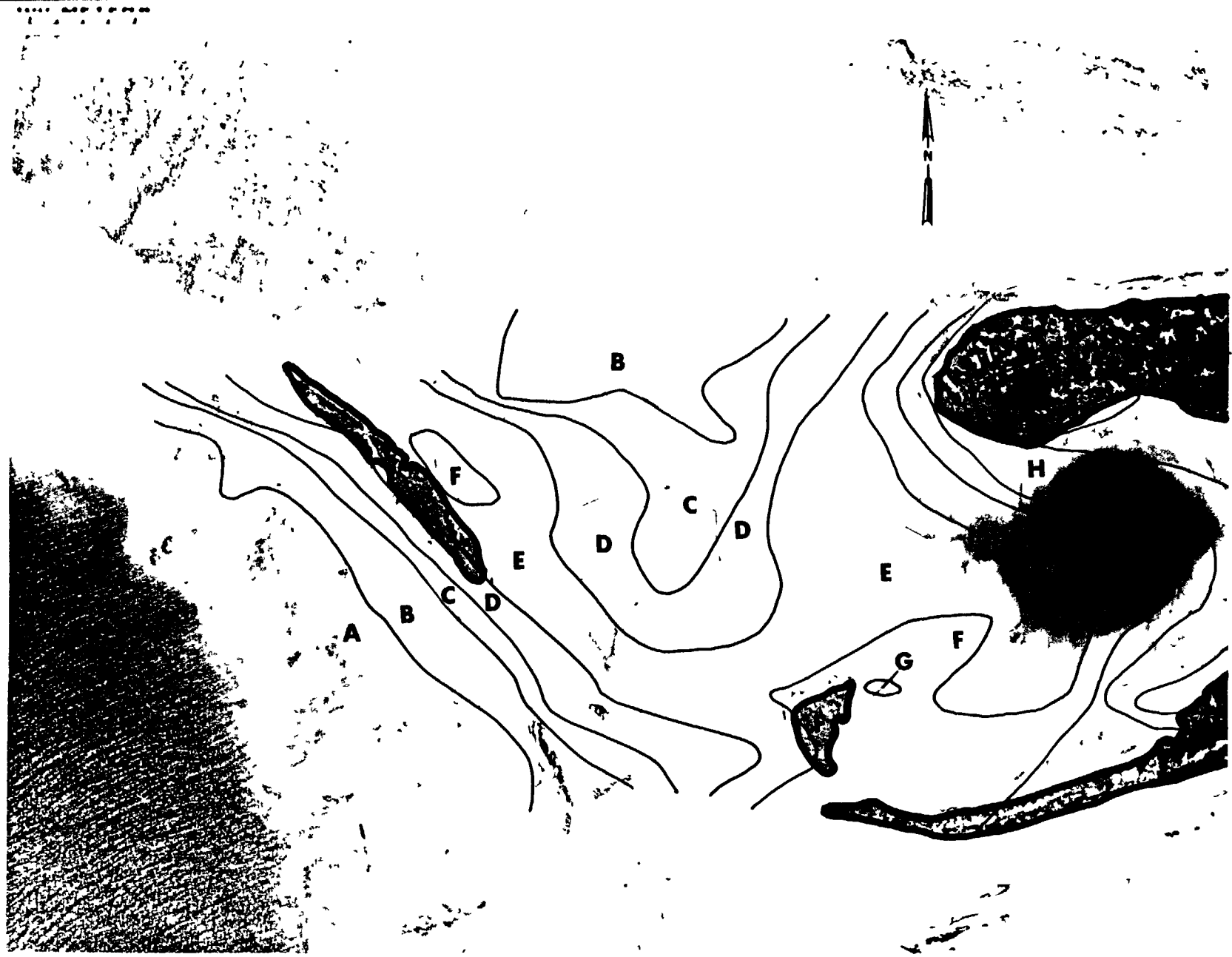
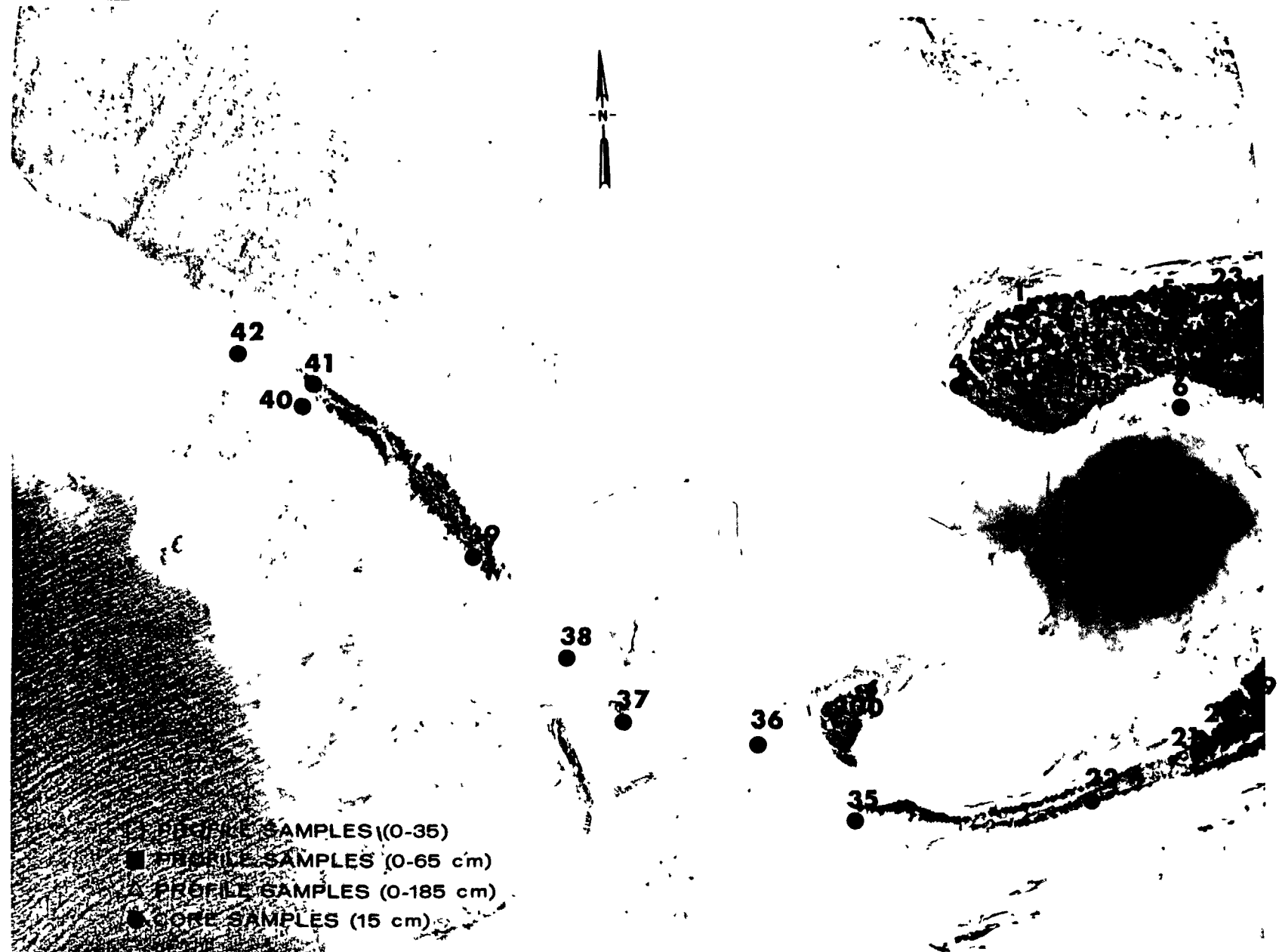


Fig. B.6.1.b. Gross count isosexposure contours. (Refer to alphabetic symbol key in this appendix.)



Fig. B.6.1.d. The gamma background exposure rate ( $\mu\text{R/hr}$ ) at 1 m above the ground, measured with a portable NaI scintillation counter.

1000 METERS



- PROFILE SAMPLES (0-35)
- PROFILE SAMPLES (0-65 cm)
- ▲ PROFILE SAMPLES (0-185 cm)
- CORE SAMPLES (15 cm)

Fig. B.6.1.f. Soil-sample locations.



Fig. B.6.1.g. Vegetation sample locations.

1000 METERS

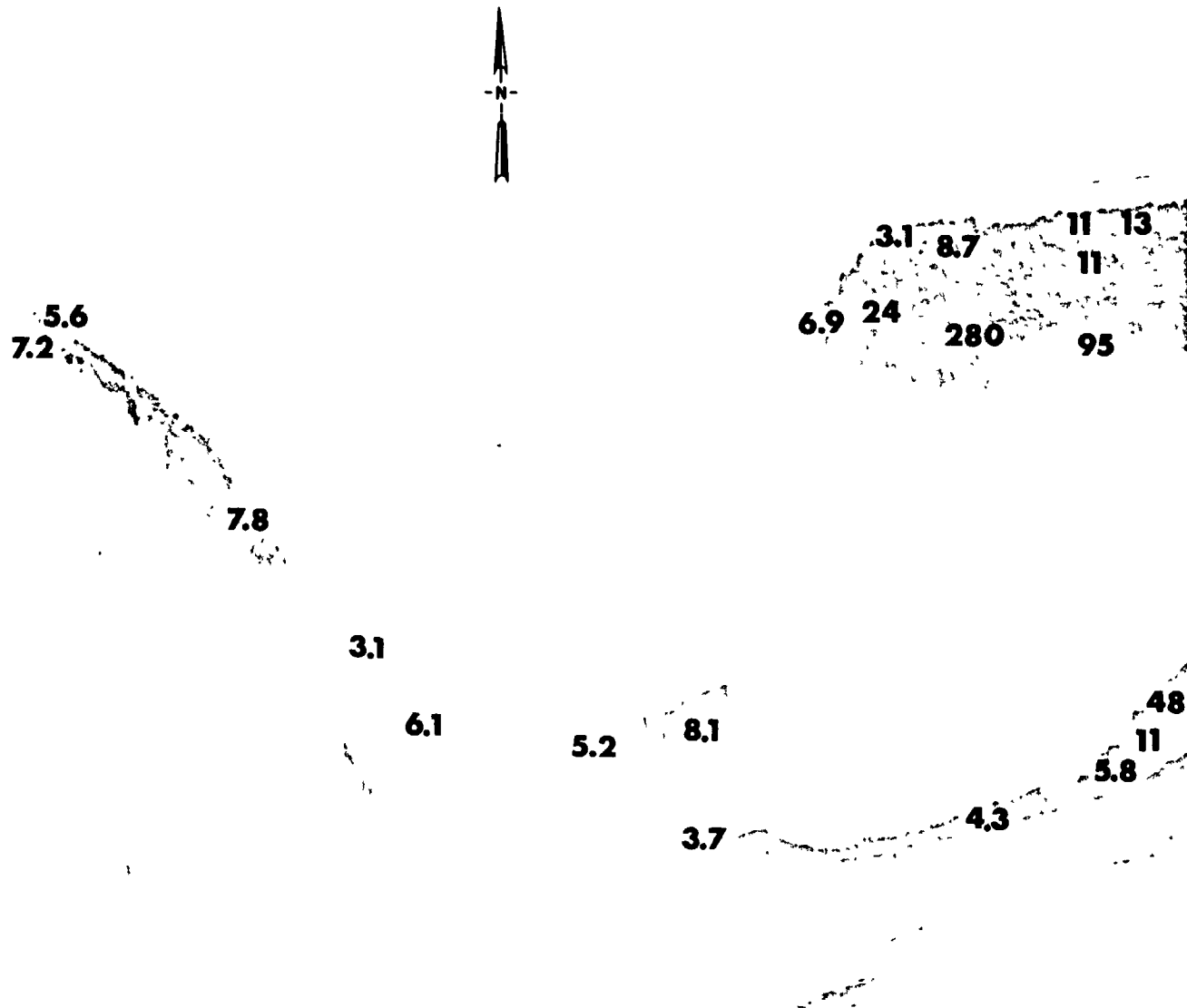


Fig. B.6.1.1. The average  $^{239}\text{Pu}$  activities (pCi/gm) in soil samples collected to a depth of 15 cm.

1000  
500  
0  
500  
1000

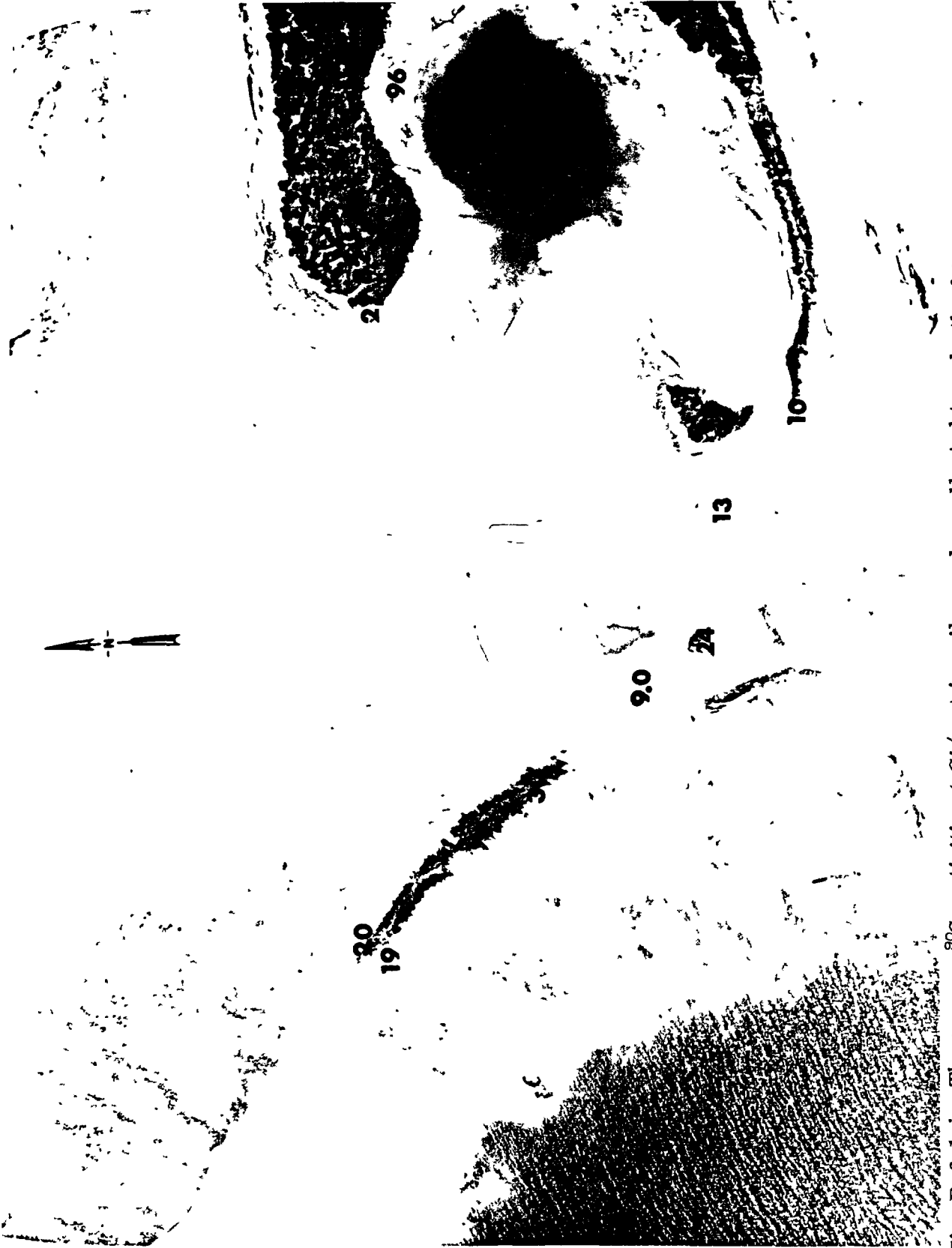


Fig. B.6.1.j. The average  $^{90}\text{Sr}$  activities (pCi/gm) in soil samples collected to a depth of 15 cm.

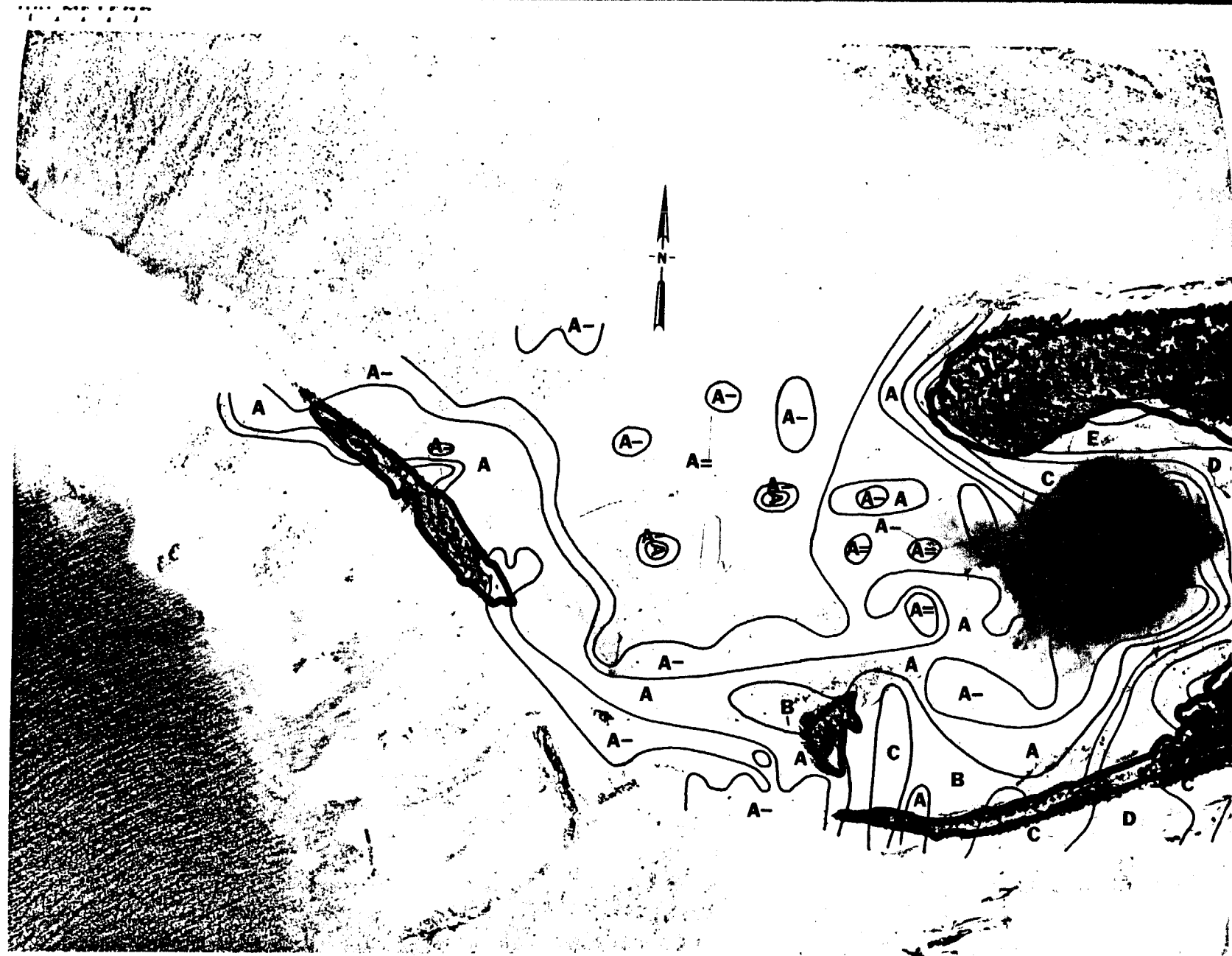


Fig. B.6.1.k.  $^{137}\text{Cs}$  isoexposure and isoconcentration contours. (Refer to alphabetic symbol key in this appendix.)



100 METERS

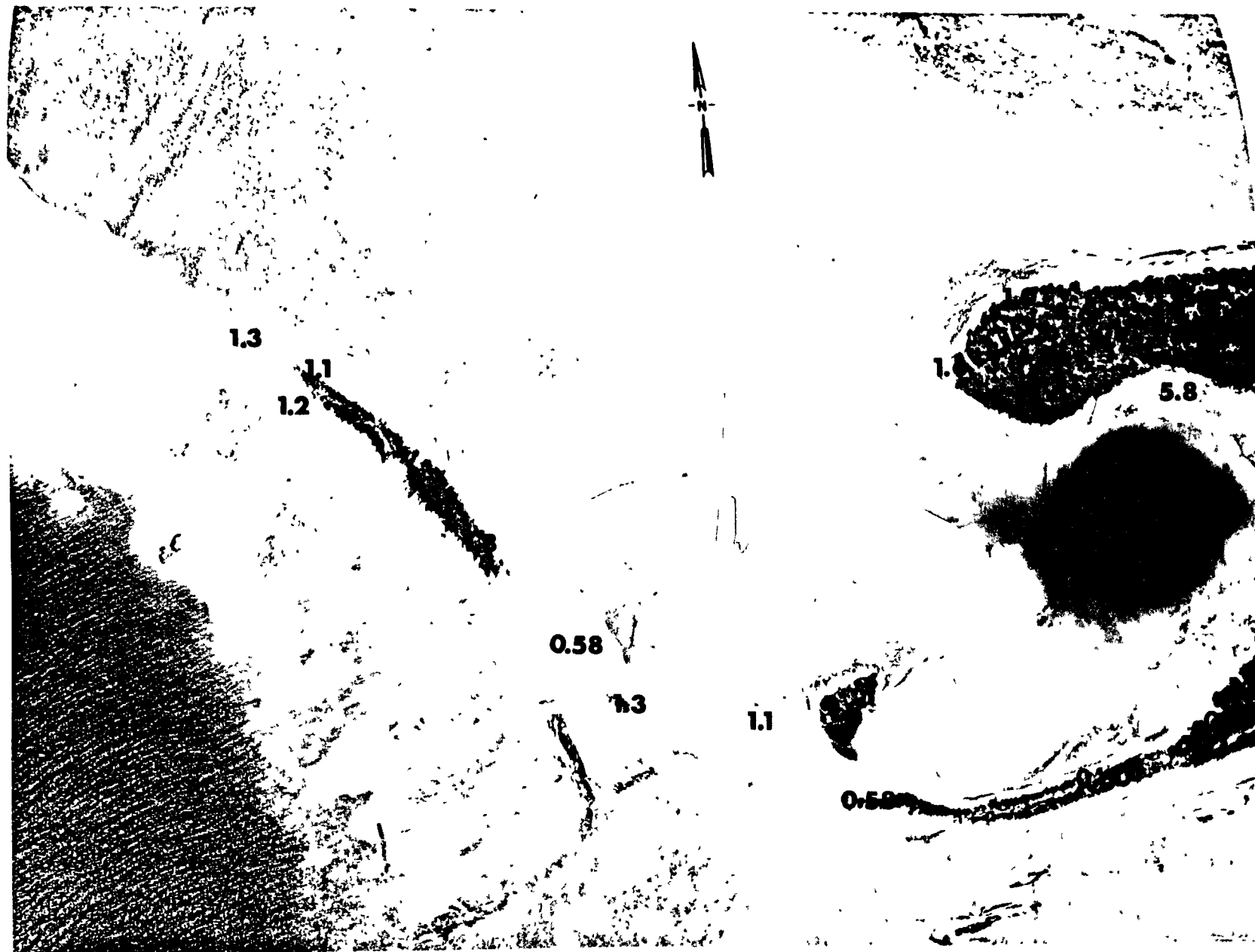


Fig. B.6.1.1. The average  $^{137}\text{Cs}$  activities (pCi/gm) in soil samples collected to a depth of 15 cm.



Fig. B.6.1.m. <sup>60</sup>Co isoexposure and isoconcentration contours. (Refer to alphabetic symbol key in this appendix.)

100 METERS

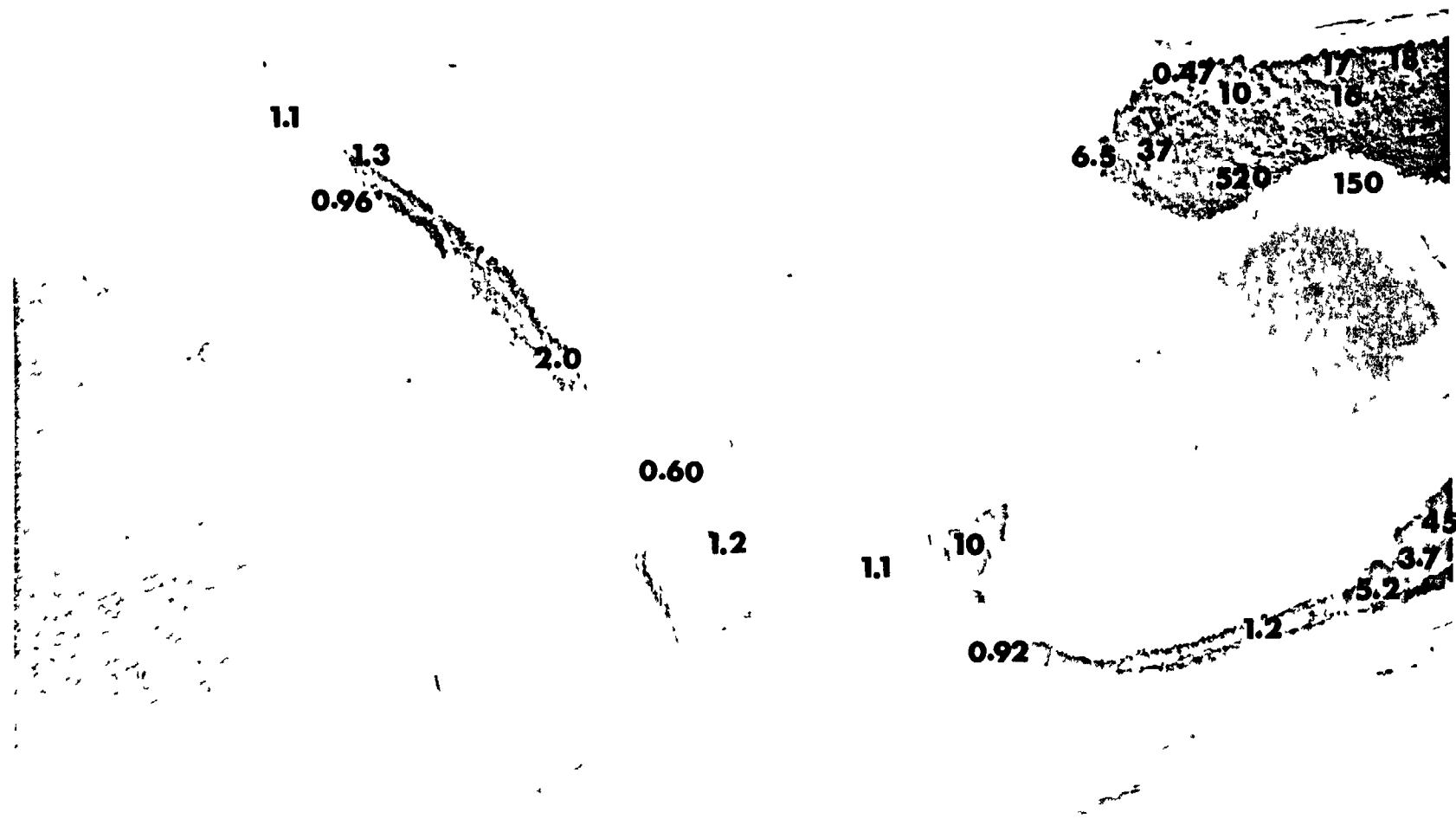
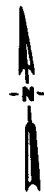


Fig. B.6.1.n. The average  $^{60}\text{Co}$  activities (pCi/gm) in soil samples collected to a depth of 15 cm.

1:10000



Fig. B.6.1.o. Terrestrial animal sample locations.

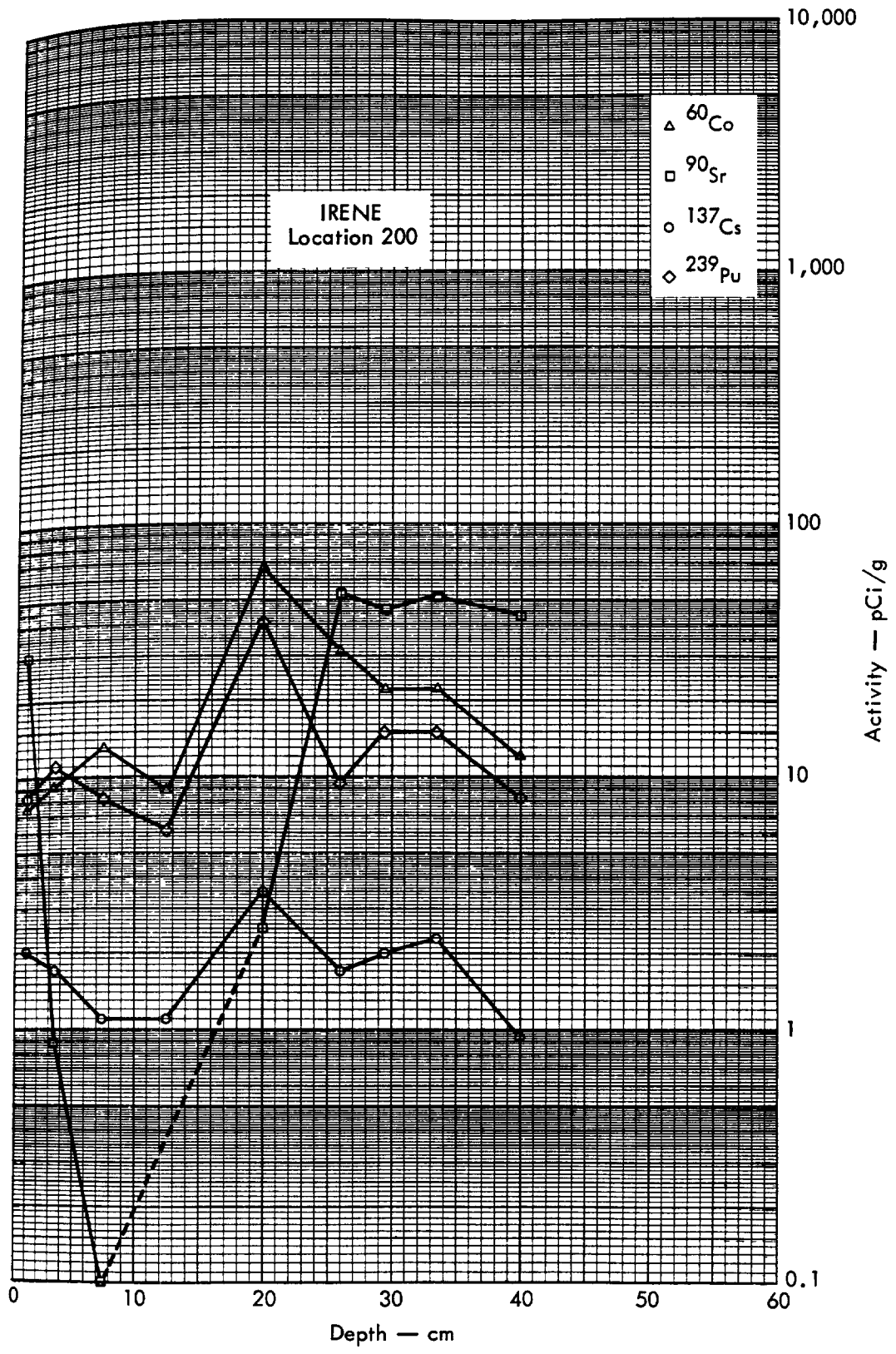


Fig. B. 6.2a. Activities of selected radionuclides as a function of soil depth.

100 METERS



IRENE B

Fig. B.7.1.a.

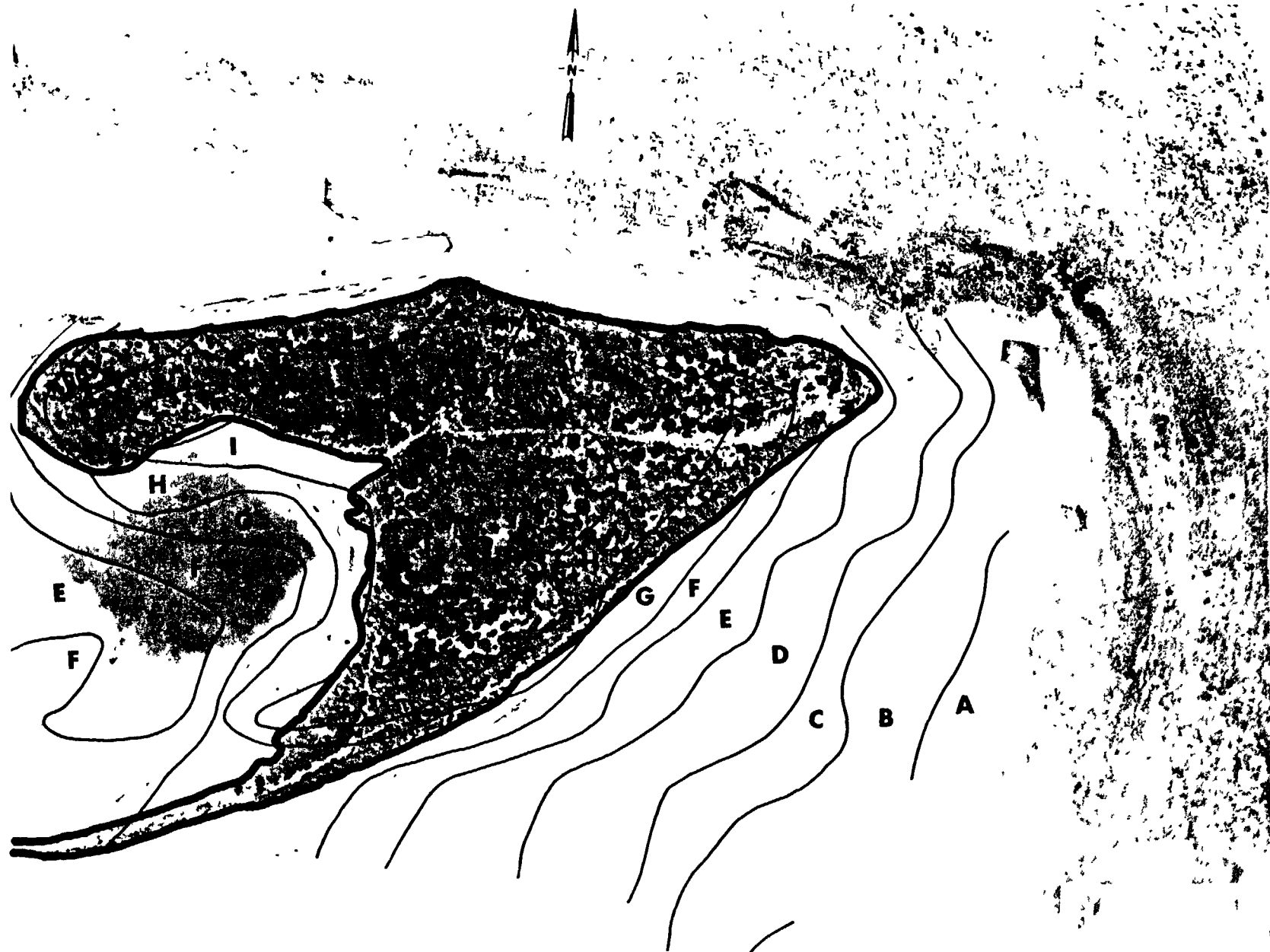


Fig. B.7.1.b. Gross count isoexposure contours. (Refer to alphabetic symbol key in this appendix.)

100 METERS

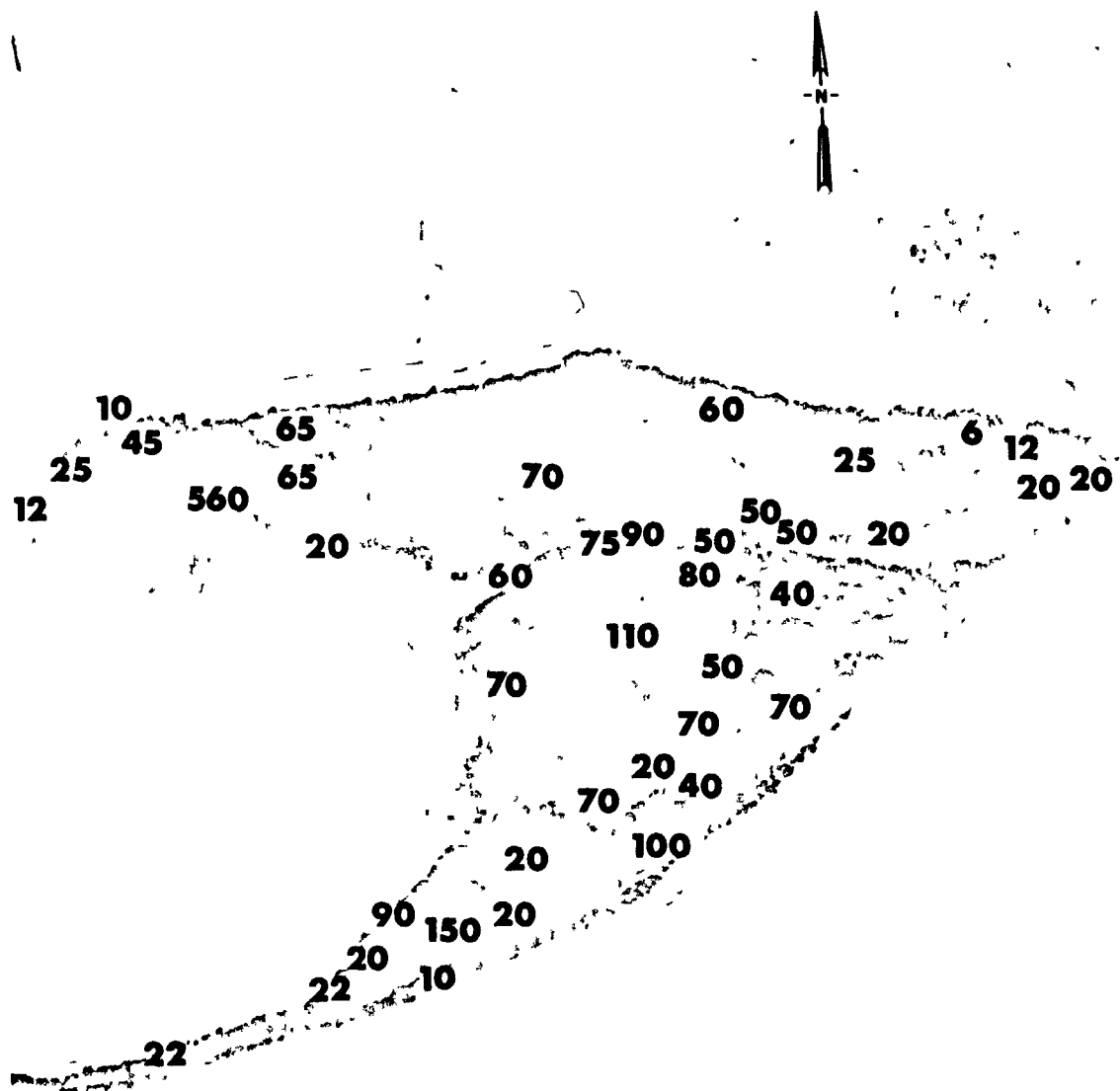


Fig. B.7.1.d. The gamma background exposure rate ( $\mu\text{R/hr}$ ) at 1 m above the ground, measured with a portable NaI scintillation counter.



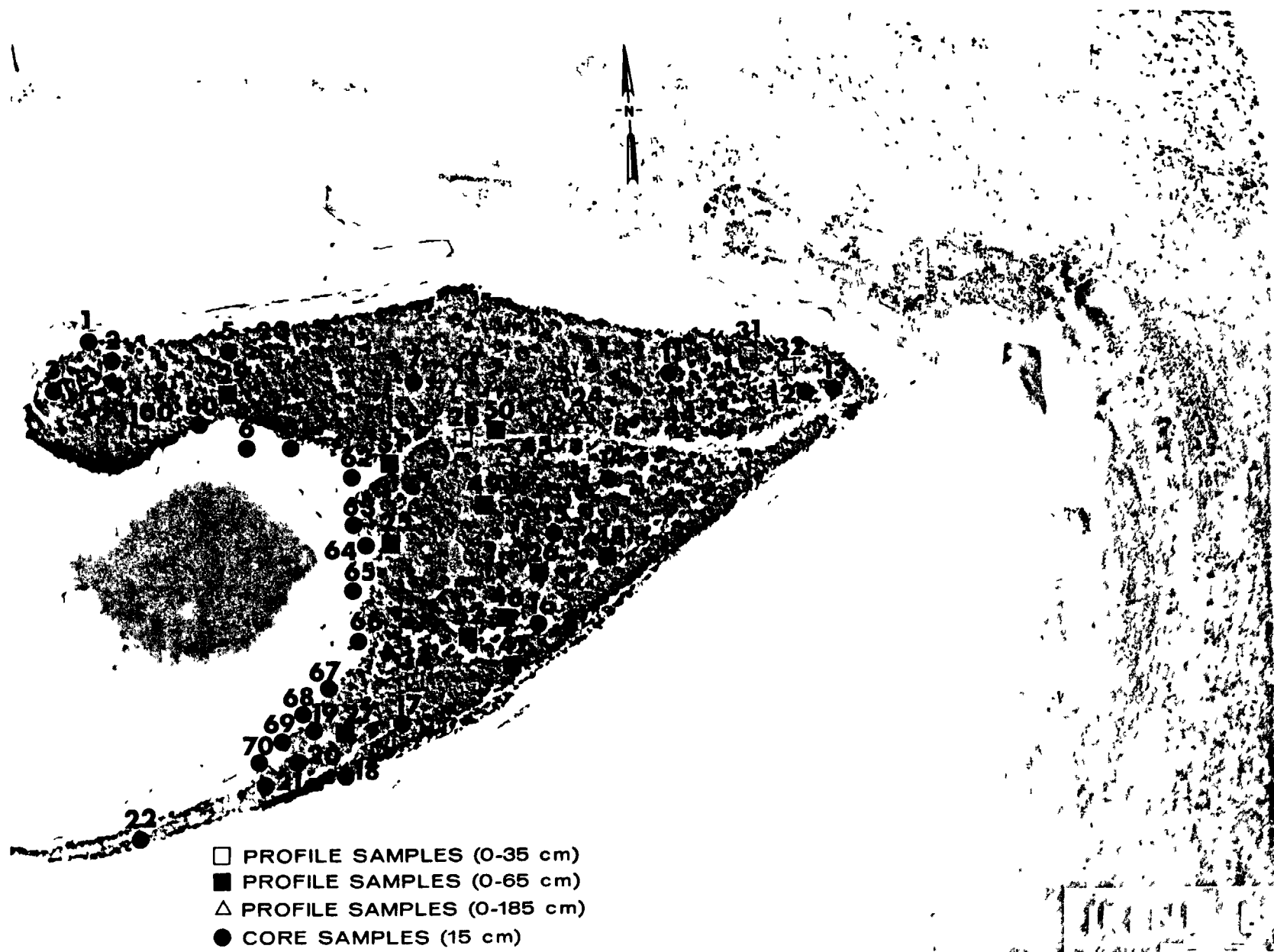


Fig. B.7.1.f. Soil-sample locations.

100 METERS



△ △ △ MESSERSCHMIDIA  
○ ○ ○ SCAEVOLA  
□ GUETTARDA

▽ LEPTURUS  
⊕ SURIANA  
⊗ SEDGE

● COCONUT

**IRENE B**

Fig. B.7.1.g. Vegetation sample locations.

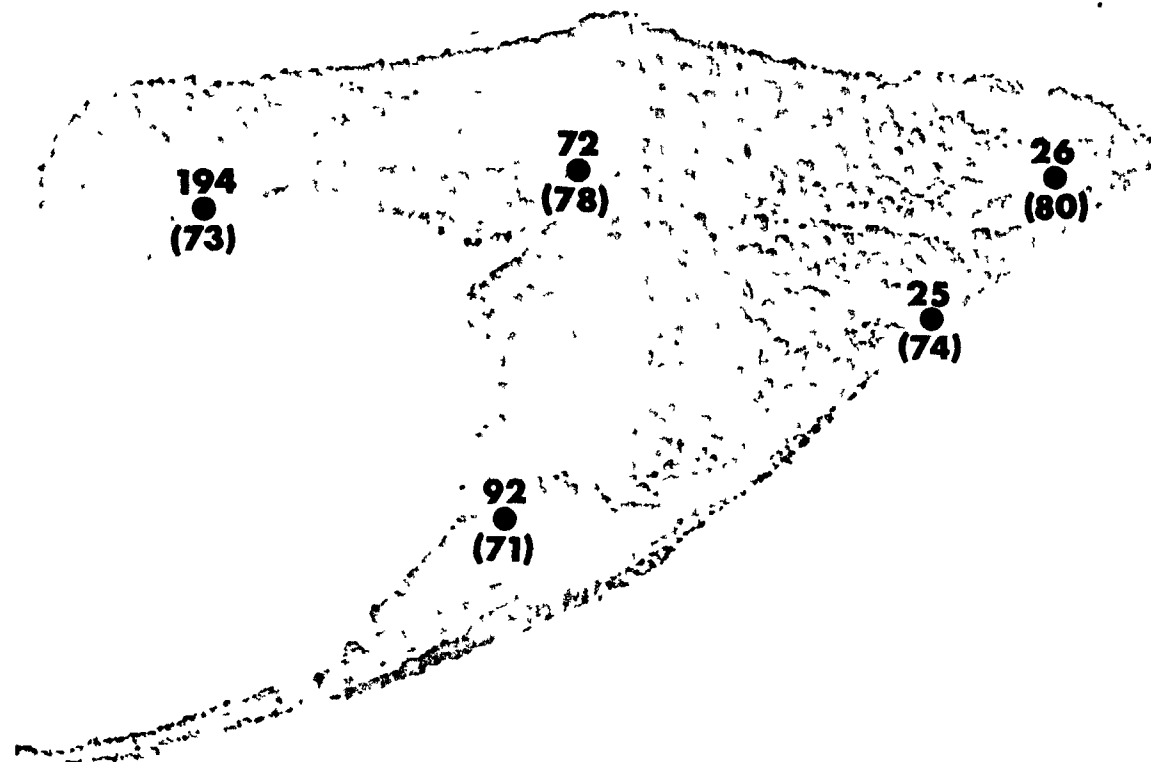


Fig. B.7.1.h. The gamma-ray exposure rates ( $\mu\text{R/hr}$ ) measured 1 m above the ground by the LiF thermoluminescent dosimeters (TLD). The numbers shown in parentheses denote the location identification numbers.

100 METERS

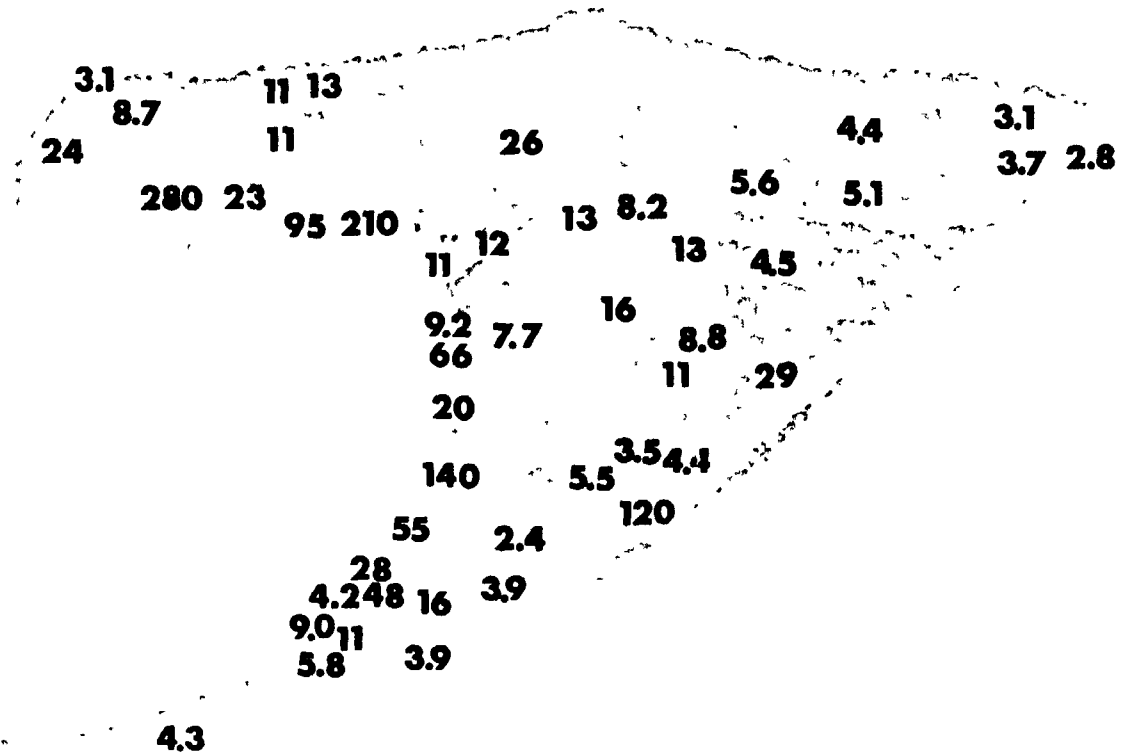
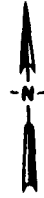


Fig. B.7.1.i. The average  $^{239}\text{Pu}$  activities (pCi/gm) in soil samples collected to a depth of 15 cm.



Fig. B.7.1.j. The average  $^{90}\text{Sr}$  activities (pCi/gm) in soil samples collected to a depth of 15 cm.

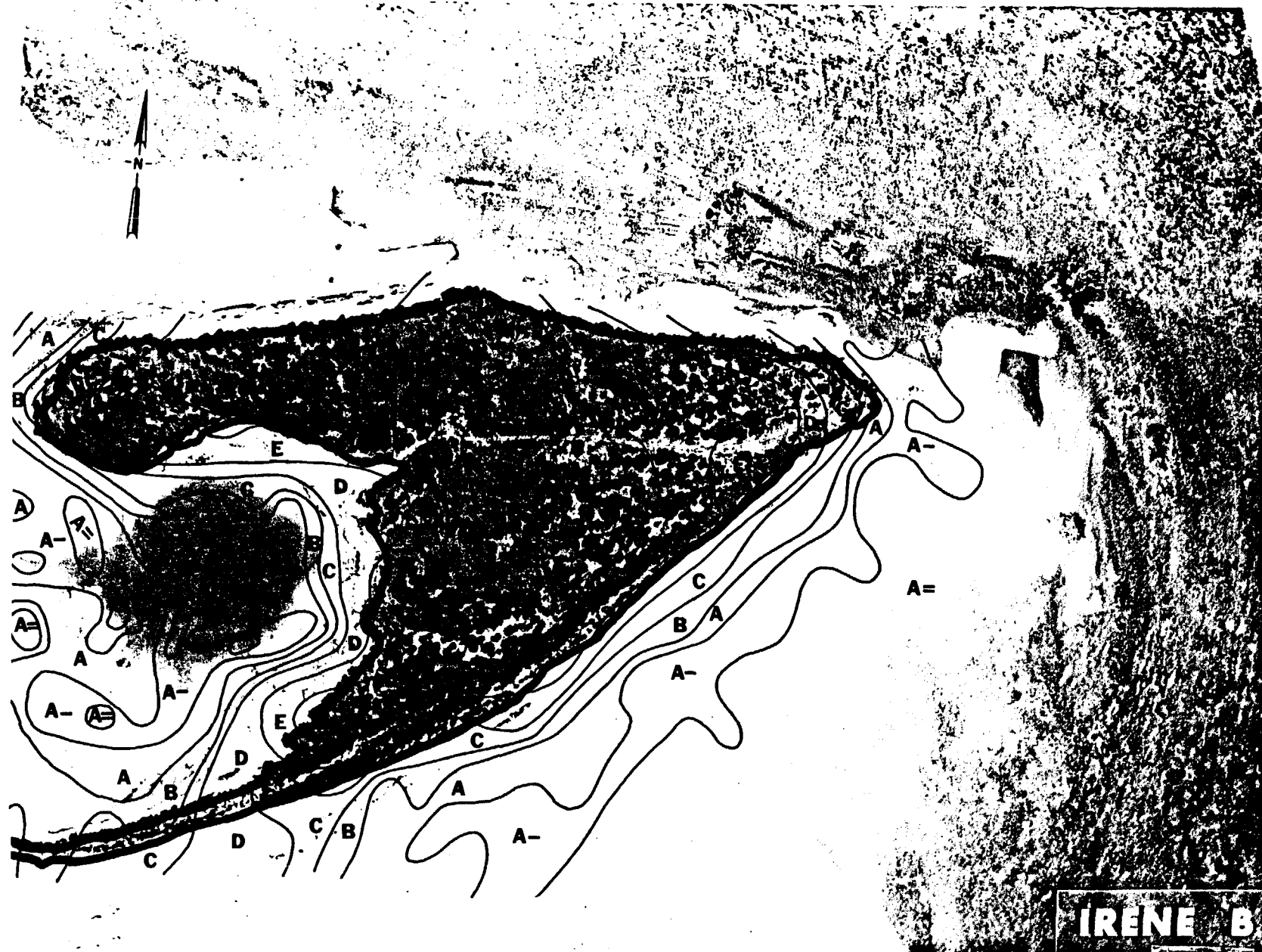
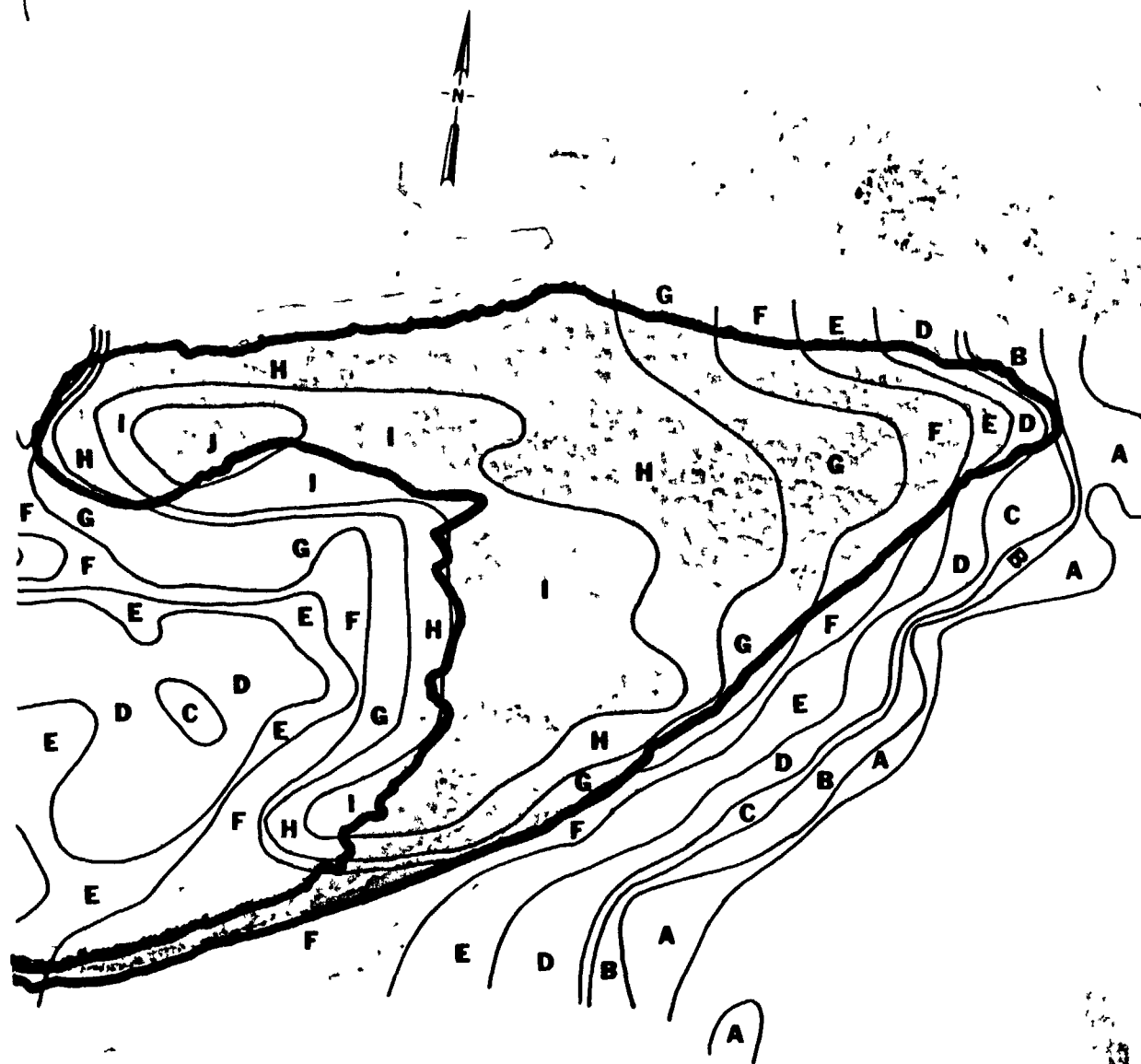


Fig. B.7.1.k. <sup>137</sup>Cs isoexposure and isoconcentration contours. (Refer to alphabetic symbol key in this appendix.)





**IRENE B**

Fig. B.7.1.m. <sup>60</sup>Co Isoexposure and isoconcentration contours. (Refer to alphabetic symbol key in this appendix.)



SCALE 1:1000

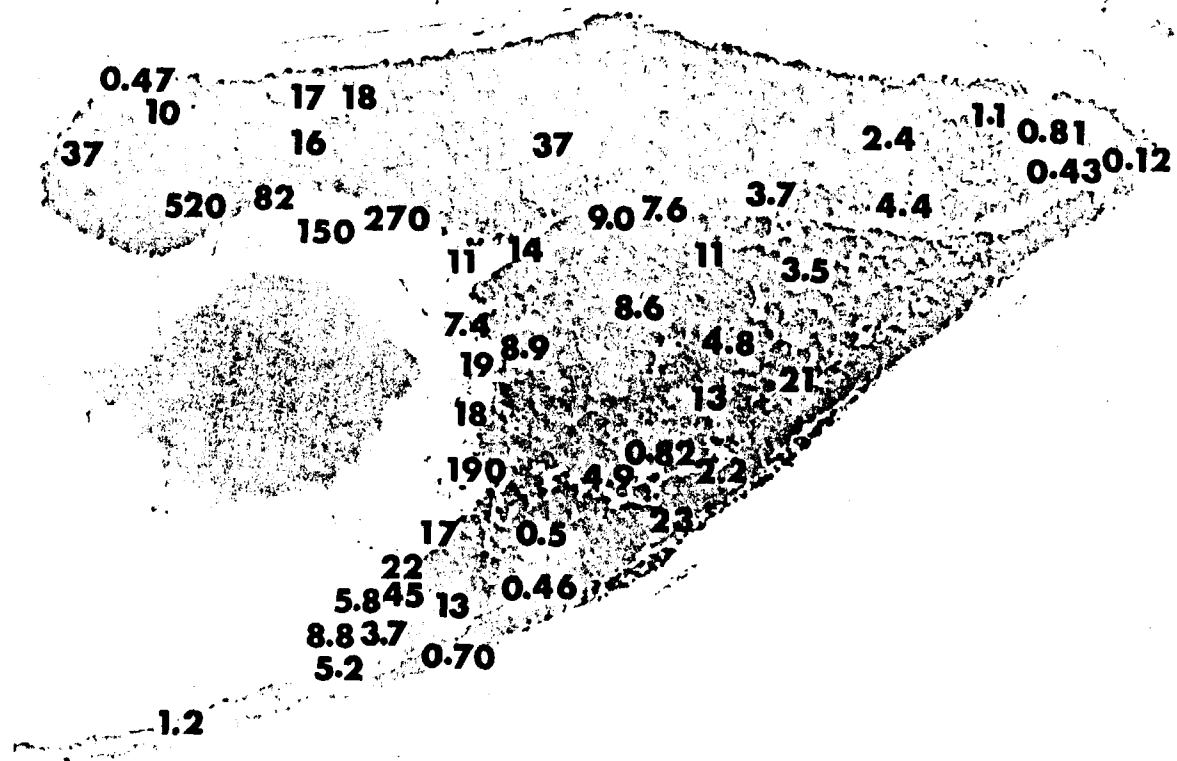
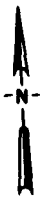


Fig. B.7.1.n. The average <sup>60</sup>Co activities (pCi/gm) in soil samples collected to a depth of 15 cm.

SCALE BAR

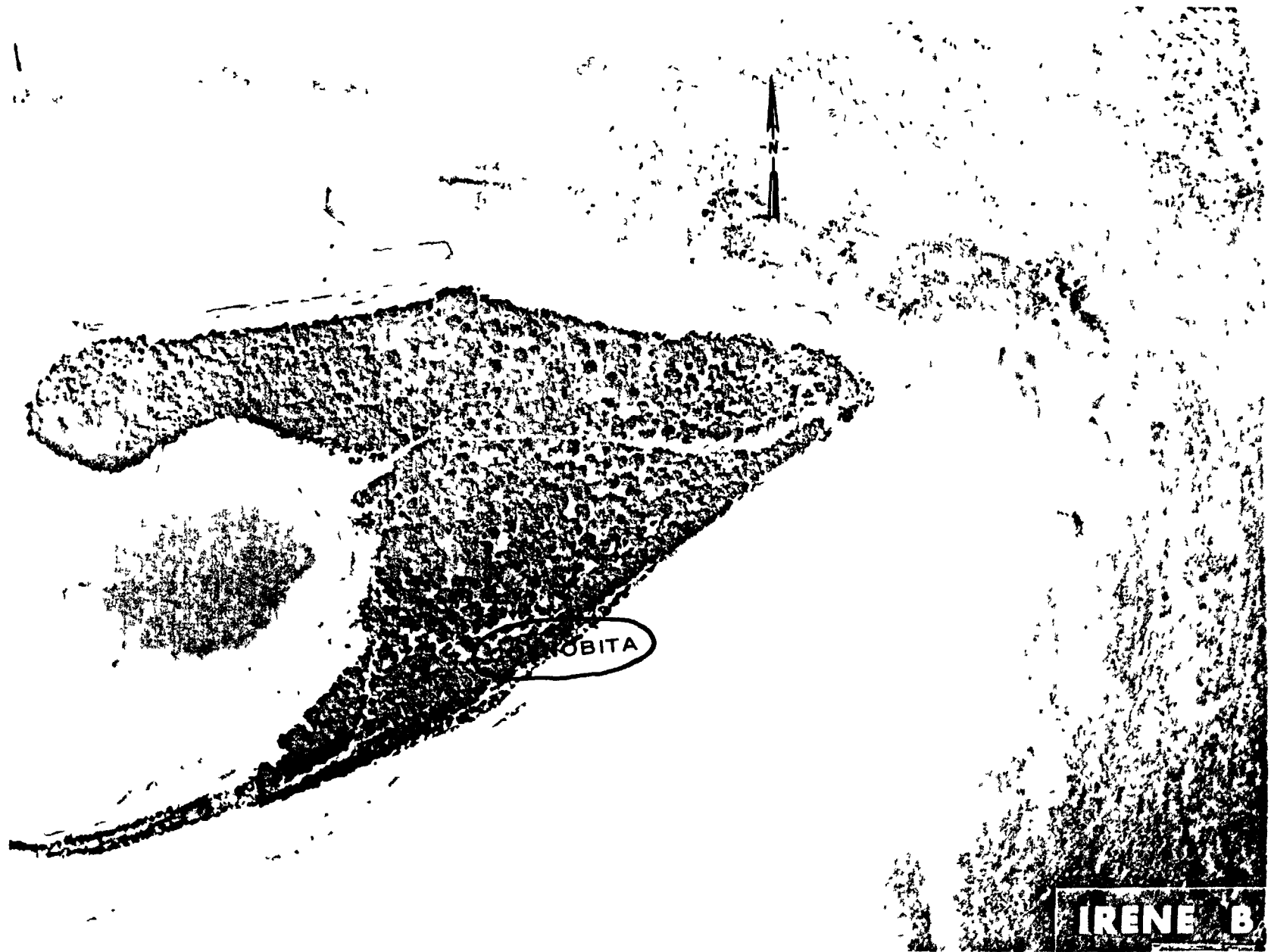


Fig. B.7.1.o. Terrestrial animal sample locations.

IRENE B

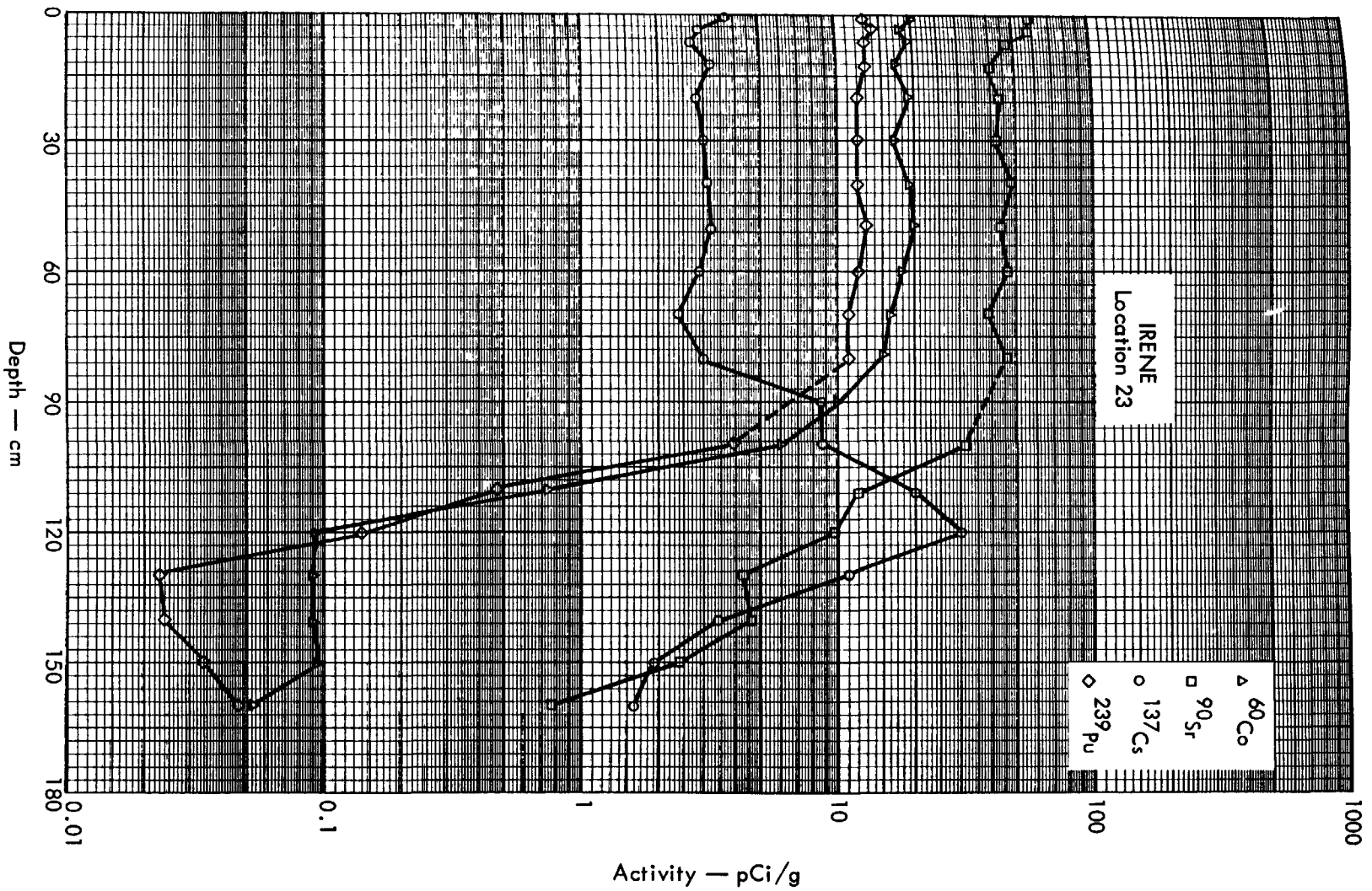


Fig. B.7.2a. Activities of selected radionuclides as a function of soil depth.

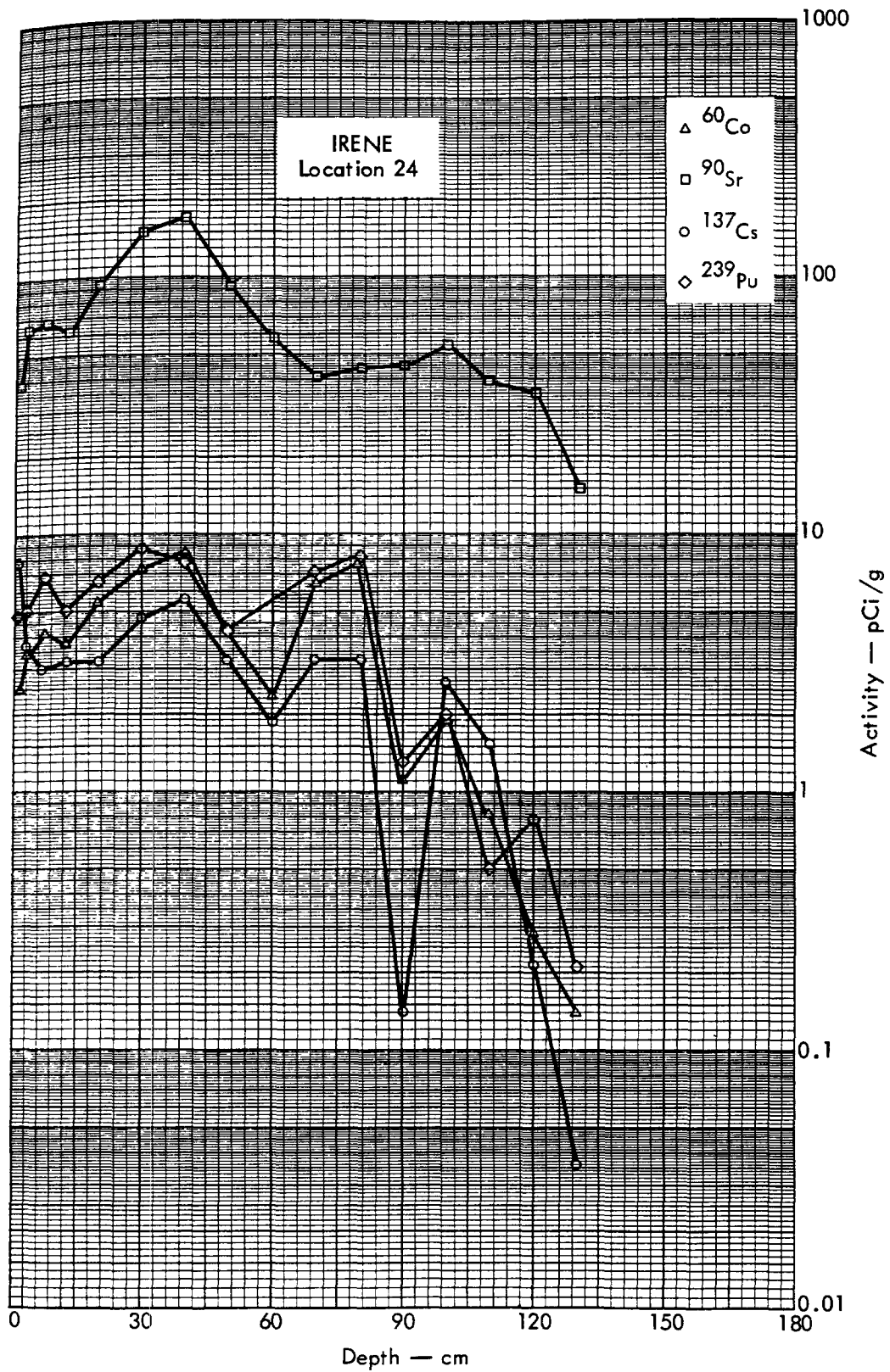


Fig. B.7.2b. Activities of selected radionuclides as a function of soil depth.

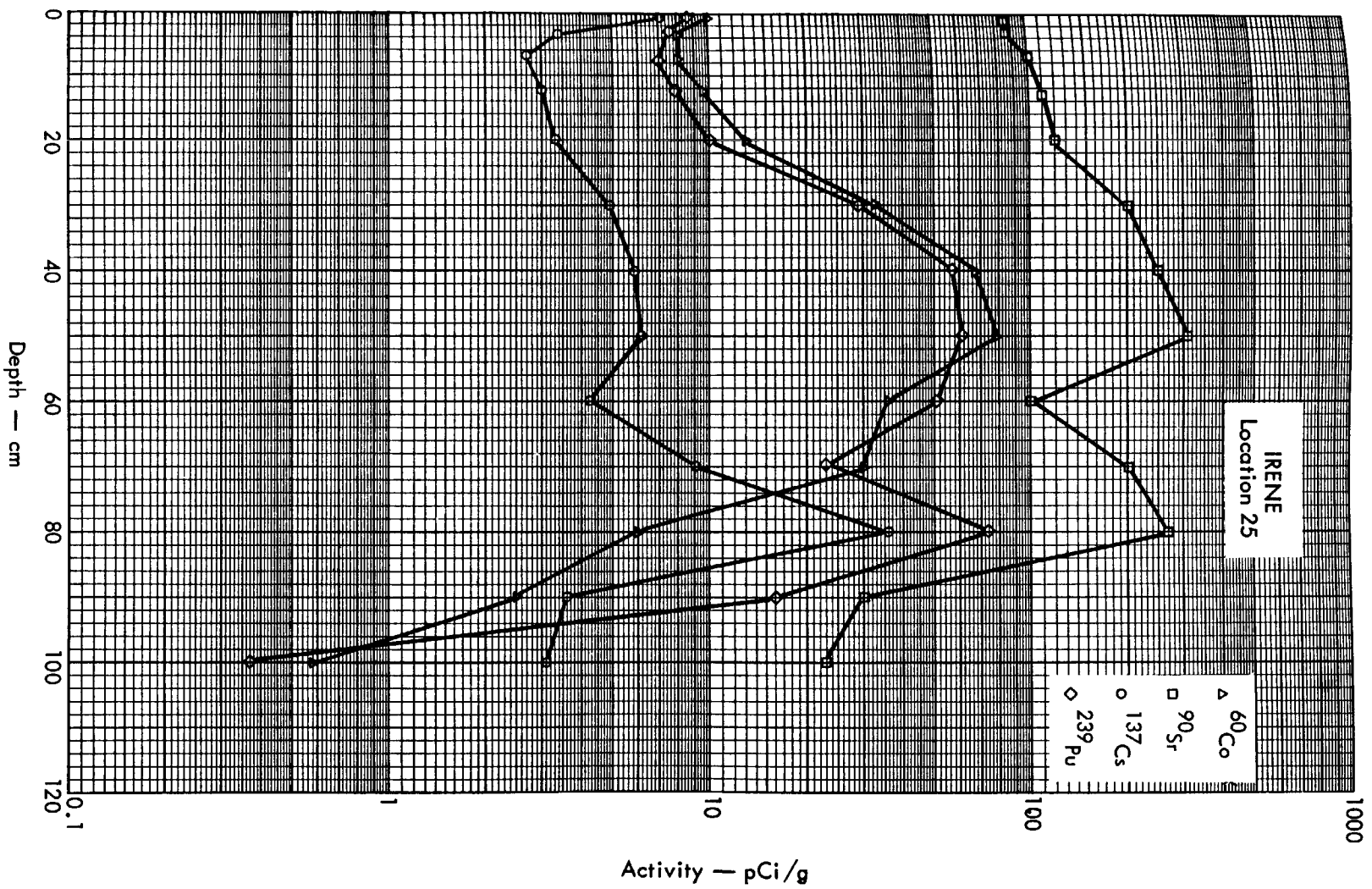


Fig. B.7.2c. Activities of selected radionuclides as a function of soil depth.

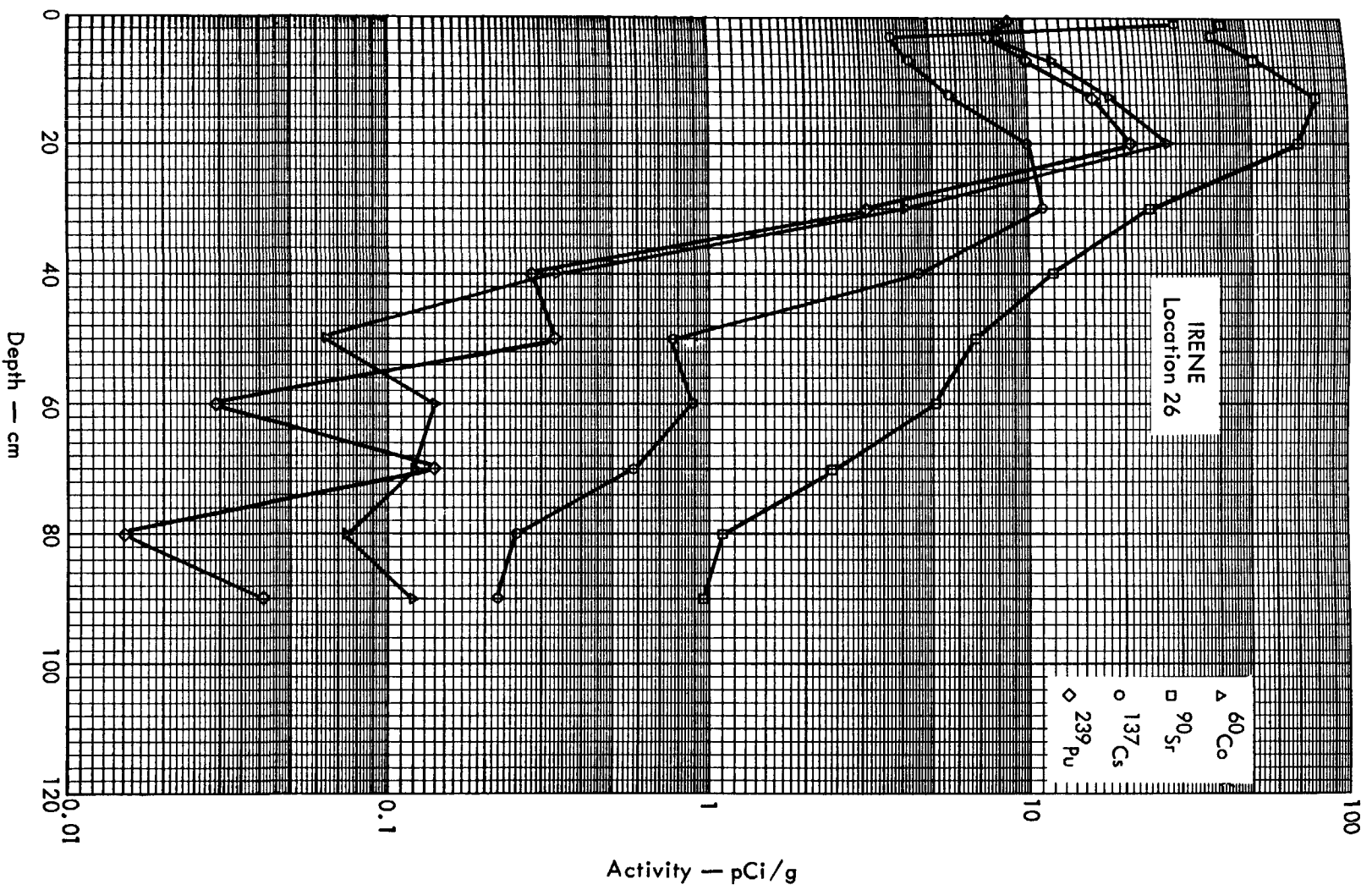


Fig. B.7.2d. Activities of selected radionuclides as a function of soil depth.

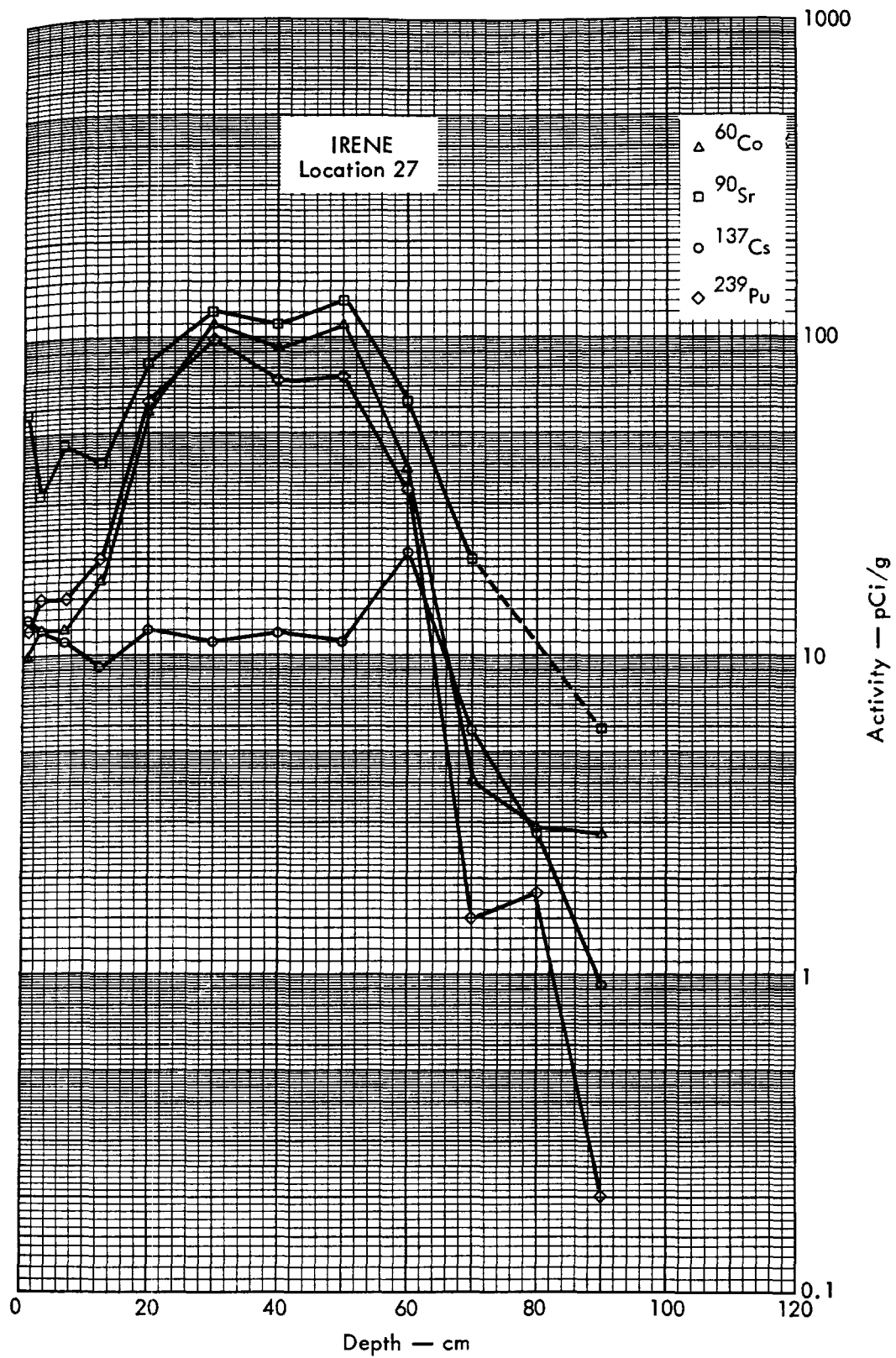


Fig. B.7.2e. Activities of selected radionuclides as a function of soil depth.

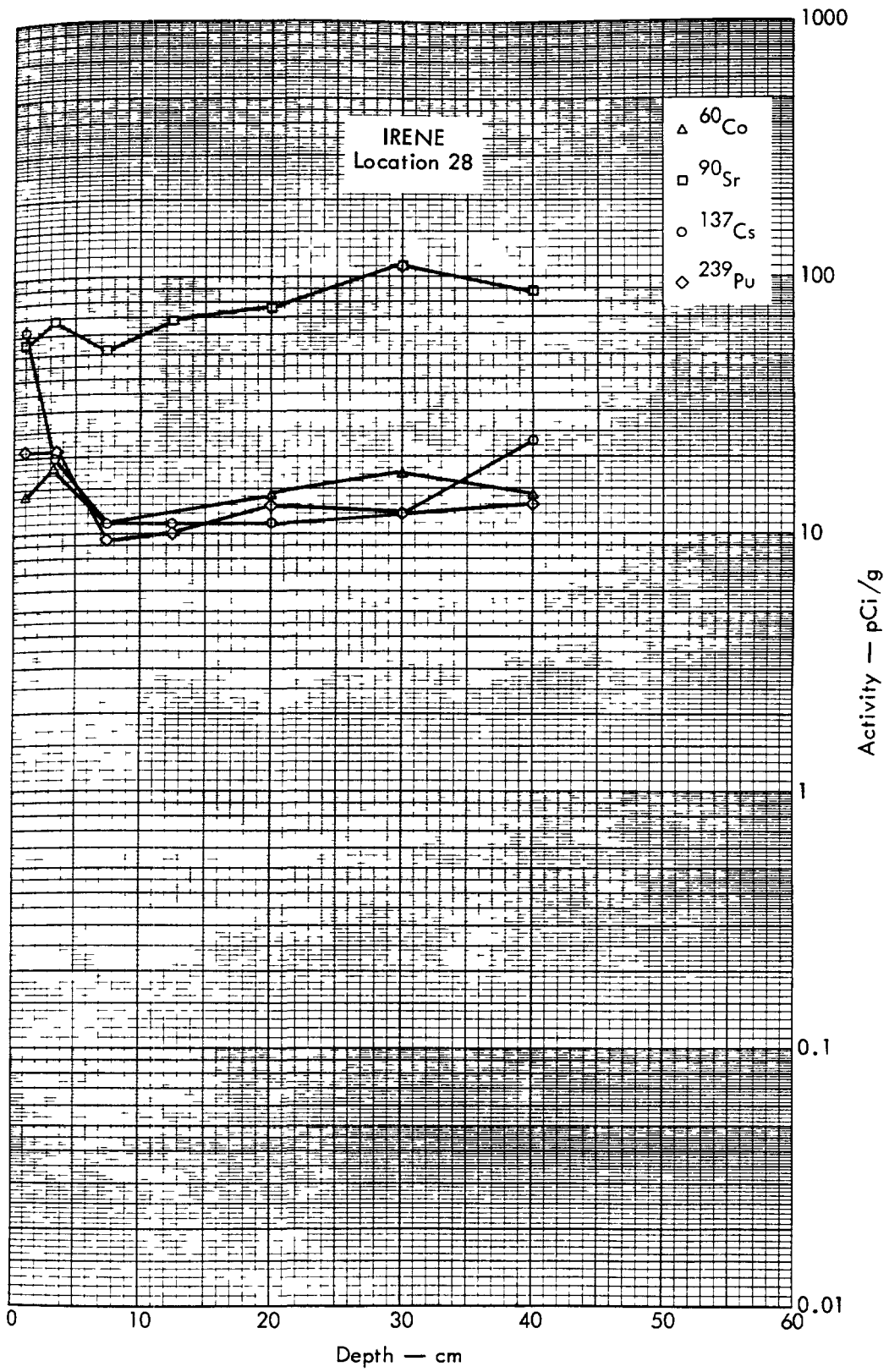


Fig. B. 7.2f. Activities of selected radionuclides as a function of soil depth.



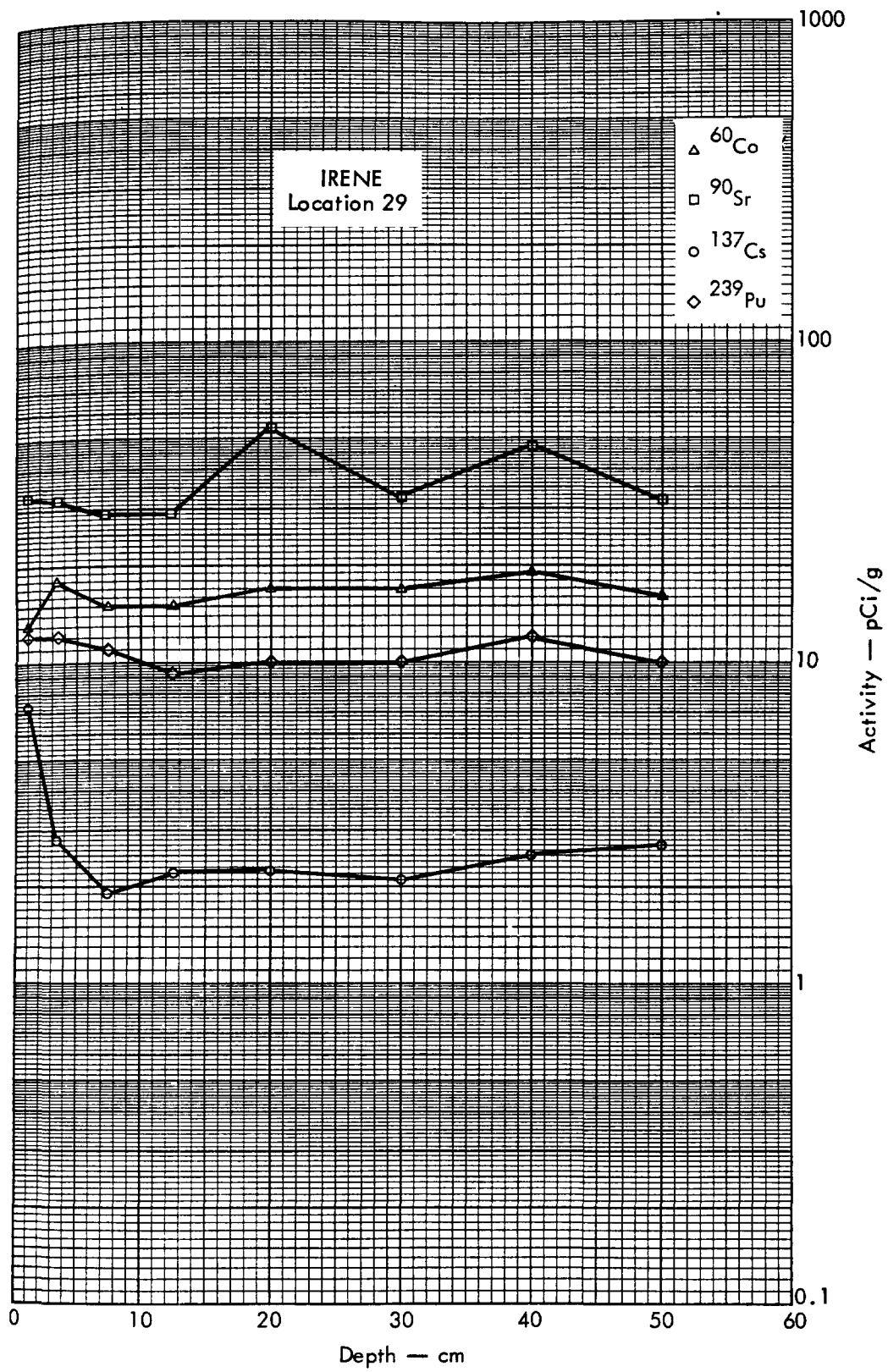


Fig. B.7.2g. Activities of selected radionuclides as a function of soil depth.

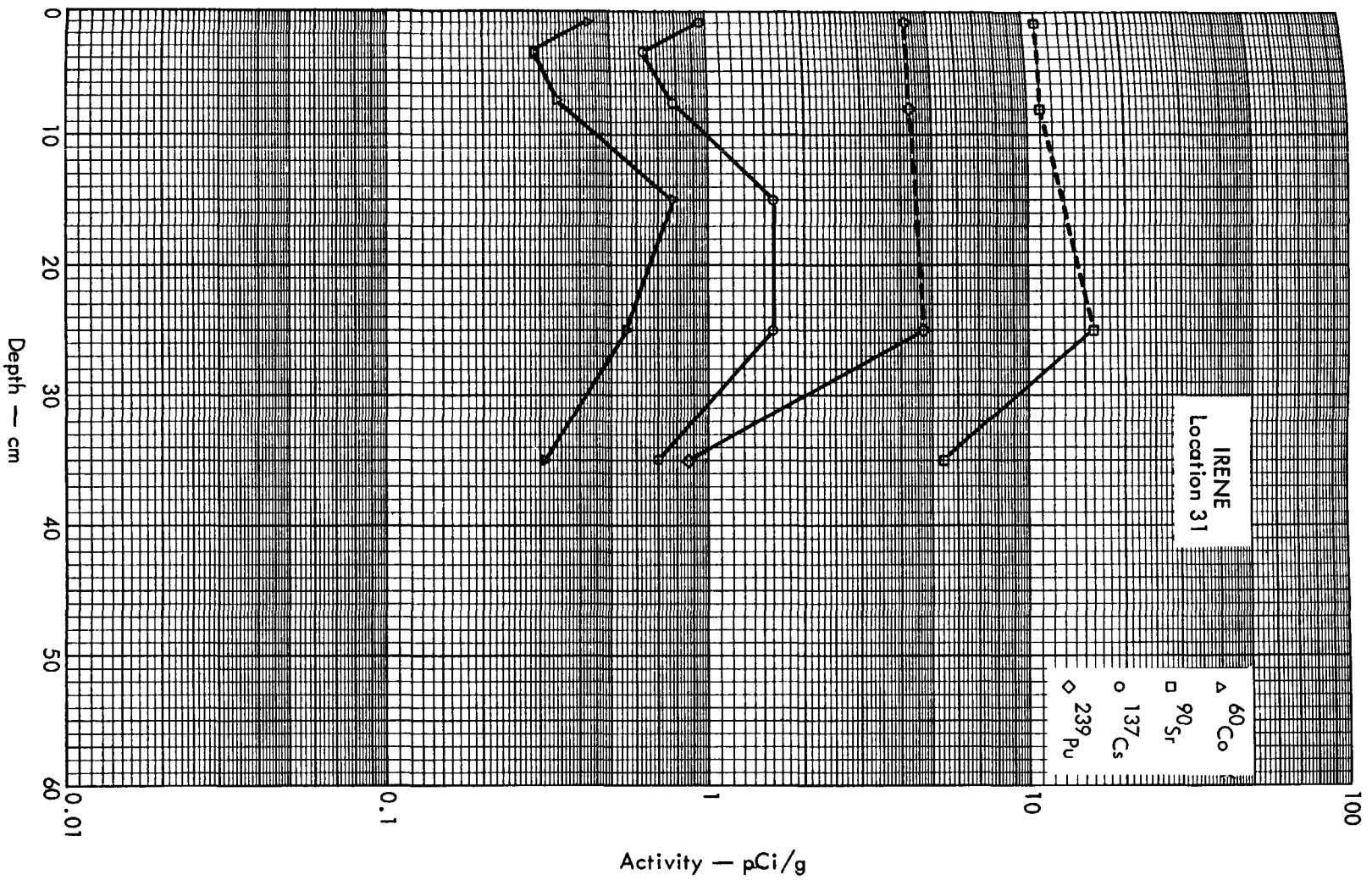


Fig. B.7.2h. Activities of selected radionuclides as a function of soil depth.

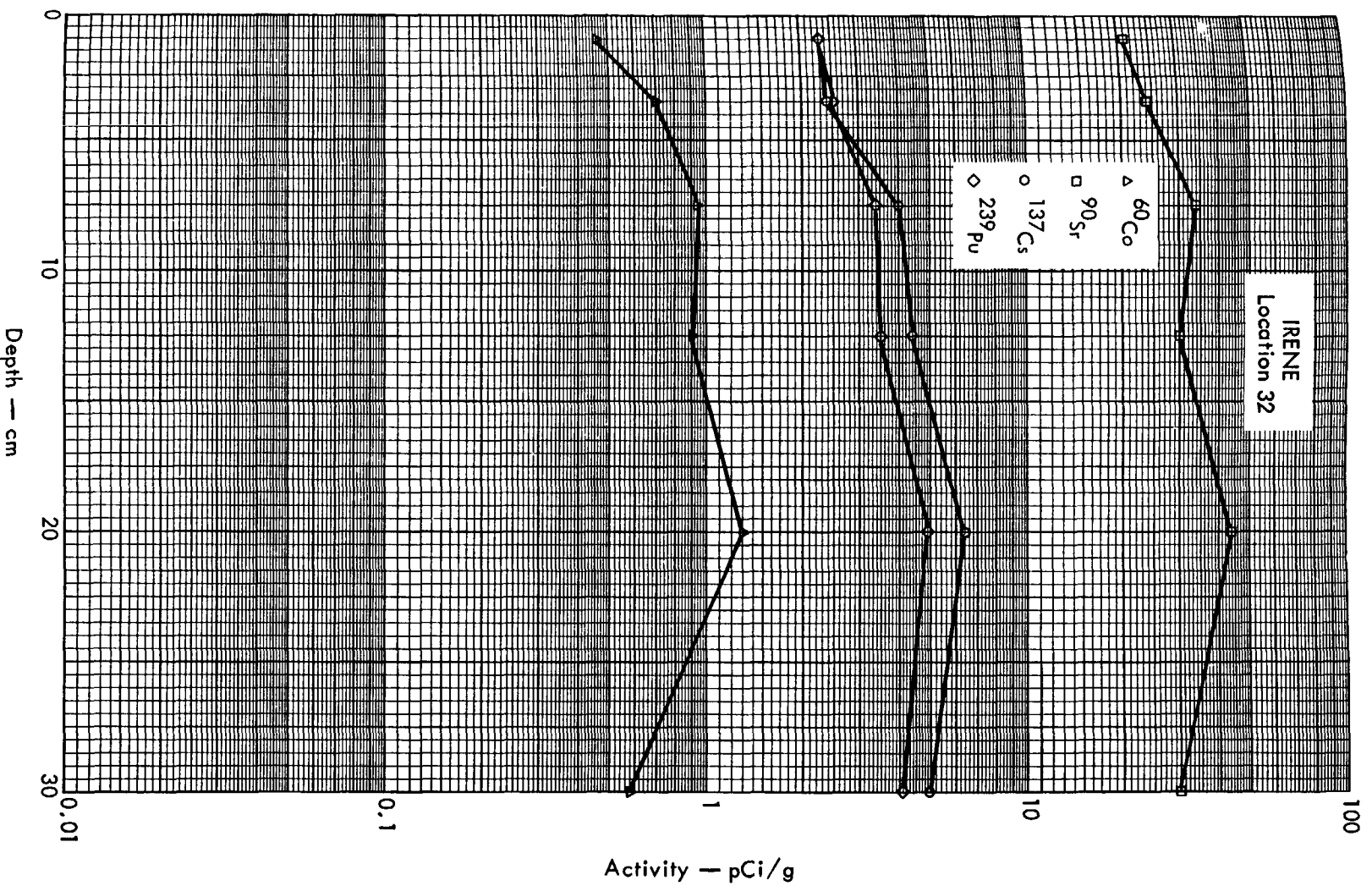


Fig. B. 7.2i. Activities of selected radionuclides as a function of soil depth.

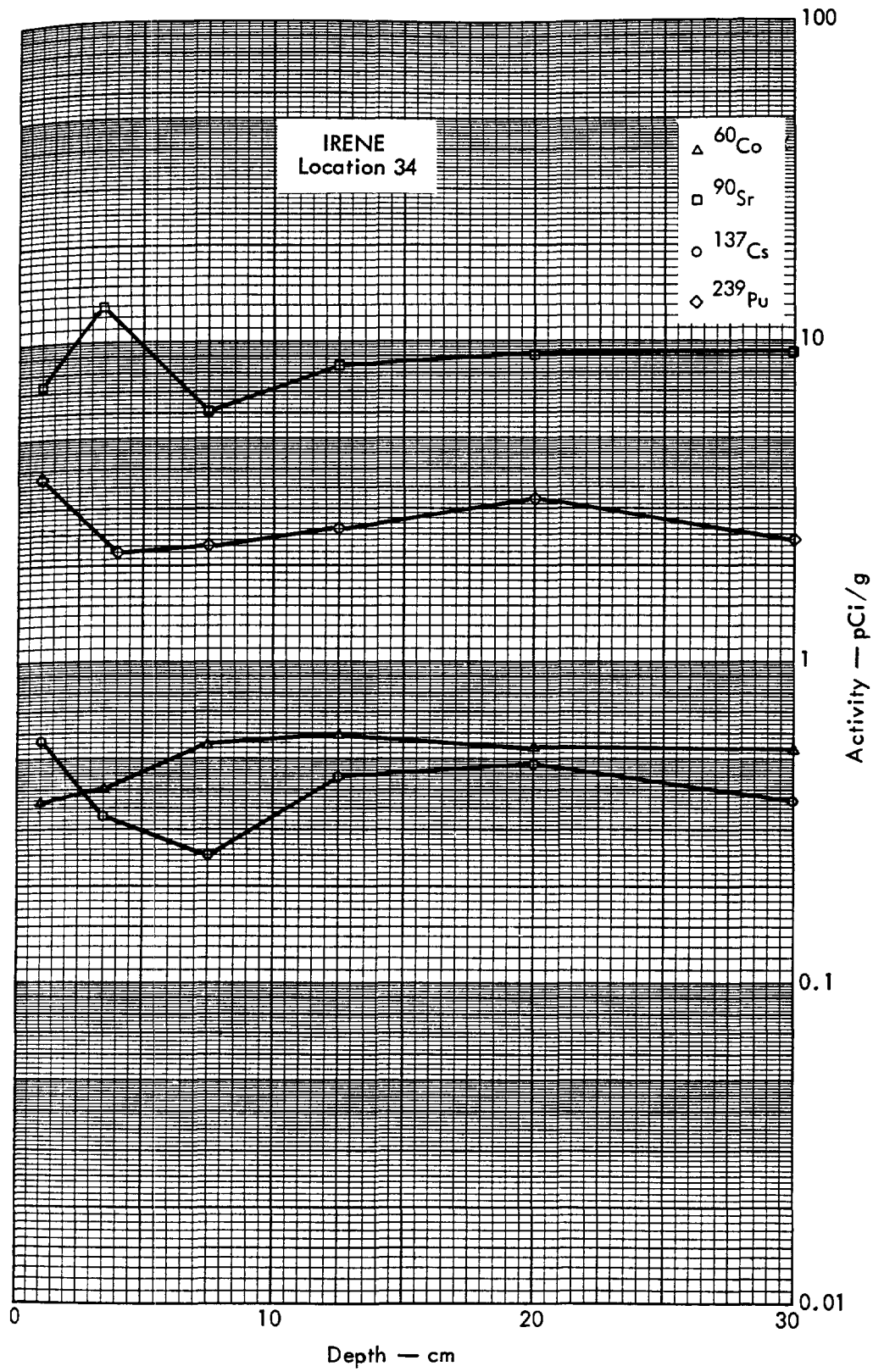


Fig. B. 7.2j. Activities of selected radionuclides as a function of soil depth.

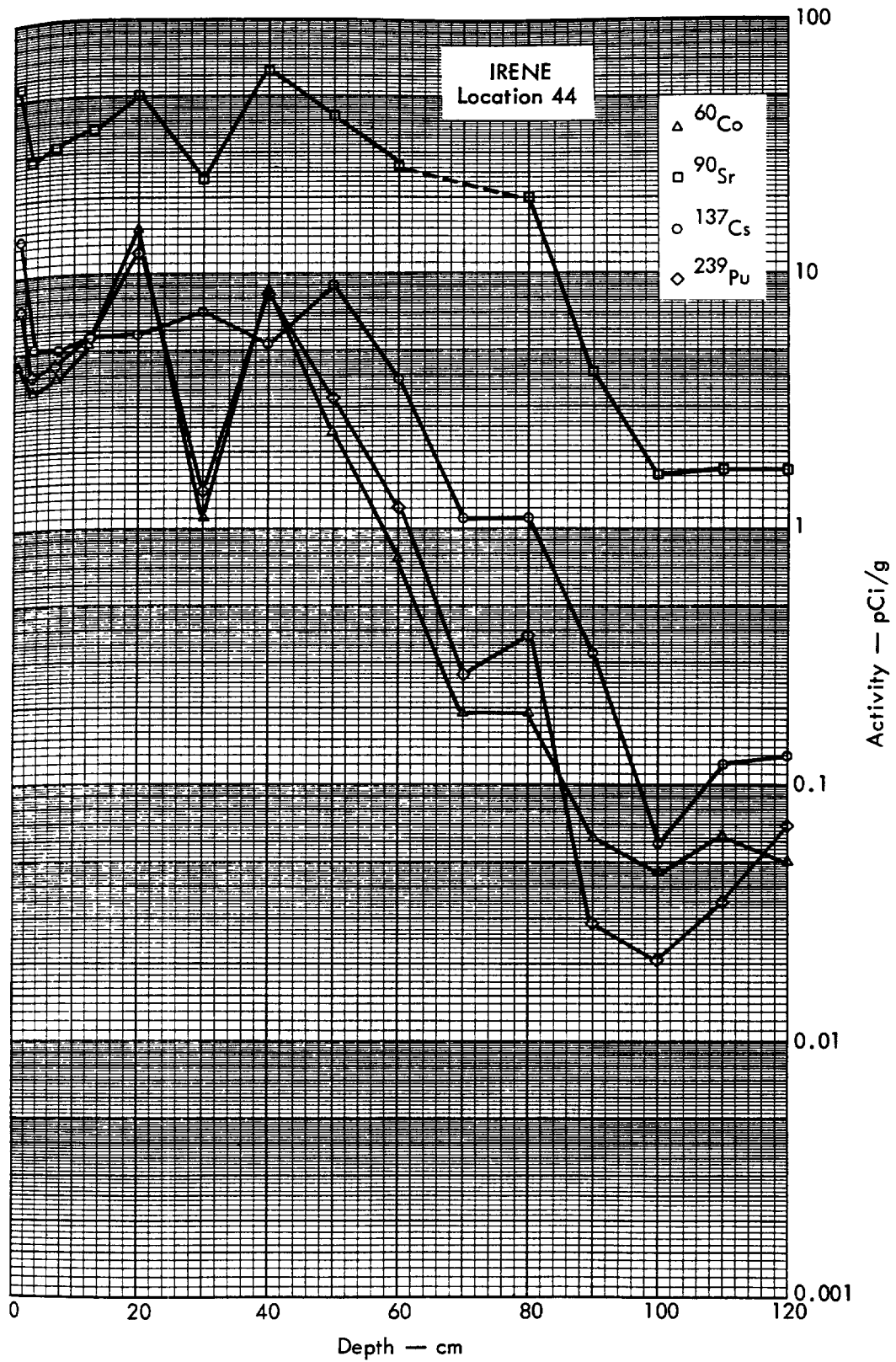


Fig. B.7.2k. Activities of selected radionuclides as a function of soil depth.

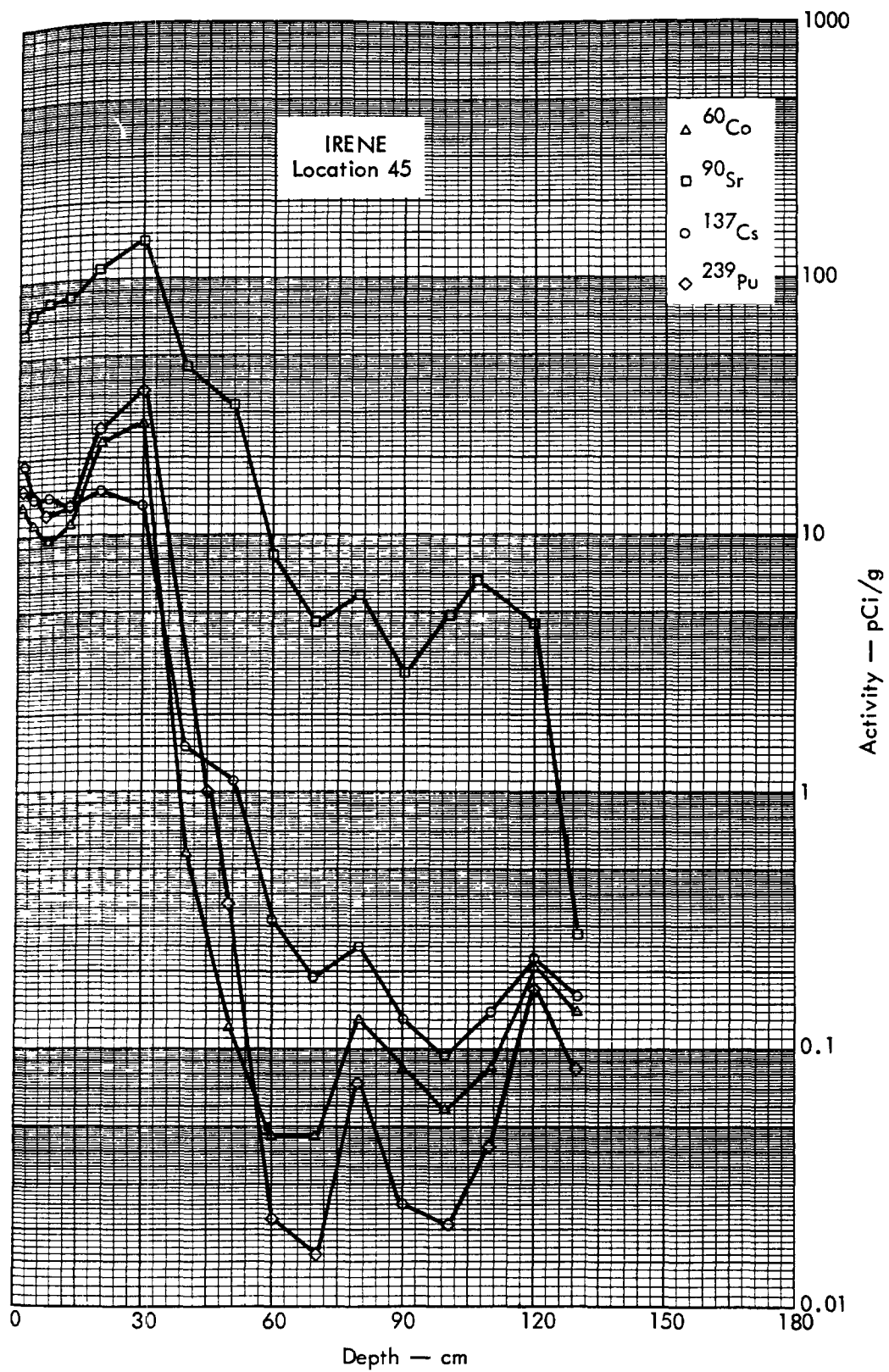


Fig. B. 7.21. Activities of selected radionuclides as a function of soil depth.

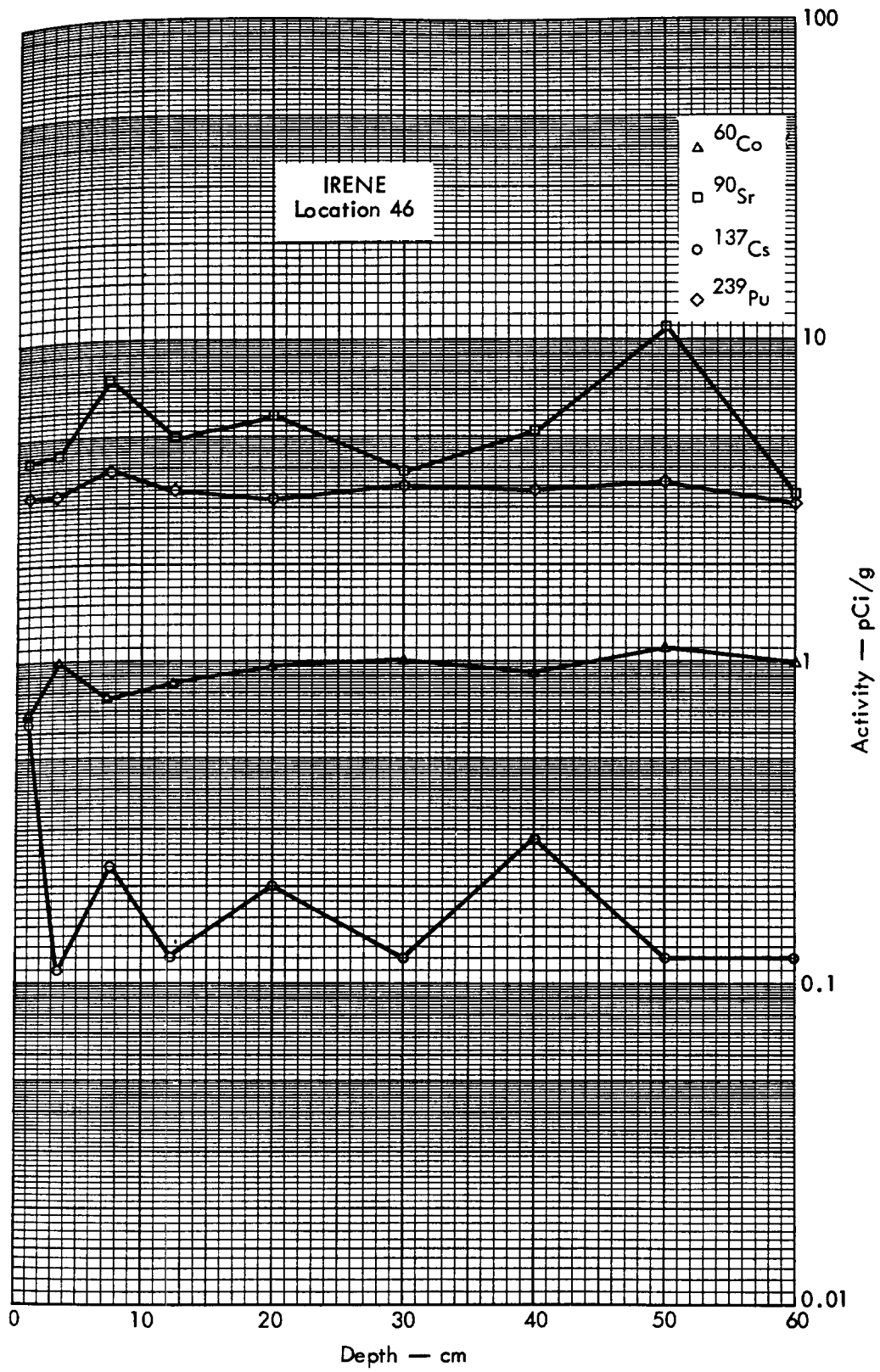


Fig. B. 7.2m. Activities of selected radionuclides as a function of soil depth.

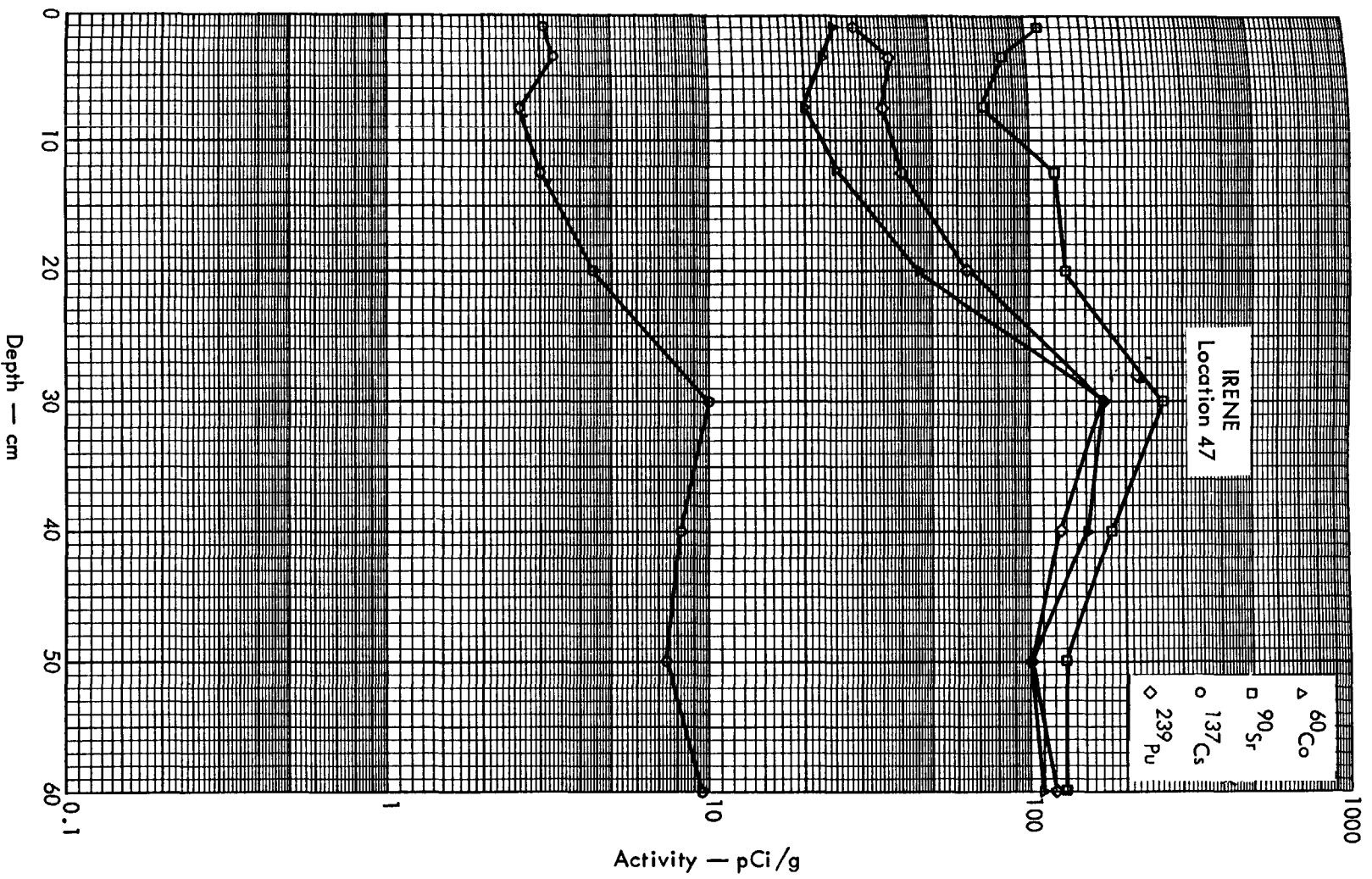


Fig. B.7.2n. Activities of selected radionuclides as a function of soil depth.



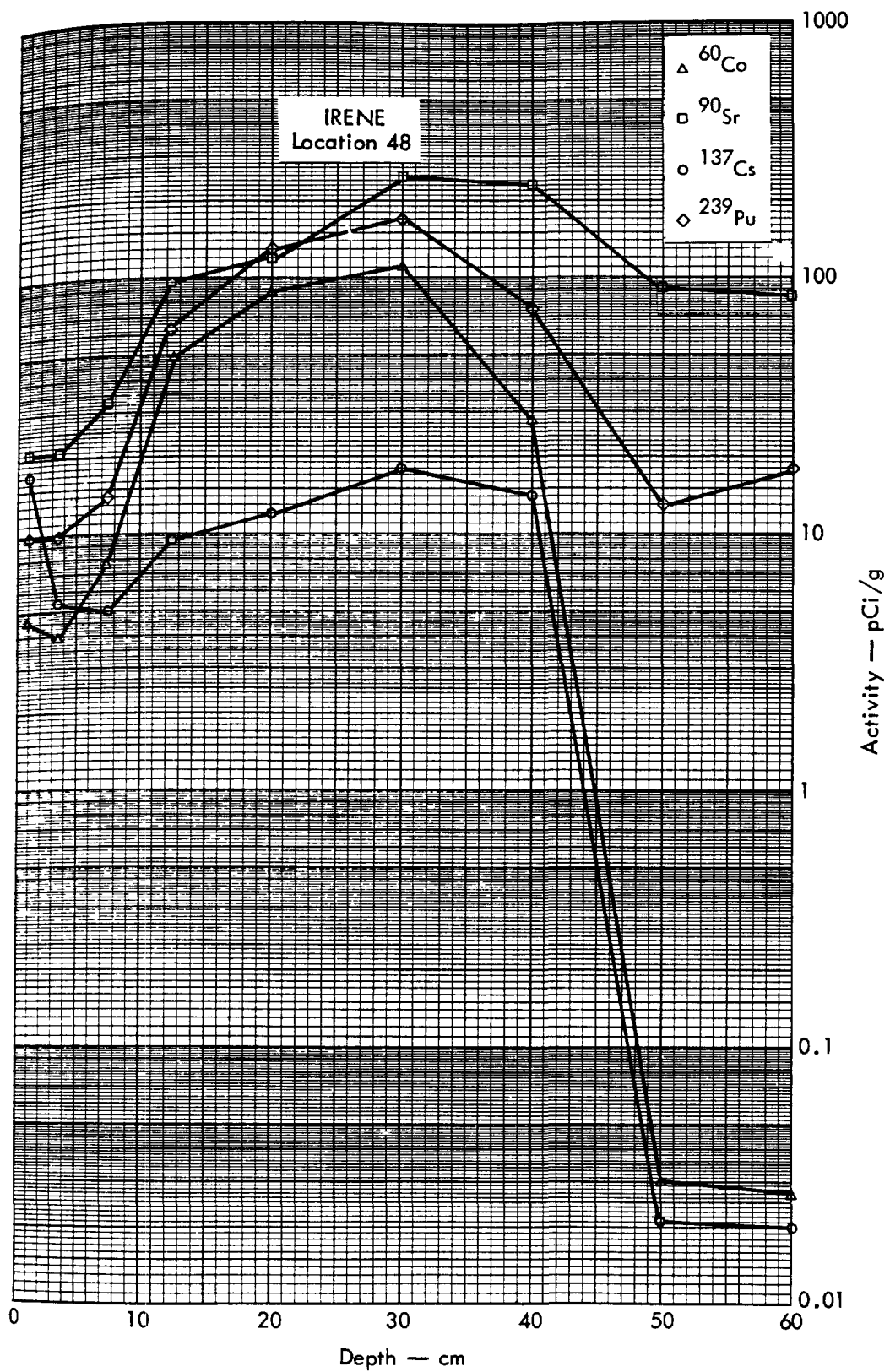


Fig. B.7.2o. Activities of selected radionuclides as a function of soil depth.

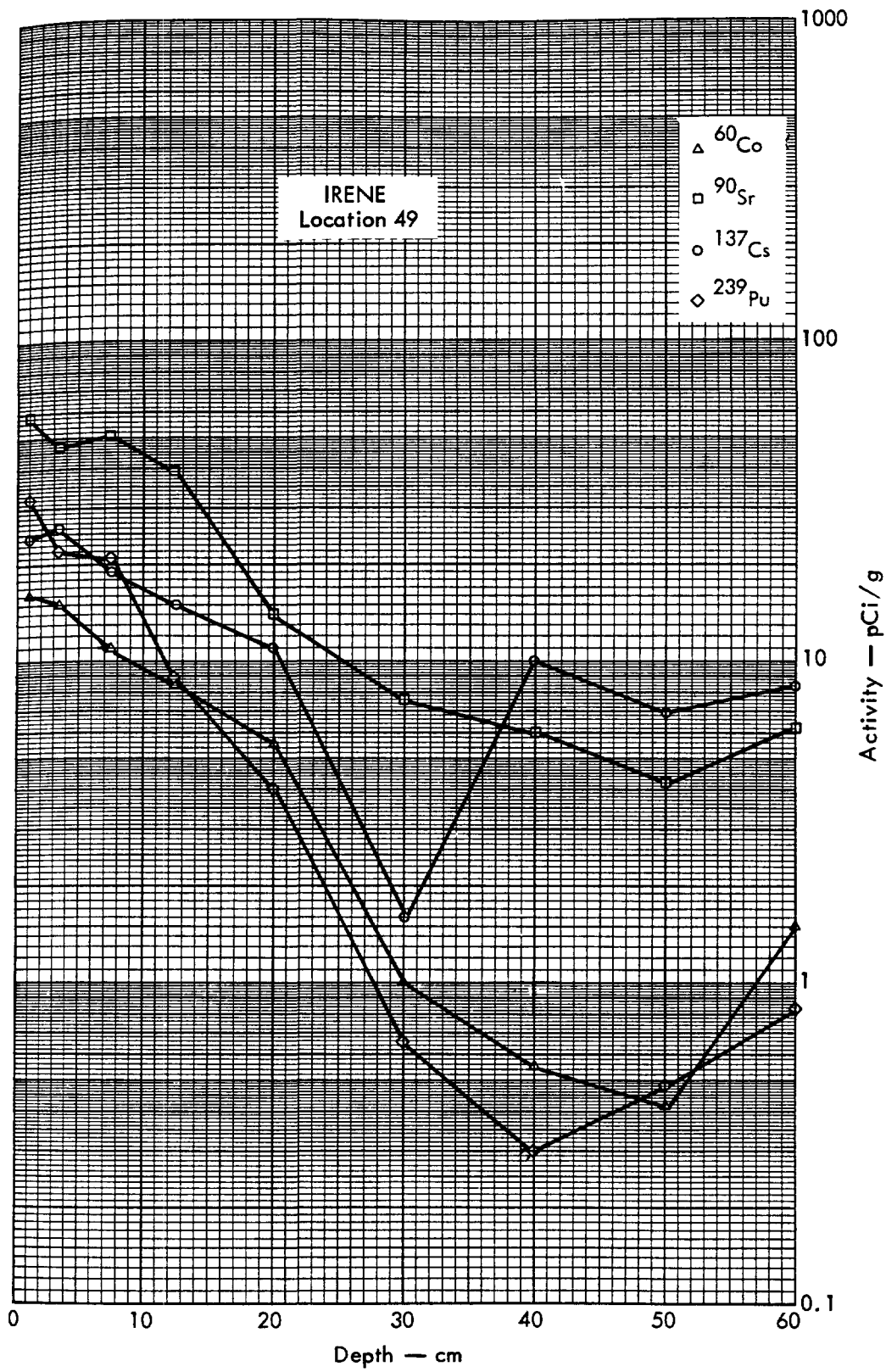


Fig. B. 7.2p. Activities of selected radionuclides as a function of soil depth.

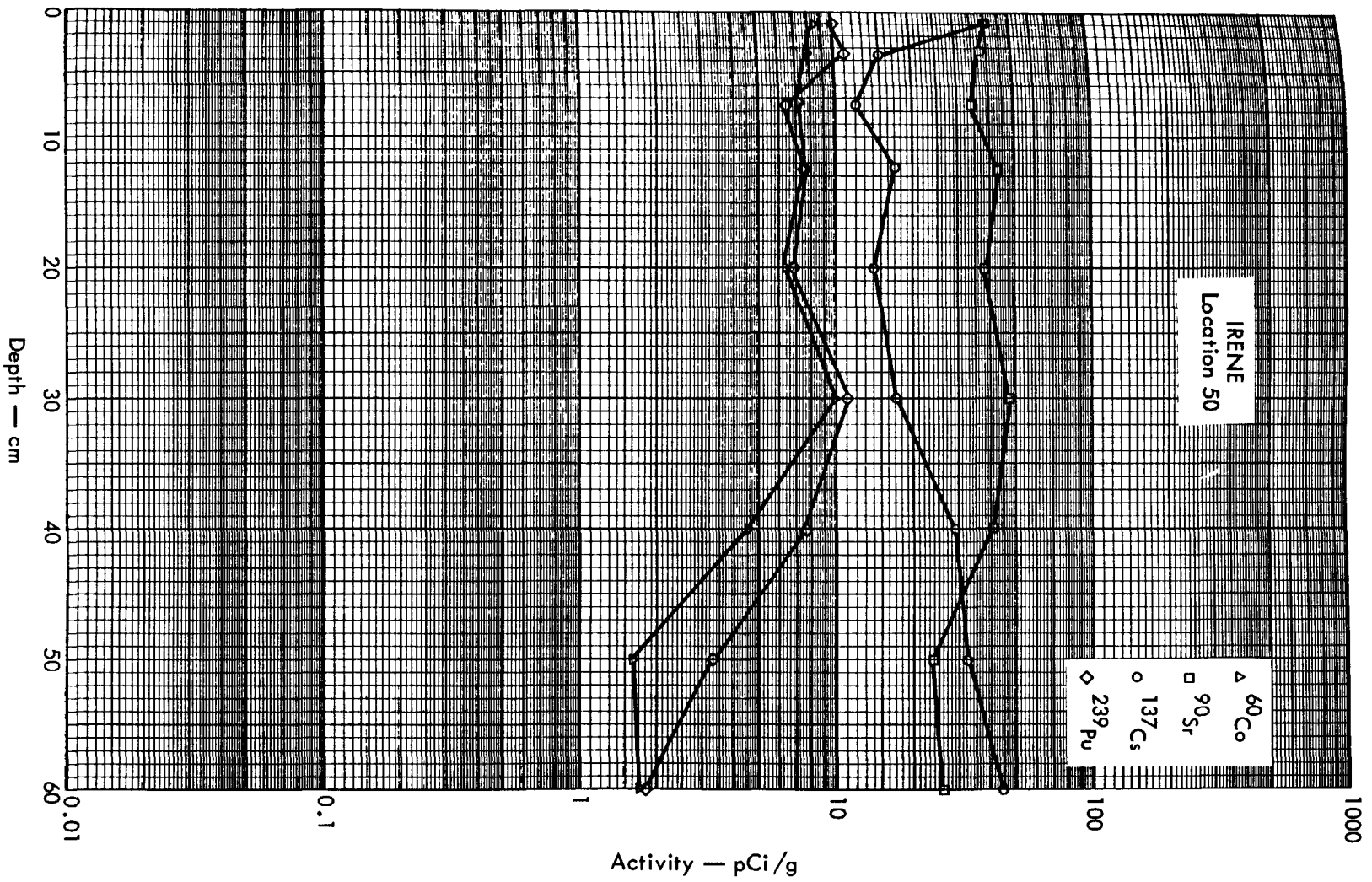


Fig. B.7.2q. Activities of selected radionuclides as a function of soil depth.

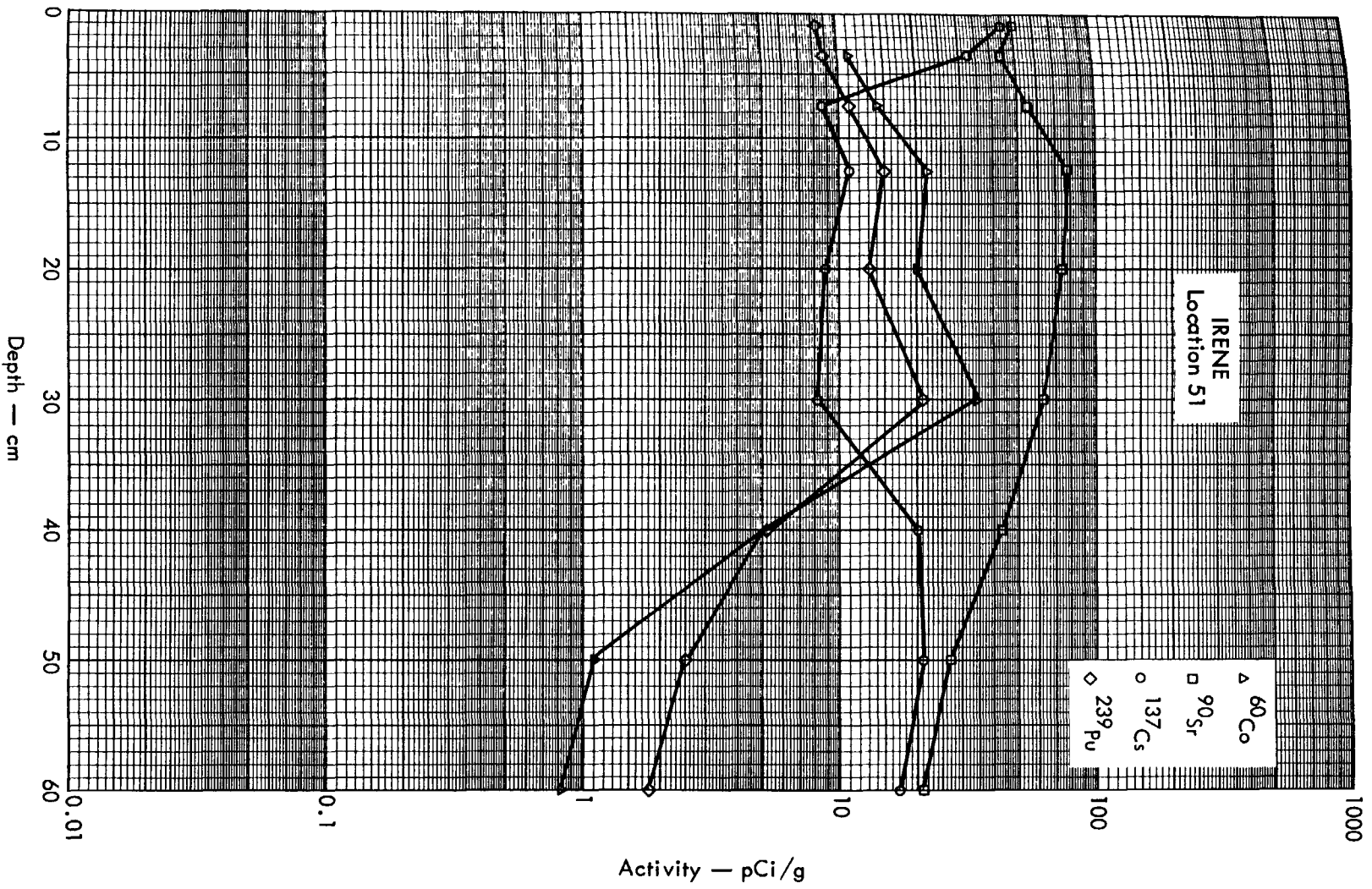


Fig. B.7.2r. Activities of selected radionuclides as a function of soil depth.

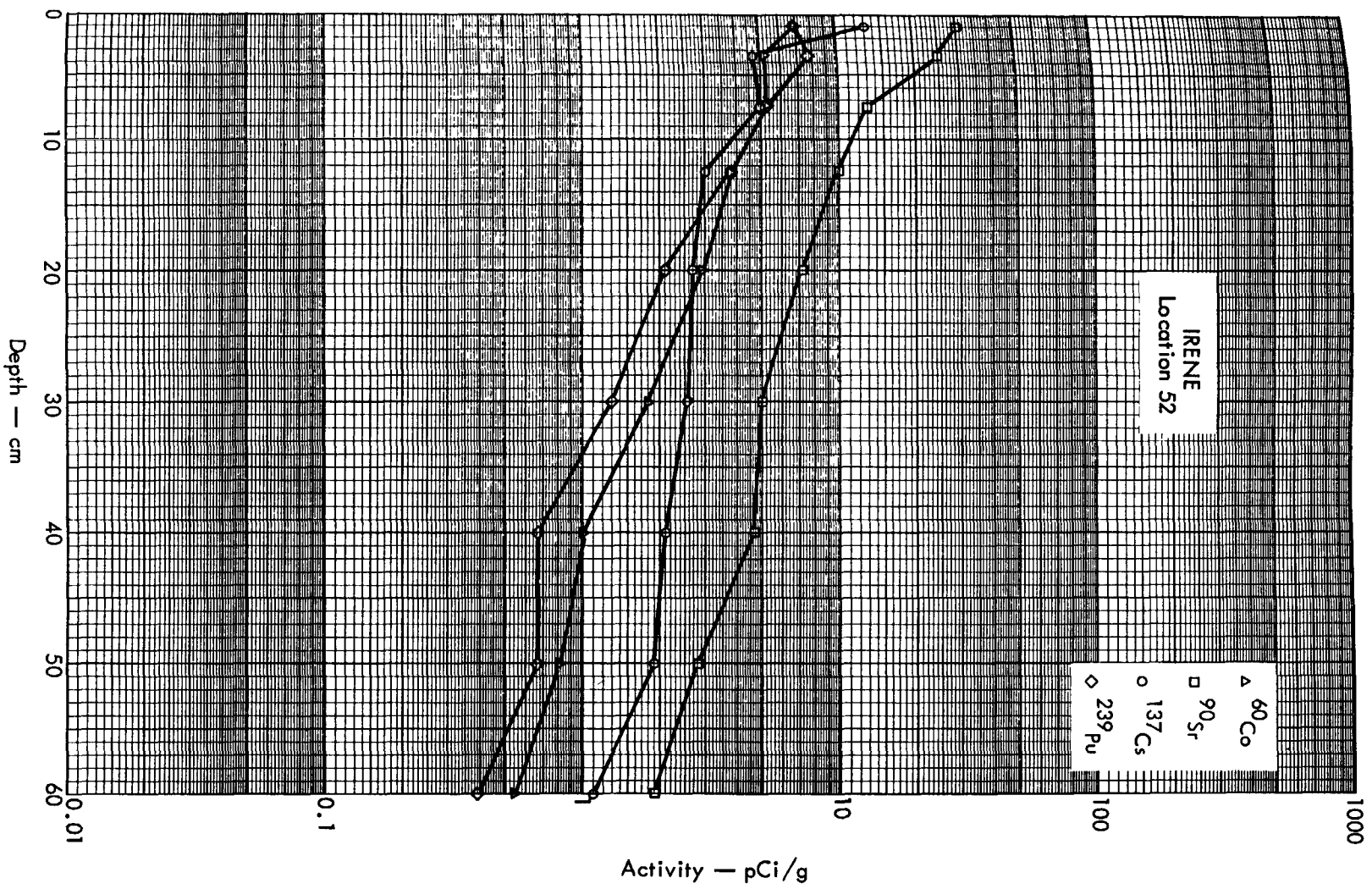


Fig. B.7.2s. Activities of selected radionuclides as a function of soil depth.

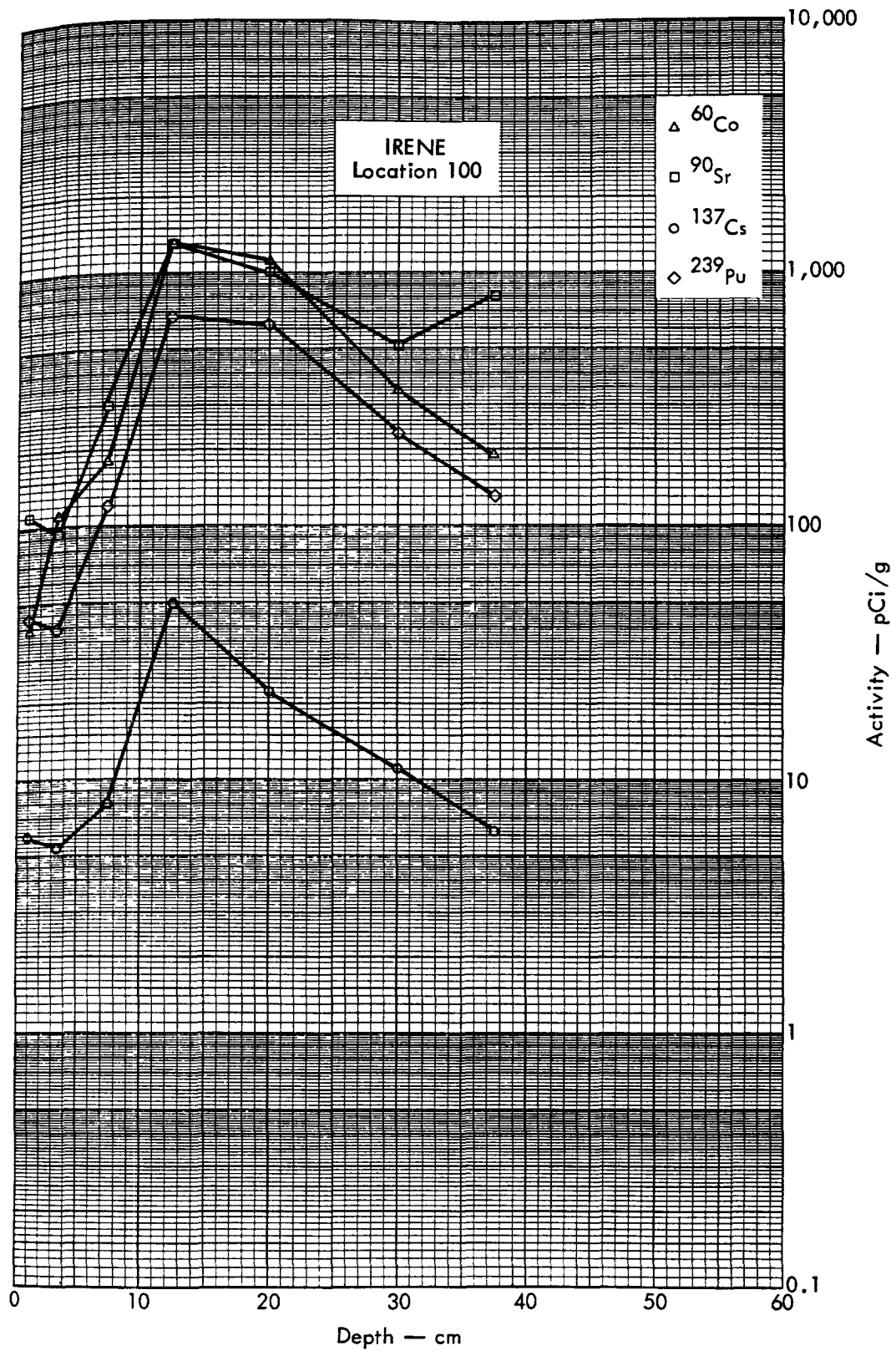
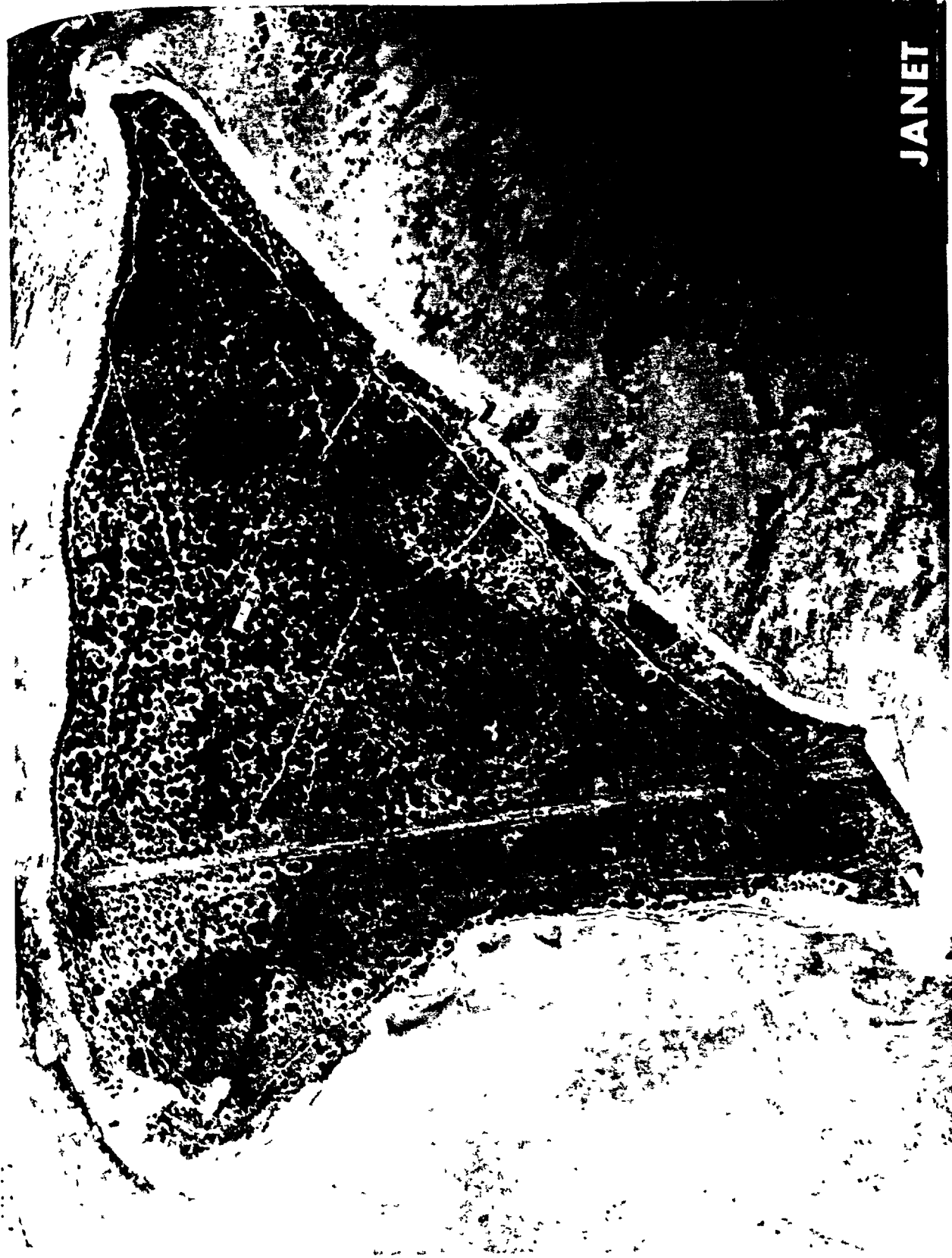


Fig. B. 7.2t. Activities of selected radionuclides as a function of soil depth.



JANET

Fig. B.8.1.a.





Fig. B. 8. 1. b. Gross count isoelevation contours. (Refer to alphabetic symbol key in this appendix.)

JANET



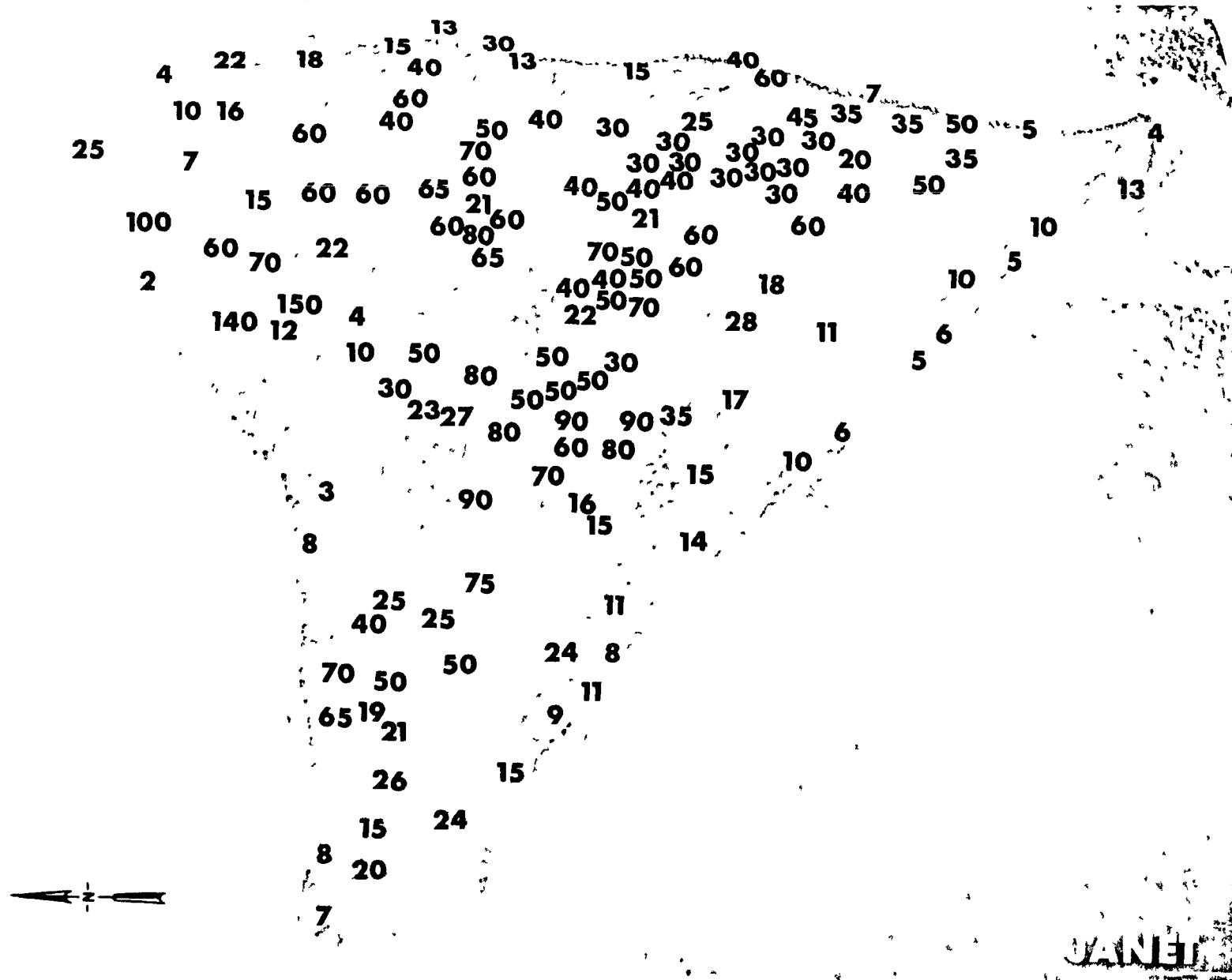


Fig. B.8.1.d. The gamma background exposure rate ( $\mu\text{R/hr}$ ) at 1 m above the ground, measured with a portable NaI scintillation counter.



Fig. B.8.1.f. Soil-sample locations.

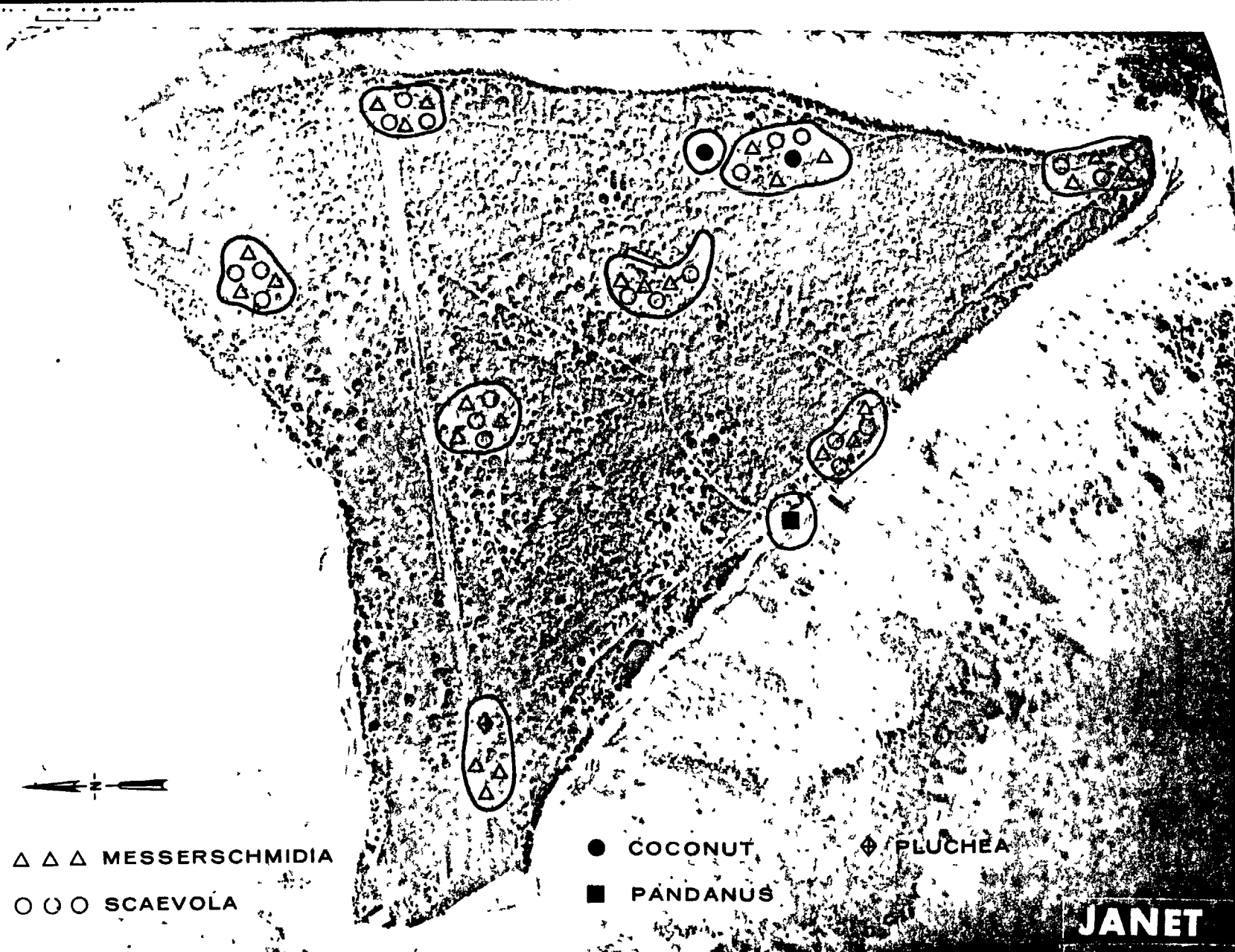


Fig. B.8.1.g. Vegetation sample locations.



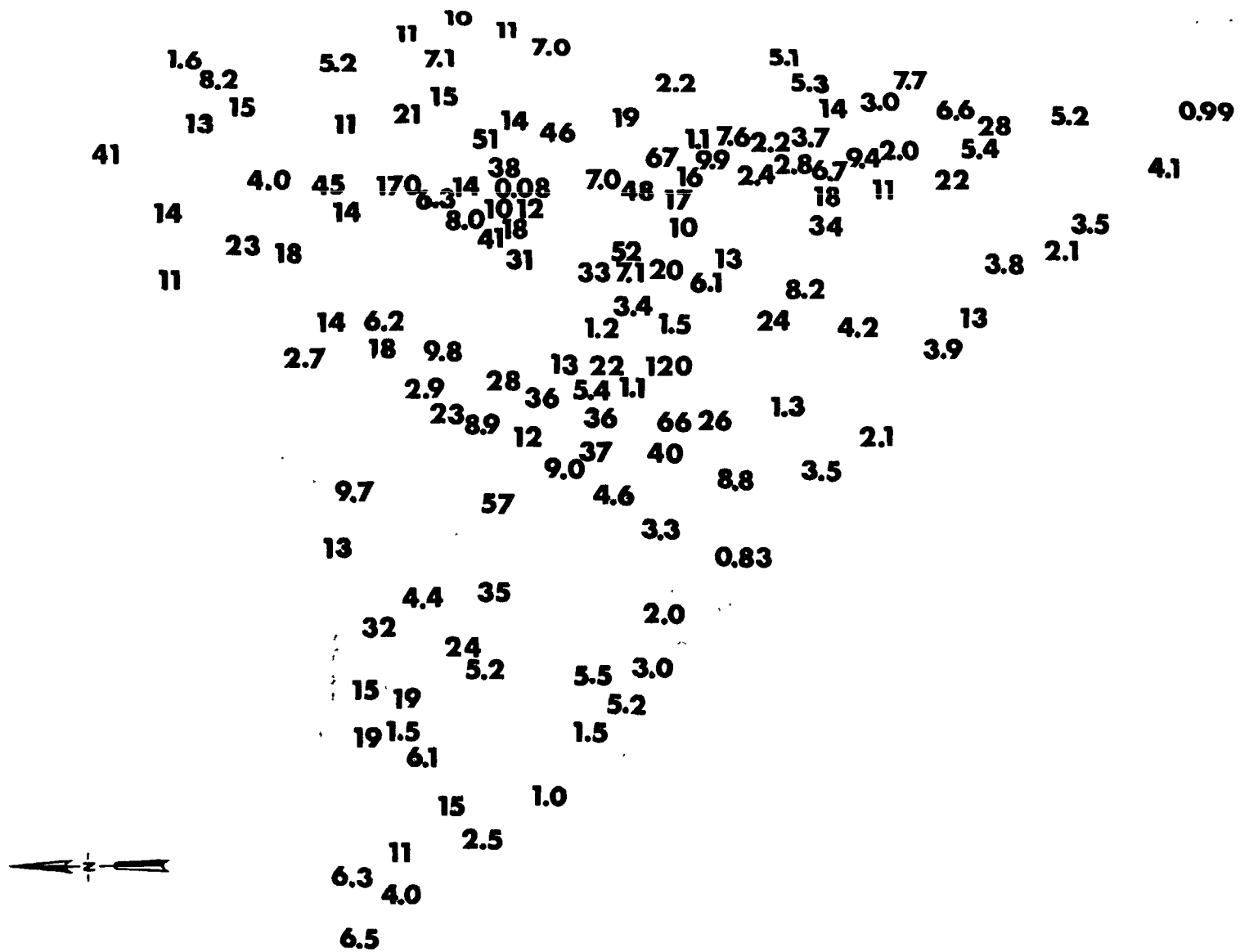


Fig. B.8.1.1. The average  $^{239}\text{Pu}$  activities (pCi/gm) in soil samples collected to a depth of 15 cm.

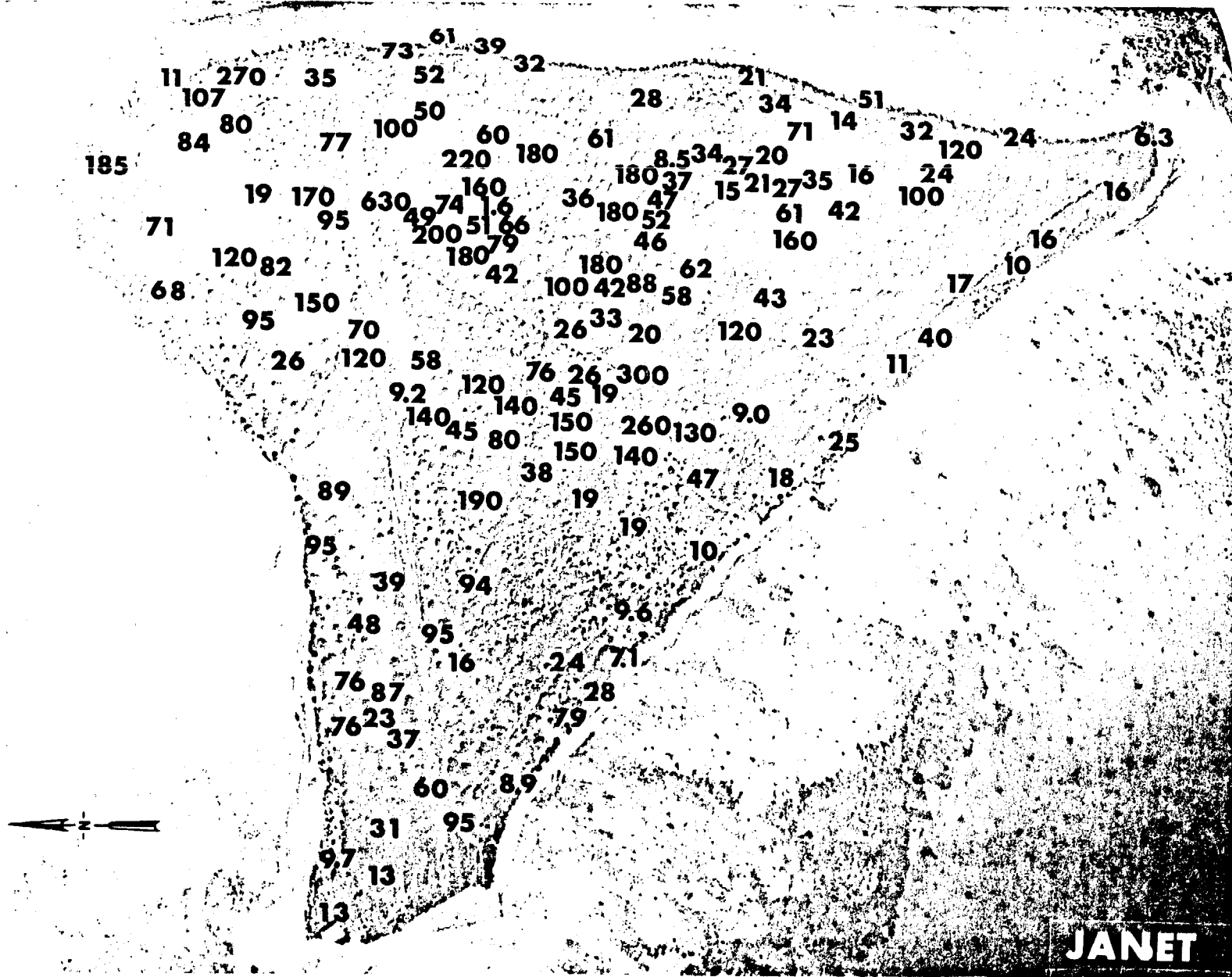


Fig. B.8.1.j. The average  $^{90}\text{Sr}$  activities (pCi/gm) in soil samples collected to a depth of 15 cm.

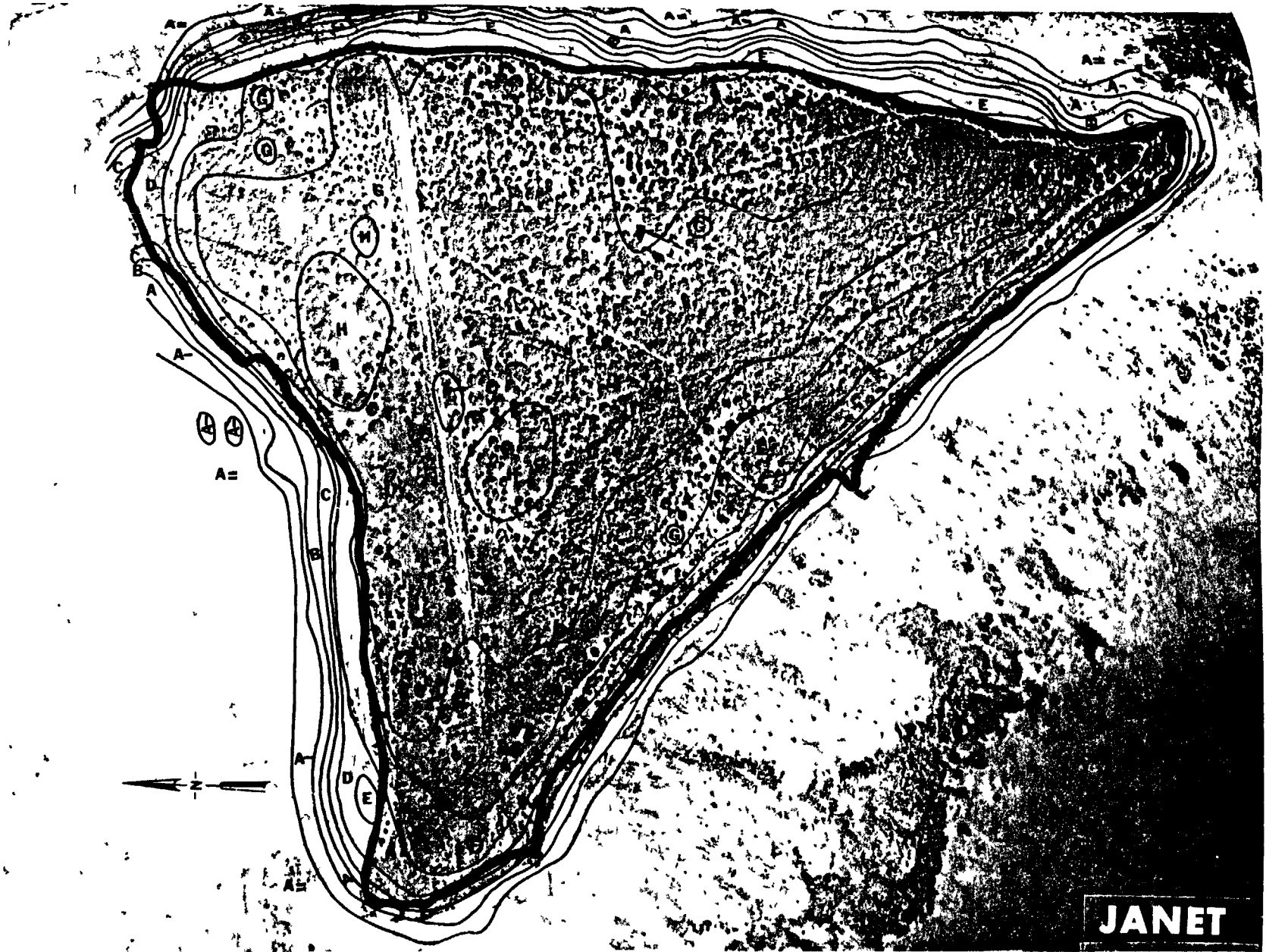


Fig. B.8.1.k. <sup>137</sup>Cs isoexposure and isoconcentration contours. (Refer to alphabetic symbol key in this appendix.)

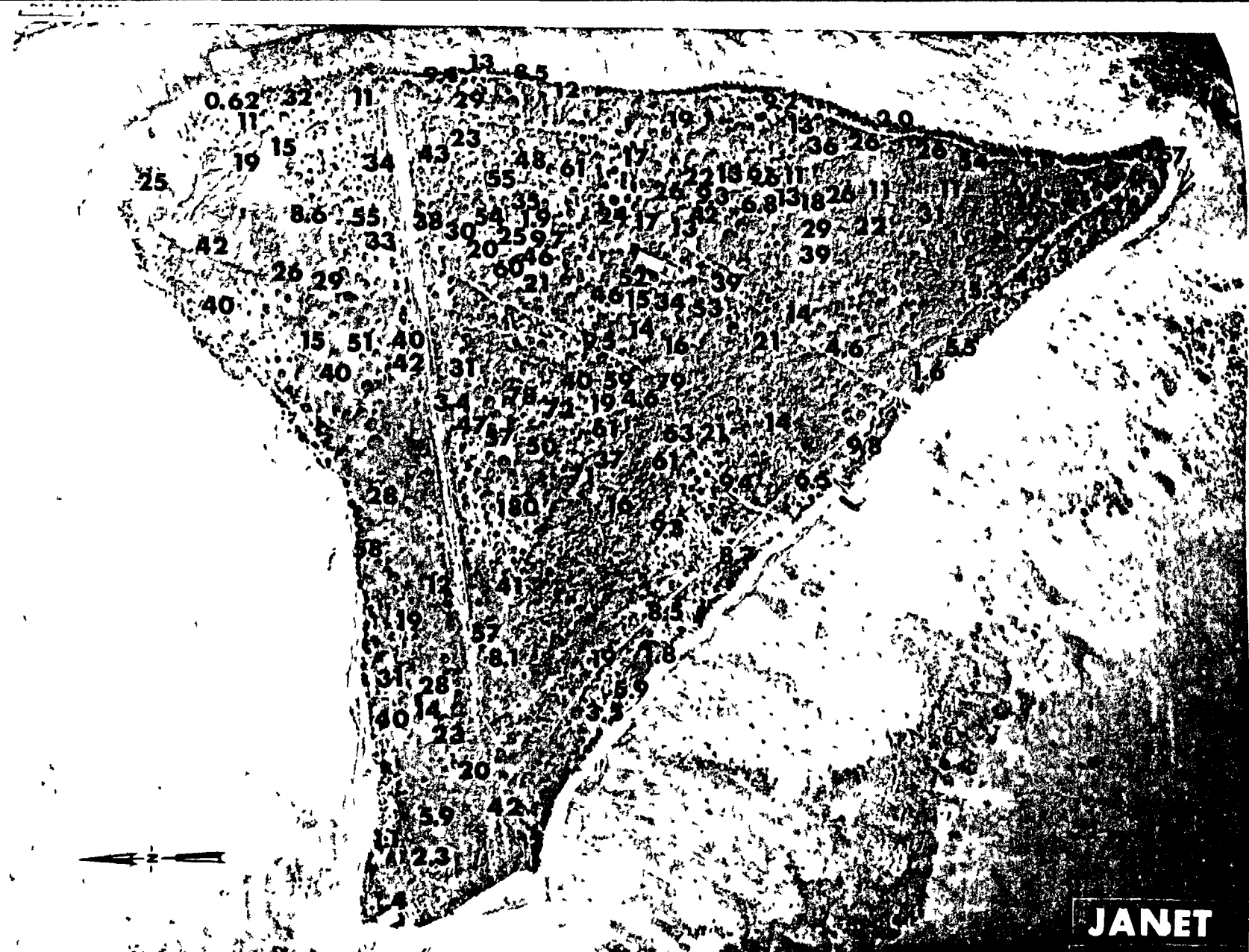


Fig. B.8.1.1. The average <sup>137</sup>Cs activities (pCi/gm) in soil samples collected to a depth of 15 cm.



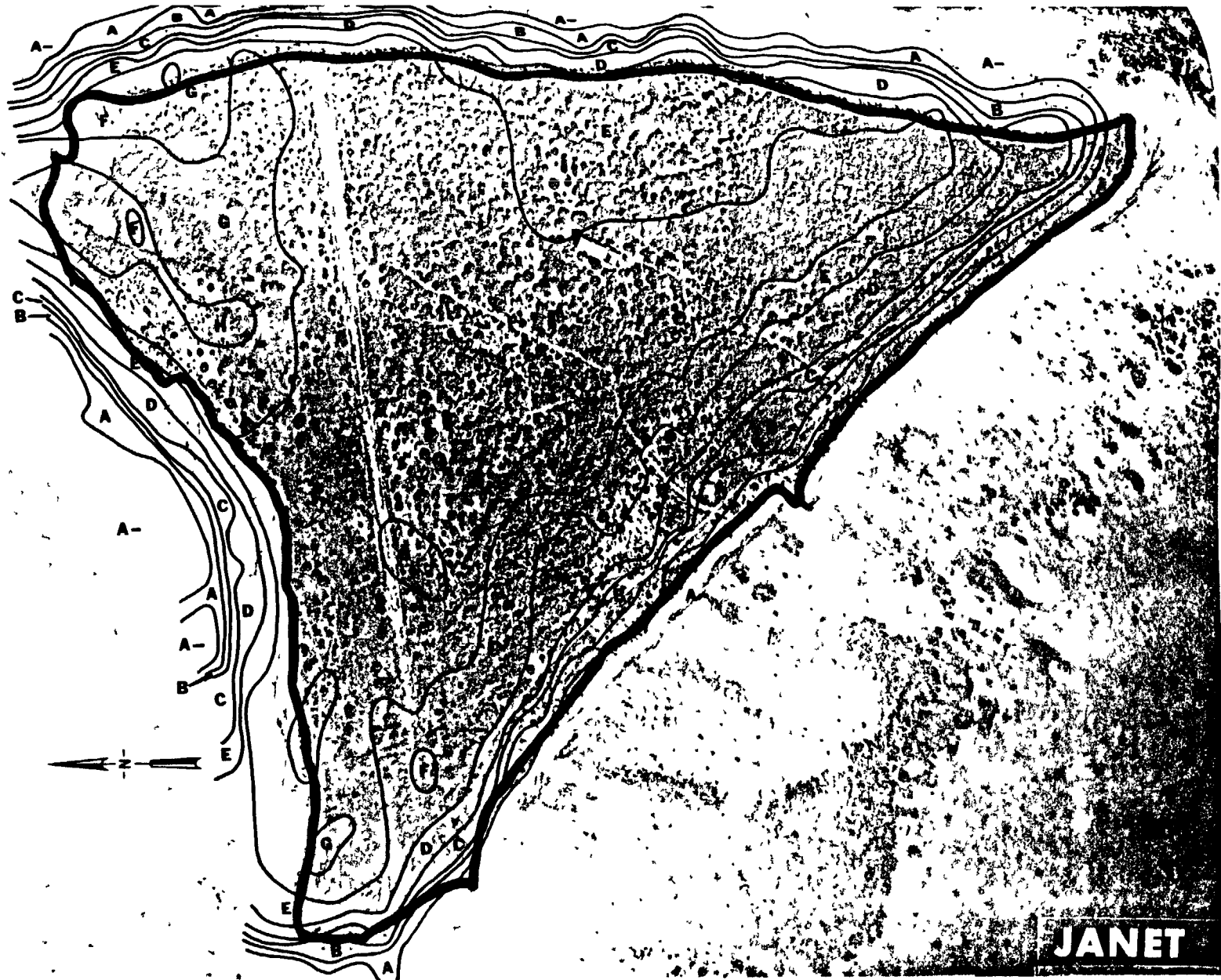


Fig. B.8.1.m.  $^{60}\text{Co}$  isoexposure and isoconcentration contours. (Refer to alphabetic symbol key in this appendix.)

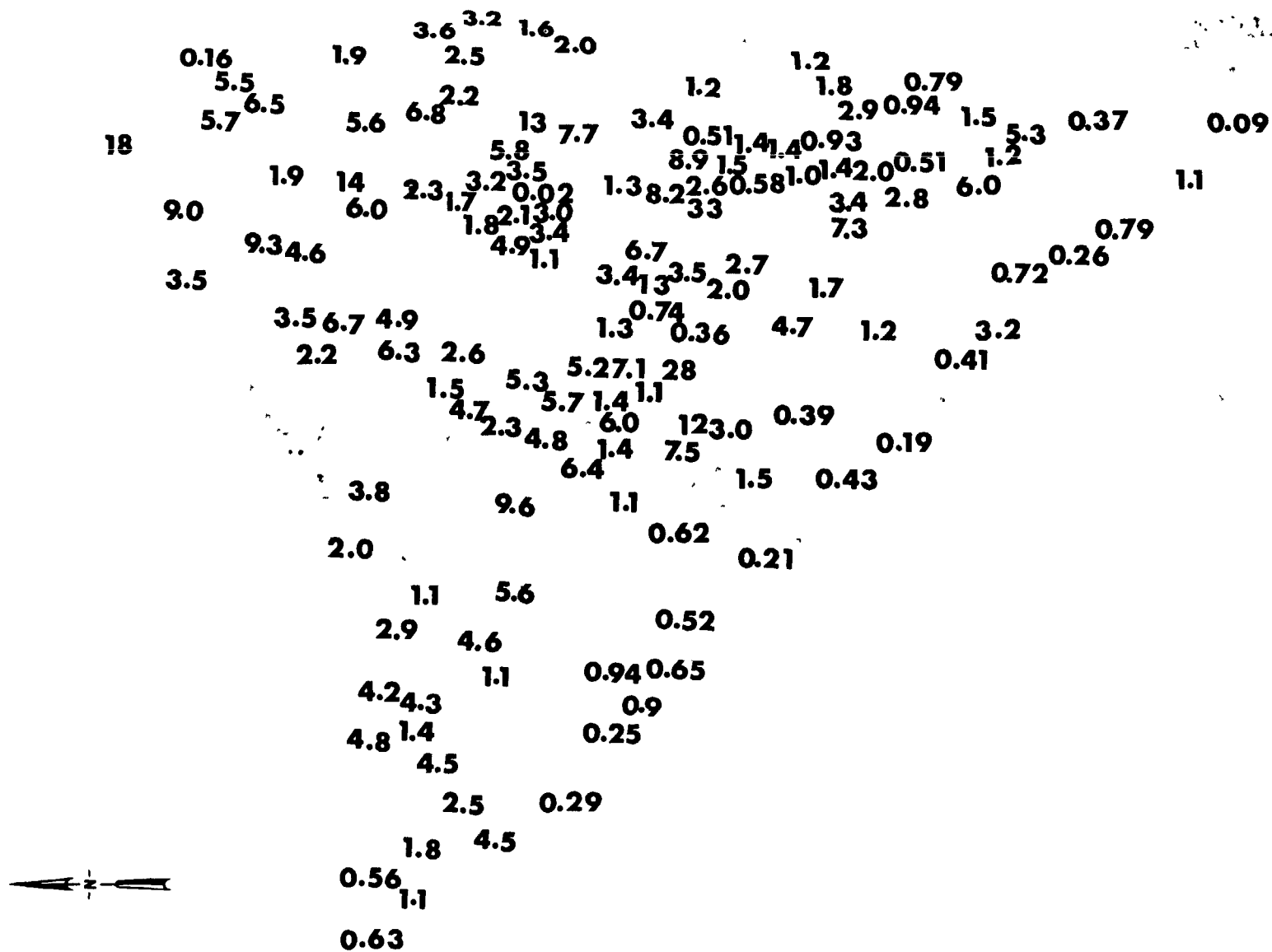


Fig. B.8.1.n. The average  $^{60}\text{Co}$  activities (pCi/gm) in soil samples collected to a depth of 15 cm.

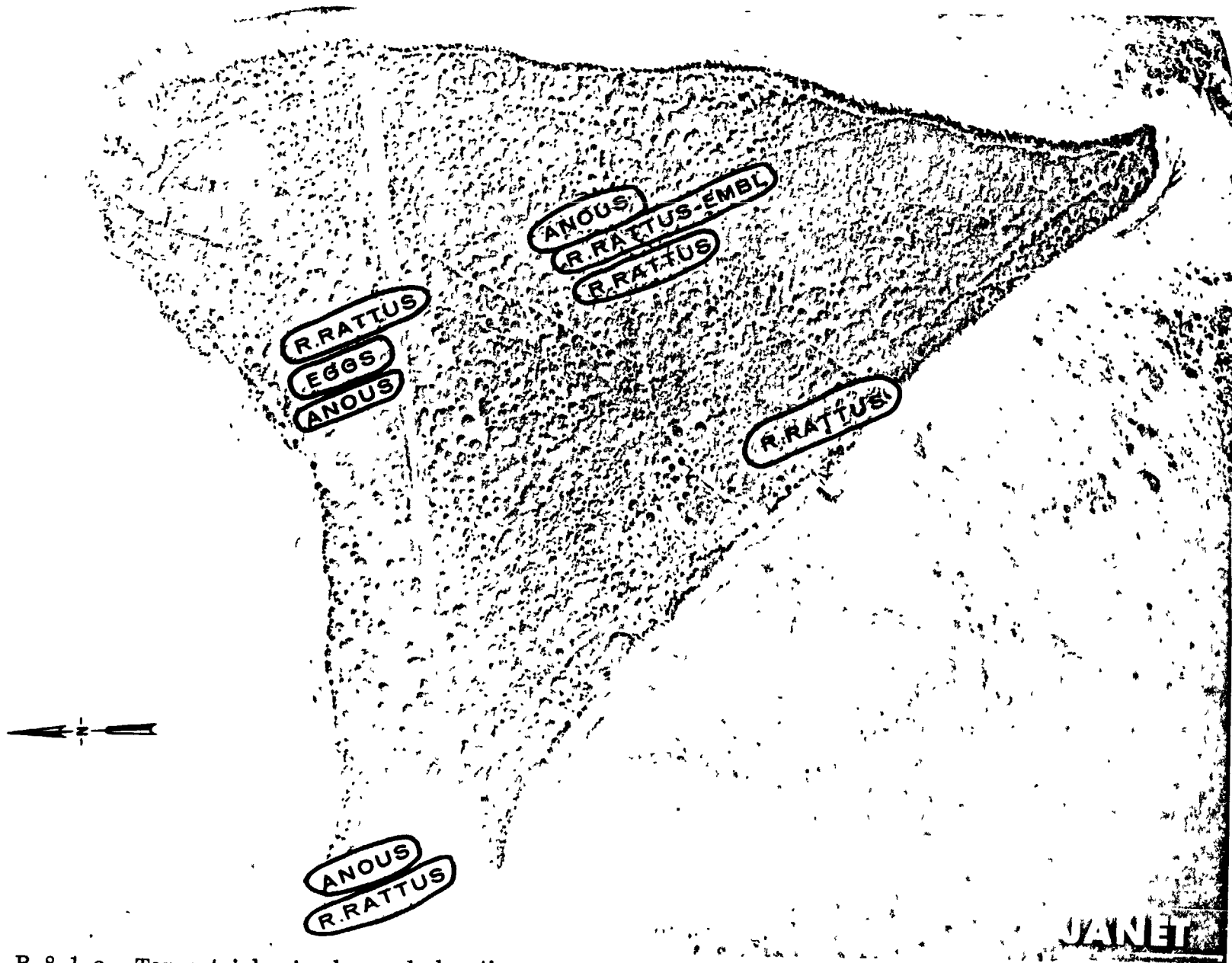


Fig. B.8.1.o. Terrestrial animal sample locations.

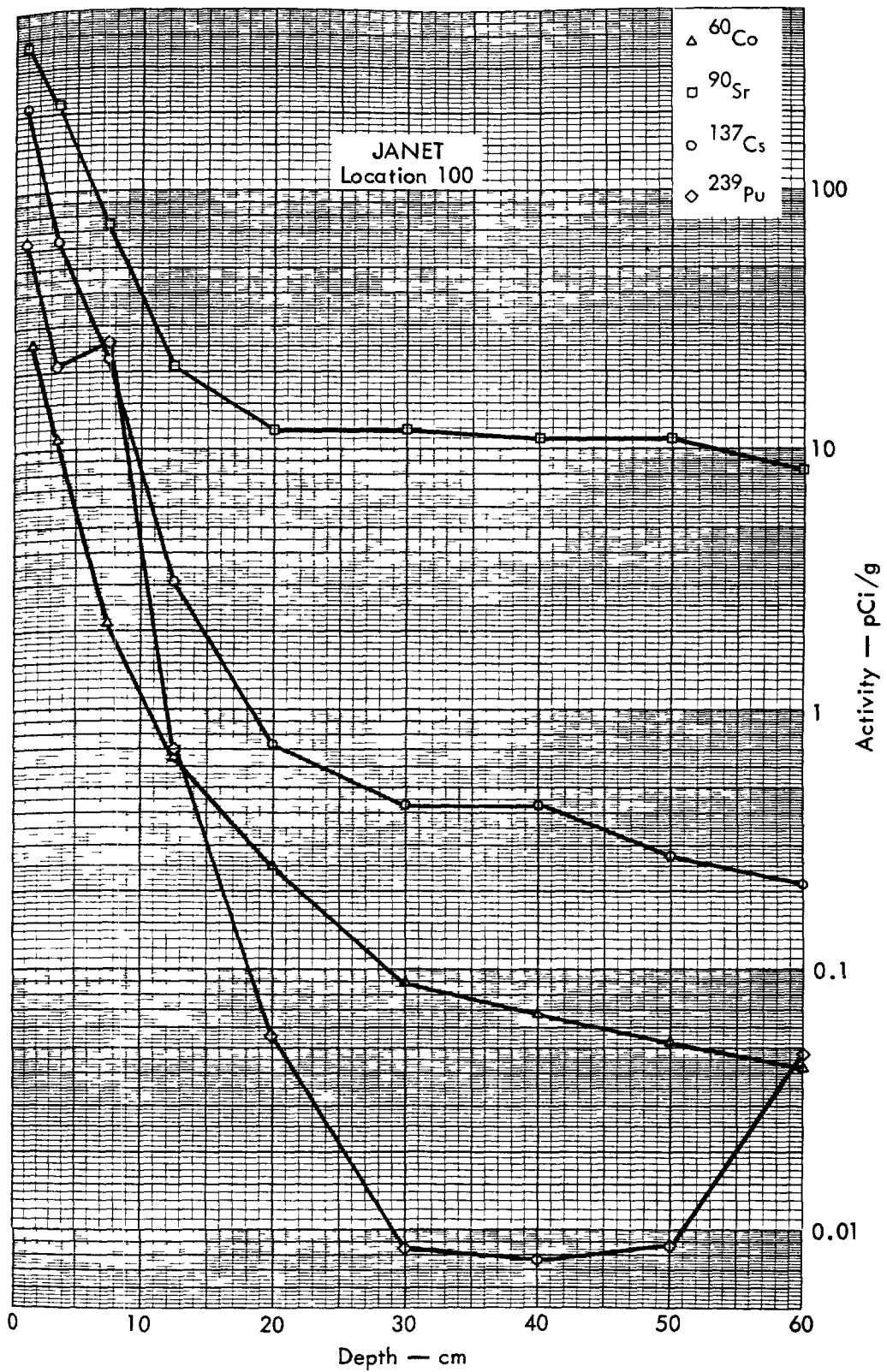


Fig. B.8.2a. Activities of selected radionuclides as a function of soil depth.

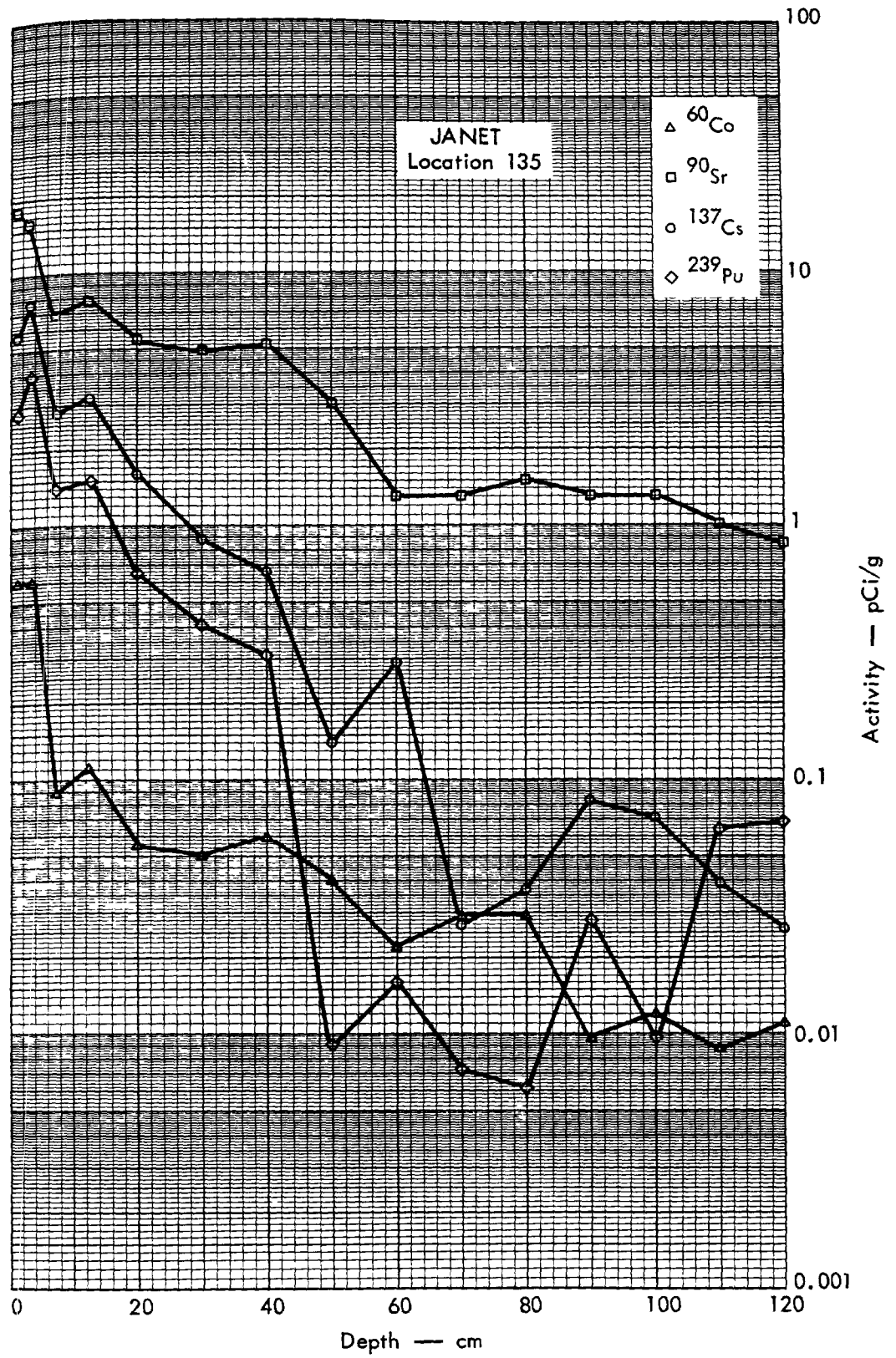


Fig. B. 8.2b. Activities of selected radionuclides as a function of soil depth.

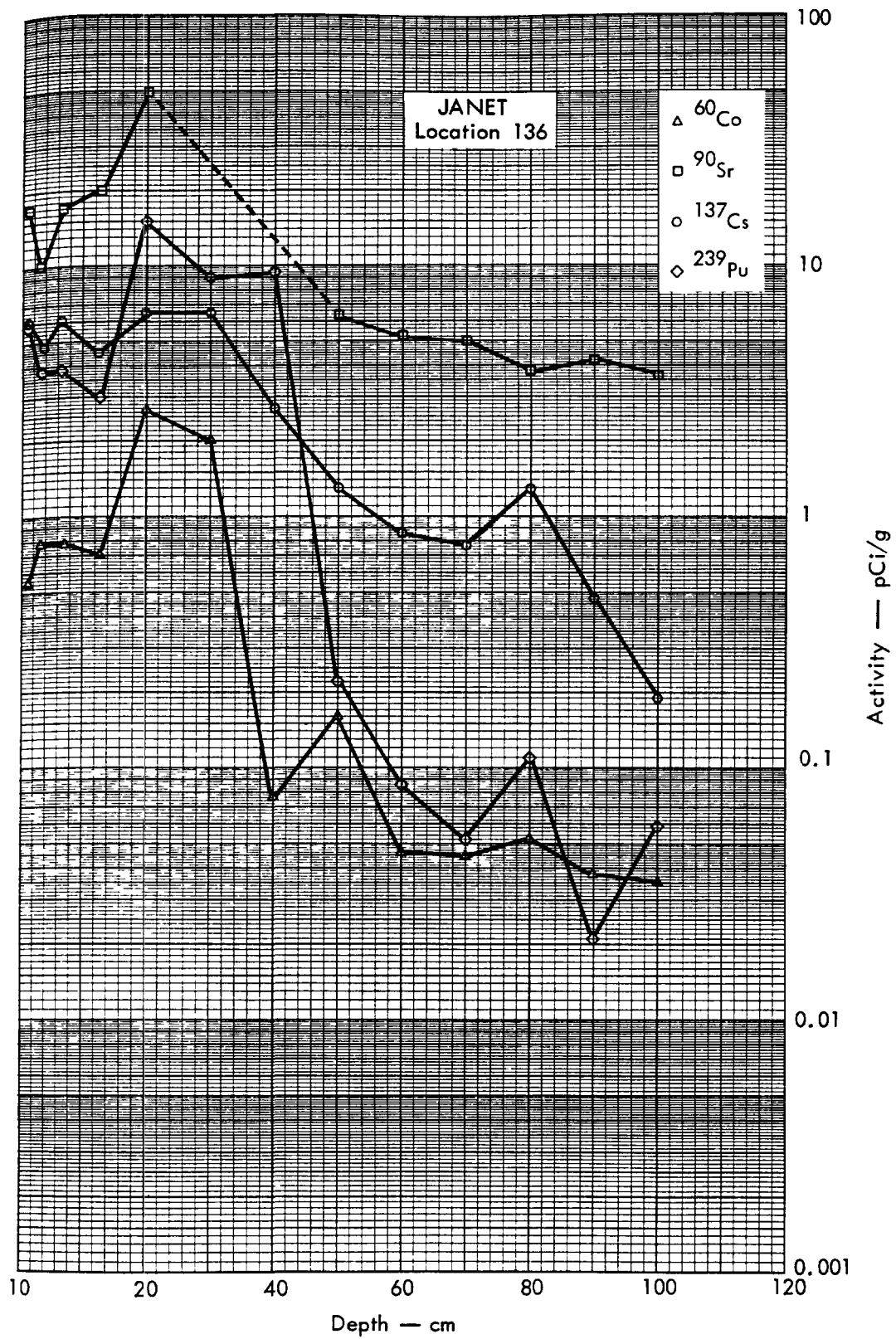


Fig. B.8.2c. Activities of selected radionuclides as a function of soil depth.

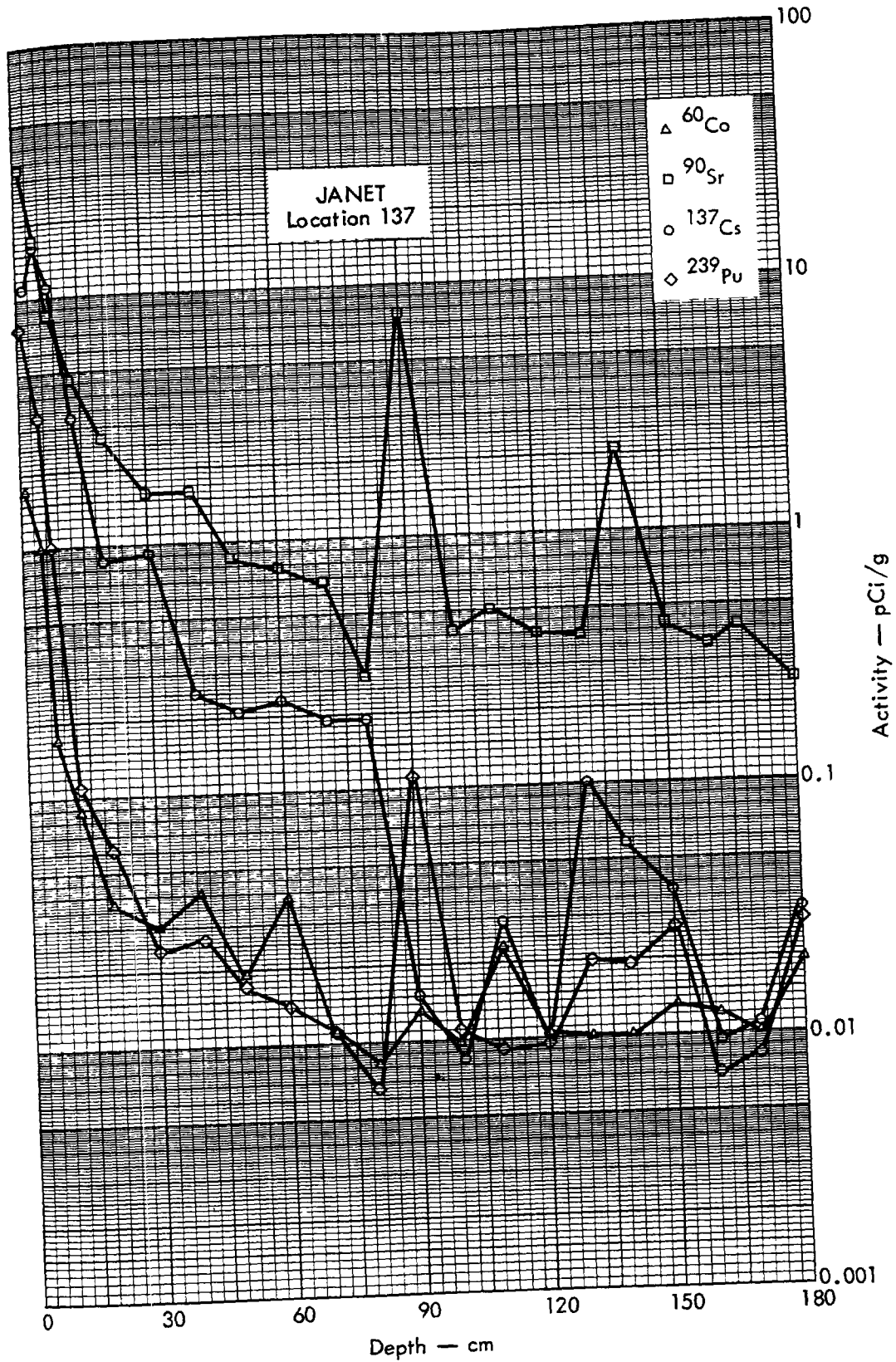


Fig. B. 8.2d. Activities of selected radionuclides as a function of soil depth.



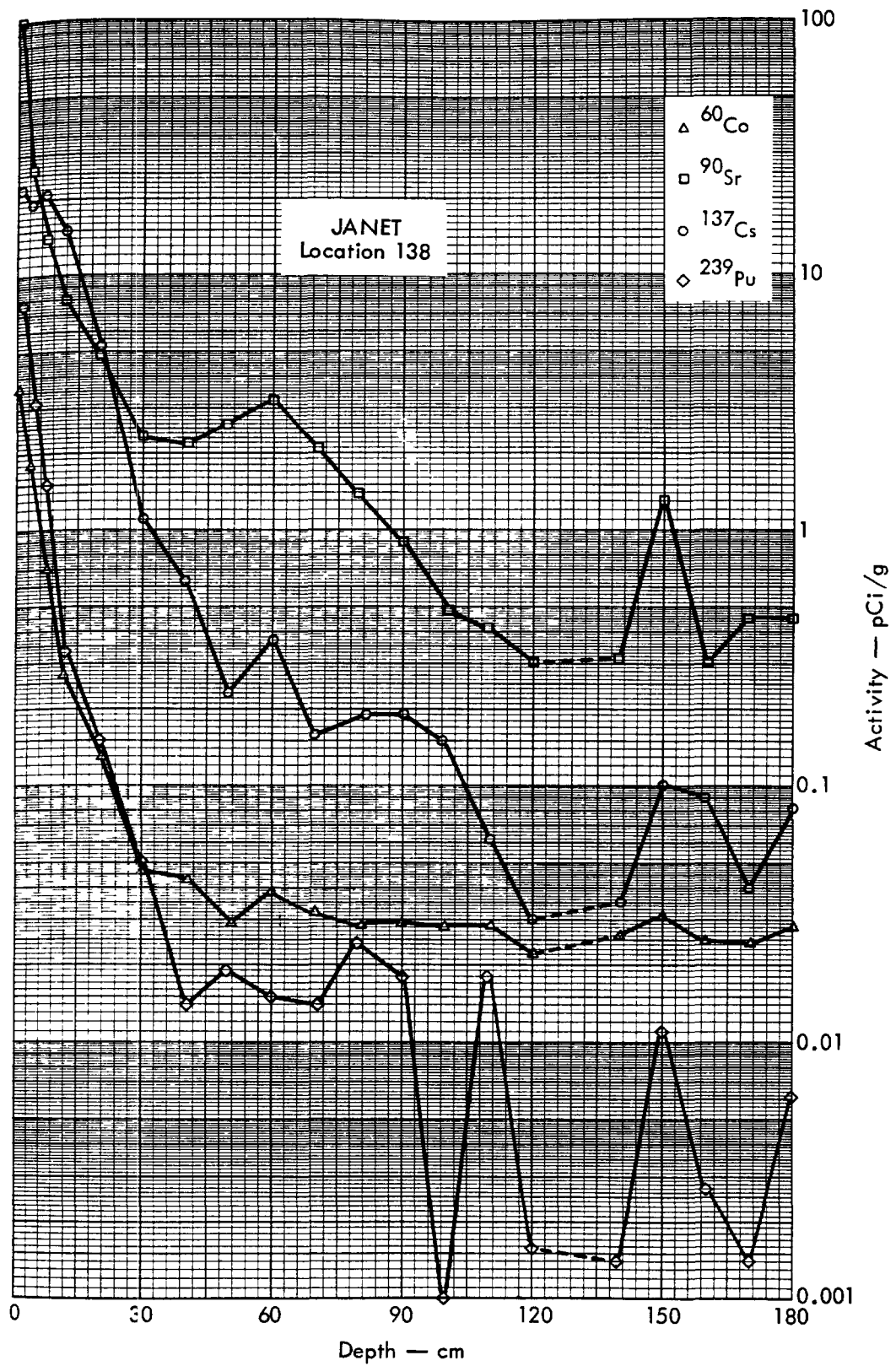


Fig. B. 8.2e. Activities of selected radionuclides as a function of soil depth.



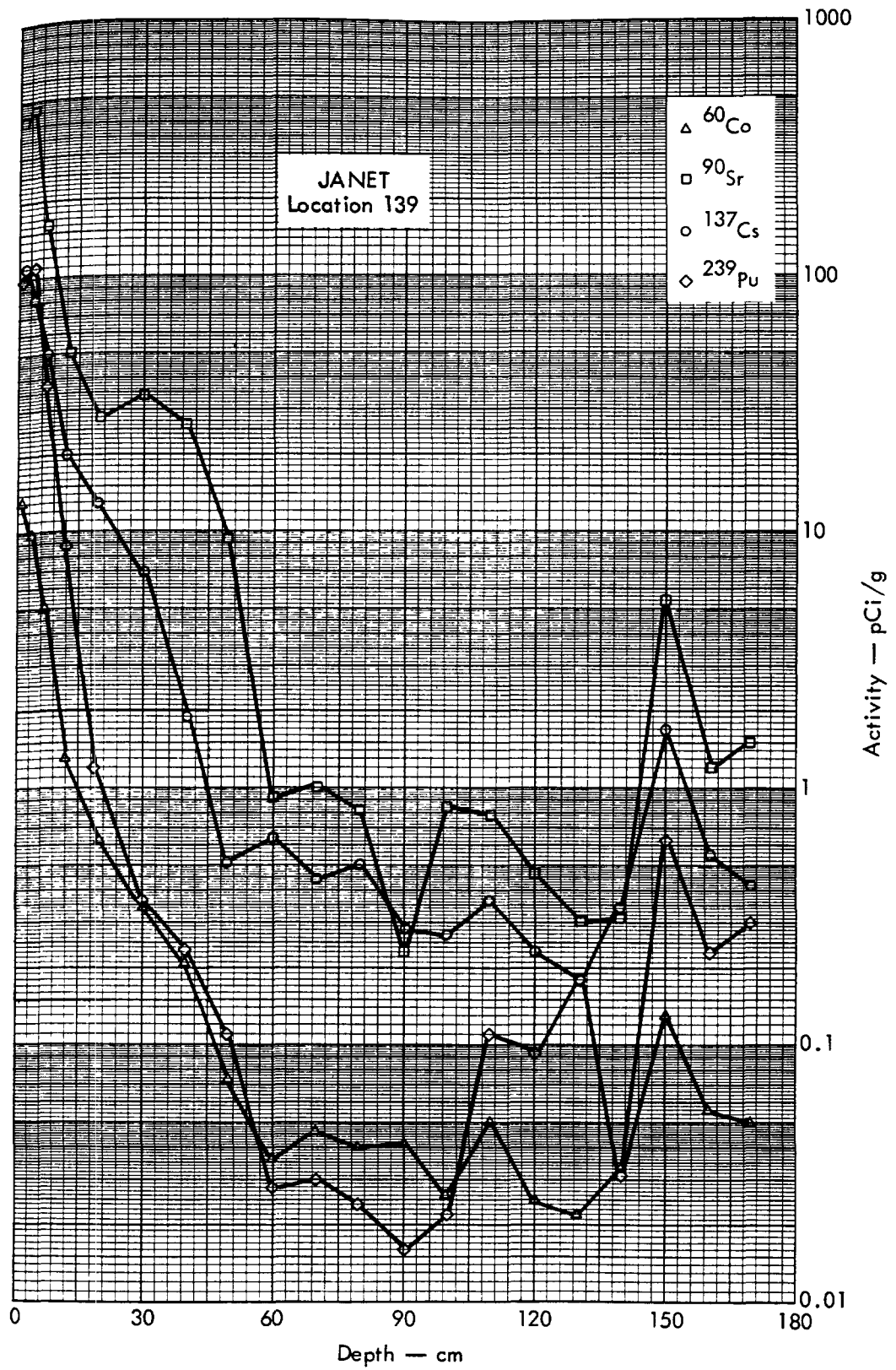


Fig. B. 8.2f. Activities of selected radionuclides as a function of soil depth.

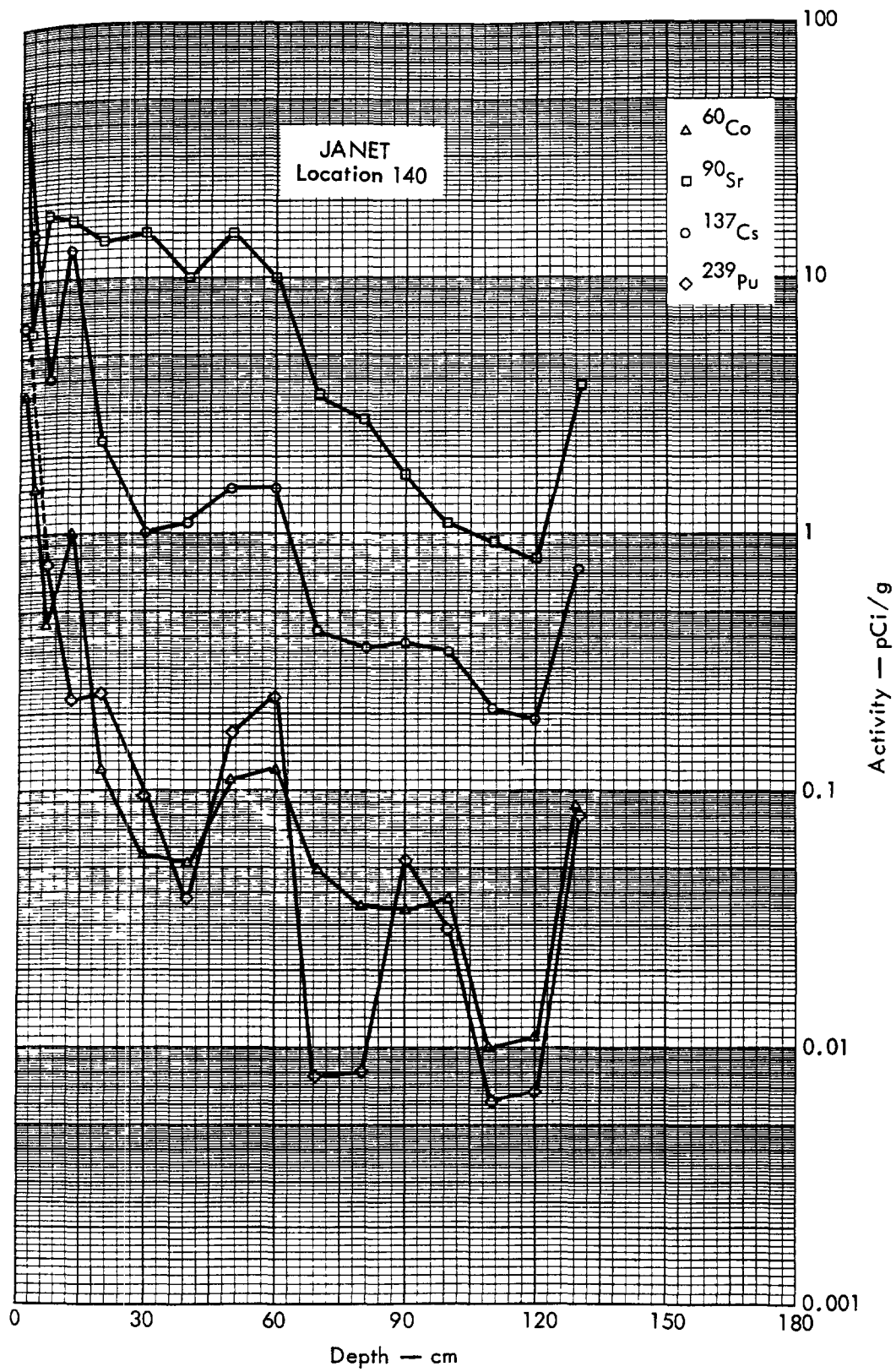


Fig. B. 8.2g. Activities of selected radionuclides as a function of soil depth.

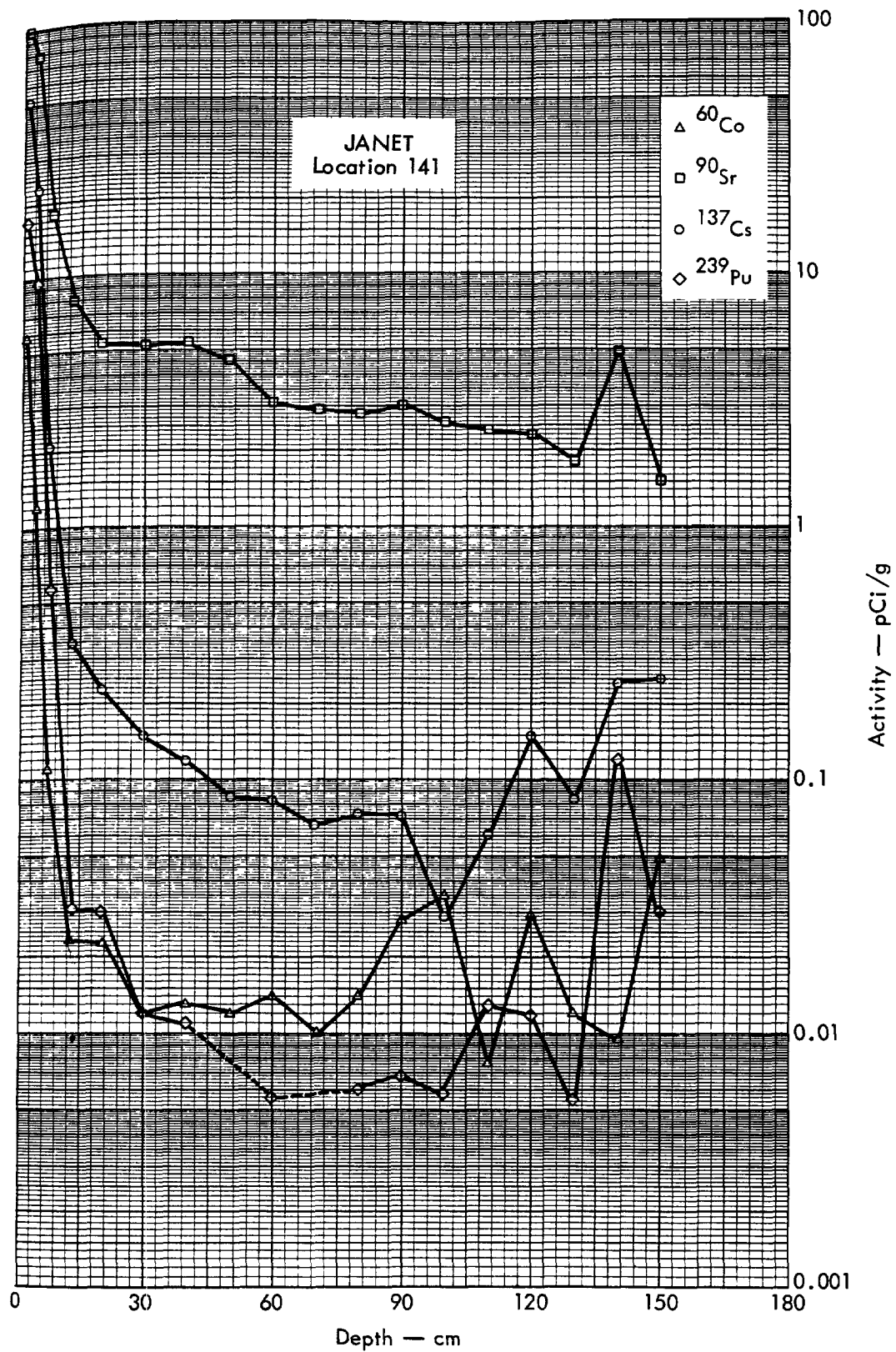


Fig. B. 8.2h. Activities of selected radionuclides as a function of soil depth.

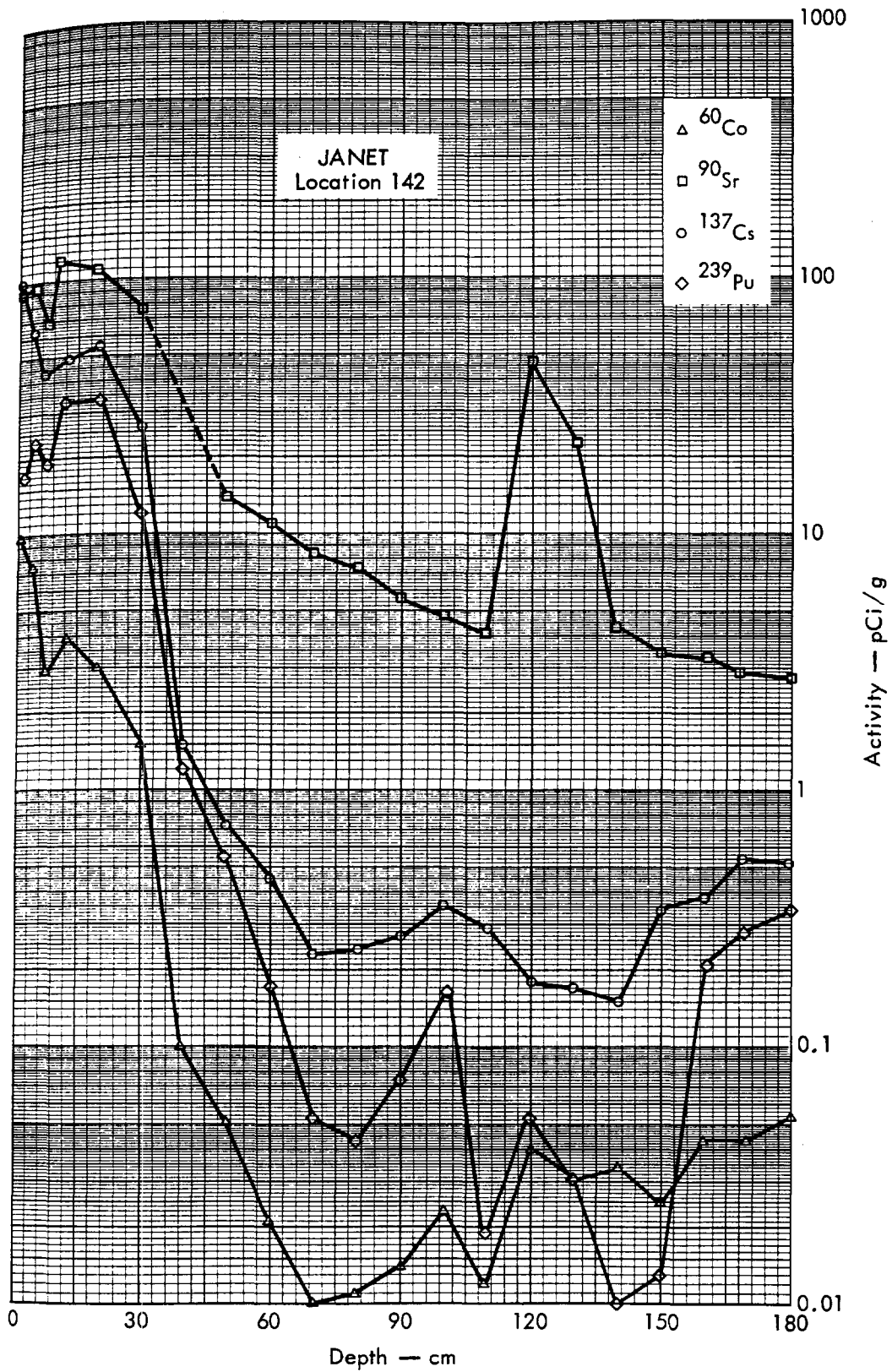


Fig. B. 8.2i. Activities of selected radionuclides as a function of soil depth.

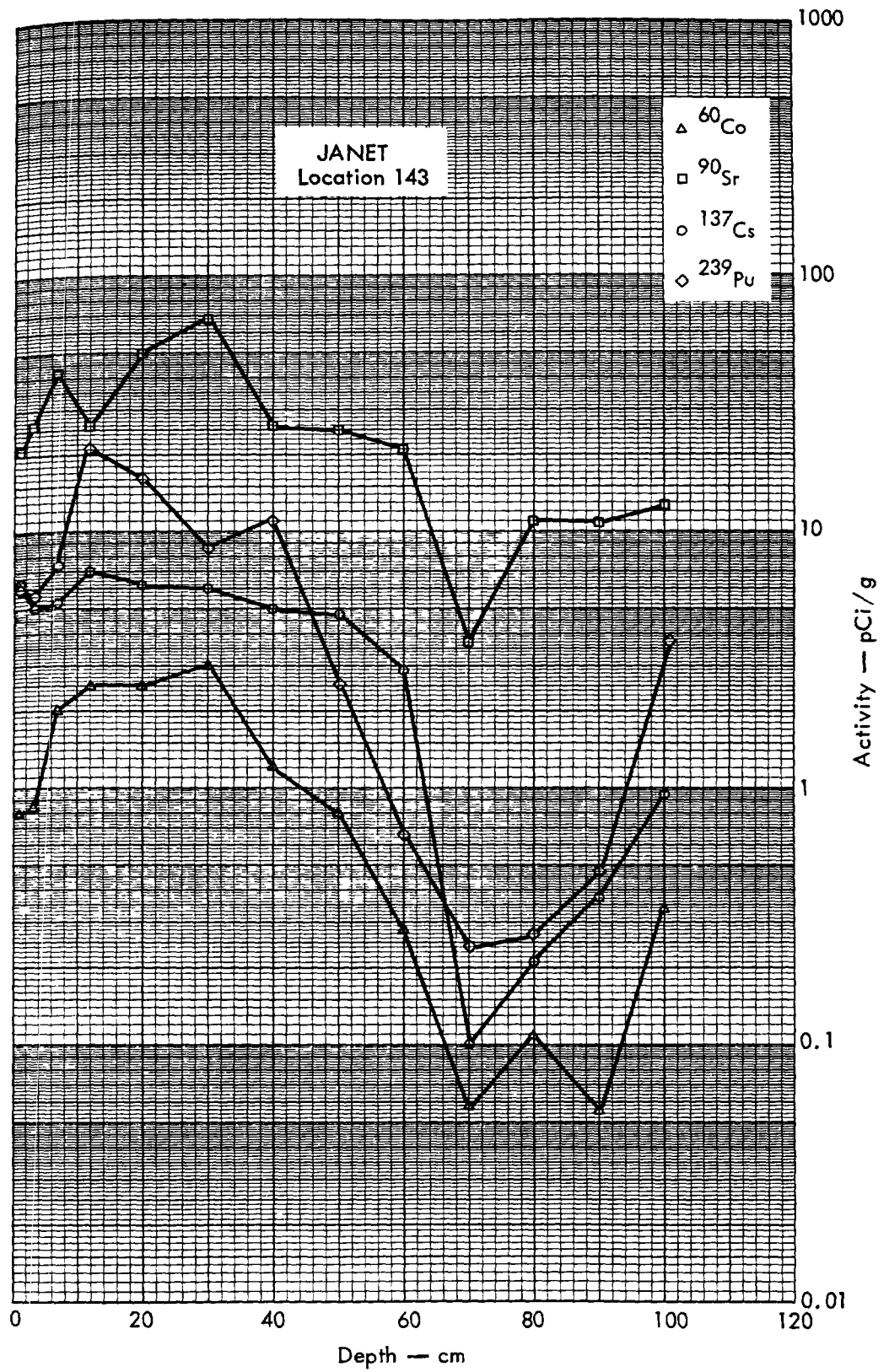


Fig. B. 8.2j. Activities of selected radionuclides as a function of soil depth.

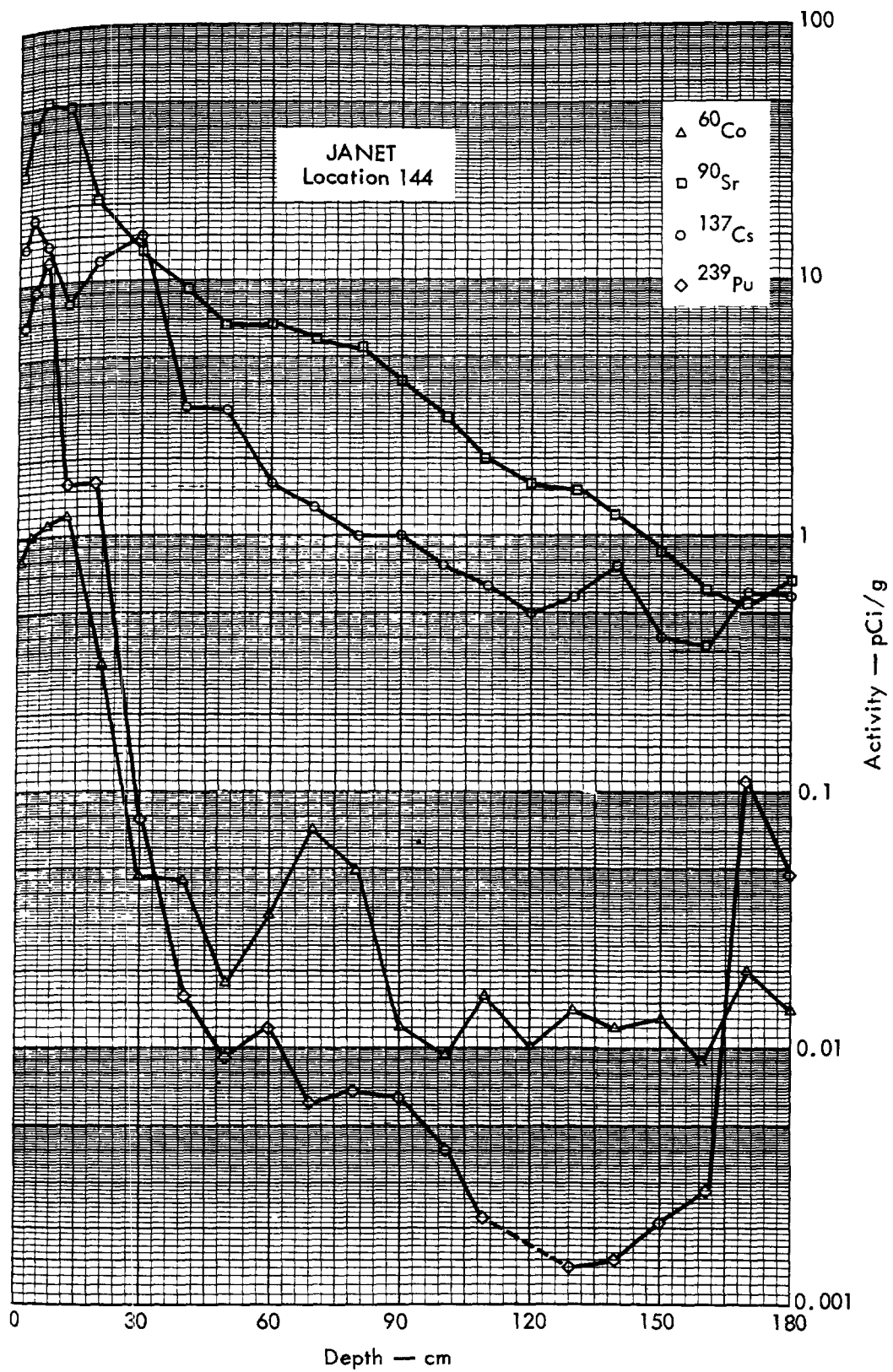


Fig. B. 8.2k. Activities of selected radionuclides as a function of soil depth.



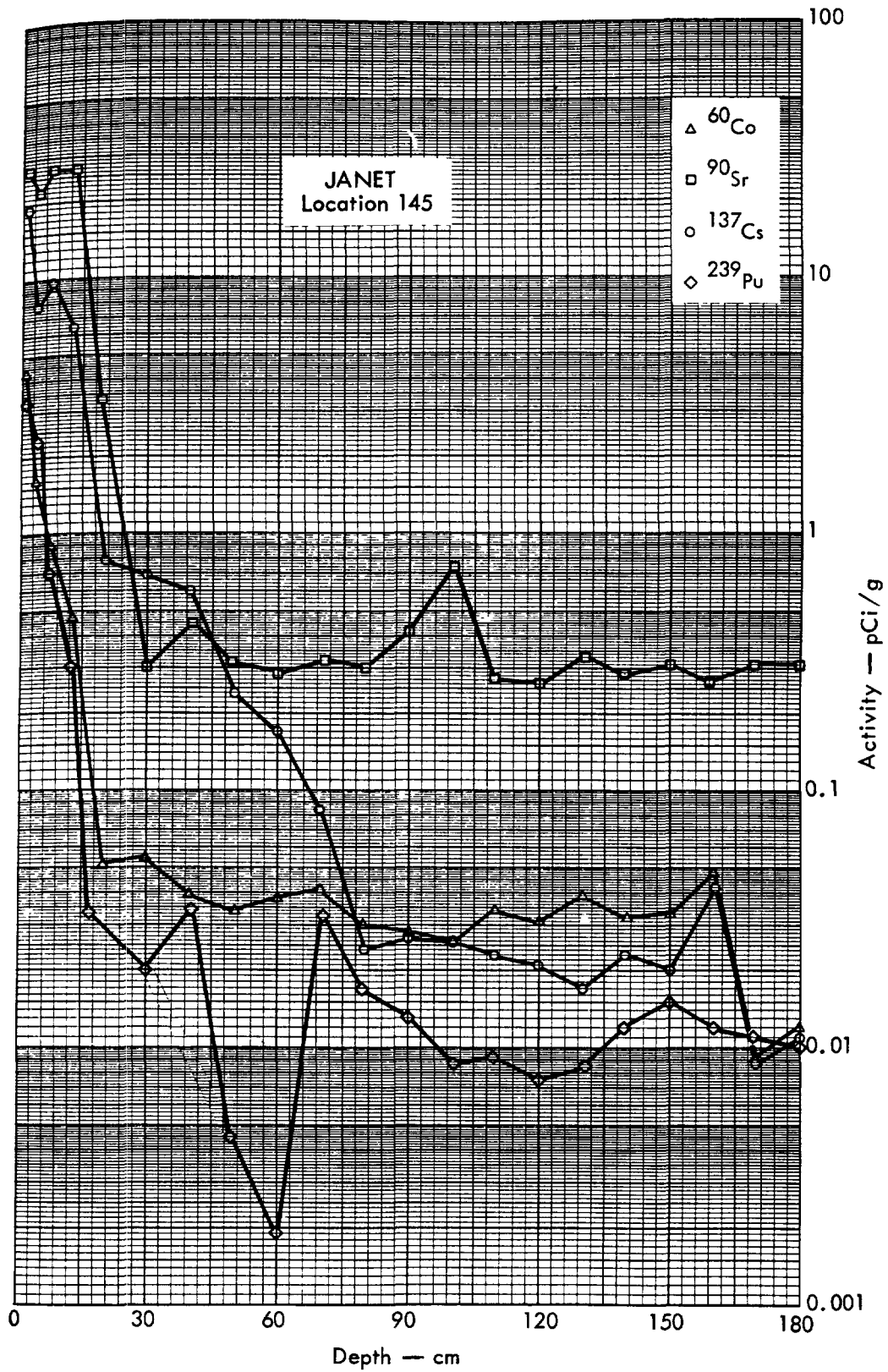


Fig. B. 8.21. Activities of selected radionuclides as a function of soil depth.

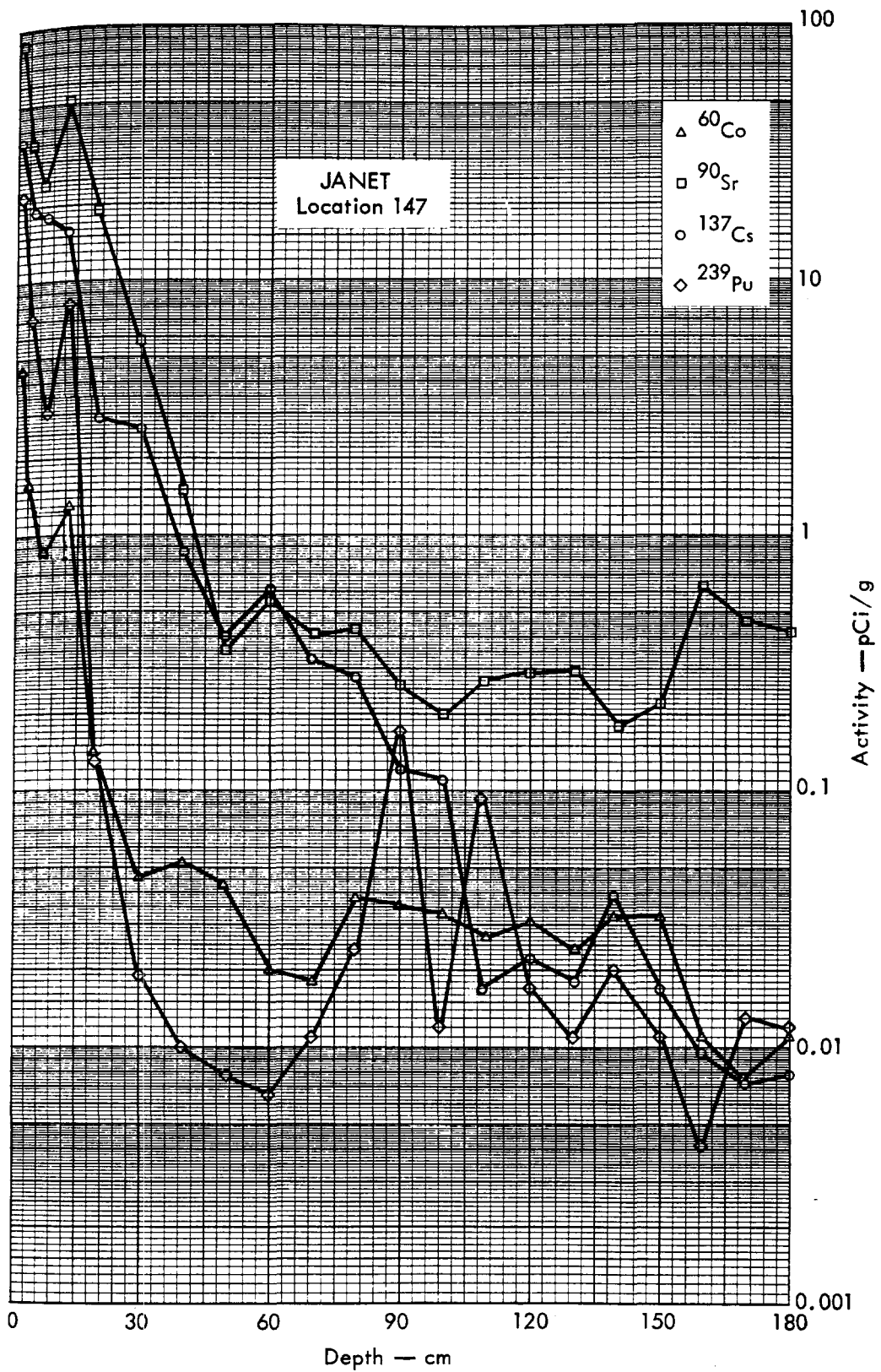


Fig. B.8.2m. Activities of selected radionuclides as a function of soil depth.



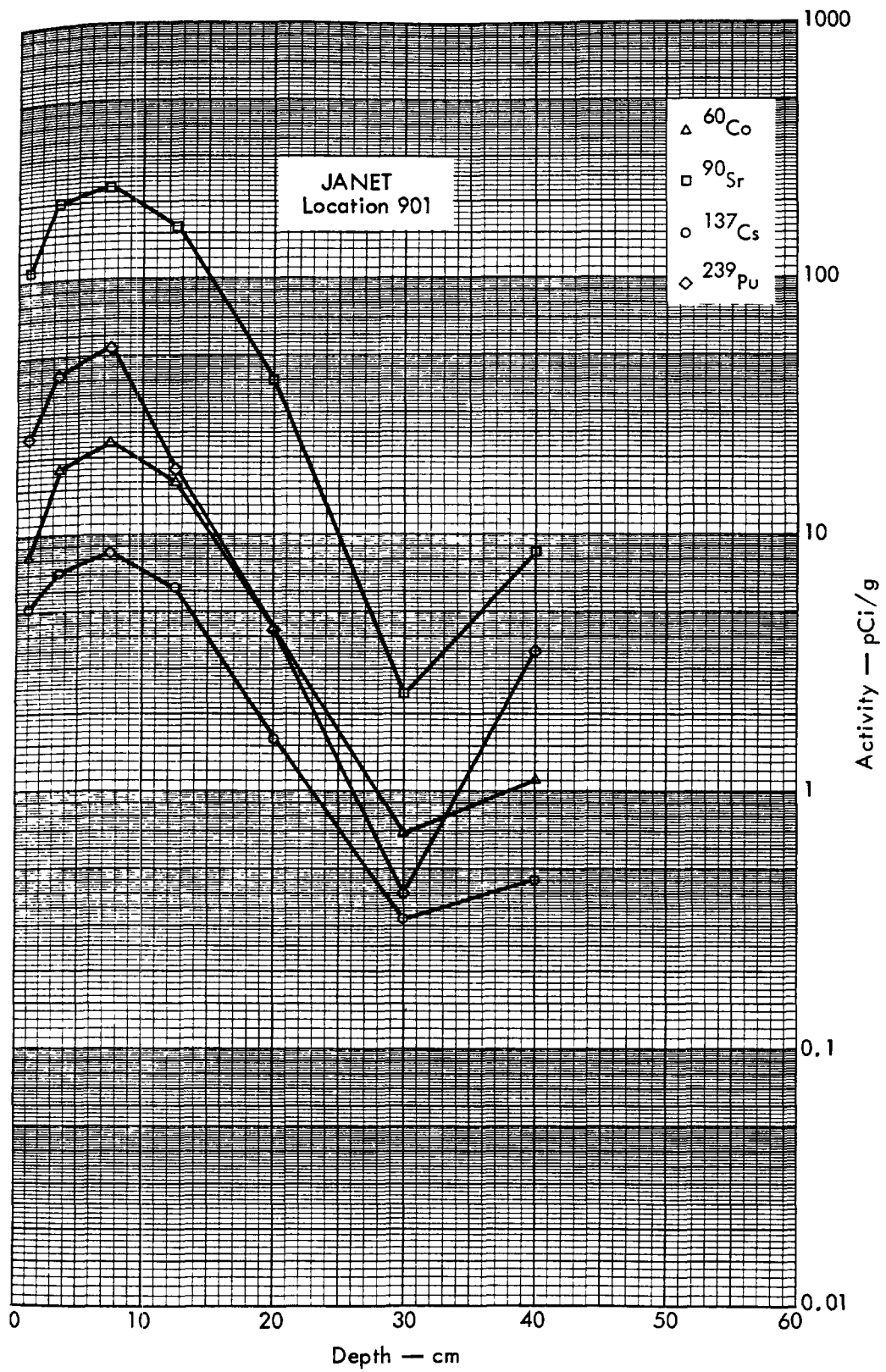


Fig. B. 8.2n. Activities of selected radionuclides as a function of soil depth.



Fig. B.9.1.a.



Fig. 2-1-1. Glass count isosexposure contours. (Refer to alphabetic symbol key in this appendix.)

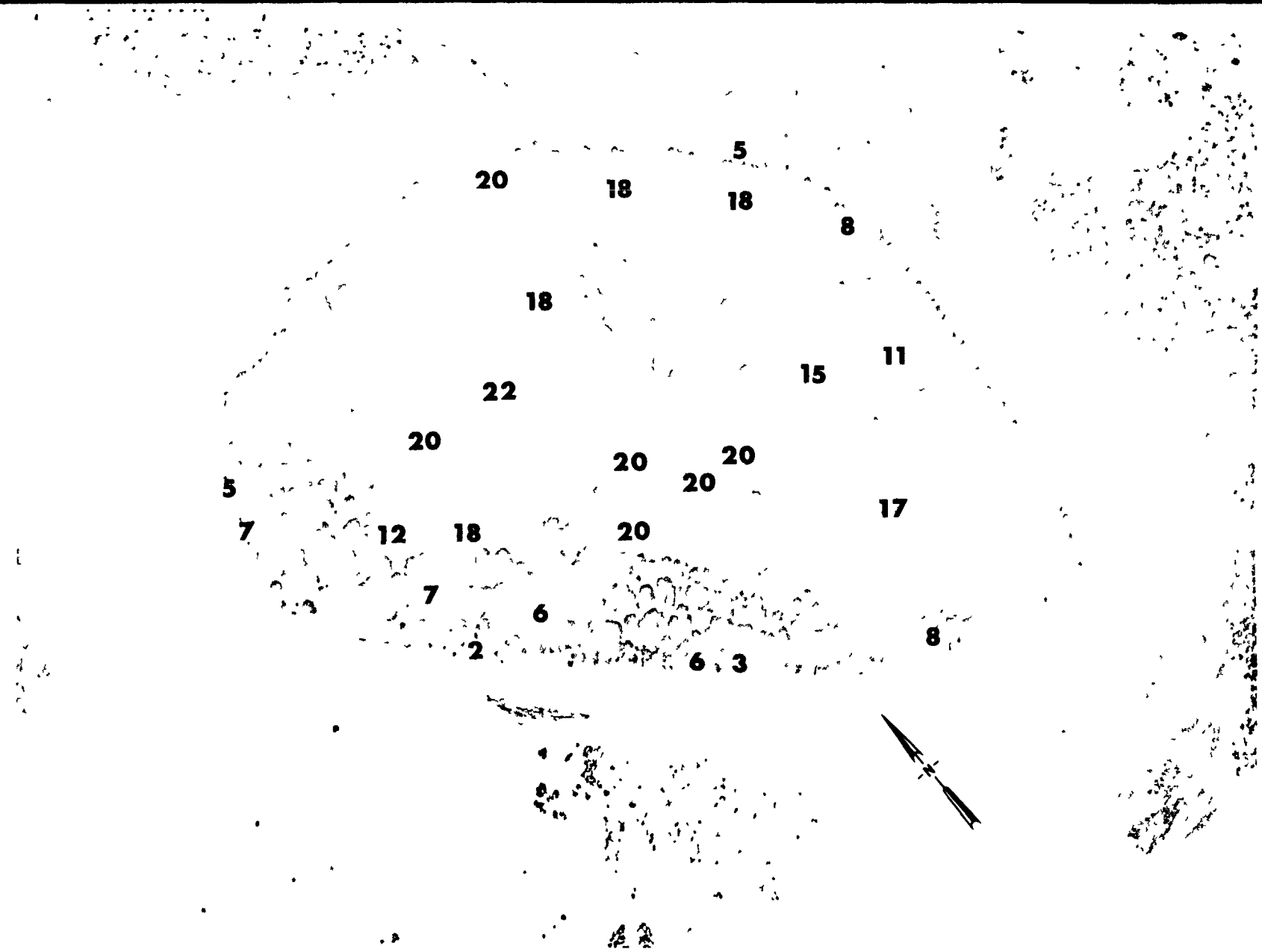
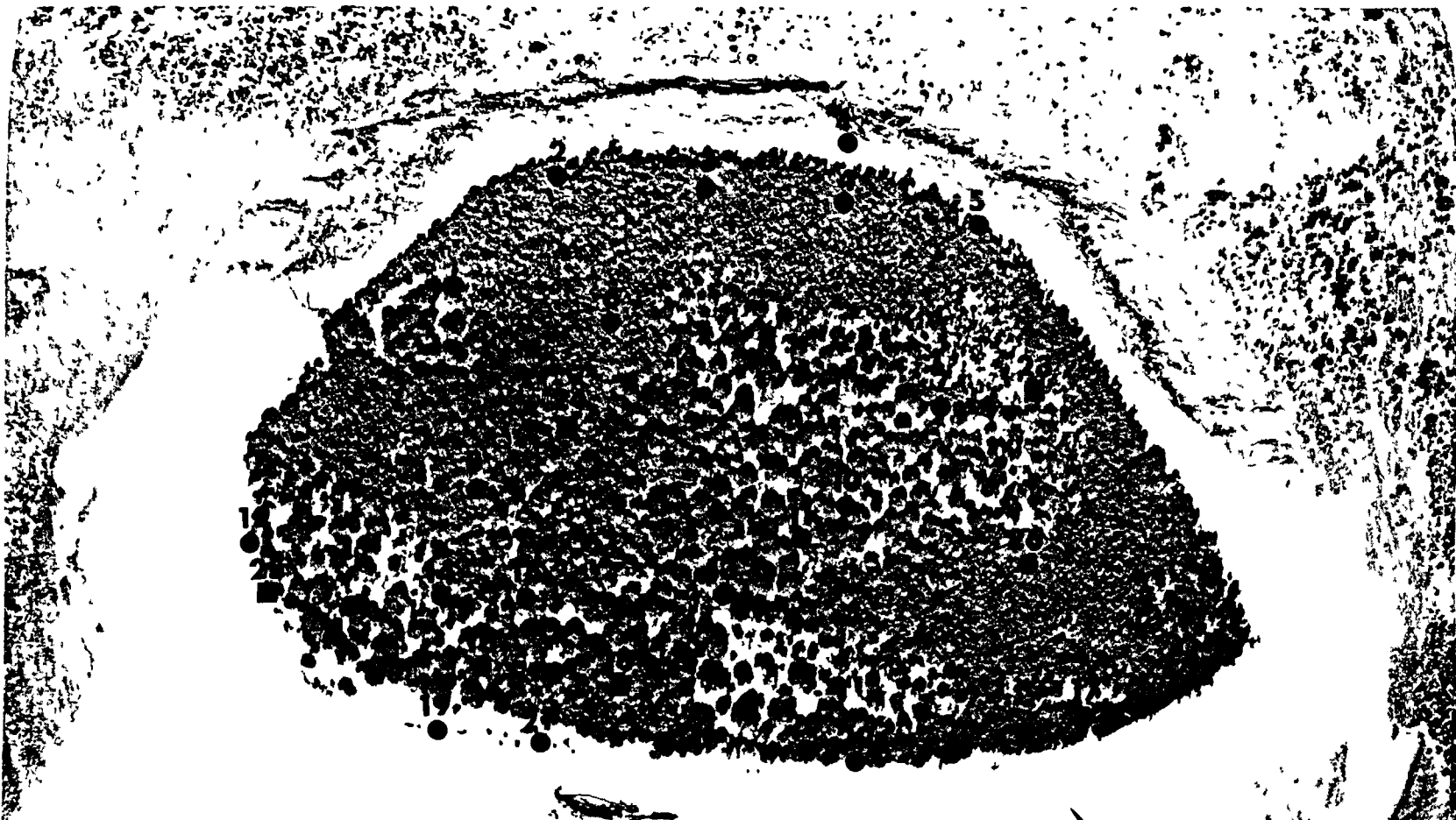


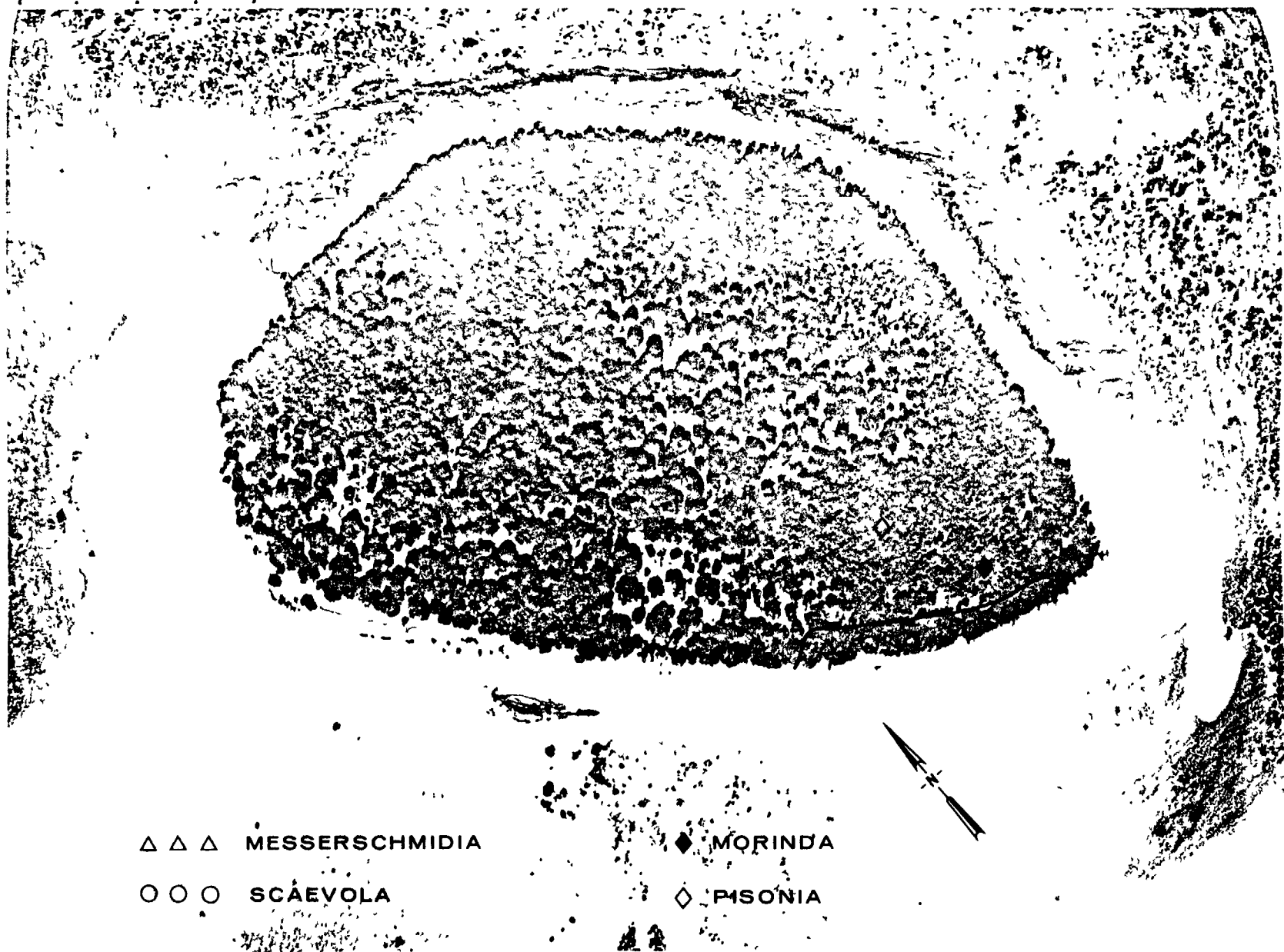
Fig. B.9.1.d. The gamma background exposure rate ( $\mu\text{R/hr}$ ) at 1 m above the ground, measured with a portable NaI scintillation counter.



■ PROFILE SAMPLES (0-65 cm)

● CORE SAMPLES (15 cm)

Fig. B.9.1.f. Soil-sample locations.



△ △ △ MESSERSCHMIDIA

○ ○ ○ SCAEVOLA

◆ MORINDA

◇ PISONIA

Fig. B.9.1.g. Vegetation sample locations.

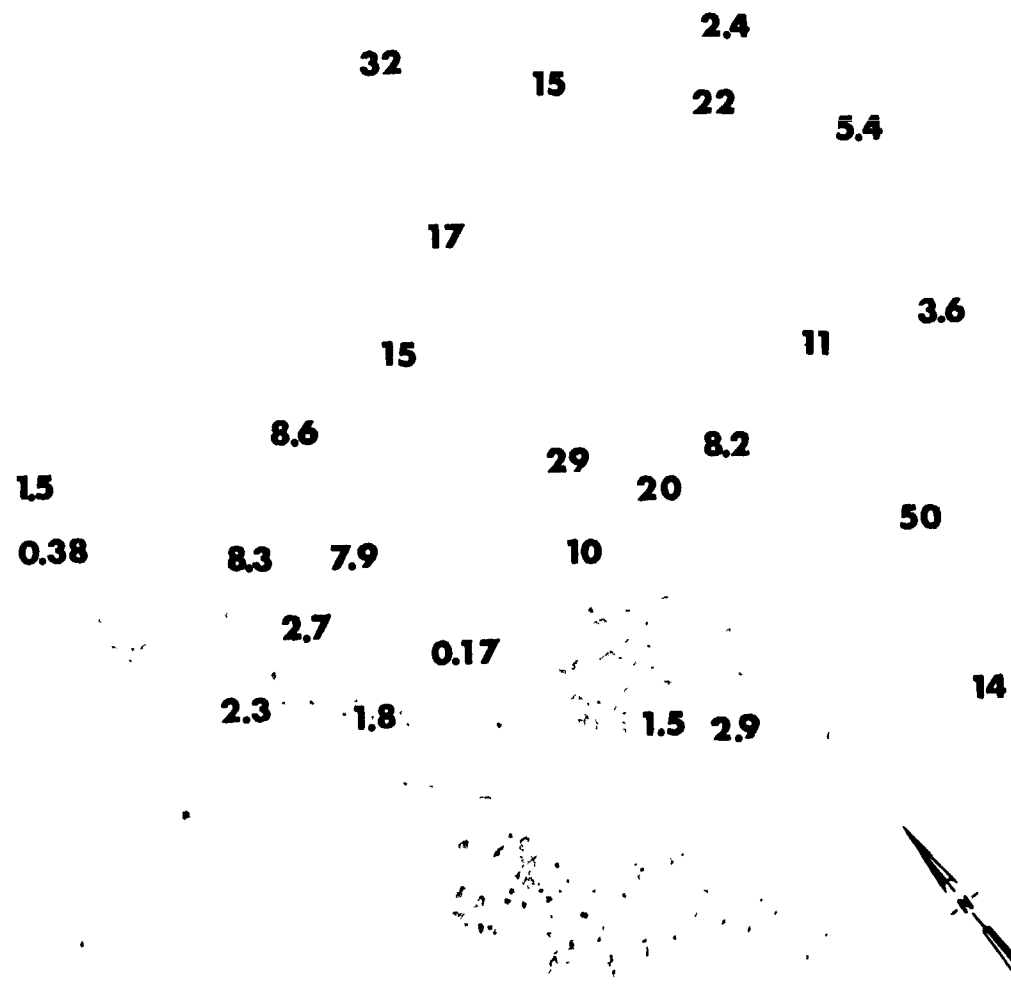


Fig. B.9.1.1. The average  $^{239}\text{Pu}$  activities (pCi/g) in soil samples collected to a depth of 15 cm.



Fig. B.9.1.j. The average  $^{90}\text{Sr}$  activities (pCi/g) in soil samples collected to a depth of 15 cm.



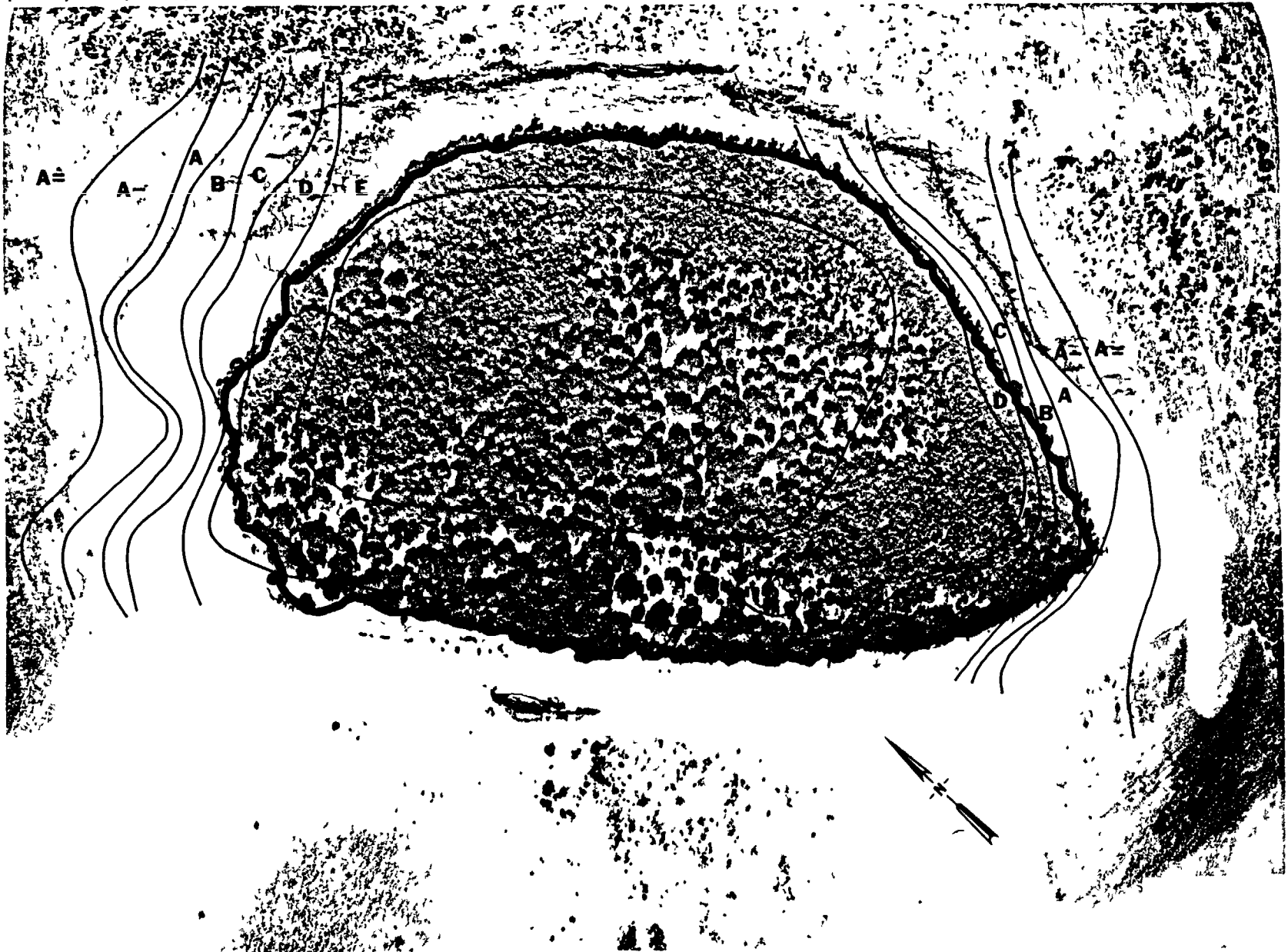


Fig. B.9.1.k. <sup>137</sup>Cs isosexposure and isoconcentration contours. (Refer to alphabetic symbol key in this appendix.)

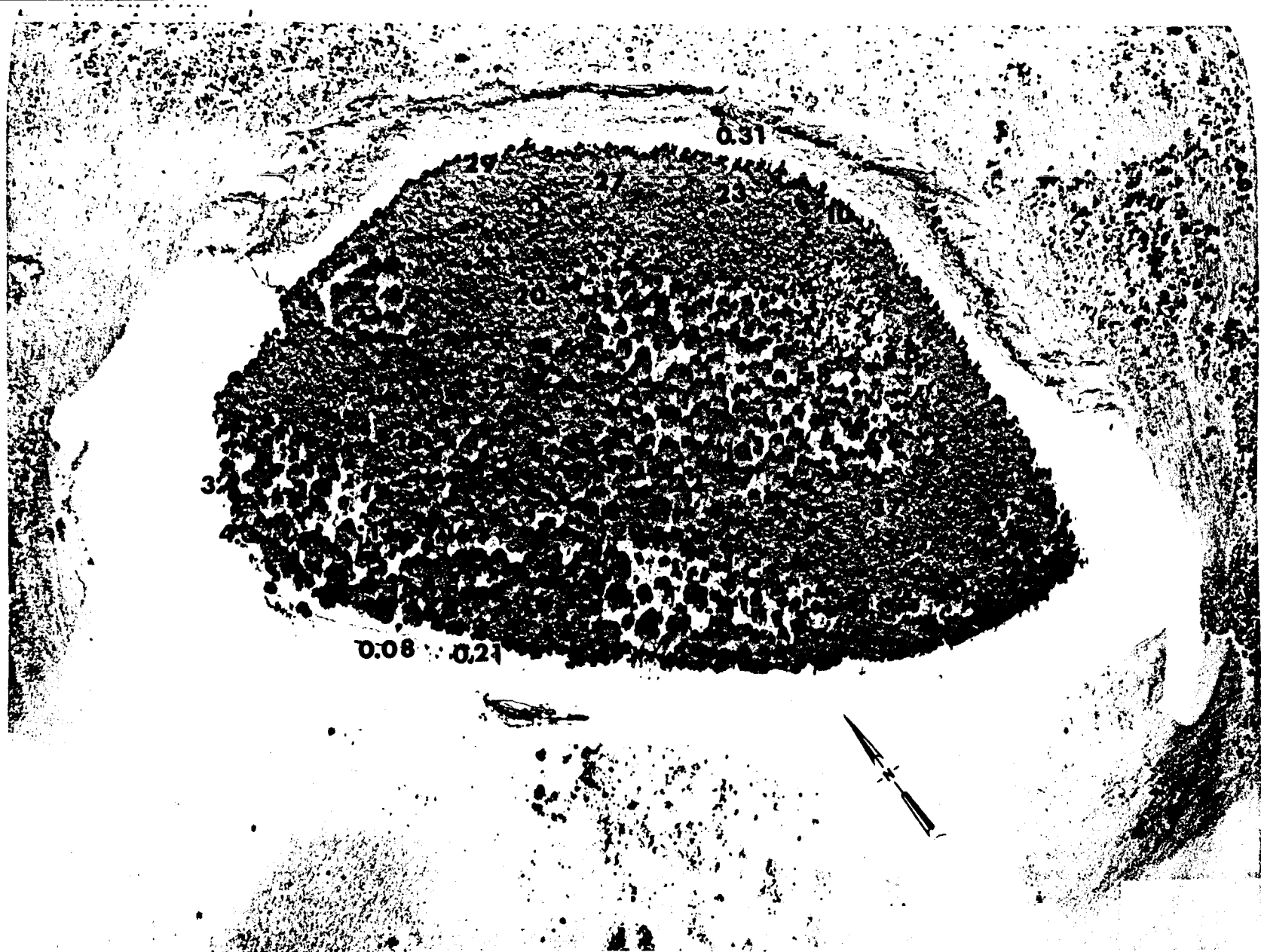


Fig. B.9.1.1. The average <sup>137</sup>Cs activities (pCi/g) in soil samples collected to a depth of 15 cm.



Fig. B.9.1.m.  $^{60}\text{Co}$  isosexposure and isoconcentration contours. (Refer to alphabetic symbol key in this appendix.)

STATE OF TEXAS

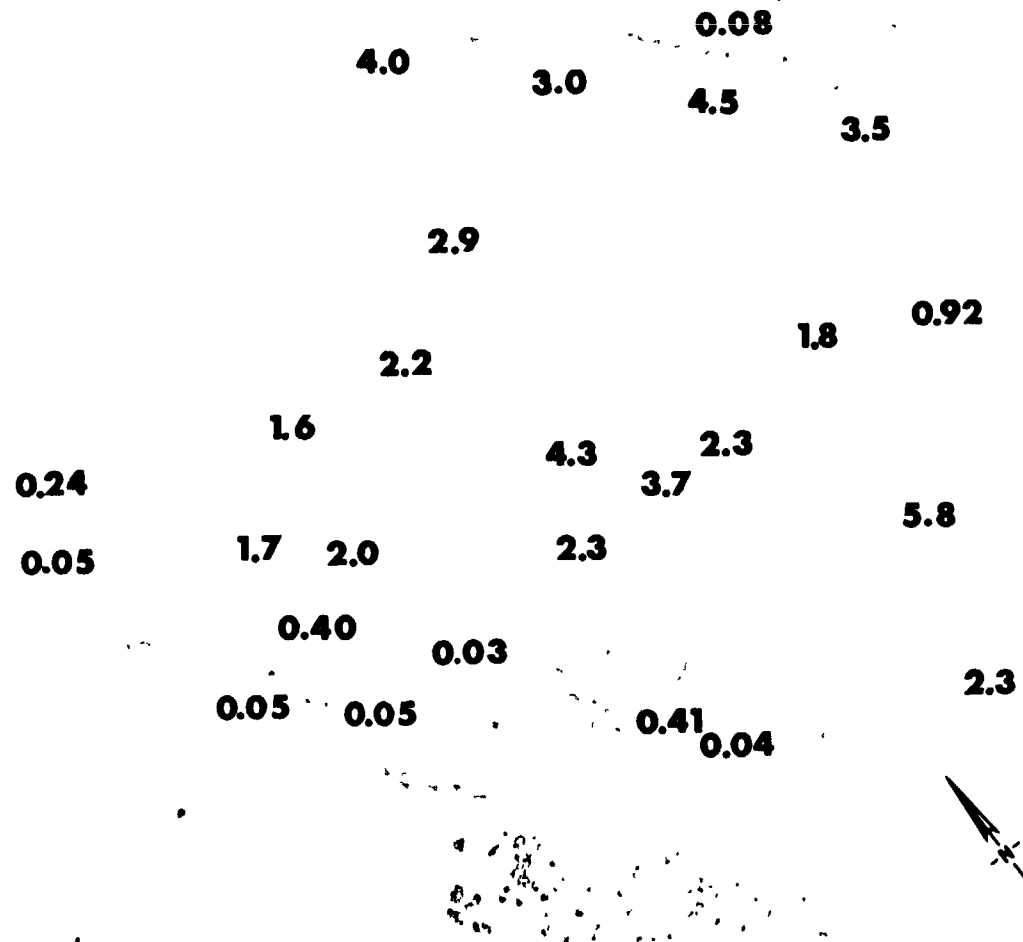


Fig. B.9.1.n. The average <sup>60</sup>Co activities (pCi/g) in soil samples collected to a depth of 15 cm.

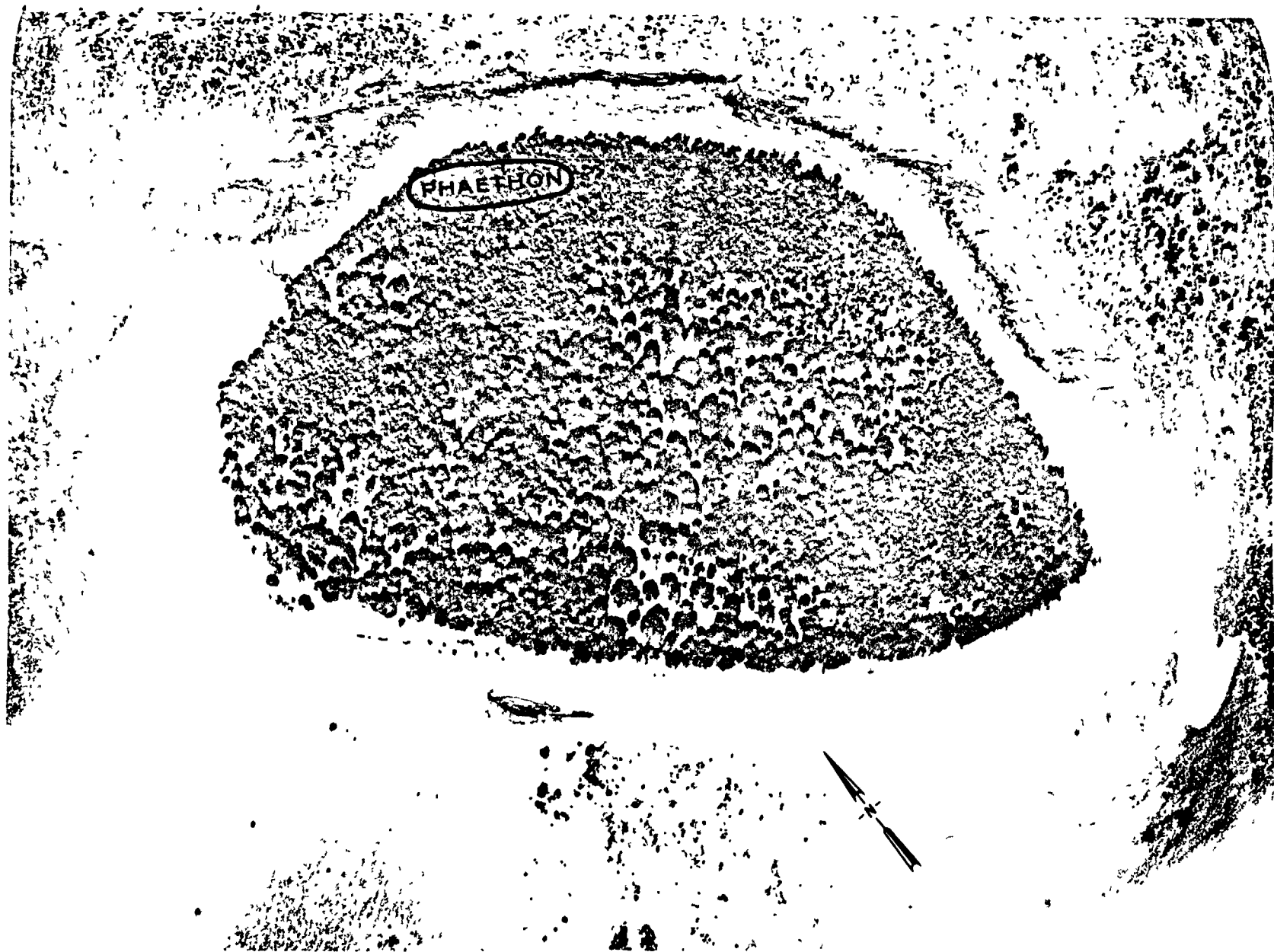


Fig. B.9.1.o. Terrestrial animal sample locations.

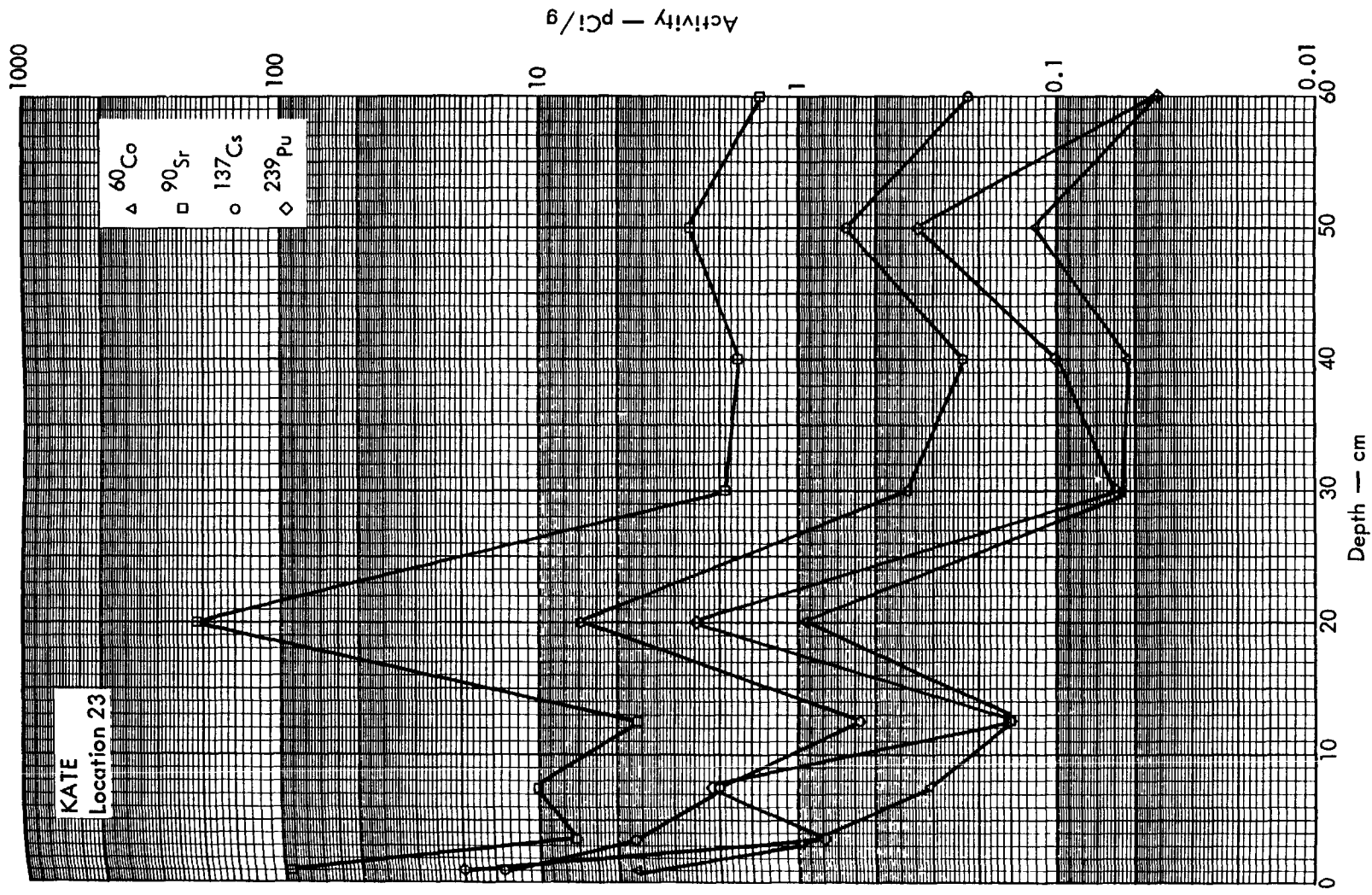


Fig. B. 9. 2a. Activities of selected radionuclides as a function of soil depth.

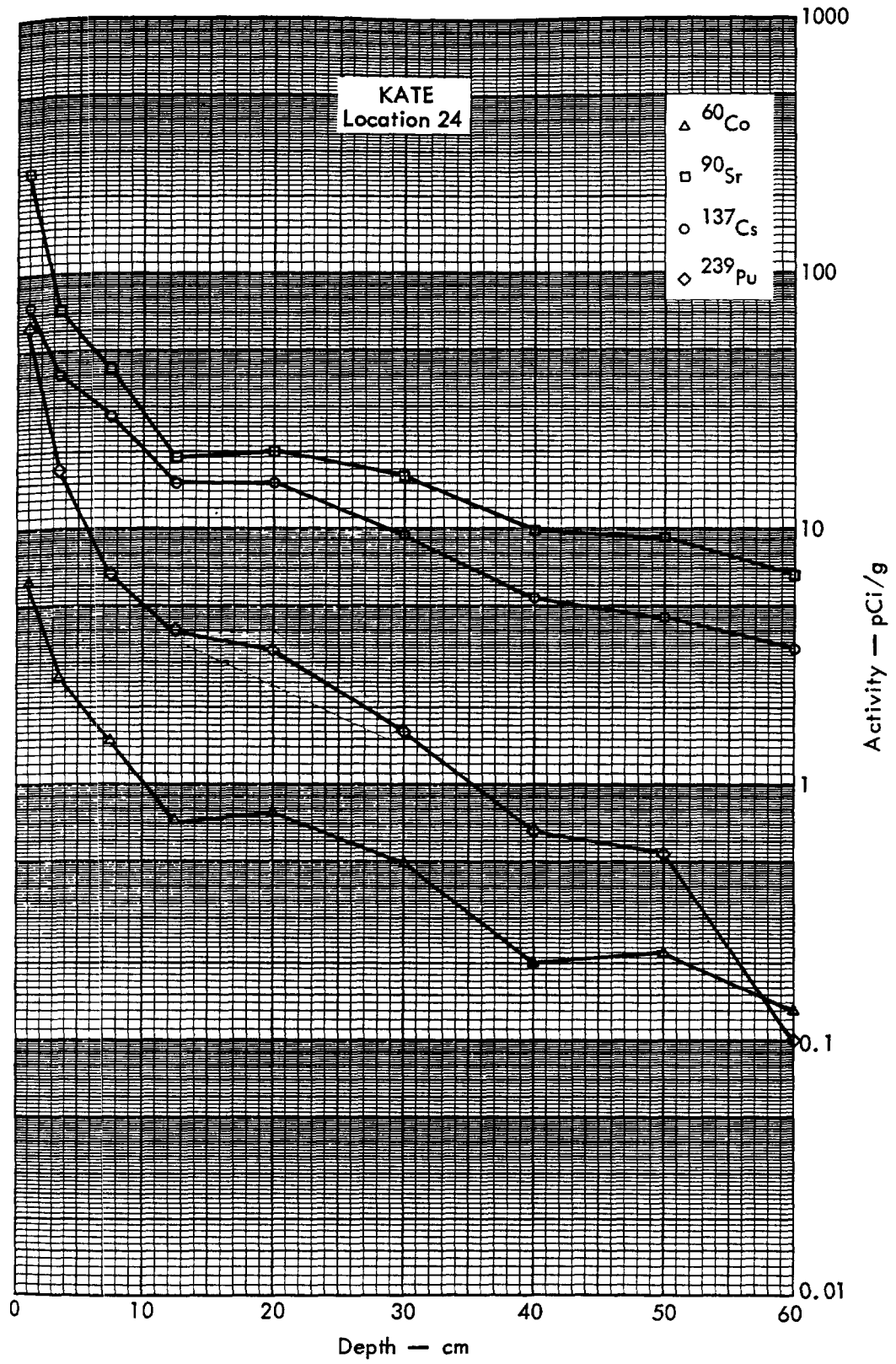


Fig. B. 9. 2b. Activities of selected radionuclides as a function of soil depth.

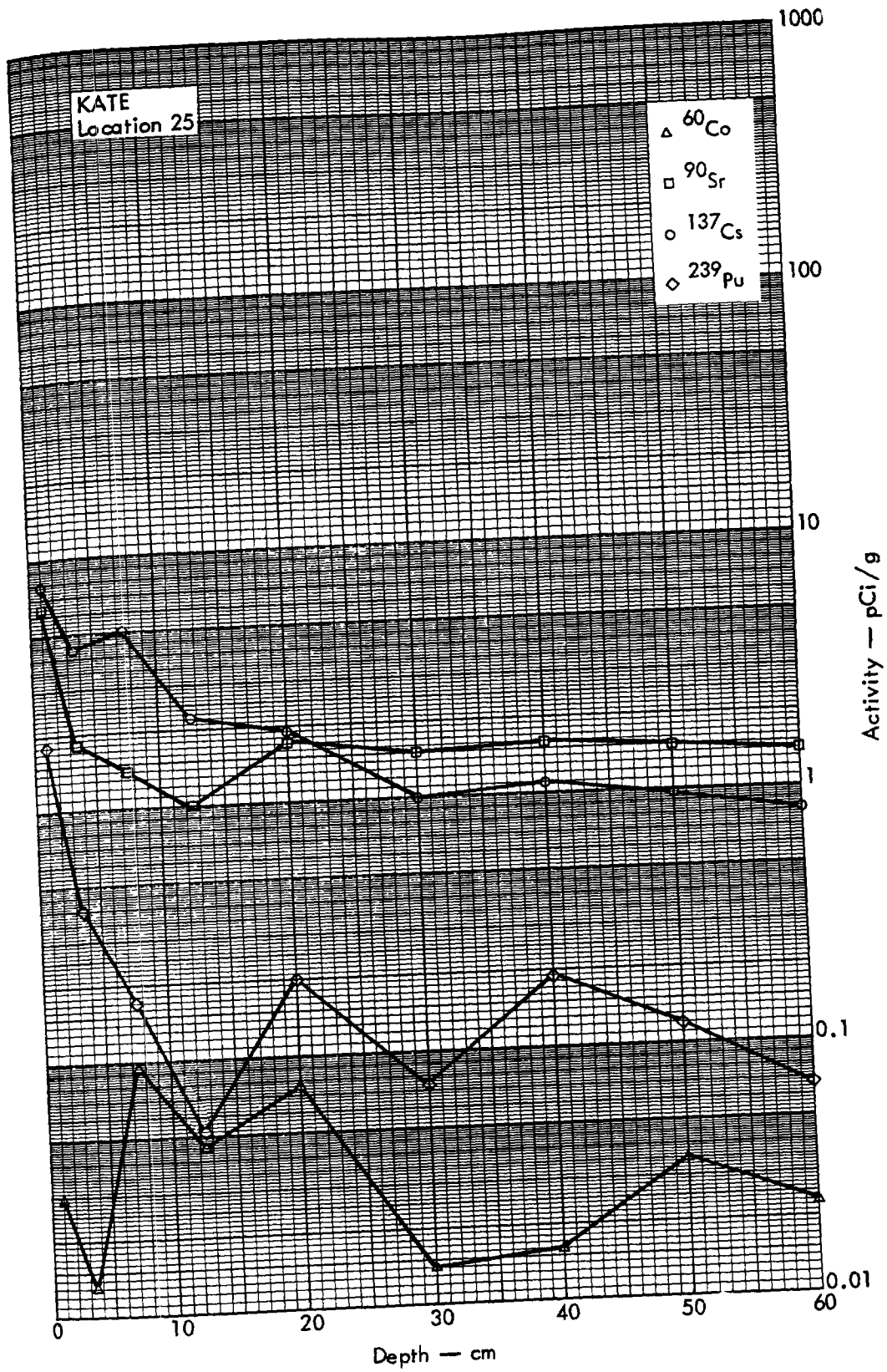


Fig. B.9.2c. Activities of selected radionuclides as a function of soil depth.





Fig. B.10.1.a.



Fig. B.10.1.b. Gross count isosexposure contours. (Refer to alphabetic symbol key in this appendix.)

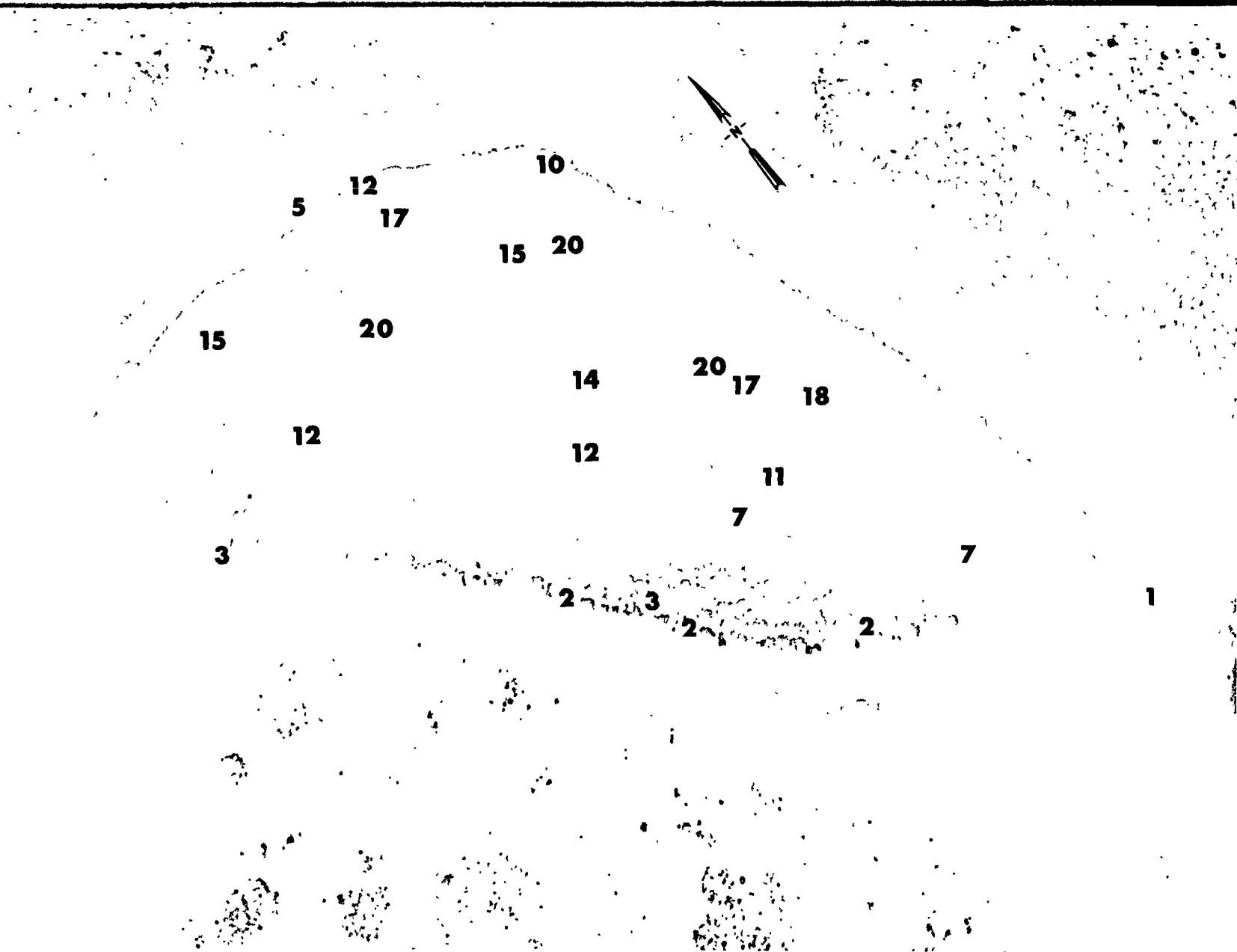


Fig. B.10.1.d. The gamma background exposure rate ( $\mu\text{R/hr}$ ) at 1 m above the ground, measured with a portable NaI scintillation counter.



Fig. B.10.1.f. Soil-sample locations.



△ △ △ MESSERSCHMIDIA  
○ ○ ○ SCAEVOLA

Fig. B.10.1.g. Vegetation sample locations.

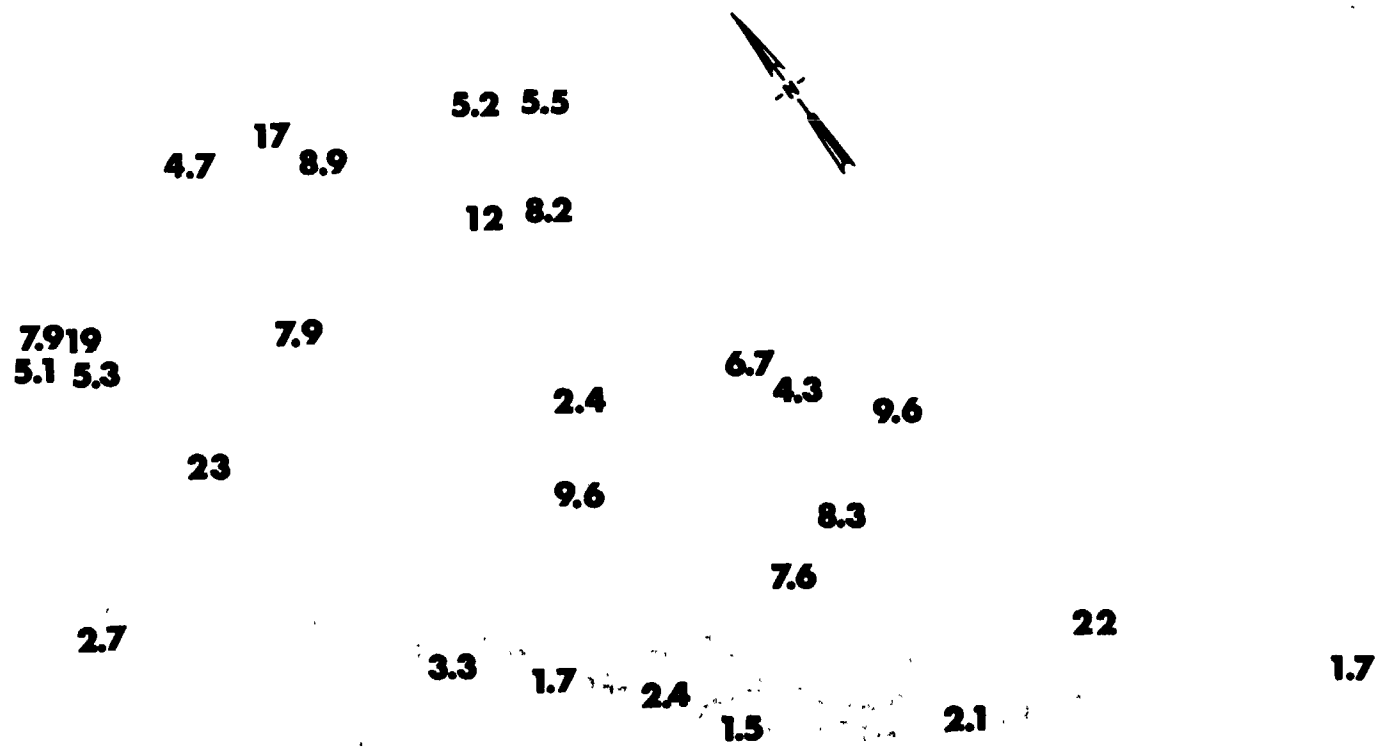


Fig. B.10.1.1. The average  $^{239}\text{Pu}$  activities (pCi/g) in soil samples collected to a depth of 15 cm.



Fig. B.10.1.j. The average <sup>90</sup>Sr activities (pCi/g) in soil samples collected to a depth of 15 cm.



Fig. B.10.1.k.  $^{137}\text{Cs}$  isoexposure and isoconcentration contours. (Refer to alphabetic symbol key in this appendix.)





Fig. R 10 1 The organism 18700 containing 100% of the material



Fig. B.10.1.n. The average  $^{60}\text{Co}$  activities (pCi/g) in soil samples collected to a depth of 15 cm.



Fig. B.10.1.o. Terrestrial animal sample locations.

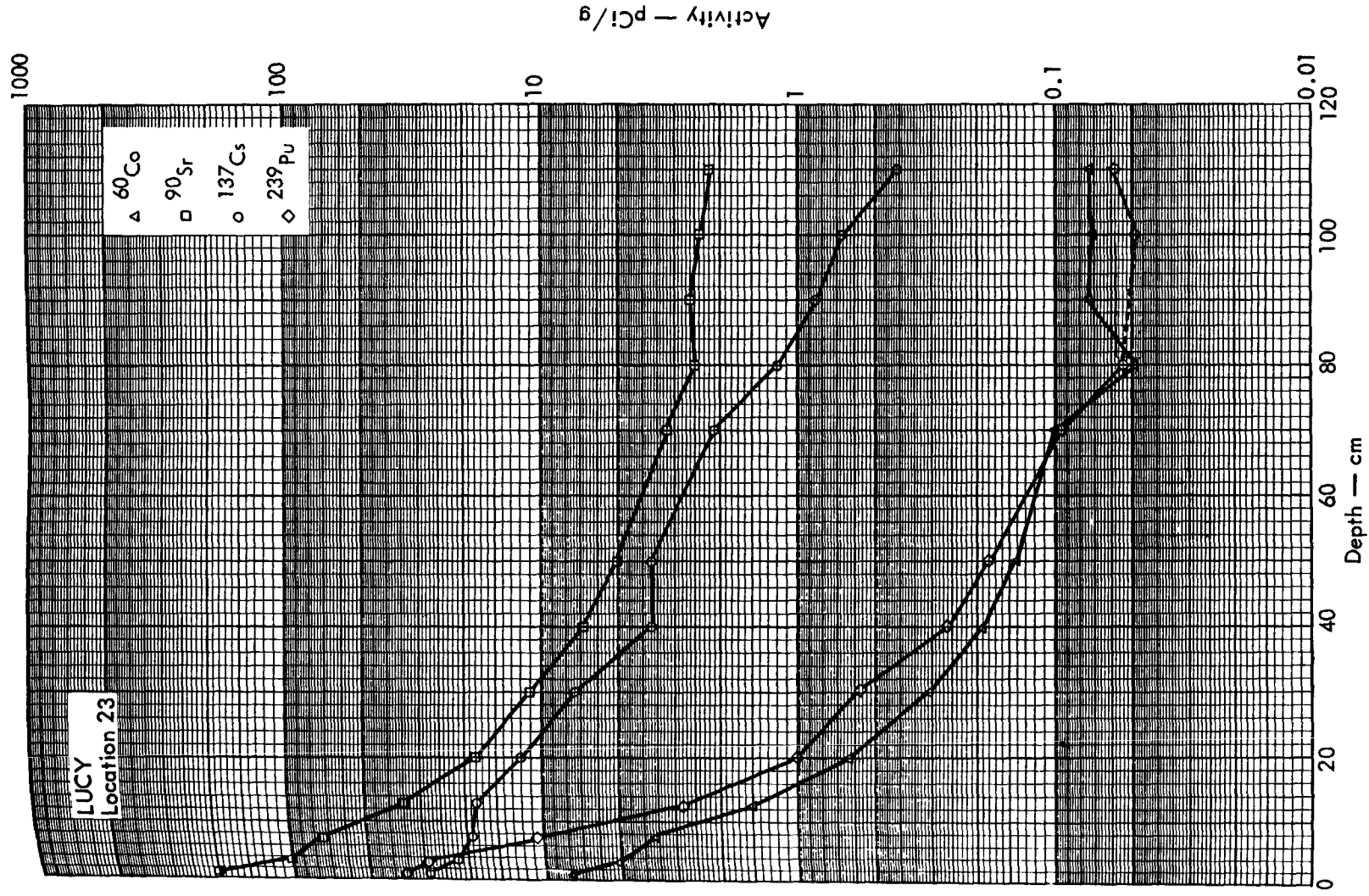


Fig. B.10.2a. Activities of selected radionuclides as a function of soil depth.

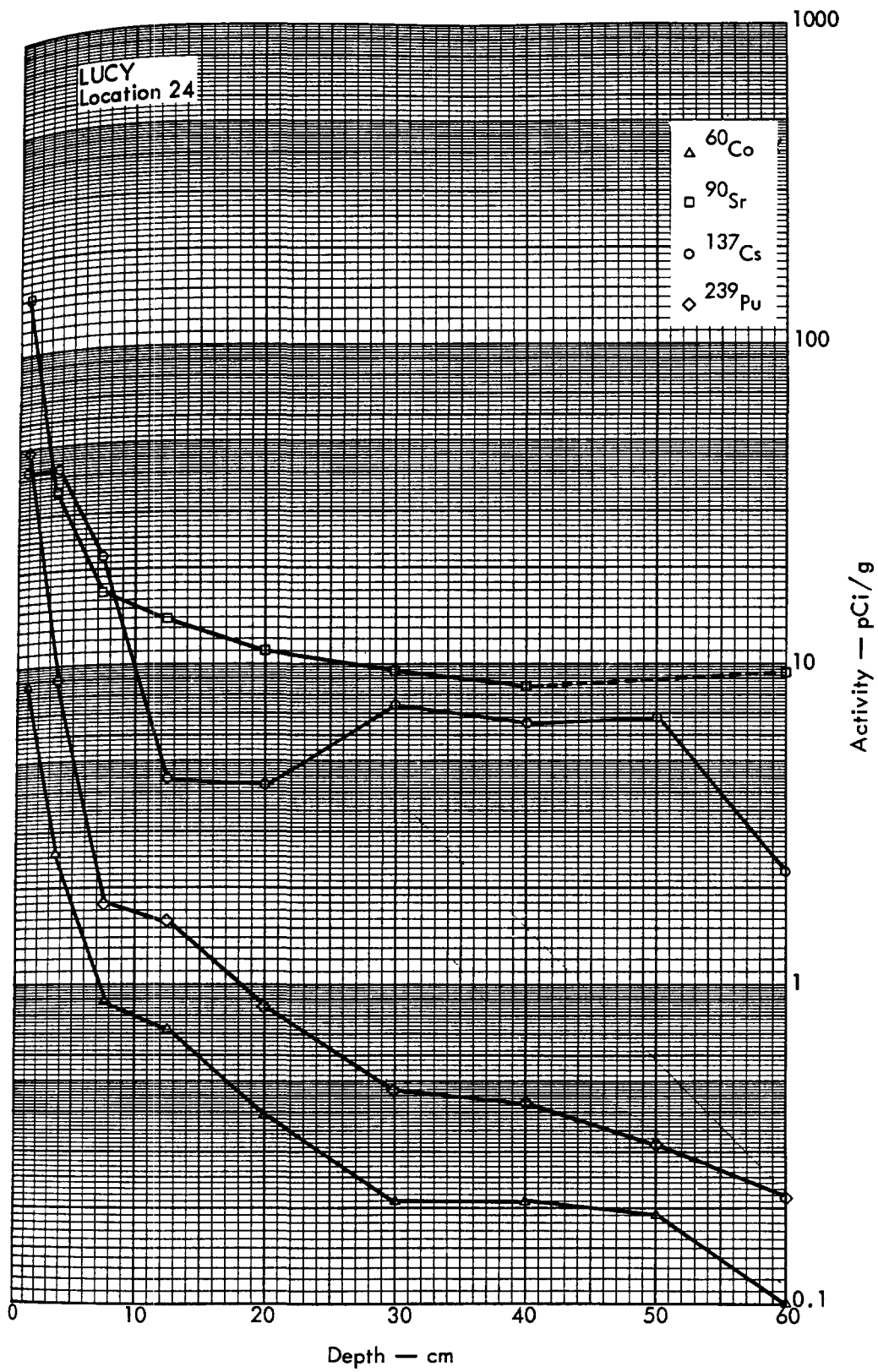


Fig. B.10.2b. Activities of selected radionuclides as a function of soil depth.

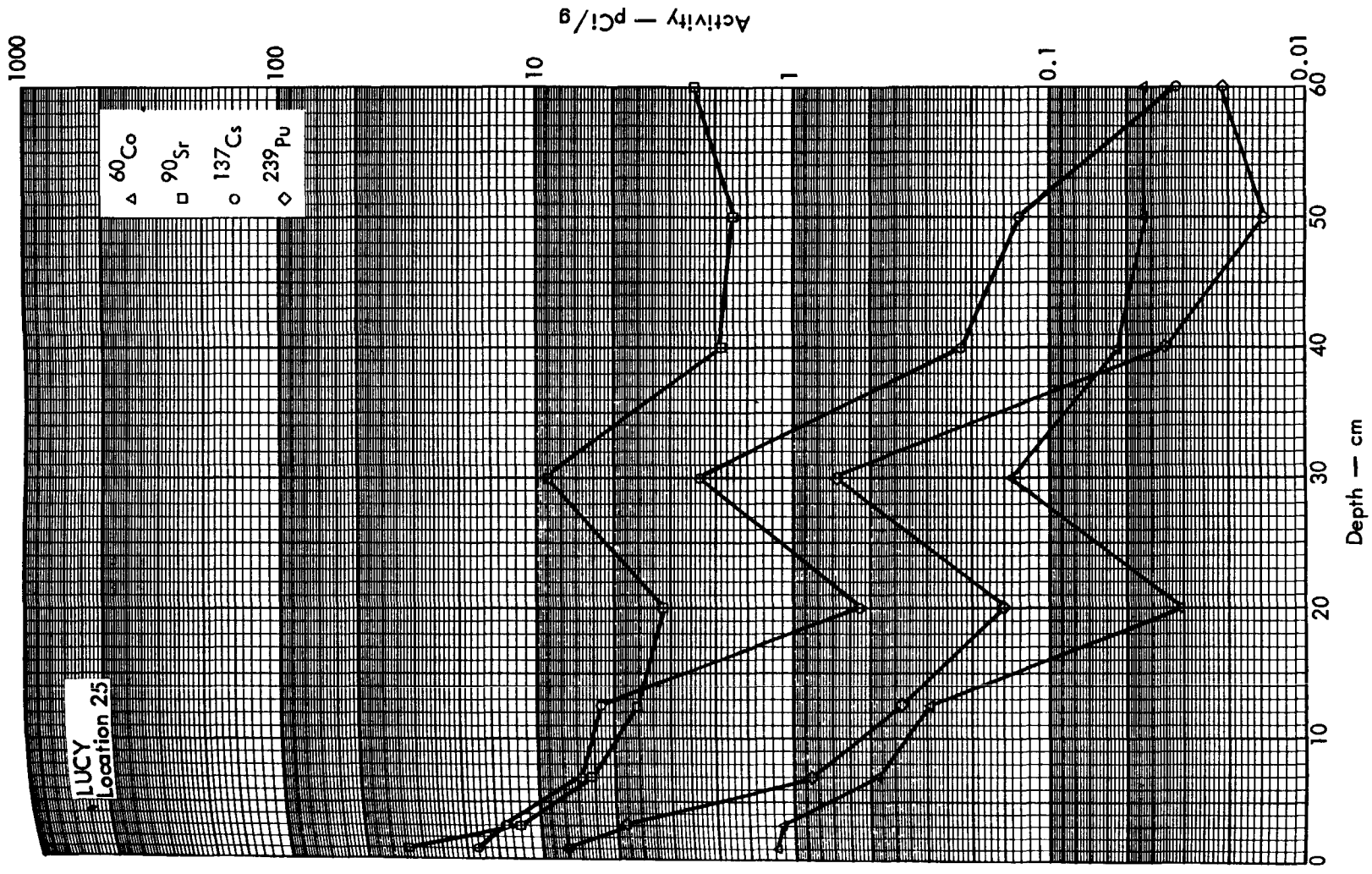


Fig. B.10.2c. Activities of selected radionuclides as a function of soil depth.

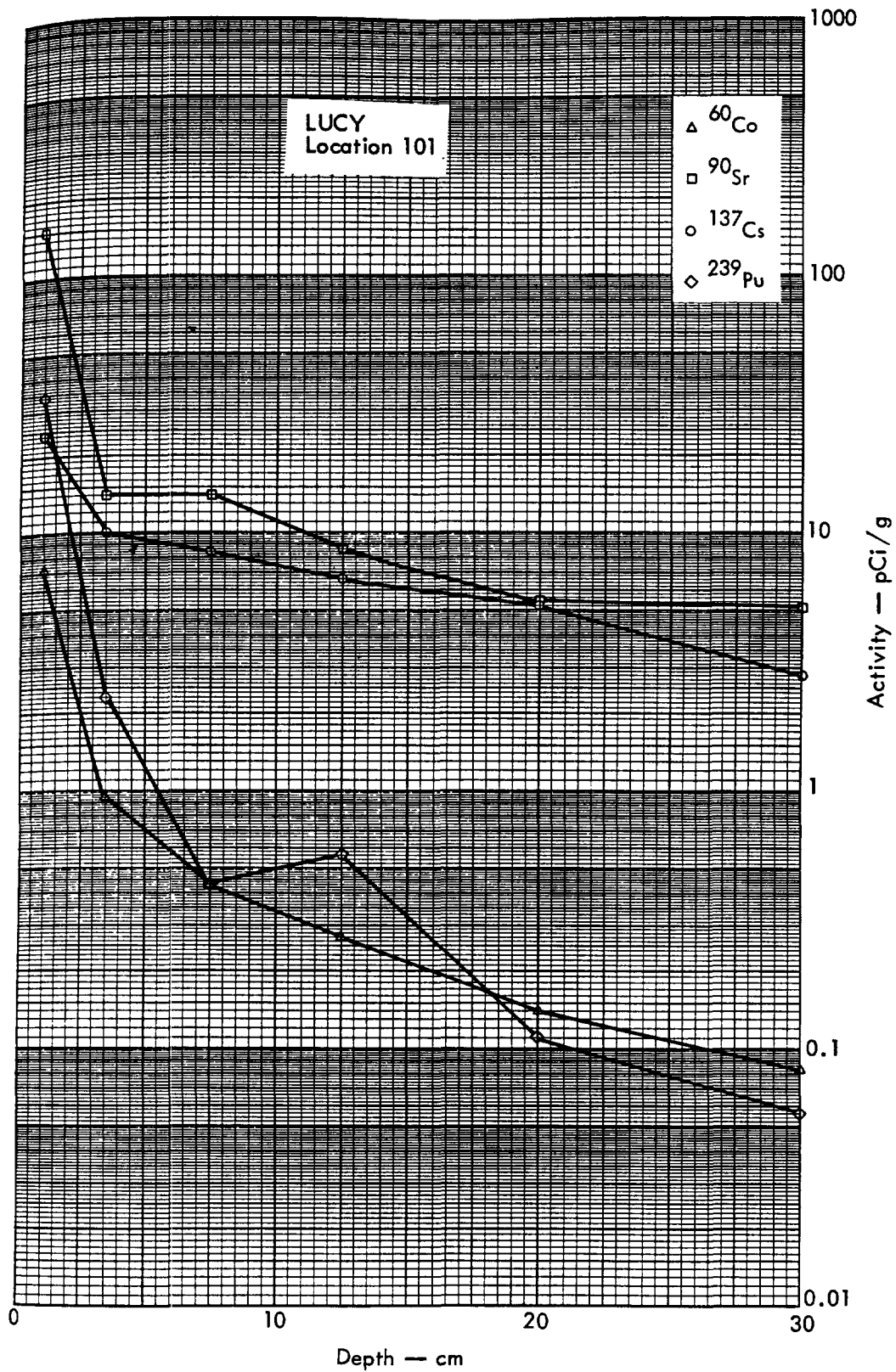


Fig. B.10.2d. Activities of selected radionuclides as a function of soil depth.

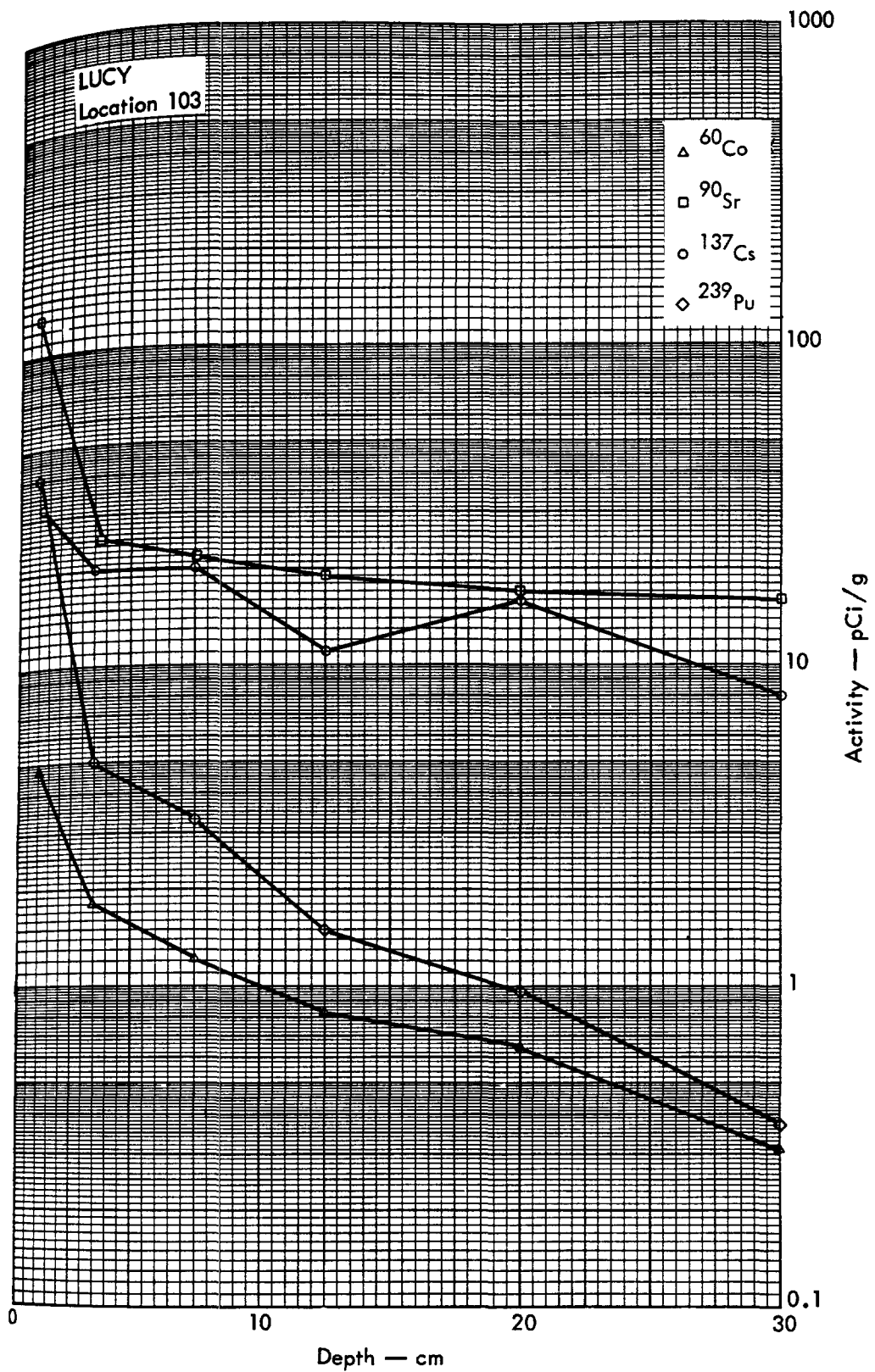


Fig. B.10.2e. Activities of selected radionuclides as a function of soil depth.



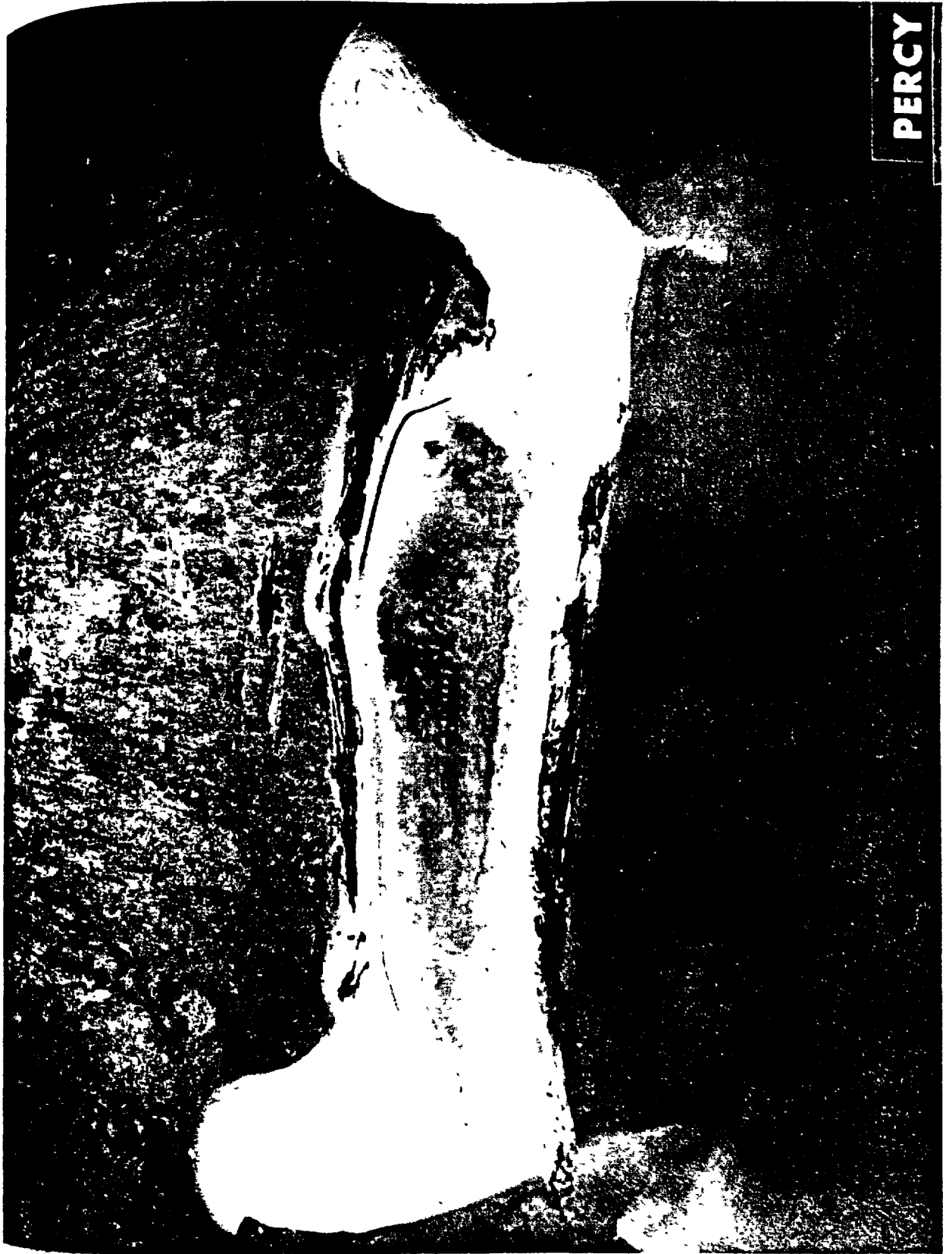


Fig. B.11.1.a.

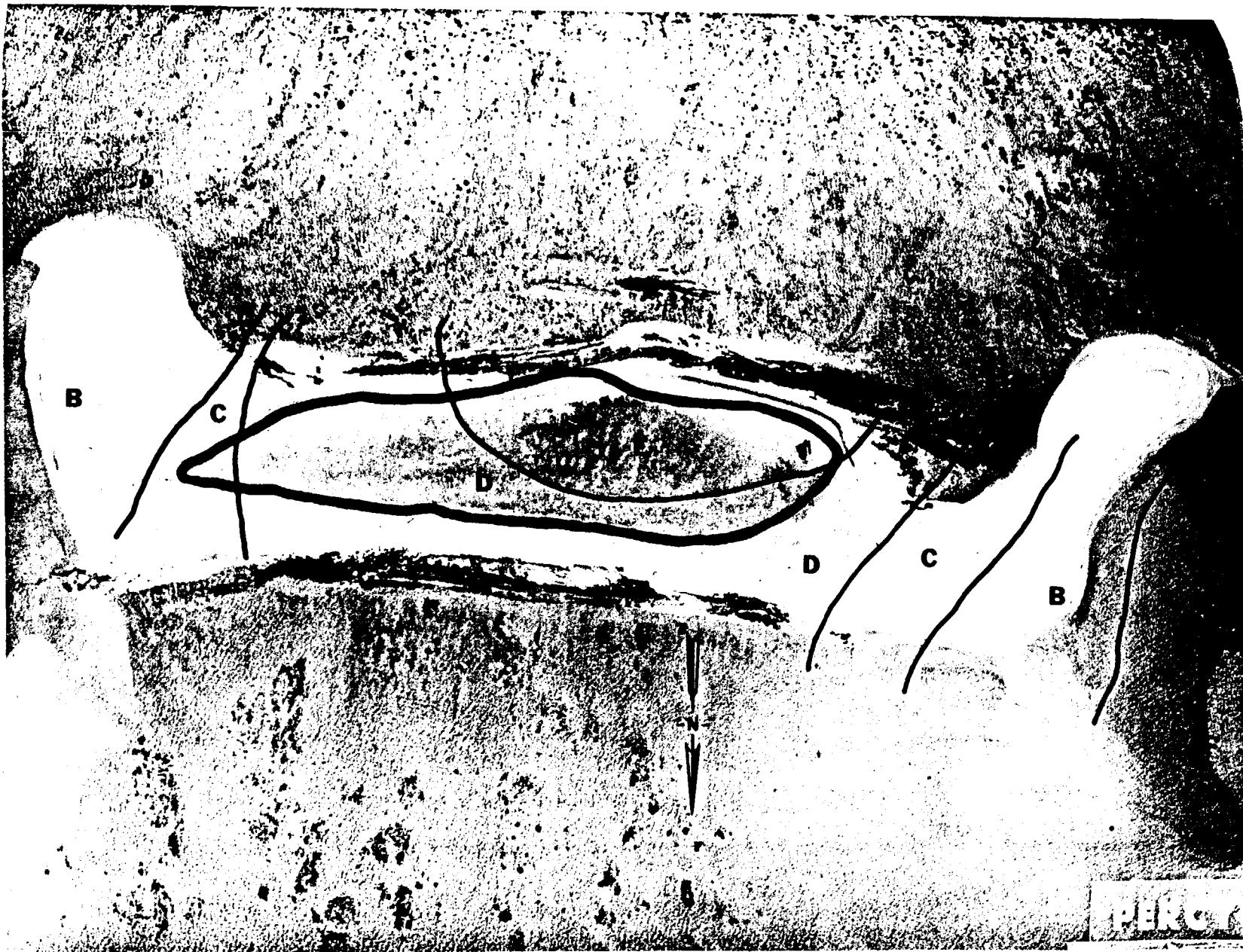


Fig. B.11.1.b. Gross count isosexposure contours. (Refer to alphabetic symbol key in this appendix.)

2

5

10

11

6

2

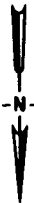


Fig. B.11.1.d. The gamma background exposure rate ( $\mu\text{R/hr}$ ) at 1 m above the ground, measured with a portable NaI scintillation counter.

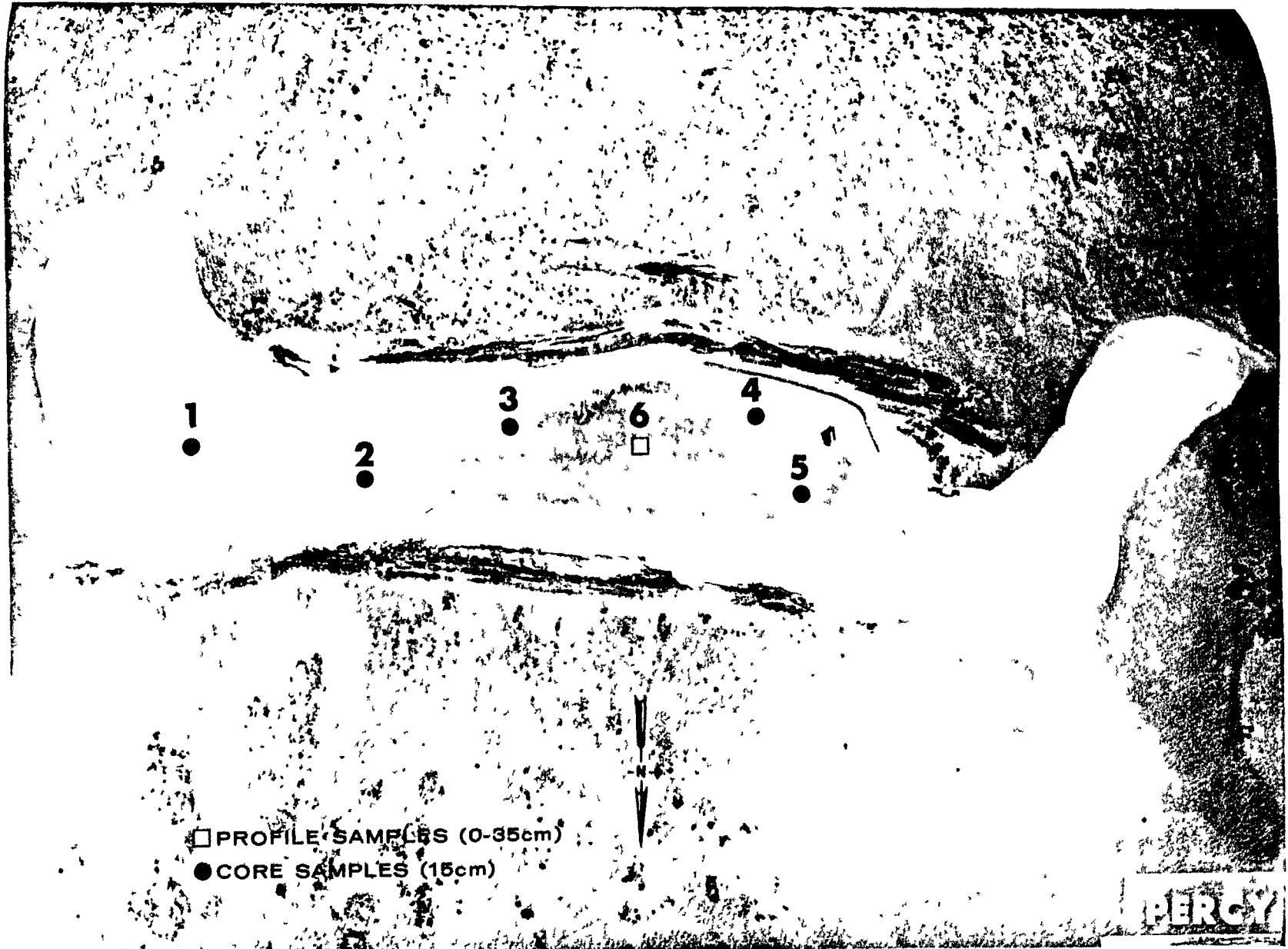


Fig. B.11.1.f. Soil-sample locations.

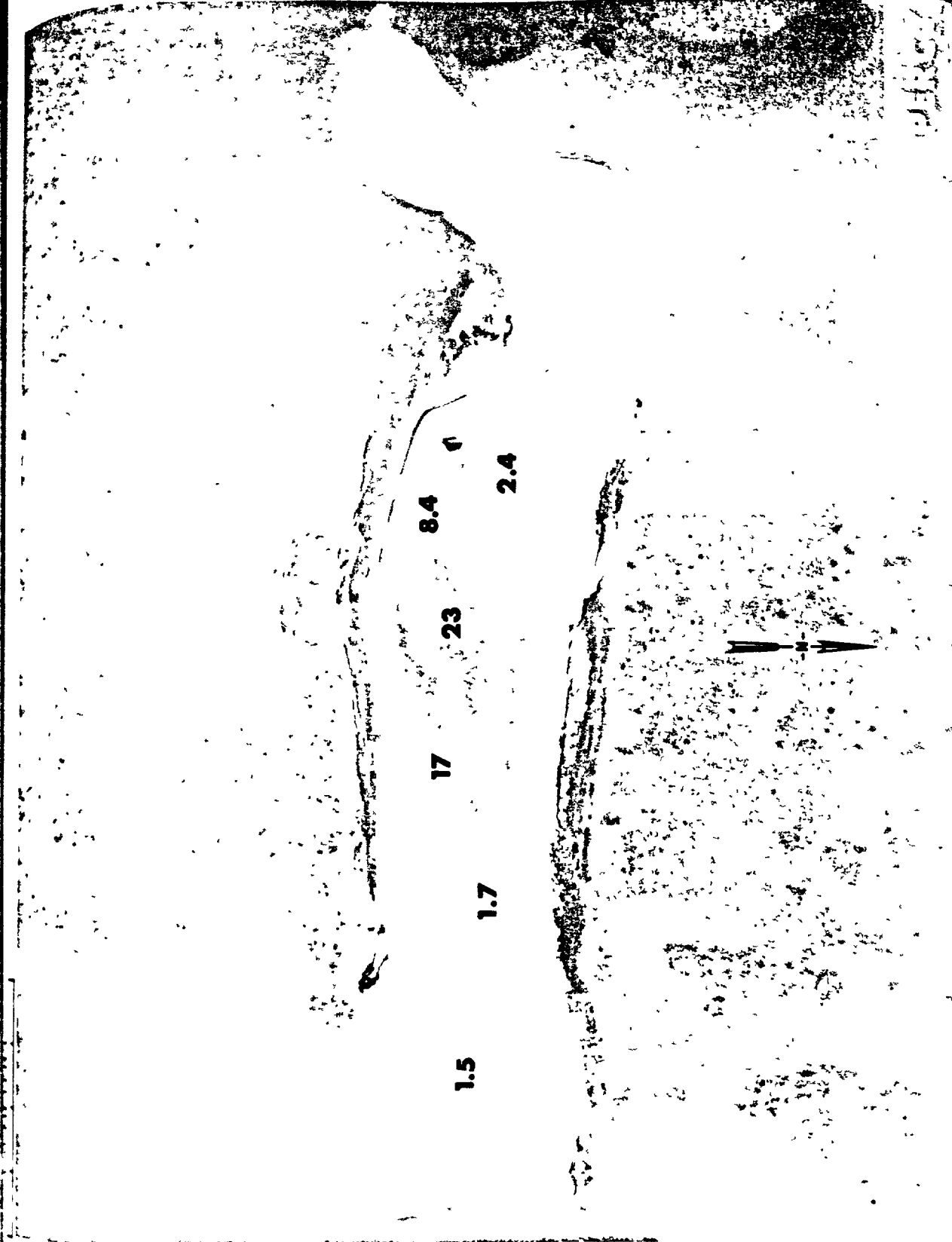


Fig. B.11.1.i. The average  $^{239}\text{Pu}$  activities (pCi/g) in soil samples collected to a depth of 15 cm.

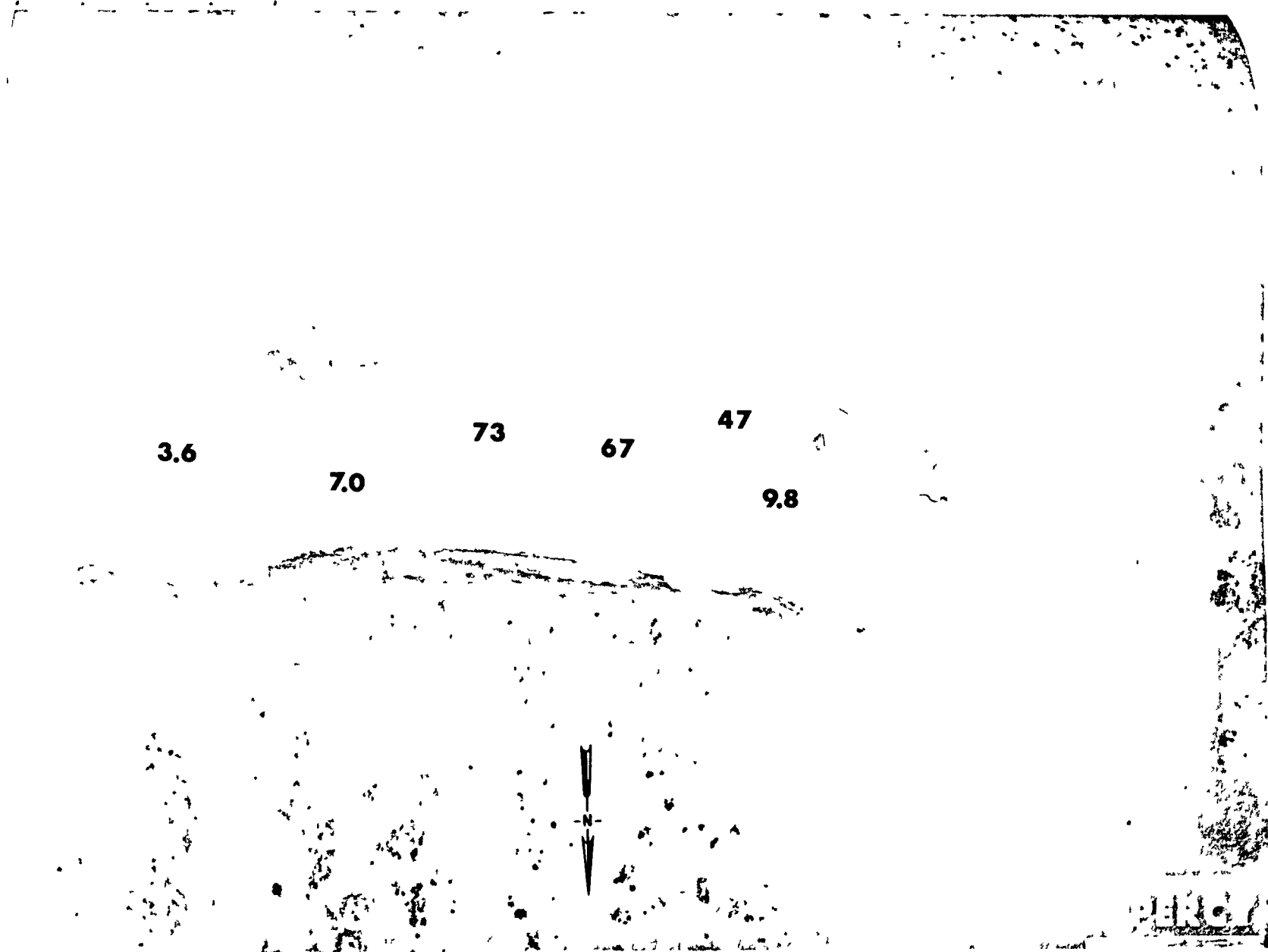


Fig. B.11.1.j. The average  $^{90}\text{Sr}$  activities (pCi/g) in soil samples collected to a depth of 15 cm.

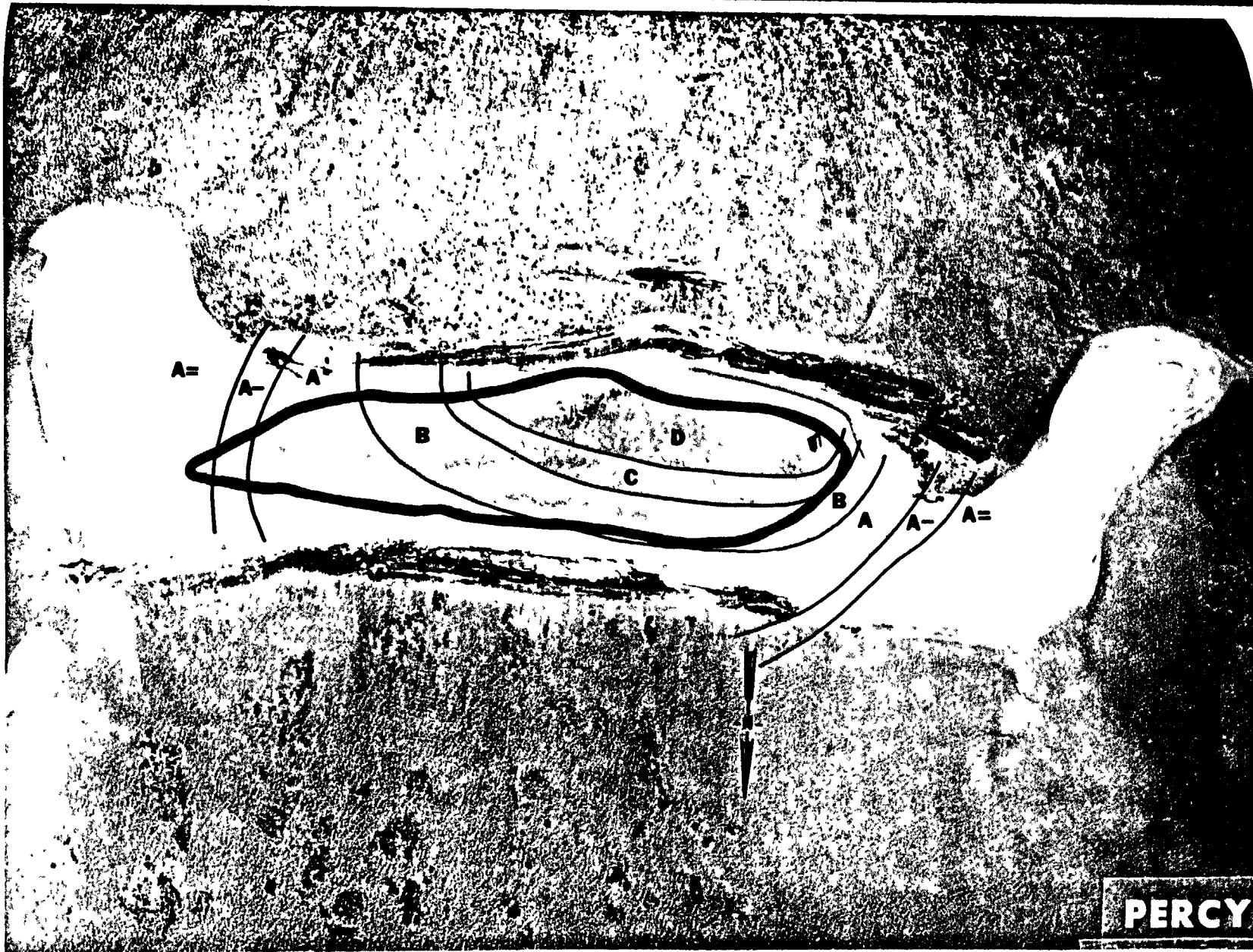


Fig. B.11.1.k. <sup>137</sup>Cs isoexposure and isoconcentration contours. (Refer to alphabetic symbol key in this appendix.)

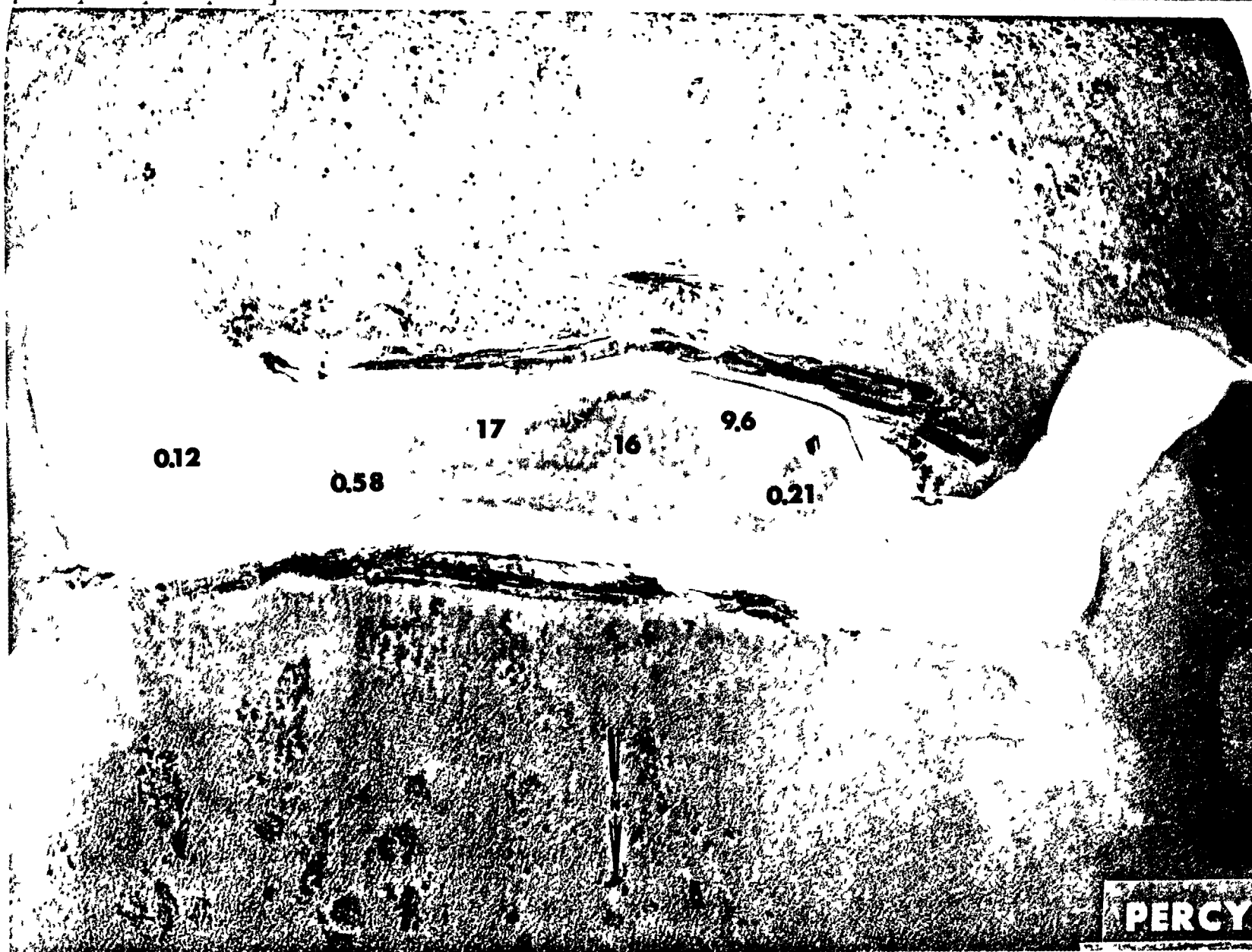


Fig. B.11.1.1. The average <sup>137</sup>Cs activities (pCi/g) in soil samples collected to a depth of 15 cm.



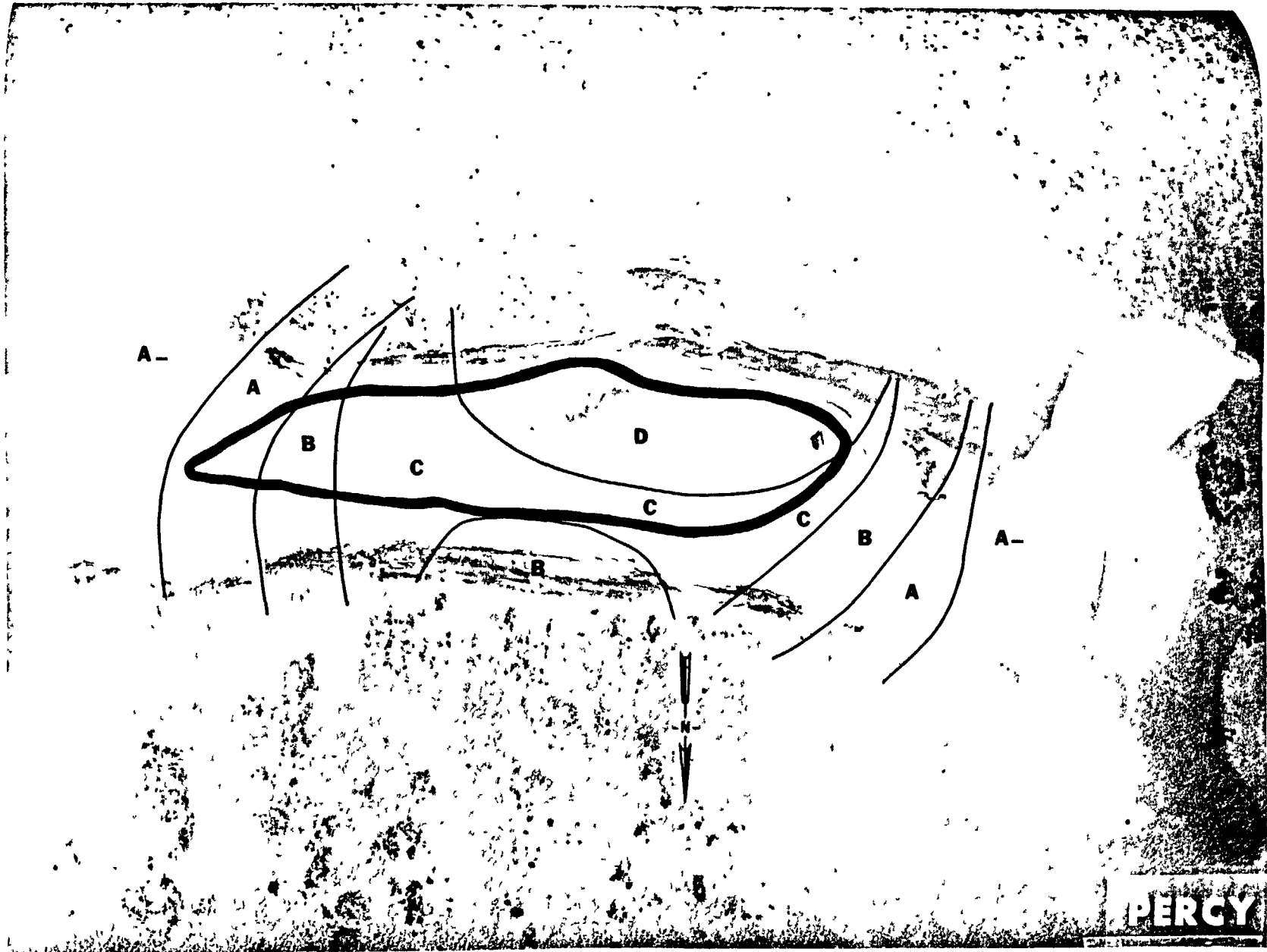


Fig. B.11.1.m.  $^{60}\text{Co}$  isosexposure and isoconcentration contours. (Refer to alphabetic symbol key in this appendix.)



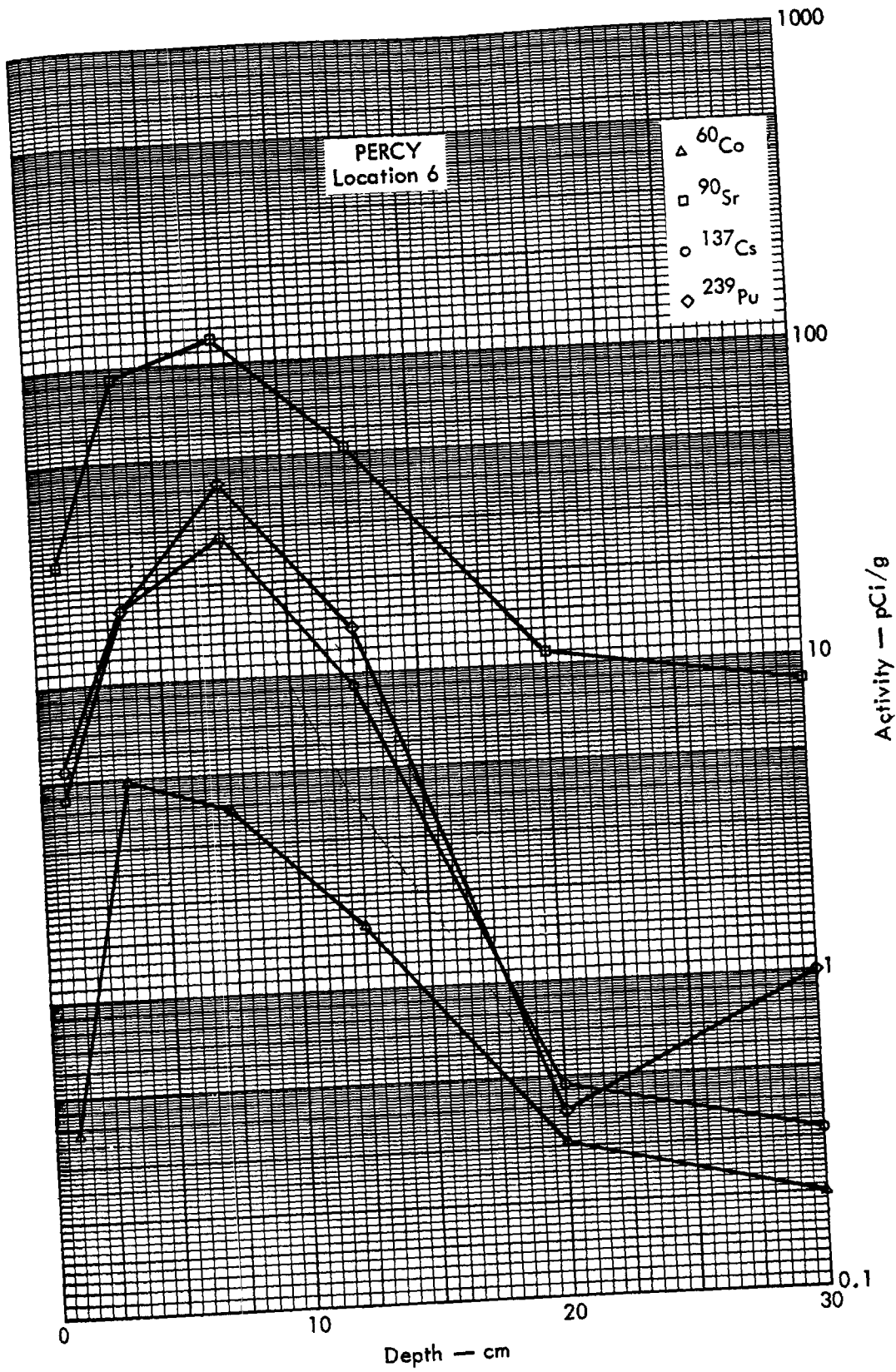
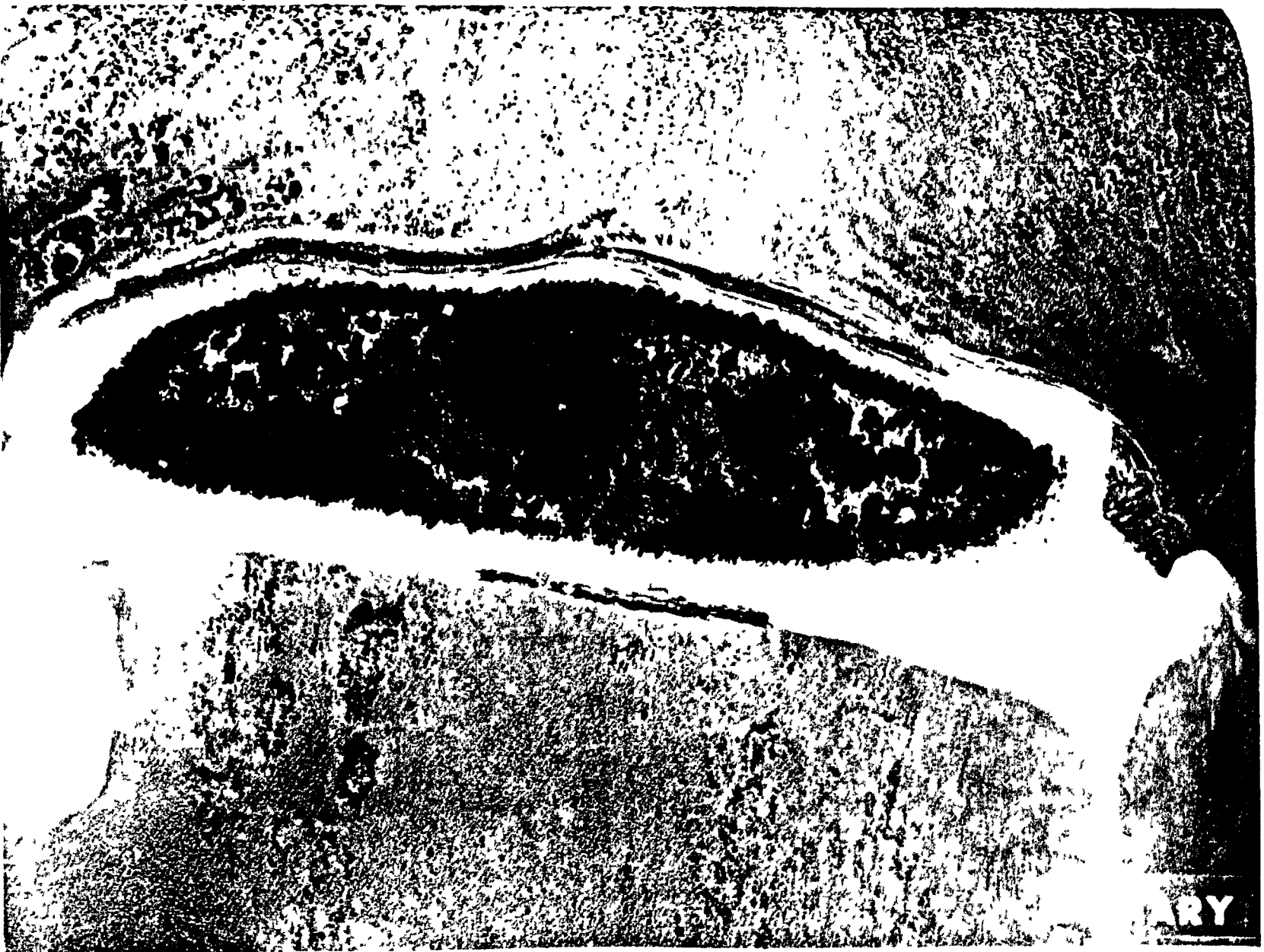


Fig. B. 11. 2a. Activities of selected radionuclides as a function of soil depth.



ARY

Fig. B.12.1.a.

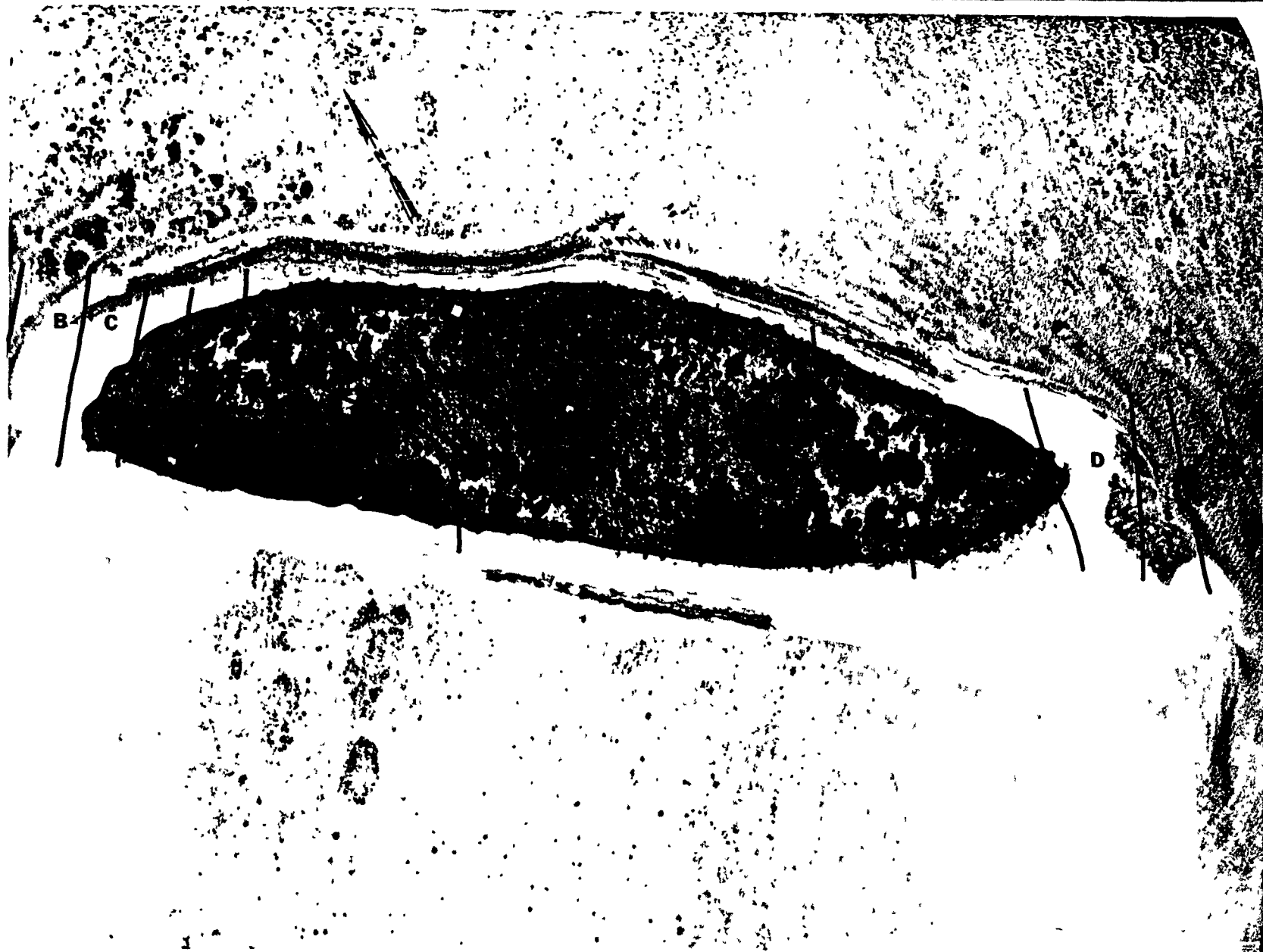


Fig. B. 12.1.b. Gross count isoexposure contours. (Refer to alphabetic symbol key in this appendix.)

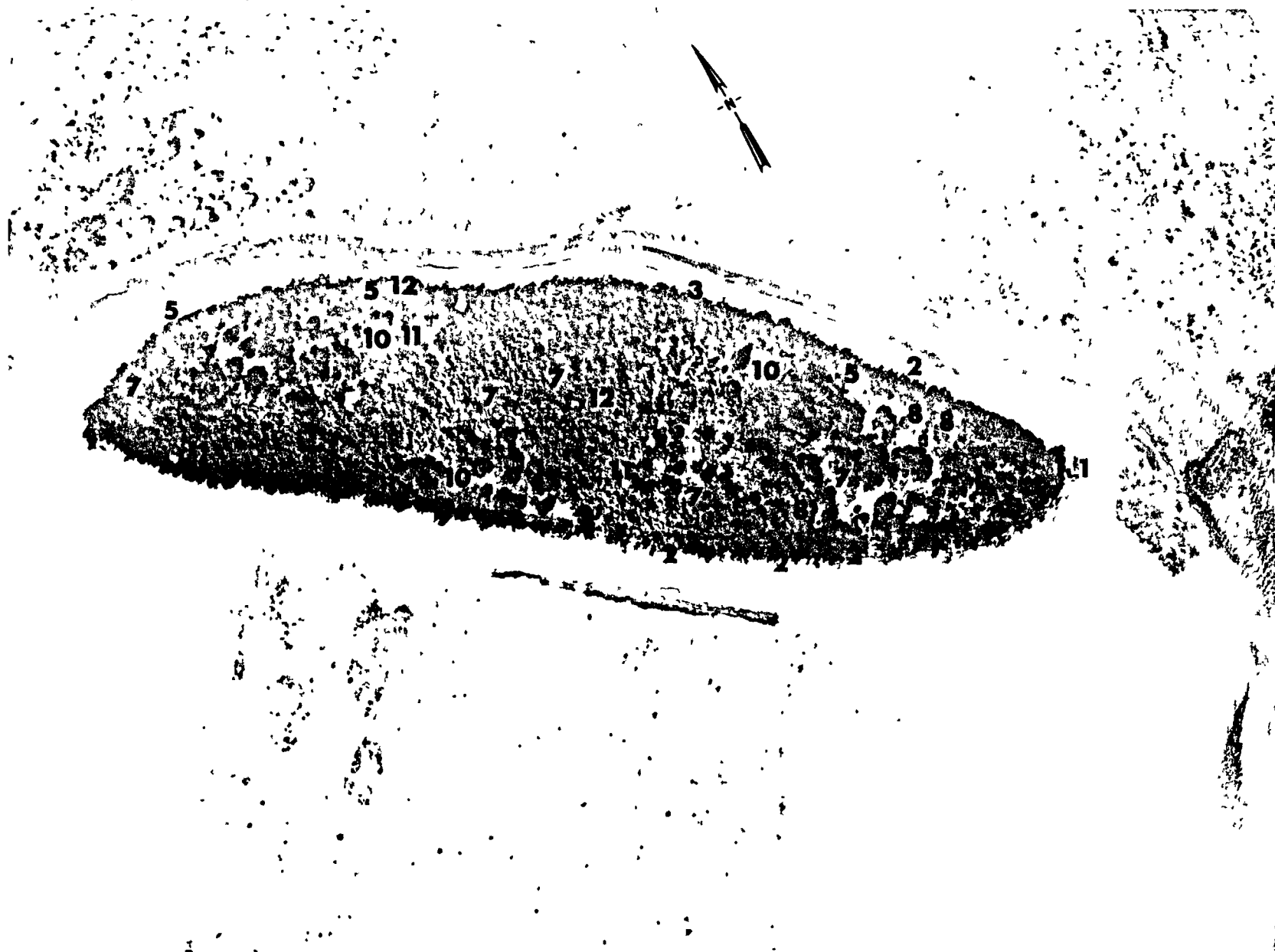
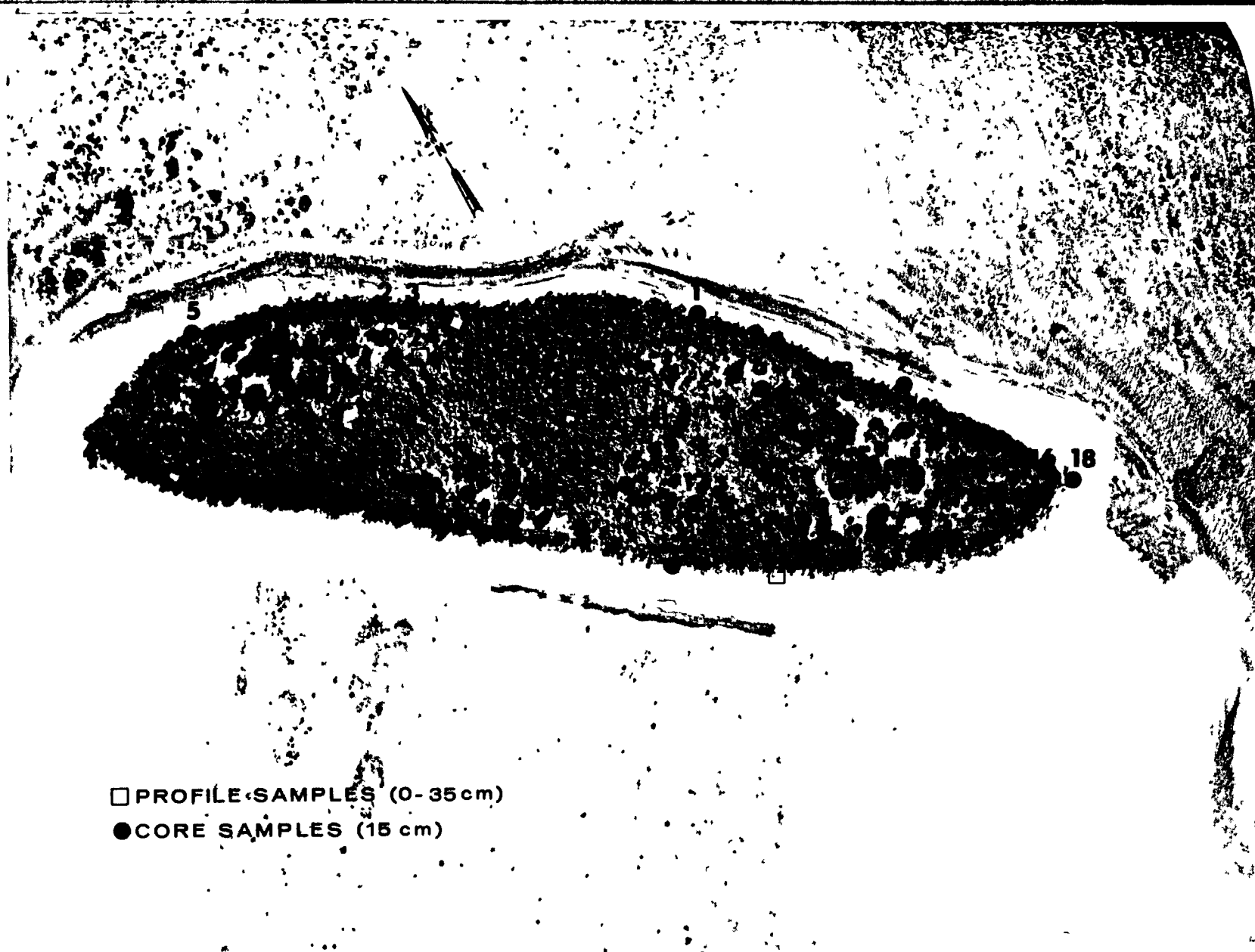


Fig. B.12.1.d. The gamma background exposure rate ( $\mu\text{R/hr}$ ) at 1 m above the ground, measured with a portable NaI scintillation counter.



□ PROFILE SAMPLES (0-35 cm)  
● CORE SAMPLES (15 cm)

Fig. B.12.1.f. Soil-sample locations.

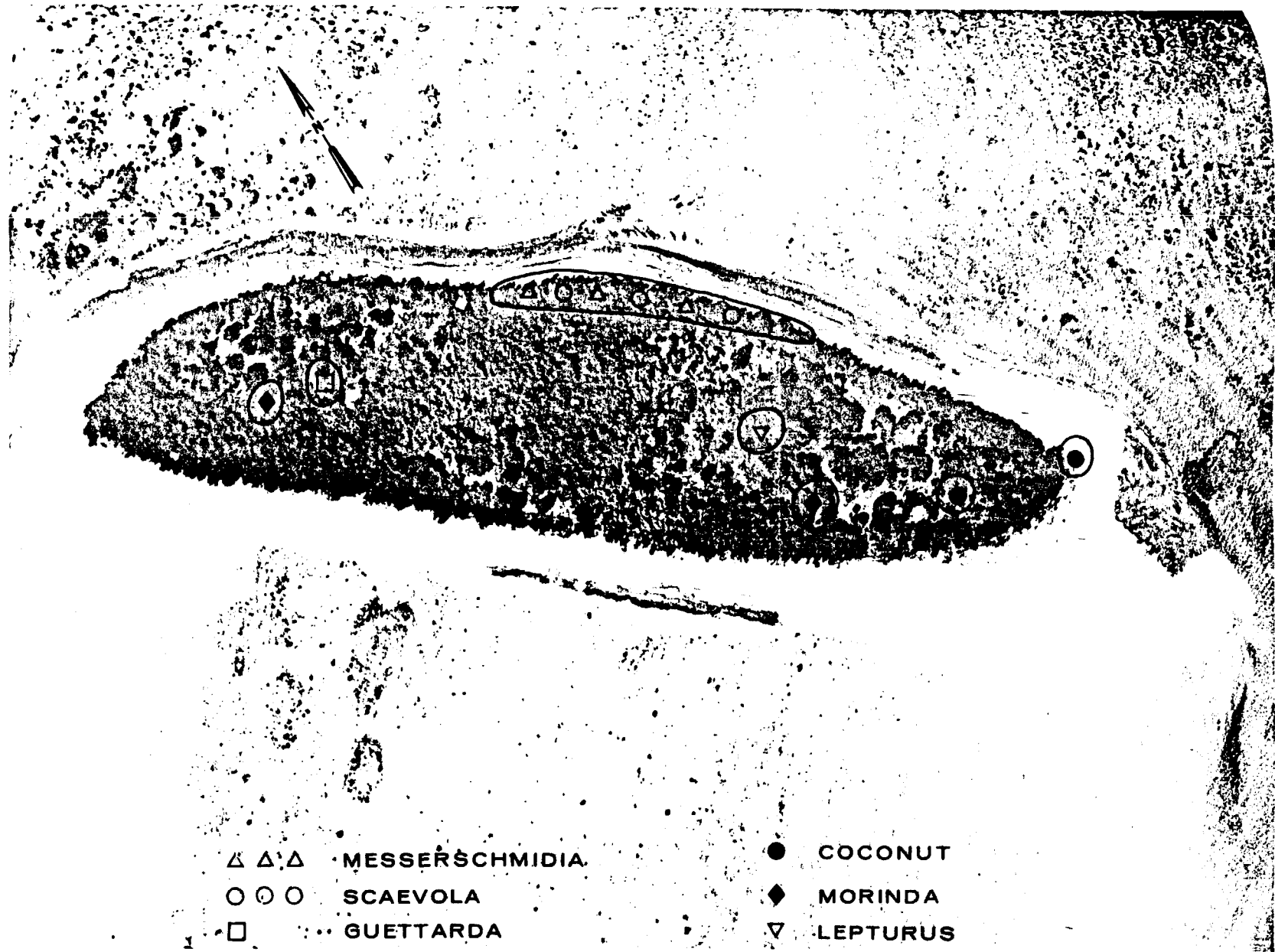


Fig. B.12.1.g. Vegetation sample locations.



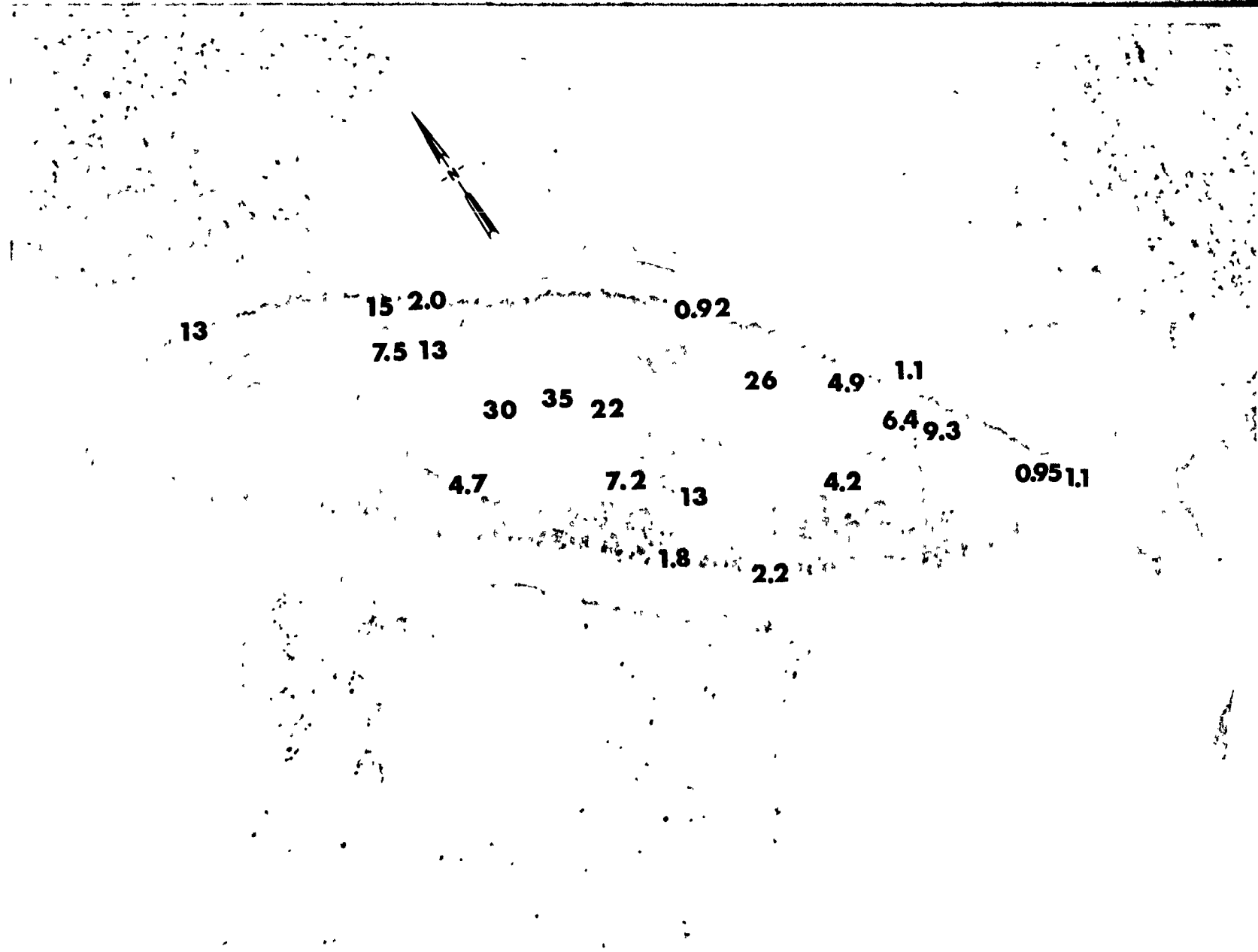


Fig. B.12.1.1. The average  $^{239}\text{Pu}$  activities (pCi/g) in soil samples collected to a depth of 15 cm.



Fig. B.12.1.j. The average  $^{90}\text{Sr}$  activities (pCi/g) in soil samples collected to a depth of 15 cm.



Fig. B.12.1.k.  $^{137}\text{Cs}$  isoexposure and isoconcentration contours. (Refer to alphabetic symbol key in this appendix.)



Fig. B.12.1.1. The average <sup>137</sup>Cs activities (pCi/g) in soil samples collected to a depth of 15 cm.

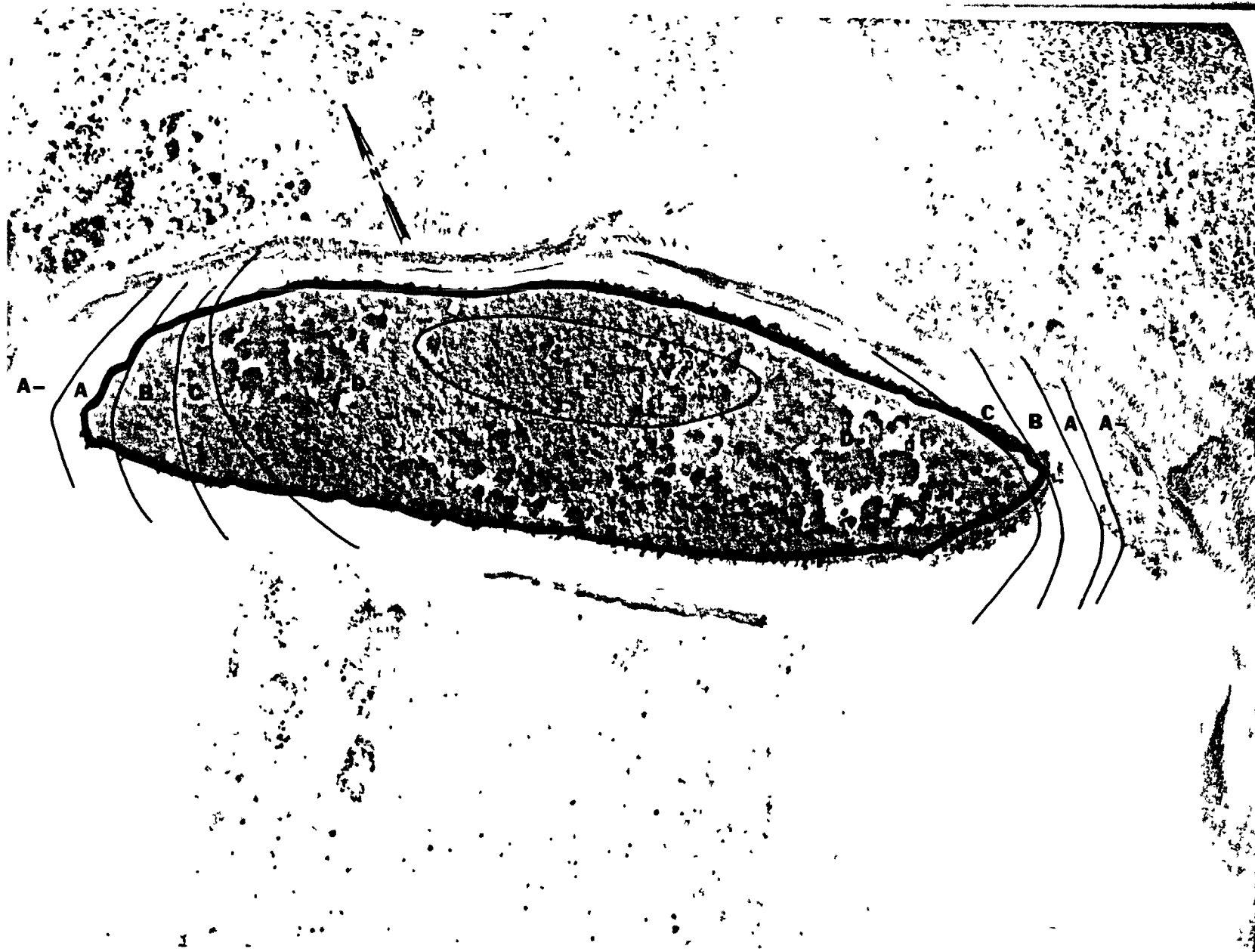


Fig. B.12.1.m.  $^{60}\text{Co}$  isoexposure and isoconcentration contours. (Refer to alphabetic symbol key in this appendix.)

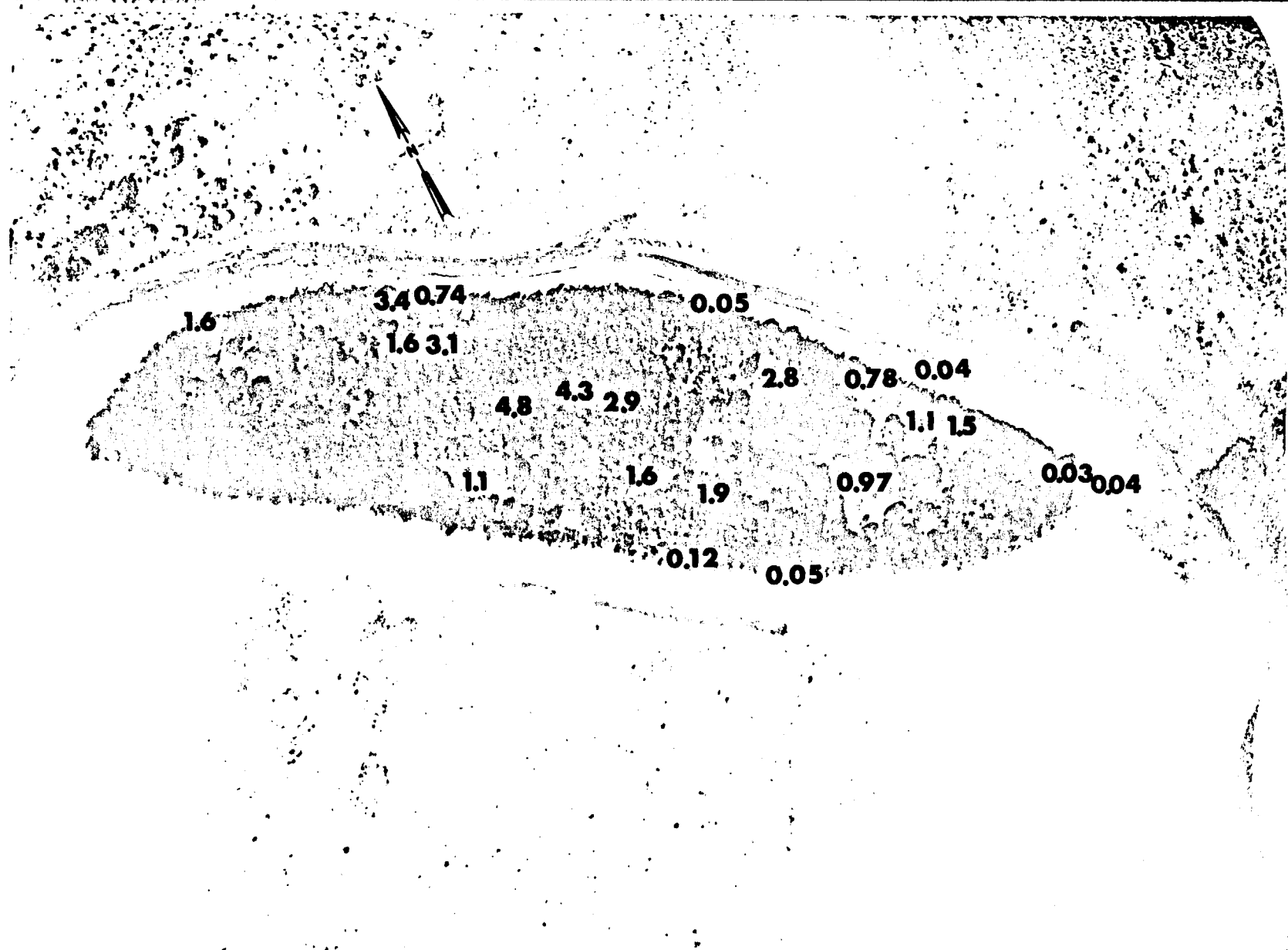


Fig. B.12.1.n. The average  $^{60}\text{Co}$  activities (pCi/g) in soil samples collected to a depth of 15 cm.

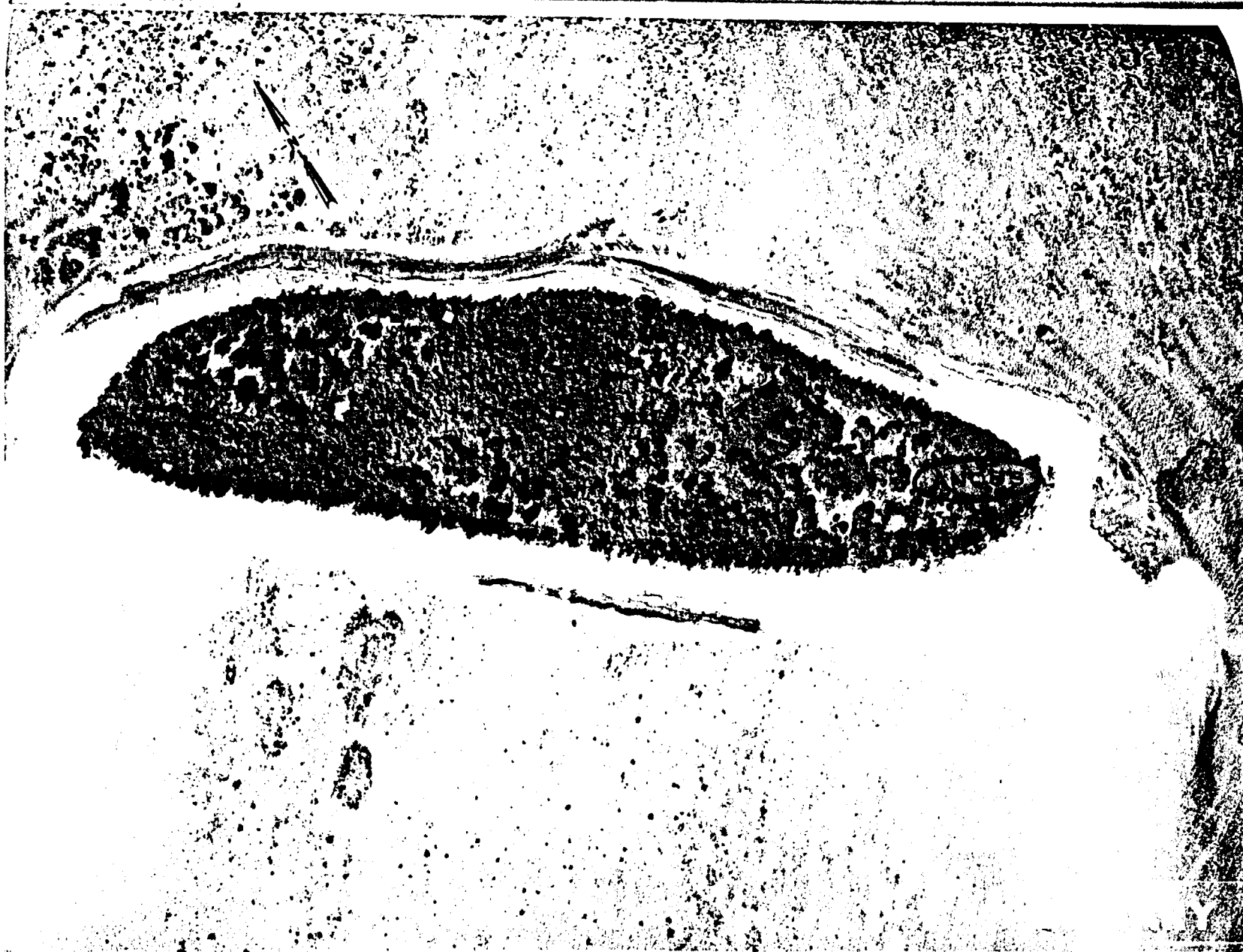


Fig. B.12.1.o. Terrestrial animal sample locations.

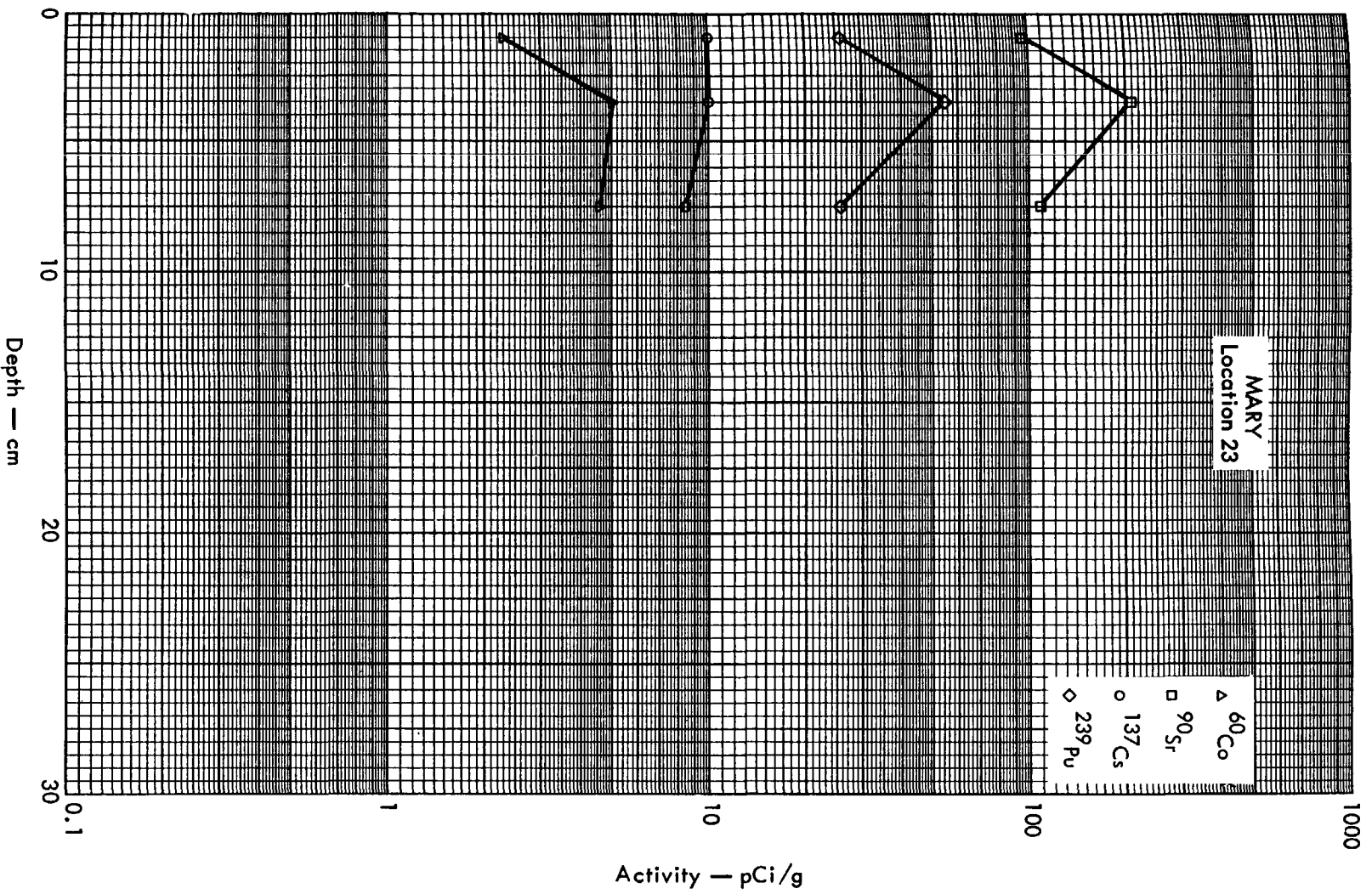


Fig. B. 12. 2a. Activities of selected radionuclides as a function of soil depth.



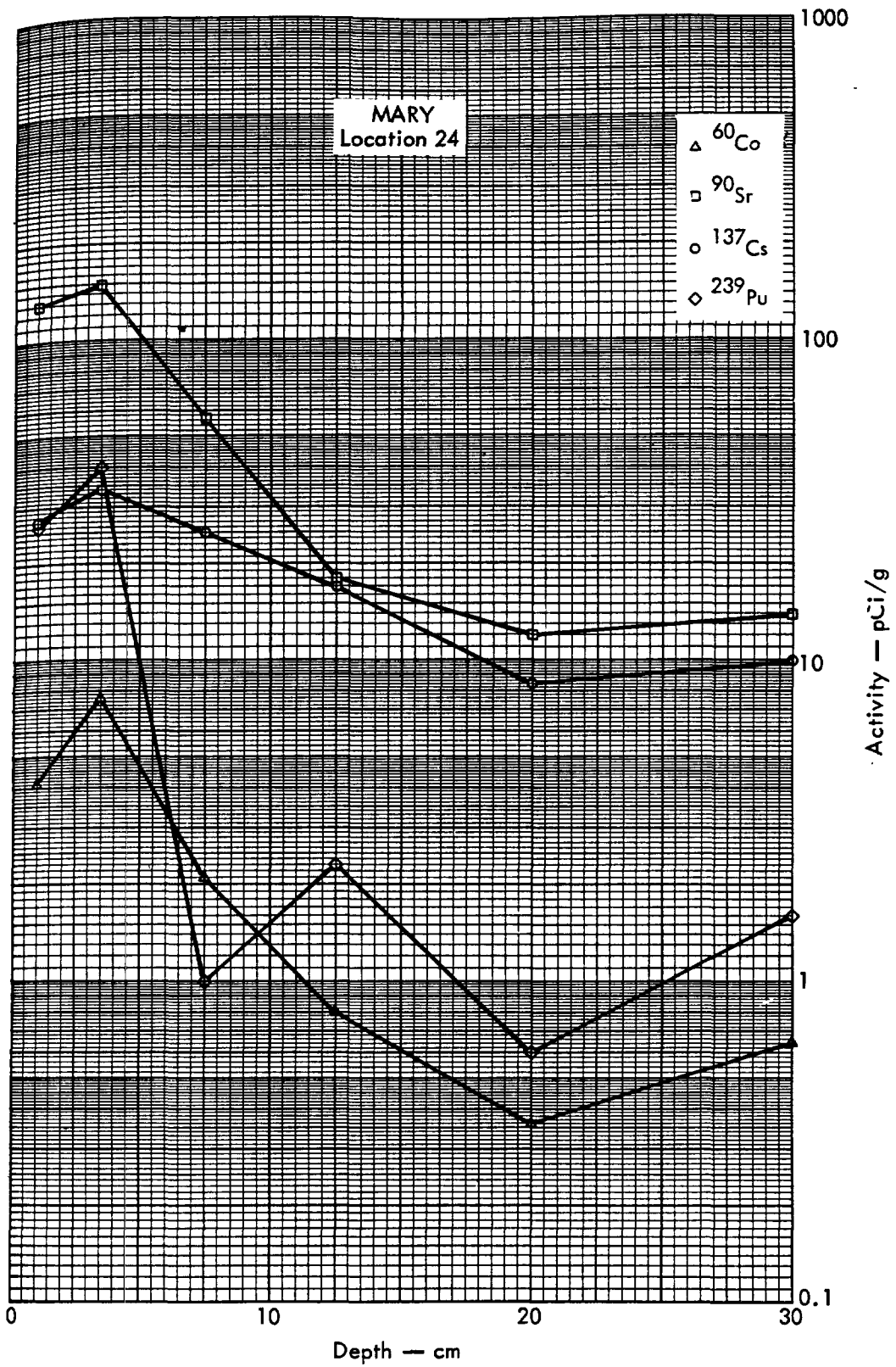


Fig. B.12.2b. Activities of selected radionuclides as a function of soil depth.

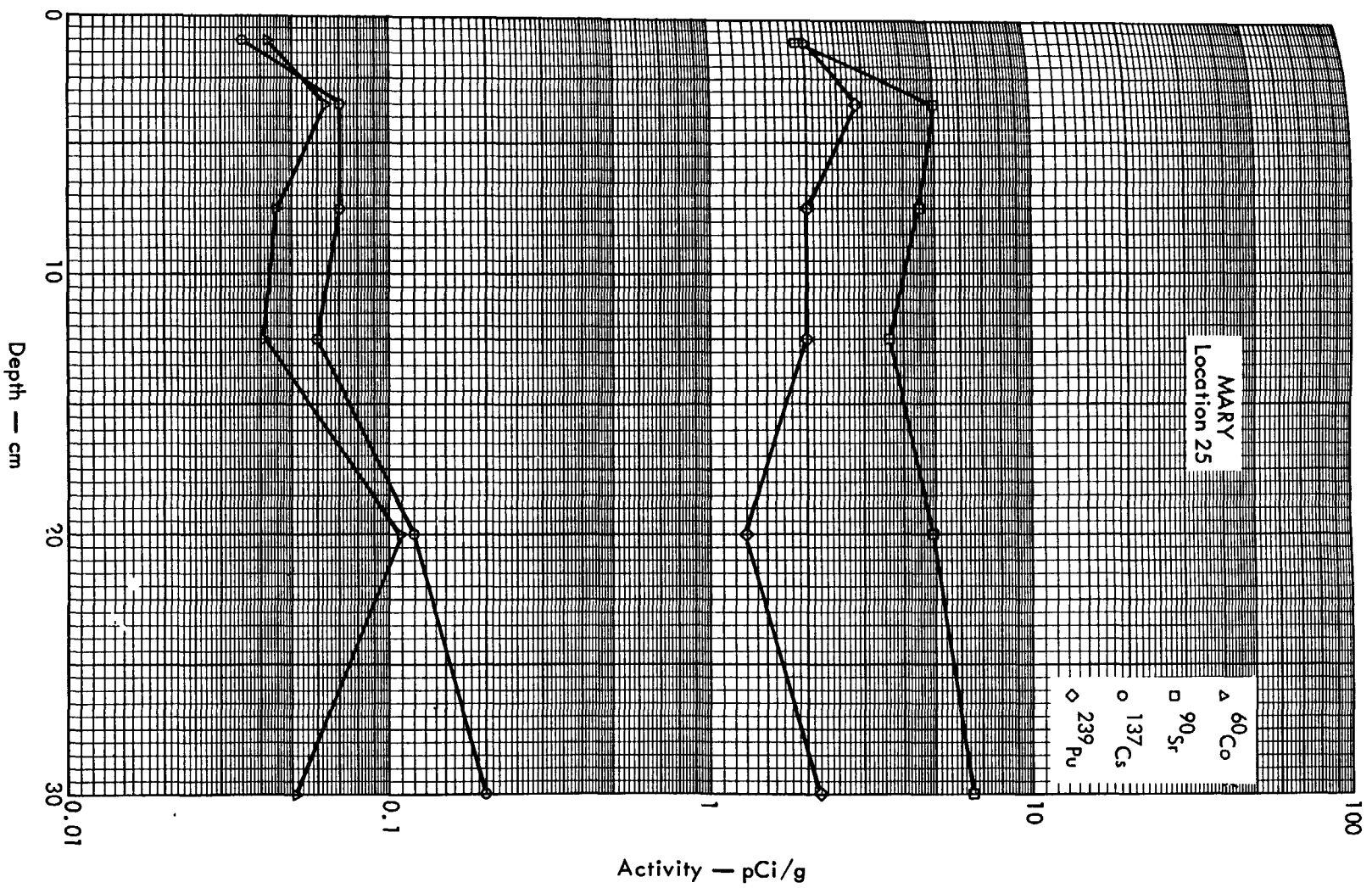


Fig. B. 12. 2c. Activities of selected radionuclides as a function of soil depth.



ANCY

Fig. B.13.1.a.

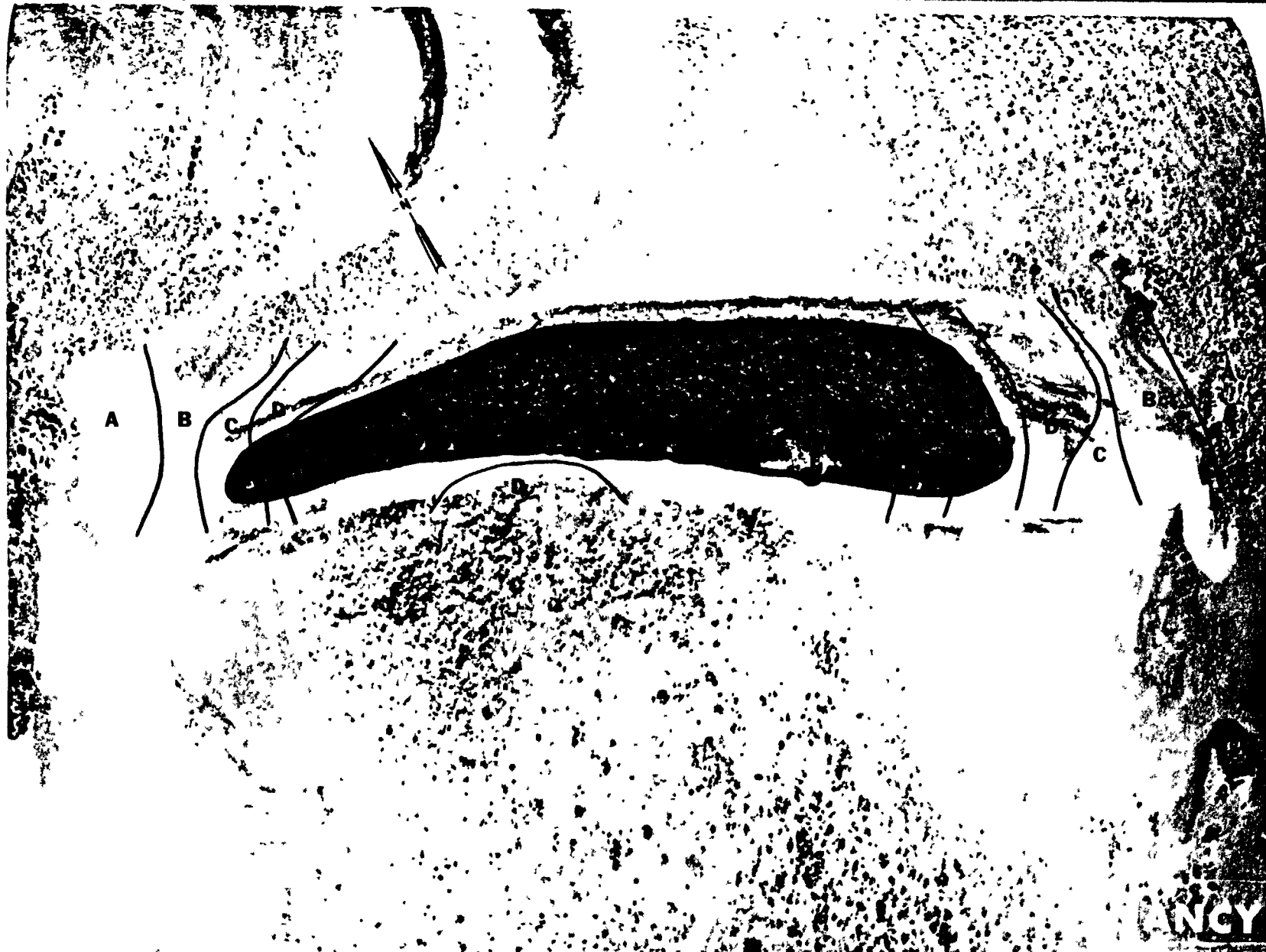


Fig. B.13.1.b. Gross count isoexposure contours. (Refer to alphabetic symbol key in this appendix.)

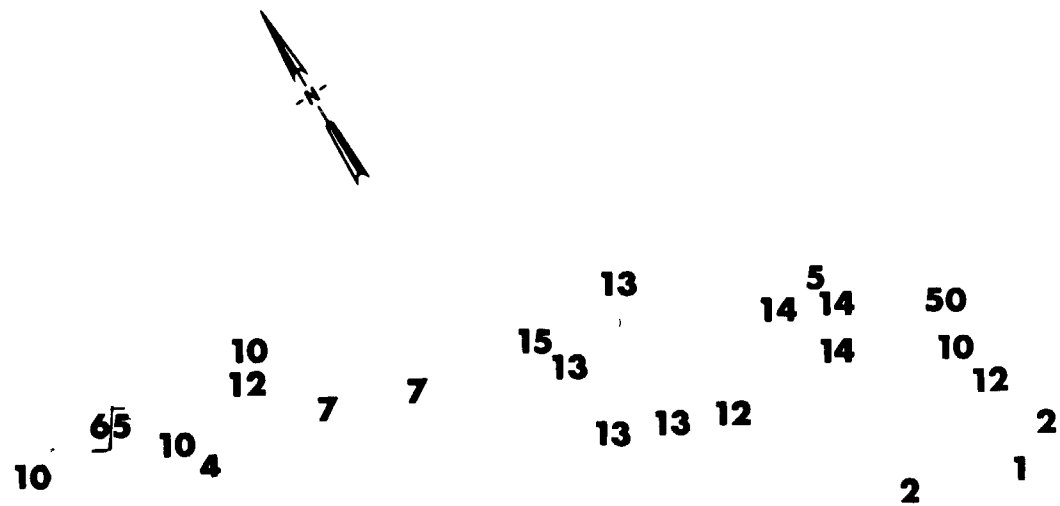


Fig. B.13.1.d. The gamma background exposure rate ( $\mu\text{R/hr}$ ) at 1 m above the ground, measured with a portable NaI scintillation counter.

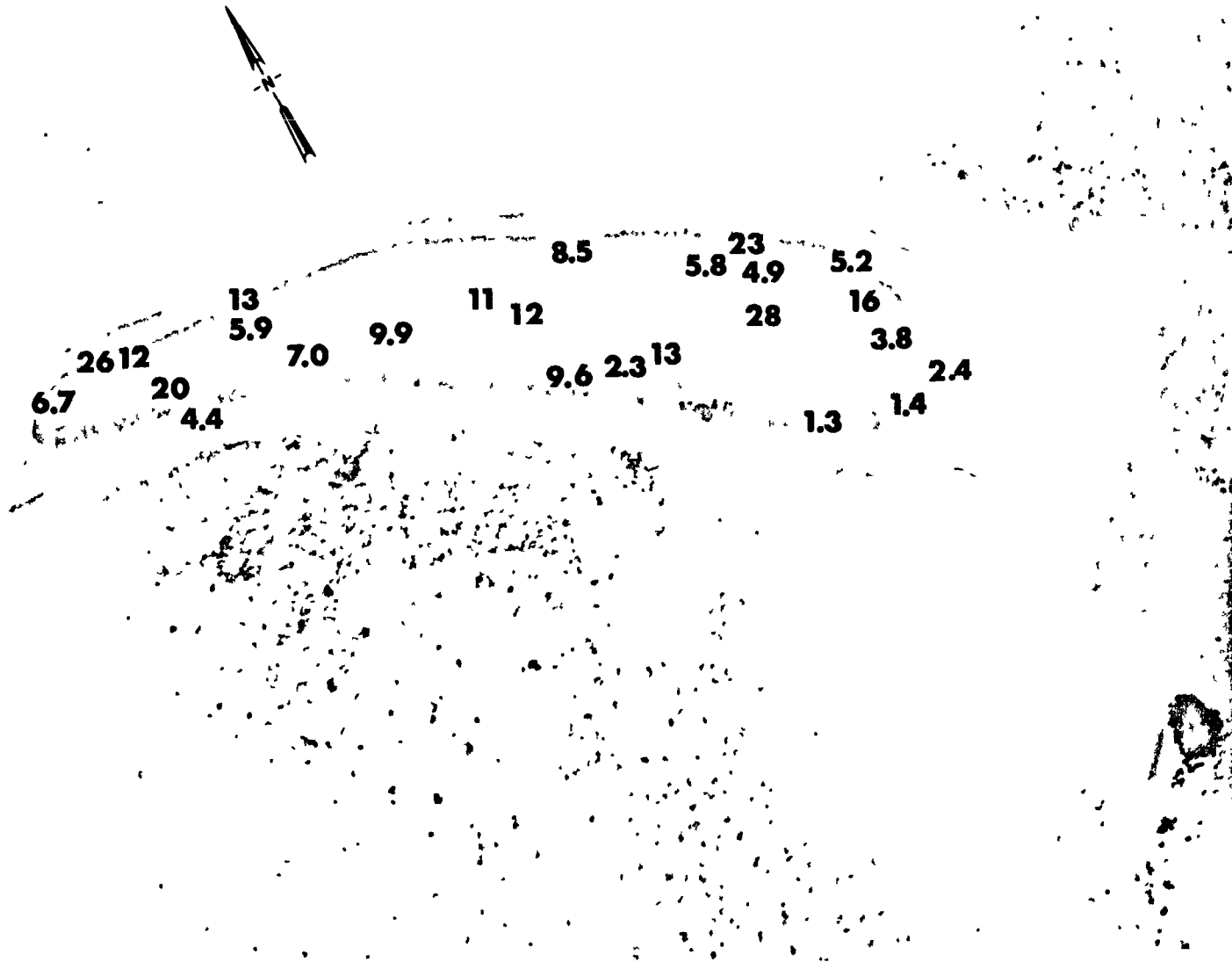


Fig. B.13.1.f. Soil-sample locations.



Fig. B.13.1.g. Vegetation sample locations.

Fig. B.13.1.1. The average  $^{239}\text{Pu}$  activities (pCi/g) in soil samples collected to a depth of 15 cm.





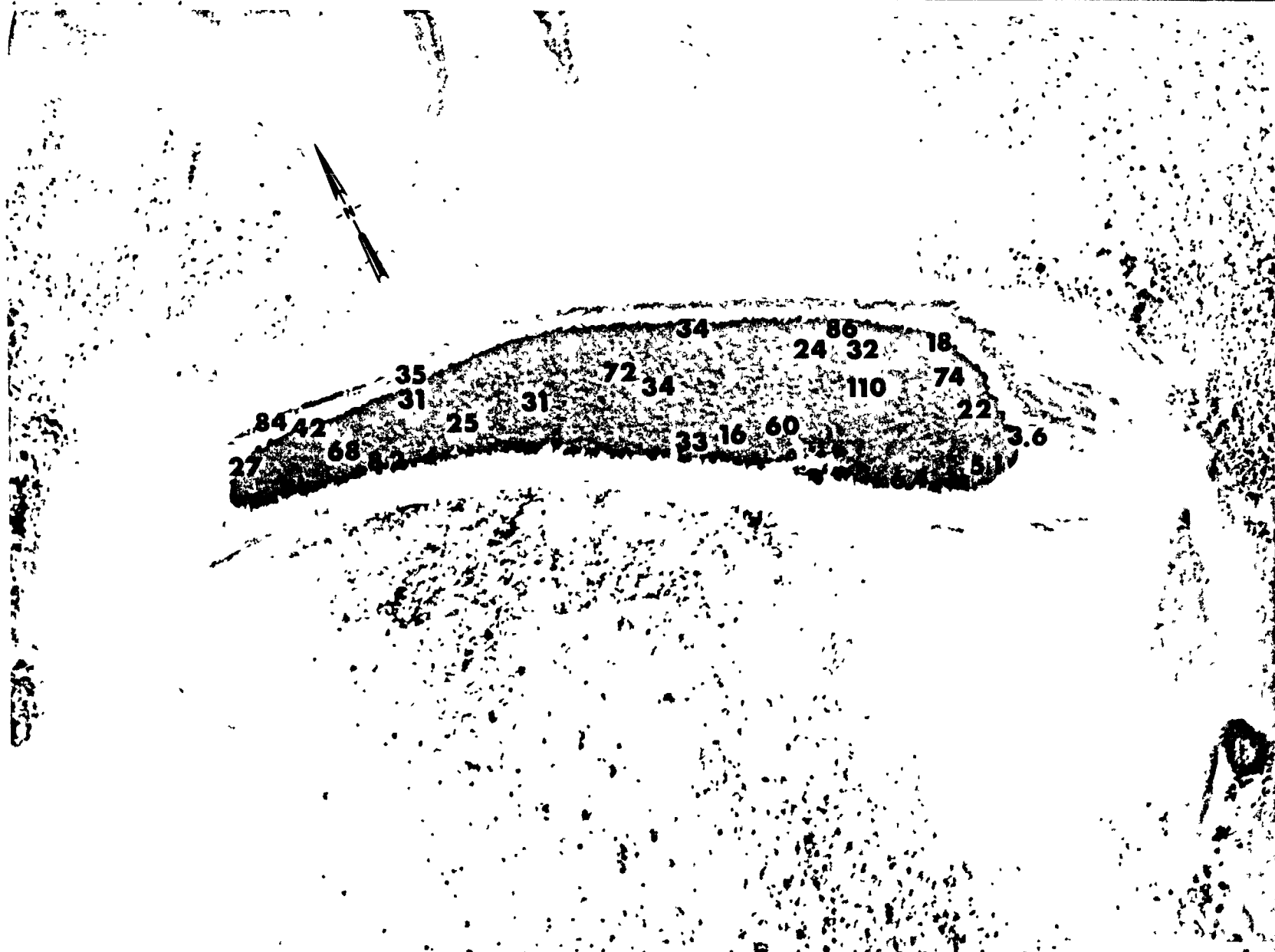


Fig. B.13.1.j. The average  $^{90}\text{Sr}$  activities (pCi/g) in soil samples collected to a depth of 15 cm.



Fig. B.13.1.k.  $^{137}\text{Cs}$  isoexposure and isoconcentration contours. (Refer to alphabetic symbol key in this appendix.)



Fig. B.13.1.1. The average  $^{137}\text{Cs}$  activities (pCi/g) in soil samples collected to a depth of 15 cm.

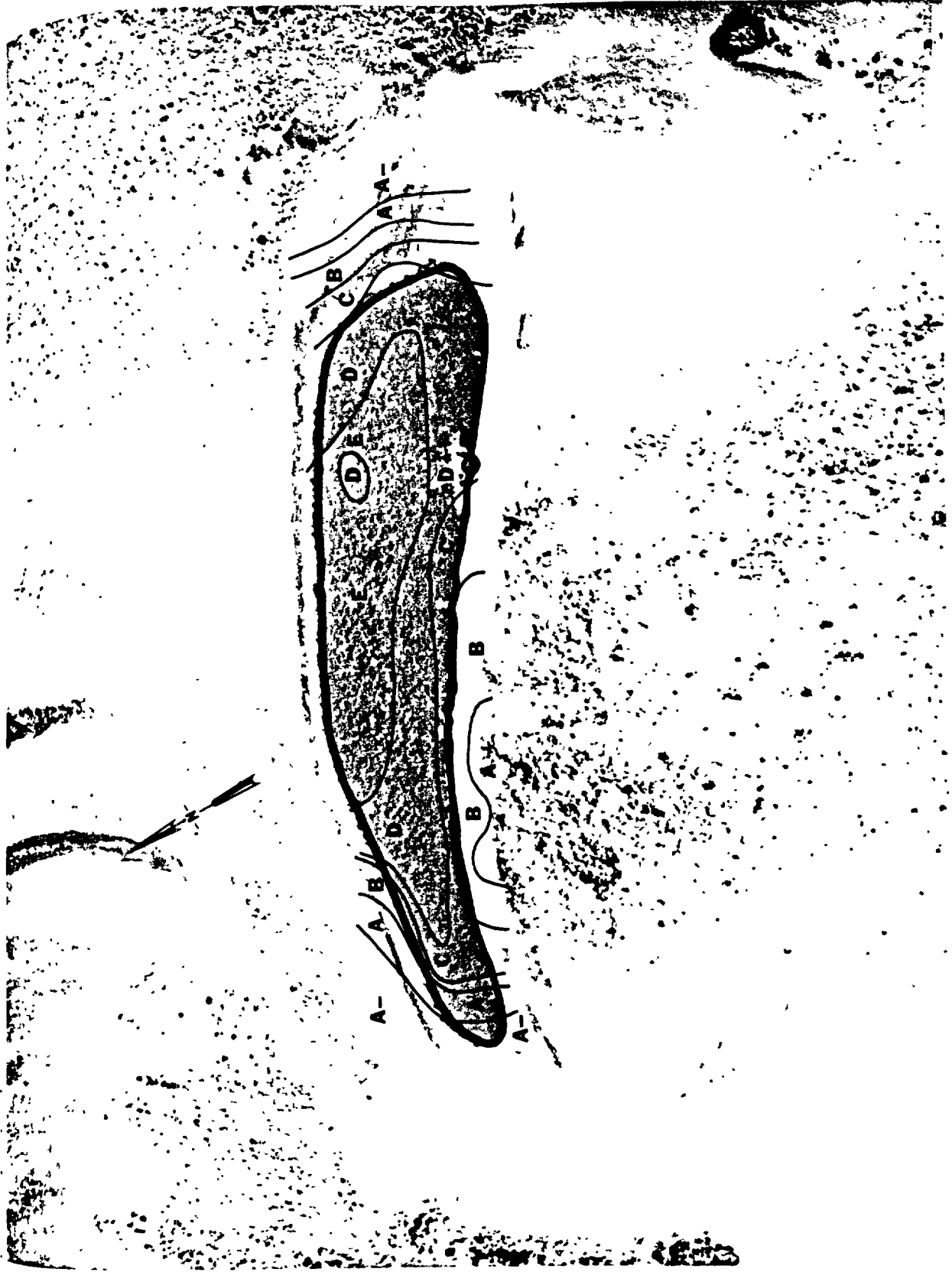


Fig. B.13. 1. m.  $^{60}\text{Co}$  isoexposure and isoconcentration contours. (Refer to alphabetic symbol key in this appendix.)

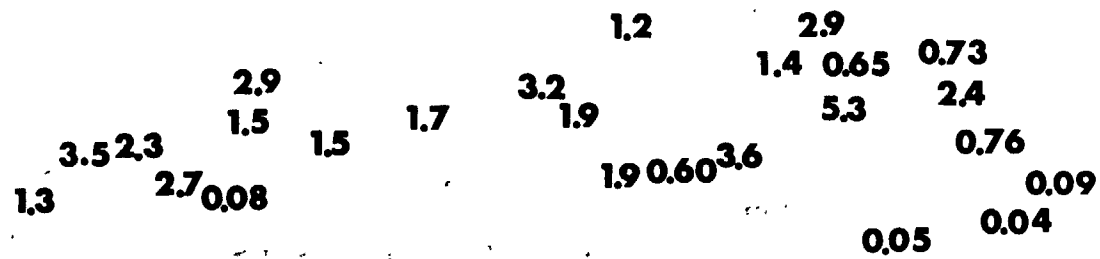


Fig. B.13.1.n. The average  $^{60}\text{Co}$  activities (pCi/g) in soil samples collected to a depth of 15 cm.

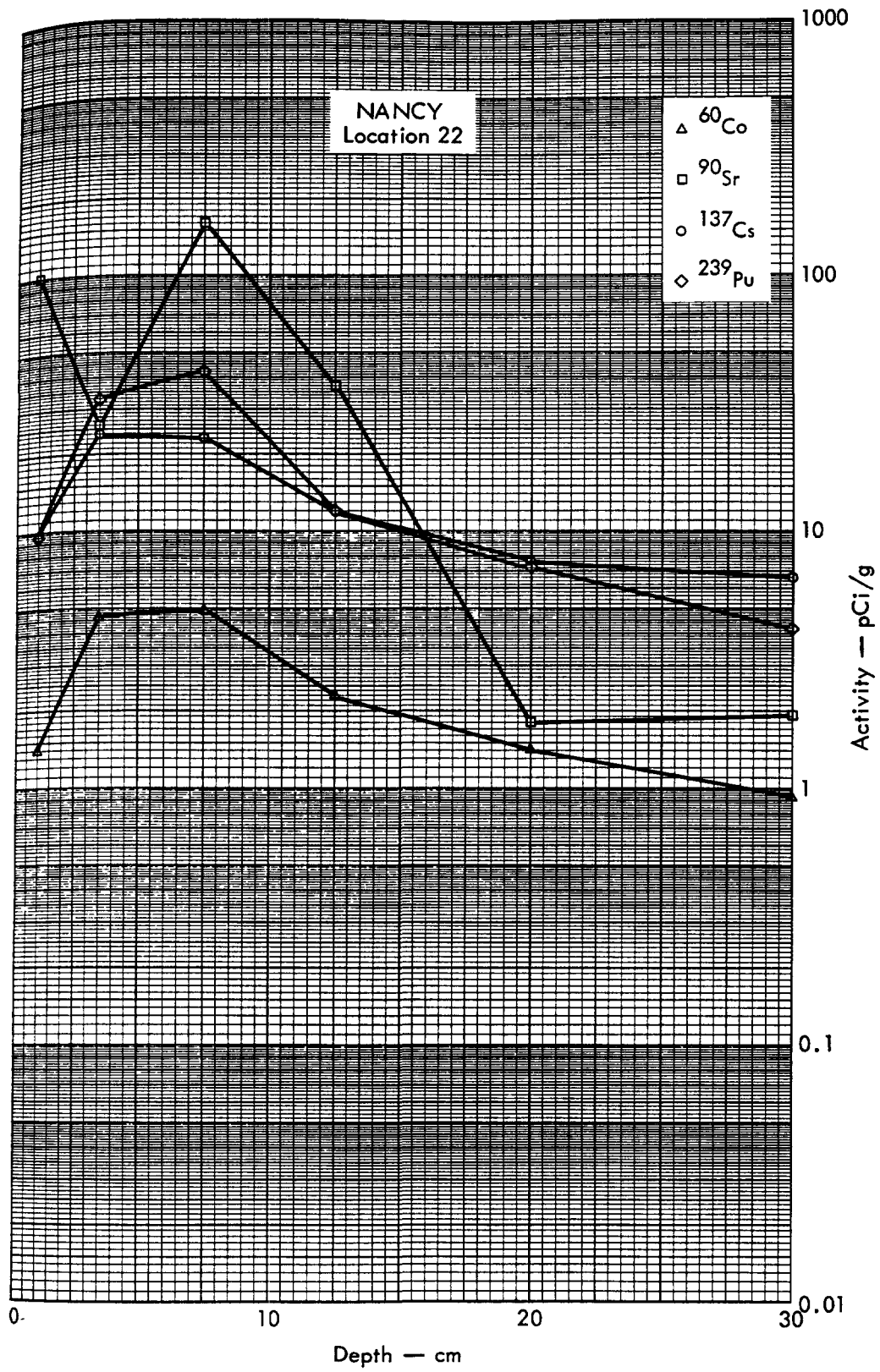


Fig. B. 13.2a. Activities of selected radionuclides as a function of soil depth.

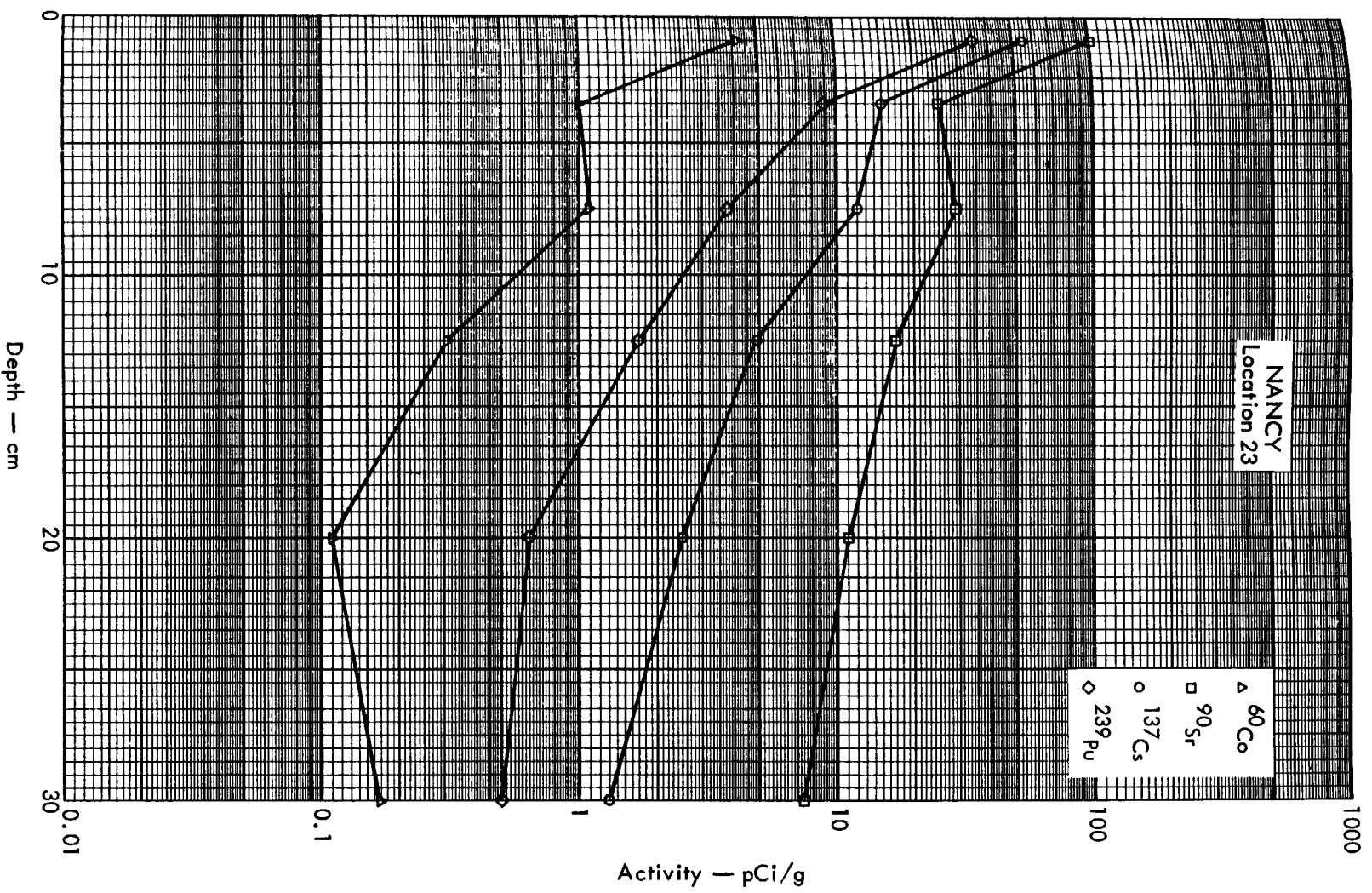


Fig. B. 13. 2b. Activities of selected radionuclides as a function of soil depth.

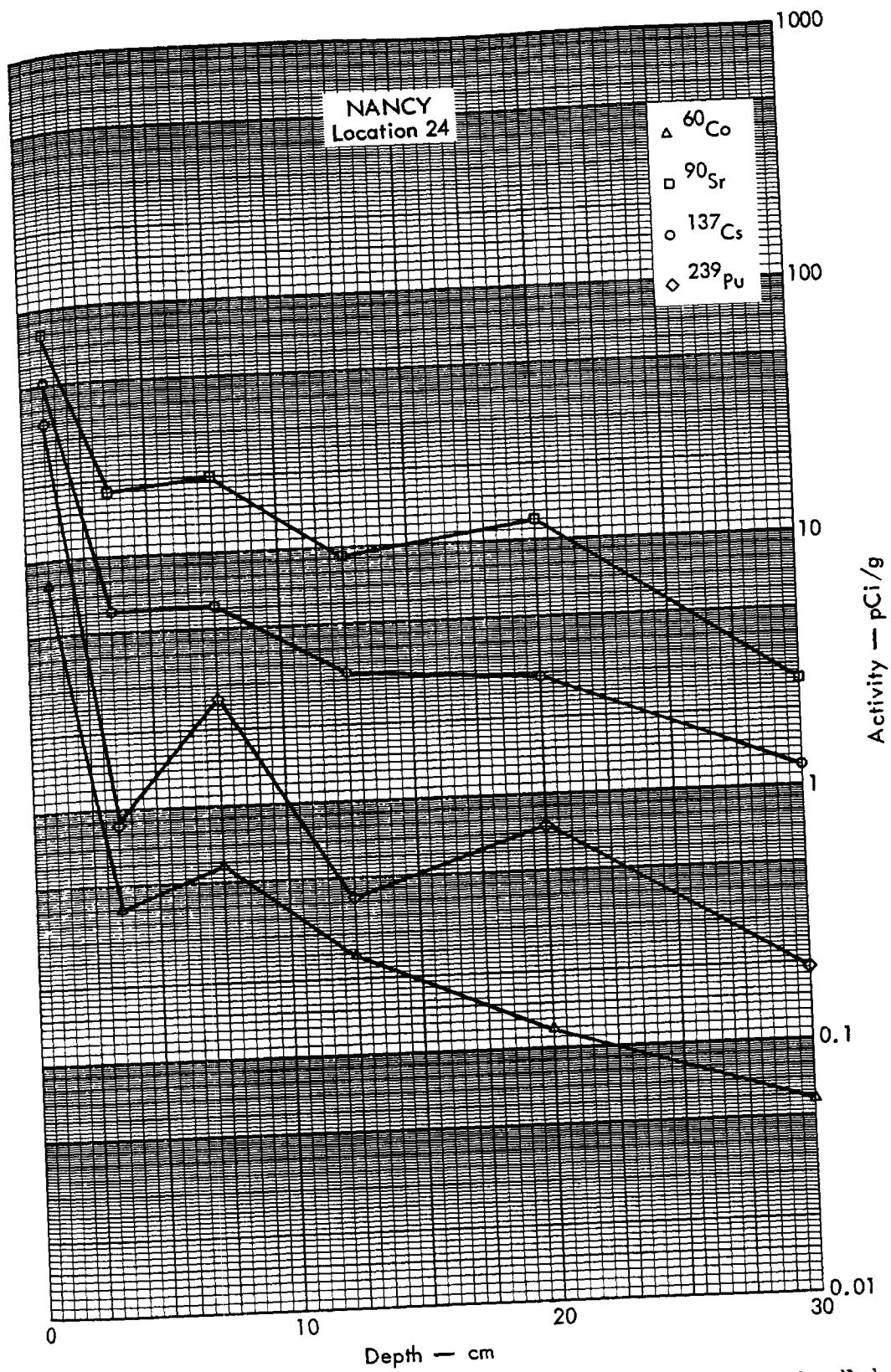


Fig. B. 13. 2c. Activities of selected radionuclides as a function of soil depth.



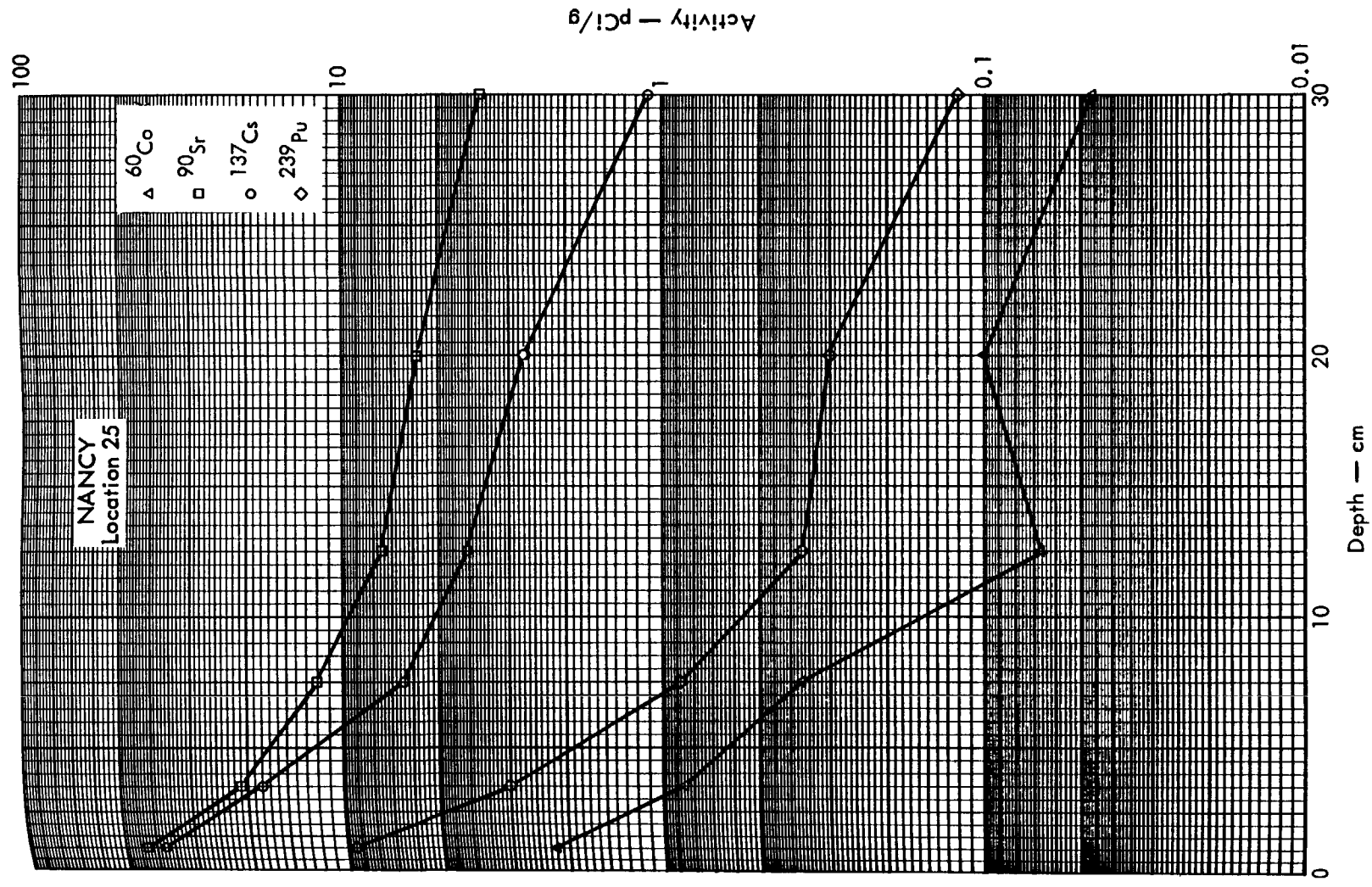


Fig. B. 13. 2d. Activities of selected radionuclides as a function of soil depth.



Fig. B.14.1.a.

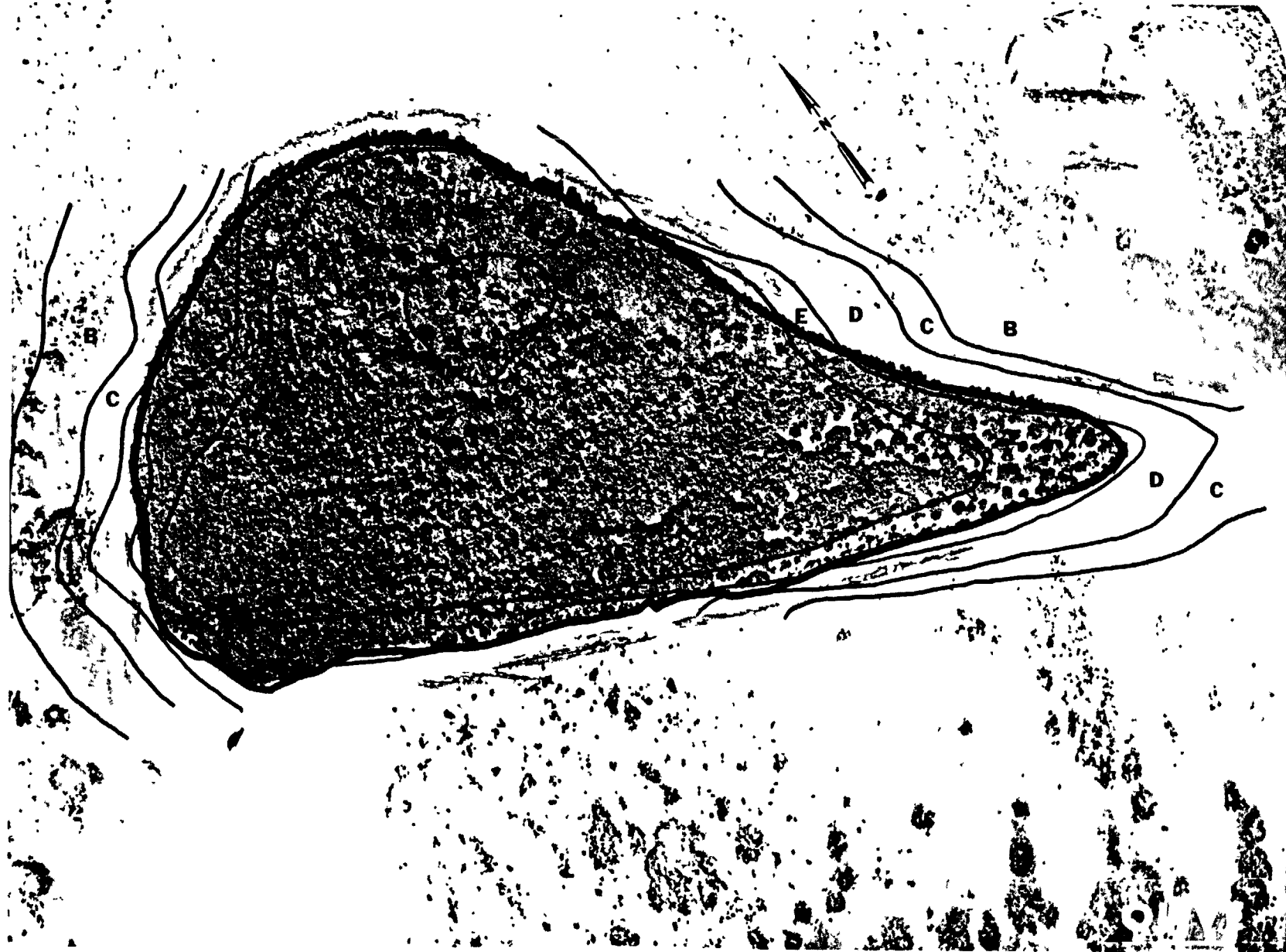


Fig. B.14.1.b. Gross count isoexposure contours. (Refer to alphabetic symbol key in this appendix.)



Fig. B.14.1.d. The gamma background exposure rate ( $\mu\text{R/hr}$ ) at 1 m above the ground, measured with a portable NaI scintillation counter.

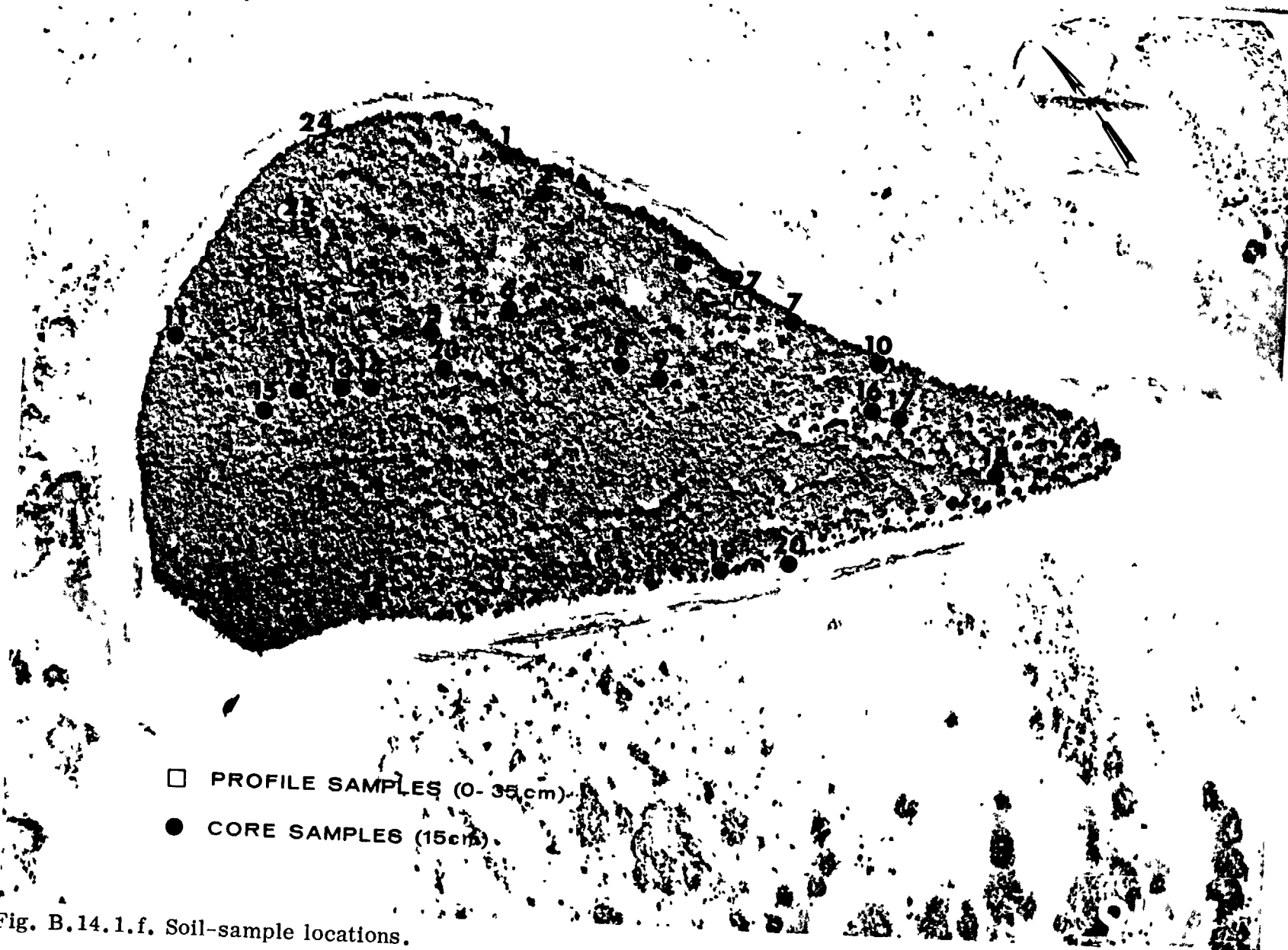


Fig. B.14.1.f. Soil-sample locations.

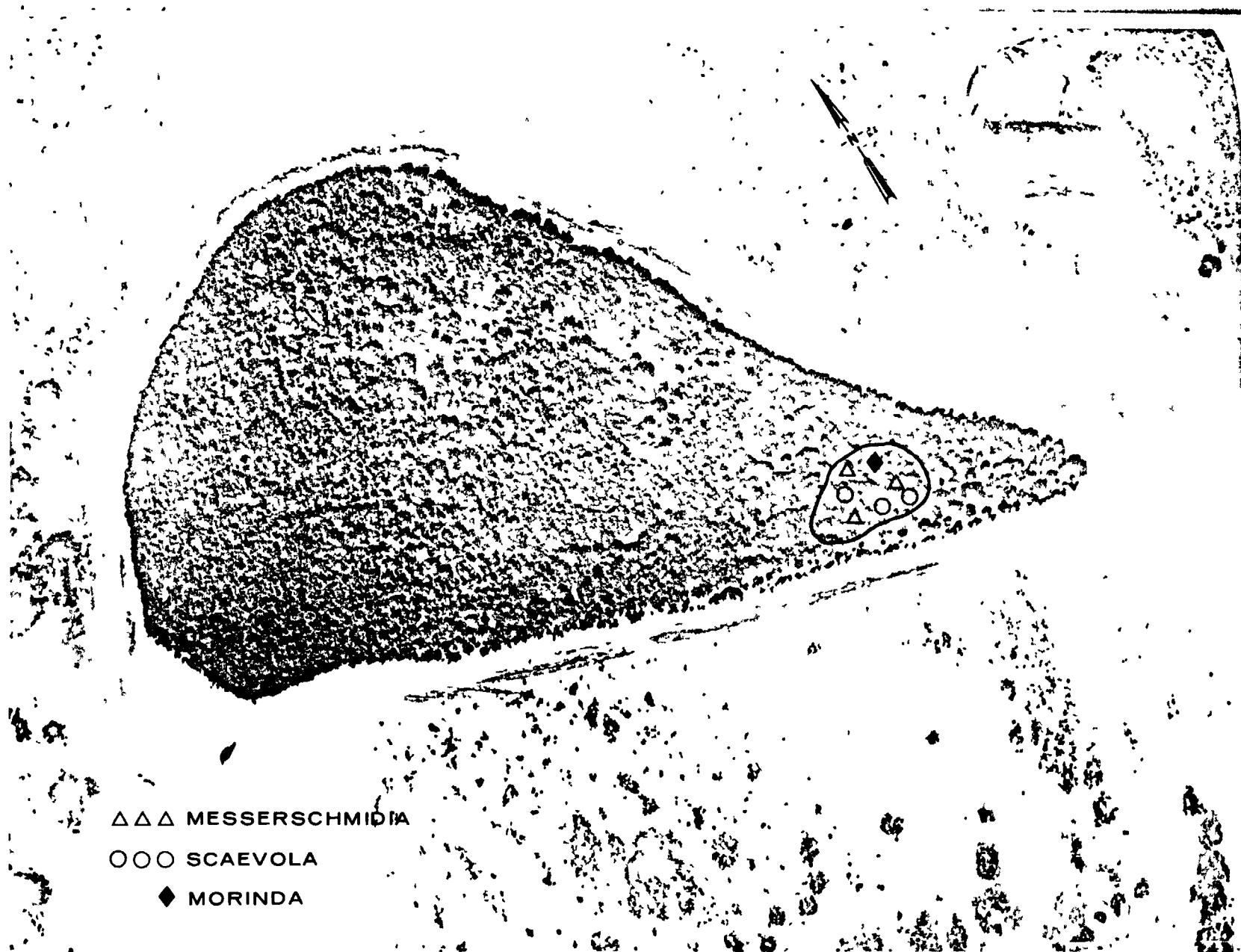


Fig. B.14.1.g. Vegetation sample locations.

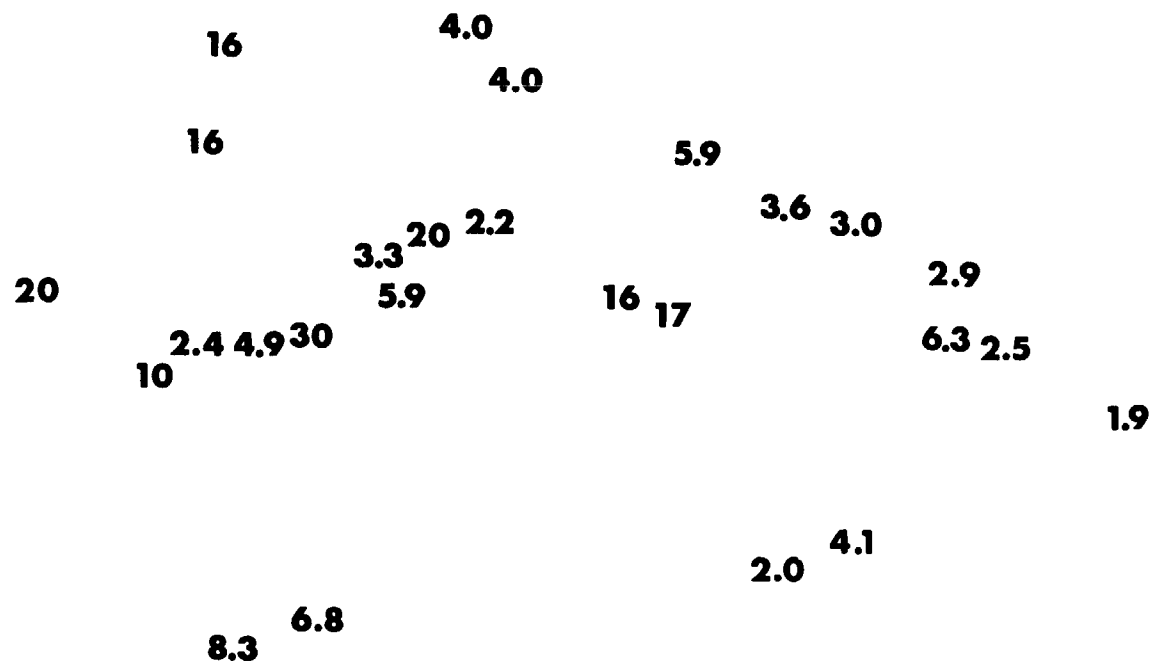


Fig. B.14.1.i. The average  $^{239}\text{Pu}$  activities (pCi/g) in soil samples collected to a depth of 15 cm.

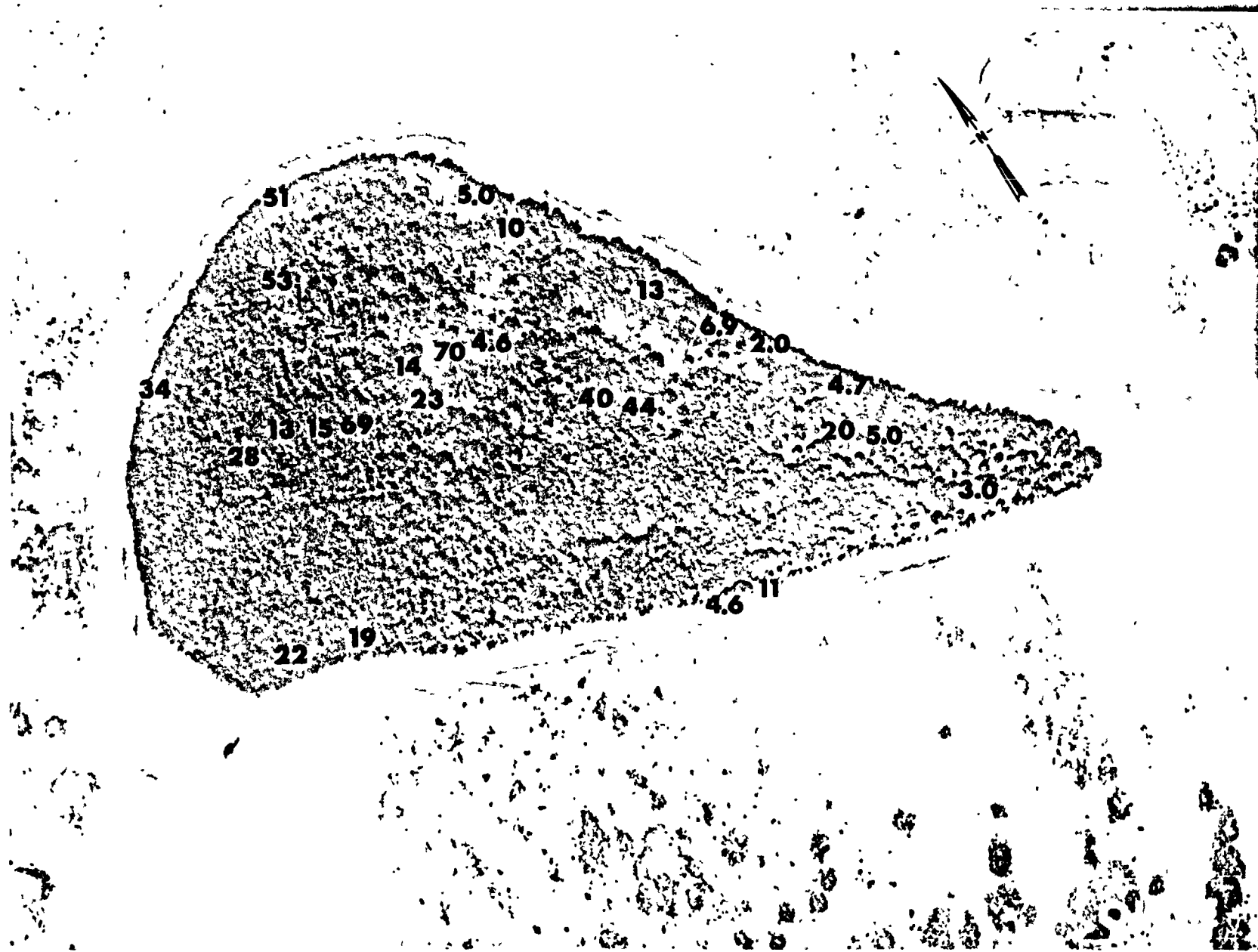


Fig. B.14.1.j. The average <sup>90</sup>Sr activities (pCi/g) in soil samples collected to a depth of 15 cm.



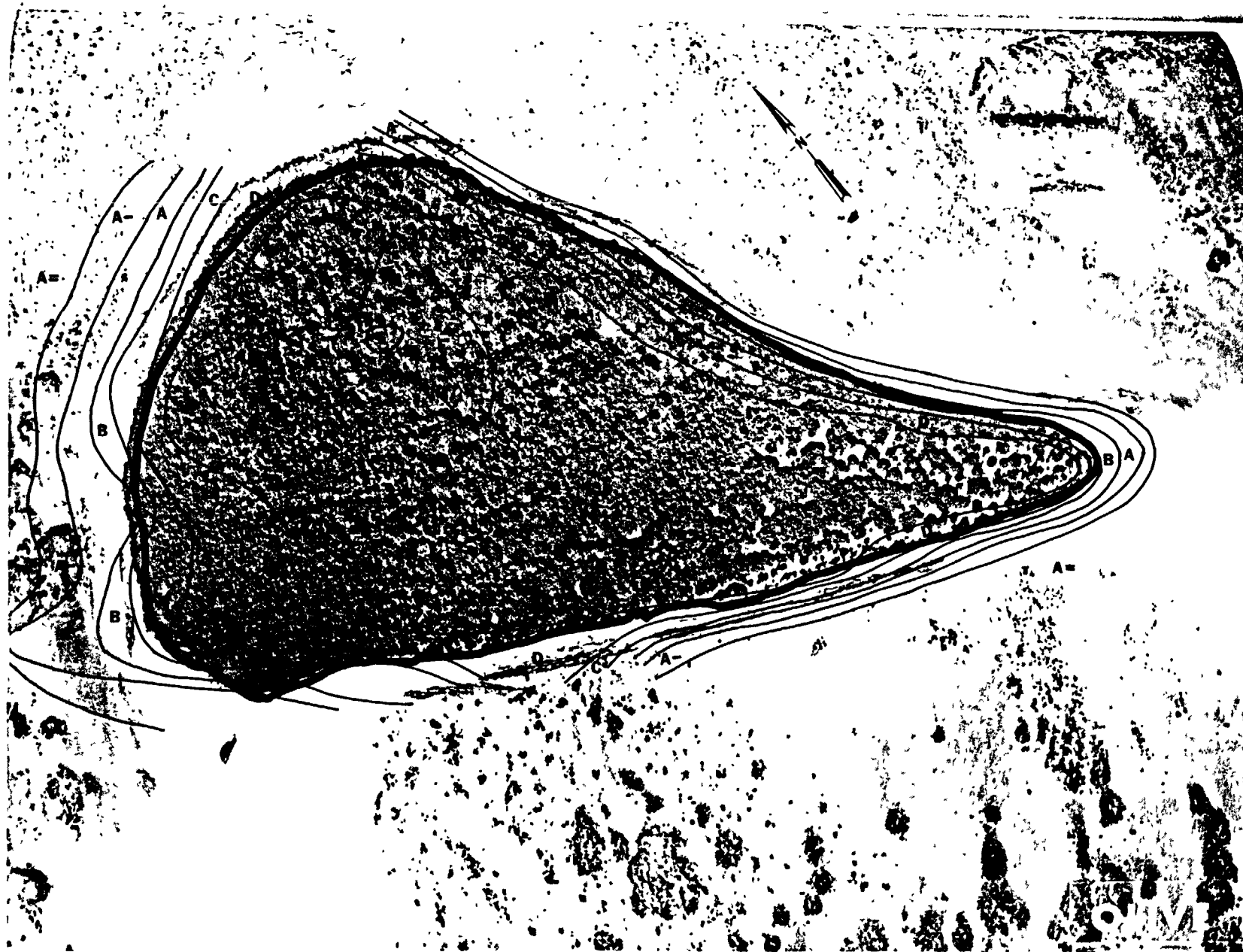


Fig. B.14.1.k.  $^{137}\text{Cs}$  isoexposure and isoconcentration contours. (Refer to alphabetic symbol key in this appendix.)

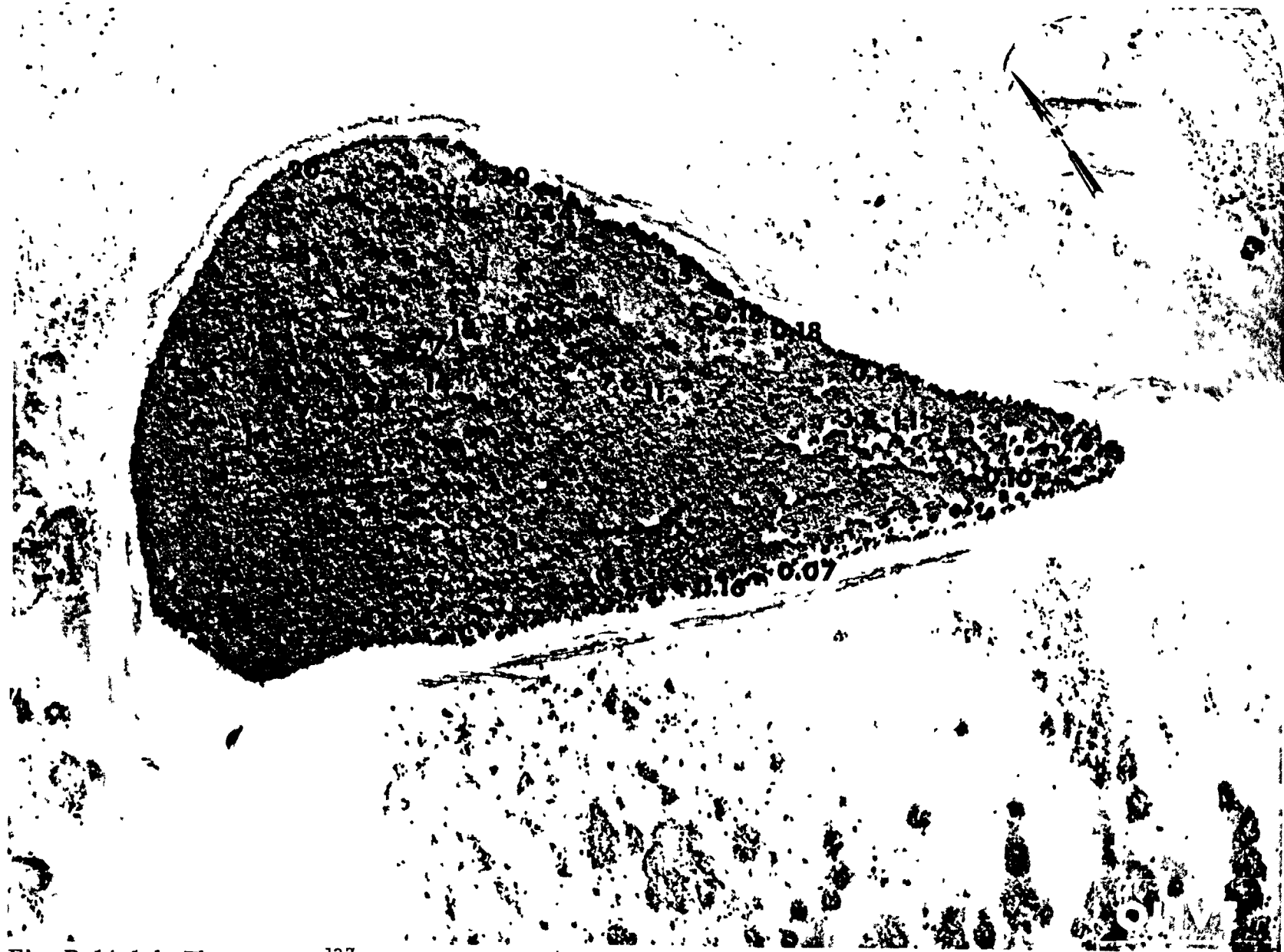


Fig. B.14.1.1. The average  $^{137}\text{Cs}$  activities (pCi/g) in soil samples collected to a depth of 15 cm.

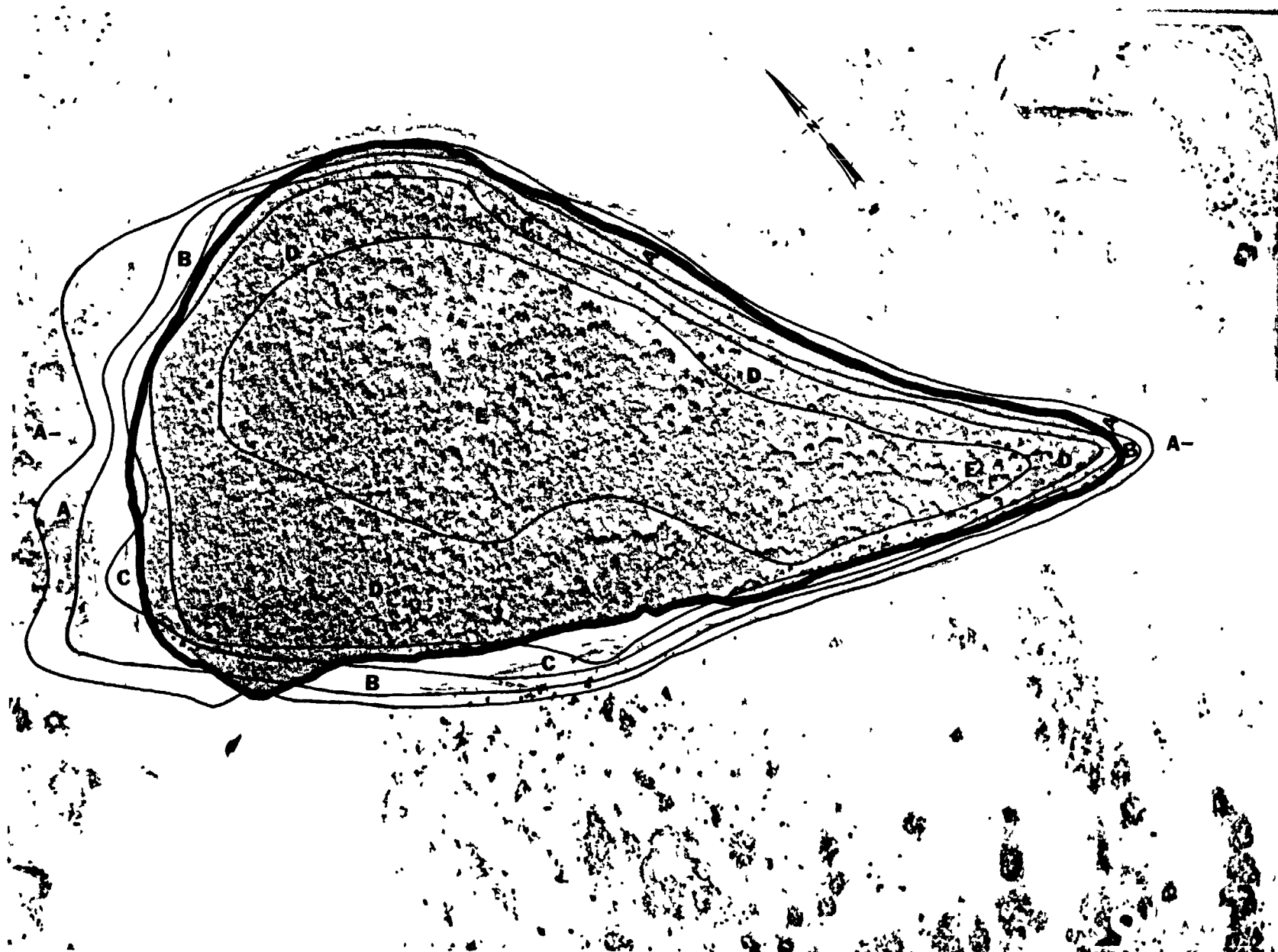


Fig. B.14.1.m. <sup>60</sup>Co isoexposure and isoconcentration contours. (Refer to alphabetic symbol key in this appendix.)

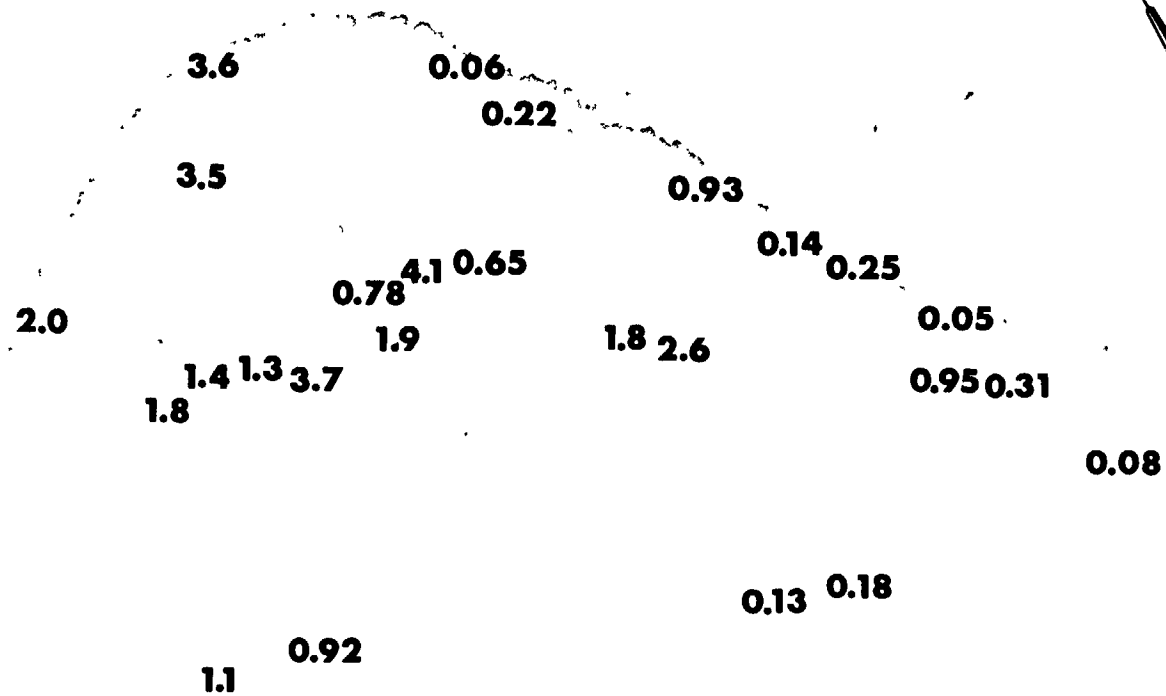


Fig. B.14.1.n. The average <sup>60</sup>Co activities (pCi/g) in soil samples collected to a depth of 15 cm.

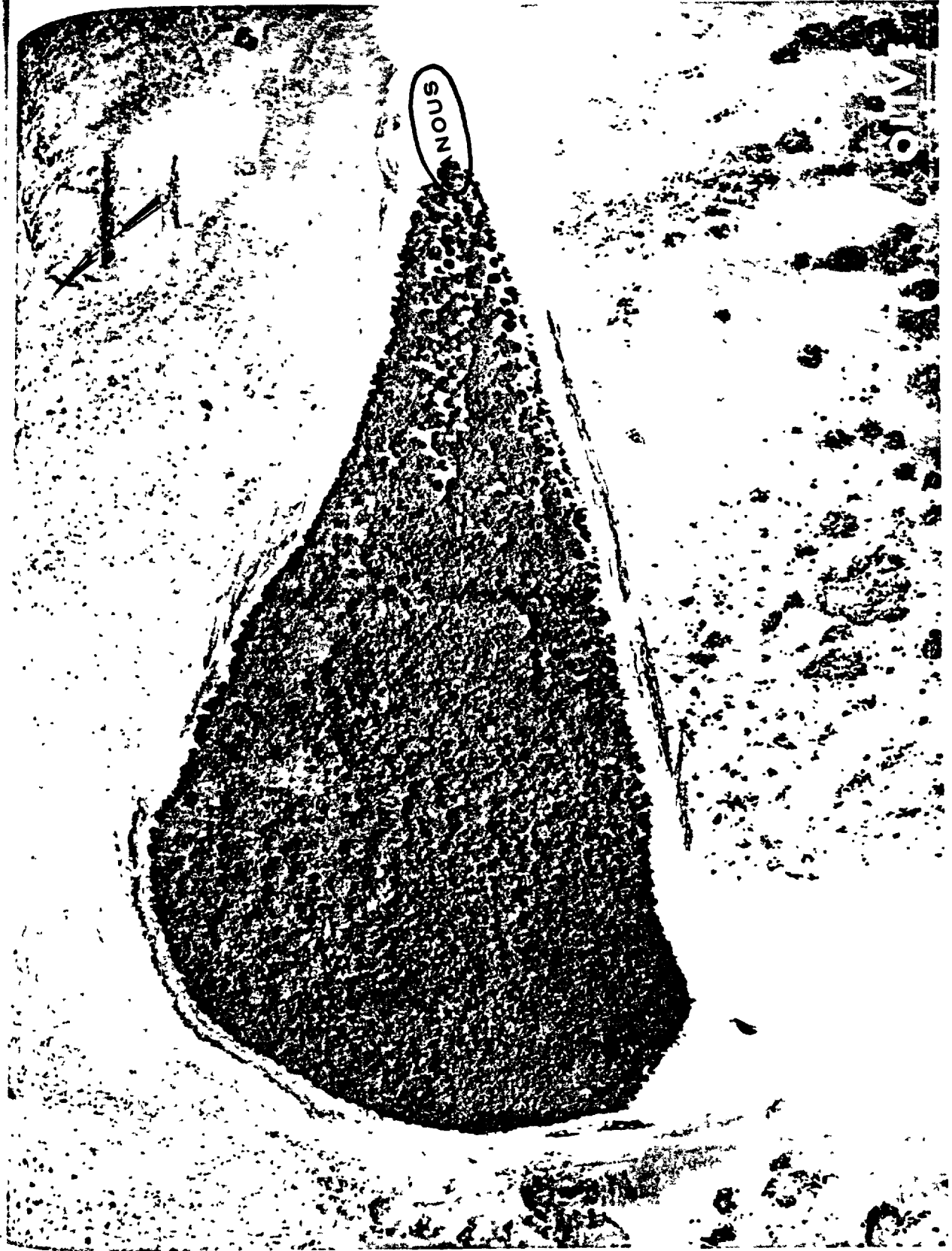


Fig. B.14.1.o. Terrestrial animal sample locations.

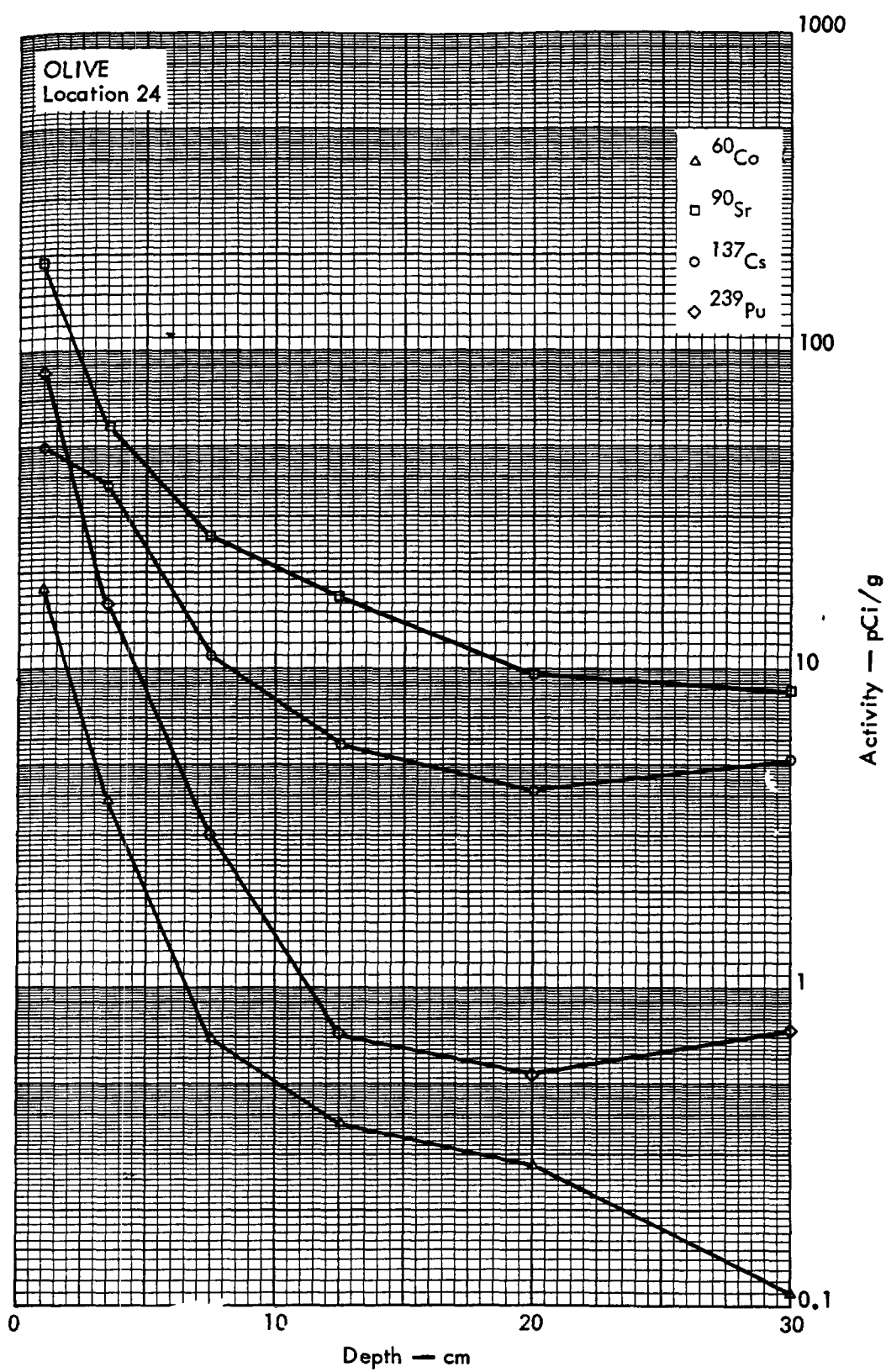


Fig. B. 14. 2a. Activities of selected radionuclides as a function of soil depth.

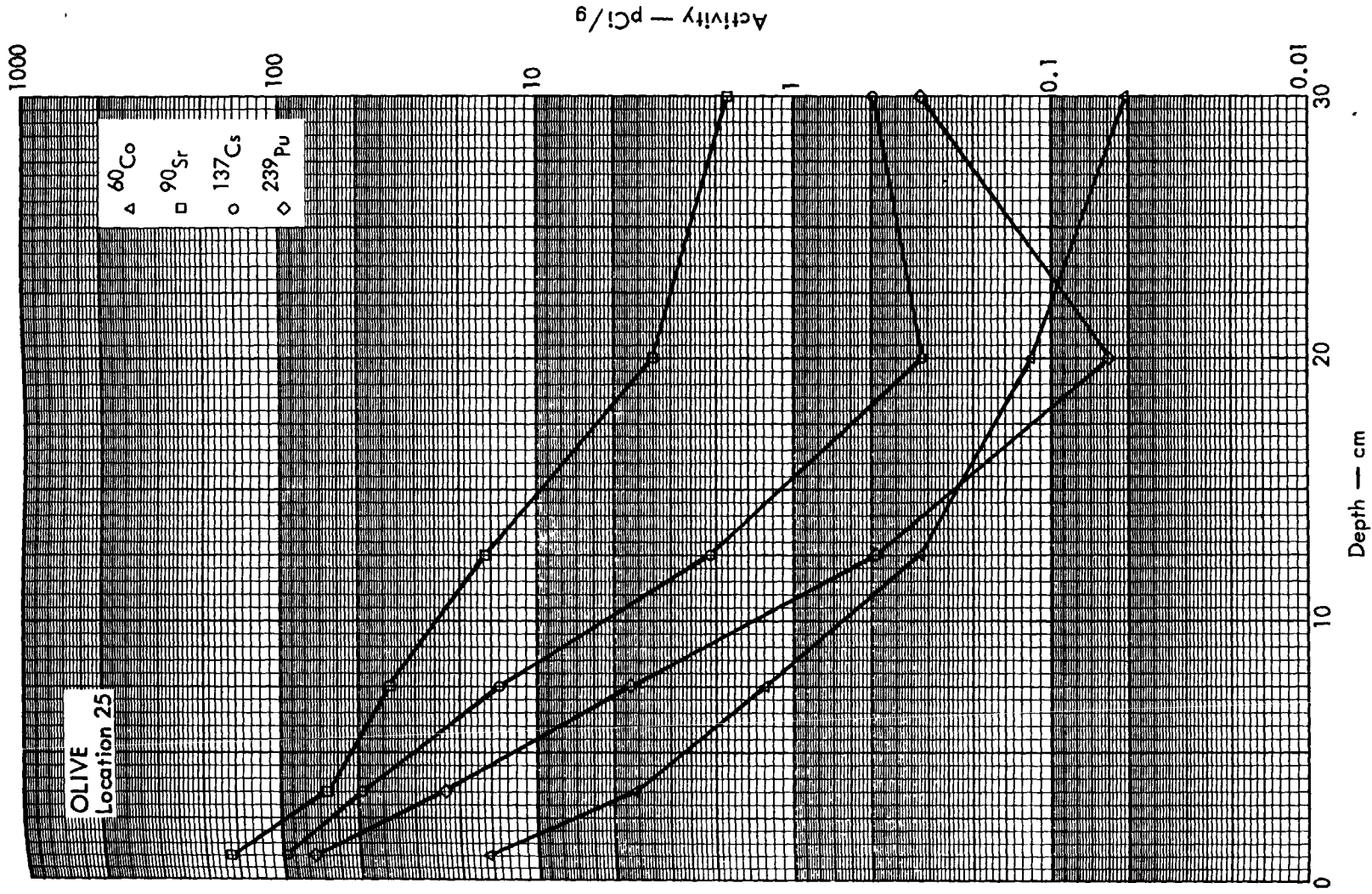


Fig. B. 14. 2b. Activities of selected radionuclides as a function of soil depth.

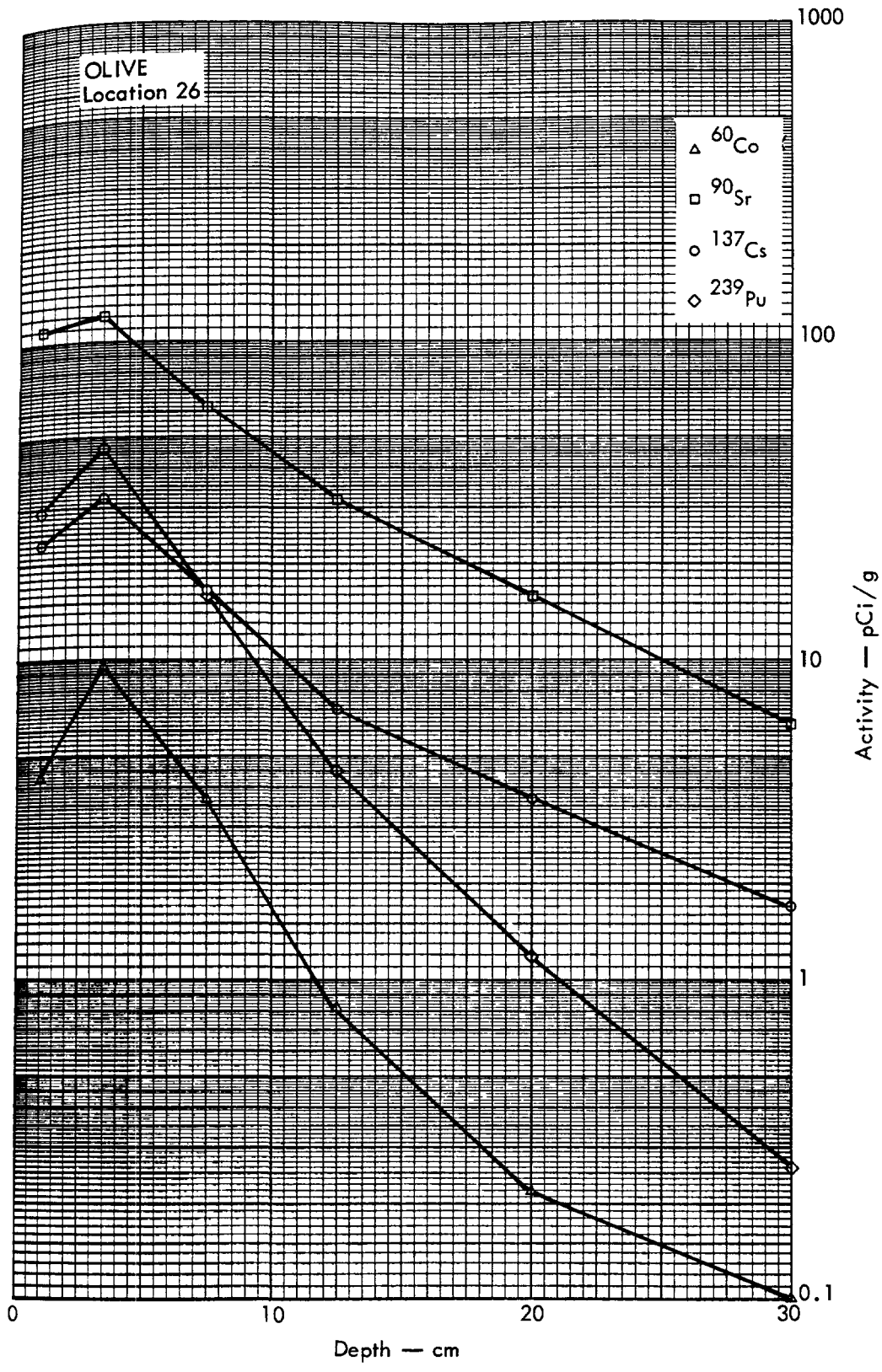


Fig. B. 14.2c. Activities of selected radionuclides as a function of soil depth.



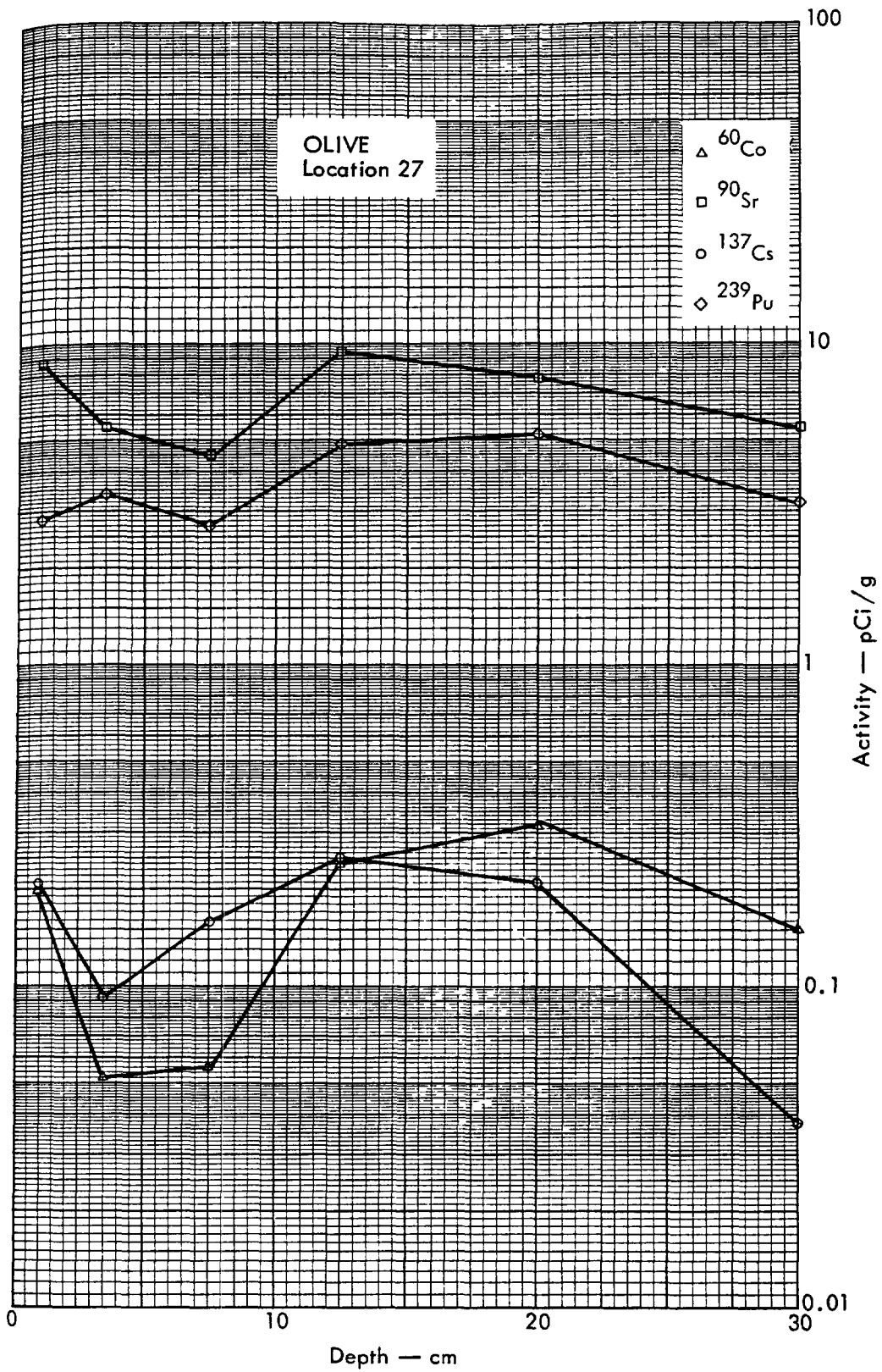
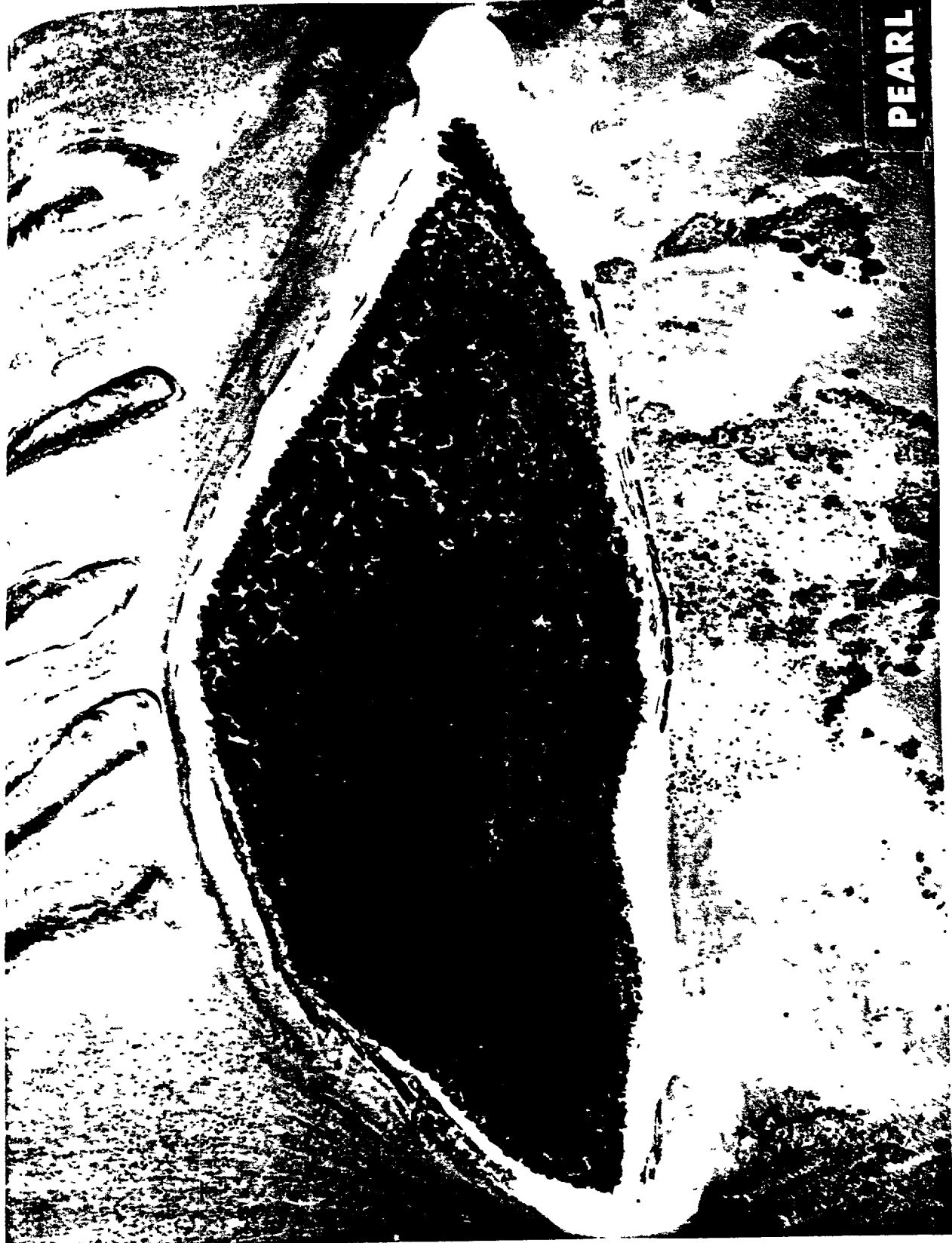


Fig. B. 14.2d. Activities of selected radionuclides as a function of soil depth.



PEARL

Fig. B.15.1.a.

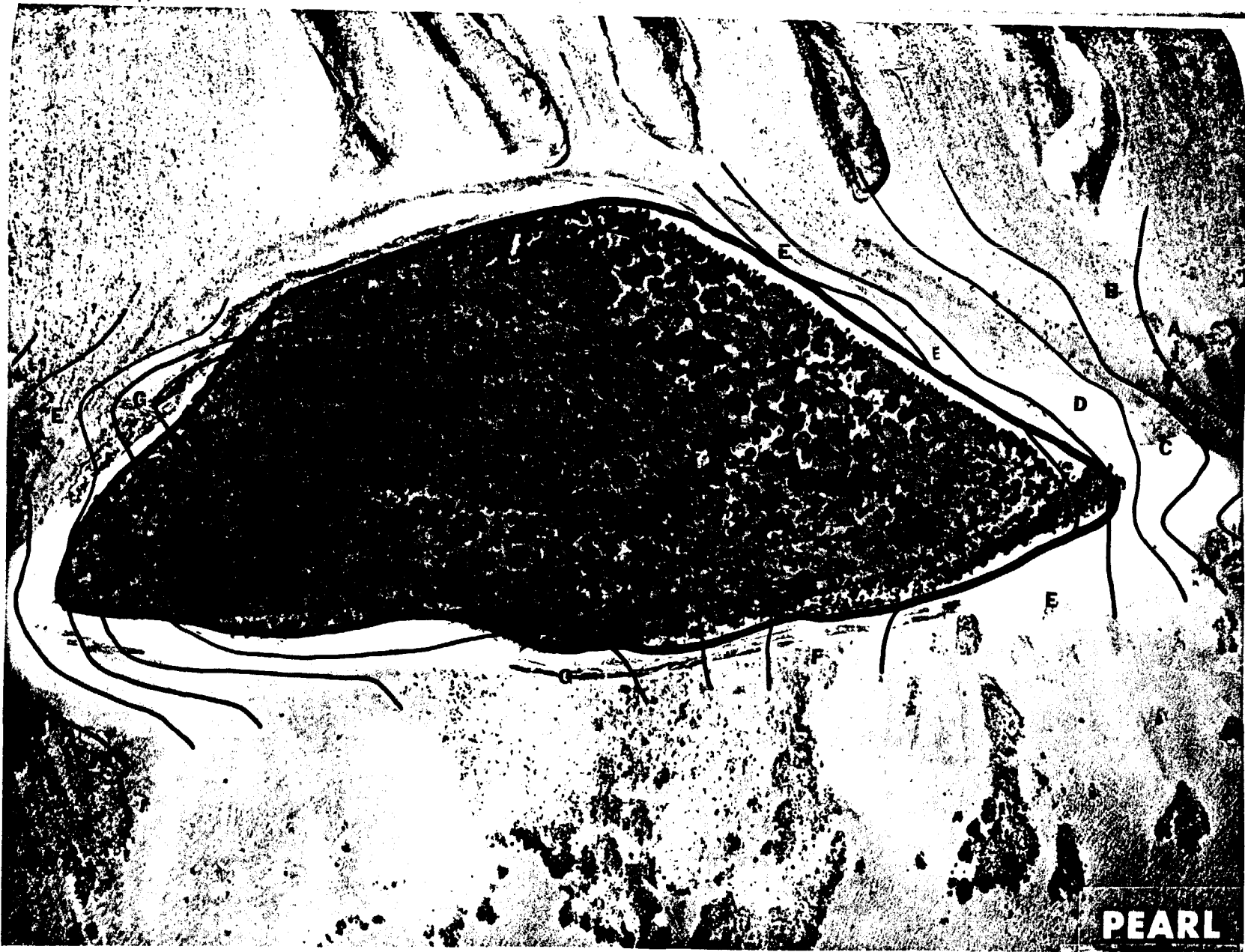


Fig. B.15.1.b. Gross count isoexposure contours. (Refer to alphabetic symbol key in this appendix.)



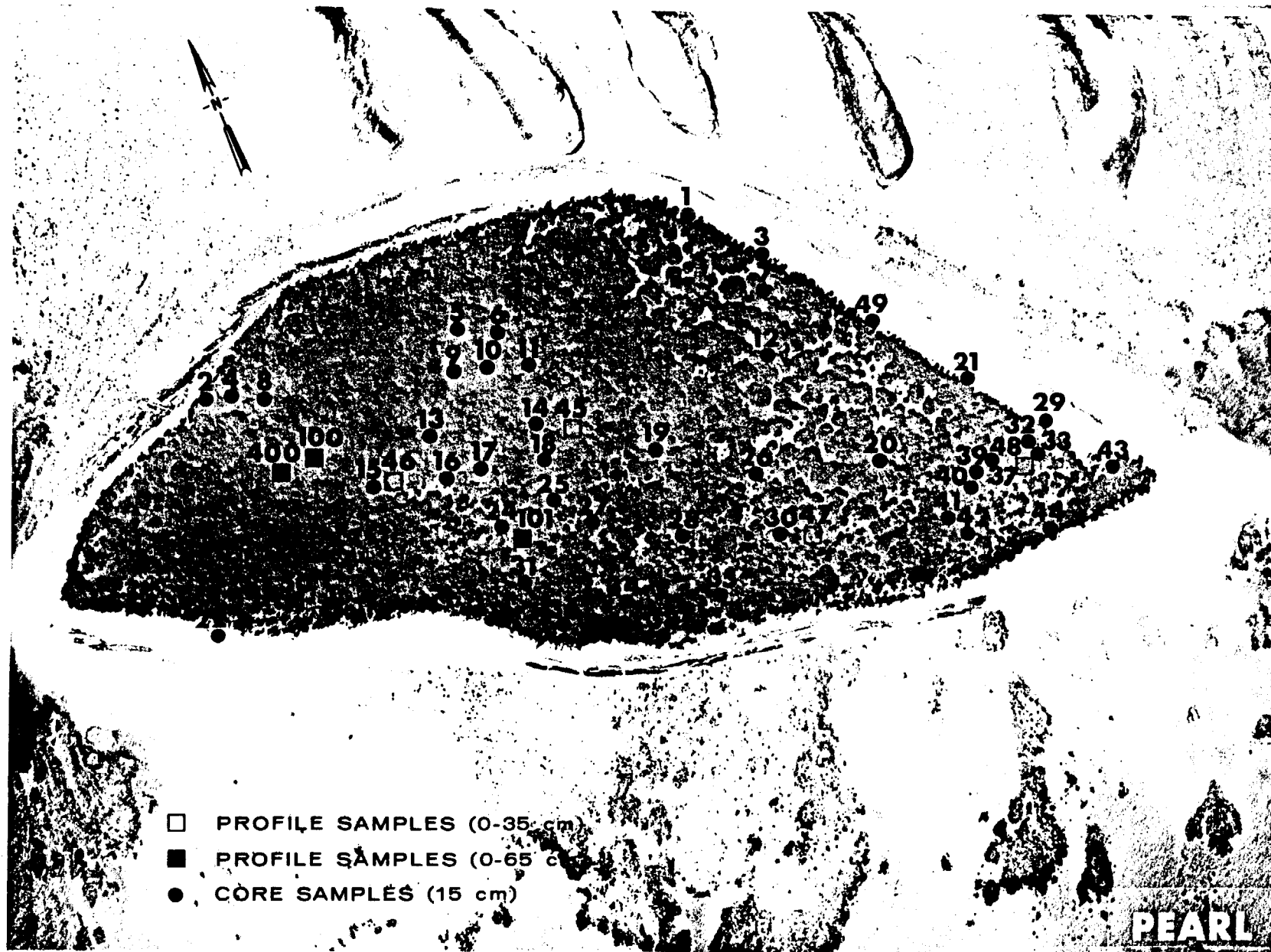


Fig. B.15.1.f. Soil-sample locations.

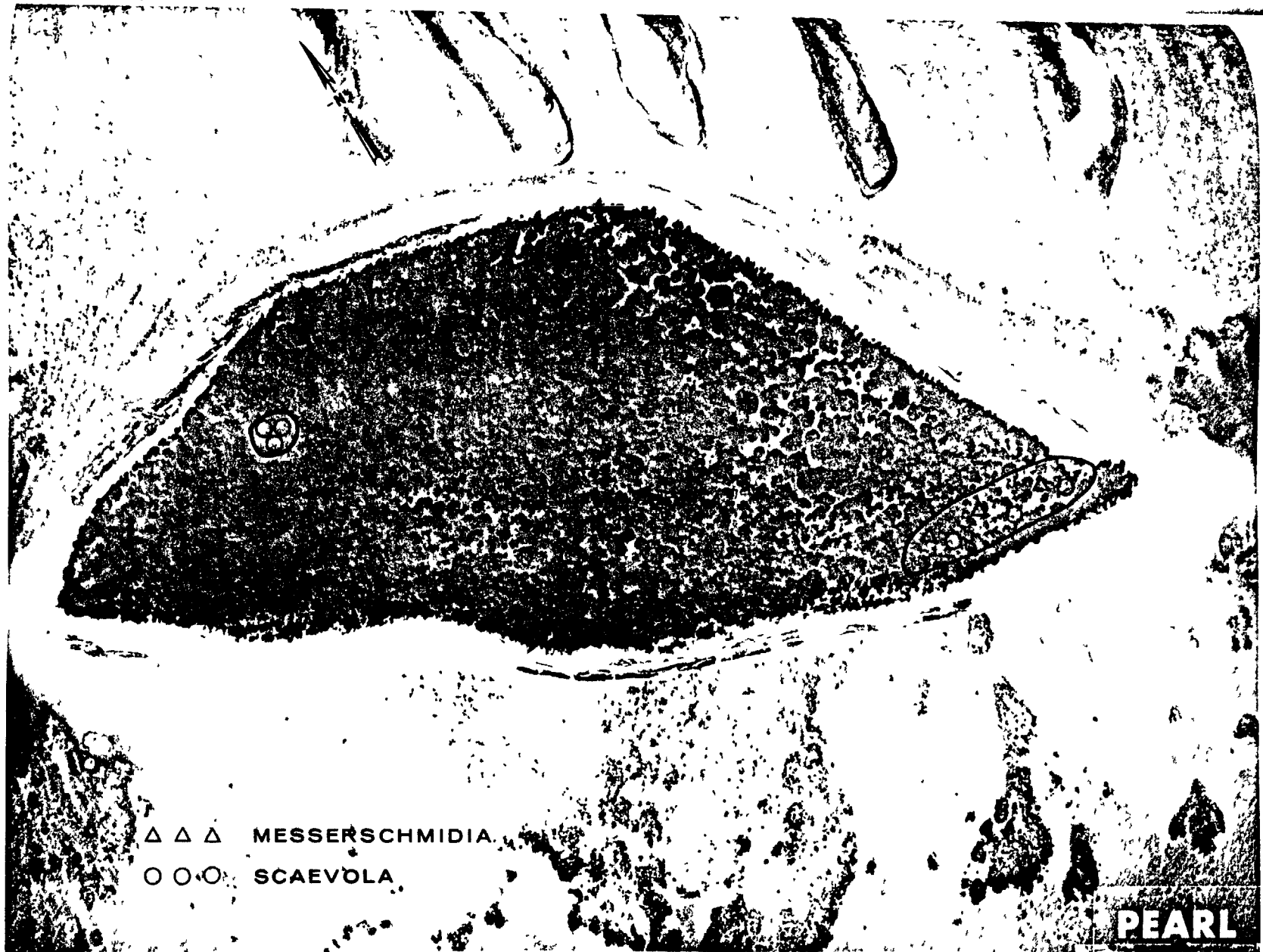


Fig. B.15.1.g. Vegetation sample locations.

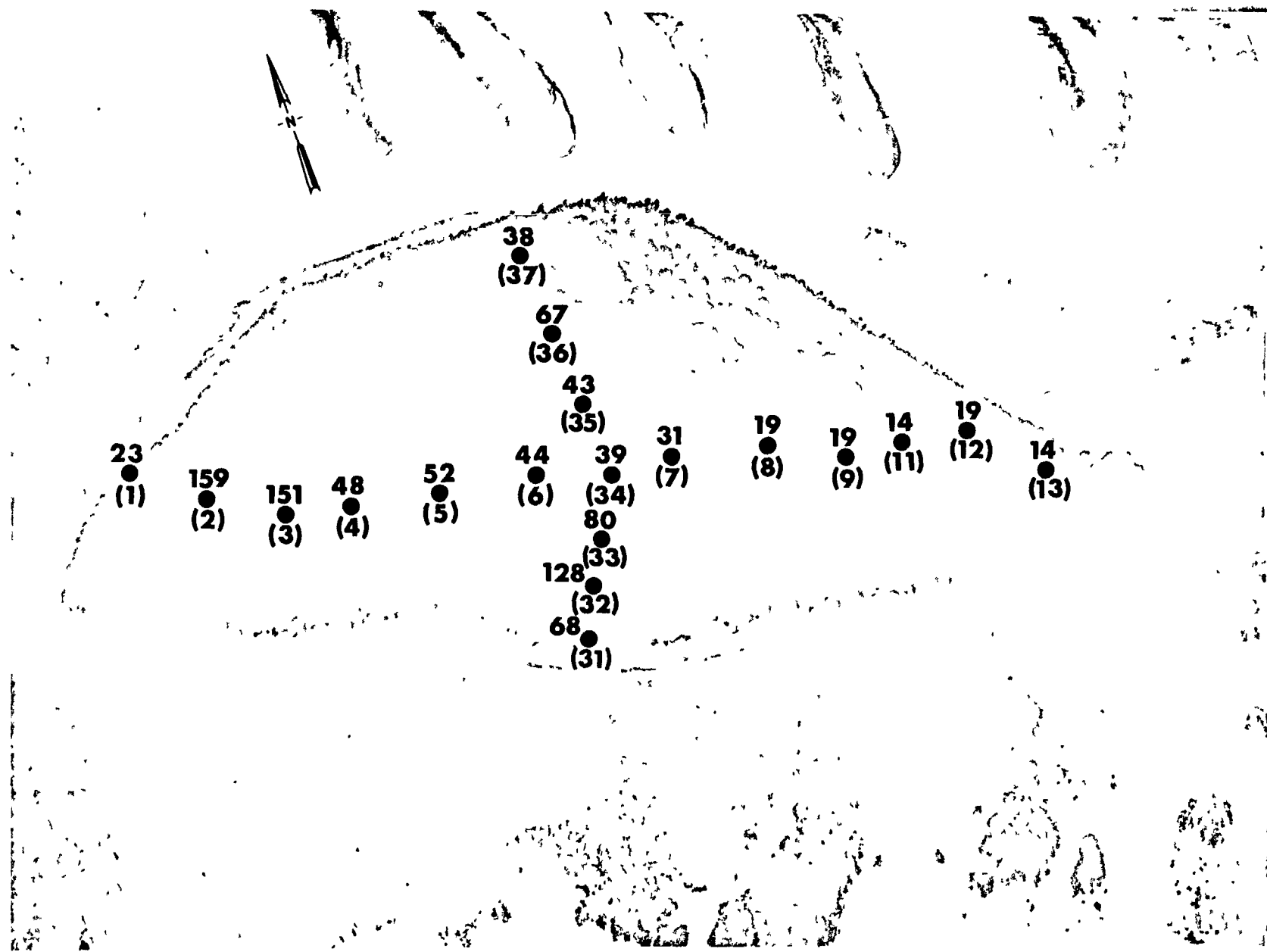


Fig. B.15.1.h. The gamma-ray exposure rates ( $\mu\text{R/hr}$ ) measured 1 m above the ground by the LiF thermoluminescent dosimeters (TLD). The numbers shown in parentheses denote the location identification numbers.







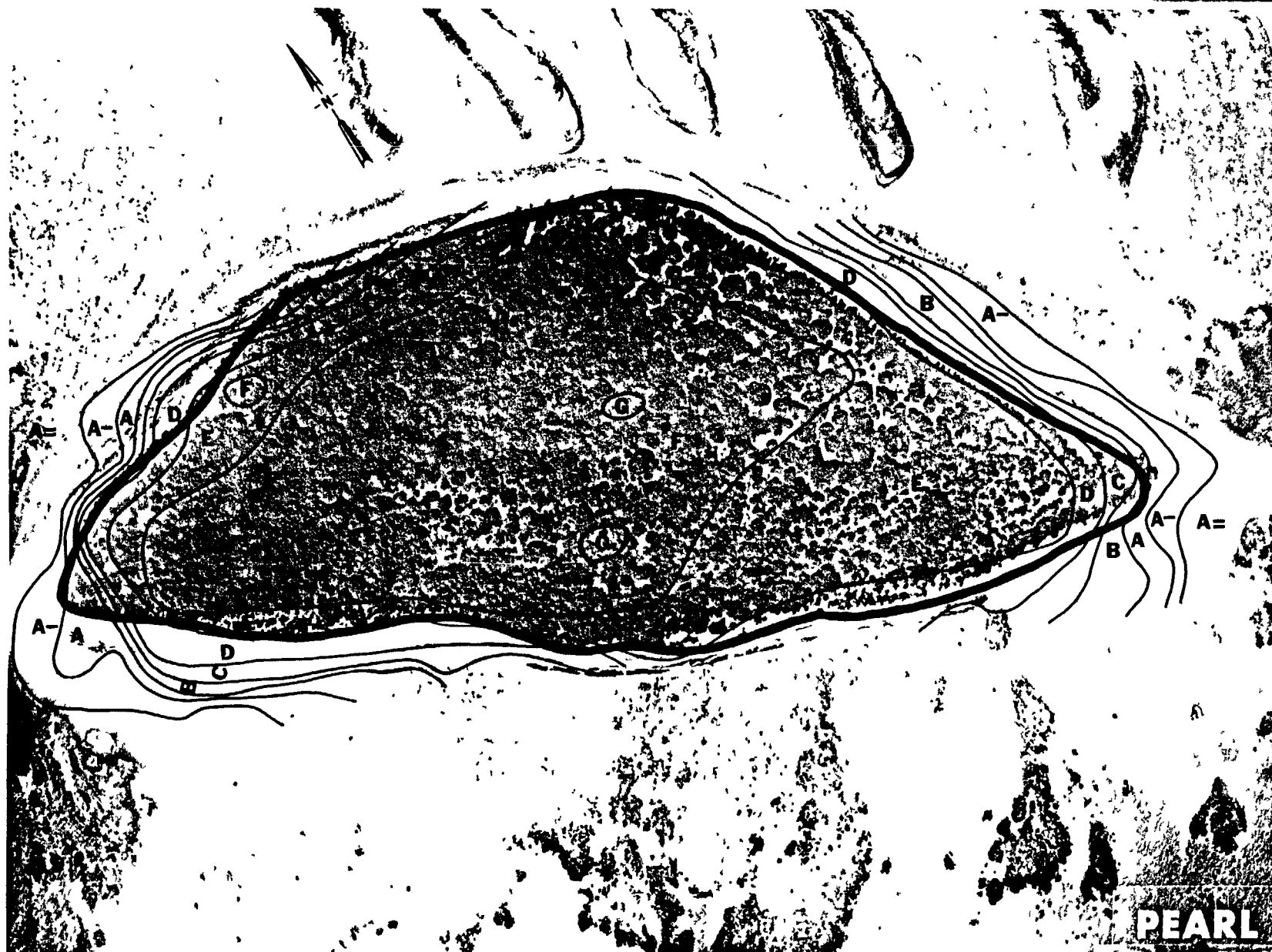


Fig. B.15.1.k. <sup>137</sup>Cs isoexposure and isoconcentration contours. (Refer to alphabetic symbol key in this appendix.)



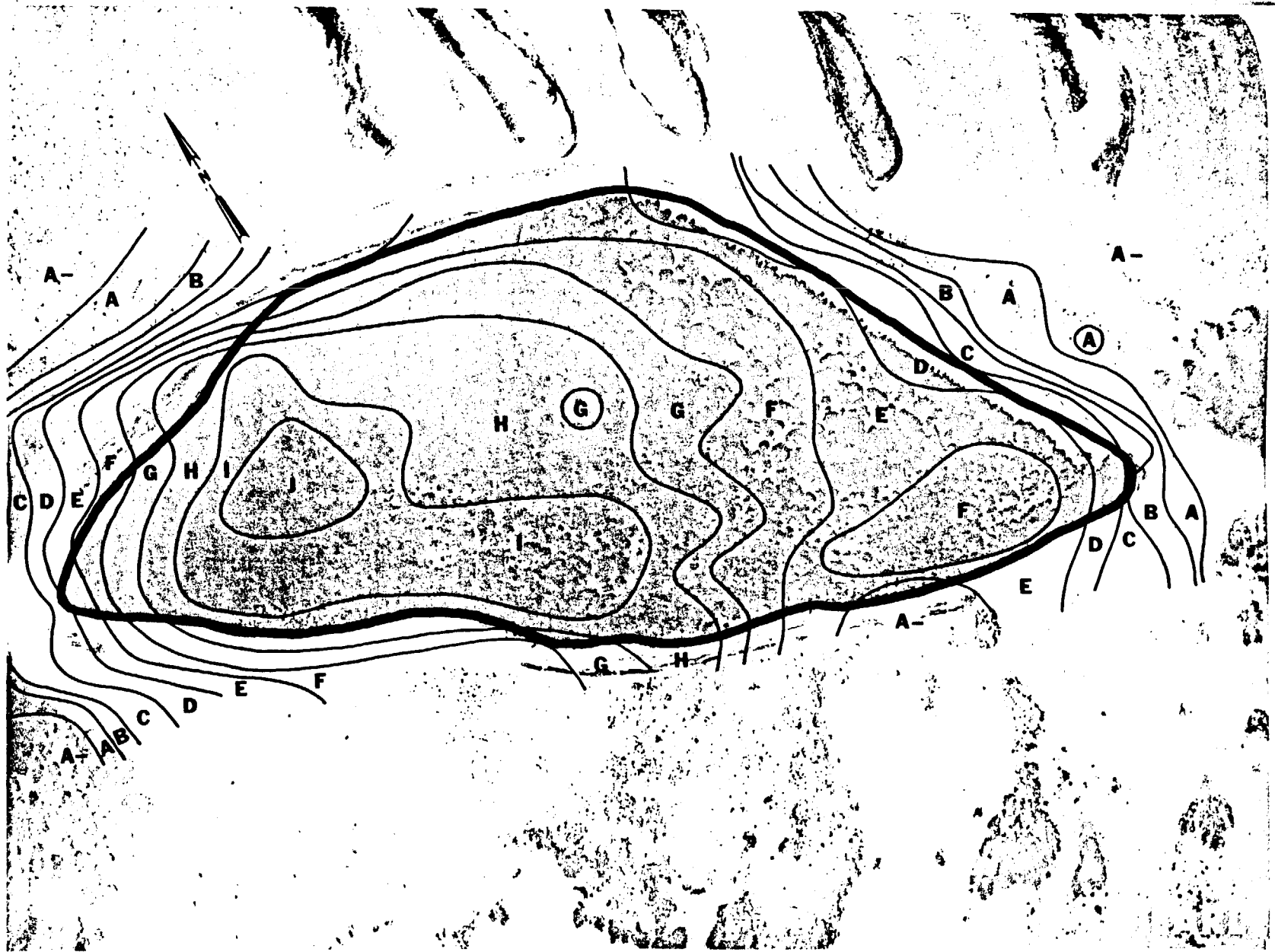


Fig. B.15.1.m.  $^{60}\text{Co}$  isoexposure and isoconcentration contours. (Refer to alphabetic symbol key in this appendix.)

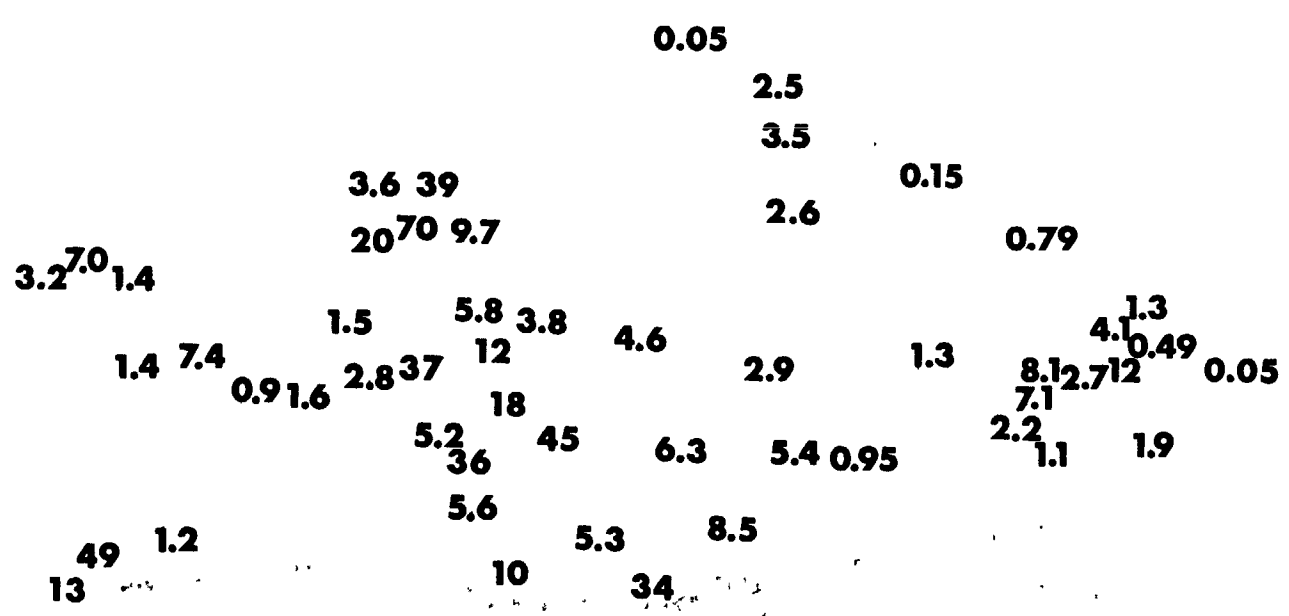
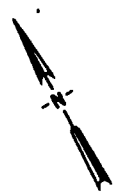


Fig. B.15.1.n. The average <sup>60</sup>Co activities (pCi/gm) in soil samples collected to a depth of 15 cm.

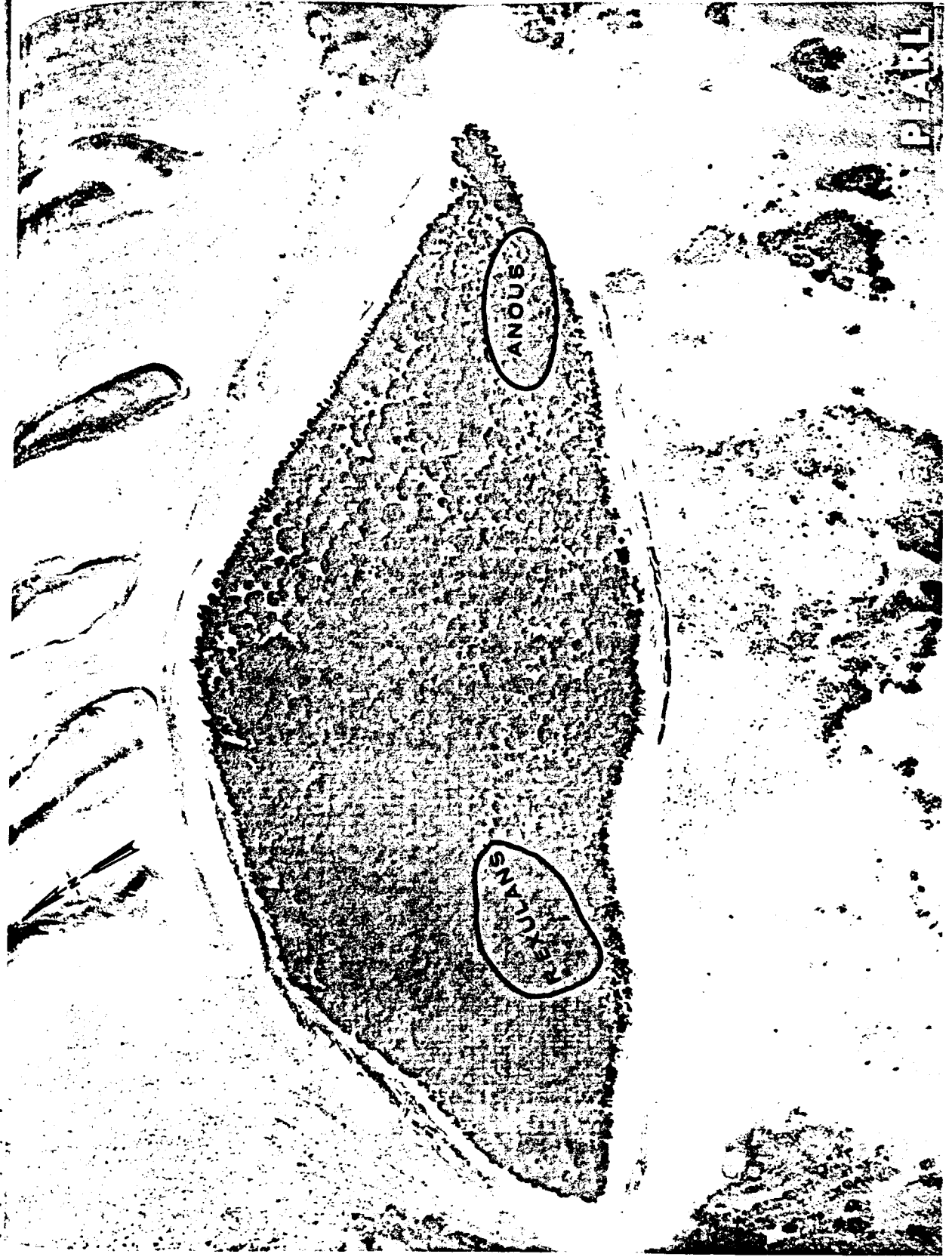


Fig. B.15.1.o. Terrestrial animal sample locations.

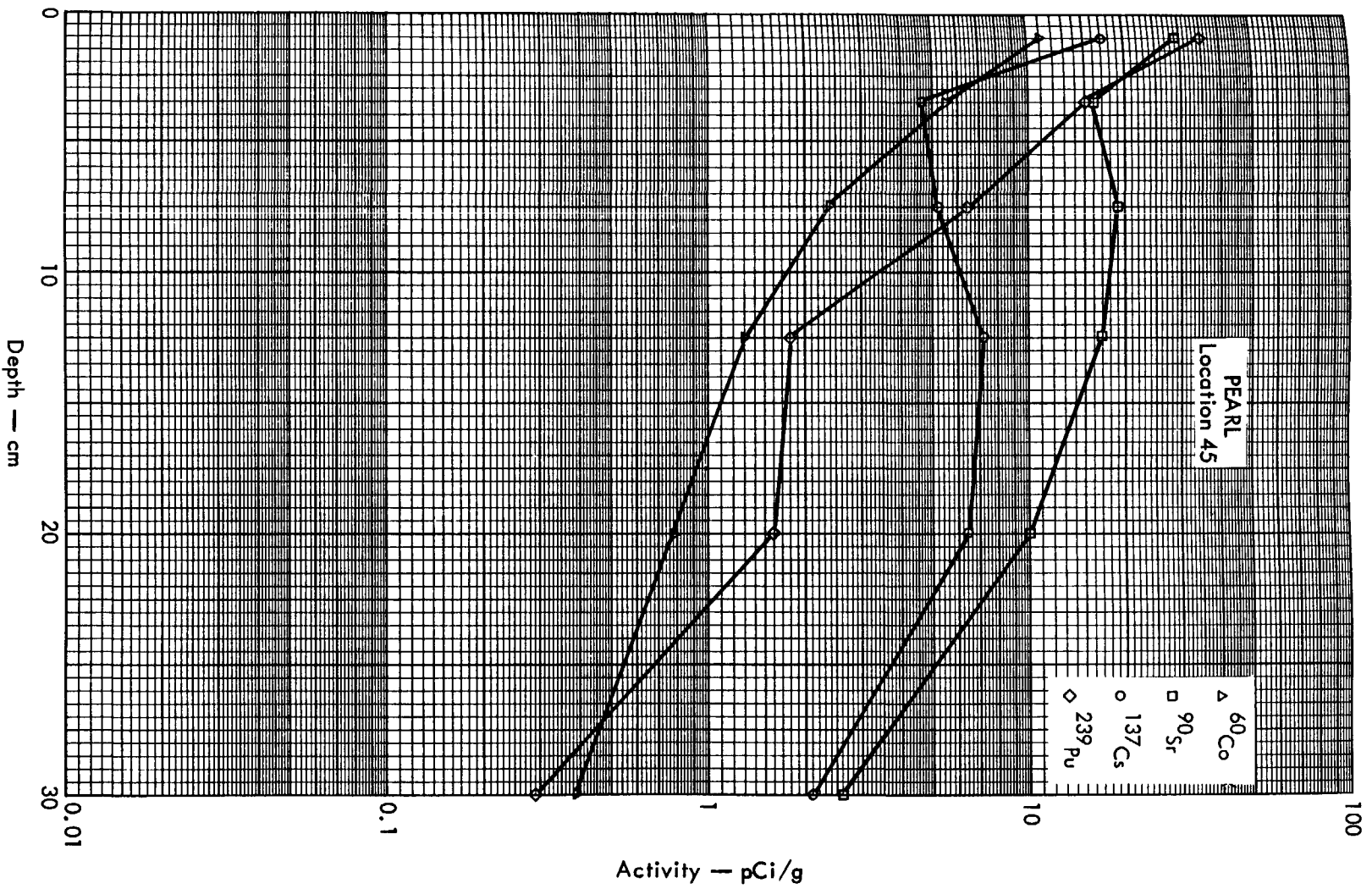


Fig. B. 15.2a. Activities of selected radionuclides as a function of soil depth.

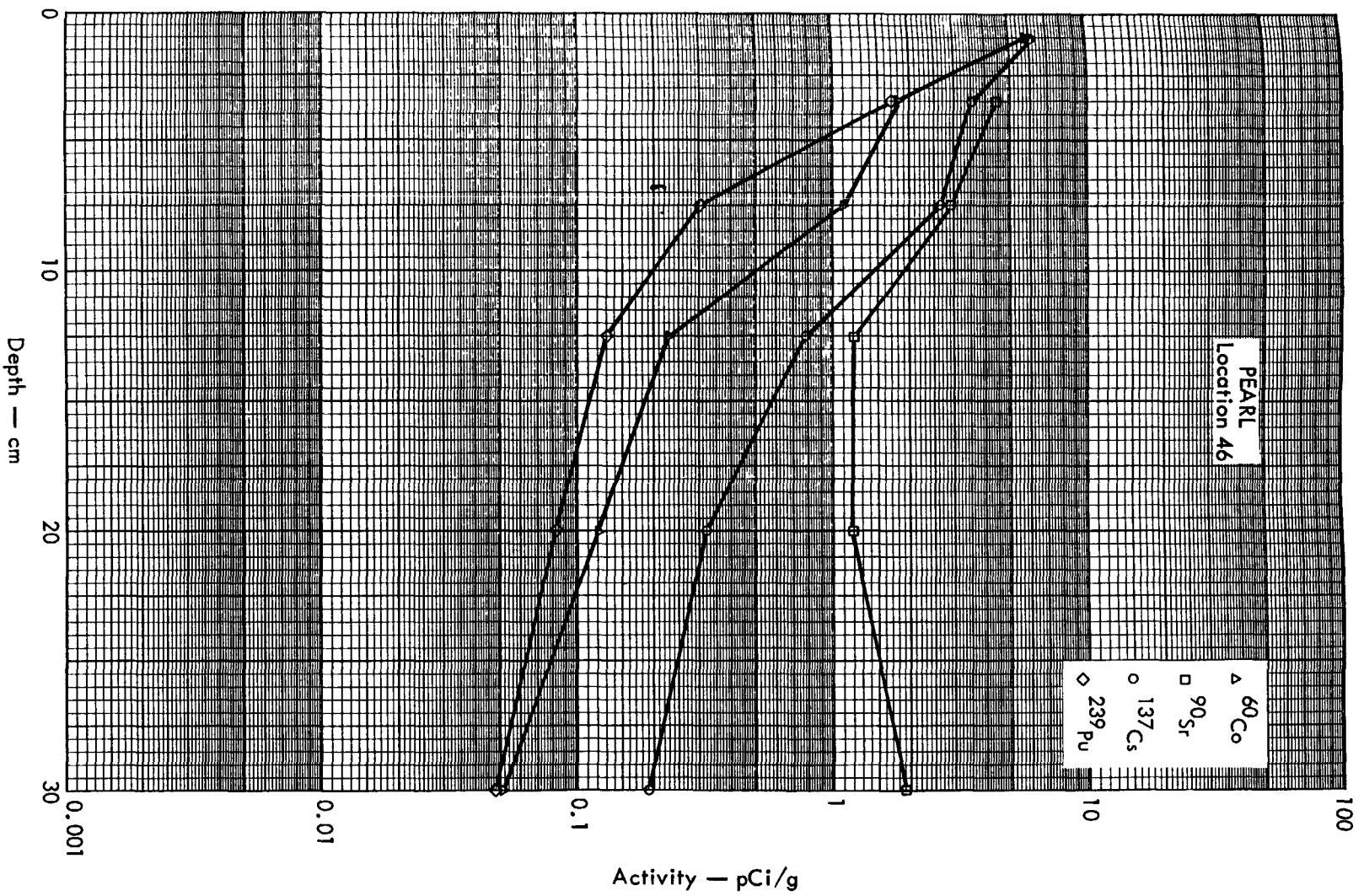


Fig. B. 15. 2b. Activities of selected radionuclides as a function of soil depth.



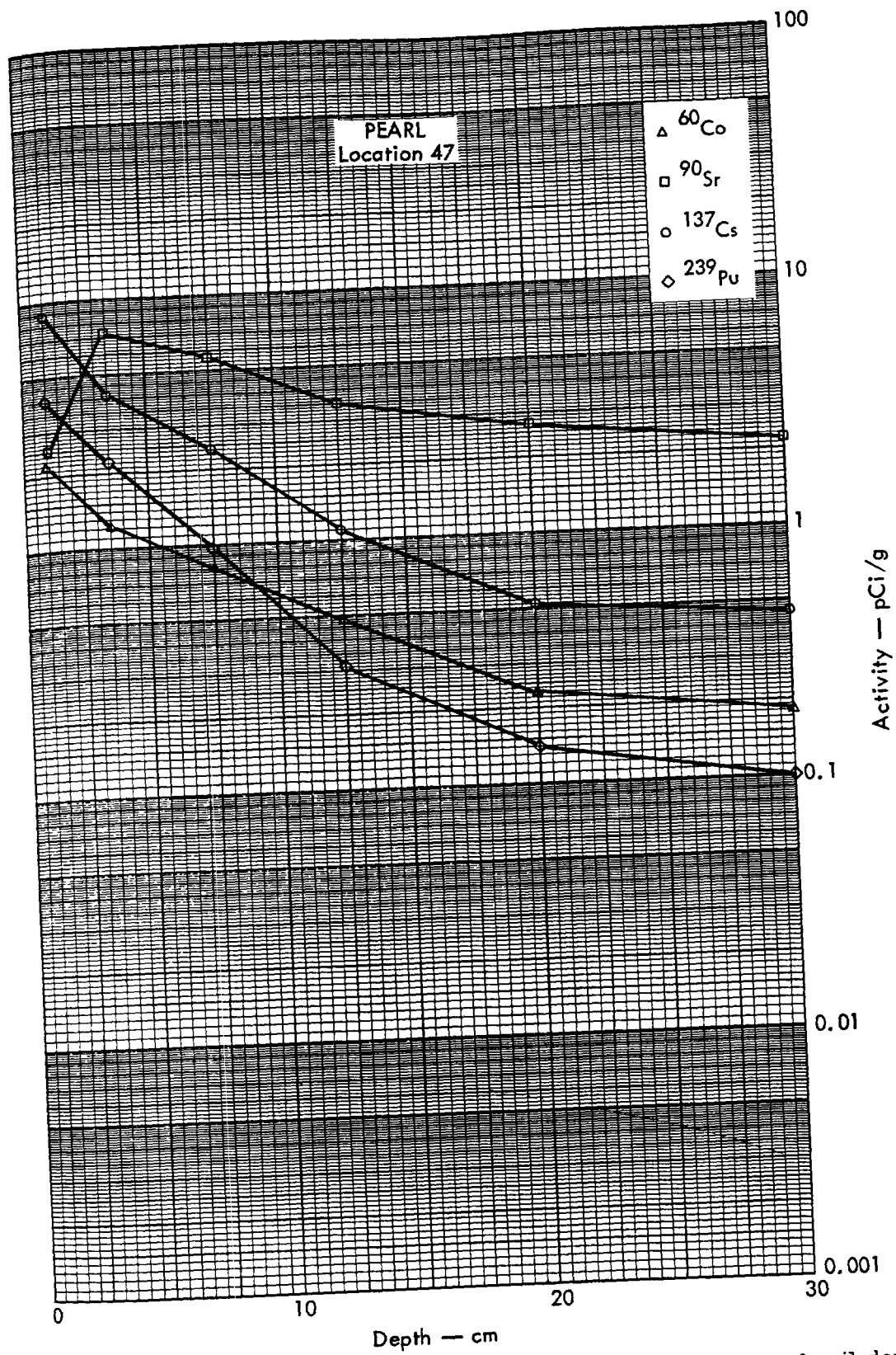


Fig. B.15.2c. Activities of selected radionuclides as a function of soil depth.

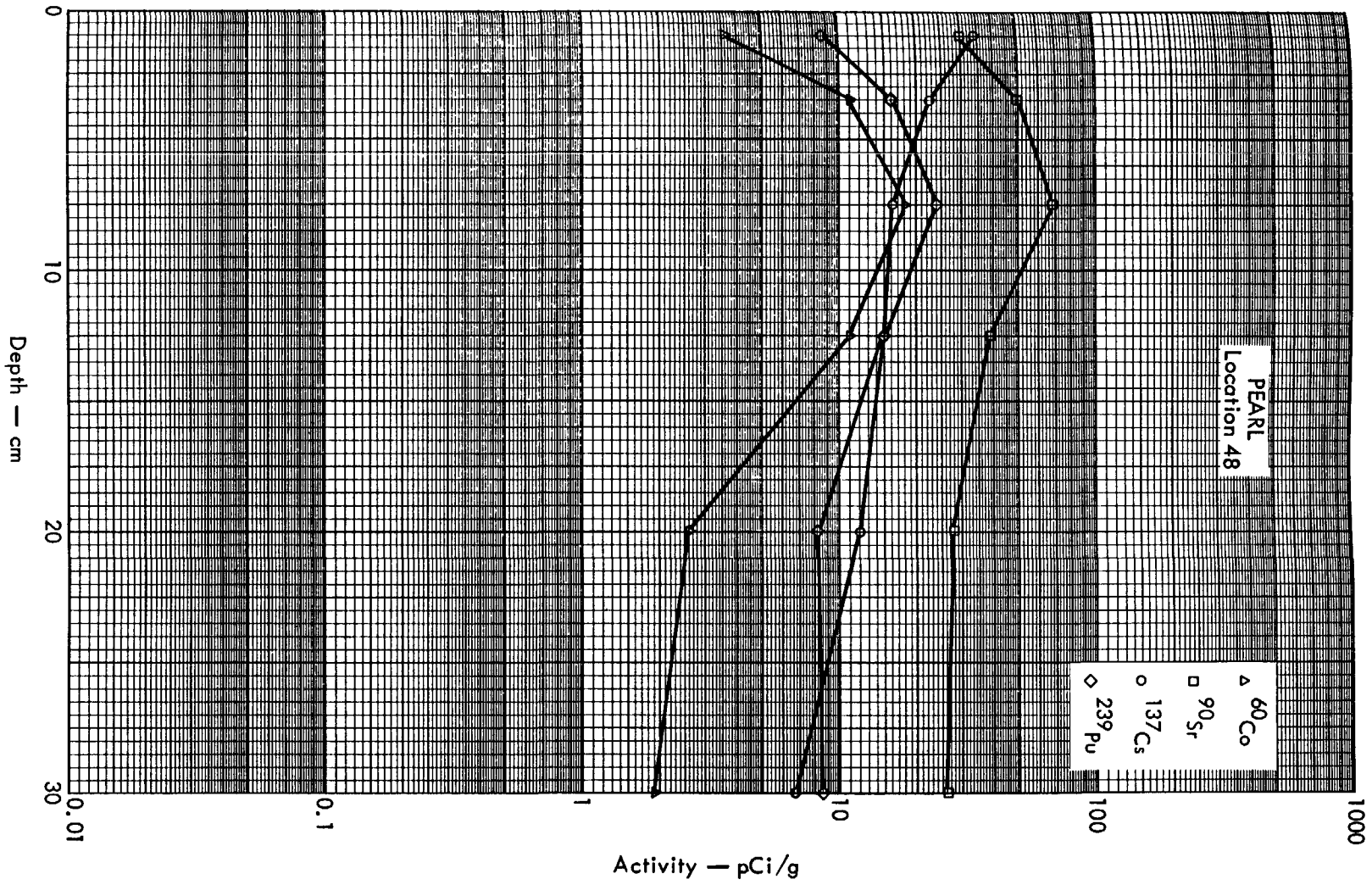


Fig. B. 15.2d. Activities of selected radionuclides as a function of soil depth.

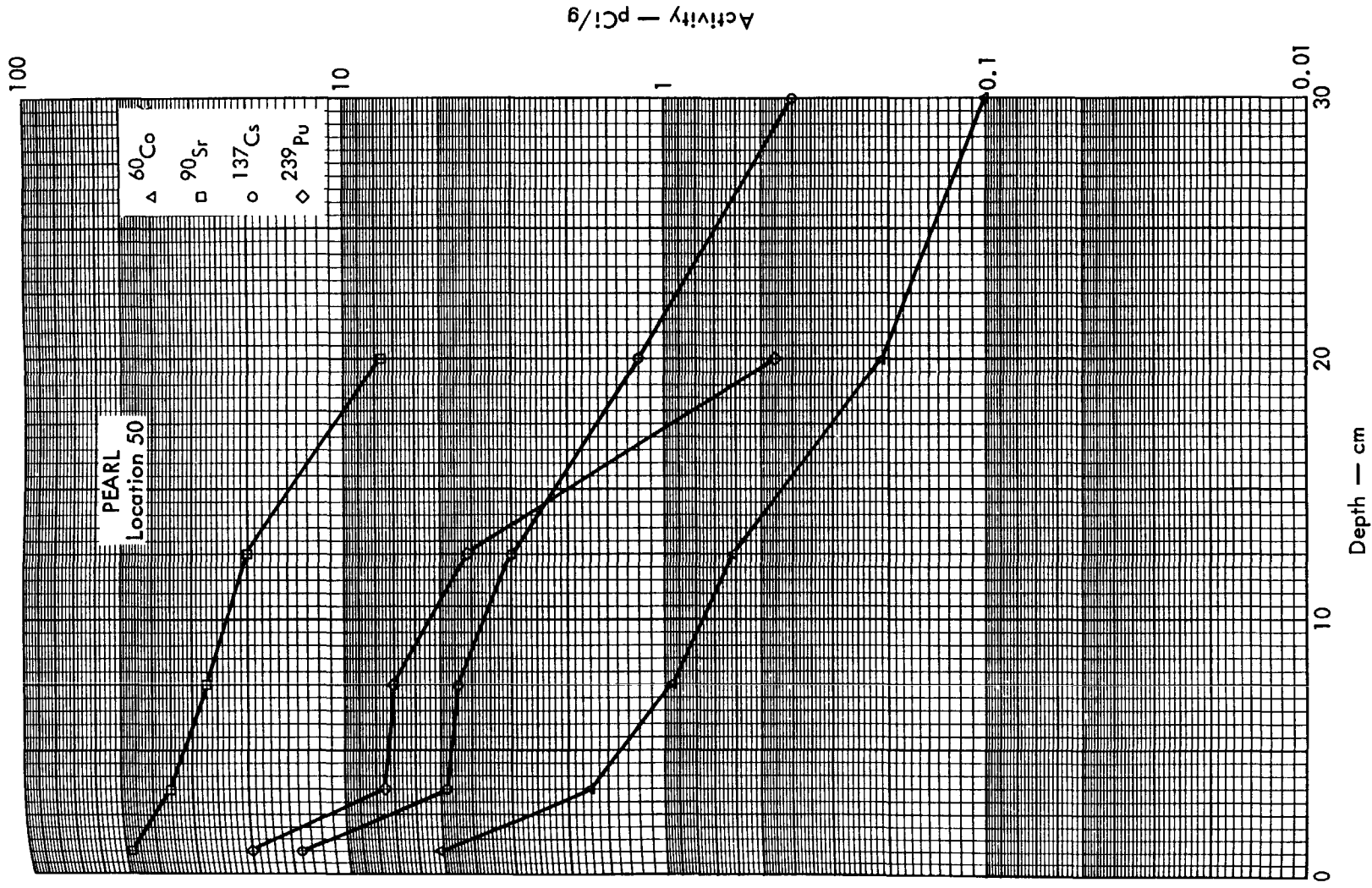


Fig. B. 15. 2e. Activities of selected radionuclides as a function of soil depth.

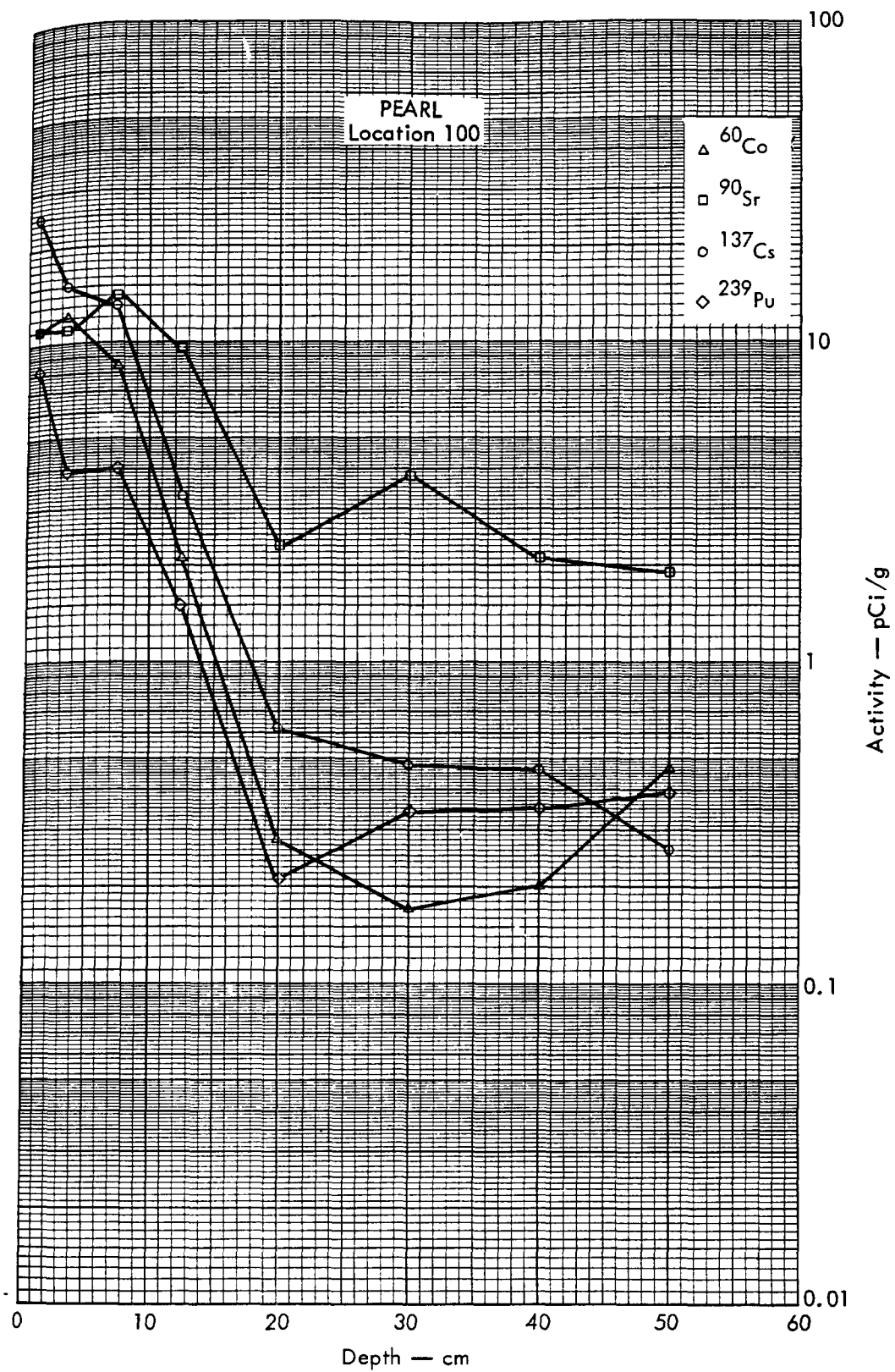


Fig. B. 15. 2f. Activities of selected radionuclides as a function of soil depth.

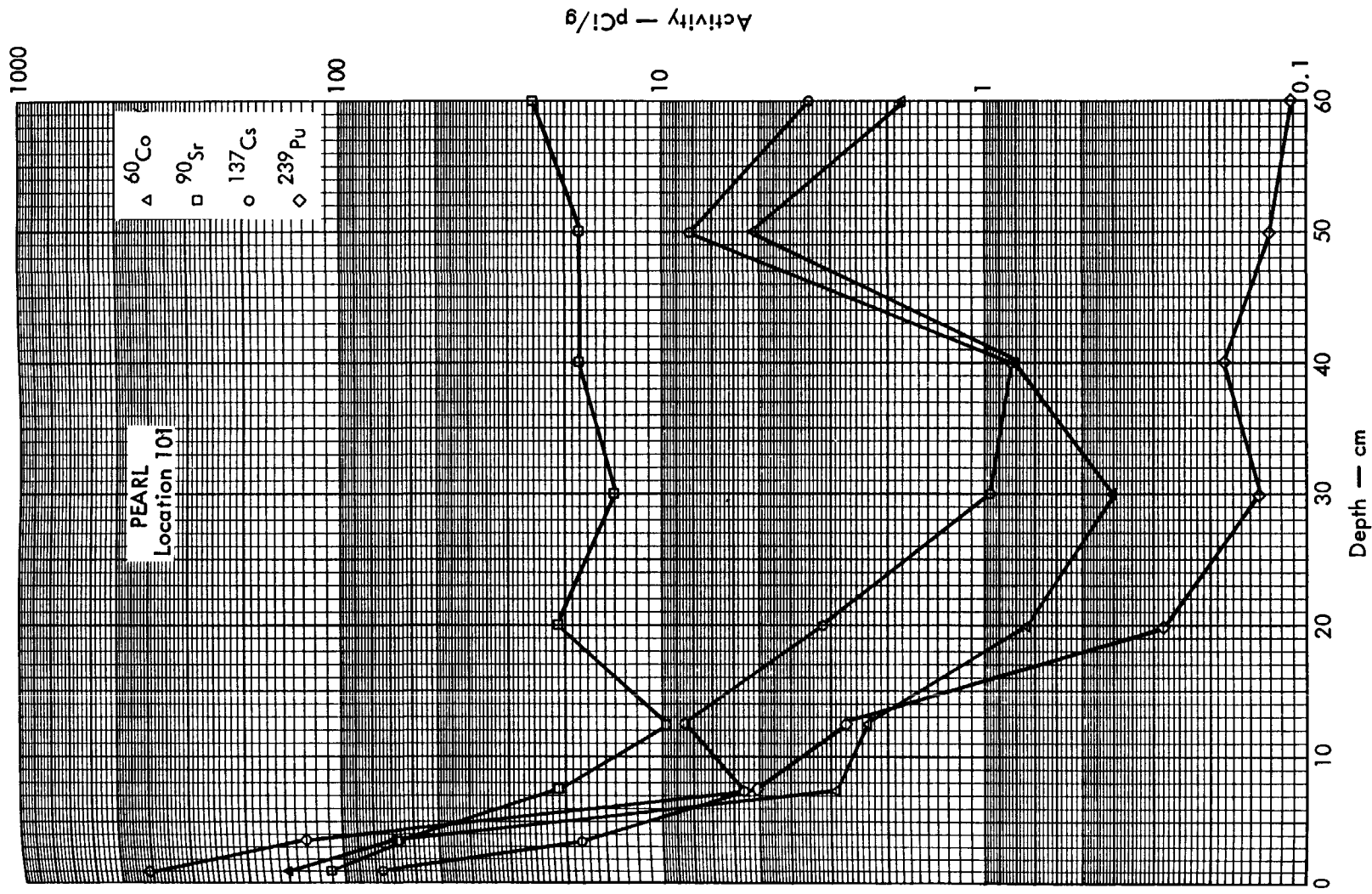


Fig. B. 15. 2g. Activities of selected radionuclides as a function of soil depth.

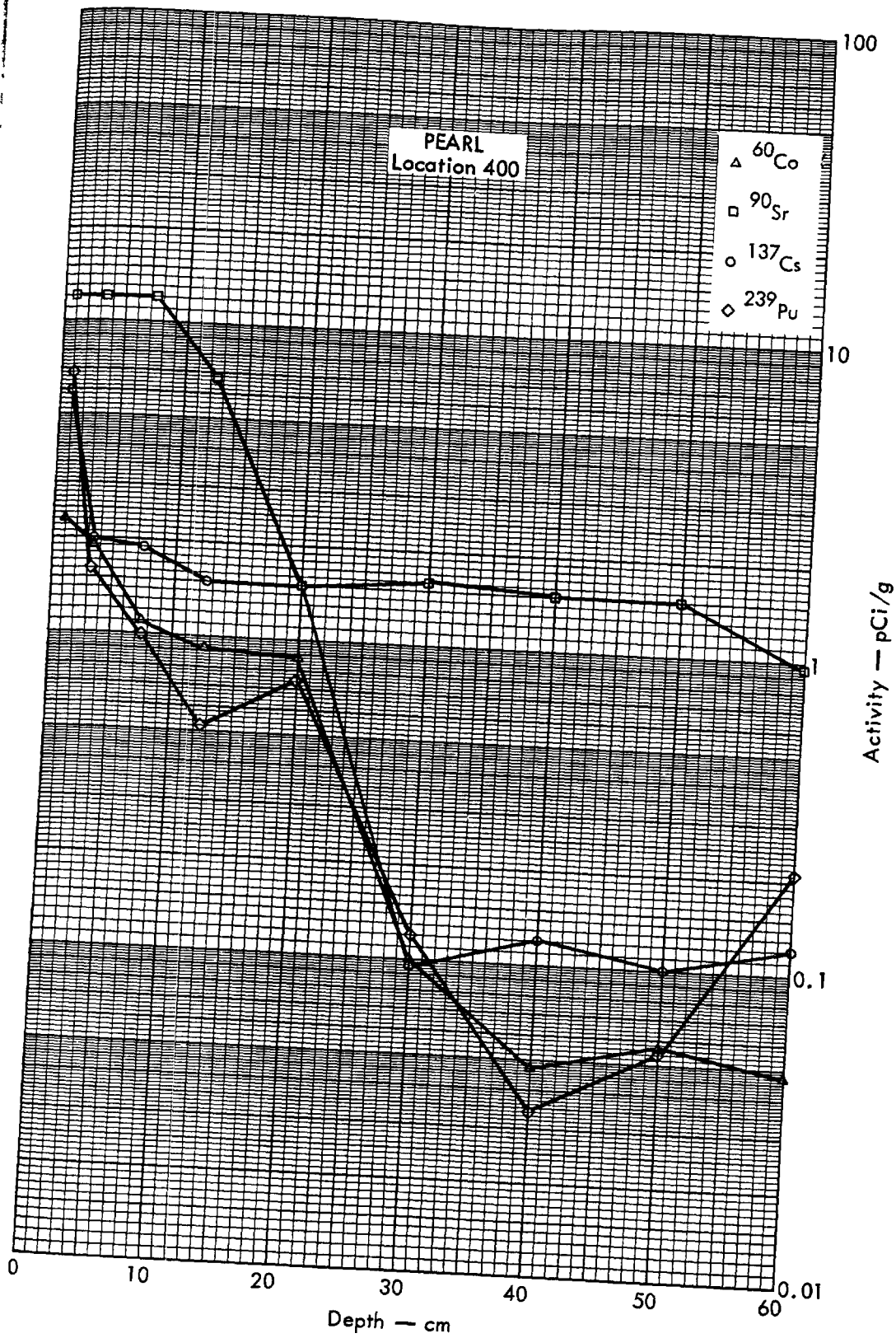


Fig. B. 15.2h. Activities of selected radionuclides as a function of soil depth.

RUBY

FIG. B.16.1.a.







Fig. B.16.1.b. Gross count isoexposure contours. (Refer to alphabetic symbol key in this appendix.)



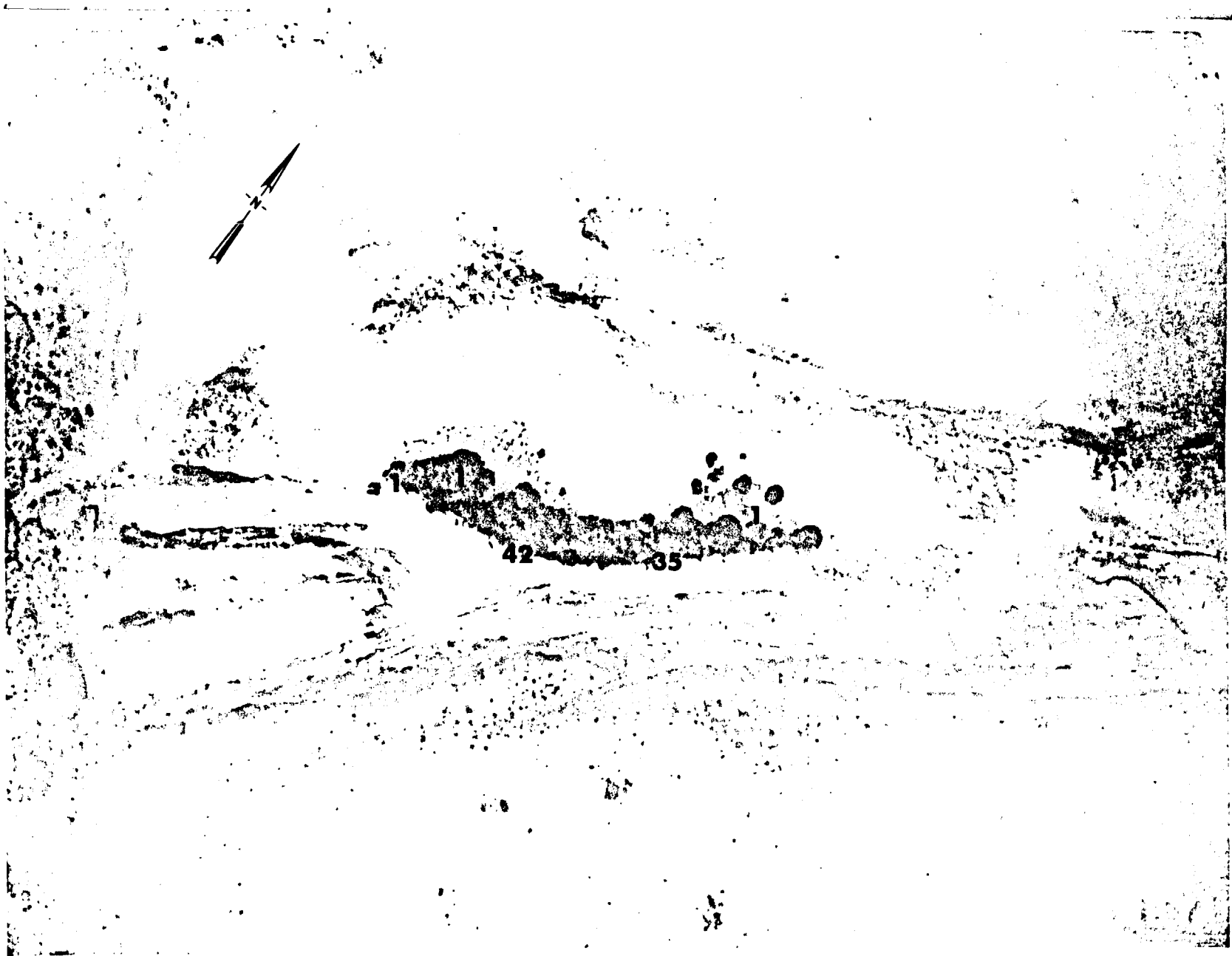


Fig. B.16.1.d. The gamma background exposure rate ( $\mu\text{R/hr}$ ) at 1 m above the ground, measured with a portable NaI scintillation counter.



Fig. B.16.1.f. Soil-sample locations.



Fig. B.16.1.g. Vegetation sample locations.

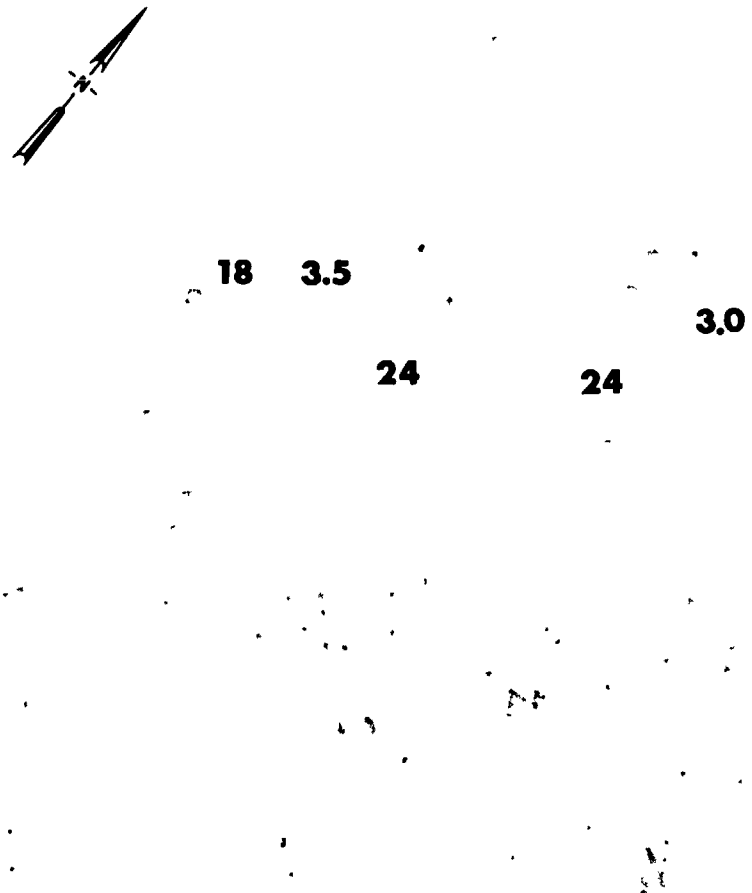


Fig. B.16.1.i. The average  $^{239}\text{Pu}$  activities (pCi/g) in soil samples collected to a depth of 15 cm.



Fig. B.16.1.j. The average  $^{90}\text{Sr}$  activities ( $\mu\text{Ci/g}$ ) in soil samples collected to a depth of 15 cm.

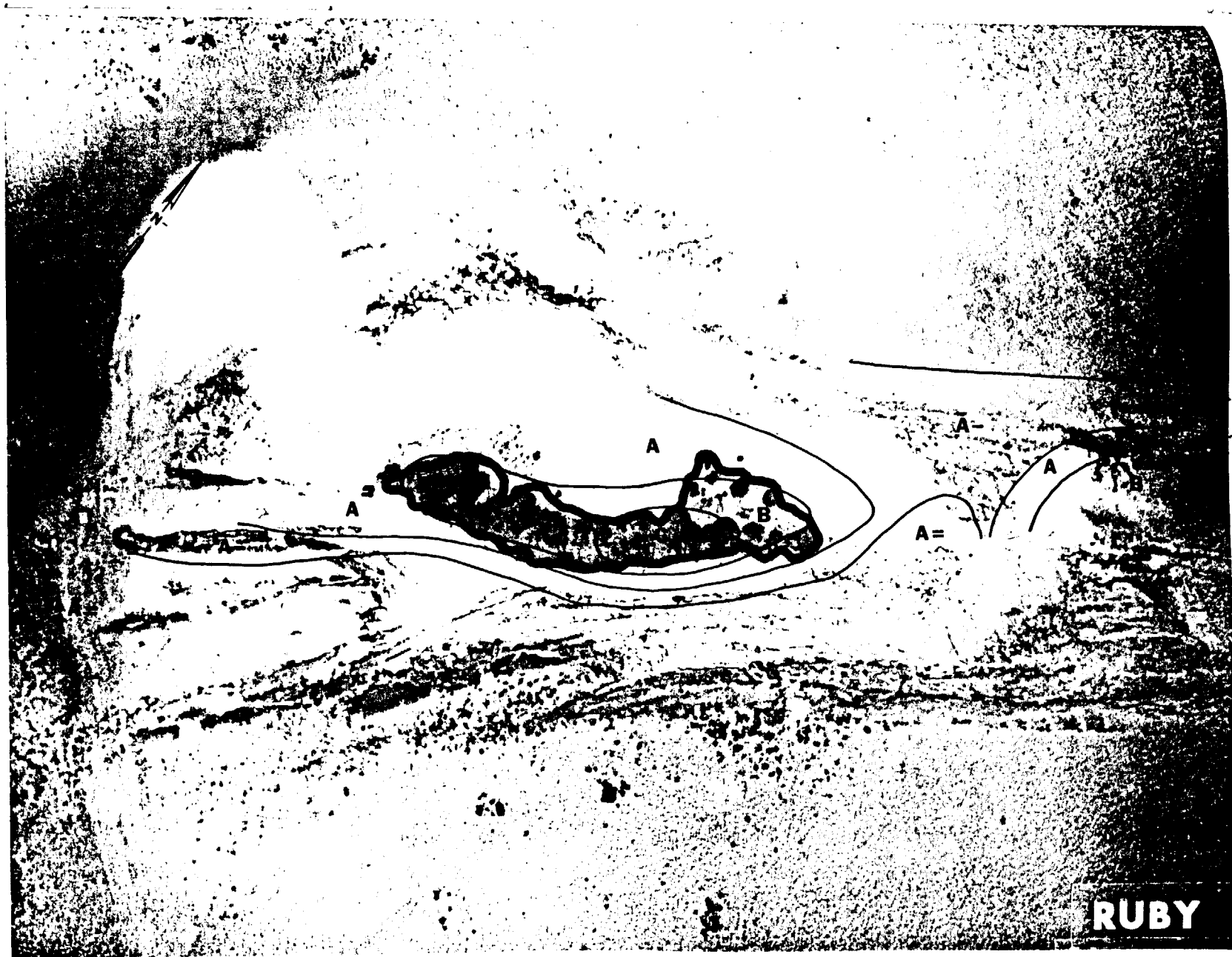


Fig. B.16.1.k.  $^{137}\text{Cs}$  isoexposure and isoconcentration contours. (Refer to alphabetic symbol key in this appendix.)



Fig. B.16.1.1. The average  $^{137}\text{Cs}$  activities (pCi/g) in soil samples collected to a depth of 15 cm.

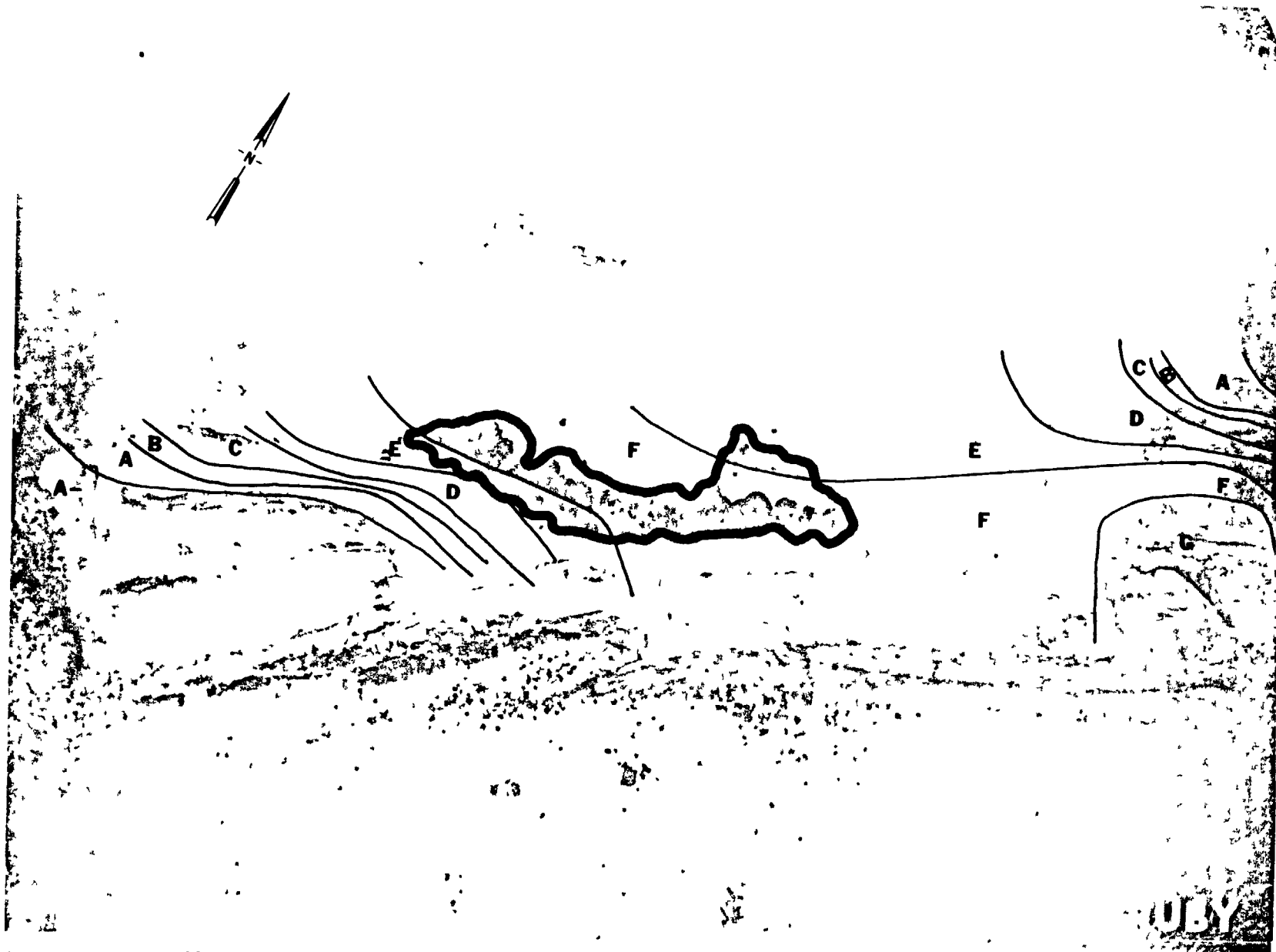
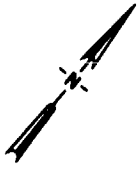
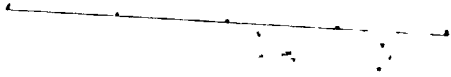


Fig. B.16.1.m.  $^{60}\text{Co}$  isoexposure and isoconcentration contours. (Refer to alphabetic symbol key in this appendix.)





**0.37 0.29**

**16**

**15**

**0.82**

Fig. B.16.1.n. The average  $^{60}\text{Co}$  activities (pCi/g) in soil samples collected to a depth of 15 cm.

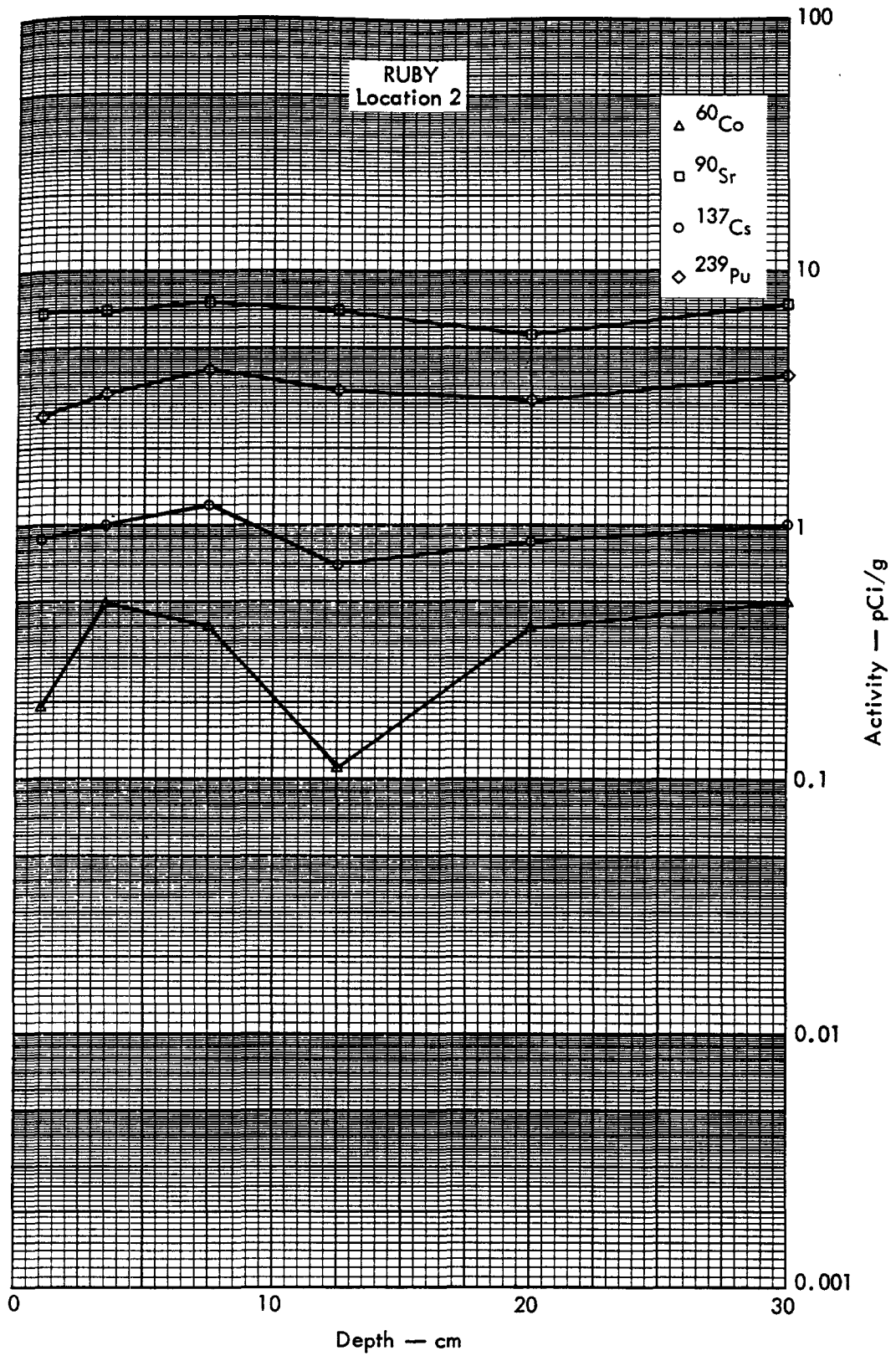


Fig. B. 16. 2a. Activities of selected radionuclides as a function of soil depth.



Fig. B.17.1.a.



Fig. B.17.1.b. Gross count isosexposure contours. (Refer to alphabetic symbol key in this appendix.)

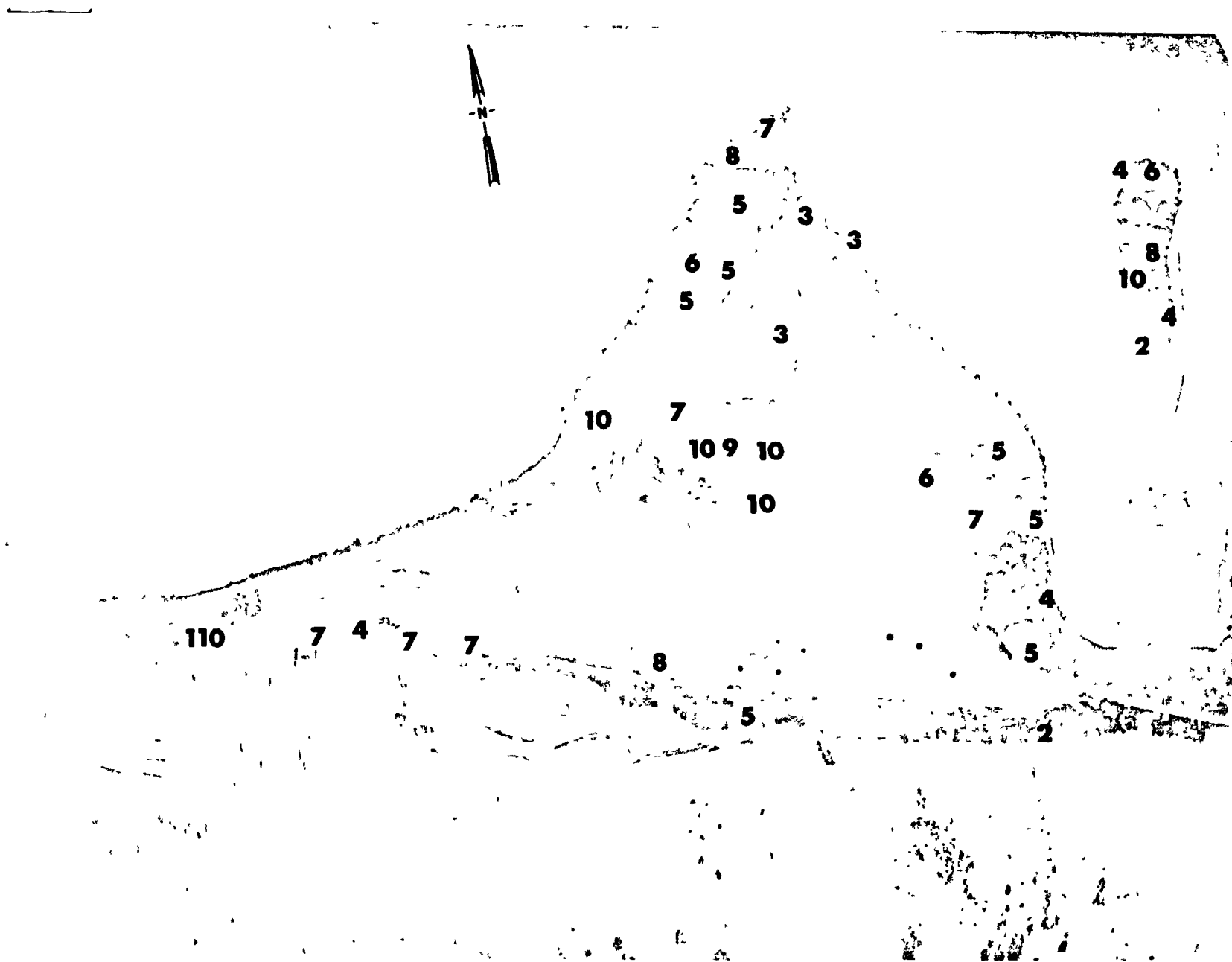


Fig. B.17.1.d. The gamma background exposure rate ( $\mu\text{R/hr}$ ) at 1 m above the ground, measured with a portable NaI scintillation counter.

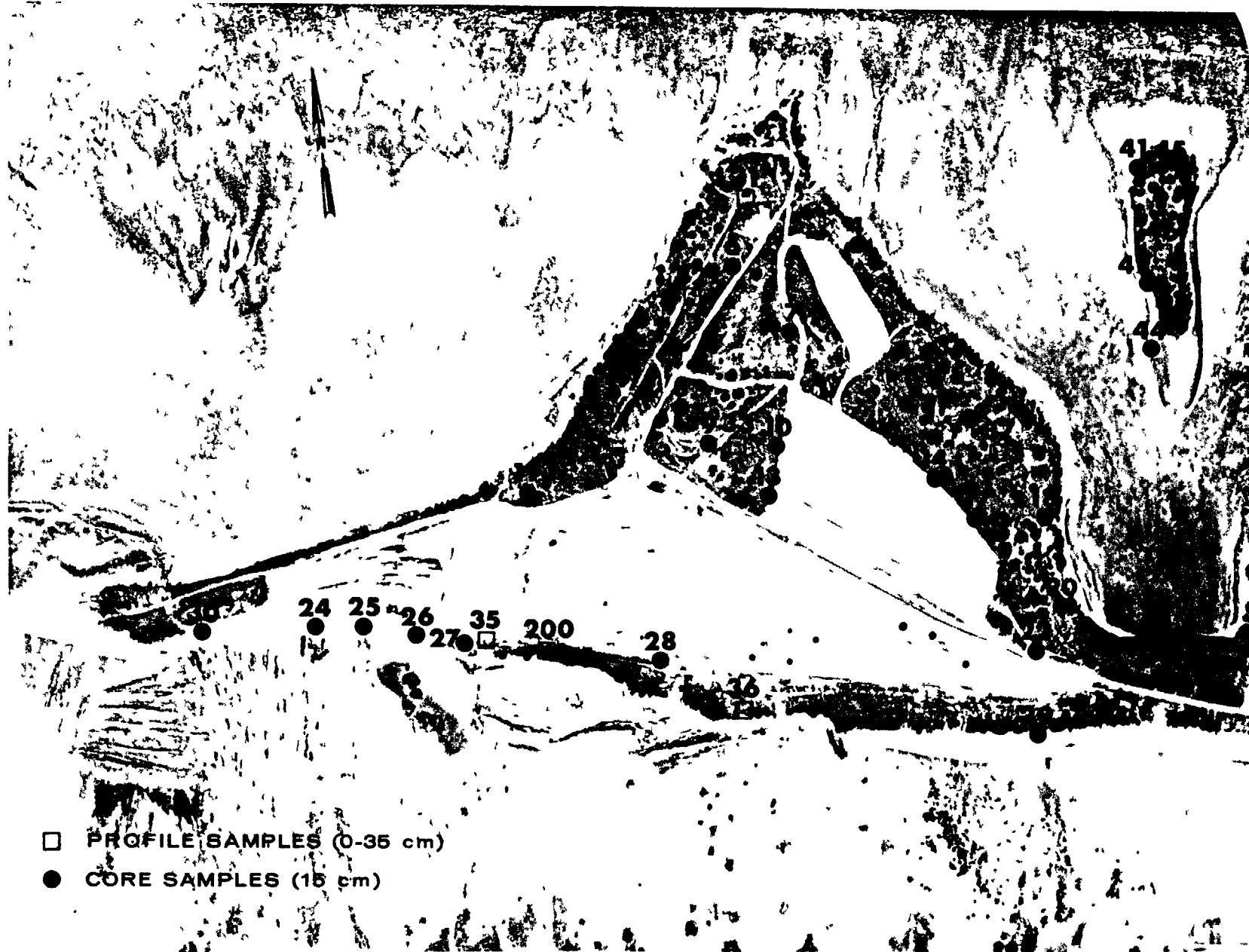


Fig. B.17.1.f. Soil-sample locations.

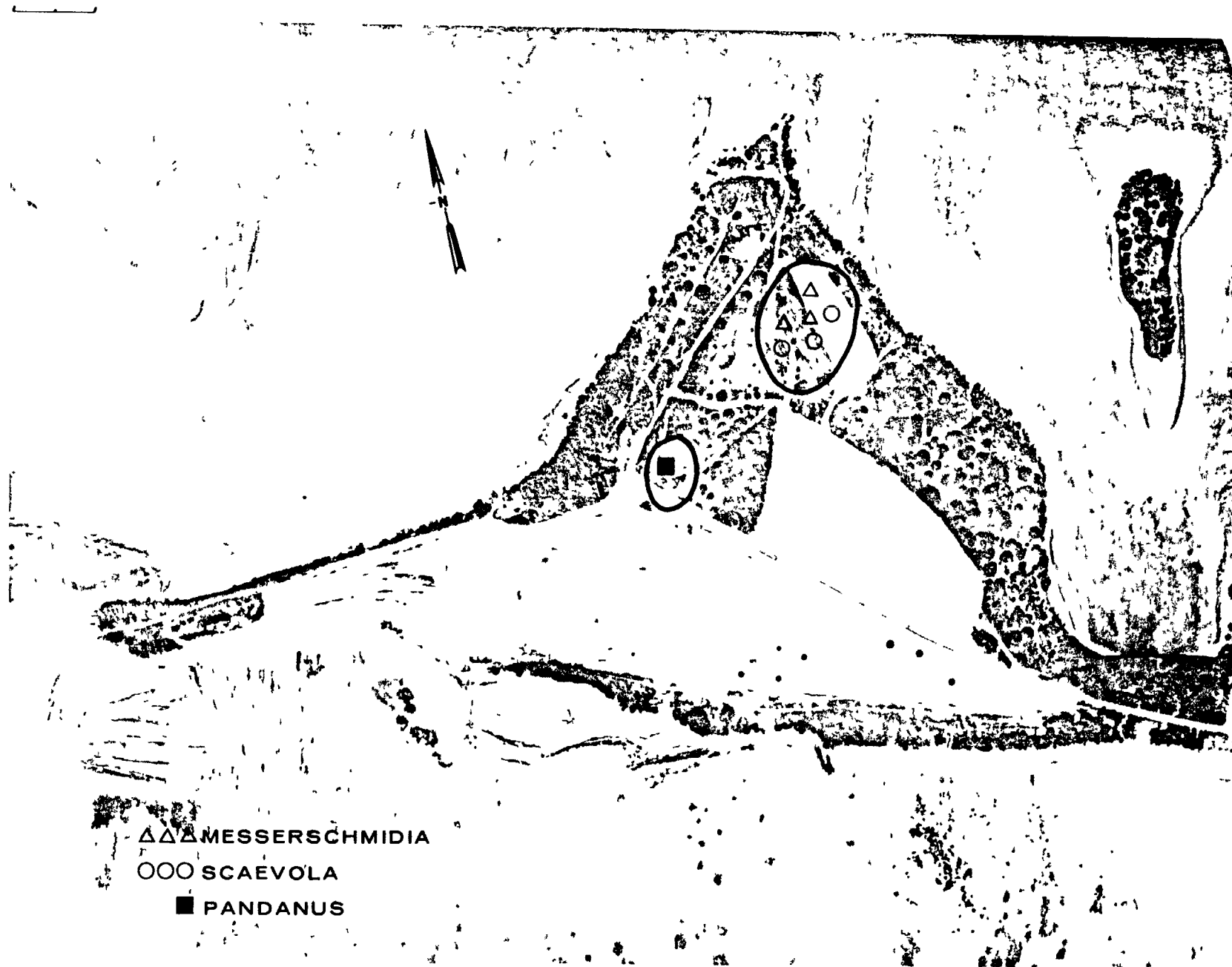


Fig. B.17.1.g. Vegetation sample locations.

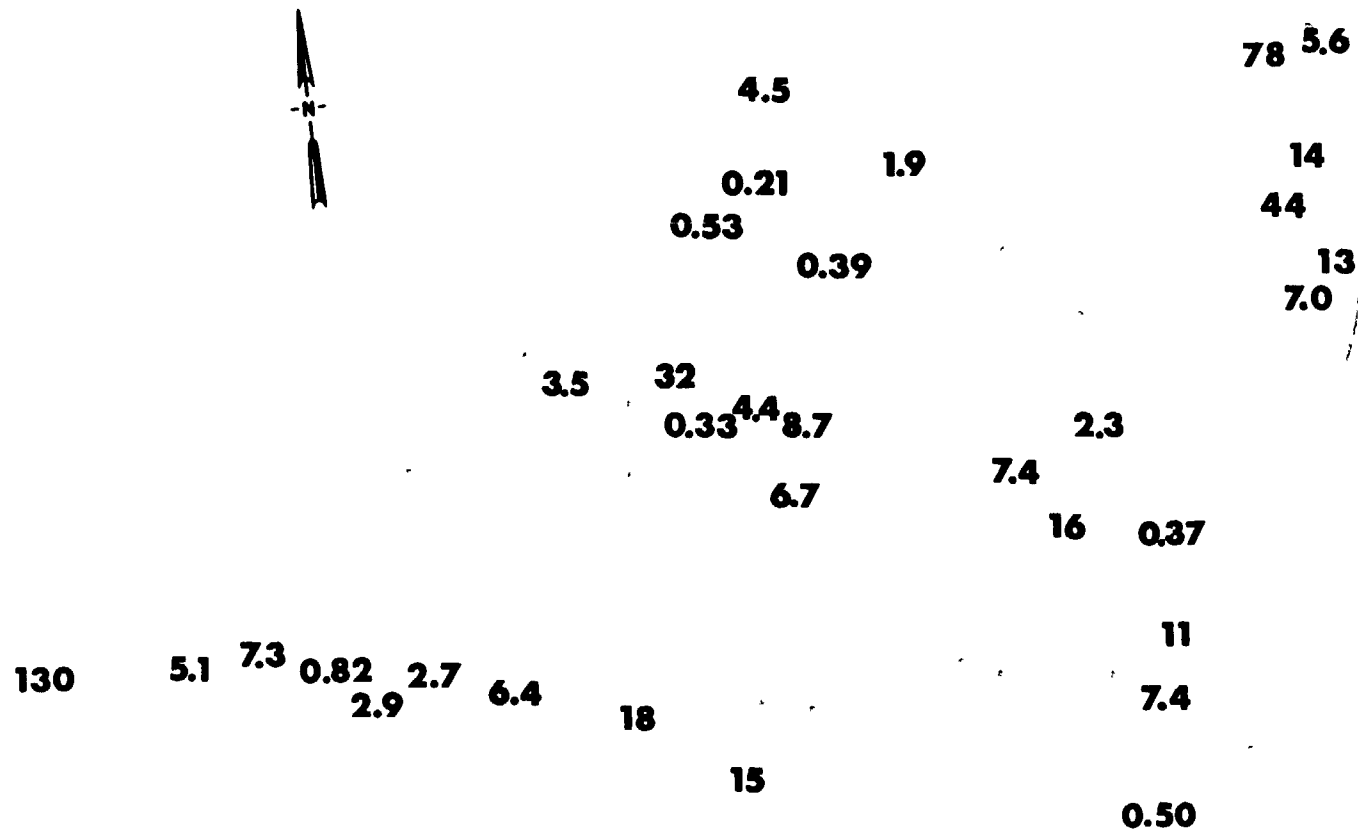


Fig. B.17.1.1. The average  $^{239}\text{Pu}$  activities (pCi/gm) in soil samples collected to a depth of 15 cm.



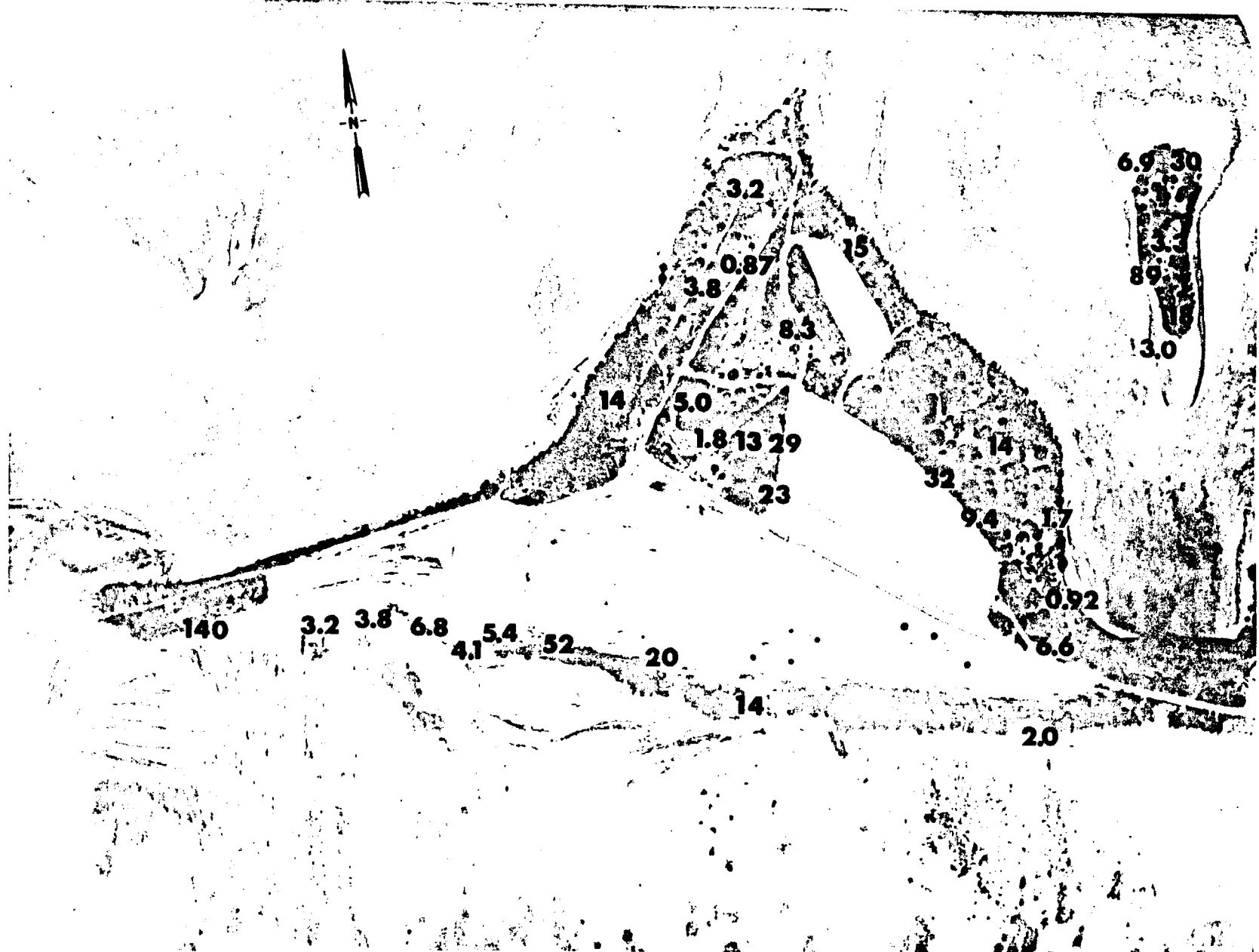


Fig. B.17.1.j. The average <sup>90</sup>Sr activities (pCi/gm) in soil samples collected to a depth of 15 cm.



Fig. B.17.1.k.  $^{137}\text{Cs}$  isoexposure and isoconcentration contours. (Refer to alphabetic symbol key in this appendix.)

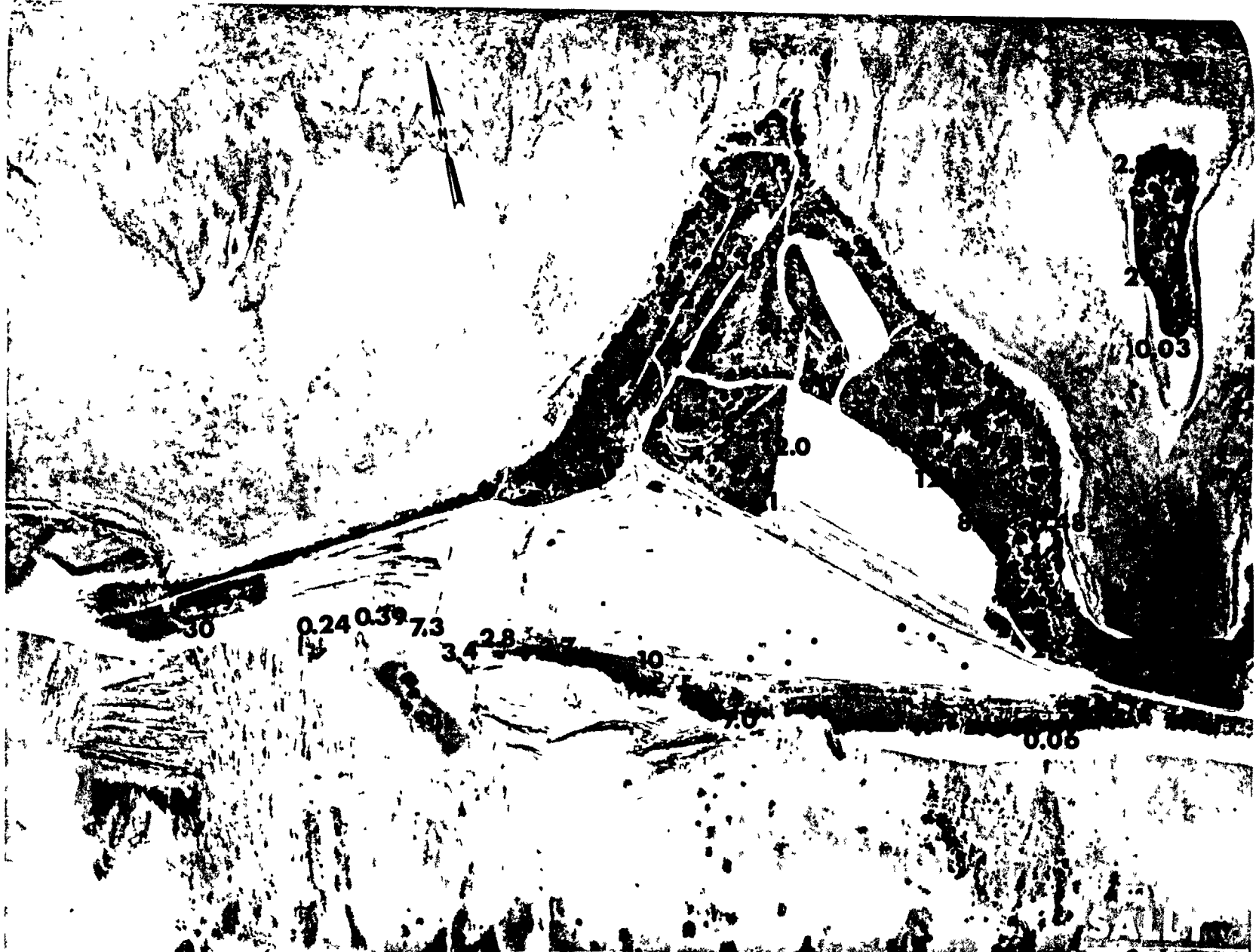


Fig. B.17.1.1. The average <sup>137</sup>Cs activities (pCi/gm) in soil samples collected to a depth of 15 cm.



Fig. B.17.1.m.  $^{60}\text{Co}$  isoexposure and isoconcentration contours. (Refer to alphabetic symbol key in this appendix.)



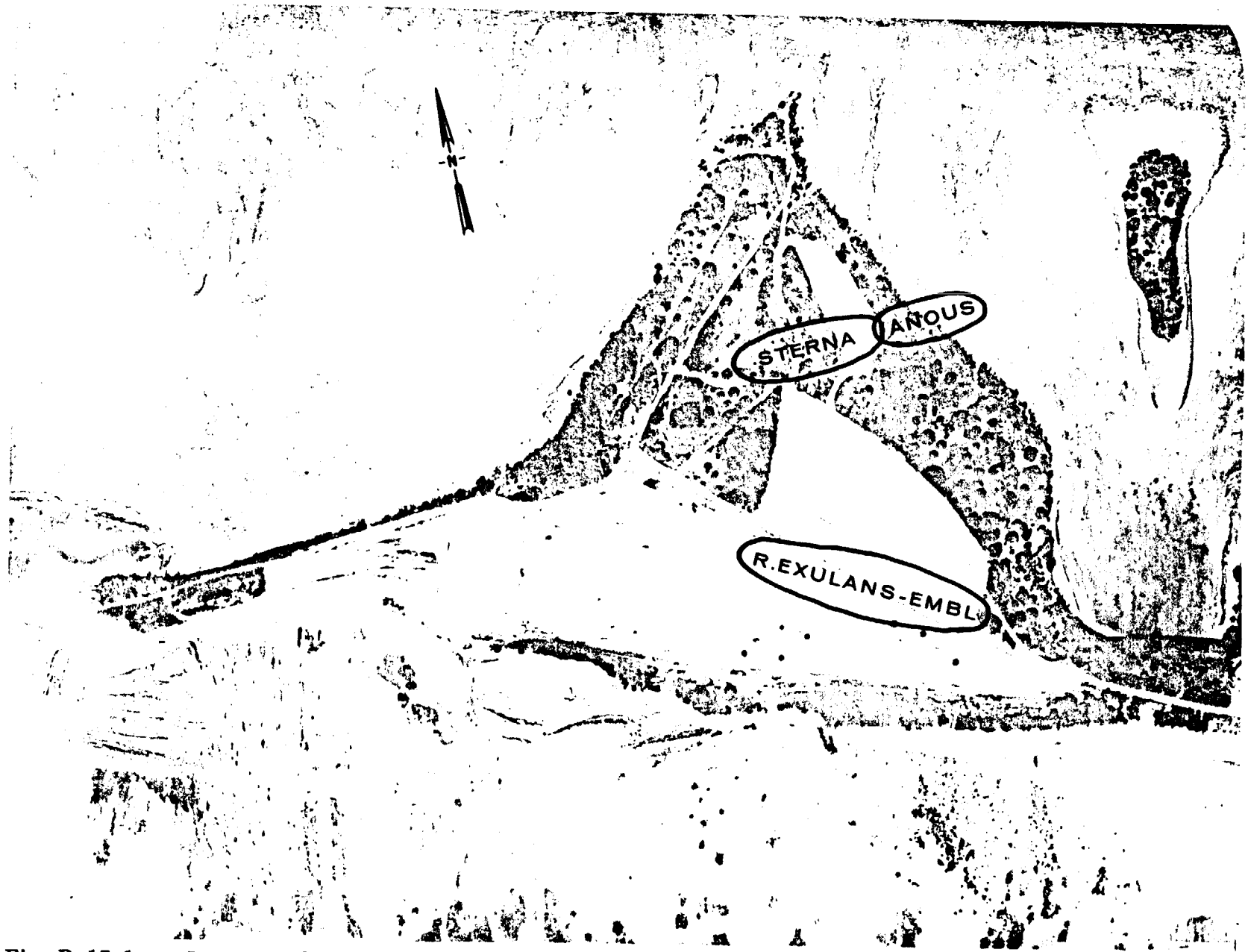


Fig. B.17.1.o. Terrestrial animal sample locations.

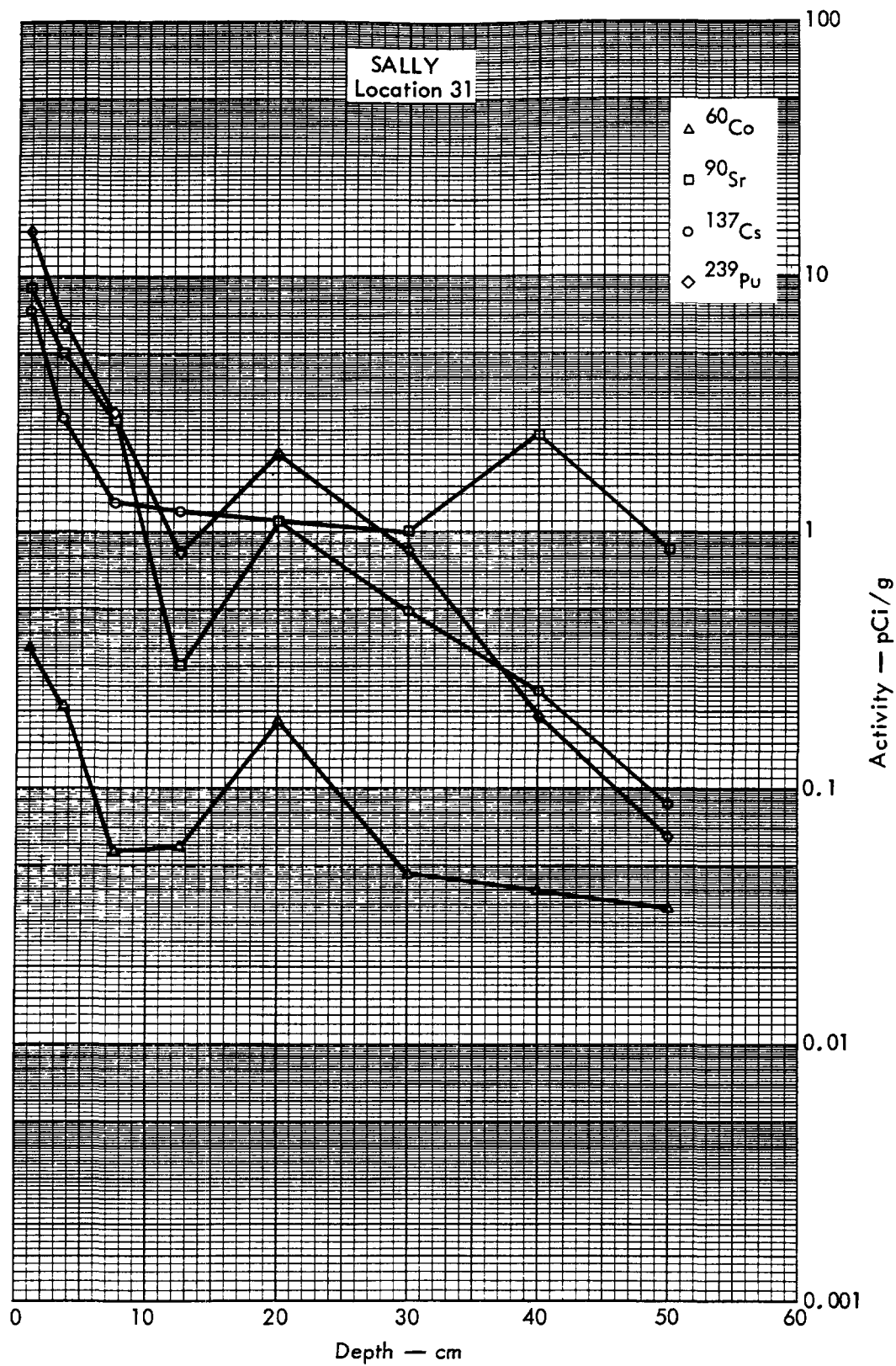


Fig. B.17.2a. Activities of selected radionuclides as a function of soil depth.

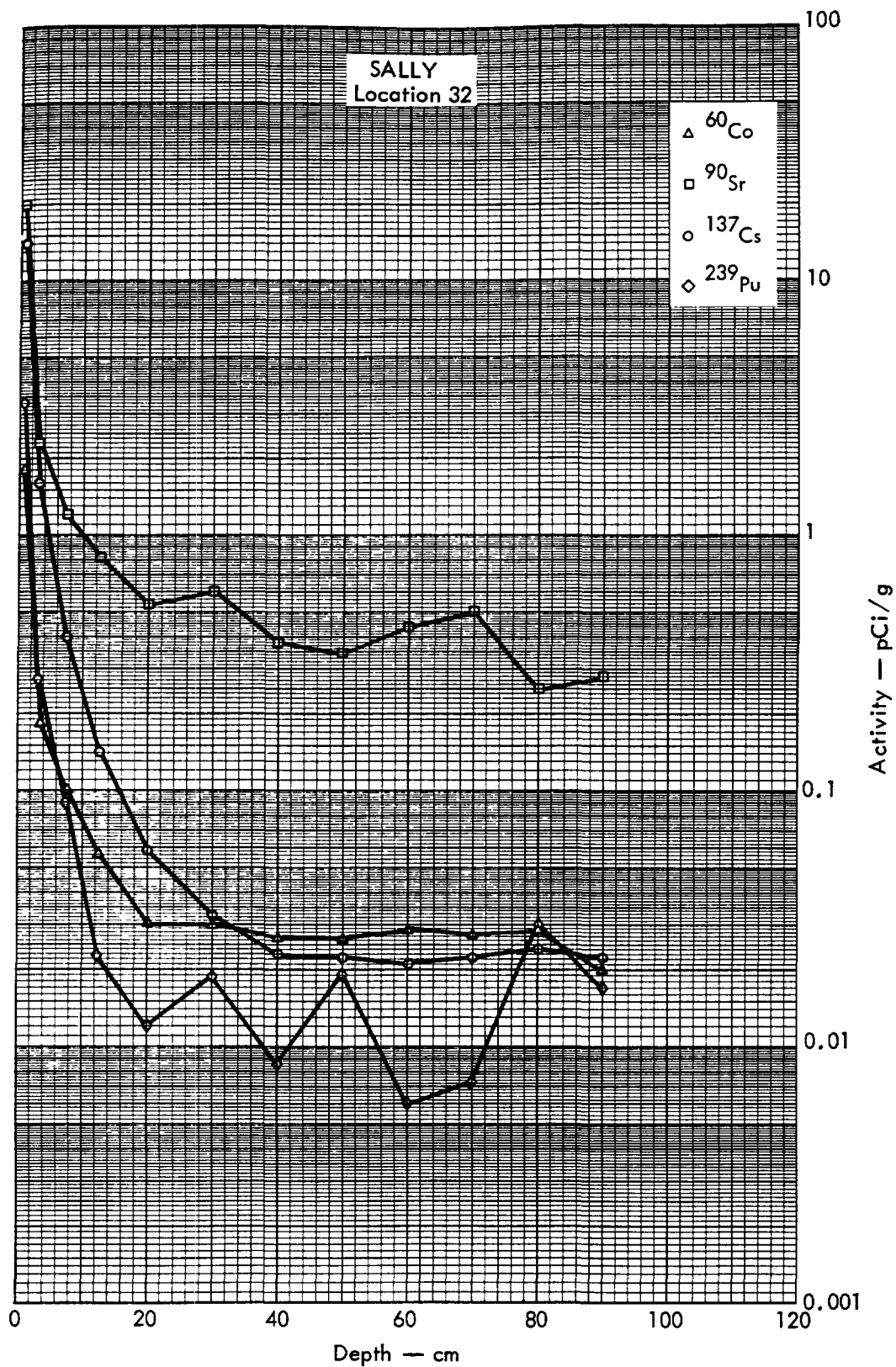


Fig. B.17.2b. Activities of selected radionuclides as a function of soil depth.



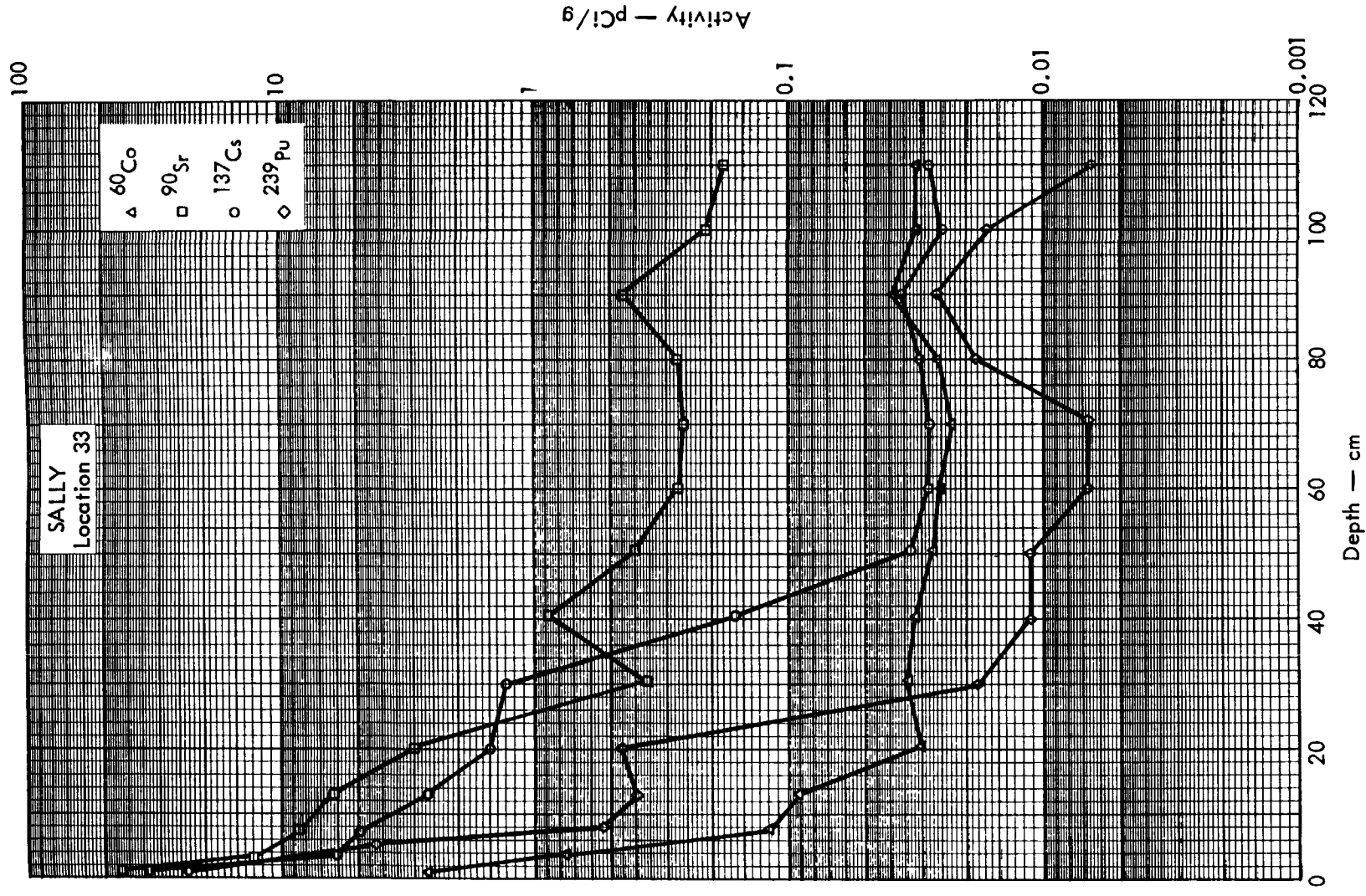


Fig. B. 17.2c. Activities of selected radionuclides as a function of soil depth.

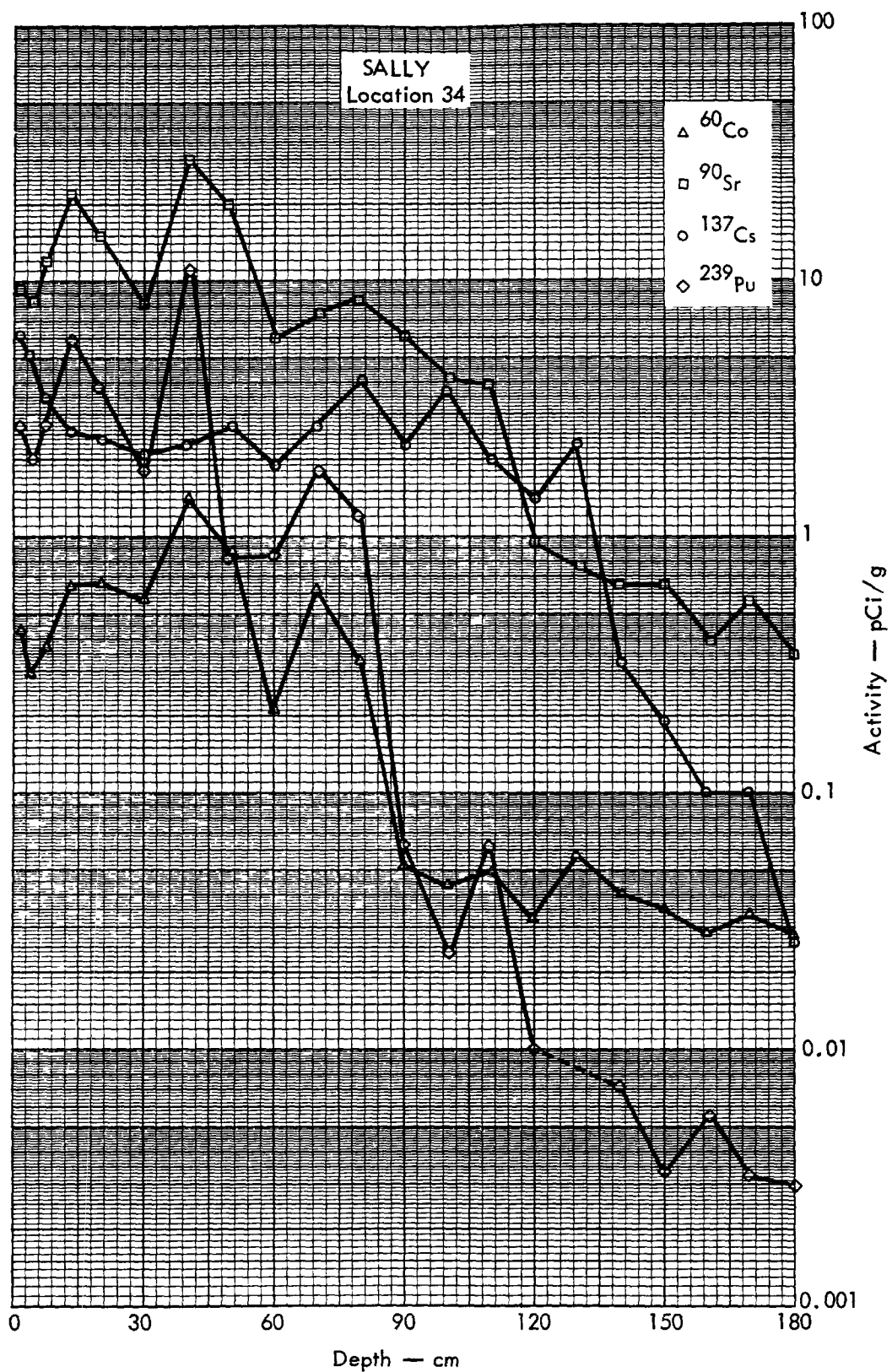


Fig. B.17.2d. Activities of selected radionuclides as a function of soil depth.

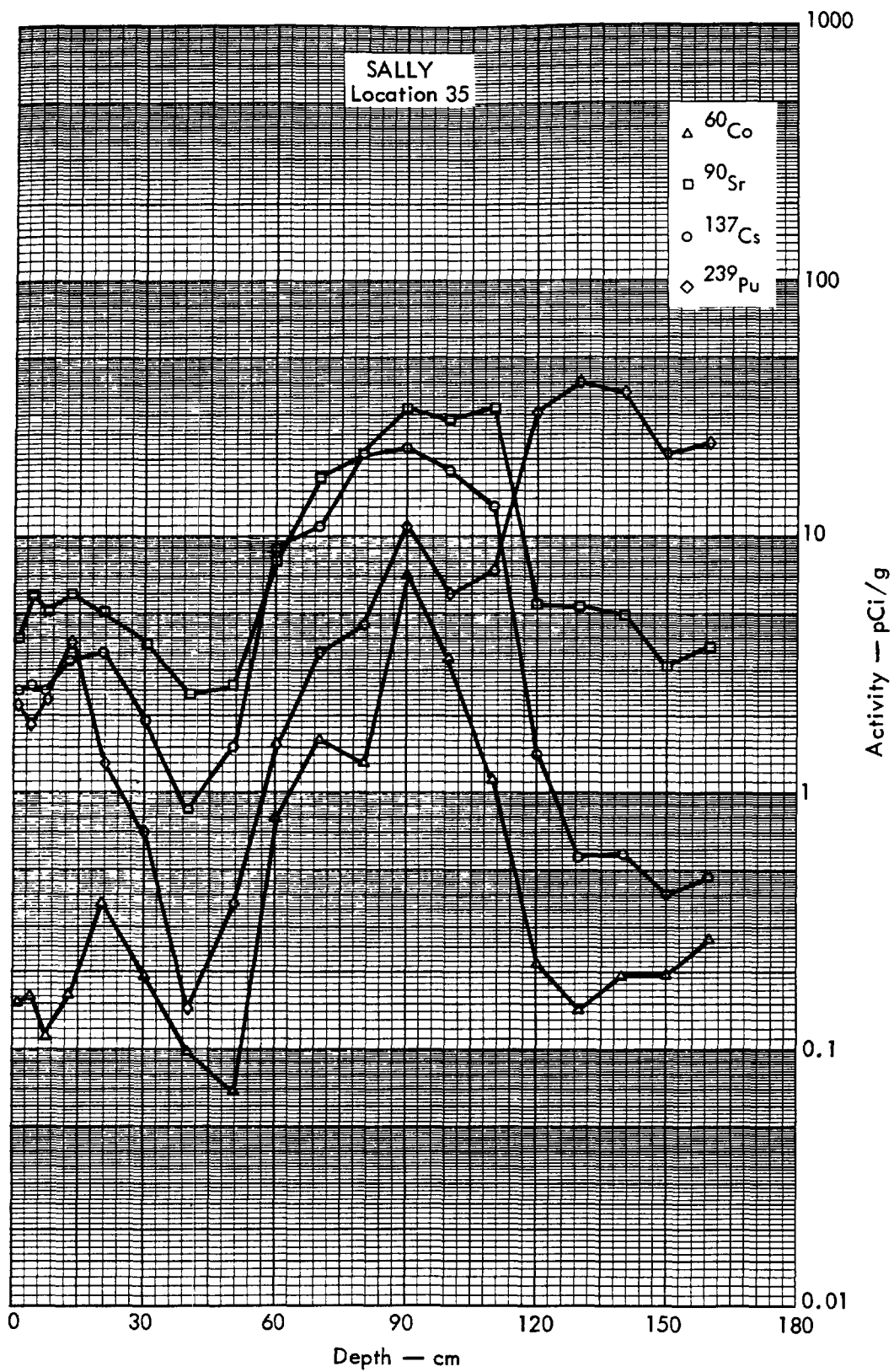


Fig. B.17.2e. Activities of selected radionuclides as a function of soil depth.

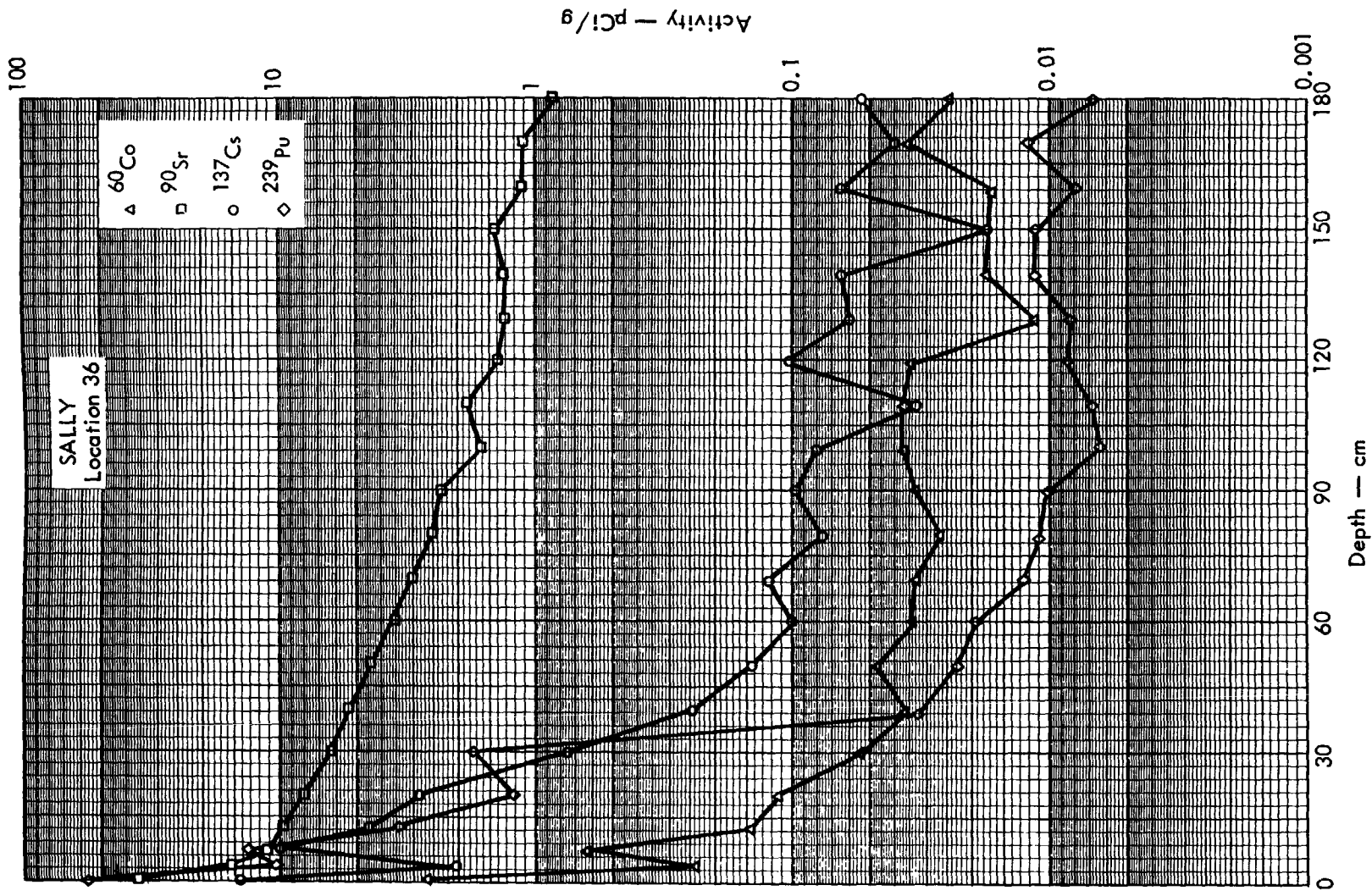


Fig. B. 17.2f. Activities of selected radionuclides as a function of soil depth.

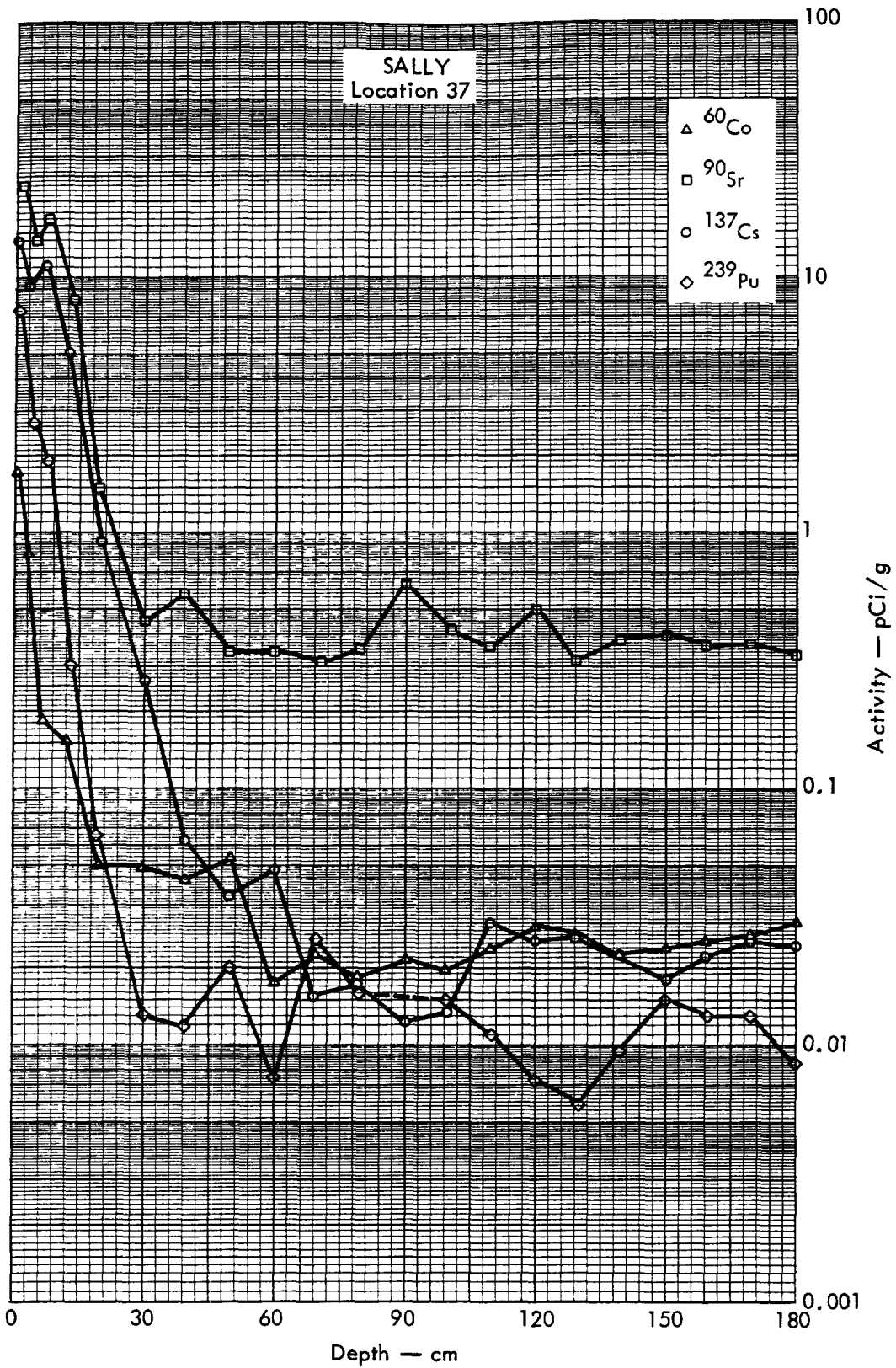


Fig. B.17.2g. Activities of selected radionuclides as a function of soil depth.

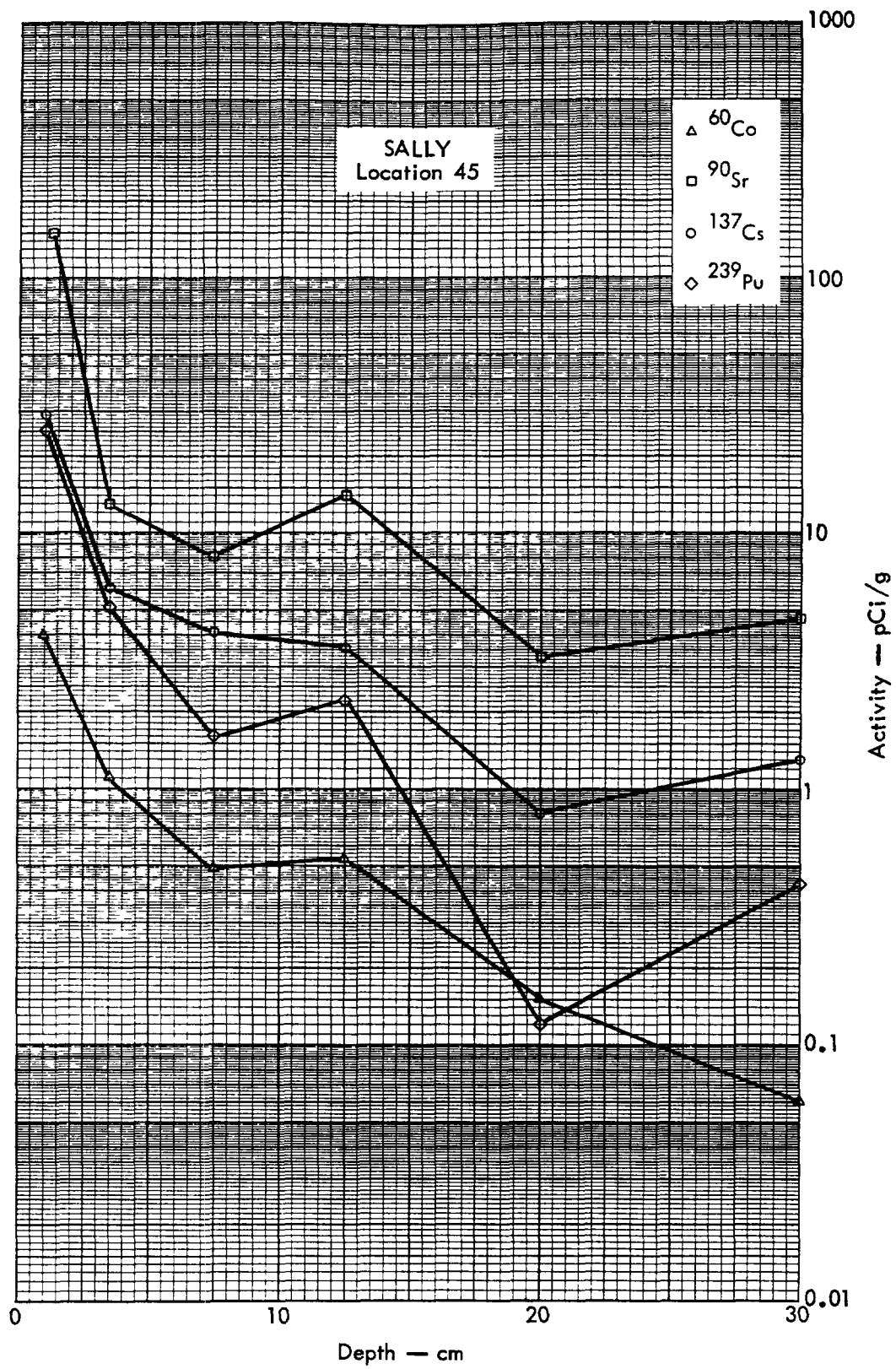


Fig. B. 17.2h. Activities of selected radionuclides as a function of soil depth.

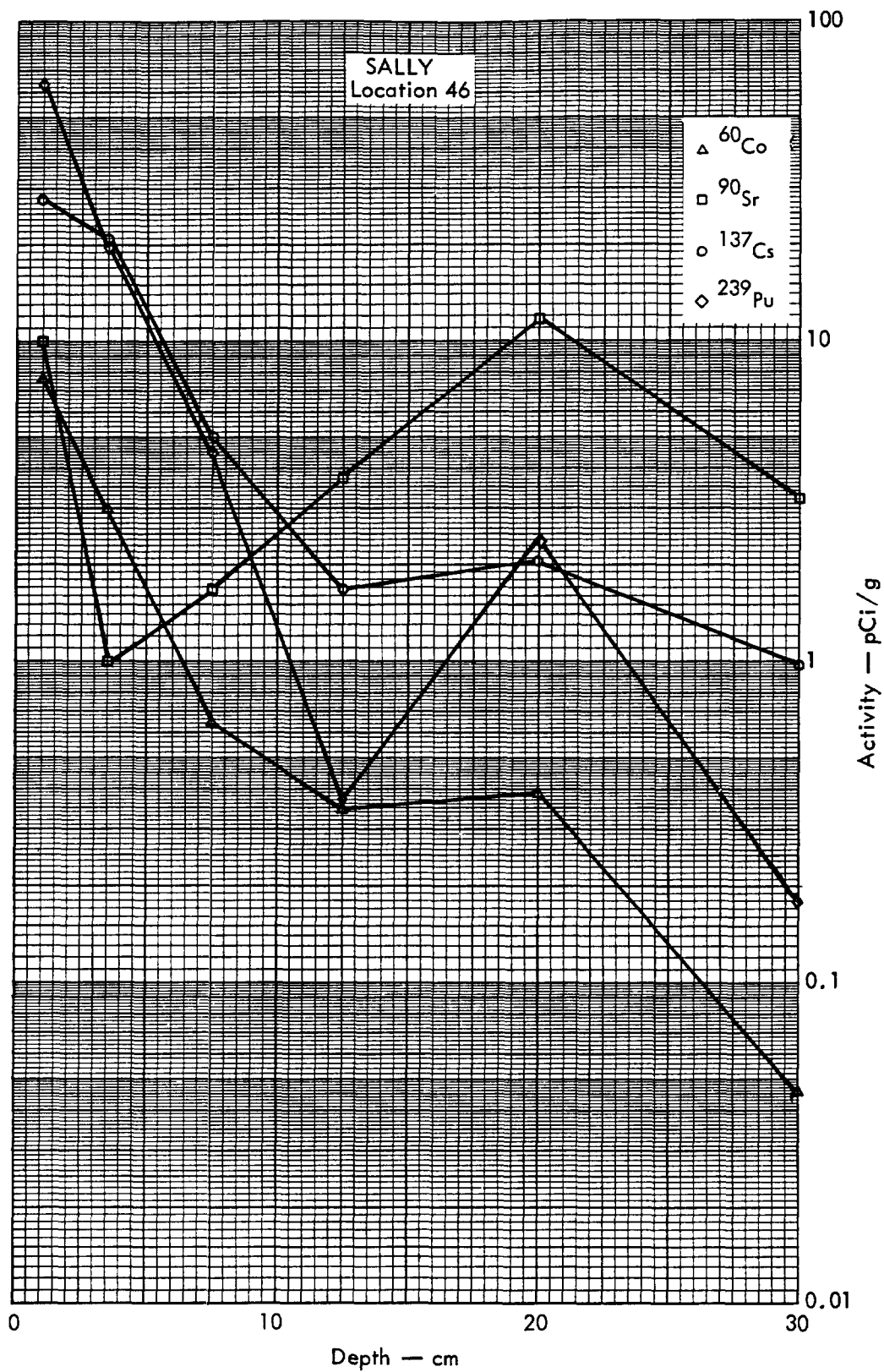


Fig. B. 17. 2i. Activities of selected radionuclides as a function of soil depth.



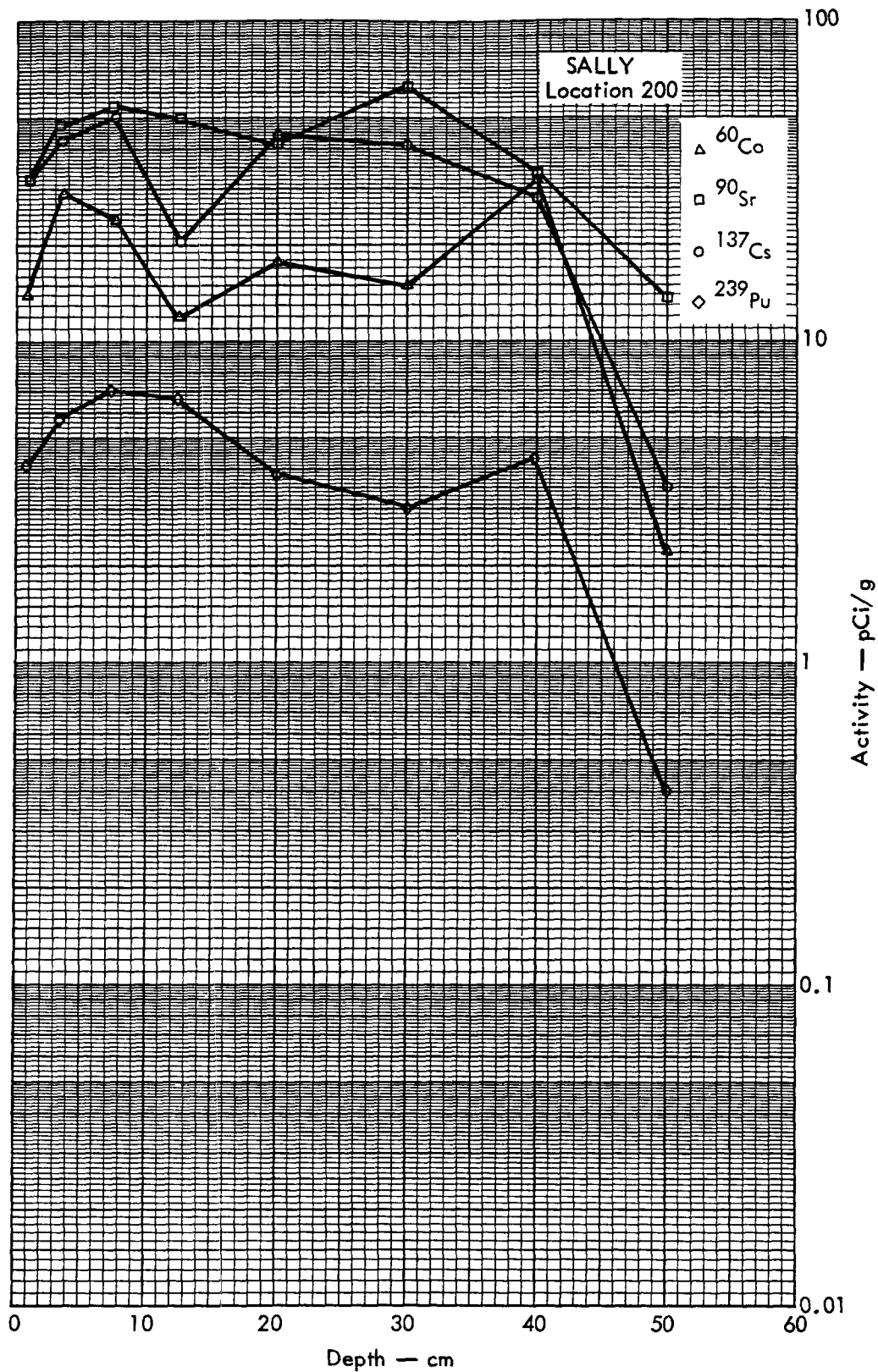


Fig. B. 17.2j. Activities of selected radionuclides as a function of soil depth.





Fig. B.18.1.a.



Fig. B.18.1.b. Gross count isoexposure contours. (Refer to alphabetic symbol key in this appendix.)

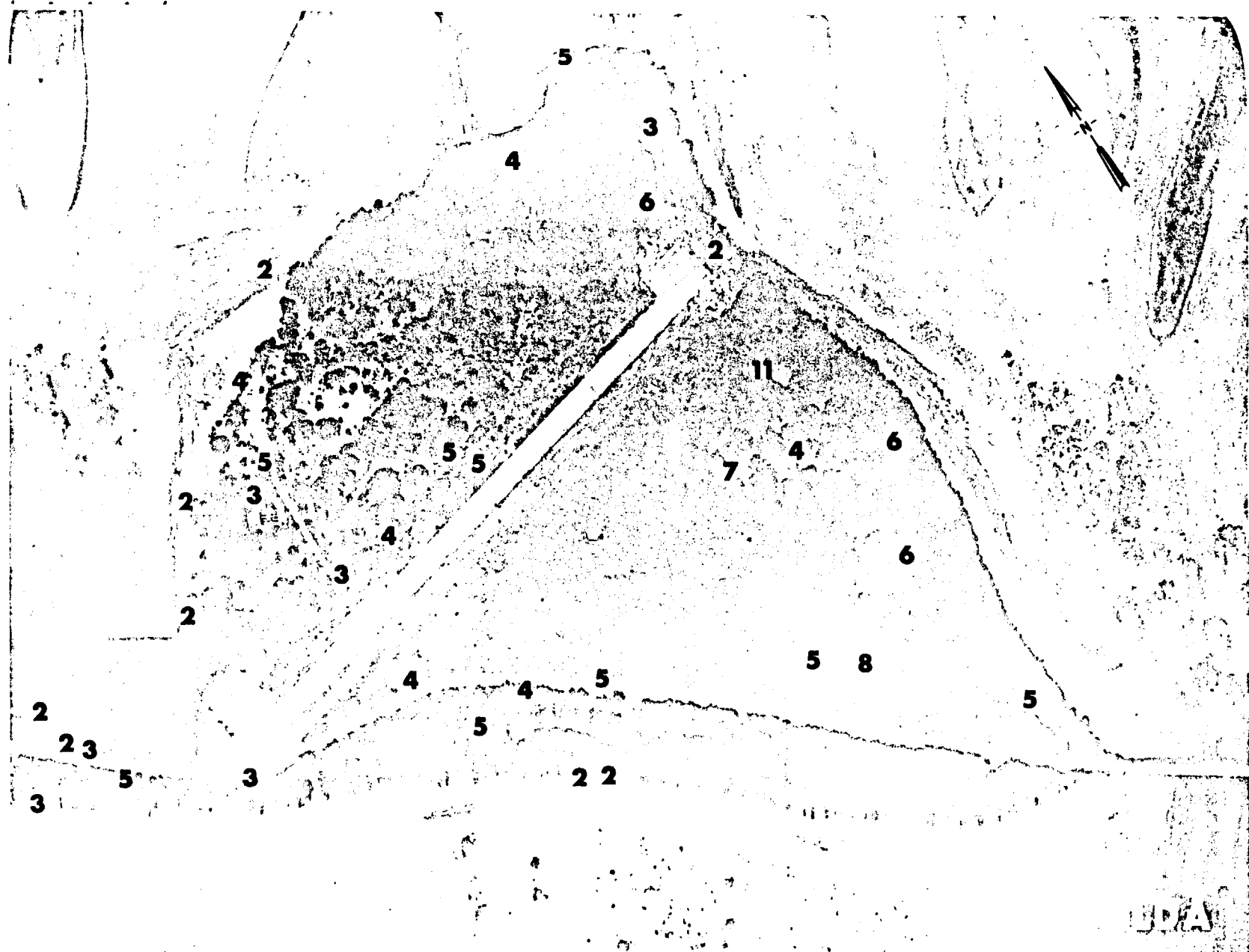


Fig. B.18.1.d. The gamma background exposure rate ( $\mu\text{R/hr}$ ) at 1 m above the ground, measured with a portable NaI scintillation counter.

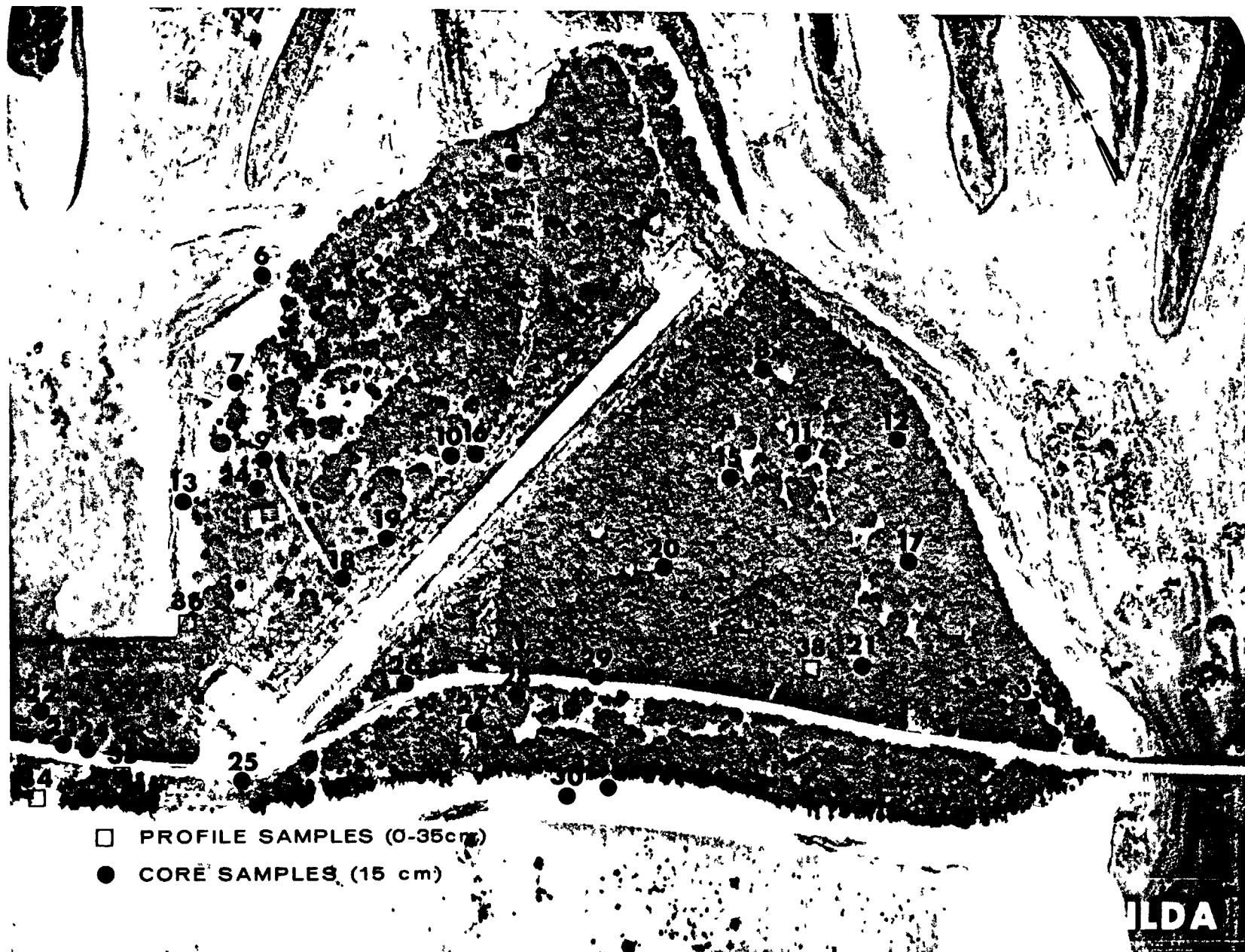


Fig. B.18.1.f. Soil-sample locations.

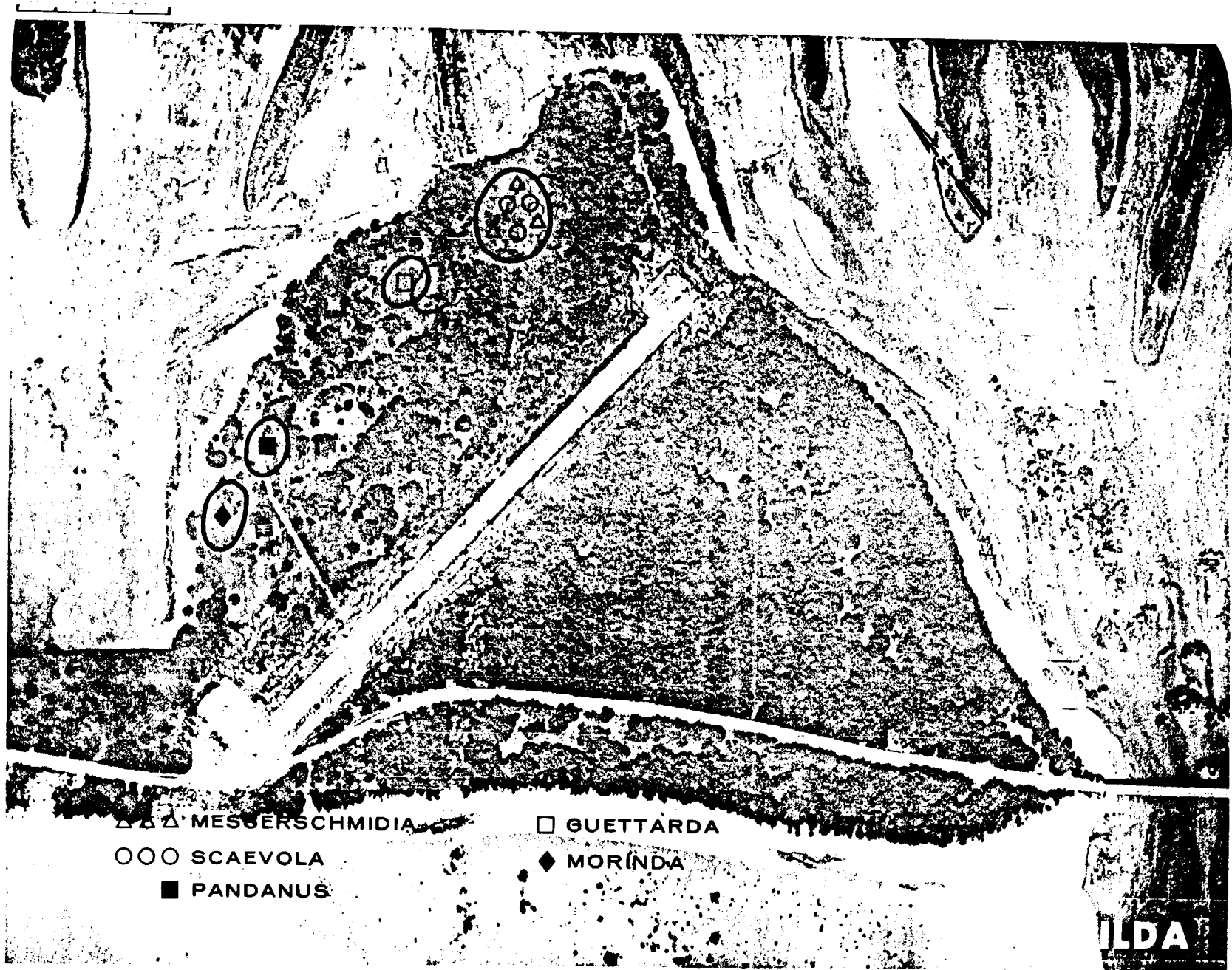


Fig. B.18.1.g. Vegetation sample locations.

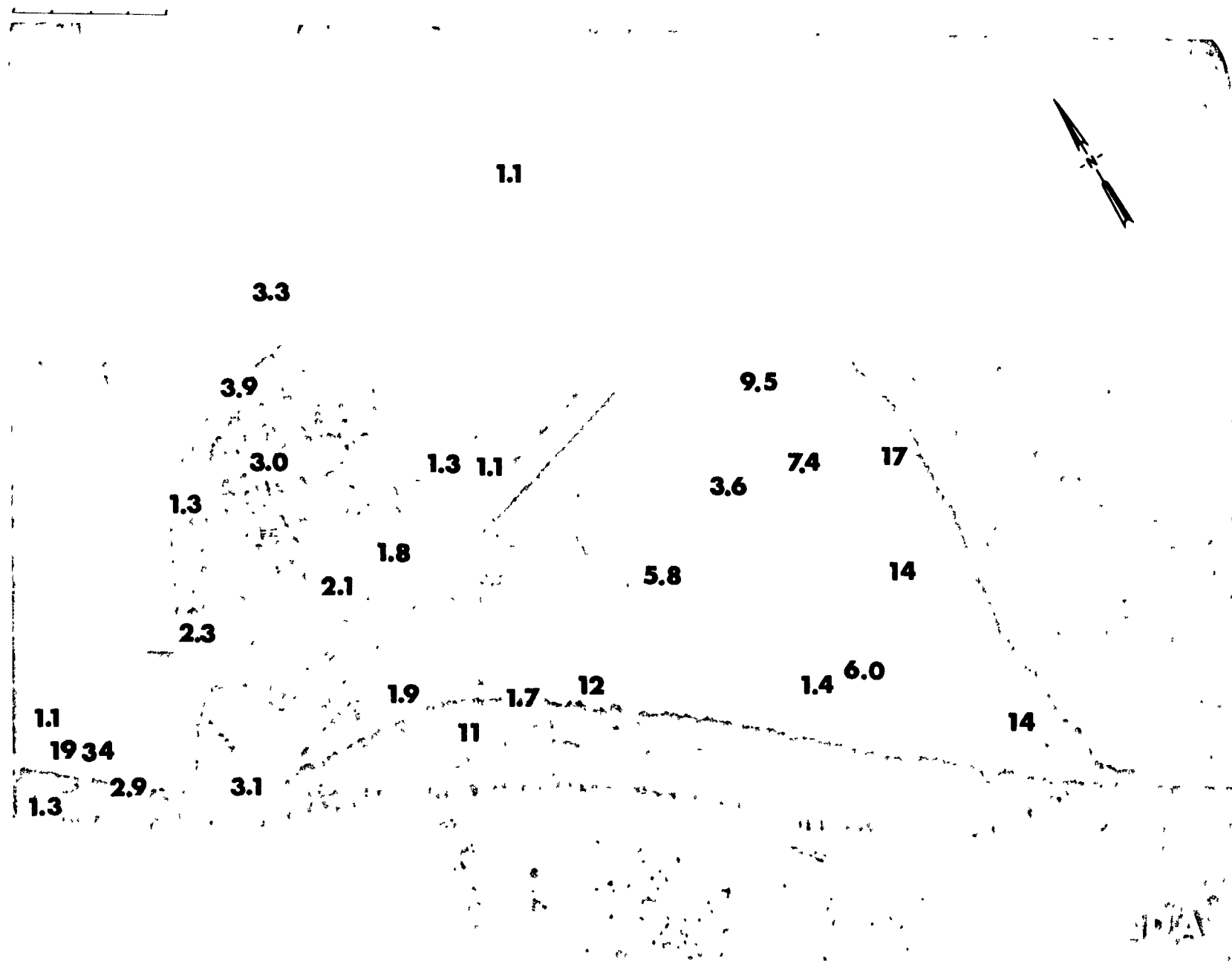


Fig. B.18.1.i. The average  $^{239}\text{Pu}$  activities (pCi/gm) in soil samples collected to a depth of 15 cm.

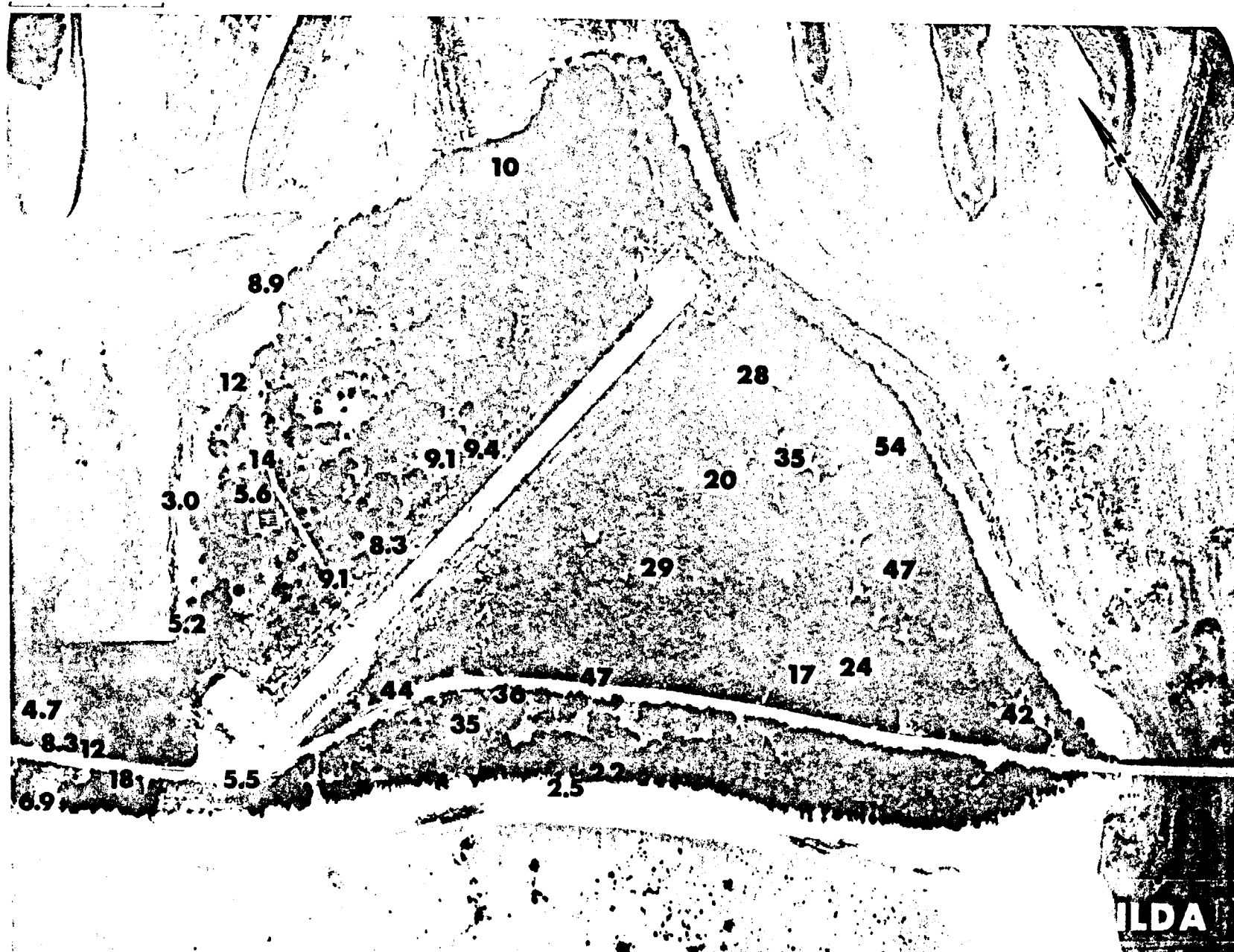


Fig. B.18.1.j. The average  $^{90}\text{Sr}$  activities (pCi/gm) in soil samples collected to a depth of 15 cm.

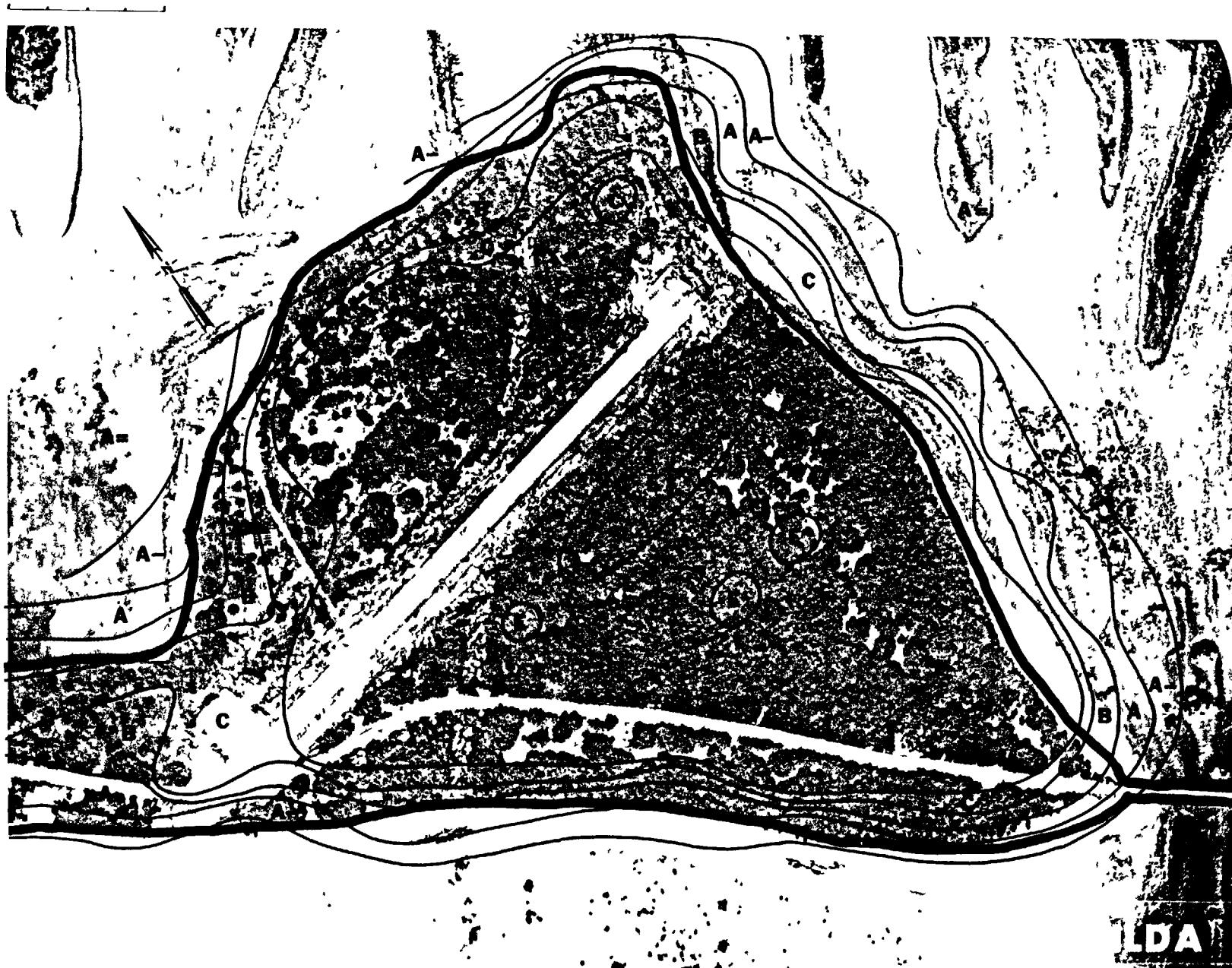


Fig. B.18.1.k.  $^{137}\text{Cs}$  isoexposure and isoconcentration contours. (Refer to alphabetic symbol key in this appendix.)



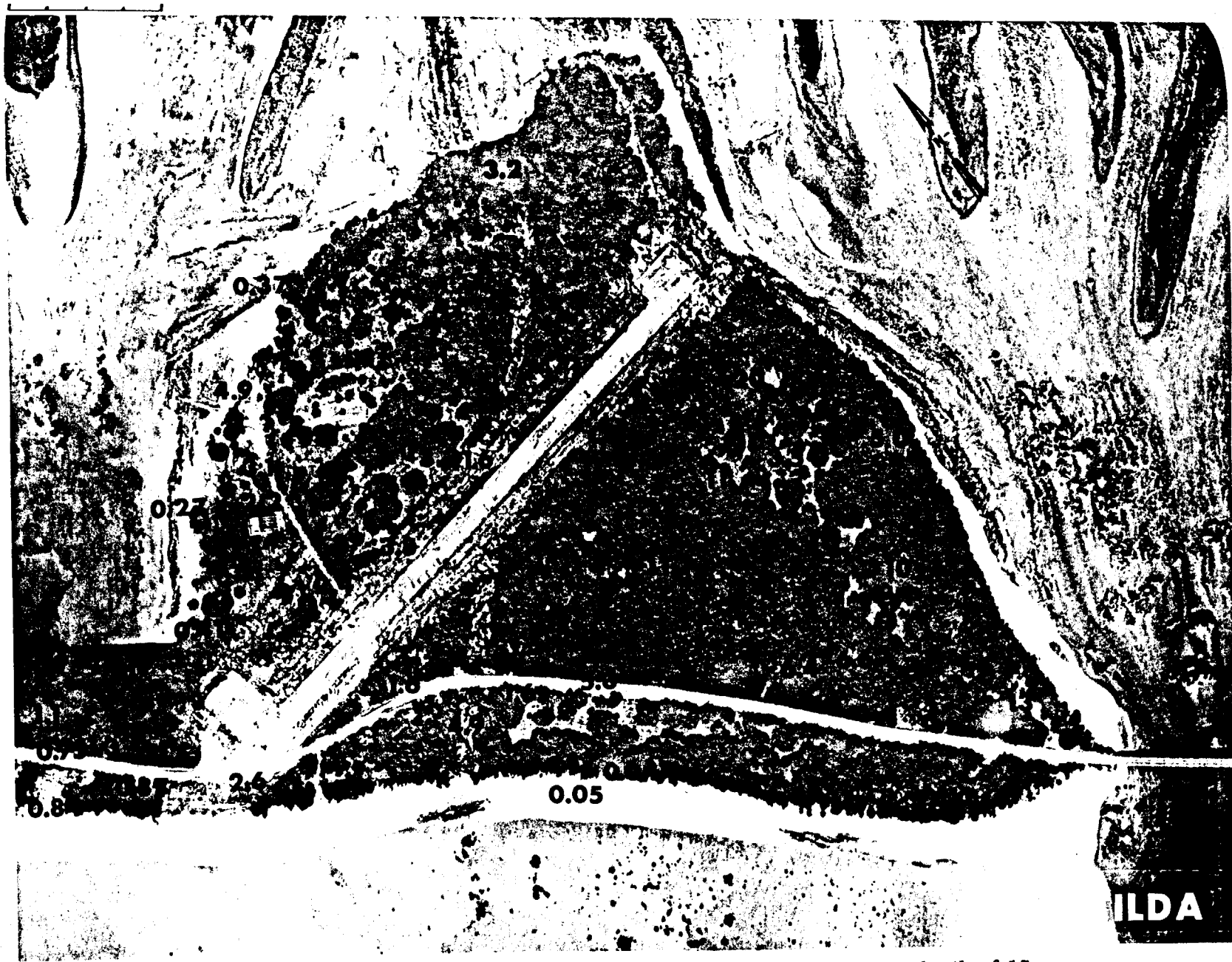


Fig. B.18.1.1. The average <sup>137</sup>Cs activities (pCi/gm) in soil samples collected to a depth of 15 cm.

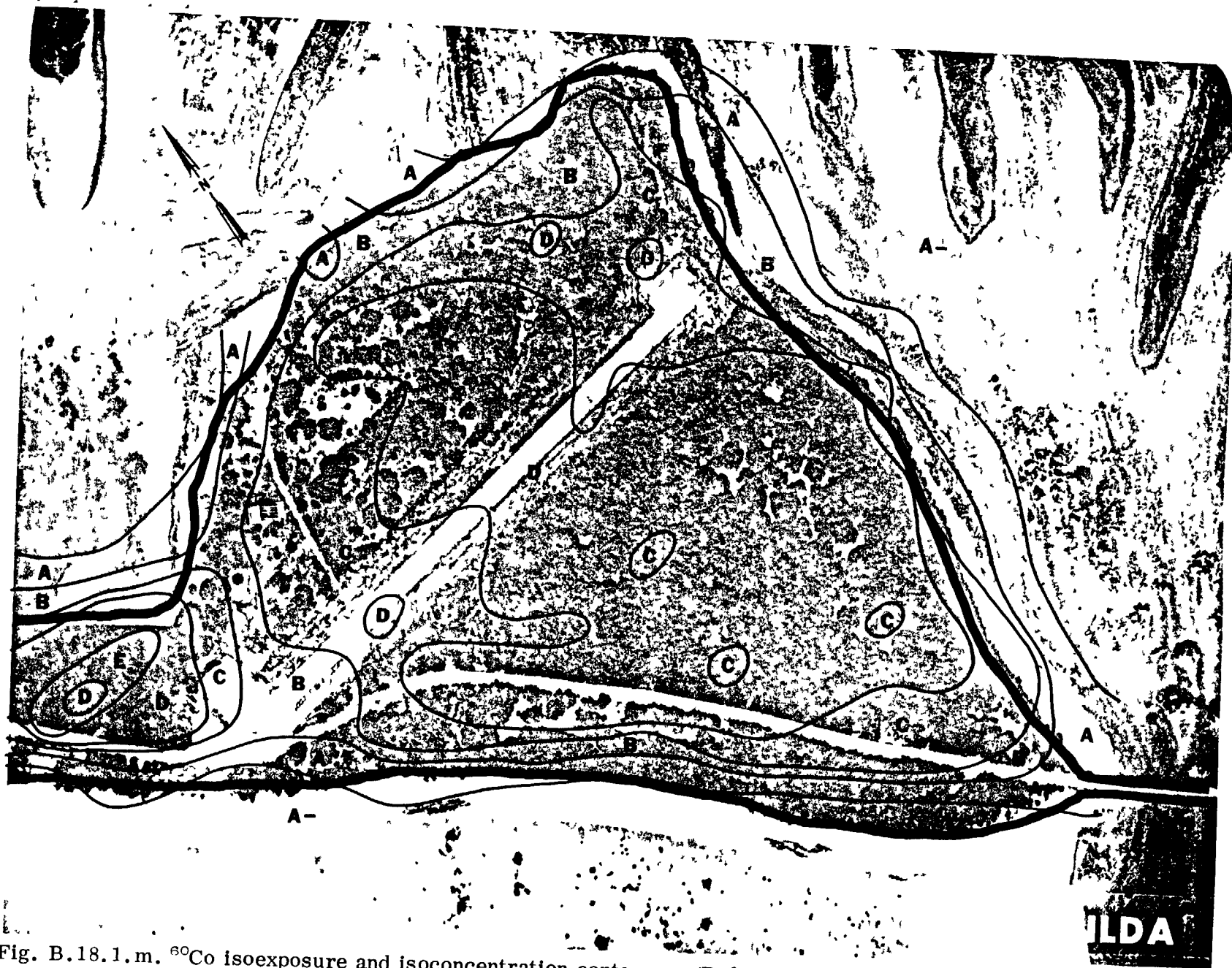


Fig. B.18.1.m. <sup>60</sup>Co isosexposure and isoconcentration contours. (Refer to alphabetic symbol key in this appendix.)

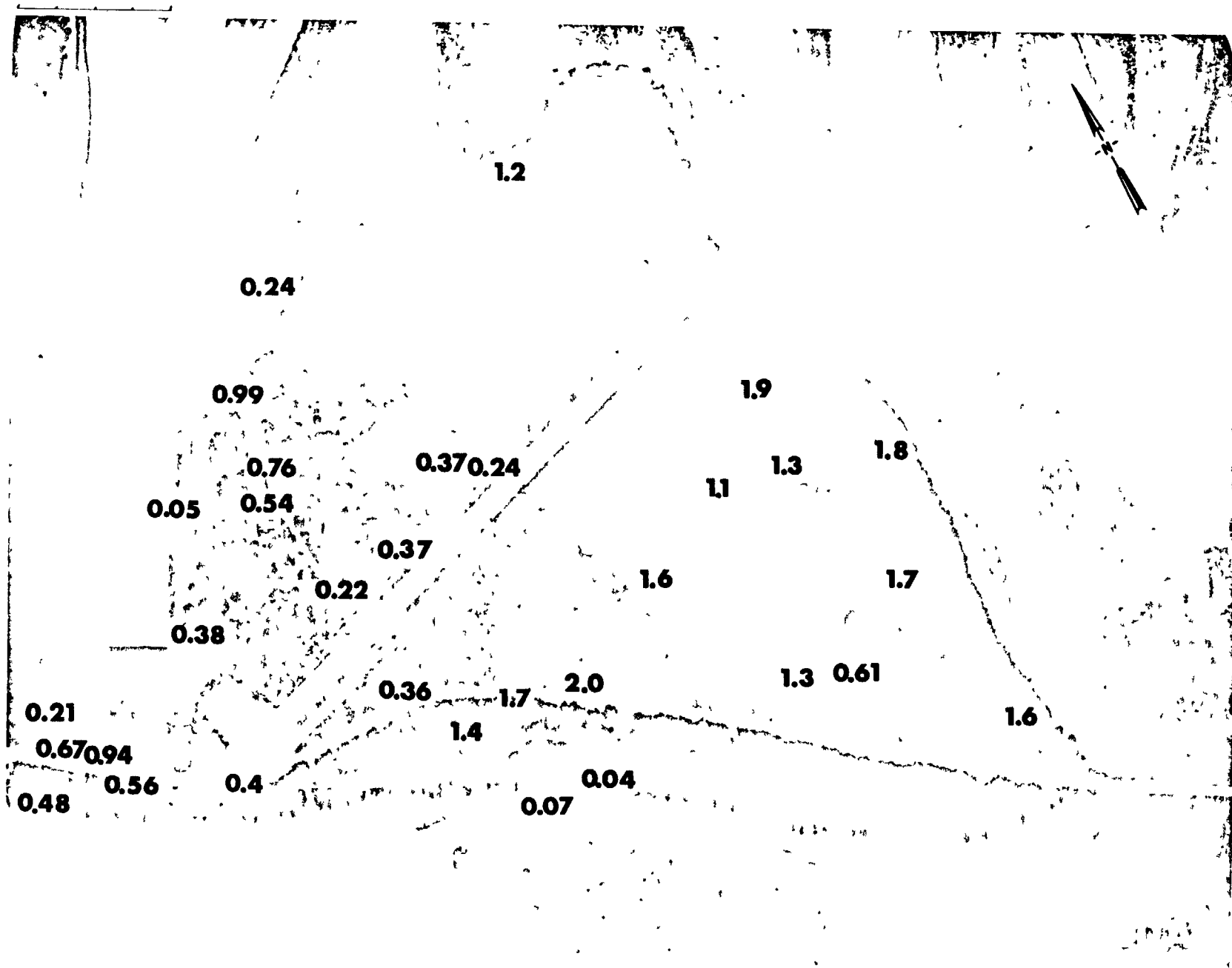


Fig. B.18.1.n. The average  $^{60}\text{Co}$  activities (pCi/gm) in soil samples collected to a depth of 15 cm.

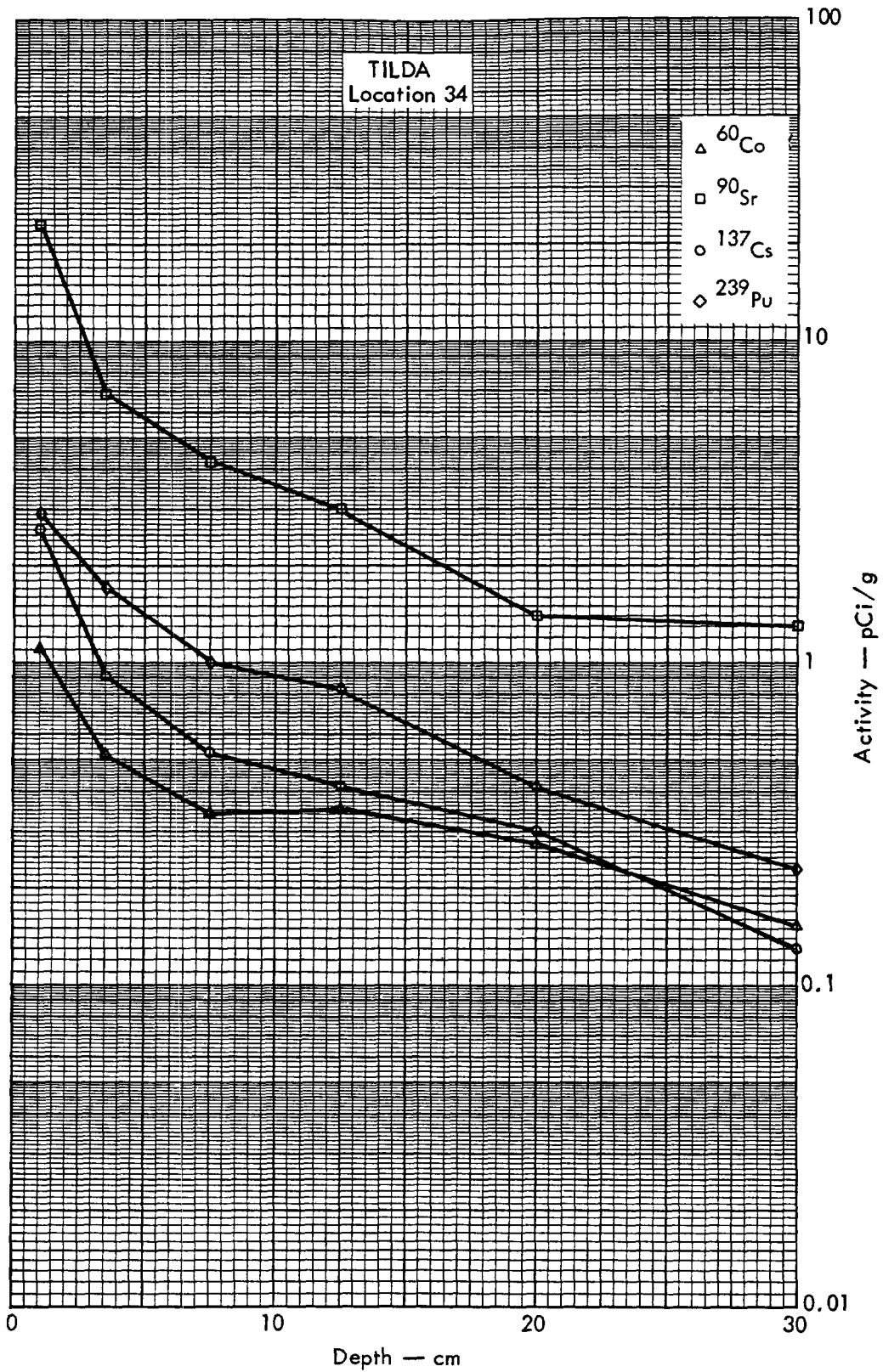


Fig. B. 18. 2a. Activities of selected radionuclides as a function of soil depth.

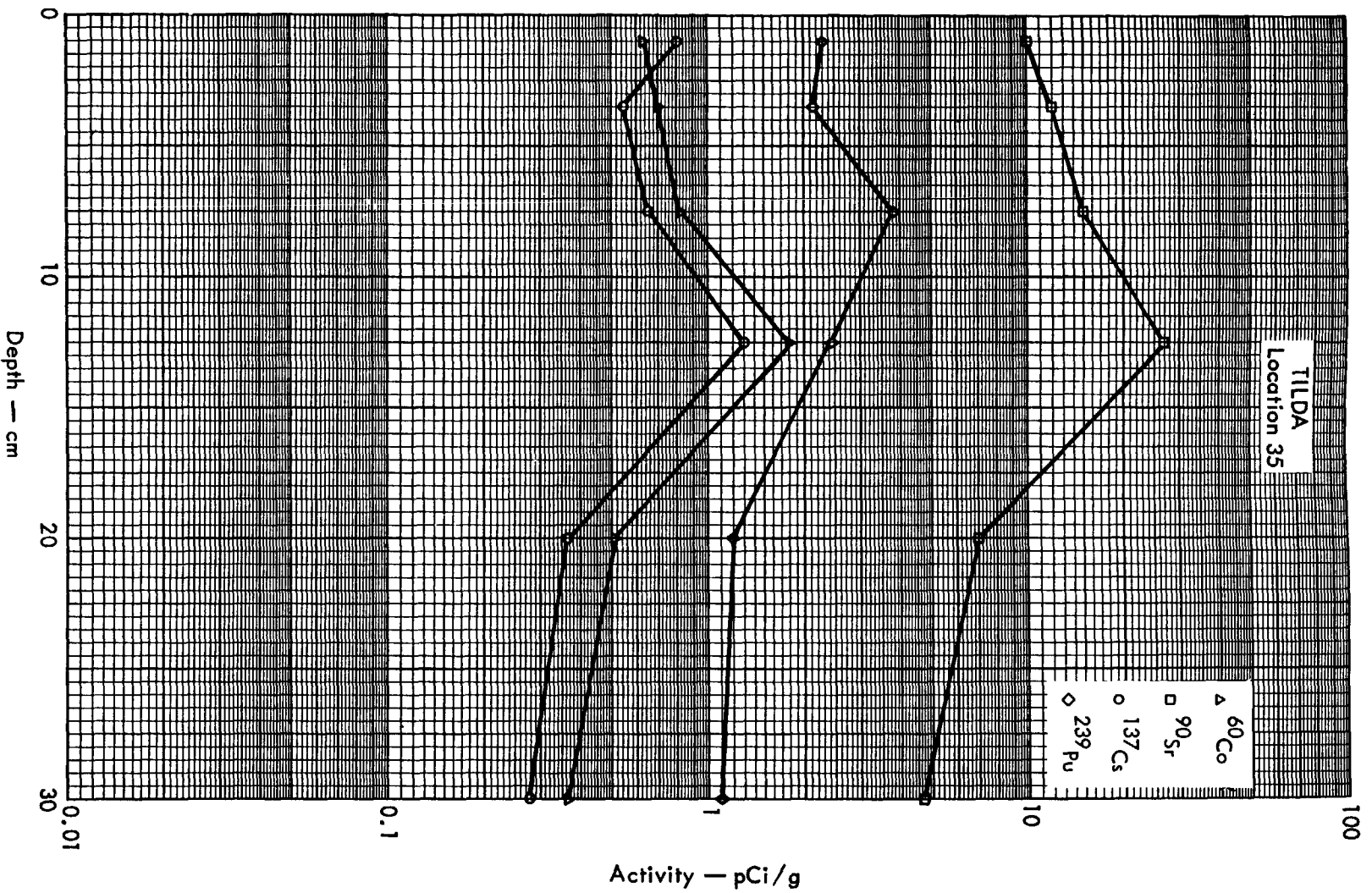


Fig. B.18. 2b. Activities of selected radionuclides as a function of soil depth.

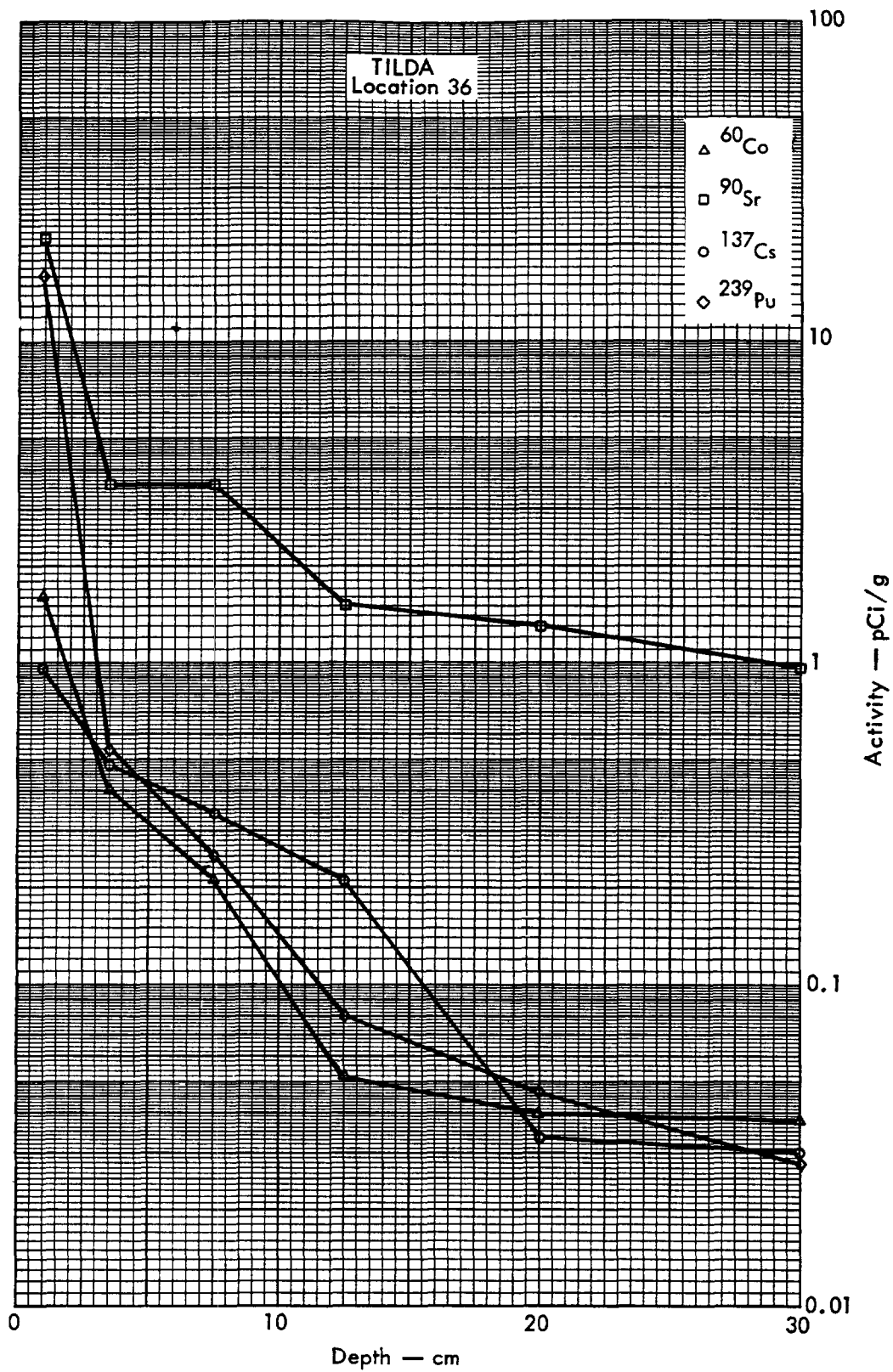


Fig. B.18.2c. Activities of selected radionuclides as a function of soil depth.

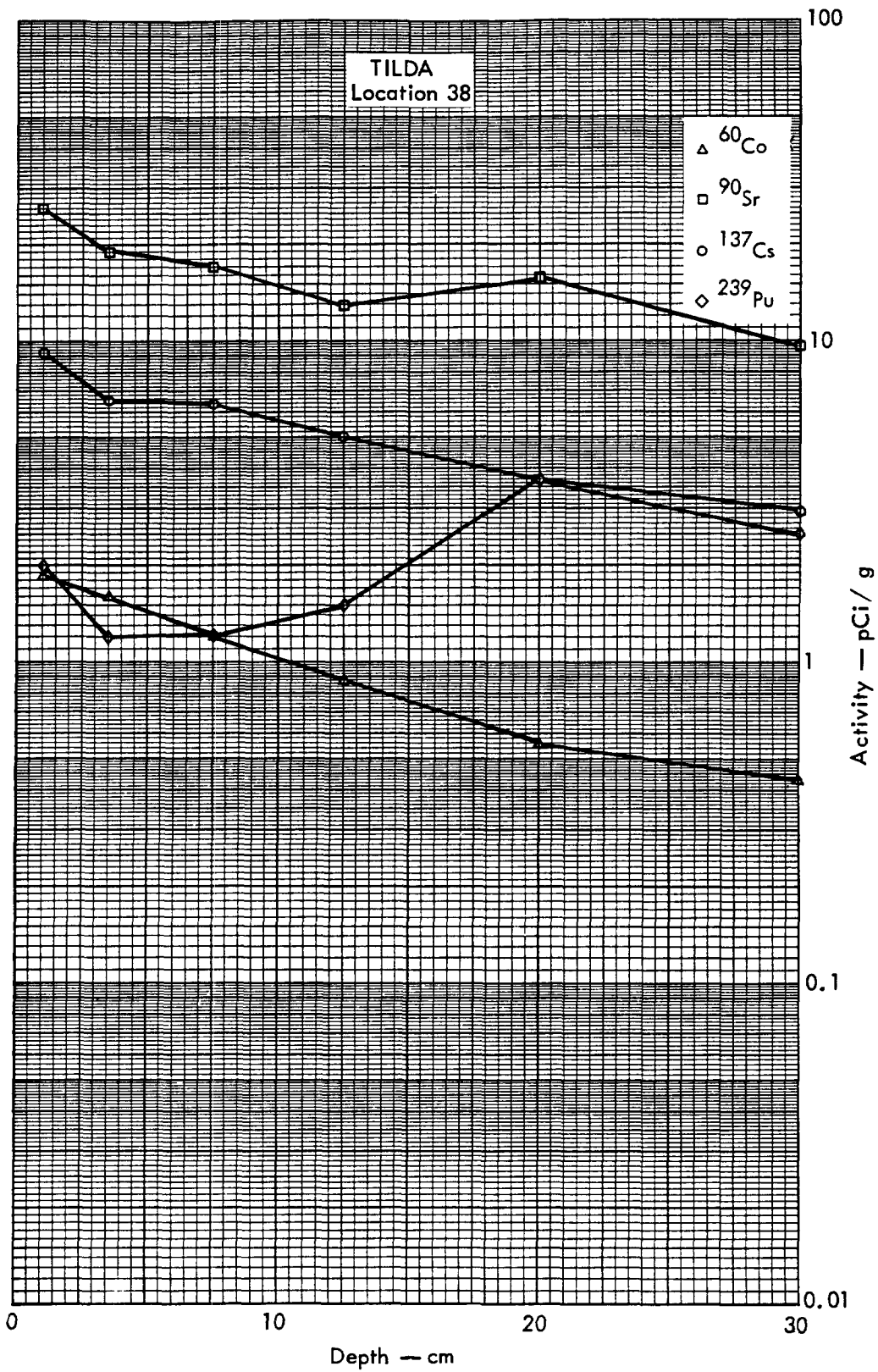


Fig. B. 18. 2d. Activities of selected radionuclides as a function of soil depth.



Fig. B.19.1.a.



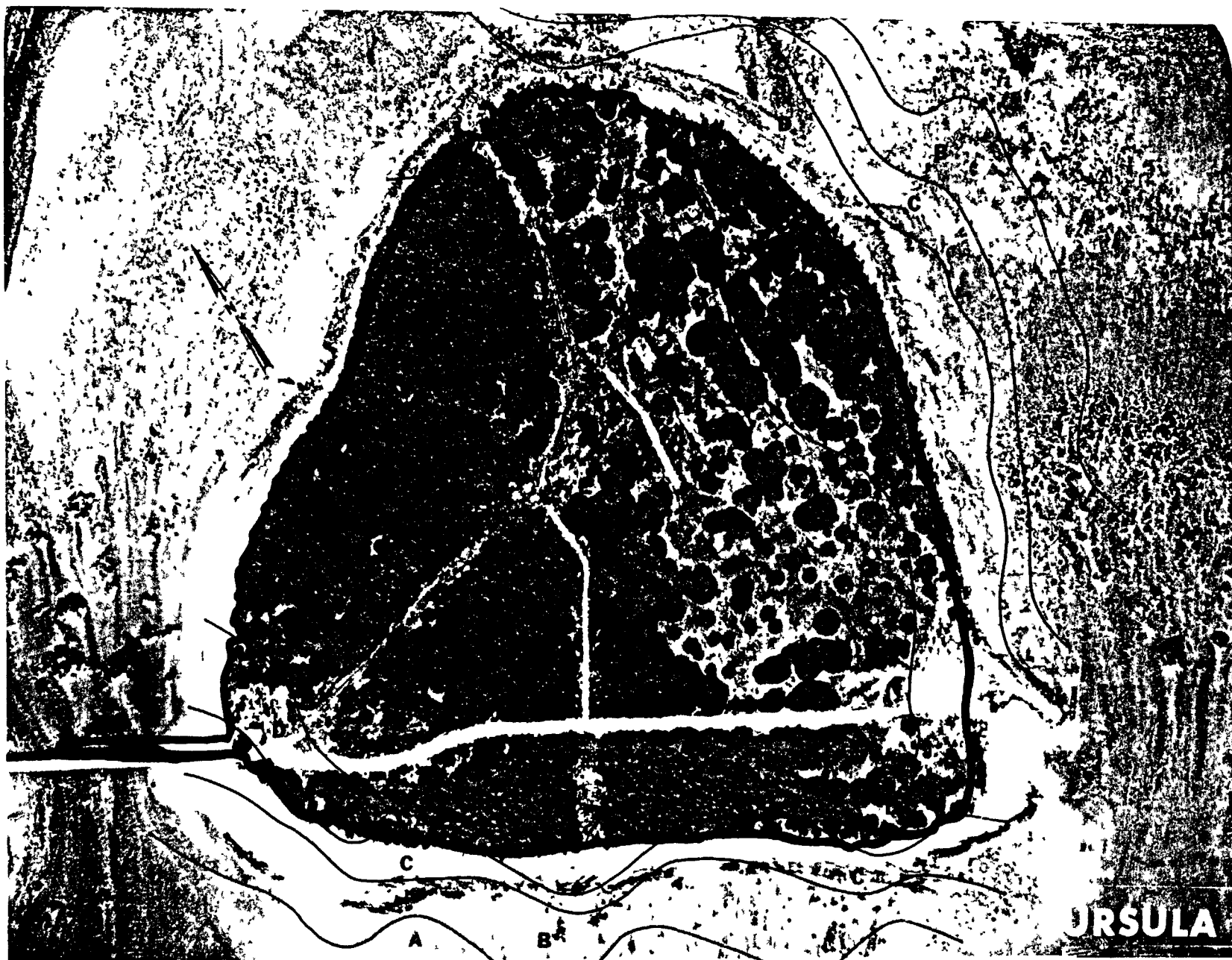


Fig. B.19.1.b. Gross count isoexposure contours. (Refer to alphabetic symbol key in this appendix.)

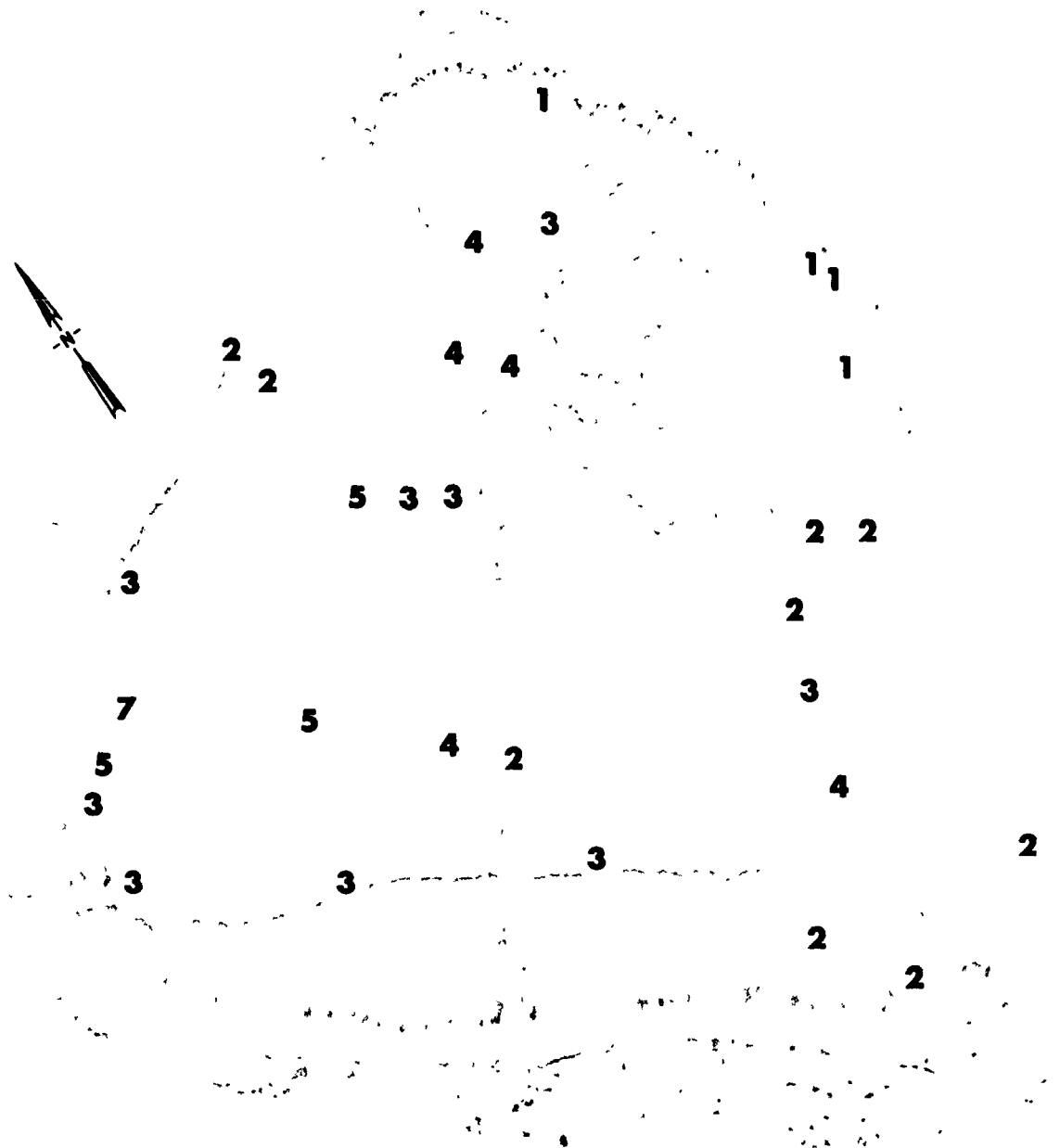
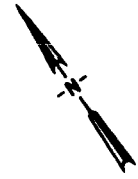
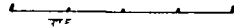


Fig. B.19.1.d. The gamma background exposure rate ( $\mu\text{R/hr}$ ) at 1 m above the ground, measured with a portable NaI scintillation counter.

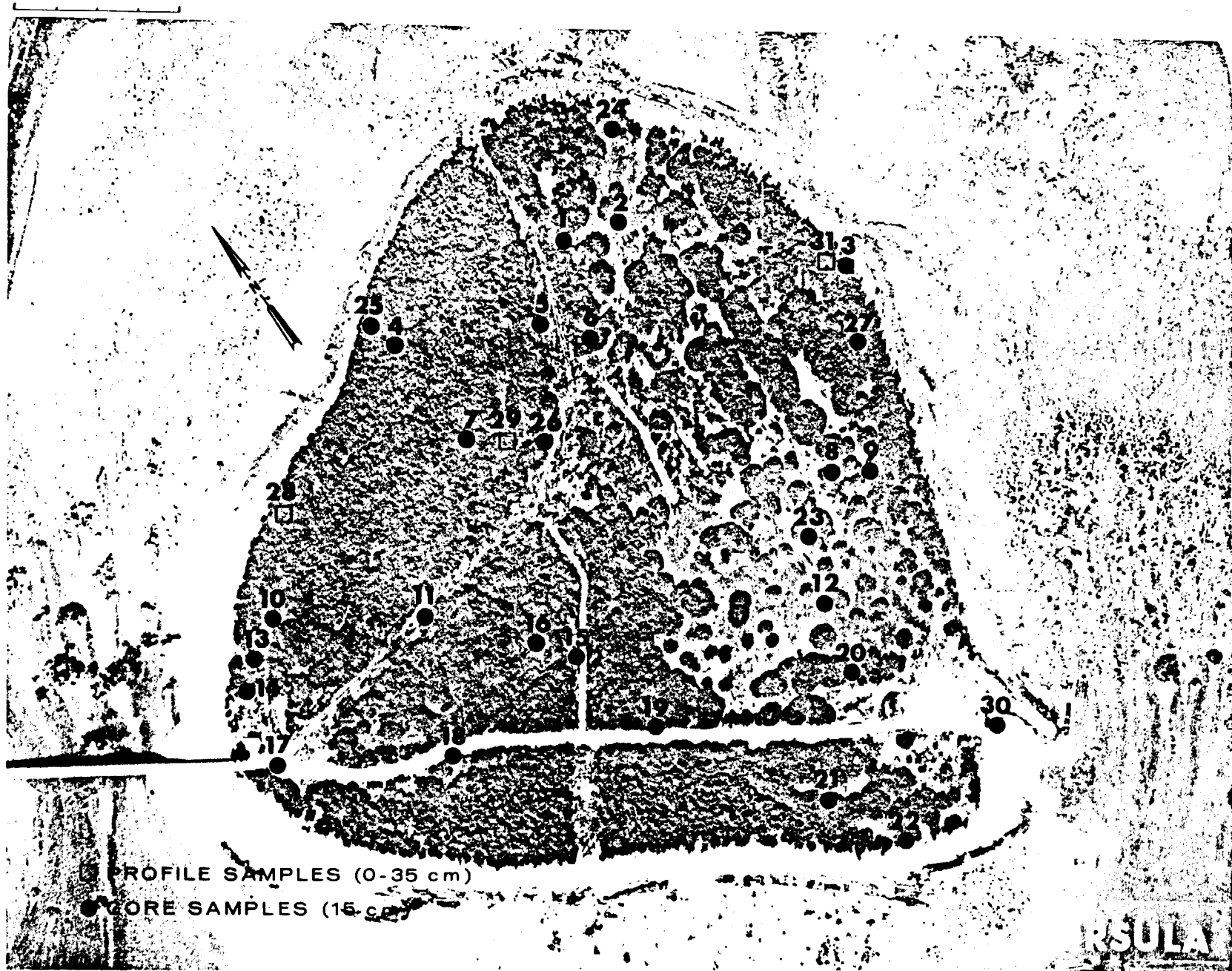


Fig. B.19.1.f. Soil-sample locations.

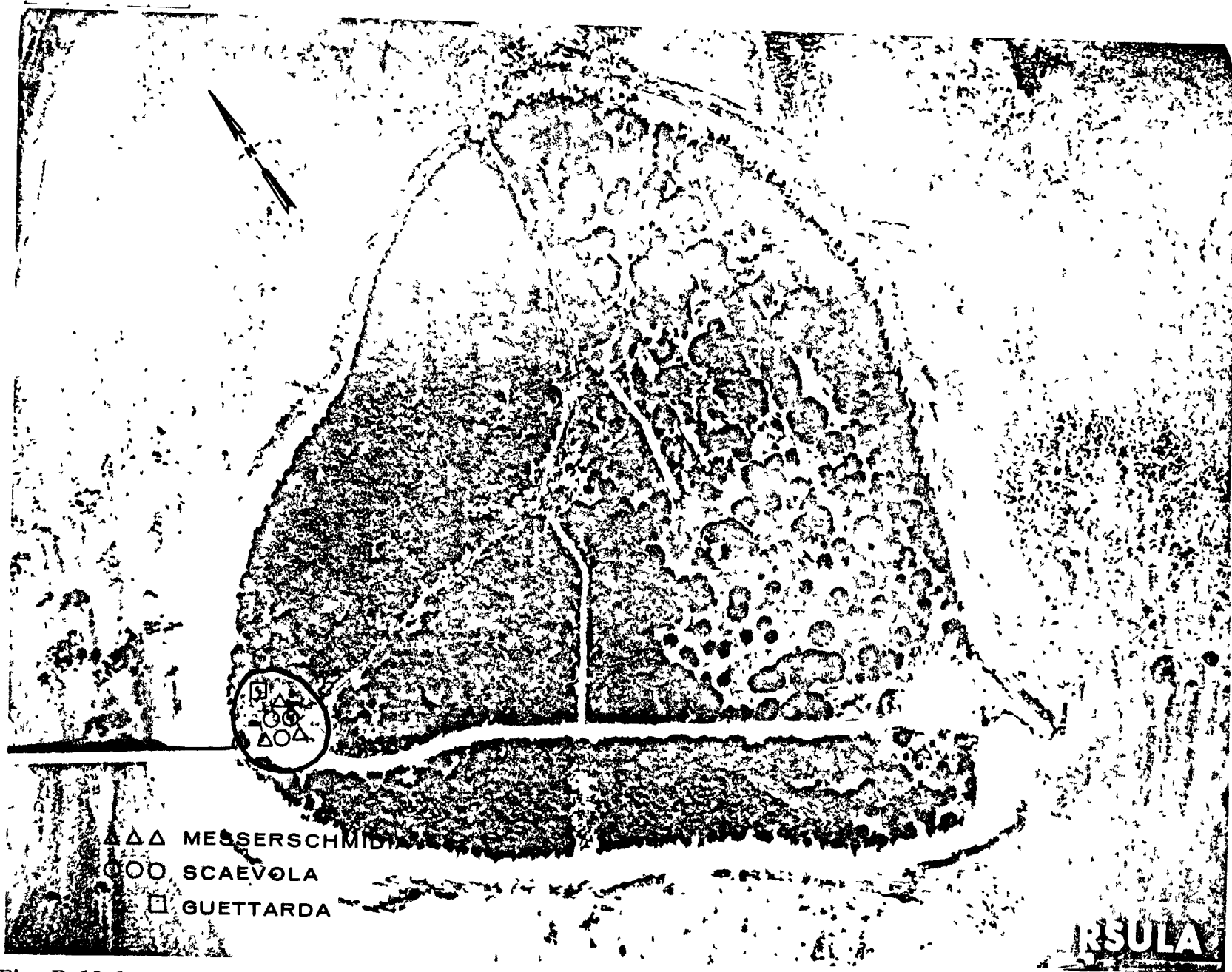


Fig. B.19.1.g. Vegetation sample locations.

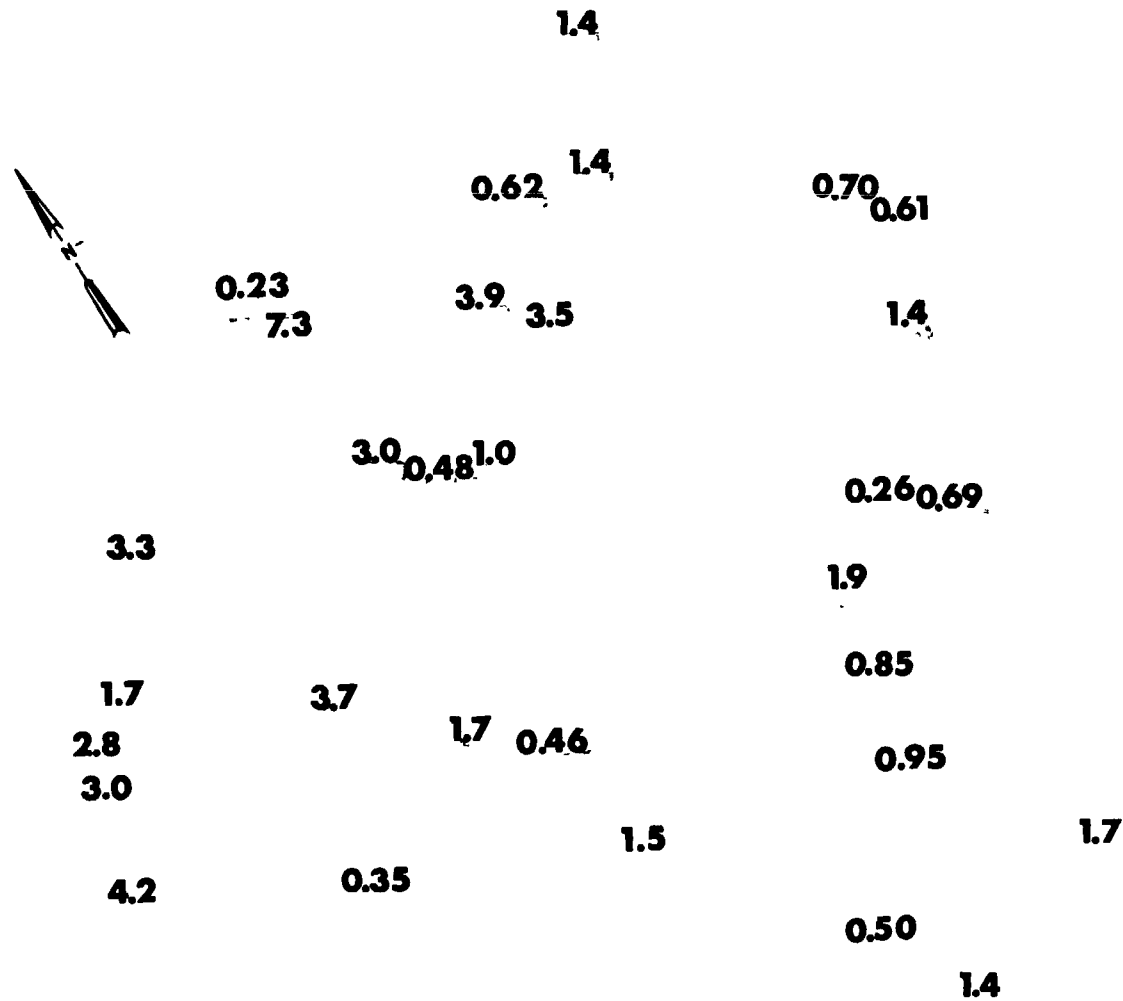


Fig. B.19.1.1. The average  $^{239}\text{Pu}$  activities (pCi/g) in soil samples collected to a depth of 15 cm.

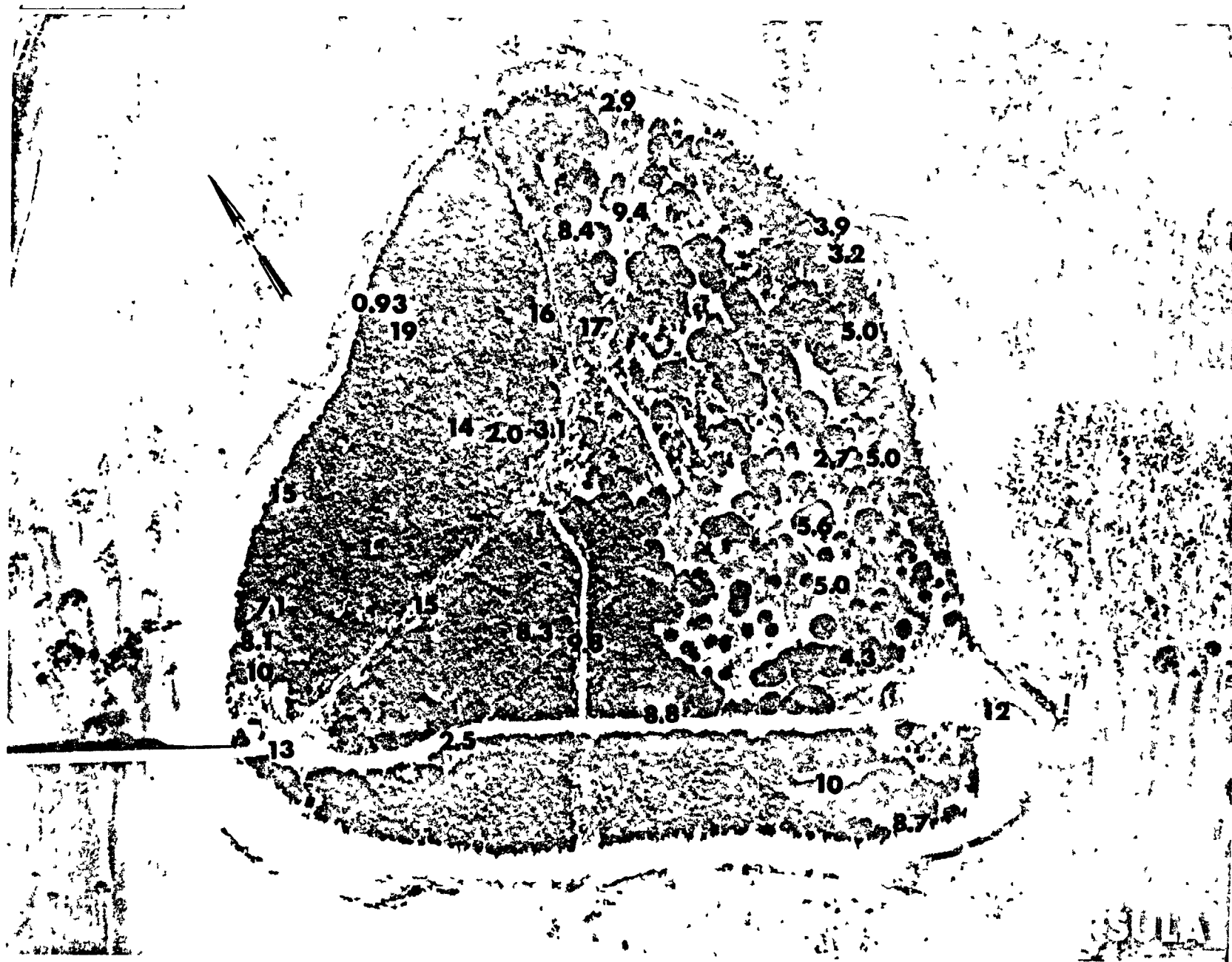


Fig. B.19.1.j. The average  $^{90}\text{Sr}$  activities (pCi/g) in soil samples collected to a depth of 15 cm.

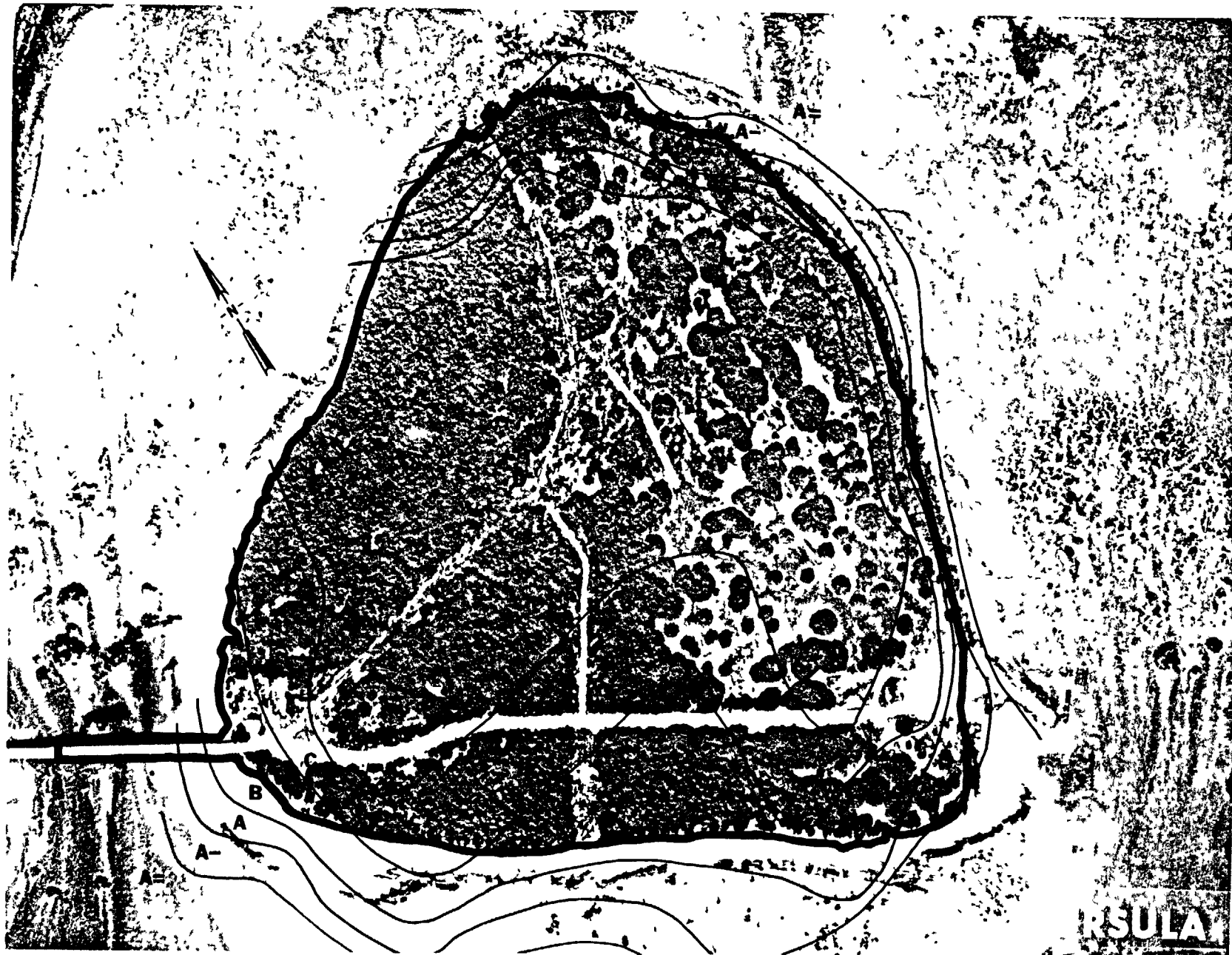


Fig. B.19.1.k. <sup>137</sup>Cs isoexposure and isoconcentration contours. (Refer to alphabetic symbol key in this appendix.)

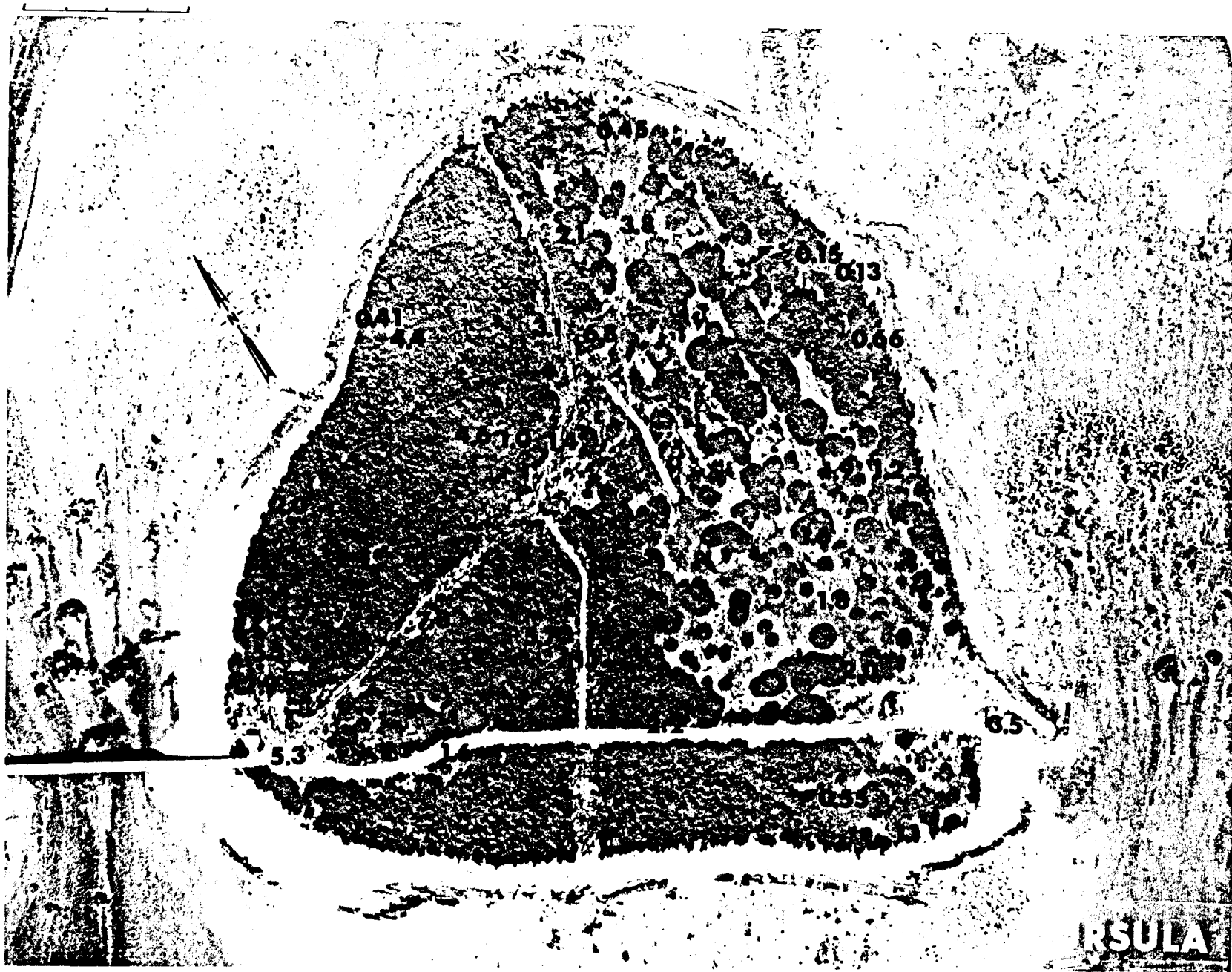


Fig. B.19.1.1. The average <sup>137</sup>Cs activities (pCi/g) in soil samples collected to a depth of 15 cm.



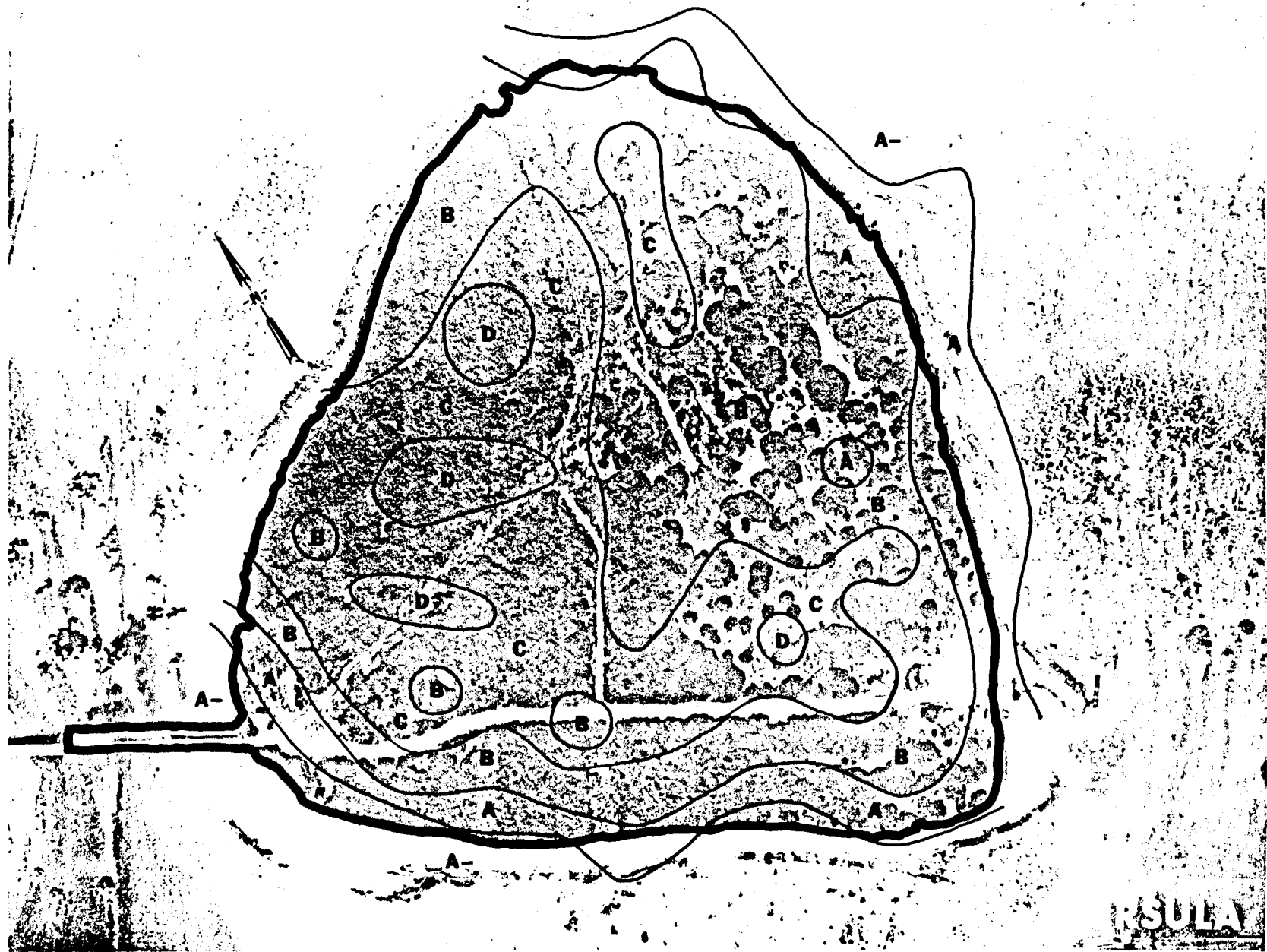


Fig. B.19.1.m.  $^{60}\text{Co}$  isoexposure and isoconcentration contours. (Refer to alphabetic symbol key in this appendix.)

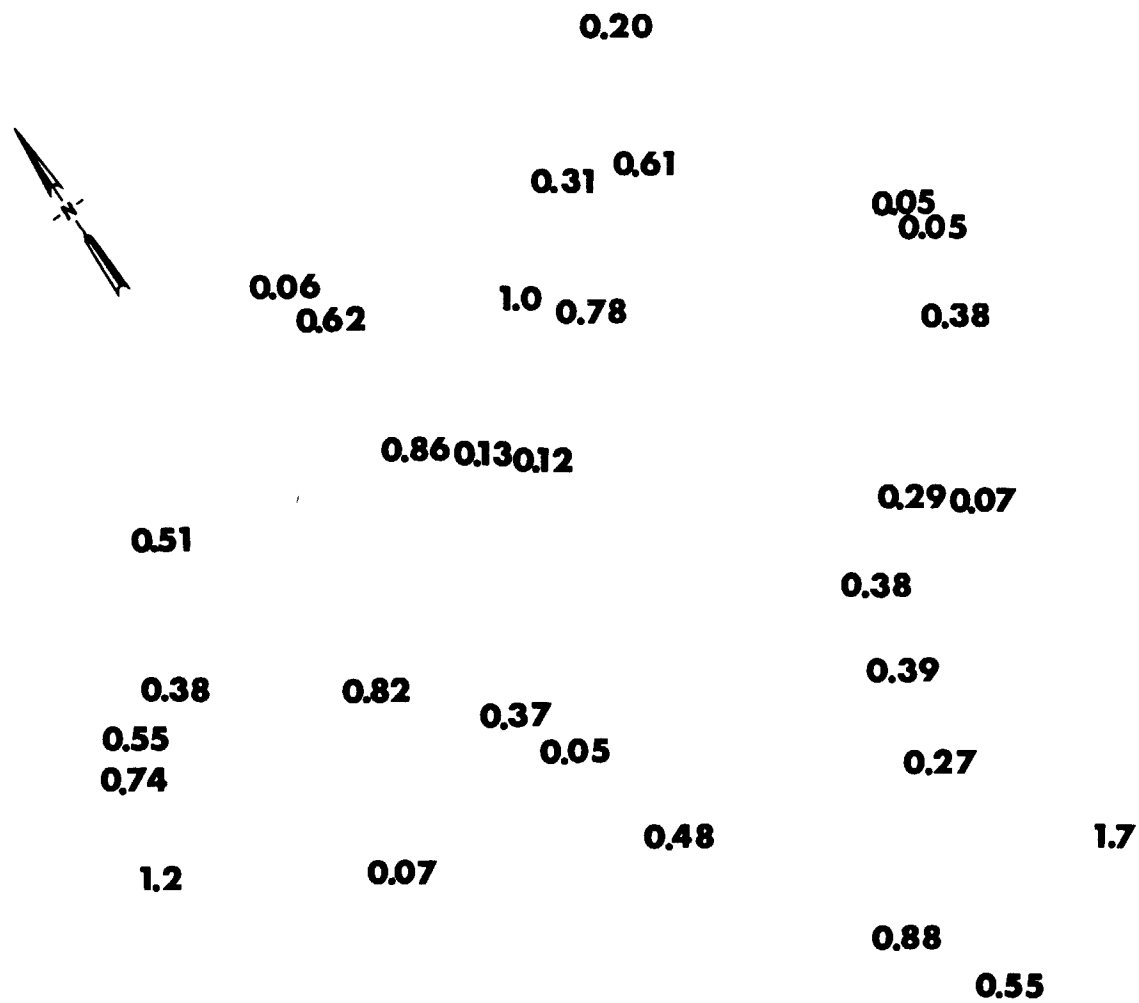


Fig. B.19.1.n. The average  $^{60}\text{Co}$  activities (pCi/g) in soil samples collected to a depth of 15 cm.

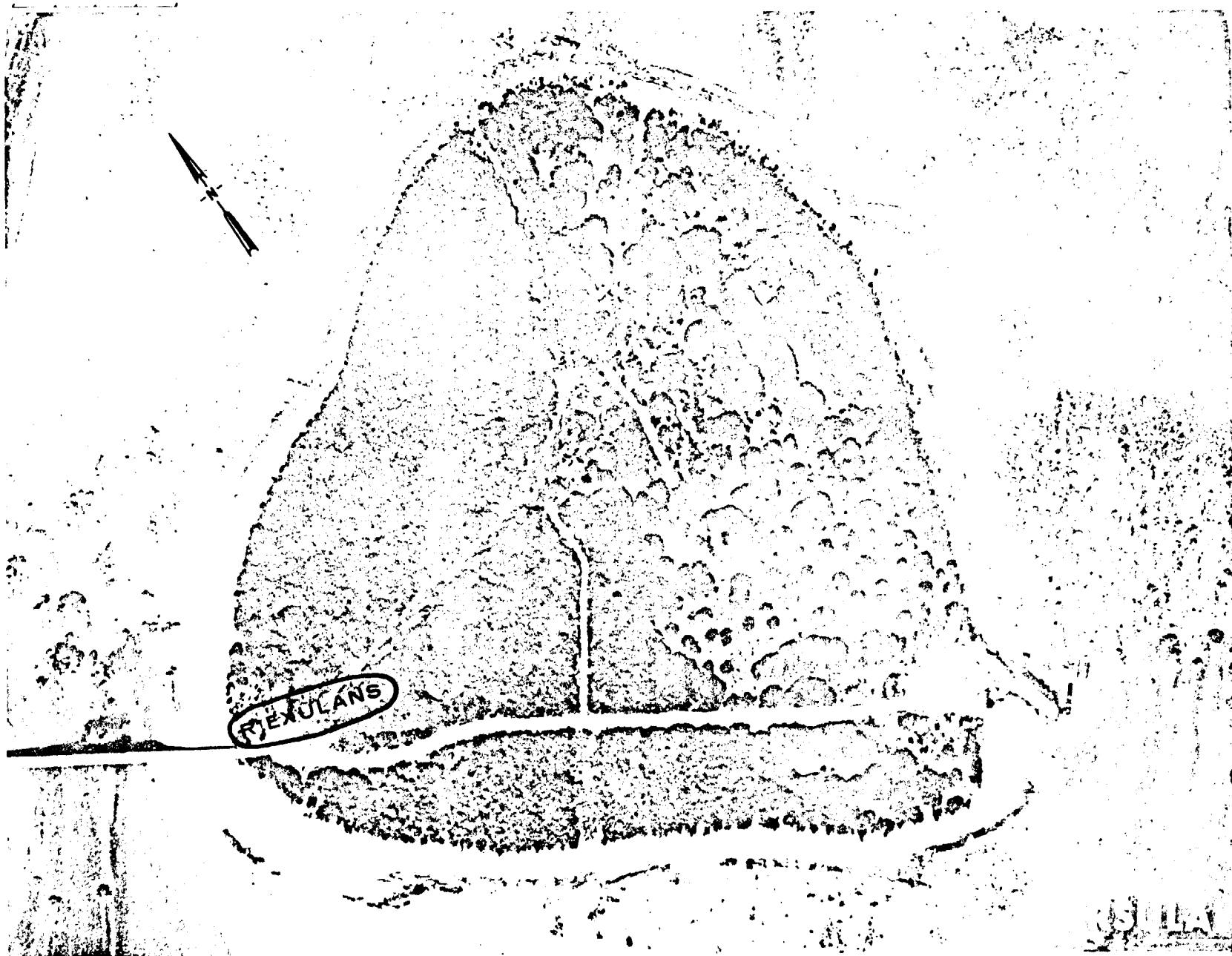


Fig. B.19.1.o. Terrestrial animal sample locations.

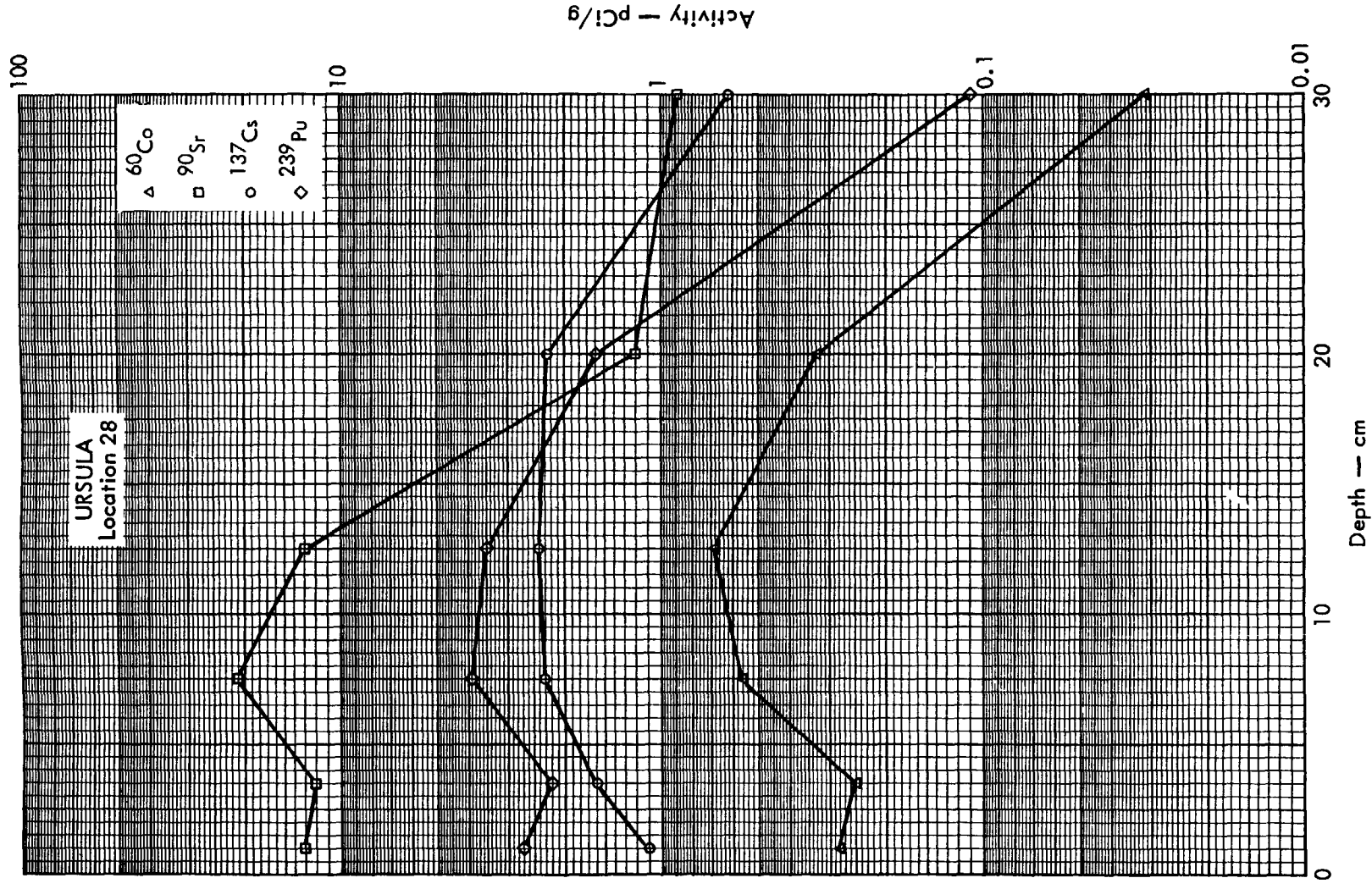


Fig. B. 19. 2a. Activities of selected radionuclides as a function of soil depth.

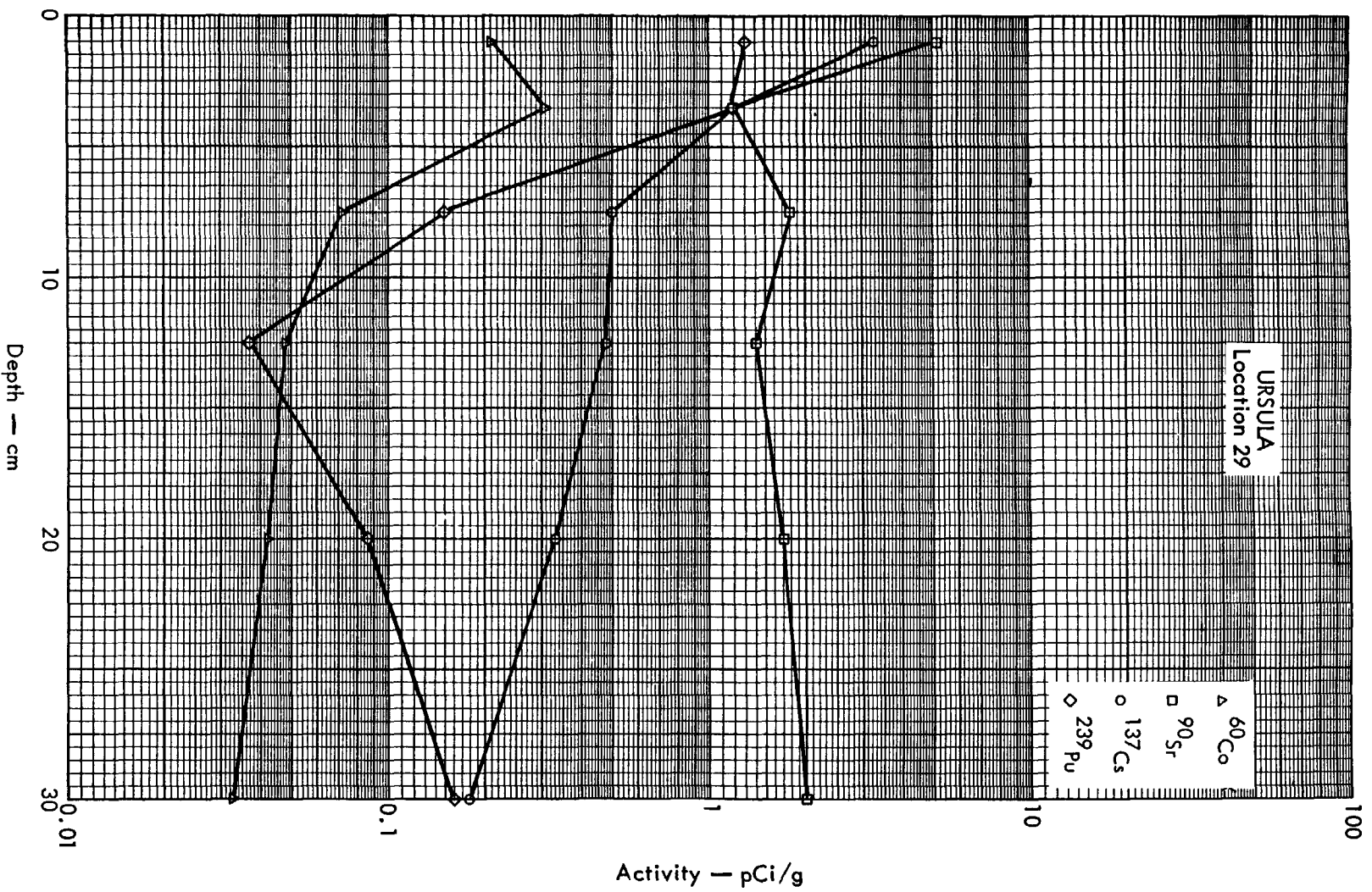


Fig. B. 19. 2b. Activities of selected radionuclides as a function of soil depth.

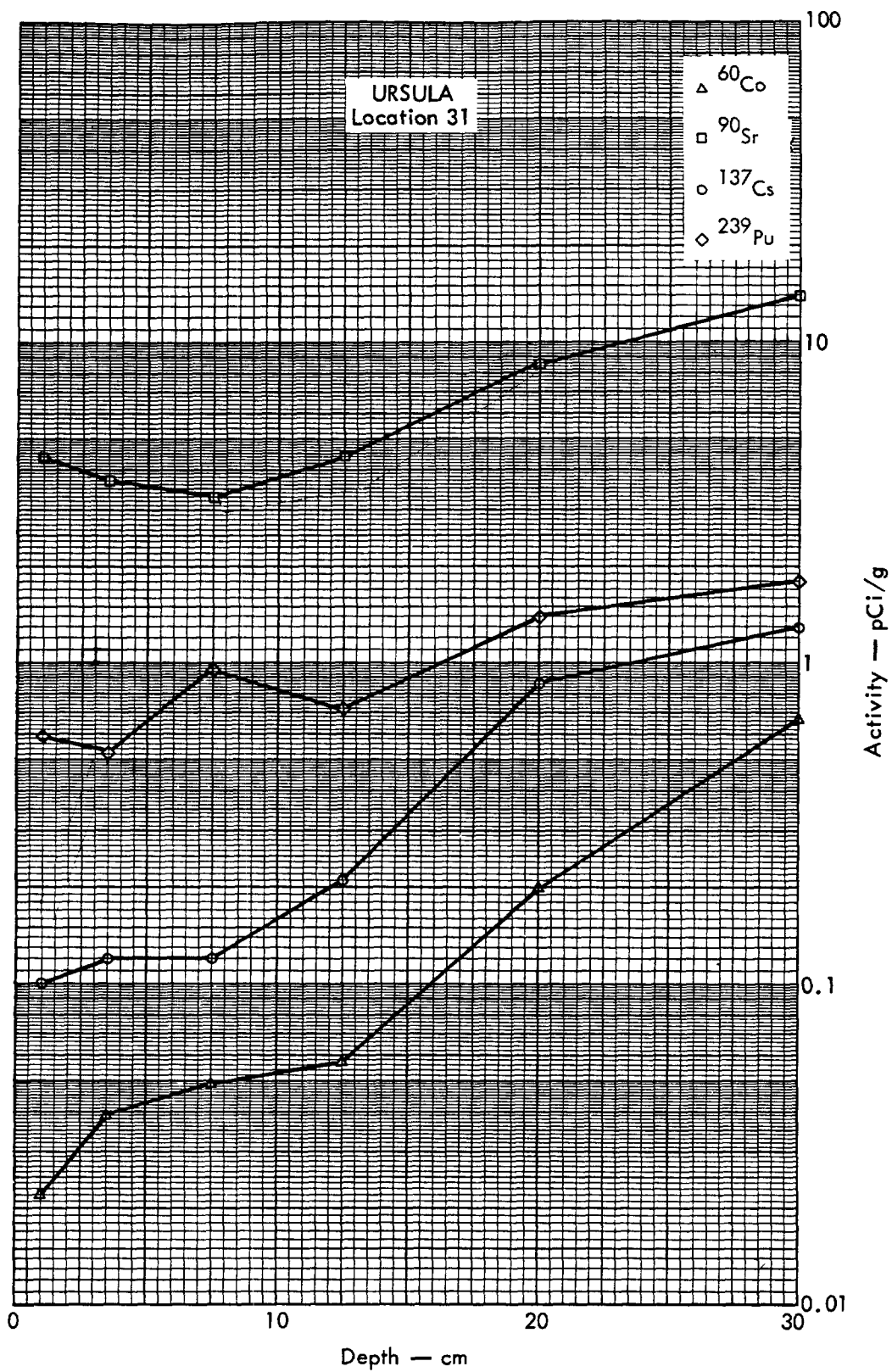


Fig. B.19. 2c. Activities of selected radionuclides as a function of soil depth.

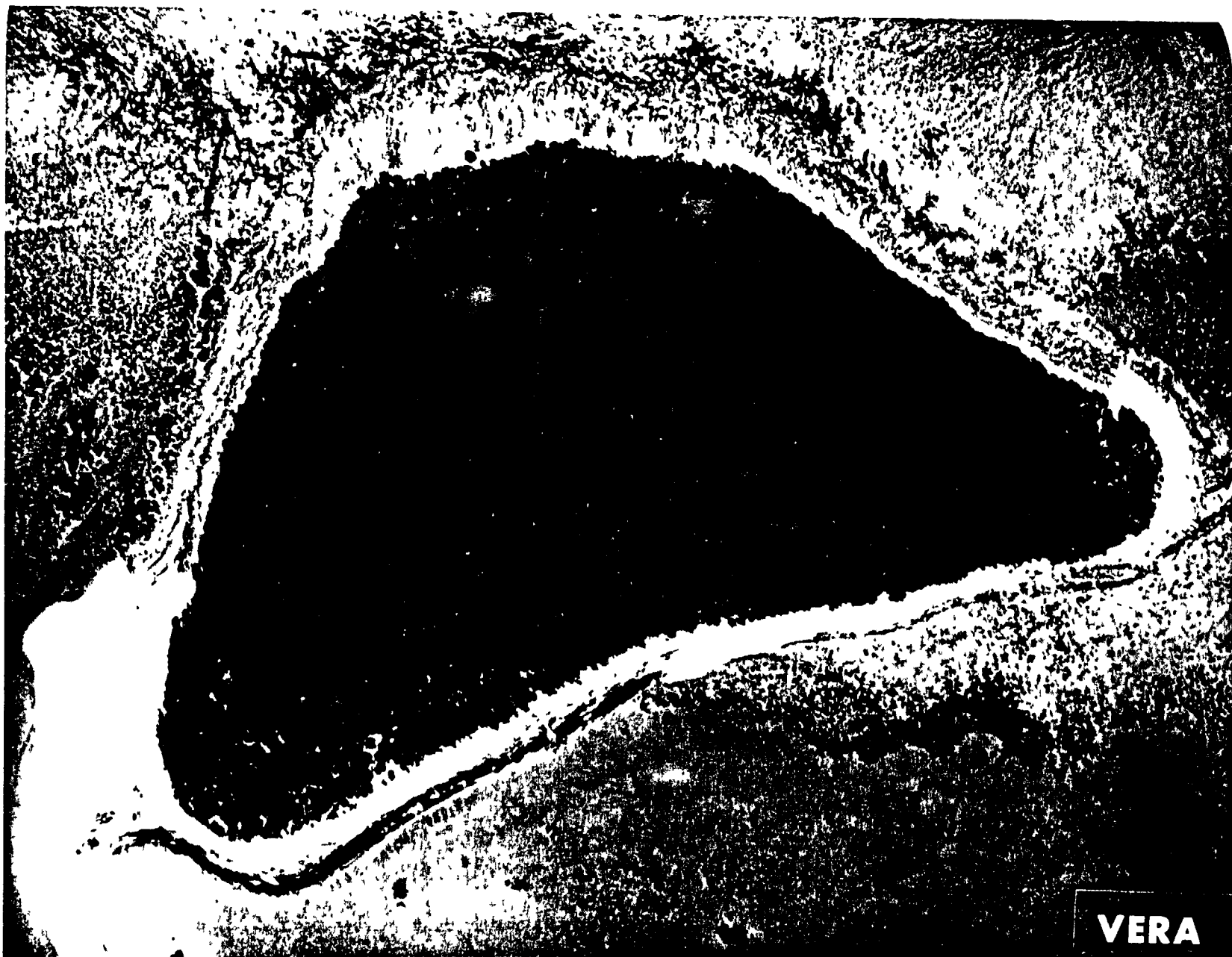


Fig. B.20.1.a.



Fig. B.20.1.b. Gross count isosexposure contours. (Refer to alphabetic symbol key in this appendix.)





Fig. B.20.1.d. The gamma background exposure rate ( $\mu\text{R/hr}$ ) at 1 m above the ground, measured with a portable NaI scintillation counter.

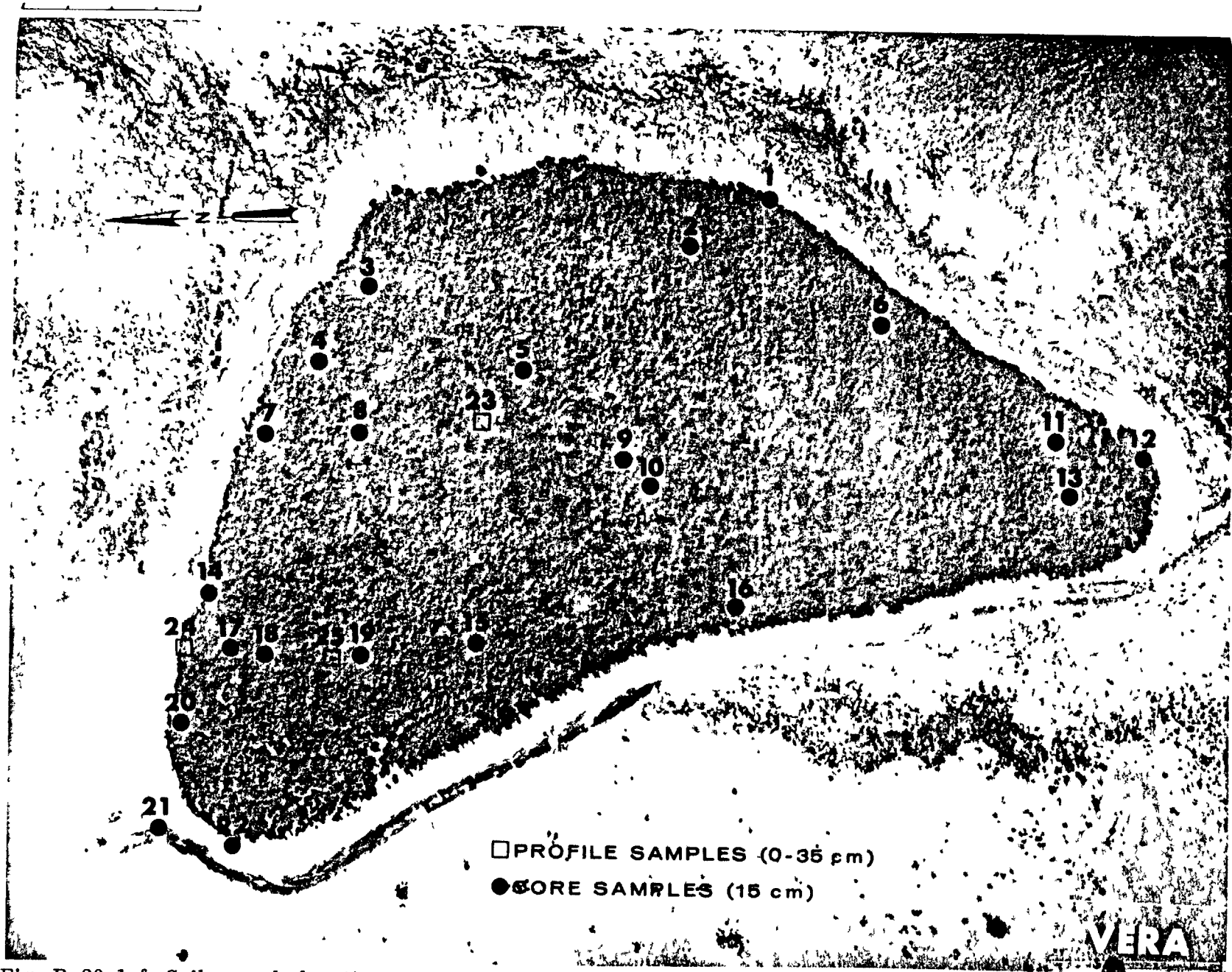
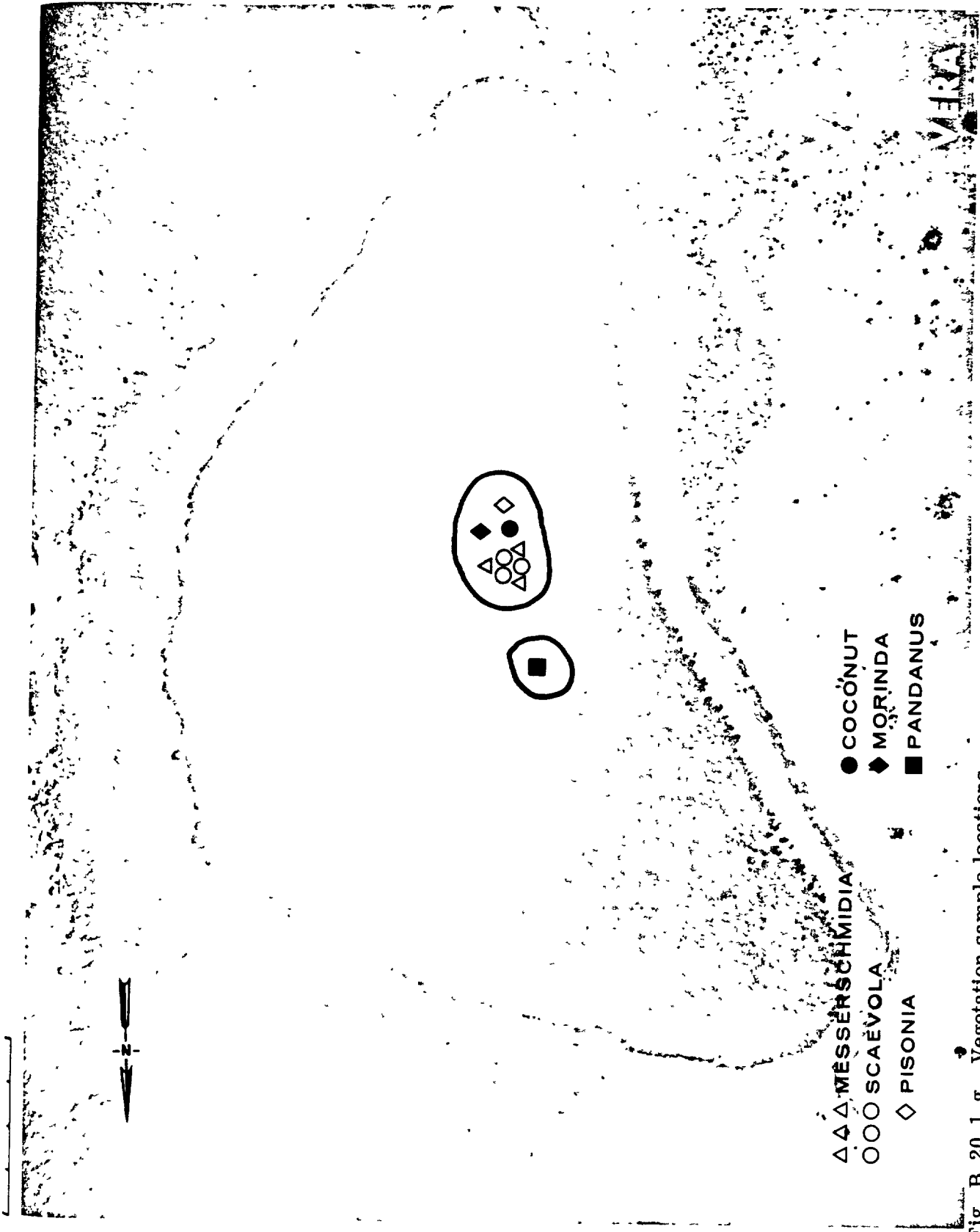


Fig. B.20.1.f. Soil-sample locations.



- △△ MESSERSCHMIDIA
- SCAEVOLA
- ◇ PISONIA
- COCÓNUT
- ◆ MORINDA
- PANDANUS

Fig. B.20.1.g. Vegetation sample locations.

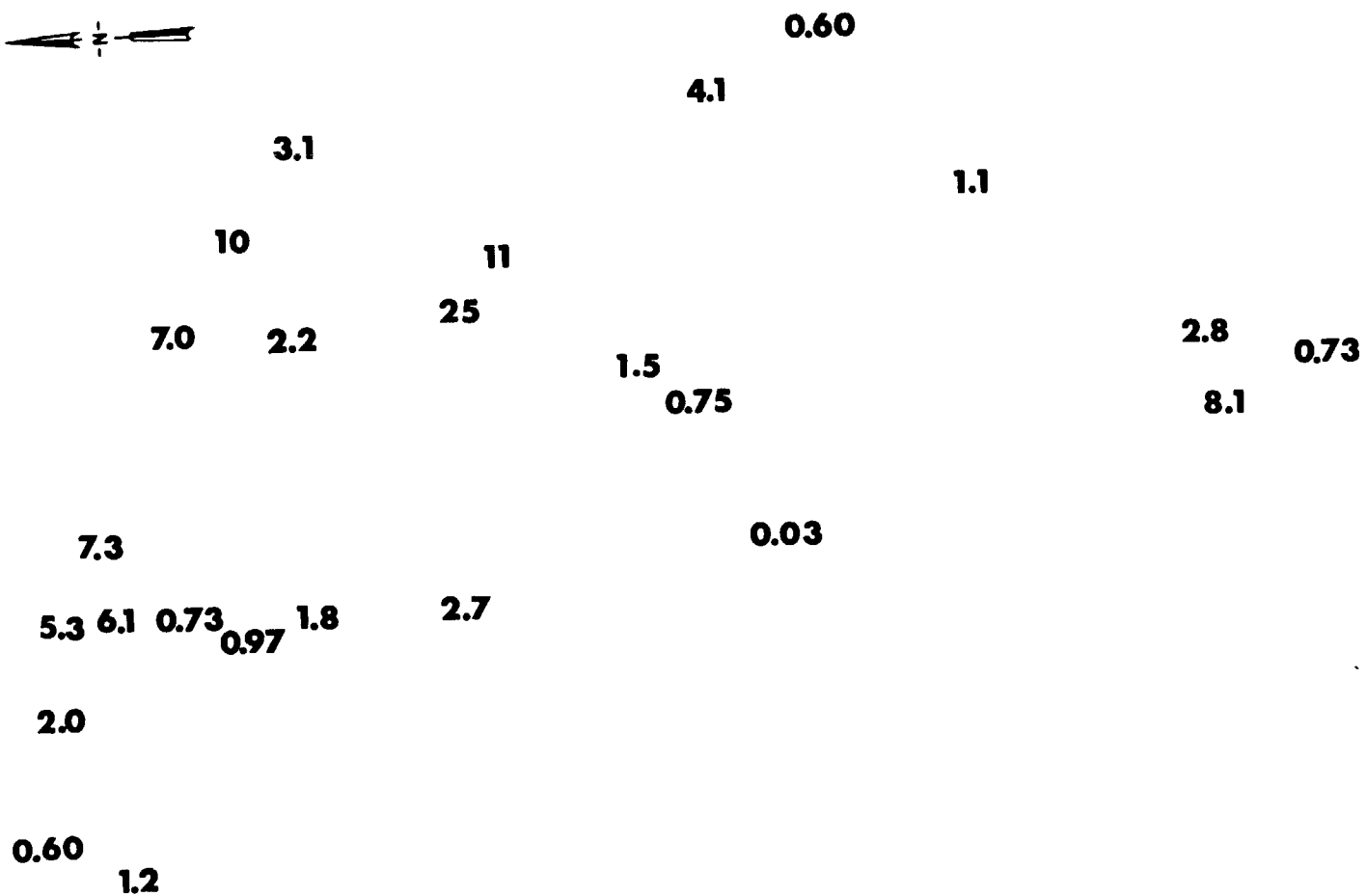
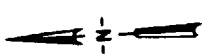


Fig. B.20.1.i. The average  $^{239}\text{Pu}$  activities (pCi/g) in soil samples collected to a depth of 15 cm.

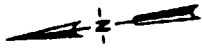
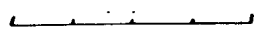


Fig. B.20.1.j. The average <sup>90</sup>Sr activities (pCi/g) in soil samples collected to a depth of 15 cm.

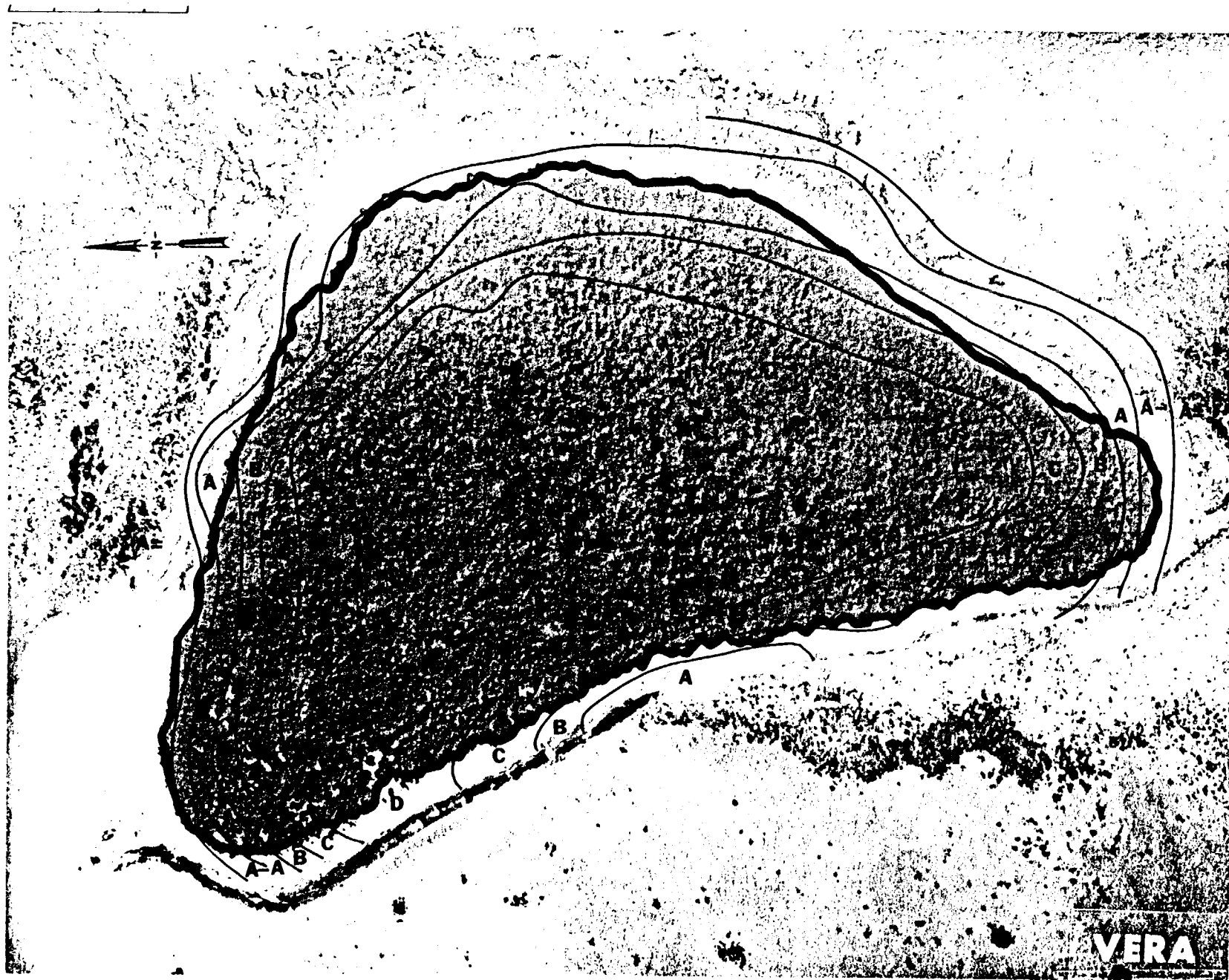


Fig. B.20.1.k. <sup>137</sup>Cs isoexposure and isoconcentration contours. (Refer to alphabetic symbol key in this appendix.)

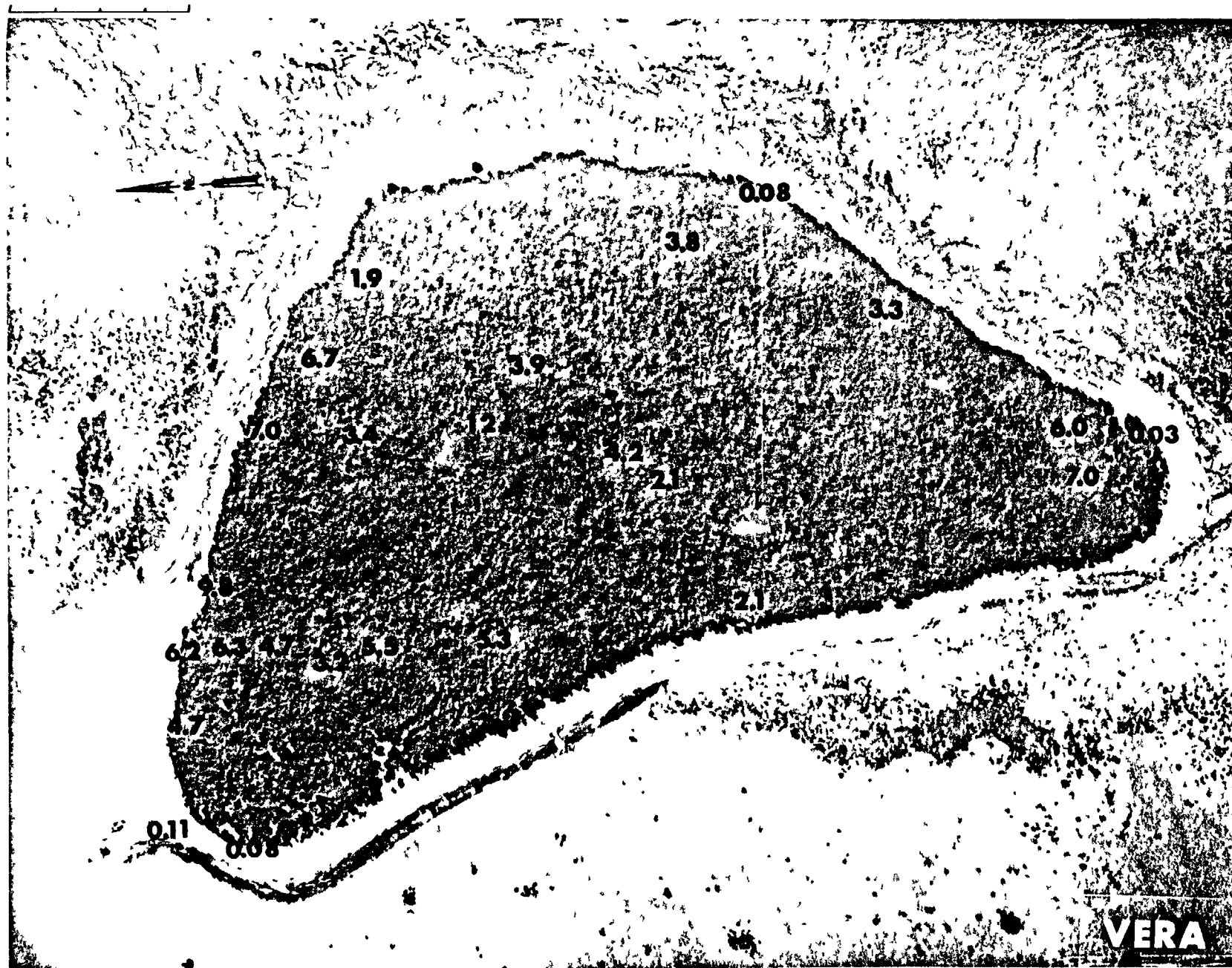


Fig. B.20.1.1. The average  $^{137}\text{Cs}$  activities (pCi/g) in soil samples collected to a depth of 15 cm.

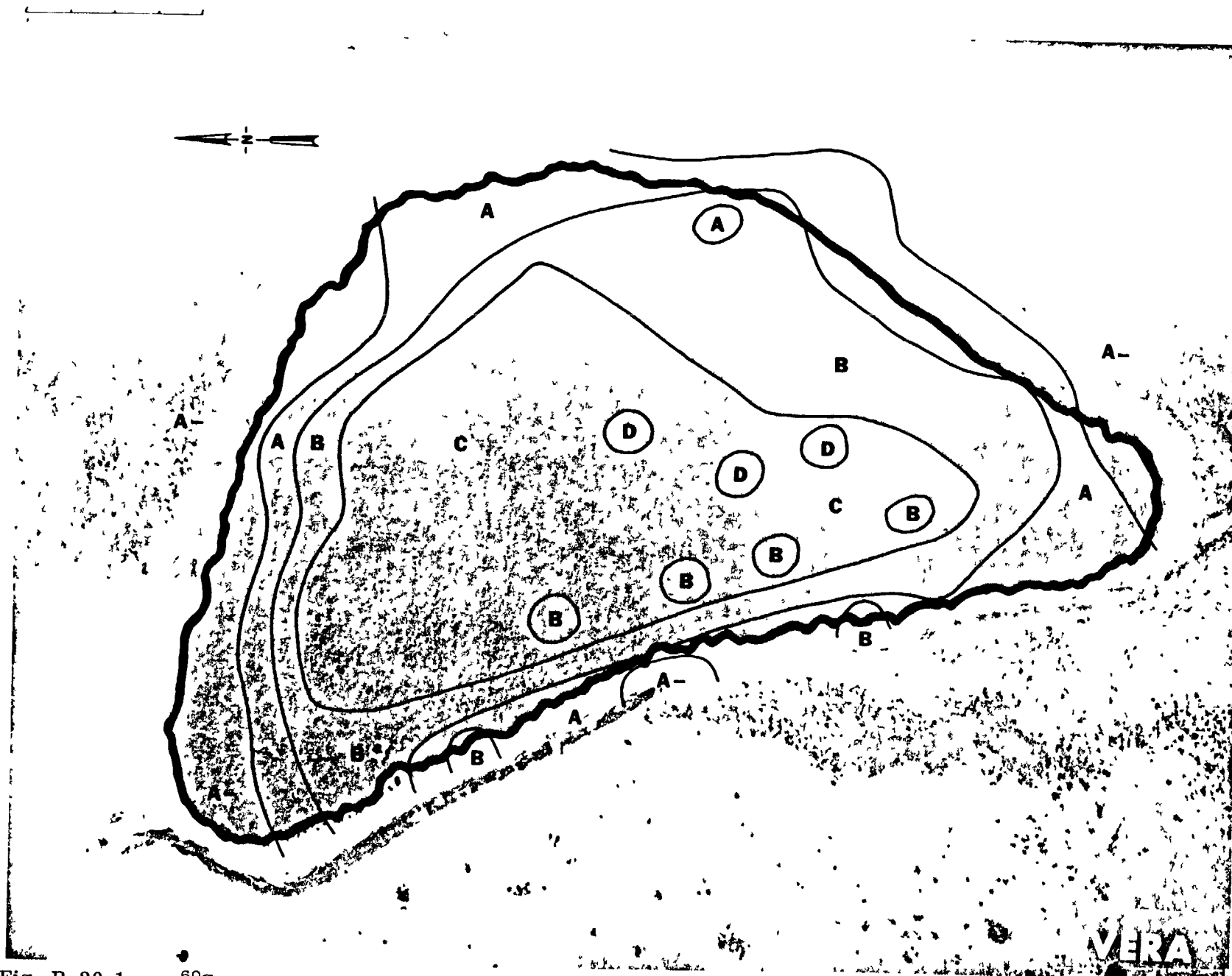


Fig. B.20.1.m.  $^{60}\text{Co}$  isoexposure and isoconcentration contours. (Refer to alphabetic symbol key in this appendix.)



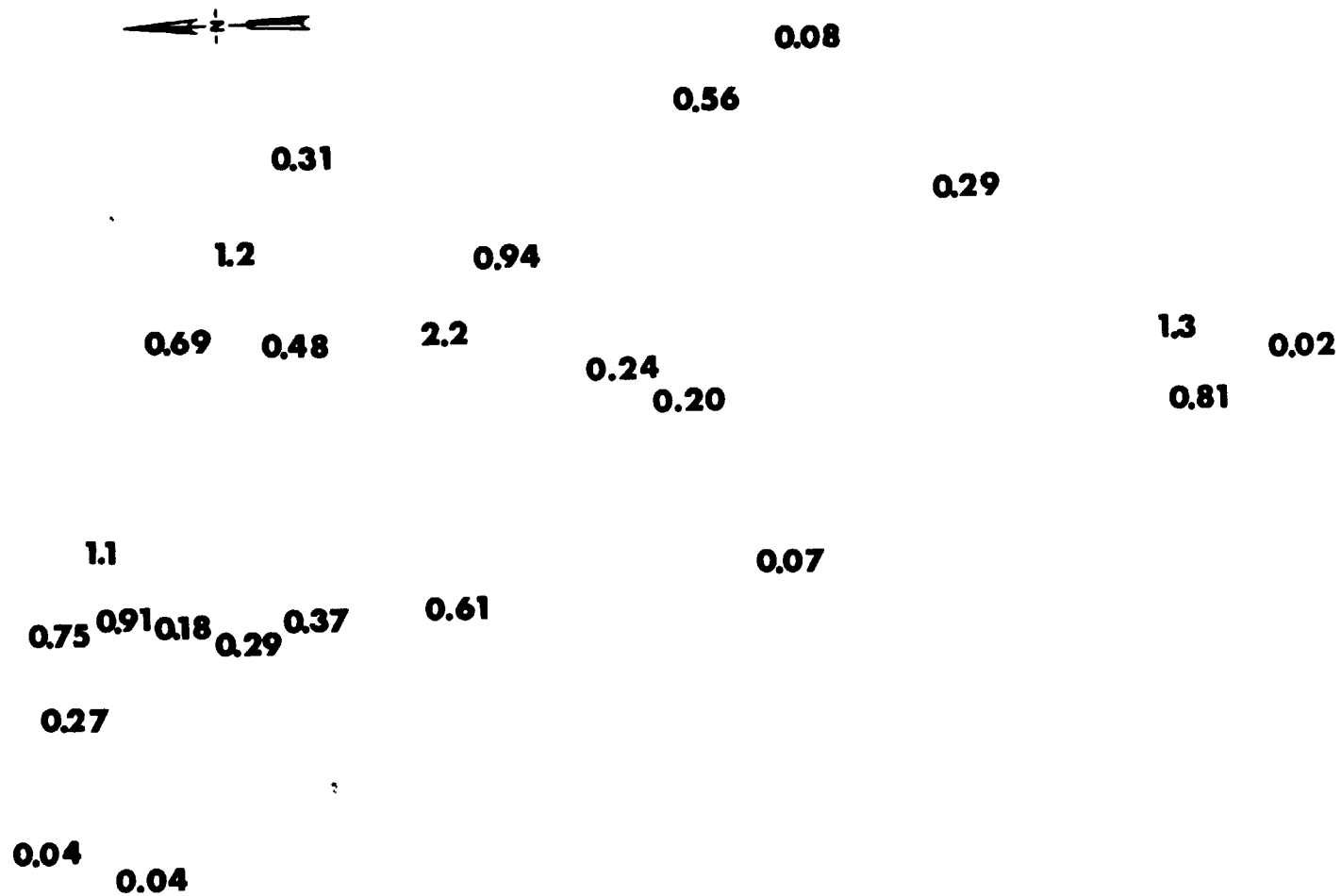


Fig. B.20.1.n. The average  $^{60}\text{Co}$  activities (pCi/g) in soil samples collected to a depth of 15 cm.

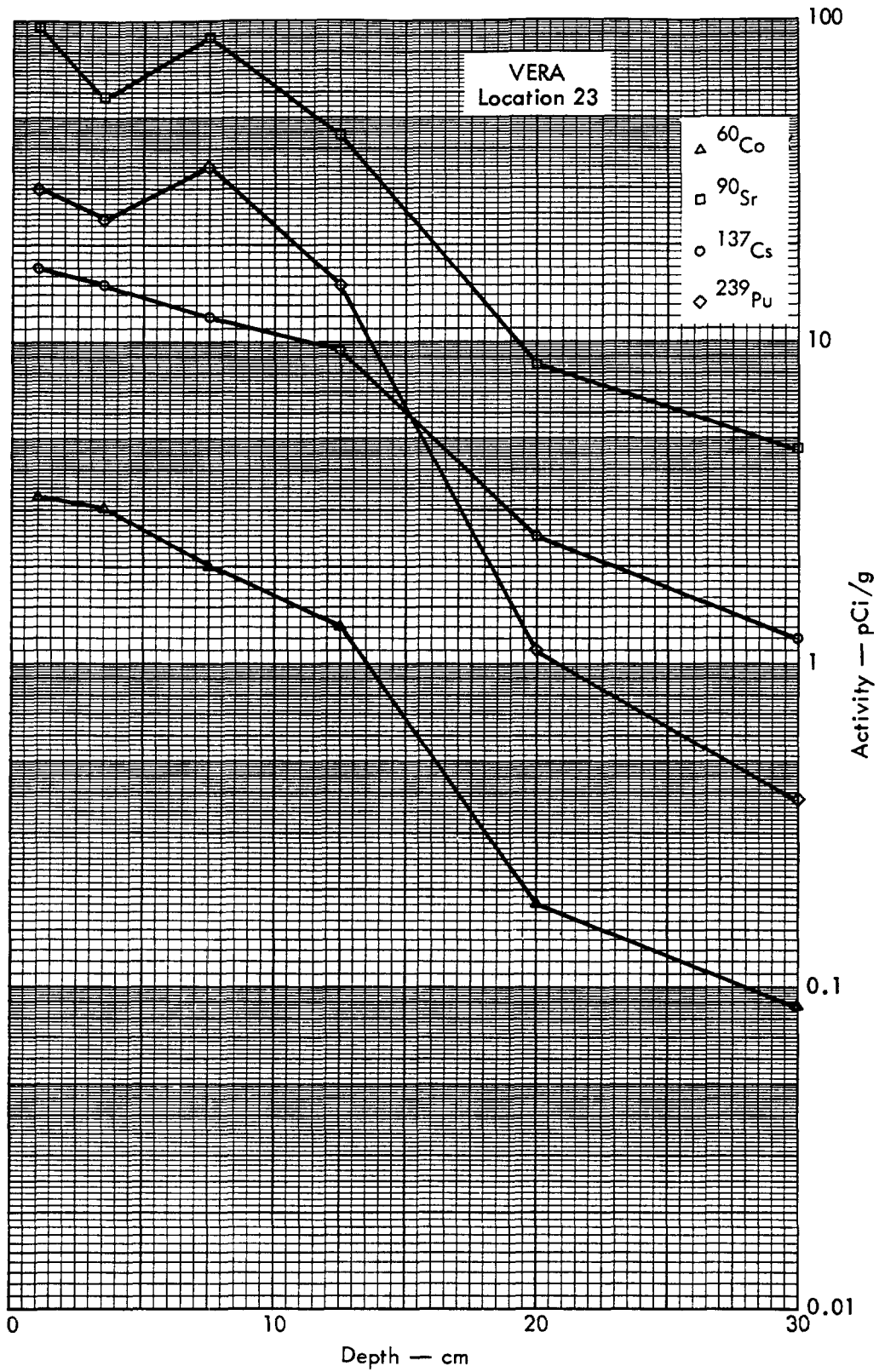


Fig. B. 20.2a. Activities of selected radionuclides as a function of soil depth.

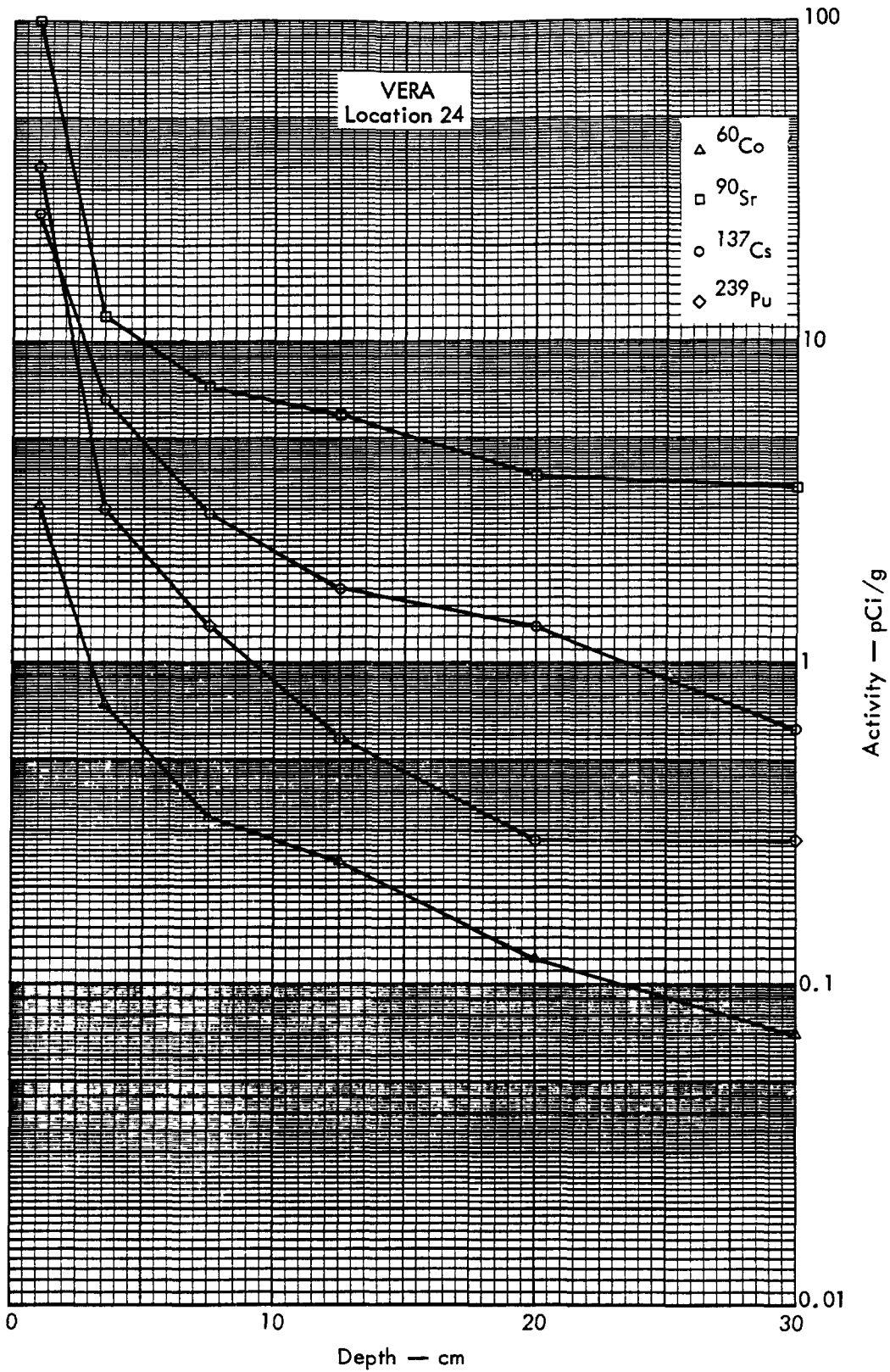


Fig. B. 20. 2b. Activities of selected radionuclides as a function of soil depth.

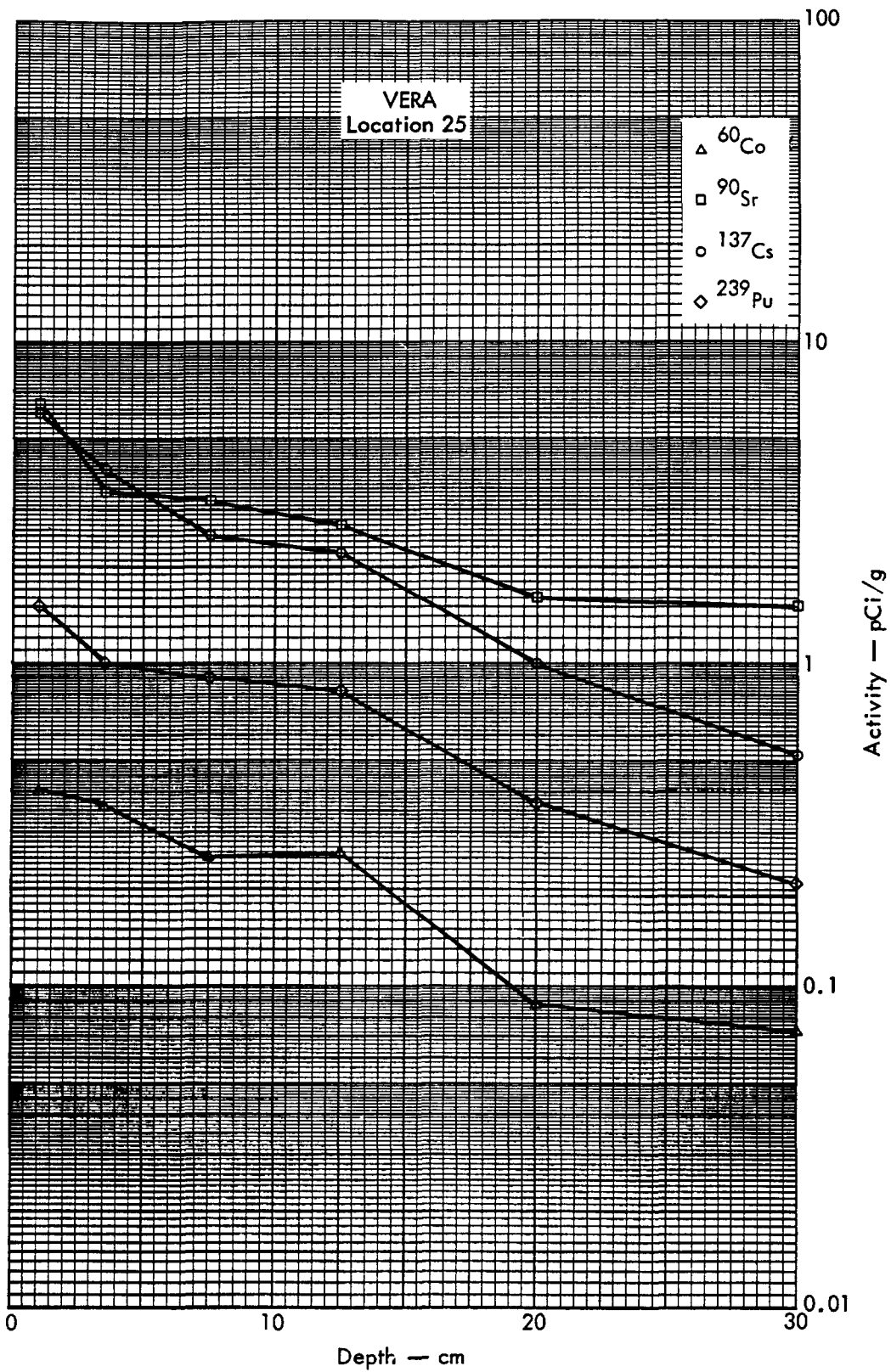


Fig. B. 20. 2c. Activities of selected radionuclides as a function of soil depth.

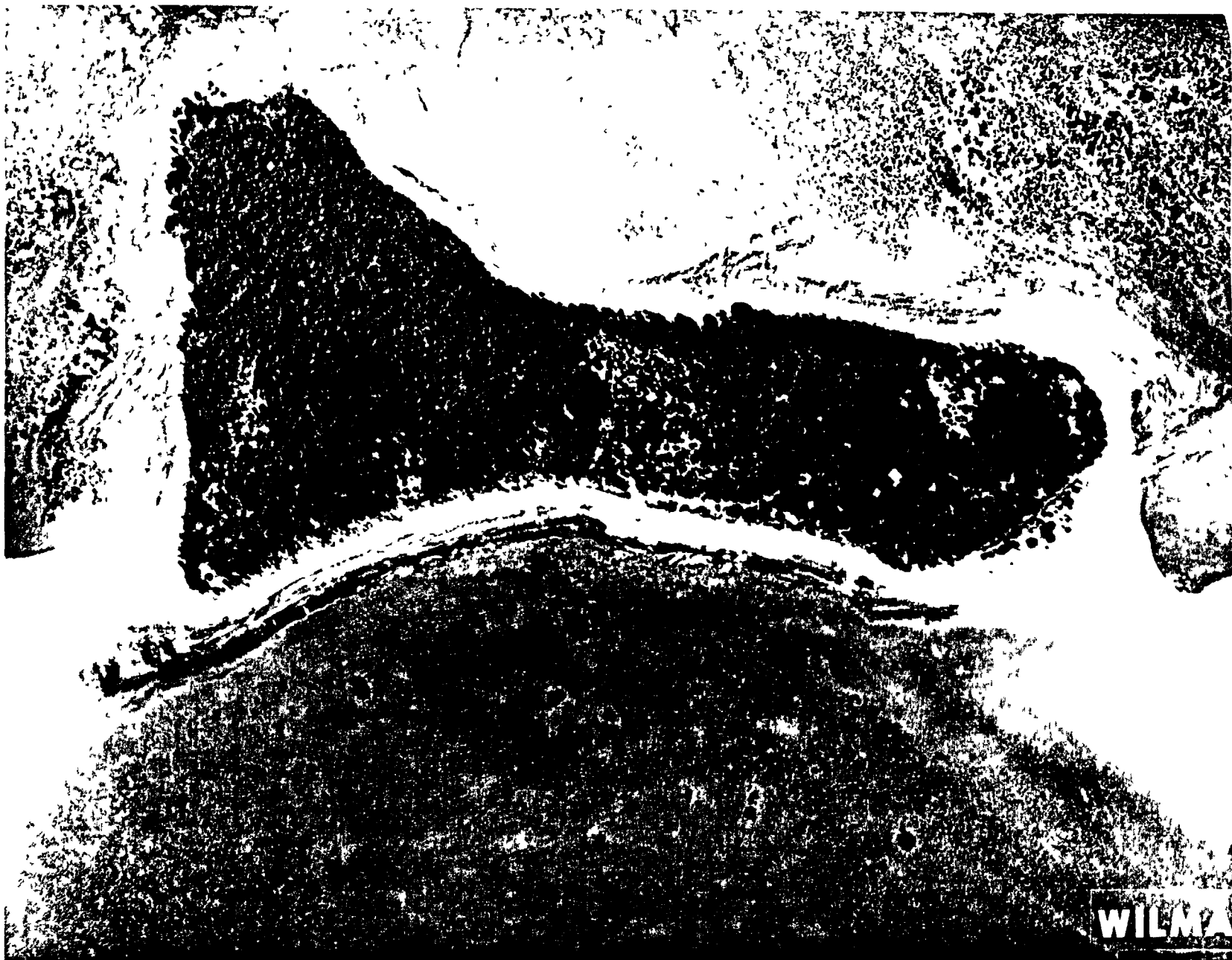


Fig. B.21.1.a.



Fig. B.21.1.b. Gross count isoexposure contours. (Refer to alphabetic symbol key in this appendix.)

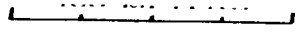


Fig. B.21.1.d. The gamma background exposure rate ( $\mu\text{R/hr}$ ) at 1 m above the ground, measured with a portable NaI scintillation counter.

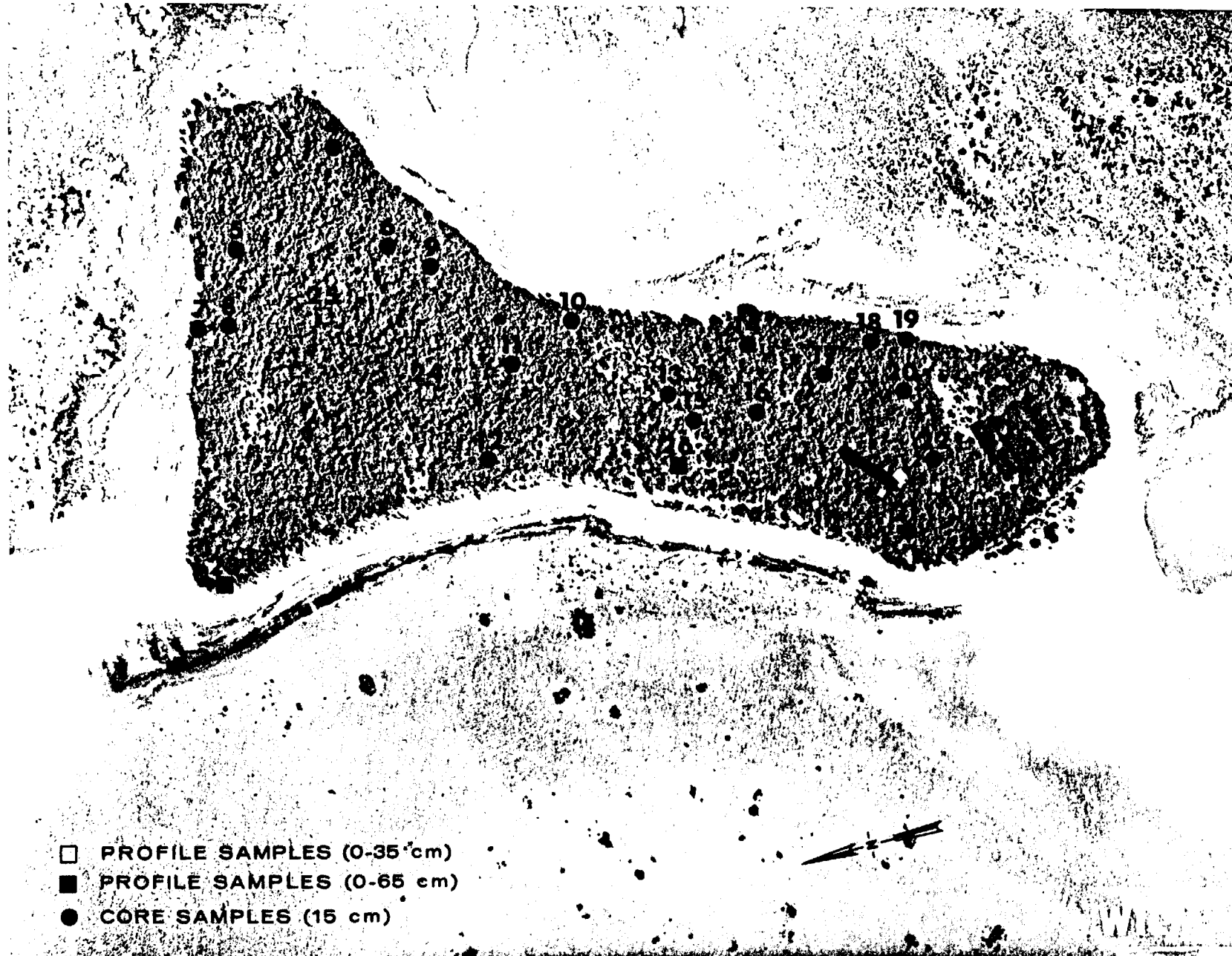


Fig. B.21.1.f. Soil-sample locations.



100 METERS

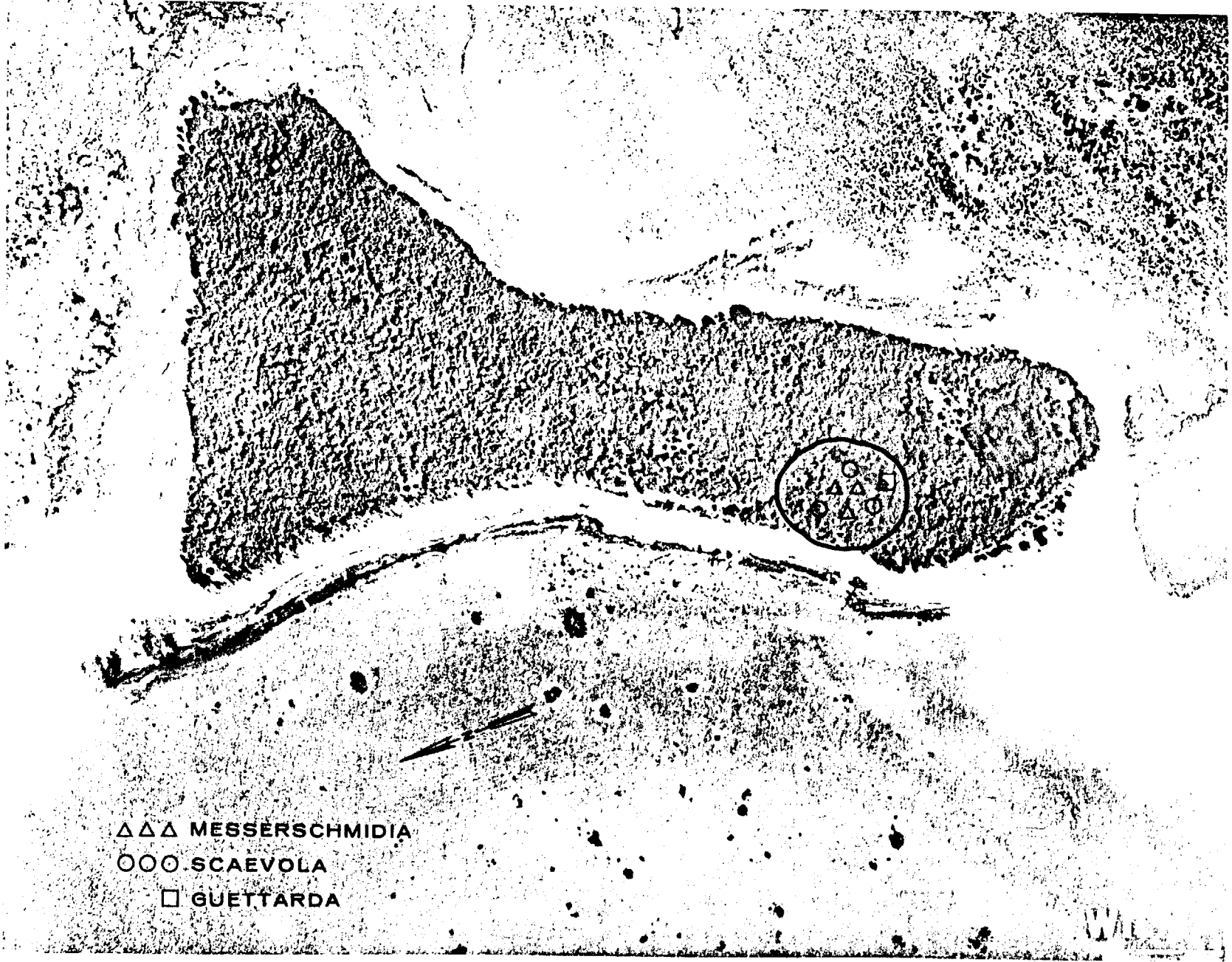


Fig. B.21.1.g. Vegetation sample locations.

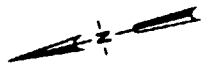
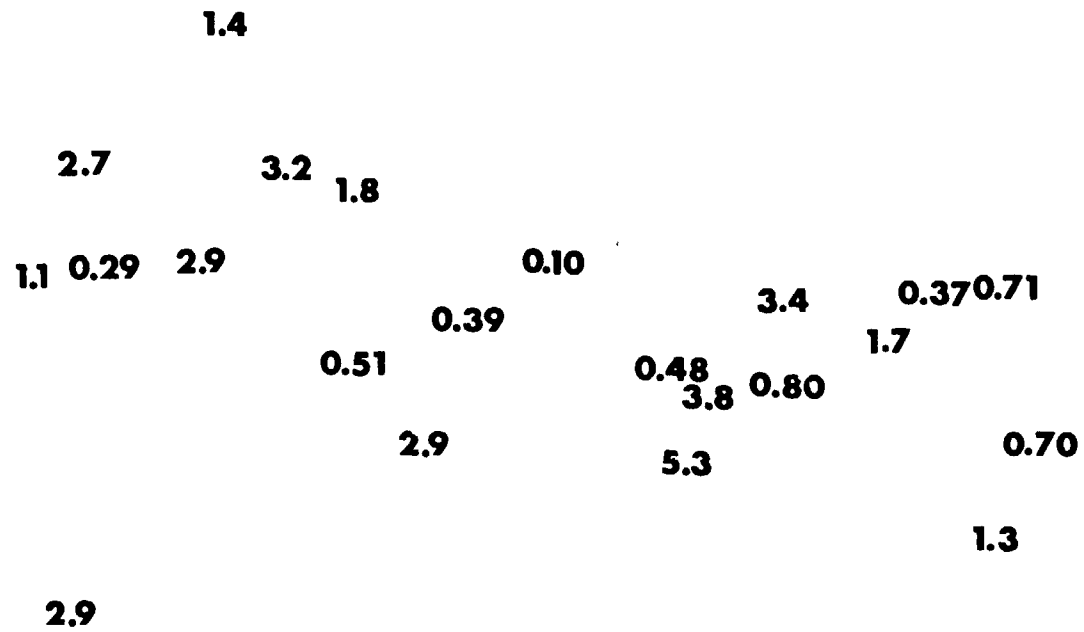
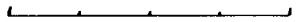


Fig. B.21.1.i. The average <sup>239</sup>Pu activities (pCi/gm) in soil samples collected to a depth of 15 cm.

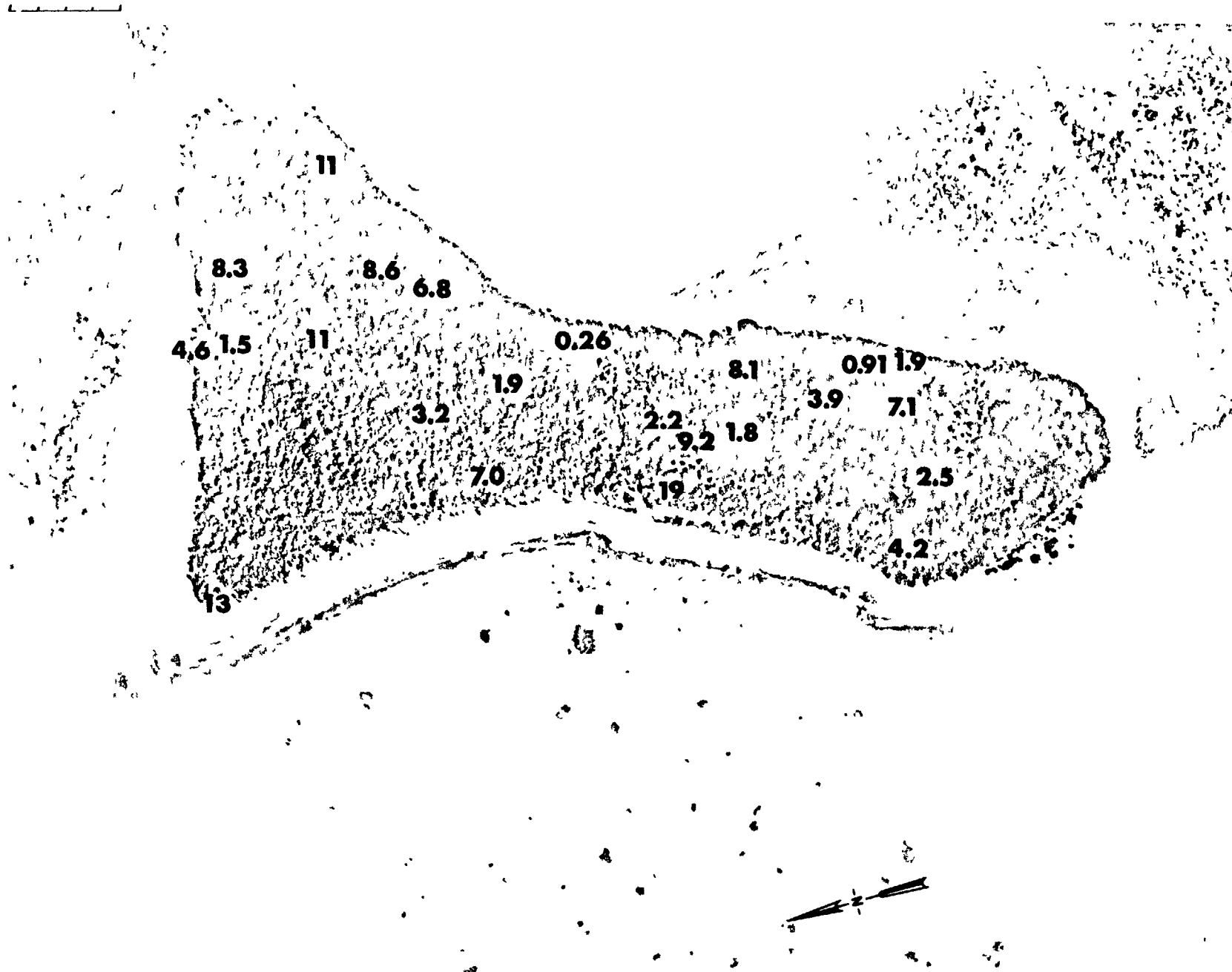


Fig. B.21.1.j. The average <sup>90</sup>Sr activities (pCi/gm) in soil samples collected to a depth of 15 cm.

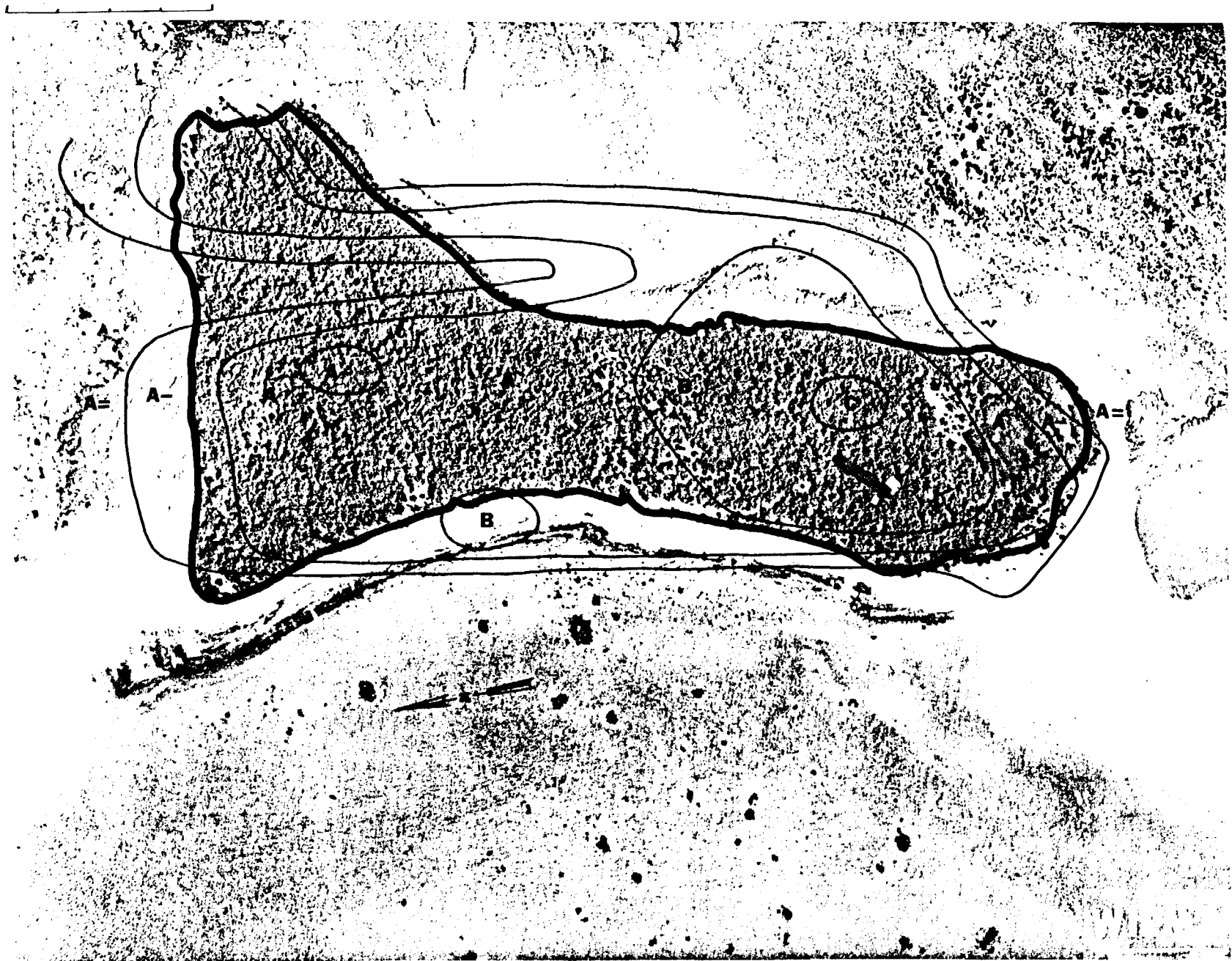


Fig. B.21.1.k.  $^{137}\text{Cs}$  isoexposure and isoconcentration contours. (Refer to alphabetic symbol key in this appendix.)

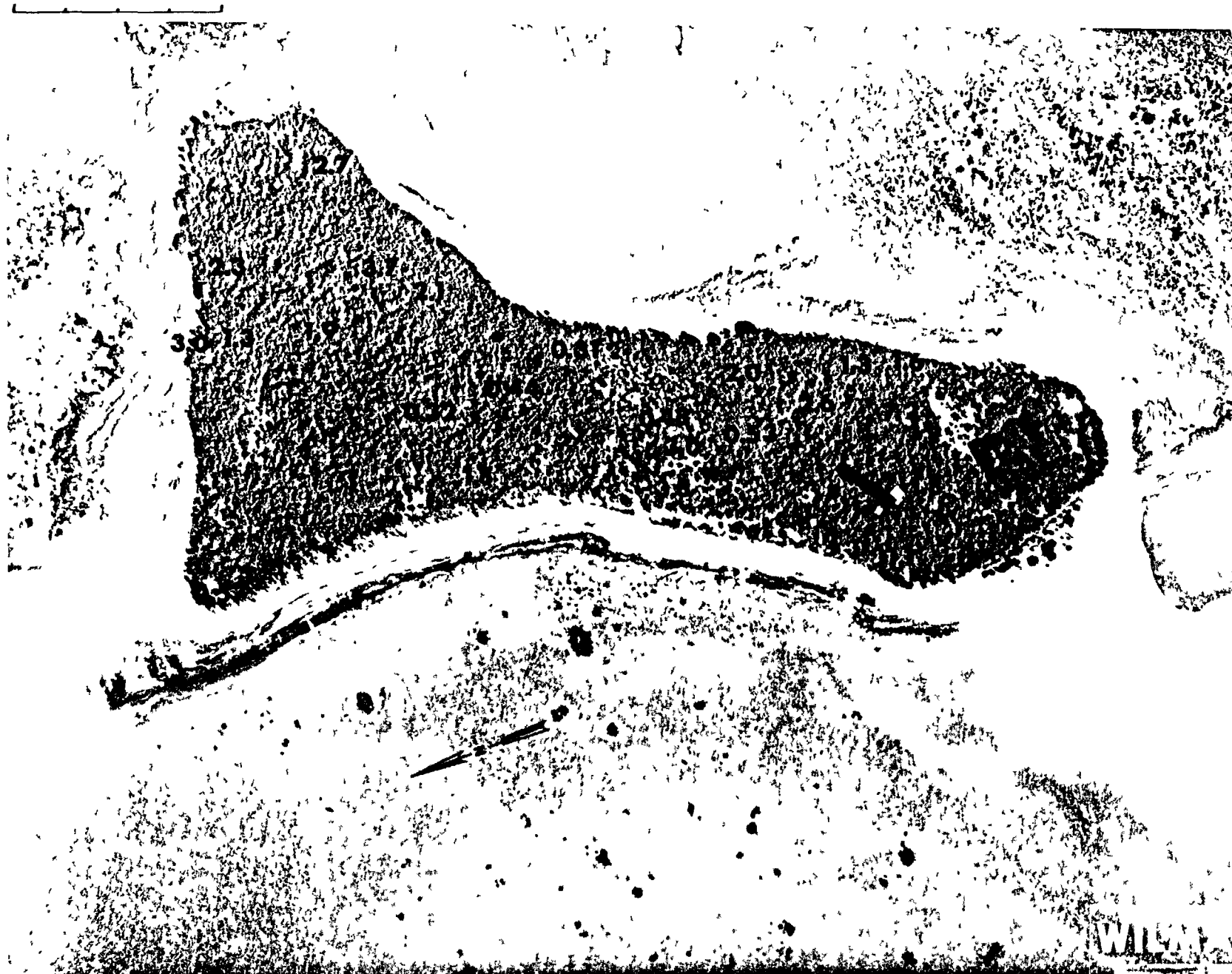


Fig. B.21.1.1. The average  $^{137}\text{Cs}$  activities (pCi/gm) in soil samples collected to a depth of 15 cm.



Fig. B.21.1.m.  $^{60}\text{Co}$  isoexposure and isoconcentration contours. (Refer to alphabetic symbol key in this appendix.)

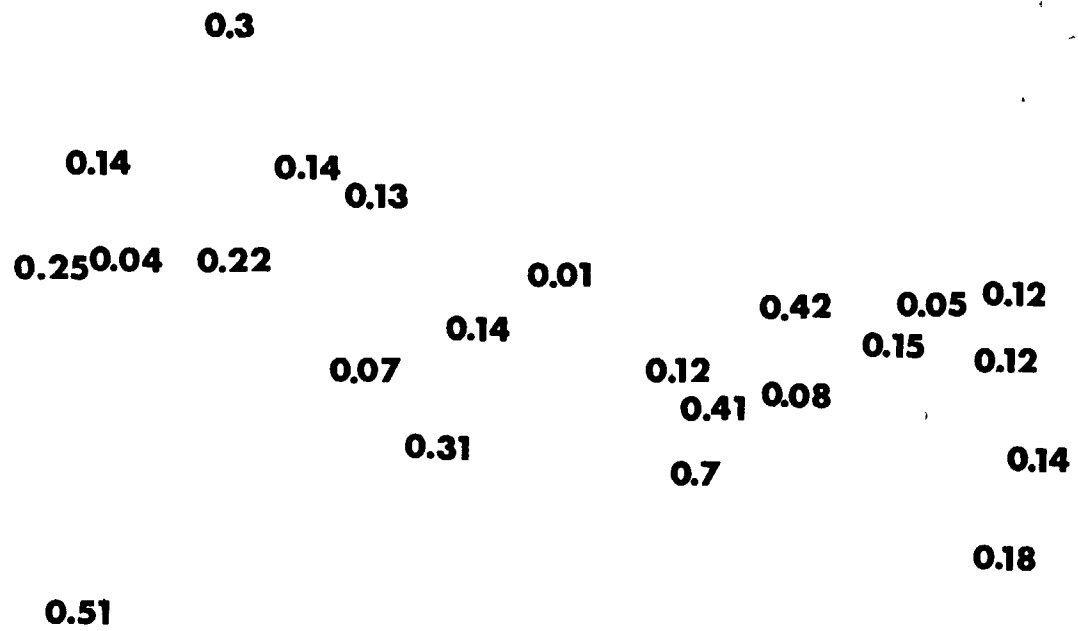


Fig. B.21.1.n. The average  $^{60}\text{Co}$  activities (pCi/gm) in soil samples collected to a depth of 15 cm.

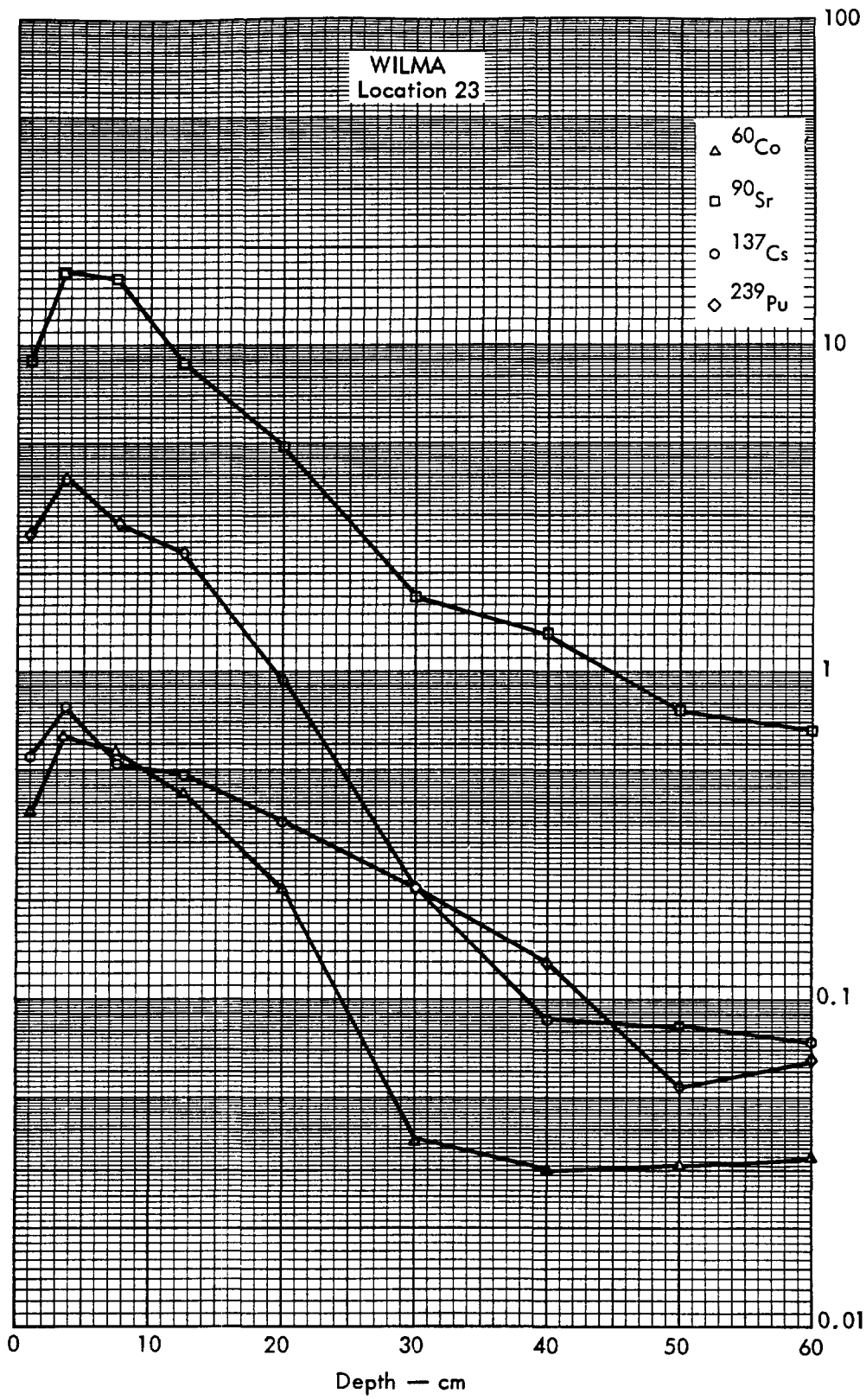


Fig. B.21.2a. Activities of selected radionuclides as a function of soil depth.



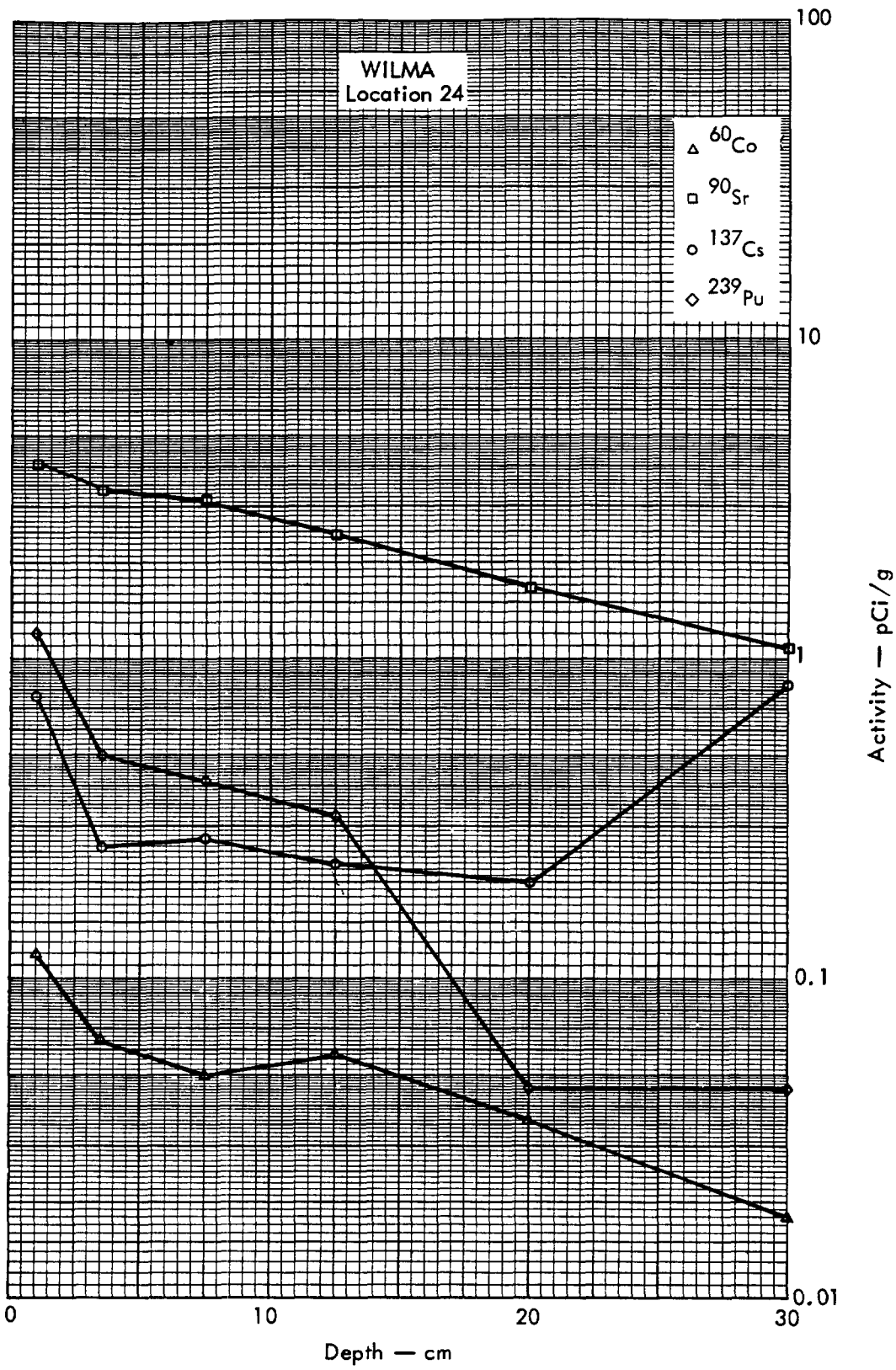


Fig. B.21.2b. Activities of selected radionuclides as a function of soil depth.

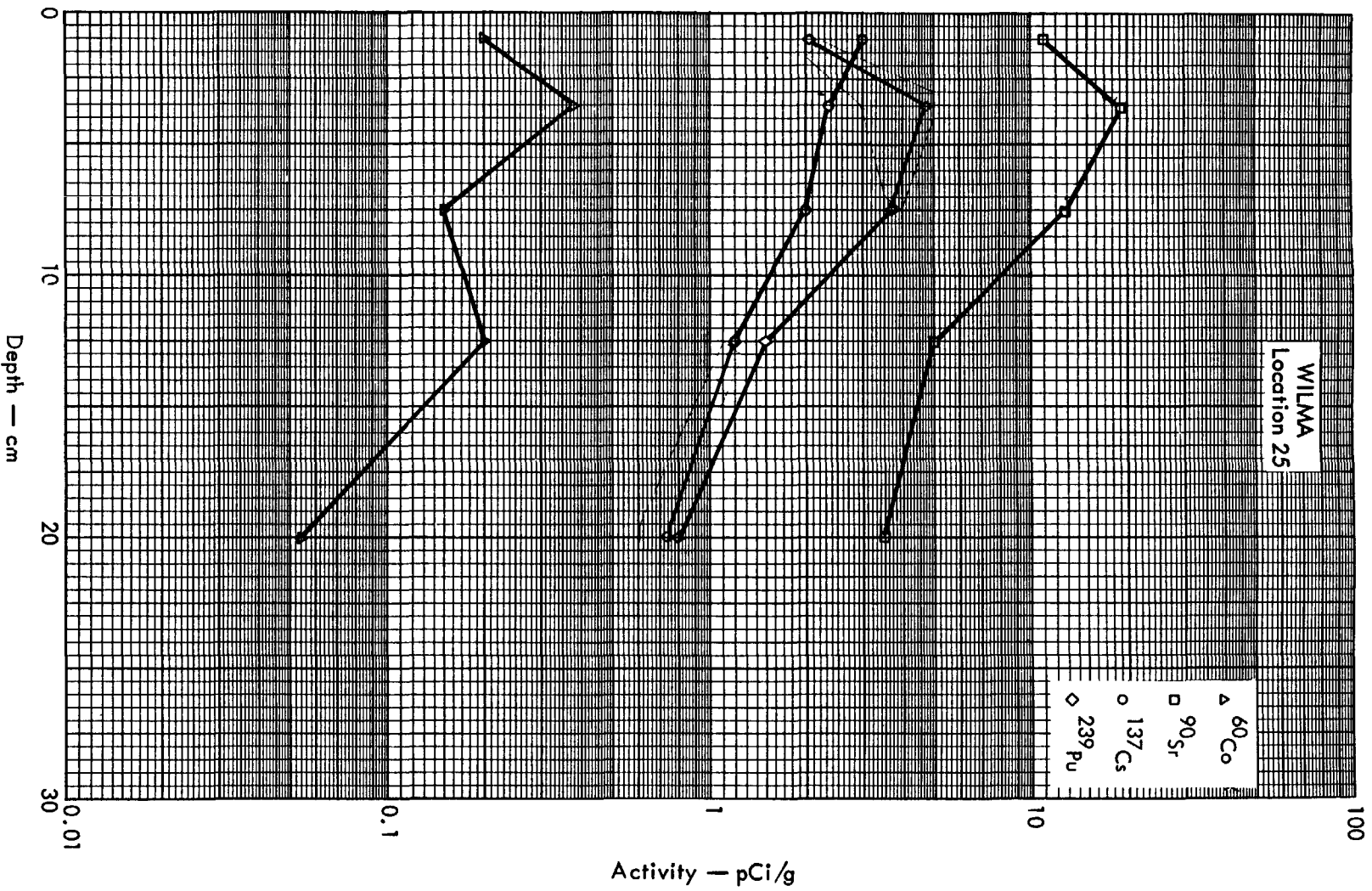


Fig. B. 21. 2c. Activities of selected radionuclides as a function of soil depth.

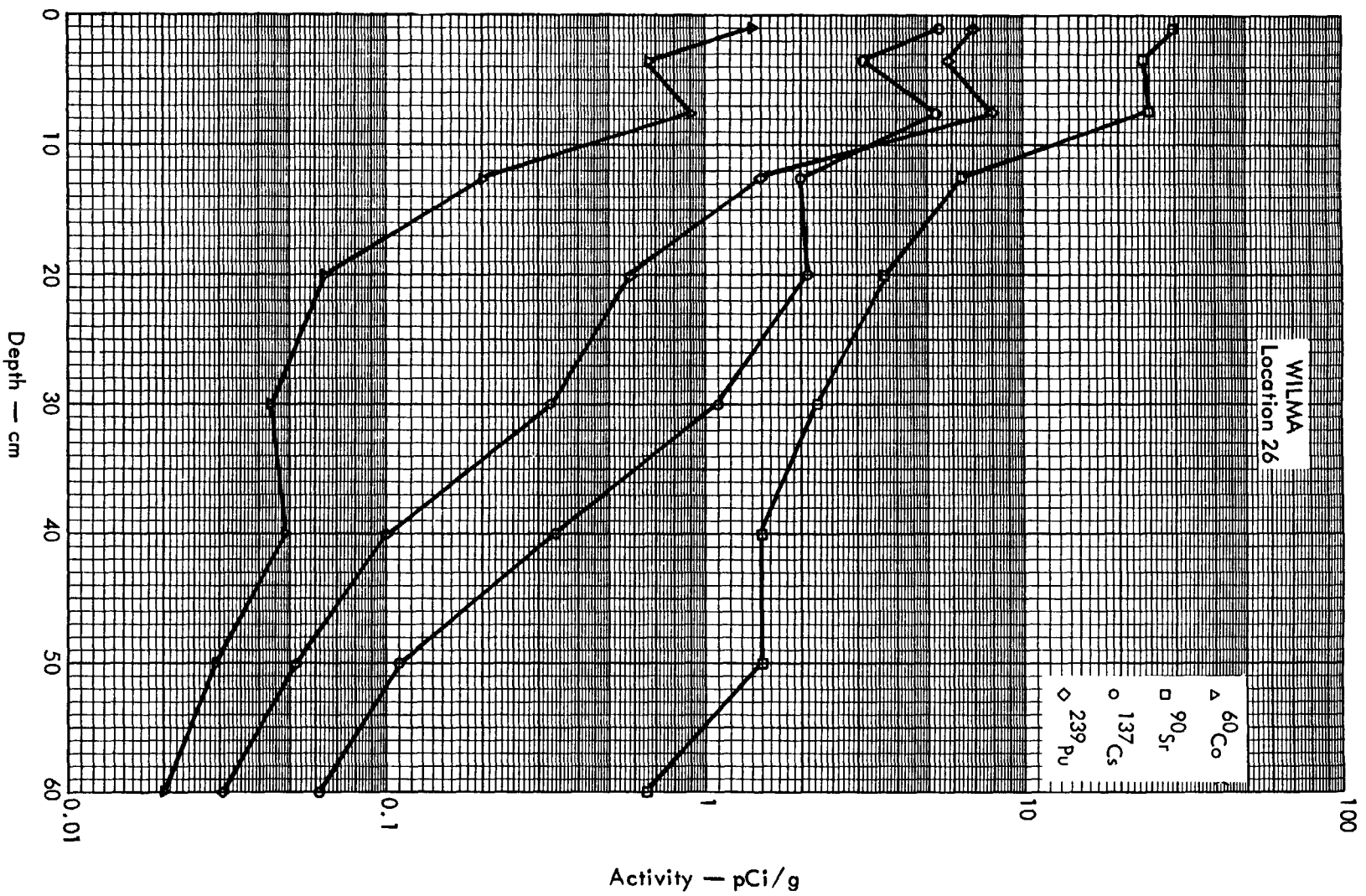


Fig. B.21.2d. Activities of selected radionuclides as a function of soil depth.

100 METERS

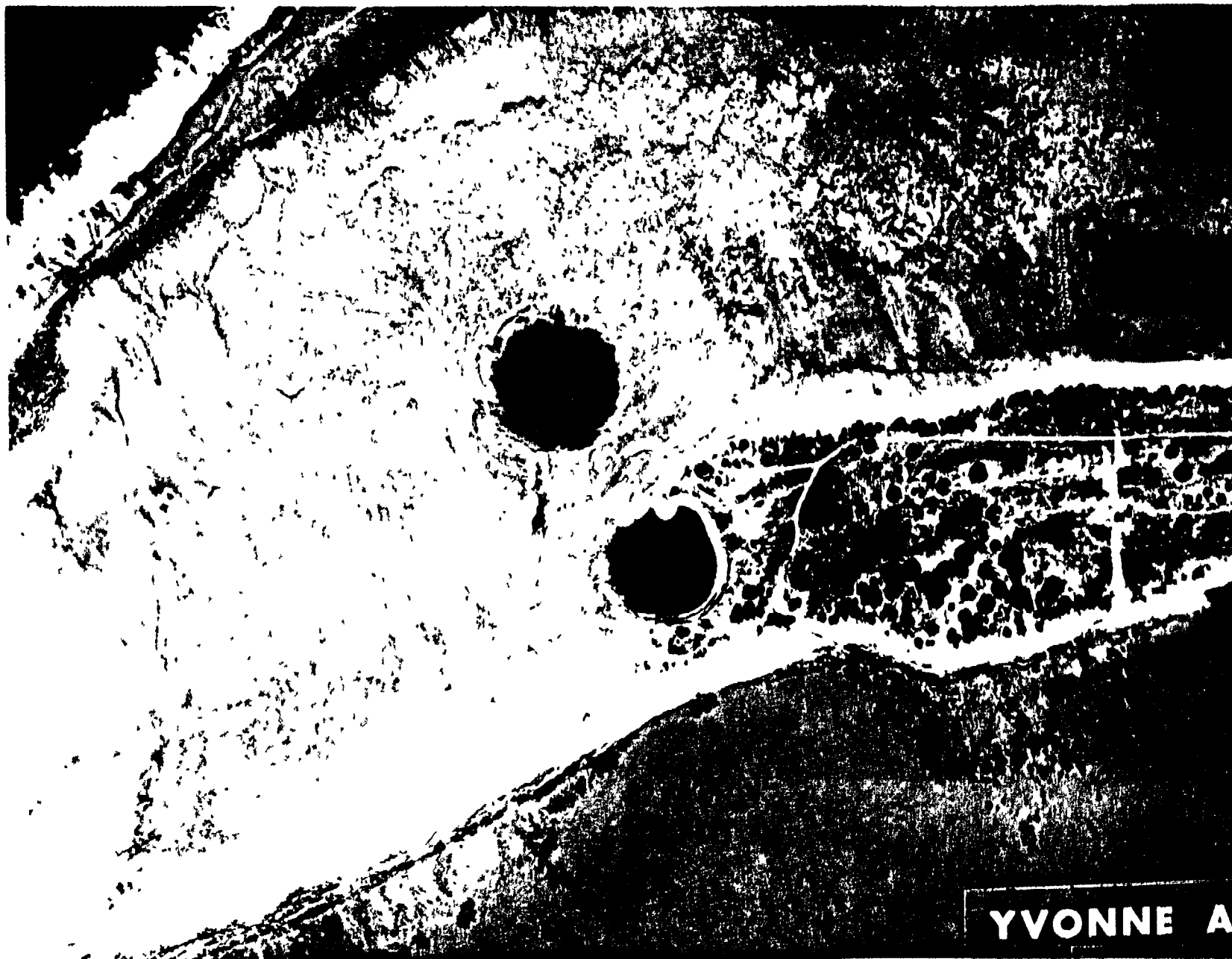


Fig. B.22.1.a.

100 METERS

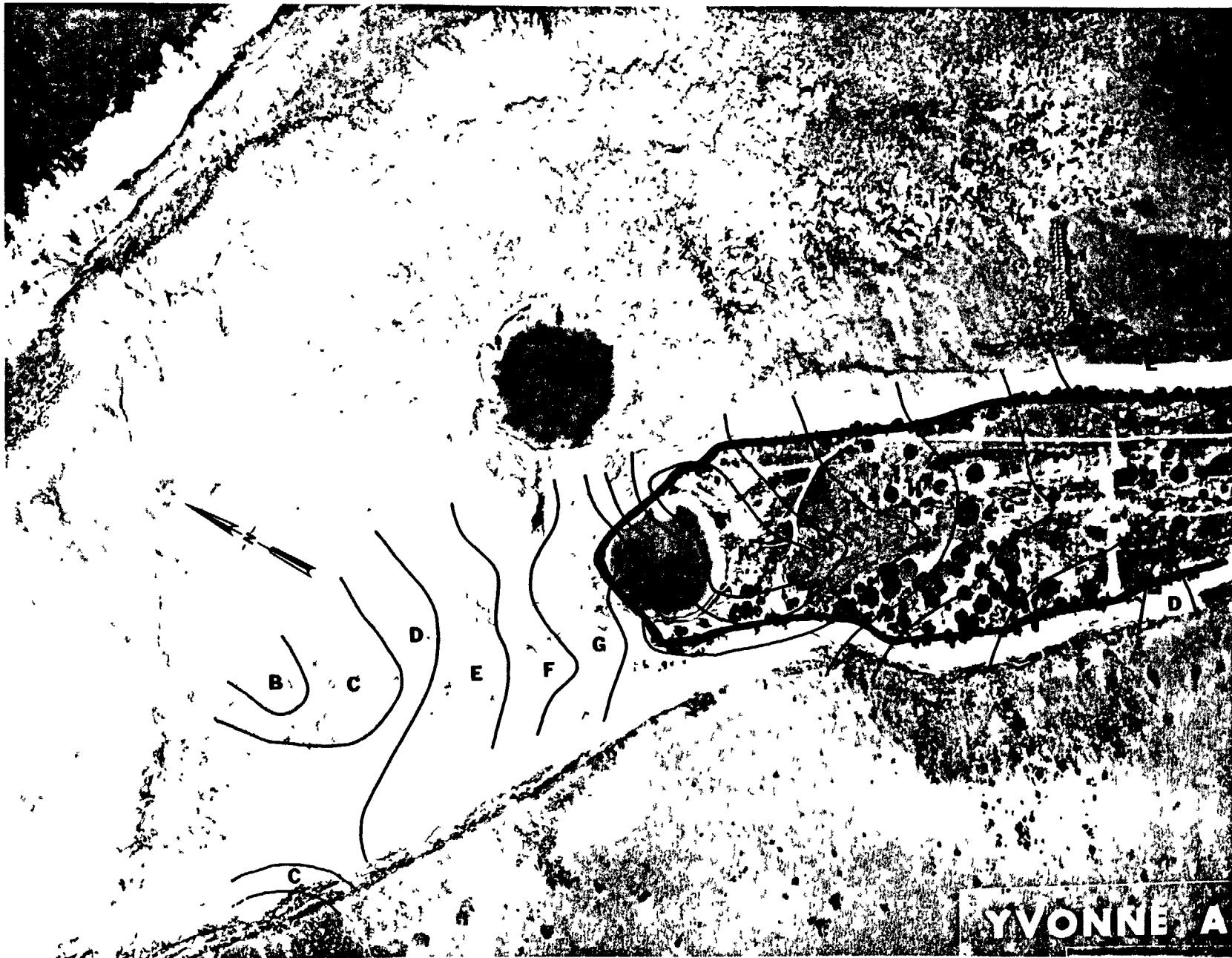
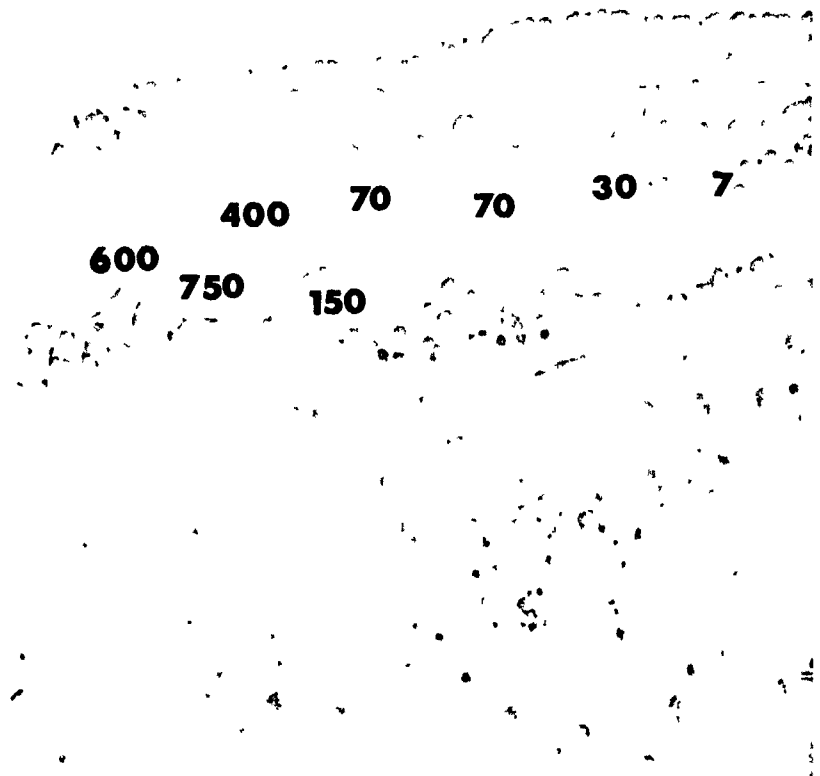
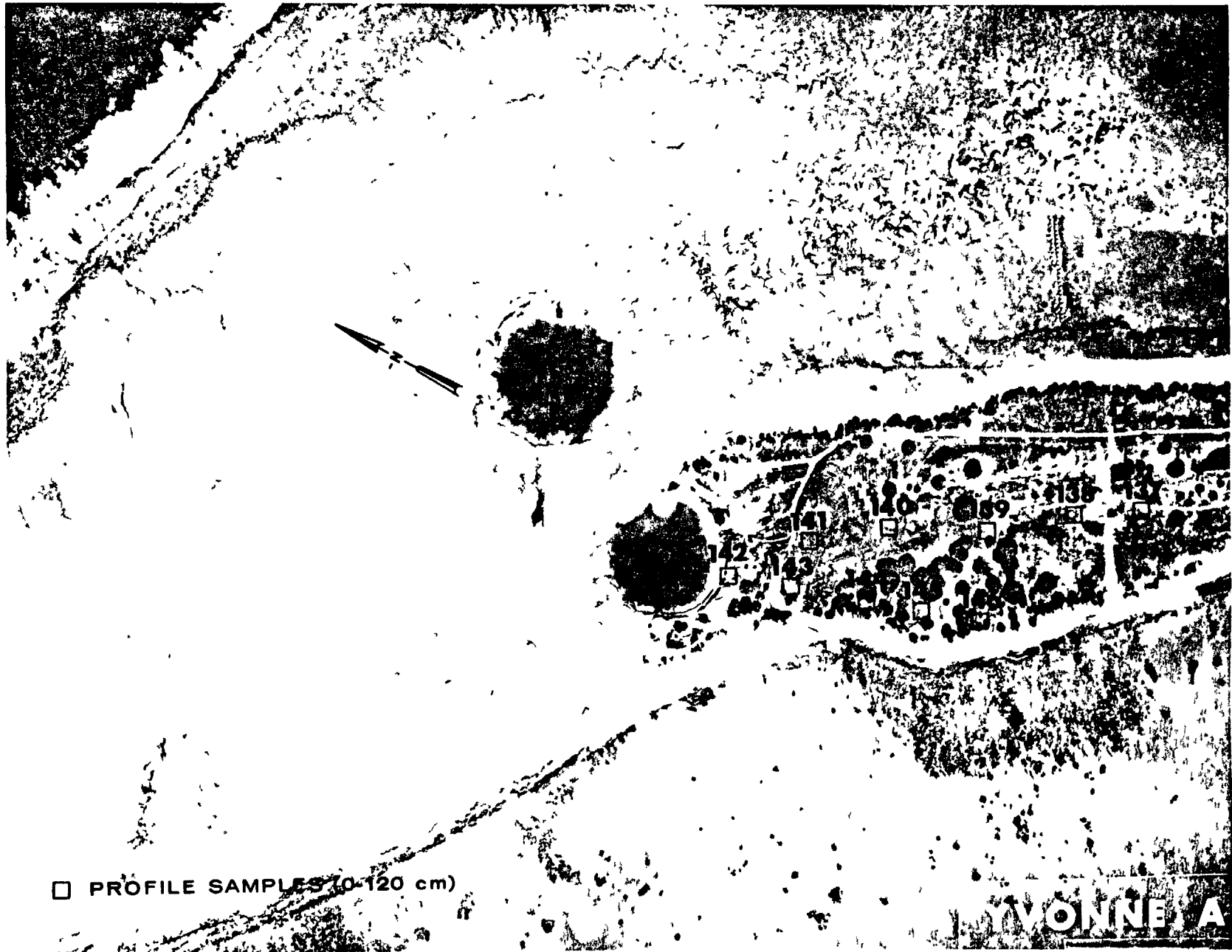


Fig. B.22.1.b. Gross count isoexposure contours. (Refer to alphabetic symbol key in this appendix.)



B.22.1.d. The gamma background exposure rate ( $\mu\text{R/hr}$ ) at 1 m above the ground, measured with a portable NaI scintillation counter.

100 METERS



□ PROFILE SAMPLES (0-120 cm)

B.22.1.f. Soil-sample locations.

100 METERS

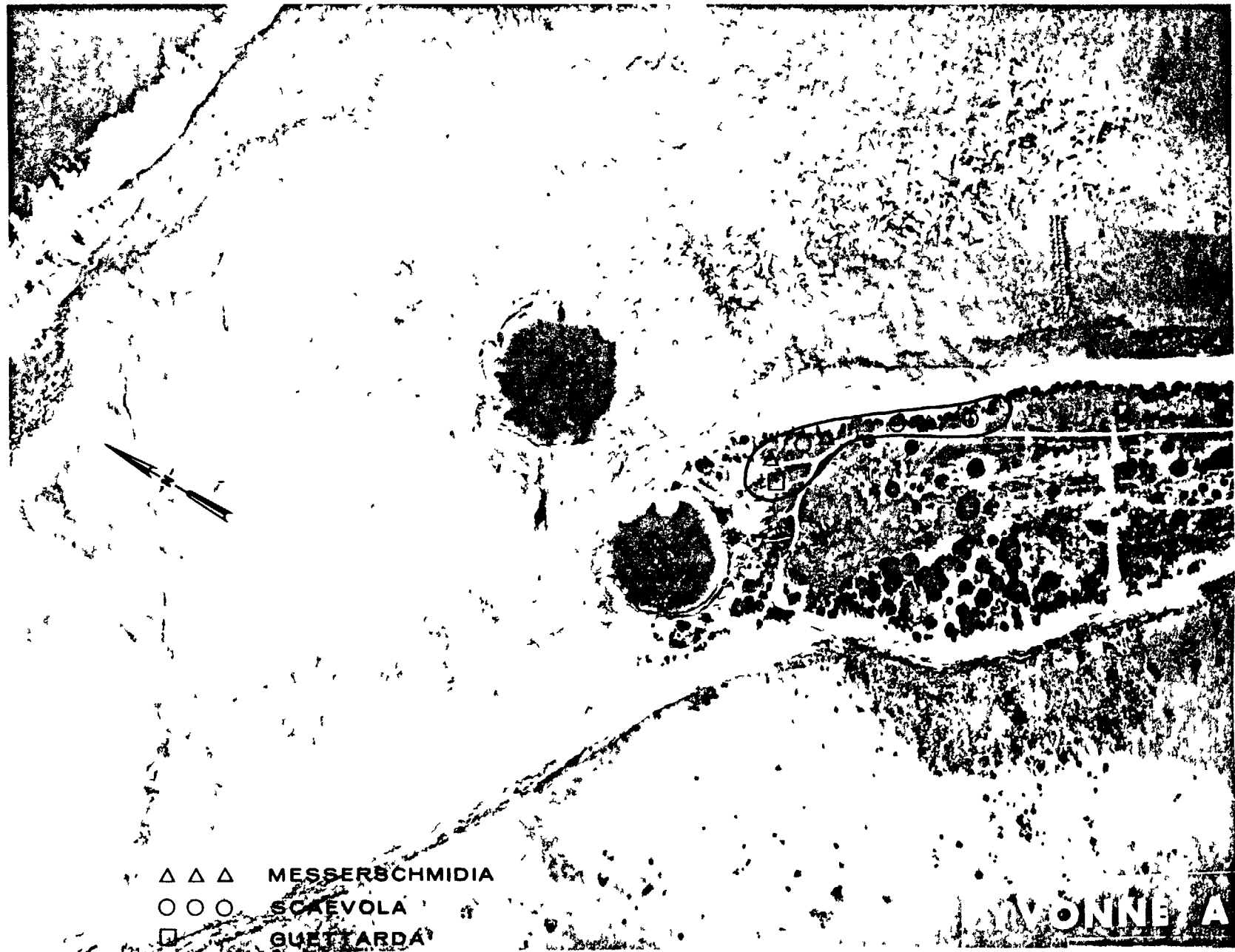
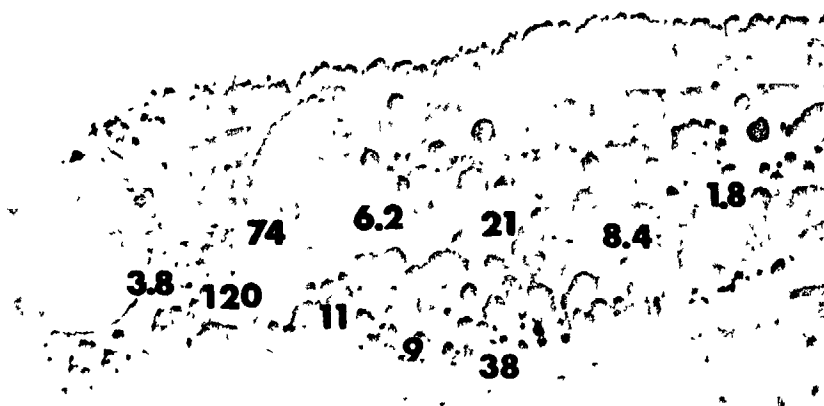


Fig. B.22.1.g. Vegetation sample locations.

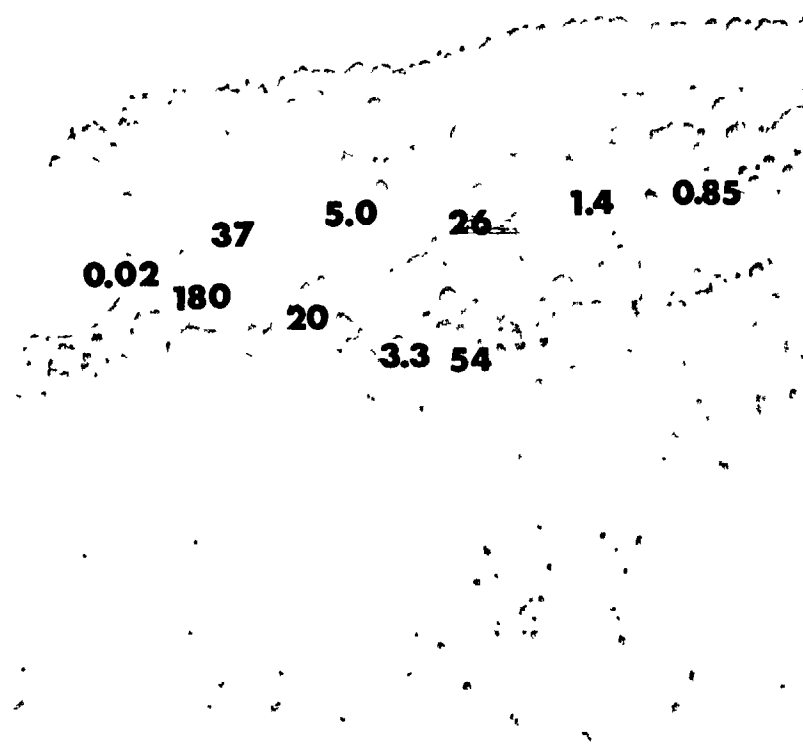


100 METERS



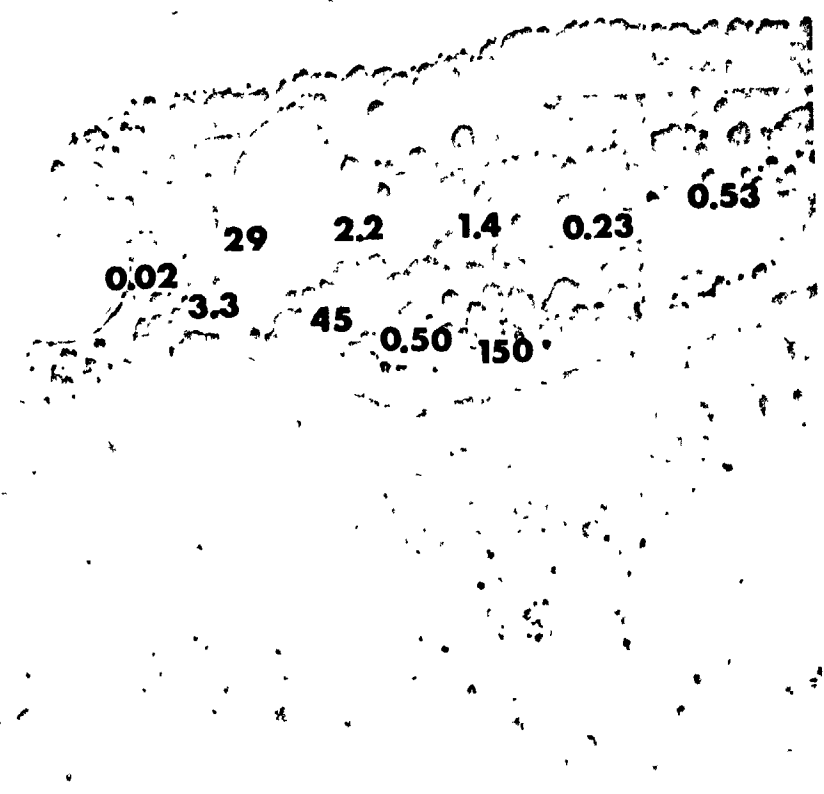
B.22.1.i.1. The average  $^{239}\text{Pu}$  activities (pCi/gm) in soil samples collected between depths of 0 and 10 cm.

100 METERS



B.22.1.1.2. The average <sup>239</sup>Pu activities (pCi/gm) in soil samples collected between depths of 10 and 20 cm.

100 METERS



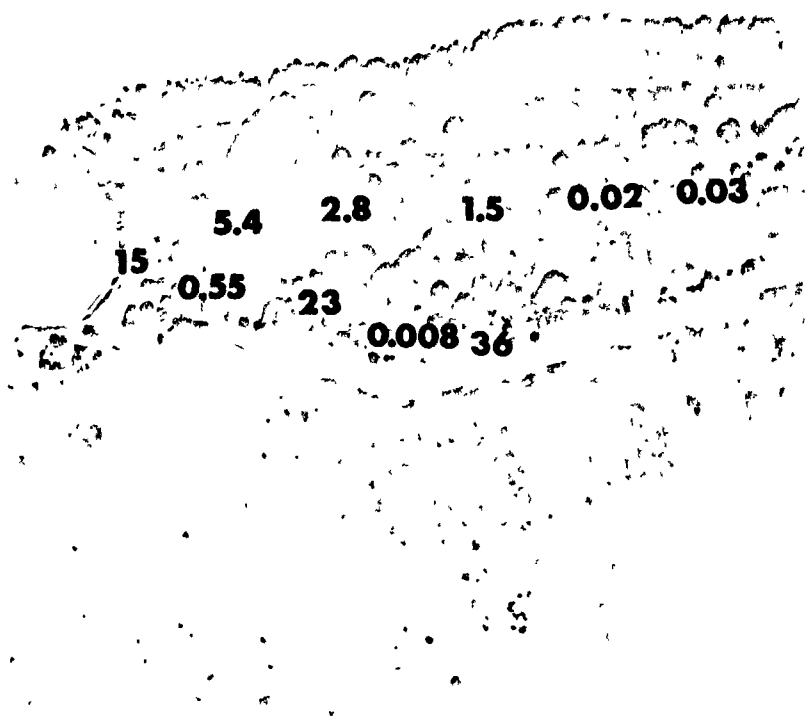
B.22.1.1.3. The average <sup>239</sup>Pu activities (pCi/gm) in soil samples collected between depths of 20 and 30 cm.

100 METERS



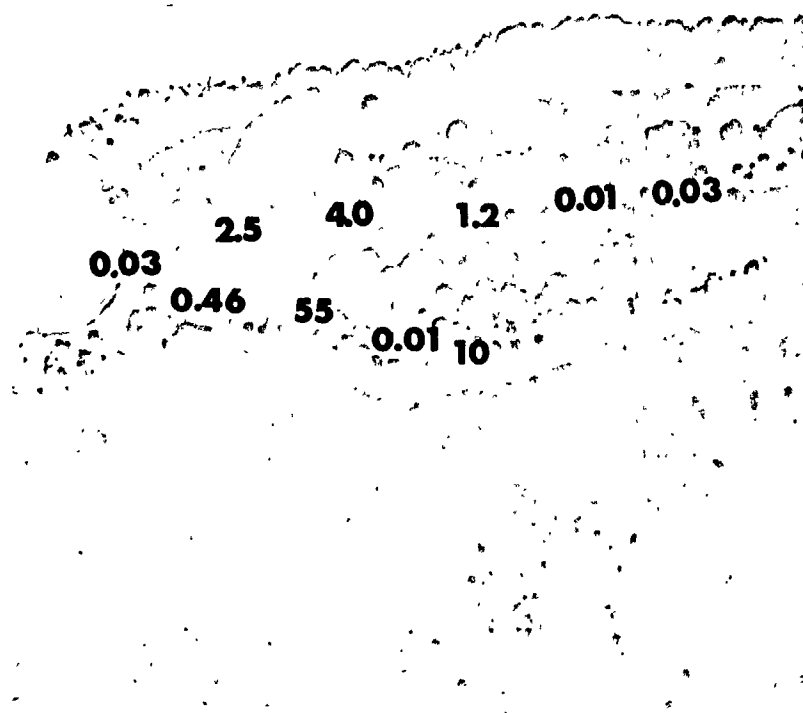
B.22.1.i.4. The average  $^{239}\text{Pu}$  activities (pCi/gm) in soil samples collected between depths of 30 and 40 cm.

100 METERS



B.22.1.1.5. The average  $^{239}\text{Pu}$  activities (pCi/gm) in soil samples collected between depths of 40 and 50 cm.

100 METERS



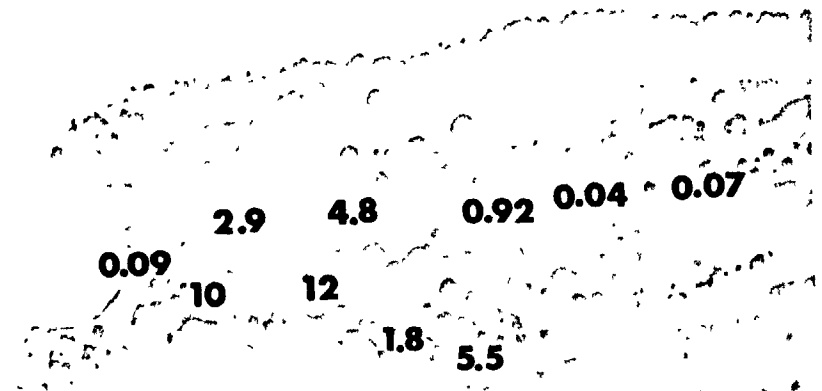
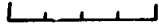
B.22.1.1.6. The average  $^{239}\text{Pu}$  activities (pCi/gm) in soil samples collected between depths of 50 and 60 cm.

100 METERS



B.22.1.1.7. The average  $^{239}\text{Pu}$  activities (pCi/gm) in soil samples collected between depths of 60 and 70 cm.

100 METERS



B.22.1.i.8. The average  $^{239}\text{Pu}$  activities (pCi/gm) in soil samples collected between depths of 70 and 80 cm.



100 METERS



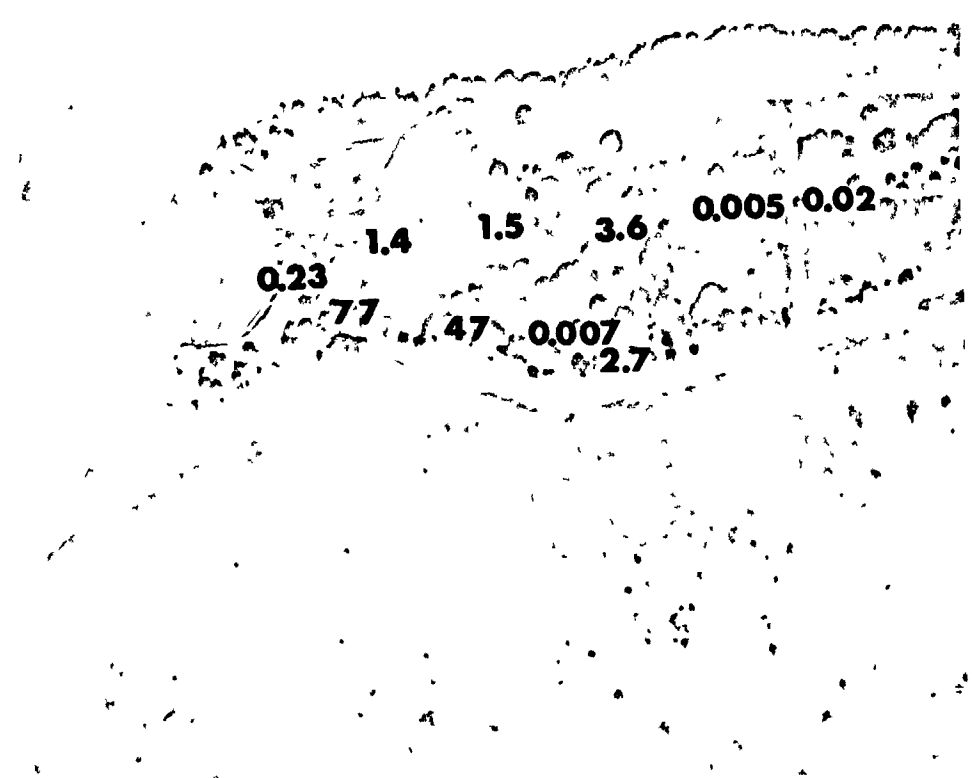
B.22.1.i.9. The average  $^{239}\text{Pu}$  activities (pCi/gm) in soil samples collected between depths of 80 and 90 cm.

100 METERS



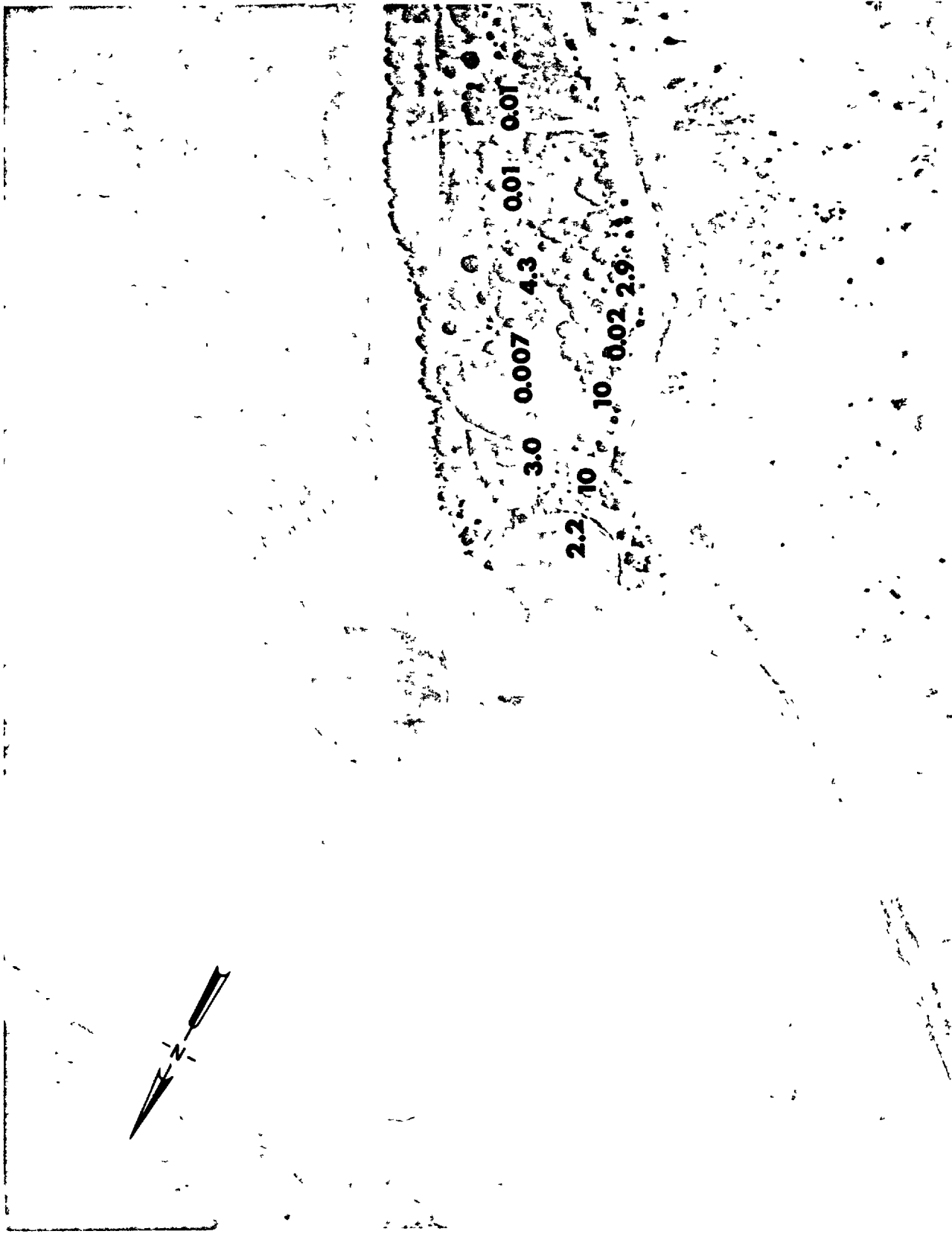
B 22.1.1.10. The average <sup>239</sup>Pu activities (pCi/gm) in soil samples collected between depths of 90 and 100 cm.

100 METERS



B.22.1.1.11. The average  $^{239}\text{Pu}$  activities (pCi/gm) in soil samples collected between depths of 100 and 110 cm.

100 METERS



B.22.1.i.12. The average  $^{239}\text{Pu}$  activities (pCi/gm) in soil samples collected between depths of 110 and 120 cm.

100 METERS

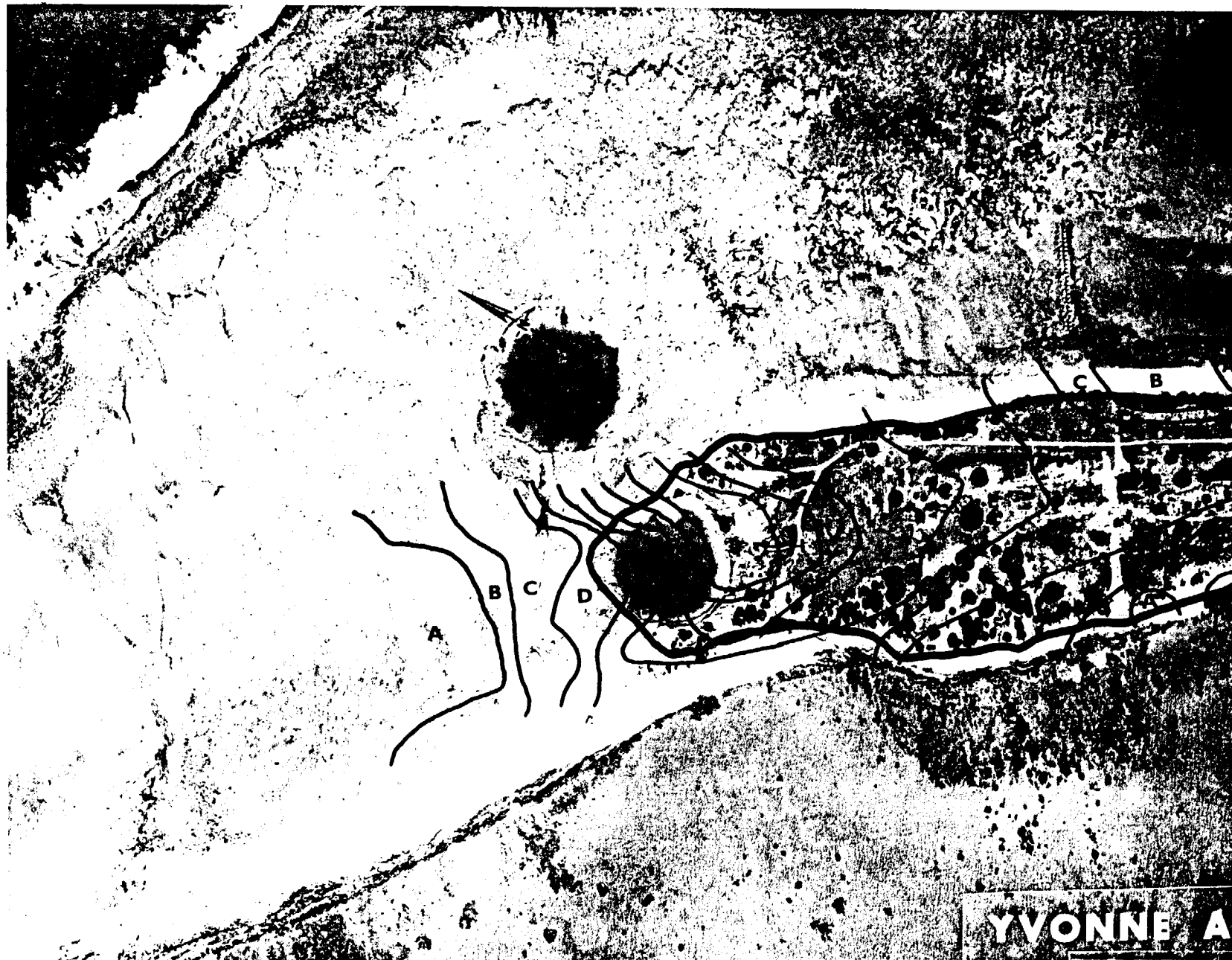


Fig. B.22.1.k.  $^{137}\text{Cs}$  isoexposure and isoconcentration contours. (Refer to alphabetic symbol key in this appendix.)

100 METERS

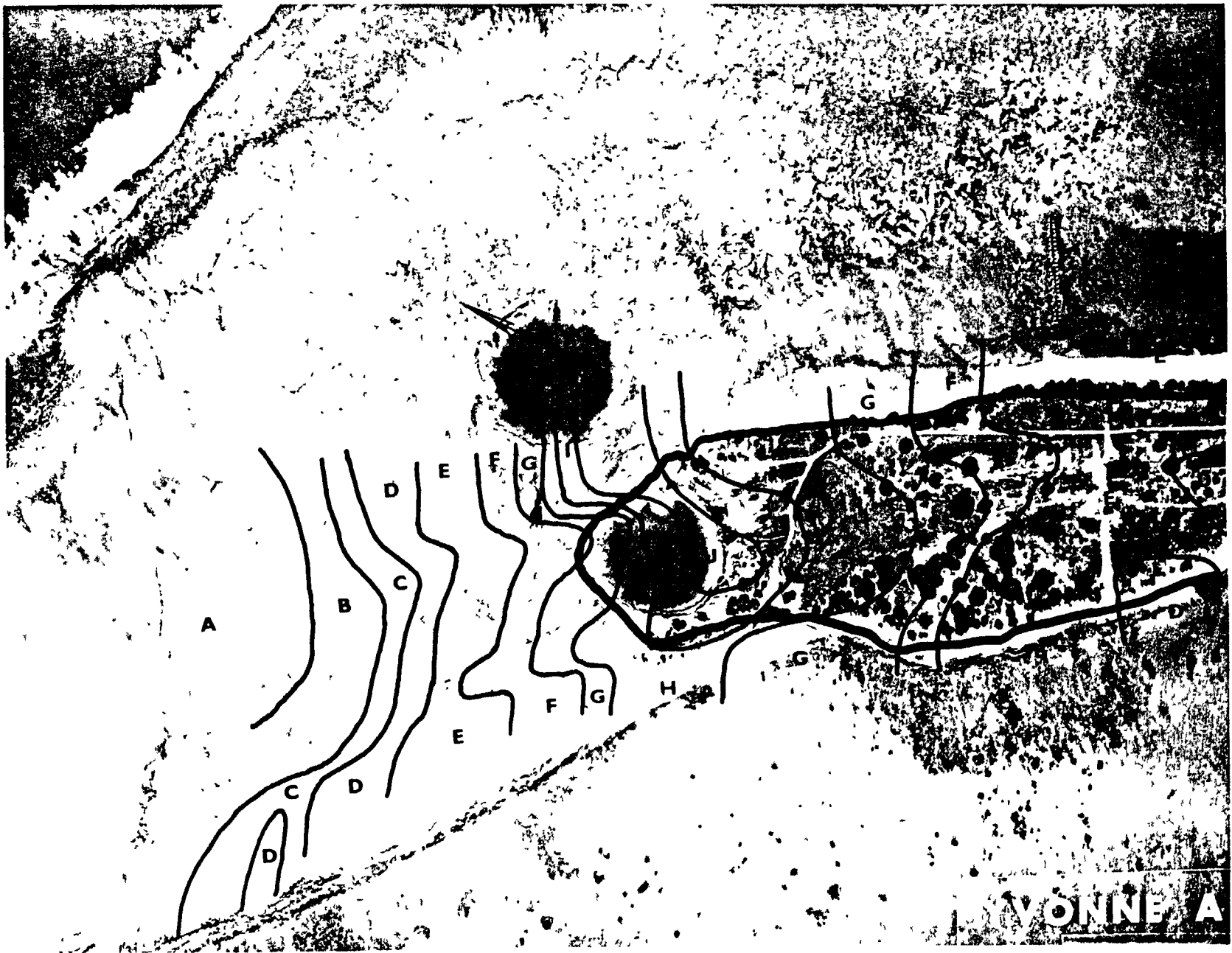


Fig. B.22.1.m.  $^{60}\text{Co}$  isoexposure and isoconcentration contours. (Refer to alphabetic symbol key in this appendix.)

100 METERS

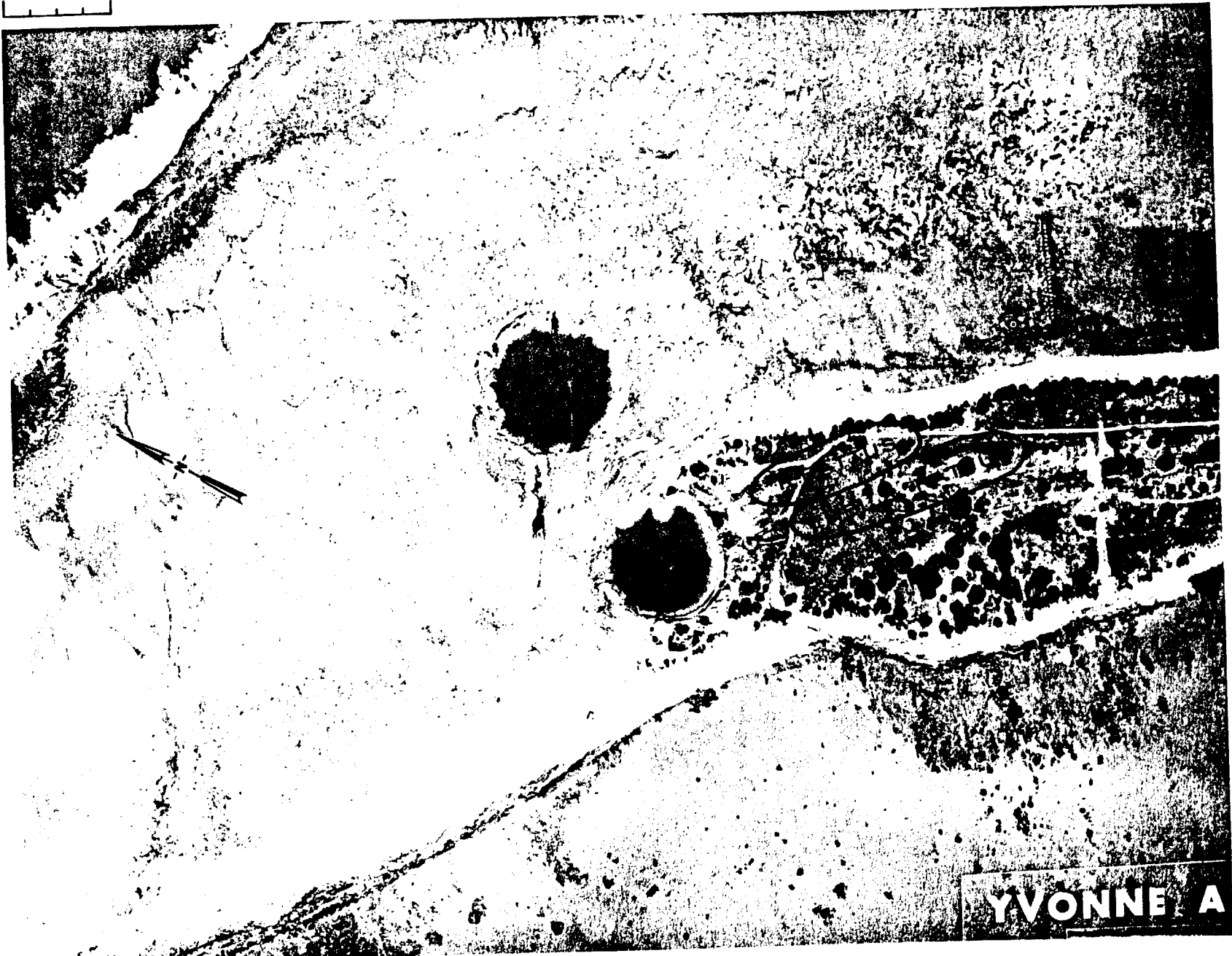


Fig. B.22.1.o. Terrestrial animal sample locations.

YVONNE A

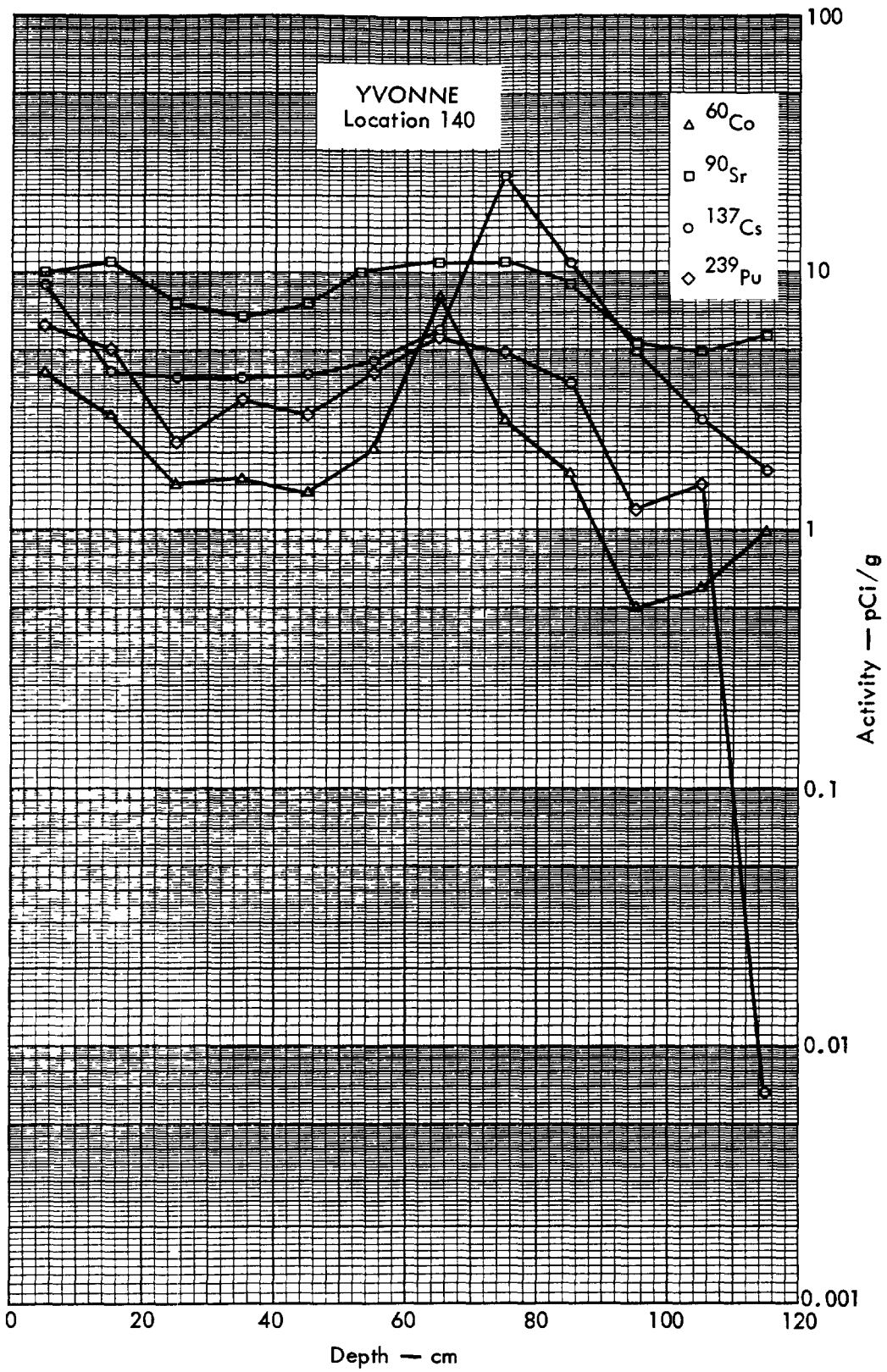


Fig. B. 22.2a. Activities of selected radionuclides as a function of soil depth.



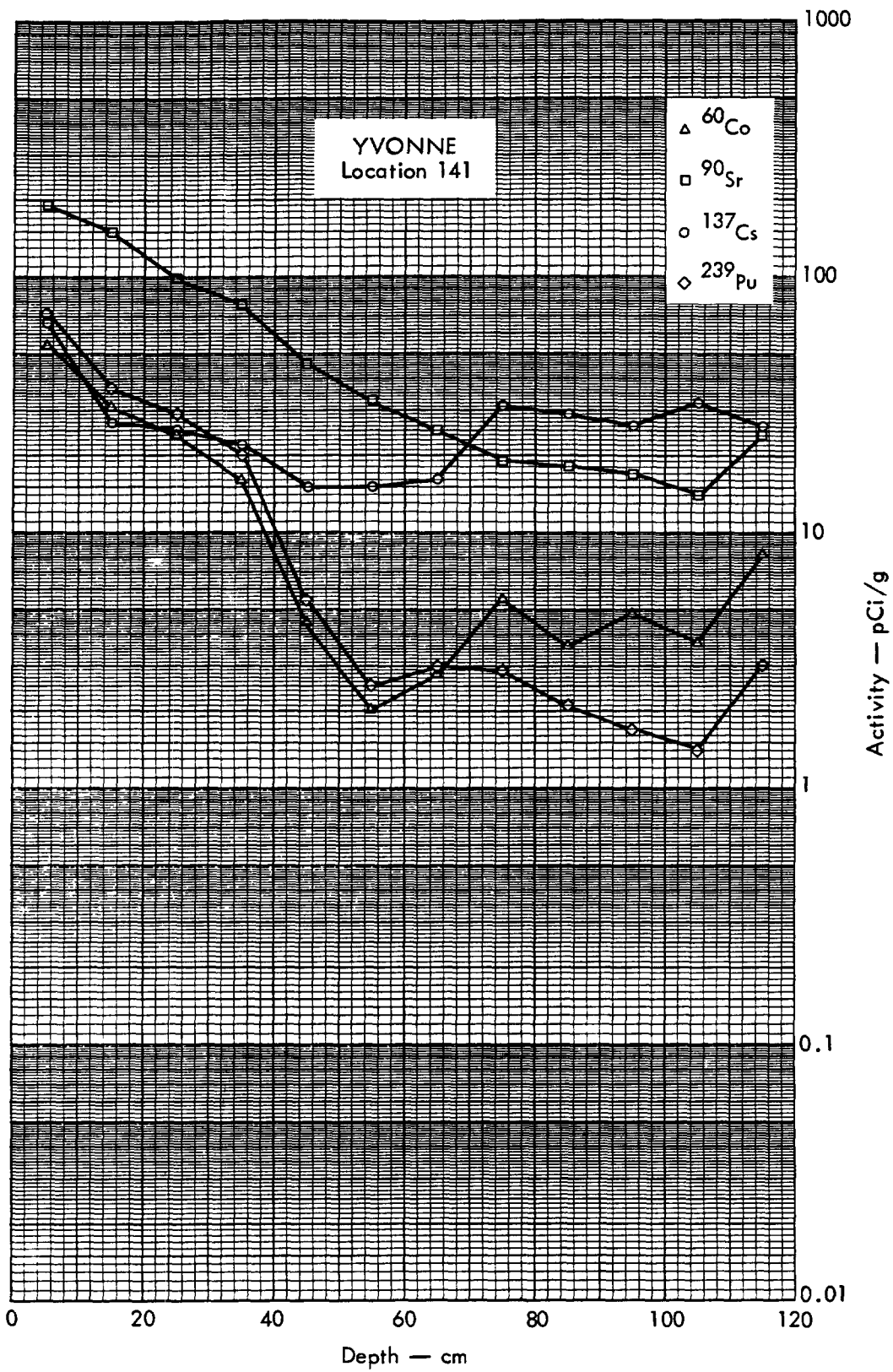


Fig. B. 22.2b. Activities of selected radionuclides as a function of soil depth.

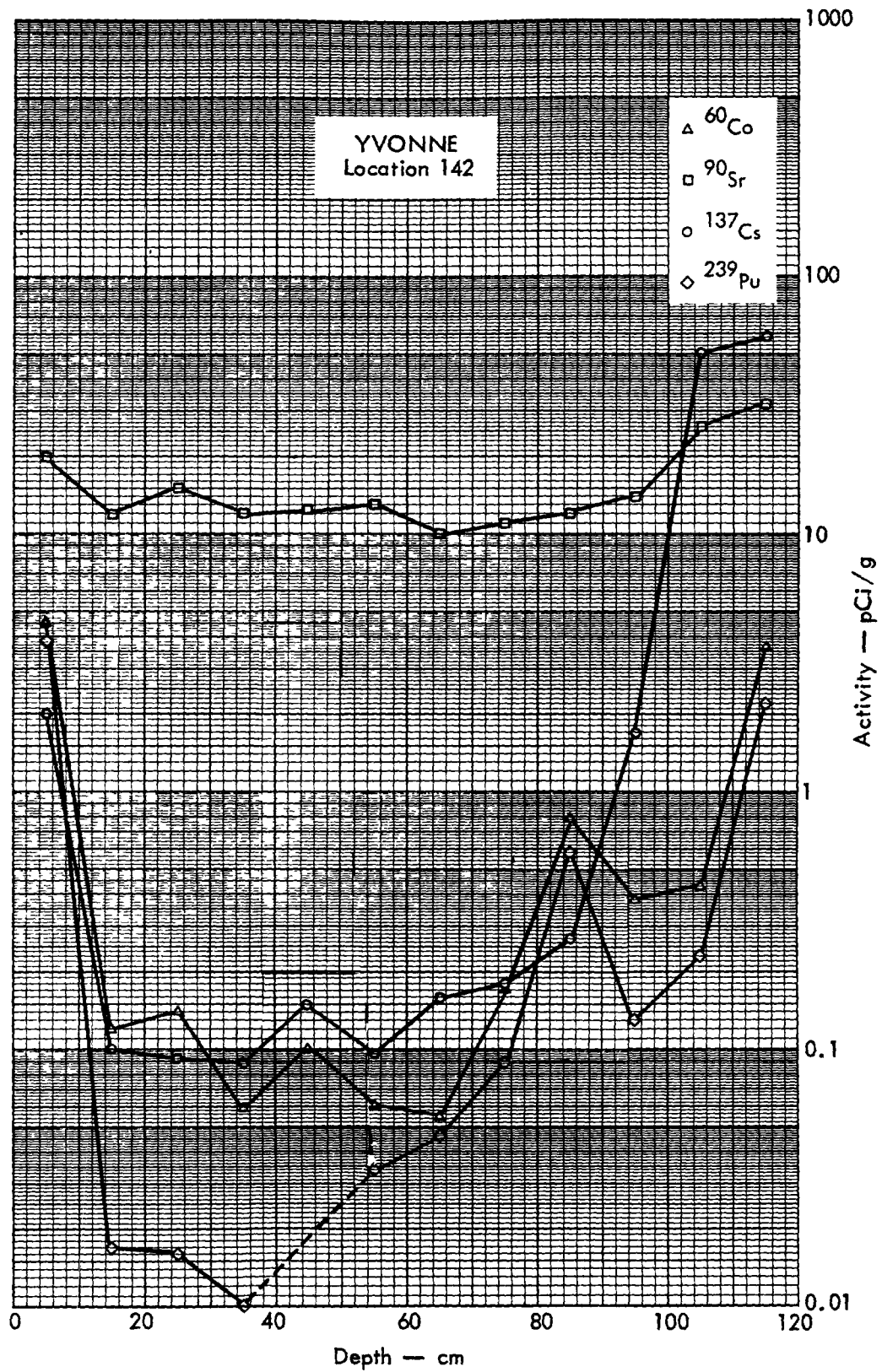


Fig. B. 22.2c. Activities of selected radionuclides as a function of soil depth.

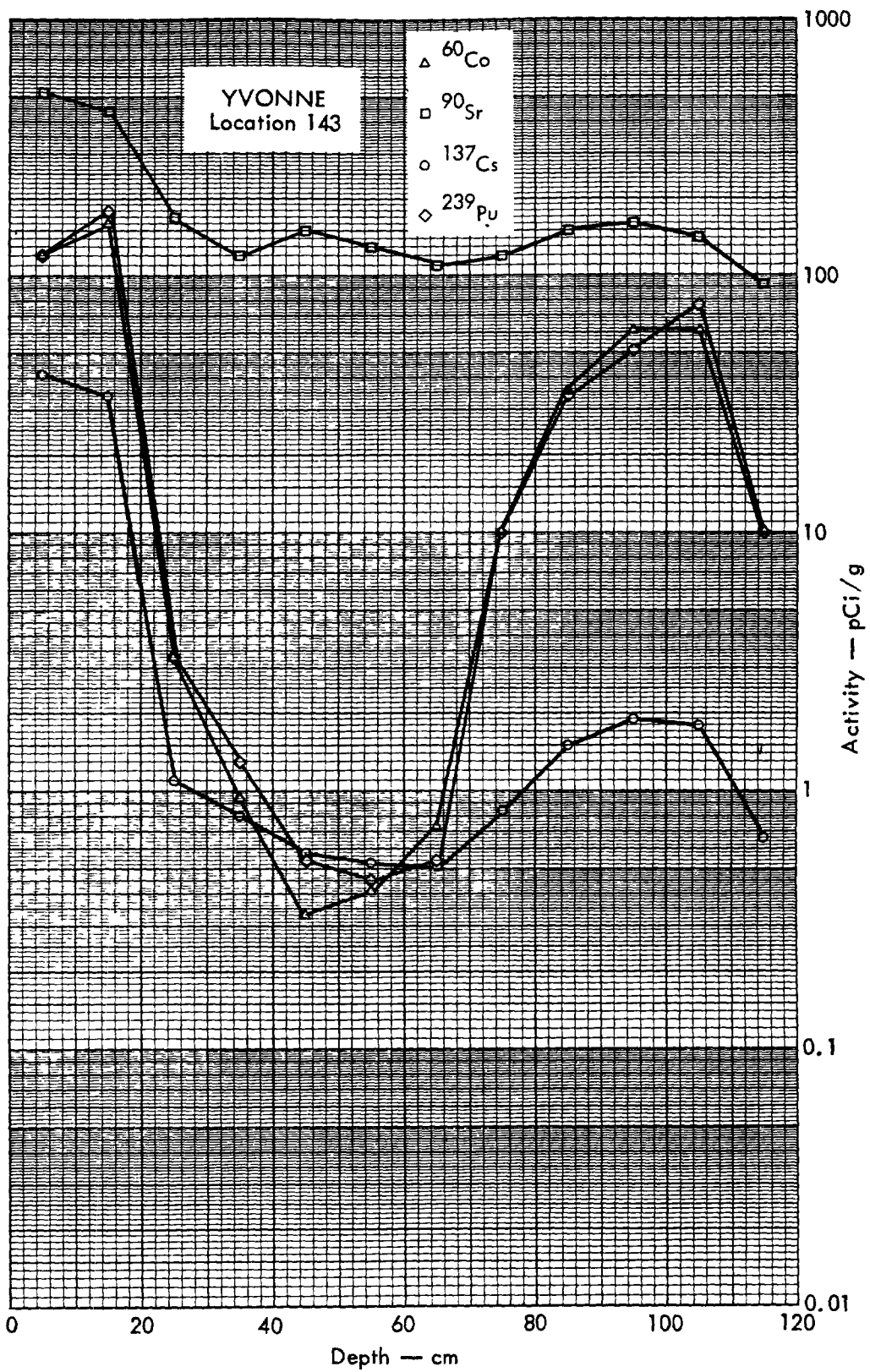


Fig. B. 22.2d. Activities of selected radionuclides as a function of soil depth.

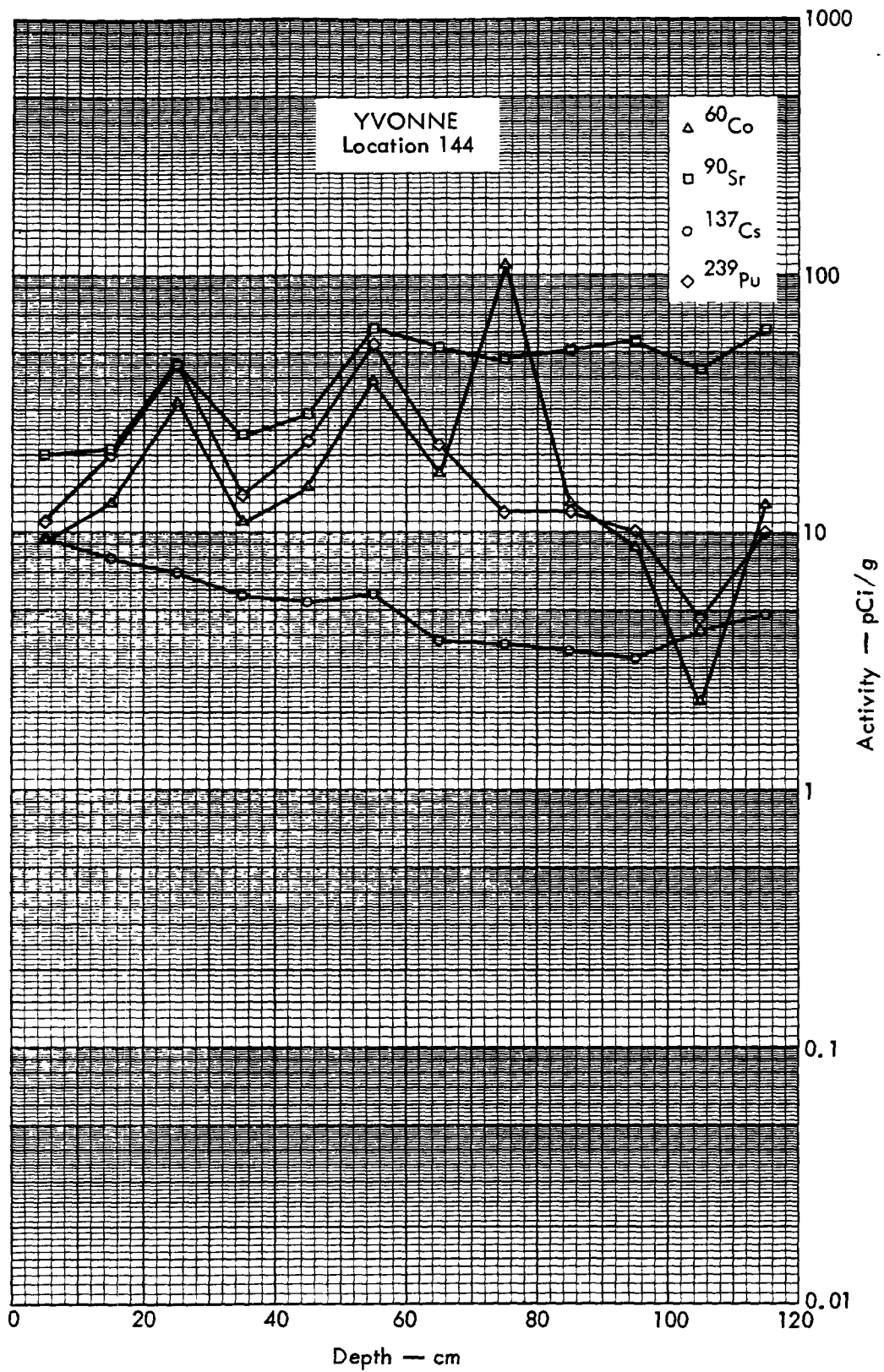


Fig. B. 22.2e. Activities of selected radionuclides as a function of soil depth.

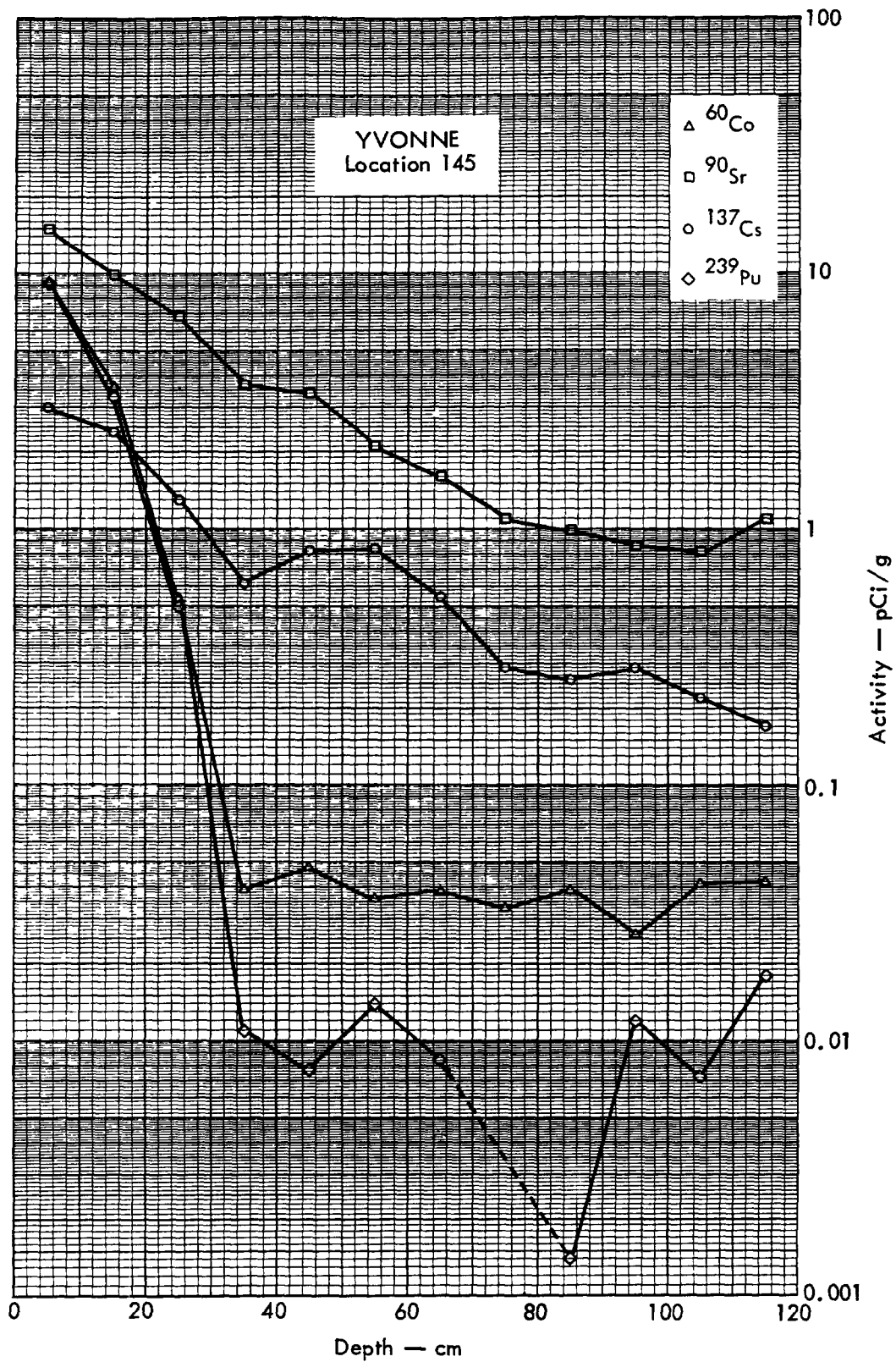


Fig. B.22.2f. Activities of selected radionuclides as a function of soil depth.

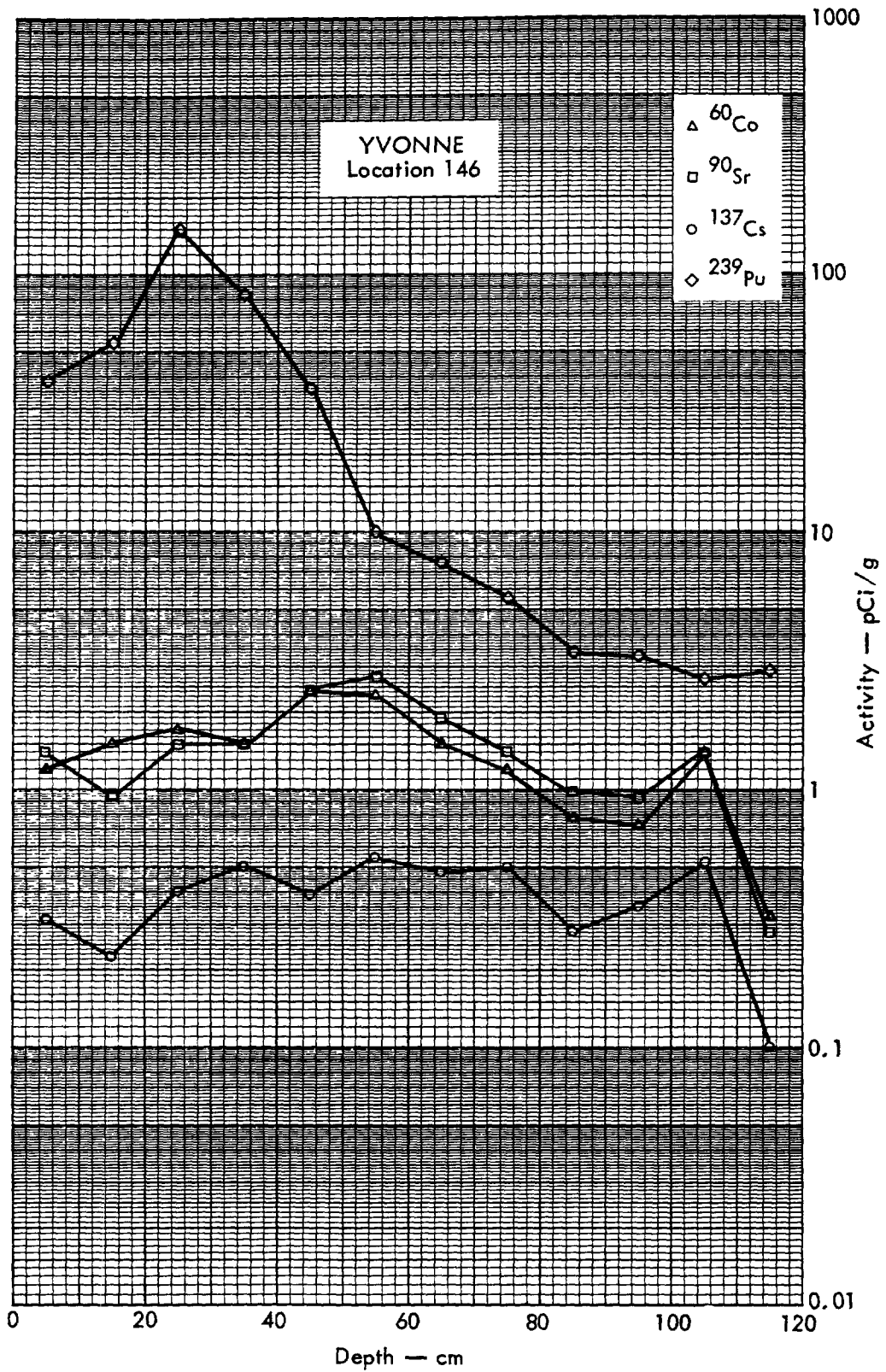


Fig. B. 22.2g. Activities of selected radionuclides as a function of soil depth.

Table C.3 Analytical data.

SET 1